Advances in Experimental Medicine and Biology 715

Dirk Linke
Adrian Goldman *Editors*

Bacterial Adhesion

Chemistry, Biology and Physics

Springer

Bacterial Adhesion

ADVANCES IN EXPERIMENTAL MEDICINE AND BIOLOGY

For further volumes:
http://www.springer.com/series/5584

Dirk Linke · Adrian Goldman
Editors

Bacterial Adhesion

Chemistry, Biology and Physics

Springer

Editors
Dirk Linke
Max Planck Institute
for Developmental Biology
Department of Protein Evolution
Spemannstr. 35
72076 Tübingen
Germany
dirk.linke@tuebingen.mpg.de

Adrian Goldman
University of Helsinki
Institute of Biotechnology
Viikinkaari 1
FIN-00014 Helsinki
Finland
adrian.goldman@helsinki.fi

ISSN 0065-2598
ISBN 978-94-007-0939-3 e-ISBN 978-94-007-0940-9
DOI 10.1007/978-94-007-0940-9
Springer Dordrecht Heidelberg London New York

Library of Congress Control Number: 2011924005

Introduction

Why a book on bacterial adhesion? Adhesion plays a major role in the bacterial lifestyle. Bacteria adhere to all surfaces and did so long before the first eukaryotes were around; stromatolites, which are calcium-based rocks in shallow seawaters formed and inhabited by cyanobacteria, are among the oldest fossils found (Battistuzzi et al., 2004). Bacteria can adhere to each other, a phenomenon referred to as autoagglutination, which is generally viewed as one of the first steps towards biofilm formation. Bacteria can also form more complex and defined structures, such as the *Myxococcus* fruiting bodies – *Myxococcus* is generally seen as a "social" bacterium with complex inter-cell interactions, and as a model for the early evolution of multicellularity (Konovalova et al., 2010). Last but not least, bacteria can adhere to other cells: different prokaryotic species in the formation of complex biofilms, or eukaryotic cells during disease. Adhesion to eukaryotic cells can serve different purposes in commensalism, symbiosis, and pathogenesis. The general principle, the expression of surface molecules to adhere to other structures, stays the same.

But why this particular book when reviews on bacterial pathogenesis are common, if not quite a dime a dozen? Our focus is: how are such adhesion phenomena best studied? Microbial genetics experiments have greatly enhanced our knowledge of what bacterial factors are involved in adhesion. For numerous reasons, though, biochemical and structural biology knowledge of the molecular interactions involved in adhesion is limited. Moreover, many of the most powerful biophysical methods available are not frequently used in adhesion research, meaning that the time dimension – the evolution of adhesion during biofilm formation remains poorly explored. The reason for this is, we believe, on the one hand microbiologists, who are experts at handling and manipulating the frequently pathogenic bacterial organisms in which adhesion is studied, lack detailed knowledge of the biophysical possibilities and have limited access to the frequently expensive instrumentation involved. On the other hand, the experts in these methods frequently do not have access to the biological materials, nor do they necessarily understand the biological questions to be answered. The purpose of this book is thus to overcome this gap in communication between researchers in biology, chemistry, and physics, and to display the many ways and means to address the topic of bacterial adhesion.

Thus, the book consists of three loosely connected parts. The first Chapters 1 to 7 deal, broadly speaking, with bacterial adhesion from a biological perspective, where different bacterial species and their repertoire of adhesion molecules are described. The chemistry section includes the biochemistry and structural biology knowledge which have been obtained on some of the adhesin systems. The physics section contains examples of biophysical methods that have been successfully applied to bacterial adhesion. For obvious reasons, we had to limit ourselves in the choice of systems and methods described in this book. The biological systems described are only examples, and mostly come from genera containing the better-studied human pathogens. We tried nonetheless to cover a broad spectrum of organisms, both Gram-positive and Gram-negative bacteria. Chapters 1 and 9 also put specific Gram-negative and Gram-positive systems into a historical perspective and describe the development of the field of infectious diseases. Many of the findings also apply to bacteria that are either non-pathogenic (Chapter 13) or pathogenic on different species and kingdoms, and Chapter 5 nicely shows that in plant pathogens, adhesins similar to those of human pathogens exist and serve comparable functions.

The chemistry section (Chapters 8 to 15), contains examples of molecular structures of the very different types of adhesins found. These are mostly from the human pathogens discussed in the biology section, again from both Gram-negative and Gram-positive bacteria. We have also included two chapters on carbohydrate structures (13 and 14), as these structures are at least as important as the proteins in bacterial pathogenesis. One pattern that emerges is that most of these adhesins contain repetitive elements, which make them long and fibrous, but which might also allow for easy recombination and thus evolution in the face of the host immune system.

The physics section (Chapters 16 to 22) originally seemed the hardest to fill: how should we identify methods useful in adhesion research, but infrequently used? Discussions with colleagues and literature searches led us to authors on such diverse methods as force measurements, electron microscopy, NMR, and optical tweezers, as well as a chapter on how bacteria adhere to medical devices and how this can be studied (Chapter 22). Moreover, the enthusiastic response of these authors showed to us that indeed, there is a need for a forum to display the panel of technical possibilities to the researchers who struggle with unsolved biological questions.

Now that the book is finished and out of our hands, we hope that it will achieve our goals – that it will be of broad interest to researchers from different fields all working on different aspects of bacterial adhesion. We hope it provides an advanced but jargon-free introduction to the state of adhesion research in 2010, one that will bring researchers together in new, exciting, and most importantly, interdisciplinary projects. The struggle for new therapies against bacterial infections is not made easier by the "Red Queen Principle" – the fact that pathogens evolve and adapt quickly in the face of new challenges (van Valen, 1973). We strongly believe that only interdisciplinary research can tackle the growing problems of multidrug

resistance, hospital-acquired infections, and other adhesion- and biofilm-related topics in human health that require new drugs, disinfectants, or vaccines.

We thank all of our authors for their hard work and Thijs van Vlijmen of Springer for being always available to answer our questions.

Tübingen — Dirk Linke
Helsinki — Adrian Goldman
November 2010

References

Battistuzzi FU, Feijao A, Hedges SB (2004) A genomic timescale of prokaryote evolution: insights into the origin of methanogenesis, phototrophy, and the colonization of land. BMC Evol Biol 4

Konovalova A, Petters T, Sogaard-Andersen L (2010) Extracellular biology of *Myxococcus xanthus*. FEMS Microbiol Rev 34:89–106

van Valen L (1973) A new evolutionary law. Evol Theory 1:1–30

Contents

Contributors

Magnus Andersson Department of Physics, Umeå Centre for Microbial Research (UCMR), Umeå University, Umeå, Sweden, magnus.andersson@physics.umu.se

Styliani Antonara Department of Molecular Biology and Microbiology, Tufts University School of Medicine, Boston, MA, USA, styliani.antonara.ctr@usuhs.mil

Ove Axner Department of Physics, Umeå Centre for Microbial Research (UCMR), Umeå University, Umeå, Sweden, ove.axner@physics.umu.se

Kateryna Bazaka School of Engineering and Physical Sciences, James Cook University, Townsville, QLD 4811, Australia, Katia.Bazaka@my.jcu.edu.au

Oscar Björnham Department of Physics, Umeå Centre for Microbial Research (UCMR), Umeå University, Umeå, Sweden, oscar.bjornham@physics.umu.se

Romain Briandet INRA, UMR 1319 MICALIS, Massy, France, romain.briandet@jouy.inra.fr

Arnaud Bridier INRA, UMR 1319 MICALIS, Massy, France; AgroParisTech, UMR 1319 MICALIS, Massy, France, arnaud.bridier@jouy.inra.fr

Mickaël Castelain Department of Physics, Umeå Centre for Microbial Research (UCMR), Umeå University, Umeå, Sweden, castelai@insa-toulouse.fr

Jenifer Coburn Division of Infectious Diseases, Medical College of Wisconsin, Milwaukee, WI 53226, USA, jcoburn@mcw.edu

Russell J. Crawford Faculty of Life and Social Sciences, Swinburne University of Technology, Hawthorn, VIC, Australia, RCrawford@swin.edu.au

Samia Daddi-Oubekka Institut des Sciences Moléculaires d'Orsay, Univ Paris-Sud, FRE 3363, Orsay, France; CNRS, Orsay, France, samia.daddi-oubekka@u-psud.fr

Asis Das Department of Molecular, Microbial and Structural Biology, University of Connecticut Health Center, Farmington, CT, USA, ADas@nso2.uchc.edu

Florence Dubois-Brissonnet AgroParisTech, UMR 1319 MICALIS, Massy, France, florence.dubois-brissonnet@jouy.inra.fr

Marie-Pierre Fontaine-Aupart Institut des Sciences Moléculaires d'Orsay, Univ Paris-Sud, FRE 3363, Orsay, France; CNRS, Orsay, France, marie-pierre.fontaine-aupart@u-psud.fr

Sebastian Geibel Institute of Structural Molecular Biology, Birkbeck and University College London, London, UK, s.geibel@mail.cryst.bbk.ac.uk

Jing Geng Laboratoire Physico-chimie Curie (CNRS UMR 168), Université Paris VI Institut Curie, Paris Cedex 05, France, Jing.GENG@danone.com

Partho Ghosh Department of Chemistry and Biochemistry, University of California, San Diego, CA, USA, pghosh@ucsd.edu

Fabiola Giusti Department of Evolutionary Biology, University of Siena, Siena, Italy, giusti10@unisi.it

Adrian Goldman Institute of Biotechnology, Viikinkaari 1, University of Helsinki, Helsinki, Finland, adrian.goldman@helsinki.fi

Iwan Grin Max Planck Institute for Developmental Biology, Tübingen, Germany, iwan.grin@tuebingen.mpg.de

Christine Heilmann Institute for Medical Microbiology, University Hospital of Münster, Münster, Germany, heilmac@uni-muenster.de

Nelly Henry Laboratoire Physico-chimie Curie (CNRS UMR 168), Université Paris VI Institut Curie, Paris Cedex 05, France, Nelly.henry@curie.fr

Michael Hensel Fachbereich Biologie/Chemie, Abteilung Mikrobiologie, Universität Osnabrück, Osnabrück, Germany, Michael.Hensel@biologie.uni-osnabrueck.de

Jean-Marie Herry INRA, UMR 1319 MICALIS, Massy, France, jean-marie.herry@jouy.inra.fr

Ferlenghi Ilaria Novartis Vaccines and Diagnostics srl, Siena, Italy, ilaria.ferlenghi@novartis.com

Elena P. Ivanova Faculty of Life and Social Sciences, Swinburne University of Technology, Hawthorn, VIC, Australia, EIvanova@swin.edu.au

Marie-Agnès Jacques Pathologie Végétale (UMR077 INRA–Agrocampus Ouest–Université d'Angers), Beaucouzé, France, Marie-Agnes.Jacques@angers.inra.fr

Patrick O. Kaiser Institut für Medizinische Mikrobiologie und Krankenhaushygiene, Universitätsklinikum, Johann Wolfgang Goethe-Universität, Frankfurt am Main, Germany, Patrick.Kaiser@kgu.de

Volkhard A.J. Kempf Institut für Medizinische Mikrobiologie und Krankenhaushygiene, Universitätsklinikum, Johann Wolfgang Goethe-Universität, Frankfurt am Main, Germany, volkhard.kempf@kgu.de

Jeanna Klinth Department of Physics, Umeå Centre for Microbial Research (UCMR), Umeå University, Umeå, Sweden, jeanna.klinth@physics.umu.se

Ralf Koebnik Laboratoire Génome et Développement des Plantes (UMR5096 Université de Perpignan–CNRS–IRD), Montpellier, France, koebnik@gmx.de

Efstratios Koutris Department of Physics, Umeå Centre for Microbial Research (UCMR), Umeå University, Umeå, Sweden, stratos.koutris@physics.umu.se

Vengadesan Krishnan School of Optometry and Center for Biophysical Sciences and Engineering, University of Alabama at Birmingham, Birmingham, AL, USA, vengadesan@cbse.uab.edu

Jack C. Leo Institute of Biotechnology, Viikinkaari 1, University of Helsinki, Helsinki, Finland, jack.leo@helsinki.fi

Dirk Linke Department of Protein Evolution, Max Planck Institute for Developmental Biology, Tübingen, Germany, dirk.linke@tuebingen.mpg.de

Steven K. Lower Ohio State University, Columbus, OH, USA, lower.9@osu.edu

Andrzej Łyskowski University of Graz, ACIB GmbH c/o Institute of Molecular Biosciences, Humboldstraße 50, III, A-8010 Graz, Austria; Institute of Biotechnology, Viikinkaari 1, University of Helsinki, Helsinki, Finland, andrzej.lyskowski@uni-graz.at

Nadia Mhedbi-Hajri Pathologie Végétale (UMR077 INRA–Agrocampus Ouest–Université d'Angers), Beaucouzé, France, Nadia.Mhedbi-Hajri@angers.inra.fr

Sthanam V.L. Narayana Center for Biophysical Sciences and Engineering, University of Alabama at Birmingham, Birmingham, AL, USA, narayana@uab.edu

Evgeny L. Nazarenko Pacific Institute of Bioorganic Chemistry, Far-East Branch of the Russian Academy of Sciences, Vladivostok-22, 690022, Russian Federation, elnaz@piboc.dvo.ru

Fiona O'Rourke Institut für Medizinische Mikrobiologie und Krankenhaushygiene, Universitätsklinikum, Johann Wolfgang Goethe-Universität, Frankfurt am Main, Germany, ORourke@med.uni-frankfurt.de

Roland J. Pieters Department of Medicinal Chemistry and Chemical Biology, Utrecht Institute for Pharmaceutical Sciences, Utrecht University, Utrecht, The Netherlands, R.J.Pieters@pharm.uu.nl

Laura Ristow Division of Infectious Diseases, Medical College of Wisconsin, Milwaukee, WI, USA; Center for Infectious Disease Research, Medical College of Wisconsin, Milwaukee, WI, USA, lristow@mcw.edu

Lígia R. Rodrigues IBB – Institute for Biotechnology and Bioengineering, Centre of Biological Engineering, University of Minho, Braga, Portugal, lrmr@deb.uminho.pt

Elizabeth A. Rogers Department of Microbiology and Molecular Genetics, University of Texas Health Science Center, Houston, TX, USA, Elizabeth.Rogers@uth.tmc.edu

Staffan Schedin Department of Applied Physics and Electronics, Umeå Centre for Microbial Research (UCMR), Umeå University, Umeå, Sweden, staffan.schedin@tfe.umu.se

Thomas Schmidgen Institut für Medizinische Mikrobiologie und Krankenhaushygiene, Universitätsklinikum, Johann Wolfgang Goethe-Universität, Frankfurt am Main, Germany, schmidgen@med.uni-frankfurt.de

Heinz Schwarz Max Planck Institute for Developmental Biology, Tübingen, Germany, heinz.schwarz@tuebingen.mpg.de

Frank Shewmaker Department of Pharmacology, Uniformed Services University of the Health Sciences, Bethesda, MD, USA, frank.shewmaker@usuhs.mil

Mikael Skurnik Haartman Institute, University of Helsinki, Helsinki, Finland, mikael.skurnik@helsinki.fi

Karine Steenkeste Institut des Sciences Moléculaires d'Orsay, Univ Paris-Sud, FRE 3363, Orsay, France; CNRS, Orsay, France, karine.steenkeste@u-psud.fr

Vincent Thomas STERIS, Fontenay-aux-Roses, Paris, France, vincent_thomas@steris.com

Ekaterina Tischenko INRA, UMR 1319 MICALIS, Massy, France; AgroParisTech, UMR 1319 MICALIS, Massy, France, ekaterina.tischenko@jouy.inra.fr

Hung Ton-That Department of Microbiology and Molecular Genetics, The University of Texas Medical School at Houston, Houston, TX, USA, Ton-That.Hung@uth.tmc.edu

Peter van Ulsen Section Molecular Microbiology, Department of Molecular Cell Biology, VU University Amsterdam, De Boelelaan 1085, HV, Amsterdam, The Netherlands, peter.van.ulsen@falw.vu.nl

Carolin Wagner Mikrobiologisches Institut, Universitätsklinikum Erlangen, Erlangen 91054, Germany, wagnercarolin@gmx.de

François Waharte Institut Curie/CNRS UMR144 PICT-IBiSA, Paris, France, francois.waharte@curie.fr

Gabriel Waksman Institute of Structural Molecular Biology, Birkbeck and University College London, London, UK, g.waksman@bbk.ac.uk

Chapter 1
Adhesins of Human Pathogens from the Genus *Yersinia*

Jack C. Leo and Mikael Skurnik

Abstract Bacteria of the Gram-negative genus *Yersinia* are environmentally ubiquitous. Three species are of medical importance: the intestinal pathogens *Y. enterocolitica* and *Y. pseudotuberculosis*, and the plague bacillus *Y. pestis*. The two former species, spread by contaminated food or water, cause a range of gastrointestinal symptoms and, rarely, sepsis. On occasion, the primary infection is followed by autoimmune sequelae such as reactive arthritis. Plague is a systemic disease with high mortality. It is a zoonosis spread by fleas, or more rarely by droplets from individuals suffering from pneumonic plague. *Y. pestis* is one of the most virulent of bacteria, and recent findings of antibiotic-resistant strains together with its potential use as a bioweapon have increased interest in the species. In addition to being significant pathogens in their own right, the yersiniae have been used as model systems for a number of aspects of pathogenicity. This chapter reviews the molecular mechanisms of adhesion in yersiniae. The enteropathogenic species share three adhesins: invasin, YadA and Ail. Invasin is the first adhesin required for enteric infection; it binds to β_1 integrins on microfold cells in the distal ileum, leading to the ingestion of the bacteria and allows them to cross the intestinal epithelium. YadA is the major adhesin in host tissues. It is a multifunctional protein, conferring adherence to cells and extracellular matrix components, serum and phagocytosis resistance, and the ability to autoagglutinate. Ail has a minor role in adhesion and serum resistance. *Y. pestis* lacks both invasin and YadA, but expresses several other adhesins. These include the pH 6 antigen and autotransporter adhesins. Also the plasminogen activator of *Y. pestis* can mediate adherence to host cells. Although the adhesins of the pathogenic yersiniae have been studied extensively, their exact roles in the biology of infection remain elusive.

J.C. Leo (✉)
Institute of Biotechnology, Viikinkaari 1, University of Helsinki, FIN-00014 Helsinki, Finland
e-mail: jack.leo@helsinki.fi

D. Linke, A. Goldman (eds.), *Bacterial Adhesion*, Advances in Experimental Medicine and Biology 715, DOI 10.1007/978-94-007-0940-9_1,

1.1 Introduction

Plague is arguably the most notorious of all diseases. This calamitous affliction is particularly virulent, and has shaped the course of history. It is estimated that the Black Death of fourteenth century Europe wiped out approximately 30% of the population (Perry and Fetherston, 1997). In 1894, Alexandre Yersin discovered the causative agent of plague to be a Gram-negative bacillus. Later, this bacterium was named *Yersinia pestis* in his honour. In addition to this infamous pathogen, two other members of the genus, *Y. enterocolitica* and *Y. pseudotuberculosis*, are known to cause human diseases.

Y. enterocolitica and *Y. pseudotuberculosis* cause food poisoning and are relatively abundant in the environment. Plague is still endemic in several regions of the world, including the Western USA and many regions in Africa, Asia and Latin America. Between 1000 and 5000 cases of human plague have been reported to the World Health Organisation per year, 100–200 leading to death, but a significant number of cases probably go unreported. Worryingly, antibiotic-resistant stains of *Y. pestis* have emerged, including some which are resistant to multiple drugs (Prentice and Rahalison, 2007).

Thus, the genus *Yersinia* is a medically important one, being prevalent and responsible for several human diseases. In addition, bacteria of the genus serve as important model organisms for various aspects of pathogenicity, including adhesion, invasion, immune evasion and effector protein delivery. This chapter gives a short overview of the biology of the human pathogenic yersiniae, followed by a more detailed discussion of the adhesins expressed by this family of bacteria.

1.2 The Human Pathogenic Yersiniae

1.2.1 Enteropathogenic Yersiniae

The yersiniae are facultative anaerobic Gram-negative pleiomorphic rods of the family Enterobacteriaceae. The genus contains 15 recognised species, with environmental, commensal and pathogenic representatives. Pathogenicity to humans correlates with the presence of the *Yersinia* 70-kb virulence plasmid pYV, found in disease-causing strains of *Y. enterocolitica*, *Y. pseudotuberculosis* and *Y. pestis*, but absent from the other species.

The two most commonly encountered human pathogenic species are *Y. enterocolitica* and *Y. pseudotuberculosis*. Like most other *Yersinia* species, both are ubiquitously found in aquatic environments, soil, and animals. Infections caused by both organisms have been reported worldwide. Although rather distantly related, *Y. enterocolitica* and *Y. pseudotuberculosis* share a number of features.

Though regarded as a single species, *Y. enterocolitica* is heterogeneous and is now considered to consist of two genetically distinguishable subspecies, *Y. enterocolitica* subsp. *enterocolitica* and *Y. enterocolitica* subsp. *palearctica* (Neubauer

et al., 2000). In addition, the species comprises 6 biogroups (1A, 1B, 2, 3, 4 and 5), based on biochemical variability, which are further subdivided into approximately 60 serotypes (Bottone, 1997). *Y. enterocolitica* has been isolated from a number of mammalian hosts, with swine being a significant reservoir for pathogenic strains of this organism. *Y. enterocolitica* is responsible for the majority of human cases of yersiniosis, and undercooked pork products have been implicated in a large number of outbreaks (Bottone, 1997).

Y. pseudotuberculosis derives its name from the tuberculosis-like granulomatous abscesses it causes in the spleen and liver of infected animals. A less common human pathogen than *Y. enterocolitica*, *Y. pseudotuberculosis* is associated with outbreaks from fresh produce like lettuce and carrots (Jalava et al., 2006). *Y. pseudotuberculosis* infections are generally more severe than those of *Y. enterocolitica*, and are more likely to require hospitalisation (Long et al., 2010). In addition to gastrointestinal infections, *Y. pseudotuberculosis* is implicated as the cause of Far East scarlet-like fever and Kawasaki disease. The former mimics symptoms often seen in scarlet fever caused by group A streptococci, including widespread scarlatinoid rash and toxic shock syndrome (Eppinger et al., 2007). The latter is an inflammatory syndrome affecting the blood vessels, lymphatics, skin, mucous membranes and heart. Though the aetiology of Kawasaki disease has not been established, epidemiological data suggest *Y. pseudotuberculosis* as a possible agent in the development of the syndrome (Vincent et al., 2007).

Infection by either organism follows a similar course. The bacteria are ingested with contaminated food or water. The bacteria then traverse the gastrointestinal tract until they reach the terminal ileum, where they cross the intestinal mucosa. Crossing is facilitated by microfold (M) cells in the intestinal epithelium (Miller et al., 2007). M cells are transcytotic epithelial cells associated with Peyer's patches, the lymphoid follicles of the intestine. They function in sampling the luminal solution for immunogenic substances, which are then transported by transcytosis to the underlying immune cells of the follicle. Yersiniae and several other enteropathogens, including *Salmonella* and *Shigella*, can hijack this transport process to gain entry to the submucosa.

Once in the follicle, yersinae replicate extracellularly. Growth of these bacteria leads to destruction of the follicle (Autenrieth and Firsching, 1996). The bacteria can then disseminate to the mesenteric lymph nodes. Usually the infection is self-limiting, but in severe cases bacteria can spread to other organs (the liver, spleen, kidneys and lungs), leading to systemic infection and bacteraemia. In addition to this infection route, it is probable that bacteria from a pool replicating in the intestinal lumen can infect the liver and spleen by some other means, possibly by disseminating through the hepatic portal vein (Barnes et al., 2006).

The symptoms of yersiniosis are varied. Cases range from mild gastroenteritis and diarrhoea to pseudoappendicular syndrome (Bottone, 1997). Enterocolitis is a typical manifestation of yersinioisis in young children, whereas terminal ileitis and mesenteric lymphadenitis (the causes of pseudoappendicitis) are usual for adults. Diarrhoea, occasionally bloody, is associated with most cases of *Y. enterocolitica* infection but is less usual for *Y. pseudotuberculosis*. Sepsis is an uncommon result

of yersiniosis. Primary infections by enteropathogenic yersiniae are infrequently followed by sequelae such as reactive arthritis (inflammation of joints), erythema nodosum (localised skin inflammation), iritis or glomerulonephritis (inflammation of the kidney) (Bottone, 1997).

1.2.2 Yersinia pestis

Three major plague pandemics have blighted recorded human history (Perry and Fetherston, 1997). The first, referred to as the Justinian plague, spread around the Mediterranean in the sixth century AD. The most famous was the second pandemic, the Black Death of Europe, which started in the fourteenth century and continued intermittently for a further 300 years. Although there is some debate as to whether *Y. pestis* was in fact the pathogen behind these historical pandemics, there is considerable evidence linking the bacterium to the Black Death (Stenseth et al., 2008). The third pandemic ("modern plague") initiated in China in the mid-nineteenth century and has since spread across the world to continue to the present, albeit at a low incidence.

Y. pestis appears to have diverged from its parent species *Y. pseudotuberculosis* within the last 20,000 years. In contrast, the *Y. pseudotuberculosis* and *Y. enterocolitica* lineages diverged between approximately 150 and 200 million years ago (Achtman et al., 1999). *Y. pestis* is thus very closely related to *Y. pseudotuberculosis*, and in fact can be considered a pathovar of this species. However, due to its historical importance and public health considerations *Y. pestis* has not been reclassified as belonging to its parent species.

Y. pestis is one of the most virulent organisms known. It is highly invasive and proliferates rapidly in host tissues. Like its enteropathogenic relatives, *Y. pestis* replicates extracellularly and the first sites for replication are within lymphatic tissues, normally lymph nodes. However, *Y. pestis* is also able to survive and replicate within macrophages (Prentice and Rahalison, 2007). The swift replication of plague bacilli in lymph nodes quickly leads to their spread into the blood stream resulting in massive bacteraemia ($\sim 10^8$ bacteria/ml blood). The mortality of plague is staggering; untreated, the disease is fatal in 40–70% of cases (Stenseth et al., 2008).

Plague is a zoonosis. The primary hosts for *Y. pestis* are rodents. Fleas, usually of the genus *Xenopsylla*, act as the vector transporting the pathogen from host to host. This form of plague (sylvatic plague) is endemic to many regions of the world (Perry and Fetherston, 1997). However, in inhabited areas of poor hygiene where rodents, particularly rats, and humans interact, the disease can be transmitted to humans (urban plague). *Xenopsylla* fleas will take blood meals from humans, and so the disease can spread from rodent to human or human to human aided by the flea vector.

When a flea takes a blood meal from a host infected with *Y. pestis* it ingests a significant number of bacteria. Once inside the flea, *Y. pestis* adheres to the spines of the proventriculus, a compartment at the beginning of the digestive tract, and

forms a biofilm that obstructs the gut of the flea. This has two effects: firstly, the flea is no longer able to digest blood meals and therefore begins to starve. This leads to increased frequency of feeding. Secondly, ingested blood washes up against the blocking biofilm, releasing *Y. pestis* cells that then enter the host as the flea regurgitates some of its blood meal. The inoculum of *Y. pestis* cells required to initiate the disease is very low, less than 10 cells (Hinnebusch, 2005).

From the primary site of infiltration, i.e. the flea bite, *Y. pestis* travels to regional lymph nodes, probably inside macrophages. In the lymph nodes, the bacteria escape the macrophages and begin to replicate extracellularly, resisting further phagocytosis. The fast, prodigious reproduction of bacteria leads to a greatly swollen lymph nodes, called "buboes". These are of course where the bubonic form of plague gets its name. The proliferation of *Y. pestis* generally leads to destruction of the lymph node and escape of the bacteria into the blood stream (septicaemic plague). The bacilli can now colonise numerous organs, particularly the liver and spleen, but on occasion also colonising the lungs (secondary pneumonic plague). This is a very serious condition, for not only is it almost invariably fatal but also allows the spread of *Y. pestis* by aerosols (Perry and Fetherston, 1997). *Y. pestis* disseminated in this manner can directly infect the lungs when contaminated aerosols are inhaled, leading to primary pneumonic plague.

1.3 Adhesins of Human Pathogenic Yersiniae

Y. enterocolitica and *Y. pseudotuberculosis* are facultative intracellular pathogens. Their primarily extracellular lifestyle necessitates factors that promote survival in host tissues: serum resistance, immune evasion, iron uptake, and adhesion. Both species elaborate at least three adhesins involved in virulence. All three are multifunctional proteins; in addition to adhesive activity they display other properties such as promoting cell invasion and serum resistance.

1.3.1 Invasin

The first adhesin required in the infection process is invasin (Inv). The chromosomally encoded *inv* gene is expressed optimally at +26°C, or under acidic conditions at +37°C, and so the protein is thought to be present in the bacteria when they reach the small intestine, allowing them to be primed for adhesion (Grassl et al., 2003). Inv binds to several cell types, including epithelial cells and platelets (Simonet et al., 1992)

Invasin is an outer membrane protein, related to intimin of enterohaemorrhagic *Escherichia coli*. The prepeptide consists of an N-terminal signal peptide followed by the transmembrane β-barrel domain. The extracellular C-terminal region is a rod-like structure formed of 3–4 all-β domains (D1-D4) belonging to the immunoglobulin fold superfamily (Fig. 1.1). The distal domain (D5) has a C-type

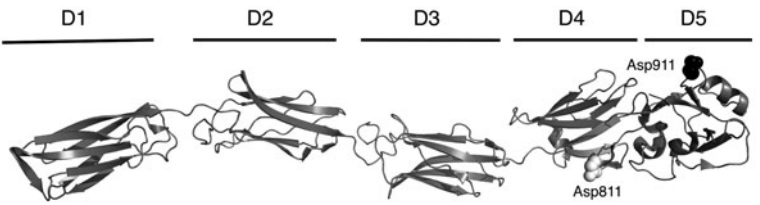

Fig. 1.1 Structure of the extracellular region of *Y. pseudotuberculosis* invasin. The crystal structure of Inv (PDB 1CWV) shows an elongated, rod-like formation. Domains D1-5 are indicated. D1-4 have an immunoglobulin-like fold, whereas D5 displays a C-type lectin fold. D4-5 are sufficient for tight binding to β_1 integrins. The two aspartate residues important for adhesion are highlighted in space-filling representation (Asp811 in *white* and Asp911 in *black*). D2 (not present in *Y. enterocolitica* Inv) is a self-association domain

lectin fold (Hamburger et al., 1999). The difference between the Inv proteins from *Y. enterocolitica* and *Y. pseudotuberculosis* is the presence of the D2 domain in the latter, lacking in the former.

Inv binds directly to β_1 integrins, which are found on the apical surface of M cells (Grassl et al., 2003). Invasin is thus required for the initial steps of host colonisation and penetration of the intestinal epithelium. D4 and D5 domains are sufficient for tight binding to the integrin. Inv binds to $\alpha_5\beta_1$ integrin with 100-fold higher affinity than its natural ligand, fibronectin. D4 and D5 form a rigid, fibronectin-like structure. Two asparagine residues, Asp911 and Asp811 (according to the numbering in the *Y. pseudotuberculosis* protein) are important for binding, with the former being more critical (Grassl et al., 2003). These are thought to form sites similar to the Arg-Gly-Asp motifs found in fibronectin.

The Inv-mediated binding to the integrin receptors normally results in internalisation of the bacteria. This requires that the density of Inv molecules on the cell surface be high. Binding and recruiting of receptors results in β_1 integrin clustering, which in turn leads to cell signalling events and the formation of adhesion foci containing e.g. phosphorylated Fac and Src proteins (Grassl et al., 2003). The subsequent rearrangement of the actin cytoskeleton triggers the internalisation of Inv-expressing bacteria (or Inv-coated beads) by a zipper mechanism. The D2 domain, present in the *Y. pseudotuberculosis* protein, is a self-association domain and enhances the effect of Inv-initiated integrin clustering (Grassl et al., 2003). In addition to cytoskeletal rearrangements, Inv-mediated signalling elicits the secretion of proinflammatory cytokines such as interleukin (IL)-1 and IL-8. Signalling events initiated by Inv-mediated integrin clustering result in the activation of the transcription factor NF-κB and upregulation of cytokine genes (Grassl et al., 2003).

1.3.2 YadA

After crossing the intestinal epithelium, the major adhesin of both enteropathogenic yersiniae is the *Yersinia* adhesin YadA, previously known as Yop1. In contrast to

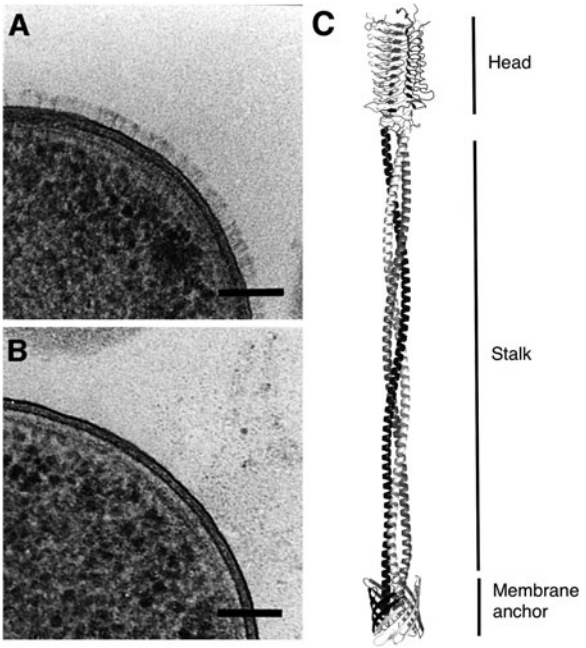

Fig. 1.2 Expression and structure of YadA. Electon micrographs of YadA-expressing *Y. enterocolitica* grown at +37°C (*panel A*) and a pYV-cured isogenic control (*panel B*). YadA is expressed at high density on the cell surface and forms a "quasi-periplasmic space" between the outer membrane and the distal head domains. A model for the structure of YadA (from *Y. enterocolitica* serotype O:8) (*panel C*). The model (Koretke et al., 2006) shows a lollipop-like organistion, with the globular head followed by an extended coiled-coil stalk and finally a 12-stranded β-barrel membrane anchor. The three chains of YadA are coloured differently. *Panels A* and *B* are reprinted by permission from Macmillan Publishers Ltd: EMBO J, Hoiczyk et al. (2000)

Inv, YadA is encoded by the virulence plasmid pYV and expressed only at +37°C. Under these conditions, it is present at very high levels, virtually coating the entire outer surface of the cell (Hoiczyk et al., 2000) (Fig. 1.2a). YadA is an obligate homotrimeric protein, and belongs to the trimeric autotransporter adhesin family. The protein is shaped like a lollipop (Fig. 1.2b), with its globular head extended from the cell surface by a coiled-coil stalk (the structure and biogenesis of YadA are discussed in more detail in Chapter 9).

YadA has multiple functions. As an adhesin, its primary targets are the large proteins of the extracellular matrix (ECM): collagen, fibronectin and laminin (El Tahir and Skurnik, 2001). The preferred ligand for YadA from *Y. enterocolitica* is collagen. YadA binds to wide range of fibrillar collagens (e.g. types I, II, III and V) and to the network-forming collagen type IV (El Tahir and Skurnik, 2001). This binding is promiscuous: collagens do not contain a specific binding sequence for YadA; rather, YadA recognises and binds to the triple-helical structure of collagen. Although YadA has no specific target sequence, it binds most tightly to regions rich

in 4-hydroxyproline (an amino acid abundant in collagens) and with a low net charge (Leo et al., 2010). The affinity of YadA for triple-helical peptides with repeats of the triplet proline-hydroxyproline-glycine is of the same order as its affinity for collagen type I, approximately 0.3 μM (Leo et al., 2008). The high density of YadA on the bacterial cell surface confers an avidity effect on this interaction, where multiple YadA molecules bind to the same collagen fibril, thus conferring a tighter overall adhesion for yersiniae to collagenous substrata. Indeed, the YadA-collagen interaction is a very stable one, resisting extremes of heat and pH. The collagen-binding activity of YadA is further associated with reactive arthritis. In a rat model, YadA was required for eliciting reactive arthritis. Bacteria expressing a deletion mutant of YadA lacking the collagen-binding activity were significantly less arthritogenic than wild type bacteria (El Tahir and Skurnik, 2001).

In contrast, *Y. pseudotuberculosis* YadA binds preferentially to fibronectin (Heise and Dersch, 2006). This change in specificity is apparently due to a 30-amino-acid extension at the N-terminus of the protein, whereas the rest of the protein sequence is highly similar between the two species. The YadA binding site(s) in fibronectin have not been determined, but the binding is independent of the Arg-Gly-Asp motifs (El Tahir and Skurnik, 2001). The collagen-binding activity of YadA in *Y. enterocolitica* is an absolute requirement for pathogenicity; however, YadA is not required for virulence in *Y. pseudotuberculosis* (El Tahir and Skurnik, 2001).

In addition to binding to the ECM, YadA mediates adhesion to a number of cell types, including epithelial cells and macrophages, and further acts as a haemagglutinin (El Tahir and Skurnik, 2001). *Y. pseudotuberculosis* YadA promotes invasion of epithelial cells and can substitute for this activity of Inv. The receptors for YadA on the epithelial cell surface also appear to be β_1 integrins. However, unlike Inv, YadA does not bind directly to the integrin but through a bridging ECM molecule (Eitel and Dersch, 2002). This binding triggers intracellular signalling cascades that lead to actin cytoskeleton rearrangements and IL-8 production, similarly to Inv (Eitel et al., 2005). The *Y. enterocolitica* YadA is not as efficient an invasin as *Y. pseudotuberculosis* YadA (Heise and Dersch, 2006).

YadA also has affinity for itself. One of its functions is to act as an autoagglutinin, which causes flocculation of the bacteria (El Tahir and Skurnik, 2001). This activity is mediated by head domains, which apparently interact in an antiparallel, zipper-like arrangement to induce autoagglutination (Hoiczyk et al., 2000). YadA also induces the formation of densely packed microcolonies of *Y. enterocolitica*, reminiscent of the microabscesses found in infected tissues, when grown in a three-dimensional collagen gel (Freund et al., 2008). Interestingly, this phenotype was not dependent on the collagen-binding activity of YadA.

A final adhesive activity of YadA is to bind to intestinal mucus. *Y. enterocolitica* binds to mucus, mucin and brush border vesicles from rabbits, and this binding correlates strongly with the expression of YadA. YadA appears to primarily interact with the carbohydrate moiety of mucin (Mantle and Husar, 1994).

As extracellular bacteria, yersiniae must survive the barrage of both innate and adaptive host immune responses. Yersiniae are serum resistant, i.e. they are able to tolerate the usually bacteriocidal effects of complement. The major player in serum

resistance of *Y. enterocolitica* is, again, YadA. The dense YadA layer covering the cell may in itself present a physical barrier that prevents opsonisation and membrane attack complex formation. In addition, YadA binds to serum factors that regulate the activity of complement. Serum factor H regulates the alternative complement pathway by promoting the cleavage of C3b to the inactive iC3b. YadA binds factor H and thus protects the bacterium from the alternative pathway of complement (Biedzka-Sarek et al., 2008a, b). In addition, YadA can recruit C4 binding protein, which is a negative regulator of the classical pathway (Kirjavainen et al., 2008). Thus, YadA plays a pivotal role in protecting yersiniae against the classical and alternative branches of complement. Furthermore, YadA mediates resistance to antimicrobial peptides produced by granulocytes (Visser et al., 1996).

In addition to its other functions, YadA also has antiphagocytic properties. The autoagglutination and densely packed microcolony formation mediated by YadA probably contribute to phagocytosis resistance (Skurnik et al., 1994; Freund et al., 2008). Additionally, YadA probably acts as a docking system: YadA binds via its N-terminus to professional phagocytes allowing the injectisome of the type III secretion system to come into contact with the target cell plasma membrane and deliver antiphagocytic effector proteins into the target cell's cytoplasm (Visser et al., 1995). This is supported by the finding that the length of the YadA stalk correlates with the length of the injectisome needle: an artificially shortened injectisome was unable to deliver effectors into target cells, but simultaneous shortening the YadA stalk rescued the secretion of effectors. Conversely, a needle of normal length no longer functioned when co-expressed with a longer version of YadA, but an abnormally long needle did (Mota et al., 2005). These data demonstrate that the injectisome must be positioned at a specific distance from other *Yersinia* cell surface structures in order to contact the host cell membrane and suggest that the injectisome has coevolved with other components, most notably YadA.

1.3.3 Ail

The third virulence-associated adhesin from enteropathogenic yersiniae is Ail (for attachment and invasion locus). This chromosomally encoded protein is, like YadA, expressed at +37°C under aerobic conditions (Pierson and Falkow, 1993). It is a small (17 kDa) outer membrane with an eight-stranded β-barrel fold. Like Inv, Ail also mediates epithelial cell binding and invasion, but only certain cell lines are targets for Ail, possibly reflecting the presence of receptors for Ail only in certain cell types (Miller and Falkow, 1988). As a small protein, Ail is usually masked by the O-antigen chains of lipopolysaccharide (LPS) and therefore only plays a minor role in pathogenesis in vivo (Wachtel and Miller, 1995).

Ail also plays a small but detectable role in serum resistance. Though usually masked by the LPS O-antigen, Ail confers serum resistance to mutant *Y. enterocolitica* strains lacking the O-antigen chain and outer core oligosaccharide (Biedzka-Sarek et al., 2005). Like YadA, Ail binds to factor H and C4 binding protein. Serum resistance in yersiniae is thus multifactorial, and is dependent on two

outer membrane proteins, YadA and Ail. The expression of O-antigen is temperature regulated in yersiniae, with more rough LPS (i.e. lacking the O-antigen chain) being expressed at +37°C (Skurnik and Bengoechea, 2003). The reduction in O-antigen expression +37°C could expose Ail, allowing it to bind the complement-regulatory factors H and C4 binding protein (Biedzka-Sarek et al., 2005).

1.3.4 Adhesins of Y. pestis

The highly virulent *Y. pestis* has adapted to a significantly different lifestyle and mode of infection than its enteropathogenic cousins. Due to the close relationship between *Y. pestis* and *Y. pseudotuberculosis* and the availability of genomic sequences, the genetic differences presumably leading to the increased virulence of *Y. pestis* have been identified (Chain et al., 2004). Surprisingly, *Y. pestis* has undergone significant gene loss; the *Y. pestis* genome contains approximately 200 pseudogenes, corresponding to ~5% of open reading frames (Chain et al., 2004). Inactivated genes include those coding for the adhesins Inv and YadA. The inactivation of the former is due to the insertion of a transposable IS*200* element in the *inv* gene, whereas a single base-pair deletion causes a frame shift in the *yadA* gene, rendering it a pseudogene (Rosqvist et al., 1988; Simonet et al., 1996). The loss of these and other genes may reflect changes in lifestyle: as *Y. pestis* no longer needs to traverse the gastrointestinal tract for infection, factors promoting invasion of the intestinal epithelium are no longer needed, so the activity of these loci is not under selection.

Much speculation has centred around the loss of YadA and its effect on *Y. pestis* virulence; it has been hypothesised that expression of this adhesin would inhibit the dissemination of the bacterium from primary infection sites. Heterologous expression of YadA in *Y. pestis* resulted in a mild decrease in virulence (Rosqvist et al., 1988). However, a recent study identified two chromosomal *yadA*-like genes, *yadBC*, both of which are expressed in *Y. pestis* and mediate epithelial cell invasion and have a role in virulence of bubonic plague (Forman et al., 2008). These genes are also present in *Y. pseudotuberculosis*, which – if they can substitute for some of the activities of YadA – may explain why this protein is not essential for virulence in either organism. In addition, *Y. pestis* expresses several other proteins with adhesive activity.

An important virulence factor of *Y. pestis* is plasminogen activator (Pla), which is encoded by a small (9.5 kb) plasmid called pPla (also pPCP1 or pPst). Pla is an outer membrane protease of the omptin family (Haiko et al., 2009) (Fig. 1.3). It activates host plasminogen, leading to the dissolution of fibrin clots, activation of matrix metalloproteases and degradation of the ECM. Pla is required for dissemination of *Y. pestis* from intradermal infection sites to lymph nodes, consistent with its activity as a "bulldozer" that allows the bacteria to clear a path from subcutaneous tissues to lymph vessels. In addition, Pla can cleave the complement factor C3, though it is not critical for the serum resistance of *Y. pestis* (Haiko et al., 2009). Pla also functions as an adhesin, mediating attachment to laminin and host cells. Though not needed

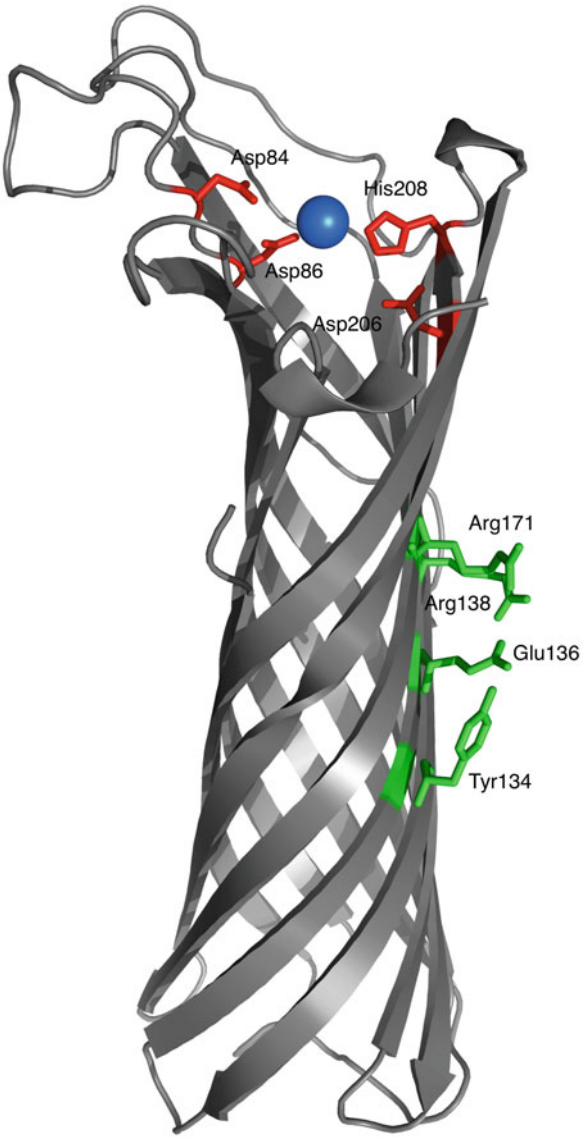

Fig. 1.3 Structure of *Y. pestis* plasminogen activator. The crystal structure of Pla (2X55) shows a narrow 10-stranded β-barrel with an elliptical cross-section. Five loops extend into the extracellular space. Catalytic residues conserved in the omptin family are depicted in *red*. In addition, the presumed nucleophilic water involved in catalysis is shown in space filling representation and coloured *blue*. The residues involved in LPS binding, which is important for Pla activity, are shown in *green* (Eren et al., 2010)

for septicaemic plague, Pla is required for the development of pneumonic plague (Lathem et al., 2007).

A chromosomally encoded virulence-related adhesin of *Y. pestis* is the pH 6 antigen. This fimbrial structure is the product of the *psa* locus and is expressed at low pH and mammalian body temperature. pH 6 antigen acts as a haemagglutinin and binds to cultured cells and β1-linked galactosyl residues in glycosphingolipids (Payne

et al., 1998). It also enhances phagocytosis resistance in a Yop-independent manner (Huang and Lindler, 2004). pH 6 antigen is possibly induced by the low pH in phagolysosomes of macrophages, and consequently protects the bacteria from later phagocytosis once they have escaped from the first macrophage. In addition to these functions, it has been reported to bind both low-density lipoprotein and human IgG Fc to protect against immunological recognition (Zav'yalov et al., 1996; Makoveichuk et al., 2003). The pH 6 antigen is also present in both *Y. pseudotuberculosis* and *Y. enterocolitica* (where it is called mucoid factor or Myf), but its role has not been studied extensively in the pathogenesis of these organisms. However, pH 6 antigen appears to mediate thermoinducible adhesion of *Y. pseudotuberculosis* to cultured cells (Yang et al., 1996).

Interestingly, possibly because *Y. pestis* produces constitutively rough LPS lacking the O-antigen, Ail (also known as OmpX) seems to have a more pronounced role in serum resistance and adhesion in *Y. pestis* (Bartra et al., 2008). Similarly, also the function of Pla appears to be blocked by O-antigen (Kukkonen et al., 2004). In *Y. pestis*, Ail substitutes for YadA in docking onto cells to allow Yop delivery, and this binding is dependent on fibronectin (Tsang et al., 2010). Ail also promotes cell invasion, and full activity of this protein is dependent on an intact LPS core structure (Kolodziejek et al., 2010).

In addition to Pla, pH 6 antigen, Ail and YadBC, chromosomal sequencing has identified numerous putative adhesins in *Y. pestis*. These include 10 classical autotransporter adhesins (Yen et al., 2007), two of which, YapC and YapE, have been studied in more detail. Recently, YapE has been shown to have a role in *Y. pestis* virulence. It mediates attachment to epithelial cells and promotes autoagglutination (Lawrenz et al., 2009). YapC also mediates host cell binding, autoagglutination and the formation of biofilm, but its effect on pathogenicity remains untested (Felek et al., 2008).

1.4 Conclusions

The human pathogenic yersiniae are group of highly adept, facultative intracellular pathogens. The diseases they cause range from mild gastroenteritis to more severe symptoms, such as terminal ileitis and mesenteric lymphadenitis, or even septicaemia. At the extreme end of this spectrum are the lethal symptoms of plague.

The virulence of all three species is heavily dependent on surface-expressed adhesins. These are multifunctional proteins, mediating attachment to cells and the ECM, but also stimulating cell invasion, conferring serum resistance, or in the case of Pla acting as a protease to promote bacterial metastasis. Although we now have a fairly detailed understanding of molecular mechanisms for many of these phenomena, the exact roles of the various adhesins in vivo remain unclear, partly due to overlapping functions and the complexity of interactions with the host. Much work still needs to be performed to clarify the contribution of these adhesins to the biology of yersiniosis.

References

Achtman M, Zurth K, Morelli G, Torrea G, Guiyoule A, Carniel E (1999) *Yersinia pestis*, the cause of plague, is a recently emerged clone of *Yersinia pseudotuberculosis*. Proc Natl Acad Sci USA 96:14043–14048

Autenrieth IB, Firsching R (1996) Penetration of M cells and destruction of Peyer's patches by *Yersinia enterocolitica*: an ultrastructural and histological study. J Med Microbiol 44: 285–294

Barnes PD, Bergman MA, Mecsas J, Isberg RR (2006) *Yersinia pseudotuberculosis* disseminates directly from a replicating bacterial pool in the intestine. J Exp Med 203:1591–1601

Bartra SS, Styer KL, O'Bryant DM, Nilles ML, Hinnebusch BJ, Aballay A, Plano GV (2008) Resistance of *Yersinia pestis* to complement-dependent killing is mediated by the Ail outer membrane protein. Infect Immun 76:612–622

Biedzka-Sarek M, Jarva H, Hyytiäinen H, Meri S, Skurnik M (2008a) Characterization of complement factor H binding to *Yersinia enterocolitica* serotype O:3. Infect Immun 76:4100–4109

Biedzka-Sarek M, Salmenlinna S, Gruber M, Lupas AN, Meri S, Skurnik M (2008b) Functional mapping of YadA- and Ail-mediated binding of human factor H to *Yersinia enterocolitica* serotype O:3. Infect Immun 76:5016–5027

Biedzka-Sarek M, Venho R, Skurnik M (2005) Role of YadA, Ail, and lipopolysaccharide in serum resistance of Y*ersinia enterocolitica* Serotype O:3. Infect Immun 73:2232–2244

Bottone EJ (1997) *Yersinia enterocolitica*: the charisma continues. Clin Microbiol Rev 10:257–276

Chain PS, Carniel E, Larimer FW, Lamerdin J, Stoutland PO, Regala WM, Georgescu AM, Vergez LM, Land ML, Motin VL, Brubaker RR, Fowler J, Hinnebusch J, Marceau M, Medigue C, Simonet M, Chenal-Francisque V, Souza B, Dacheux D, Elliott JM, Derbise A, Hauser LJ, Garcia E (2004) Insights into the evolution of *Yersinia pestis* through whole-genome comparison with *Yersinia pseudotuberculosis*. Proc Natl Acad Sci USA 101:13826–13831

Eitel J, Dersch P (2002) The YadA protein of *Yersinia pseudotuberculosis* mediates high-efficiency uptake into human cells under environmental conditions in which invasin is repressed. Infect Immun 70:4880–4891

Eitel J, Heise T, Thiesen U, Dersch P (2005) Cell invasion and IL-8 production pathways initiated by YadA of *Yersinia pseudotuberculosis* require common signalling molecules (FAK, c-Src, Ras) and distinct cell factors. Cell Microbiol 7:63–77

El Tahir Y, Skurnik M (2001) YadA, the multifaceted *Yersinia* adhesin. Int J Med Microbiol 291:209–218

Eppinger M, Rosovitz MJ, Fricke WF, Rasko DA, Kokorina G, Fayolle C, Lindler LE, Carniel E, Ravel J (2007) The complete genome sequence of *Yersinia pseudotuberculosis* IP31758, the causative agent of Far East scarlet-like fever. PLoS Genet 3:e142

Eren E, Murphy M, Goguen J, van den Berg B (2010) An active site water network in the plasminogen activator pla from *Yersinia pestis*. Structure 18:809–818

Felek S, Lawrenz MB, Krukonis ES (2008) The *Yersinia pestis* autotransporter YapC mediates host cell binding, autoaggregation and biofilm formation. Microbiology 154:1802–1812

Forman S, Wulff CR, Myers-Morales T, Cowan C, Perry RD, Straley SC (2008) *yadBC* of *Yersinia pestis*, a new virulence determinant for bubonic plague. Infect Immun 76:578–587

Freund S, Czech B, Trülzsch K, Ackermann N, Heesemann J (2008) Unusual, virulence plasmid-dependent growth behavior of *Yersinia enterocolitica* in three-dimensional collagen gels. J Bacteriol 190:4111–4120

Grassl GA, Bohn E, Muller Y, Buhler OT, Autenrieth IB (2003) Interaction of *Yersinia enterocolitica* with epithelial cells: invasin beyond invasion. Int J Med Microbiol 293:41–54

Haiko J, Suomalainen M, Ojala T, Lähteenmäki K, Korhonen TK (2009) Invited review: breaking barriers – attack on innate immune defences by omptin surface proteases of enterobacterial pathogens. Innate Immun 15:67–80

Hamburger ZA, Brown MS, Isberg RR, Bjorkman PJ (1999) Crystal structure of invasin: a bacterial integrin-binding protein. Science 286:291–295

Heise T, Dersch P (2006) Identification of a domain in *Yersinia* virulence factor YadA that is crucial for extracellular matrix-specific cell adhesion and uptake. Proc Natl Acad Sci USA 103:3375–3380

Hinnebusch BJ (2005) The evolution of flea-borne transmission in *Yersinia pestis*. Curr Issues Mol Biol 7:197–212

Hoiczyk E, Roggenkamp A, Reichenbecher M, Lupas A, Heesemann J (2000) Structure and sequence analysis of *Yersinia* YadA and *Moraxella* UspAs reveal a novel class of adhesins. EMBO J 19:5989–5999

Huang XZ, Lindler LE (2004) The pH 6 antigen is an antiphagocytic factor produced by *Yersinia pestis* independent of *Yersinia* outer proteins and capsule antigen. Infect Immun 72: 7212–7219

Jalava K, Hakkinen M, Valkonen M, Nakari UM, Palo T, Hallanvuo S, Ollgren J, Siitonen A, Nuorti JP (2006) An outbreak of gastrointestinal illness and erythema nodosum from grated carrots contaminated with *Yersinia pseudotuberculosis*. J Infect Dis 194:1209–1216

Kirjavainen V, Jarva H, Biedzka-Sarek M, Blom AM, Skurnik M, Meri S (2008) *Yersinia enterocolitica* serum resistance proteins YadA and Ail bind the complement regulator C4b-binding protein. PLoS Pathog 4:e1000140

Kolodziejek AM, Schnider DR, Rohde HN, Wojtowicz AJ, Bohach GA, Minnich SA, Hovde CJ (2010) Outer membrane protein X (Ail) contributes to *Yersinia pestis* virulence in pneumonic plague and its activity is dependent on LPS core length. Infect Immun 78:5233–5243

Koretke KK, Szczesny P, Gruber M, Lupas AN (2006) Model structure of the prototypical non-fimbrial adhesin YadA of *Yersinia enterocolitica*. J Struct Biol 155:154–161

Kukkonen M, Suomalainen M, Kyllönen P, Lähteenmäki K, Lång H, Virkola R, Helander IM, Holst O, Korhonen TK (2004) Lack of O-antigen is essential for plasminogen activation by *Yersinia pestis* and *Salmonella enterica*. Mol Microbiol 51:215–225

Lathem WW, Price PA, Miller VL, Goldman WE (2007) A plasminogen-activating protease specifically controls the development of primary pneumonic plague. Science 315:509–513

Lawrenz MB, Lenz JD, Miller VL (2009) A novel autotransporter adhesin is required for efficient colonization during bubonic plague. Infect Immun 77:317–326

Leo JC, Elovaara H, Bihan D, Pugh N, Kilpinen SK, Raynal N, Skurnik M, Farndale RW, Goldman A (2010) First analysis of a bacterial collagen-binding protein with collagen toolkits: promiscuous binding of YadA to collagens may explain how YadA interferes with host processes. Infect Immun 78:3226–3236

Leo JC, Elovaara H, Brodsky B, Skurnik M, Goldman A (2008) The Yersinia adhesin YadA binds to a collagenous triple-helical conformation but without sequence specificity. Protein Eng Des Sel 21:475–484

Long C, Jones TF, Vugia DJ, Scheftel J, Strockbine N, Ryan P, Shiferaw B, Tauxe RV, Gould LH (2010) *Yersinia pseudotuberculosis* and *Y. enterocolitica* infections, FoodNet, 1996–2007. Emerg Infect Dis 16(3):566–567

Makoveichuk E, Cherepanov P, Lundberg S, Forsberg A, Olivecrona G (2003) pH6 antigen of *Yersinia pestis* interacts with plasma lipoproteins and cell membranes. J Lipid Res 44:320–330

Mantle M, Husar SD (1994) Binding of *Yersinia enterocolitica* to purified, native small intestinal mucins from rabbits and humans involves interactions with the mucin carbohydrate moiety. Infect Immun 62:1219–1227

Miller VL, Falkow S (1988) Evidence for two genetic loci in *Yersinia enterocolitica* that can promote invasion of epithelial cells. Infect Immun 56:1242–1248

Miller H, Zhang J, Kuolee R, Patel GB, Chen W (2007) Intestinal M cells: the fallible sentinels?. World J Gastroenterol 13:1477–1486

Mota LJ, Journet L, Sorg I, Agrain C, Cornelis GR (2005) Bacterial injectisomes: needle length does matter. Science 307:1278

Neubauer H, Aleksic S, Hensel A, Finke EJ, Meyer H (2000) *Yersinia enterocolitica* 16S rRNA gene types belong to the same genospecies but form three homology groups. Int J Med Microbiol 290:61–64

Payne D, Tatham D, Williamson ED, Titball RW (1998) The pH 6 antigen of *Yersinia pestis* binds to β1-linked galactosyl residues in glycosphingolipids. Infect Immun 66:4545–4548

Perry RD, Fetherston JD (1997) *Yersinia pestis* – etiologic agent of plague. Clin Microbiol Rev 10:35–66

Pierson DE, Falkow S (1993) The *ail* gene of *Yersinia enterocolitica* has a role in the ability of the organism to survive serum killing. Infect Immun 61:1846–1852

Prentice MB, Rahalison L (2007) Plague. Lancet 369:1196–1207

Rosqvist R, Skurnik M, Wolf-Watz H (1988) Increased virulence of *Yersinia pseudotuberculosis* by two independent mutations. Nature 334:522–524

Simonet M, Riot B, Fortineau N, Berche P (1996) Invasin production by *Yersinia pestis* is abolished by insertion of an IS*200*-like element within the *inv* gene. Infect Immun 64:375–379

Simonet M, Triadou P, Frehel C, Morel-Kopp MC, Kaplan C, Berche P (1992) Human platelet aggregation by *Yersinia pseudotuberculosis* is mediated by invasin. Infect Immun 60:366–373

Skurnik M, Bengoechea JA (2003) The biosynthesis and biological role of lipopolysaccharide O-antigens of pathogenic *Yersiniae*. Carbohydr Res 338:2521–2529

Skurnik M, El Tahir Y, Saarinen M, Jalkanen S, Toivanen P (1994) YadA mediates specific binding of enteropathogenic *Yersinia enterocolitica* to human intestinal submucosa. Infect Immun 62:1252–1261

Stenseth NC, Atshabar BB, Begon M, Belmain SR, Bertherat E, Carniel E, Gage KL, Leirs H, Rahalison L (2008) Plague: past, present, and future. PLoS Med 5:e3

Tsang TM, Felek S, Krukonis ES (2010) Ail binding to fibronectin facilitates *Yersinia pestis* binding to host cells and Yop delivery. Infect Immun 78:3358–3368

Vincent P, Salo E, Skurnik M, Fukushima H, Simonet M (2007) Similarities of Kawasaki disease and *Yersinia pseudotuberculosis* infection epidemiology. Pediatr Infect Dis J 26:629–631

Visser LG, Annema A, van Furth R (1995) Role of Yops in inhibition of phagocytosis and killing of opsonized *Yersinia enterocolitica* by human granulocytes. Infect Immun 63:2570–2575

Visser LG, Hiemstra PS, van den Barselaar MT, Ballieux PA, van Furth R (1996) Role of YadA in resistance to killing of *Yersinia enterocolitica* by antimicrobial polypeptides of human granulocytes. Infect Immun 64:1653–1658

Wachtel MR, Miller VL (1995) *In vitro* and *in vivo* characterization of an *ail* mutant of *Yersinia enterocolitica*. Infect Immun 63:2541–2548

Yang Y, Merriam JJ, Mueller JP, Isberg RR (1996) The *psa* locus is responsible for thermoinducible binding of *Yersinia pseudotuberculosis* to cultured cells. Infect Immun 64:2483–2489

Yen YT, Karkal A, Bhattacharya M, Fernandez RC, Stathopoulos C (2007) Identification and characterization of autotransporter proteins of *Yersinia pestis* KIM. Mol Membr Biol 24:28–40

Zav'yalov VP, Abramov VM, Cherepanov PG, Spirina GV, Chernovskaya TV, Vasiliev AM, Zav'yalova GA (1996) pH6 antigen (PsaA protein) of *Yersinia pestis*, a novel bacterial Fc-receptor. FEMS Immunol Med Microbiol 14:53–57

Chapter 2
Adhesive Mechanisms of *Salmonella enterica*

Carolin Wagner and Michael Hensel

Abstract *Salmonella enterica* is an invasive, facultative intracellular pathogen of animal and man with the ability to colonize various niches in diverse host organisms. The pathogenesis of infections by *S. enterica* requires adhesion to various host cell surfaces, and a large number of adhesive structures can be found. Depending on the serotype of *S. enterica*, gene clusters for more than 10 different fimbrial adhesins were identified, with type I fimbriae such as Fim, Lpf (long polar fimbriae), Tafi (thin aggregative fimbriae) or the type IV pili of serotype Typhi. In addition, autotransporter adhesins such as ShdA, MisL and SadA and the type I secreted large repetitive adhesins SiiE and BapA have been identified. Although the functions of many of the various adhesins are not well understood, recent studies show the specific structural and functional properties of *Salmonella* adhesins and how they act in concert with other virulence determinants. In this chapter, we describe the molecular characteristics of *Salmonella* adhesins and link these features to their multiple functions in infection biology.

2.1 Introduction

Some bacterial pathogens are equipped with a wealth of adhesive structures. One remarkable example is *Salmonella enterica*, a frequent gastrointestinal pathogen. Although a close relative of the commensal enterobacterial species *Escherichia coli*, *S. enterica* possesses a large number of virulence factors that confer an invasive, facultative intracellular lifestyle to this pathogen. These virulence traits mainly depend on the injection of toxin-like proteins into eukaryotic target cells. Prior to these manipulations of host cells, various *Salmonella* serovars deploy an astonishingly large number of adhesive structures that belong to the various classes of fimbrial and

M. Hensel (✉)
Fachbereich Biologie/Chemie, Abteilung Mikrobiologie, Universität Osnabrück,
49076 Osnabrück, Germany
e-mail: Michael.Hensel@biologie.uni-osnabrueck.de

D. Linke, A. Goldman (eds.), *Bacterial Adhesion*, Advances in Experimental Medicine and Biology 715, DOI 10.1007/978-94-007-0940-9_2,

non-fimbrial adhesins. In this chapter, we will describe the molecular and functional properties of *Salmonella* adhesins and link these features to their role in infection biology.

2.2 Pathogenesis of Infections with *Salmonella enterica*

Salmonella enterica causes food-borne infections of animals and man. The pathogen is primarily transmitted through contaminated food and water, including poultry, egg, meat, fish and also vegetables or fruits. Infections lead to diseases that can cause severe health problems, mainly in developing countries or in patients with compromised immune status, such as children, elderly people or HIV patients. In addition, the presence of *Salmonella* in livestock animals is known to have a serious impact on economy. Diseases caused by *Salmonella* lead to different outcomes, depending on the serotype encountered and the immune status of the host. While the serovars Typhimurium or Enteritidis cause self-limiting gastroenteritis in humans, infections with serovars Typhi or Paratyphi lead to typhoid fever, a severe systemic disease.

After ingestion, successful passage through the stomach and entering the gut, *Salmonella* has to counterbalance the intestinal peristalsis and to ensure its adhesion for the colonisation of the gut. Adhesion to host tissues is a crucial step during pathogenesis: the first tight contact between host and microbe is a prerequisite for triggering distinct processes like biofilm formation or protein translocation that may be followed by entry into the host cell and later systemic dissemination. *Salmonella* has evolved various strategies to initiate adhesion and host serovars have adapted a characteristic combination of different adhesion systems. The description of diverse adhesion systems is the scope of the following sections. A detailed understanding of the molecular basis for each adhesion system is required in order to develop new strategies for treatment and for prevention of severe disease outcomes.

2.3 Atypical Adhesive Structures in *Salmonella*

The various adhesion systems present in *S. enterica* have been organised into different categories. Fimbrial and non-fimbrial adhesins are the two major groups of adhesive structures; they differ according to their assembly pathways (Soto and Hultgren, 1999) as will be discussed in detail in Sections 2.4 and 2.5, respectively. Additionally, several surface structures of *Salmonella*, whose main functions are primarily not involved in adhesion, also contribute in part to the attachment and colonisation of host tissues.

One of these surface structures is the flagellum, a long polymeric protein appendage necessary for bacterial motility. Furthermore, flagella are involved in chemotaxis and other forms of directed movement, induction of immune responses and inflammation and they contribute to attachment to and colonisation of both

mucosal tissues (reviewed in Ramos et al., 2004) and gall bladders in chronically infected carriers. A transposon mutagenesis study recently revealed that mutations in structural and assembly genes of flagella impaired the ability of the mutants to adhere to cholesterol-coated surfaces. Among these, FliC, the conserved and major subunit of flagella, was suggested to be the critical component. The attachment via FliC to cholesterol might be an initial step for *Salmonella* to colonize and form biofilms on human gall stones (Crawford et al., 2010).

A system assembled similarly to the flagellar system is the type III secretion system (T3SS). Once adhered, *Salmonella* employs the *Salmonella* pathogenicity island (SPI) 1-encoded T3SS to translocate effector proteins through a needle-like structure into the host cell leading to uptake of *Salmonella*. It has recently been shown that a complex consisting of 3 translocon proteins (SipB, SipC and SipD) is required to mediate intimate attachment of the bacterium to epithelial cells. Thus, the T3SS provides its own attachment system to translocate effector proteins into the host cell (Lara-Tejero and Galan, 2009).

In contrast to the T3SS and flagella, there is no specific attachment factor known for lipopolysaccharide (LPS). The adhesive effect of the cell wall component LPS is rather attributed to its amphiphilic character. LPS is composed of a central hydrophobic glycolipid (Lipid A) and a hydrophilic core polysaccharide and variable O-antigen side chains. LPS is an essential component of the outer membrane that protects the bacterium against defensins and other antimicrobial factors, but can also act as endotoxin that triggers a life-threatening condition in patients known septic shock. It has been shown that the entire LPS molecule is required for colonisation of host tissue; and Nevola and co-workers (1985) showed that an LPS-deficient strain was outcompeted by a wild-type strain in a mouse colonisation experiment.

2.4 Fimbrial Adhesins

The group of fimbrial adhesins comprises most of the annotated *Salmonella* adhesins. Fimbriae are proteinaceous surface appendages that appear in several copies per cell. Fimbrial adhesins are assembled by different systems: the chaperone-usher pathway, the extracellular nucleation pathway and a special system for type IV pili, which is similar to the type II secretion system. Some representative electron microscopy images of type I fimbriae, type IVB pili in *S. enterica* serovar Typhi, long polar fimbriae (Lpf) and thin aggregative fimbriae (Tafi) can be found in Korhonen et al. (1980), Tam et al. (2006), Bäumler and Heffron (1995) and Sukupolvi et al. (1997), respectively.

2.4.1 Chaperone-Usher Assembled Fimbrial Adhesins

Fimbriae assembled by the chaperone-usher pathway (CUP) have been studied in great detail. Fimbrial subunits are directed to the periplasm through the general

secretion pathway (GSP) via an N-terminal secretion sequence that is cleaved off during transport. In the periplasm, interaction with specific chaperones prevents the premature assembly of fimbrial subunits and rapid degradation by proteases. The chaperones also direct fimbrial subunits to the usher, which is composed of integral outer membrane proteins that coordinate the assembly of the fimbriae. On the tip of the completed fimbriae, the distal subunit contains the receptor-binding site that interacts with its host receptor.

According to genomic analysis of various *S. enterica* serovars, there exist at least 15 operons predicted to encode fimbrial adhesins. Each serovar is characterised by a distinct combination of fimbriae that act synergistically (summarized in Townsend et al., 2001; van der Velden et al., 1998). The varying distribution of fimbrial operons is likely to reflect the adaptation of the various serovars to different niches. However, the identification and functional characterisation of fimbrial adhesins is challenging, since many of the putative fimbrial operons are not expressed under laboratory conditions (Humphries et al., 2003). As an experimental approach, the function of fimbriae that are not synthesised in vitro may be analysed after heterologous expression in *E. coli* strains using flow cytometry or electron microscopy as has been shown for the *stc* fimbrial operon (Humphries et al., 2003). Further, the observation that antibodies against specific fimbrial antigens could be detected in the sera of mice or other species after infection with *Salmonella* indicated that most of these fimbriae are expressed in vivo (Humphries et al., 2005; Nicholson and Bäumler, 2001). The function of some of the fimbrial adhesins has already been proven in vivo. Apart from their role in attachment of the bacterium to host cell, studies involving competitive infection experiments have revealed the contribution of fimbriae to long-term colonisation in mice (Weening et al., 2005) and to biofilm formation (Ledeboer et al., 2006).

The function of these fimbrial adhesins is primarily achieved through binding to a specific receptor on the host cell. In general, the nature of these receptors may be a distinct membrane protein, sugar residues or lipid structures. However, all fimbrial adhesins characterised so far in *Salmonella* exhibit lectin-like functions. StdA binds to α(1–2)fucosylated receptors (Chessa et al., 2009), PefA binds to the LewisX blood group antigen (Chessa et al., 2008) and the best-studied fimbrial adhesin FimH, which is encoded by the *fim* operon, is highly specific for mannose residues. Fim is the only fimbrial adhesin that is synthesised in static culture in laboratory media and is present in all serovars tested (Humphries et al., 2003; Townsend et al., 2001). Fim fimbriae are members of the type 1 fimbriae family, which are characterised by mannose-sensitive hemagglutination and mannose-sensitive binding to host cells (Duguid, 1959). Type 1 fimbriae have a diameter of 6 nm and an average length of 1 μm (Korhonen et al., 1980). FimA, the major structural subunit, forms the fimbrial shaft whose impact on host tropism is still controversial (Guo et al., 2009; Thankavel et al., 1999). FimH, which represents the tip of the fimbriae, is responsible for the varying binding properties on the host cell. Whereas FimH of *E. coli* preferentially binds to bladder epithelial cells, FimH of *Salmonella* binds to enterocytes (Thankavel et al., 1999). Besides its lectin-like function, FimH was assumed to bind to glycoprotein-2, expressed on M cells (Hase et al., 2009).

Although there are only minor differences in the sequences of FimH variants, the binding pattern differs in different *Salmonella* serovars and strains (Hancox et al., 1997). These allelic variations partly account for the diverse host tropisms of the serovars.

As the fimbriae of avian-specific serovars *S*. Gallinarum and *S*. Pullorum have long been thought to represent a "non-adhesive" variant of type 1 fimbriae, they are often designated as type 2 fimbriae (Crichton et al., 1989). Compared to *S*. Typhimurium, there are minor amino acid replacements in FimH of *S*. Gallinarum and *S*. Pullorum that render the fimbriae unable to bind to mannose or to murine and human cell lines (Guo et al., 2009; Kisiela et al., 2005). However, it has been shown recently that type 2 fimbriae of *S*. Gallinarum exhibited binding to chicken leukocytes. This interaction was mannose-resistant, suggesting a different receptor in avian host tissues and accounts in part for the avian-specific host adaption of those serovars (Guo et al., 2009).

These variations in binding specificities of FimH are not restricted to various serovars. Instead, even the FimH derivatives of strains of the same serovar can exhibit differences in binding profiles. In *S*. Typhimurium, there exist "high-adhesive" and "low-adhesive" variants of FimH (Boddicker et al., 2002; Guo et al., 2009). The high-adhesive forms show a higher affinity to human epithelial cells than the low-adhesive form of FimH (Boddicker et al., 2002). The low-adhesive variant of FimH of *S*. Typhimurium shows the same characteristics as that of *S*. Enteritidis. Further, both low-adhesive variants are mannose-sensitive and bind not only to human colonic cell lines, but also to human bladder cells, known so far only as the target of *E. coli* FimH (Kisiela et al., 2006). In contrast to low-adhesive FimH, high-adhesive FimH seems to be able to discriminate between these cell types.

Other fimbrial adhesins in *S. enterica* serovar Typhimurium are Bcf, Saf, Stb, Stc, Stf, Sth, Sti and Stj. Specific for serovar Enteritidis are the Sef fimbriae, while Stg fimbriae were detected in serovar Typhi. Our knowledge of these family members is still however rather sparse.

2.4.2 Long Polar Fimbriae

The gene cluster for the long polar fimbriae (Lpf) has been initially identified as a region present in *S. enterica* serovar Typhimurium, Enteritidis and others but absent in *S*. Typhi or *E. coli*. Expression of the genes in *E. coli* resulted in the formation of long appendages at the cell poles similar to type IV fimbriae (Bäumler and Heffron, 1995). These researchers subsequently reported that Lpf played a role in the adhesion of *S*. Typhimurium to cells of the Peyer's patches (Bäumler et al., 1996). Peyer' patches are aggregates of lymphoid follicles and part of the gut-associated lymphatic tissue. As Peyer's patches are considered as sites of entry for *Salmonella* infections, this could be important for the disease outcome of *S*. Typhimurium infection. Indeed, additive effects of the adhesins Lpf, Fim, Pef and Agf in colonisation of the intestine and systemic virulence after oral infection of mice were observed

(van der Velden et al., 1998). Phase variation between on-/off-states was observed during infection of mice with *S*. Typhimurium, which allowed the colonising bacteria to evade the immune system (Norris et al., 1998) and to avoid cross-immunity between various *S. enterica* serovars with different O-antigens but a similar Lpf antigenic structure (Norris and Bäumler, 1999).

2.4.3 Thin Aggregative Fimbriae: Assembly Through the Nucleation-Precipitation Pathway

Fimbrial adhesins with morphology distinct from the fimbrial adhesins described above are designated as "*t*hin *a*ggregative *fi*mbriae" (Tafi). These structures are assembled via a unique assembly pathway, the nucleation-precipitation pathway. Tafi are fimbrial adhesins with a diameter of 3–4 nm and lead to auto-aggregation of *Salmonella*, biofilm formation and adhesion to various surfaces (Collinson et al., 1993, 1991). In *Salmonella,* Tafi are encoded by two operons, *agfDEFG* and *agfBA*. AgfD is the transcriptional regulator, AgfBA the fimbrial subunits and AgfEFG mediate assembly of the fimbriae are part of the assembly system in the outer membrane (Barnhart and Chapman, 2006; Römling et al., 1998a). The homologues of Tafi in *E. coli* are called Curli and are encoded by the operons *csgDEFG* and *csgBA* (Barnhart and Chapman, 2006; Collinson et al., 1991; Olsen et al., 1989; Römling et al., 1998a). CsgA and AgfA, which are the major aggregative subunit in *E. coli* and *S.* Typhimurium, respectively, share a 74% identity in their polypeptide sequence and also exhibit similar functions (Collinson, 1996; Hammar et al., 1996). Tafi and Curli are expressed and assembled in response to nutrient limitation, low osmolarity and low temperature (Gerstel and Römling, 2001; Olsen et al., 1989; Römling et al., 1998b).

Tafi and Curli are known to be assembled via the nucleation-precipitation pathway and have been studied in great detail in *E. coli* (Hammar et al., 1996). The subunits encoded by the *csgBA* operon are transported into the periplasm via the general secretion pathway, while CsgD regulates the transcription of *csgBA*. CsgG is an outer membrane lipoprotein required for the secretion of CsgA and CsgB across the outer membrane and interacts with CsgE (reviewed in Barnhart and Chapman, 2006). For the assembly of the fimbriae, the nucleator CsgB polymerises secreted CsgA (curlin) on the outside of the bacterial cell. Furthermore, there is also evidence for interbacterial complementation; secreted CsgA from one cell can be polymerised on CsgB of a neighbouring cell (Hammar et al., 1996). In *Salmonella* it has been shown that interbacterial complementation only occurs in the absence of LPS, suggesting that LPS is a barrier for the diffusion of CsgA (White et al., 2001, 2003). One major difference between the nucleation-precipitation pathway and the CUP is that polymerisation of the fimbrial subunit in CUP occurs from the periplasmic site of the outer membrane, whereas Curli and Tafi are assembled on the outside of the bacterial cell envelope.

Tafi and Curli interact with different extracellular matrix proteins such as fibronectin or laminin and might allow the colonisation of wounds (Collinson et al., 1993; Olsen et al., 1993, 1989). The ability of Tafi to bind the dye Congo Red

facilitates the identification of Tafi-positive *Salmonella* (Collinson et al., 1993). Tafi have been shown to be required for attachment to cultured mouse intestinal epithelial cells, to inorganic surfaces like Teflon and stainless steel where they can form biofilms, and to plants, which might be a vector for animal-to-animal transmissions (Austin et al., 1998; Barak et al., 2005; Sukupolvi et al., 1997).

2.4.4 Type IV Pili

Type IV pili are another class of fimbrial adhesins present in a large number of bacterial pathogens. In *S. enterica*, type IV pili were only detected in the strictly human-adapted serovar Typhi. The 11 genes that are necessary for type IV pilus assembly are encoded in the *pil* operon localised on *Salmonella* pathogenicity island (SPI) 7 and are required for the adhesion to and uptake into human intestinal cells (Zhang et al., 1997, 2000)

The subunits for the pilus formation are assembled in the periplasm at the inner membrane and extruded through a secretin in the outer membrane as an intact pilus (Wolfgang et al., 2000). The assembly mechanism has been studied in detail for type IVa pili of *Neisseria gonorrhoeae*. *Salmonella* pili belong to the type IVb pilus family; they differ from type IVa pili in the length of the signal peptide and in the mature sequence of the pilin subunit (reviewed in Craig and Li, 2008). The pilin subunits (PilE in *N. gonorrhoea*e and PilS in *S.* Typhi) are transported to the periplasm via the general secretion pathway where they are anchored to the inner membrane. A prepilin peptidase (PilD in *N. gonorrhoeae* and PilU in *S.* Typhi) cleaves the N-terminal leader sequence. The energy for pilus polymerisation is provided by an assembly ATPase. The assembled pilus is protruded out of the outer membrane through the action of secretin PilQ of *N. gonorrhoeae*. An additional retraction ATPase mediates the depolymerisation of the pilus leading to a movement called "twitching motility". This mechanism mediates movement along surfaces as the pilus is retracted while it is still adhered to target surface (Craig and Li, 2008). Besides twitching and gliding motility (Wall and Kaiser, 1999), type IV pili have also been shown to be required for many pathogenic processes including immune escape, DNA uptake, biofilm formation, microcolony formation and adhesion reviewed by (Craig and Li, 2008). Adhesion and uptake occur via the cystic fibrosis transmembrane conductance regulator (CFTR), a receptor mutated in cystic fibrosis patients. *S.* Typhi has been shown to upregulate and exploit CFTR as a receptor for bacterial uptake (Lyczak and Pier, 2002; Pier et al., 1998). The level of CFTR on the surface correlated with the efficiency of *S.* Typhi uptake (Pier et al., 1998). prePilS could bind to a fragment of CFTR and thus could mediate adhesion of *S.* Typhi to the membrane of gut epithelial cells (Tsui et al., 2003; Xu et al., 2004). Interestingly, the most common CFTR mutation in cystic fibrosis, ΔF508, leads to impaired uptake of *S.* Typhi into mice submucosa. Therefore, a heterozygous carrier of this mutation might be less susceptible for *S.* Typhi infection, possibly explaining the persistence of this mutation in the human population (Pier et al., 1998).

2.5 Non-fimbrial Adhesins

In contrast to fimbrial adhesins, non-fimbrial adhesins are a rather heterogeneous group of adhesins. This group comprises mono- and oligomeric adhesins that are either secreted through a type I secretion system or autotransported across the bacterial membranes.

2.5.1 Adhesins Secreted by Type I Secretion Systems

So far, two adhesins that are substrates of the type I secretion systems (T1SSs) have been identified in *S. enterica,* SiiE and BapA. These adhesins are the largest proteins of the *Salmonella* proteome and are secreted into the extracellular milieu by the action of T1SS. The T1SS are tripartite complexes consisting of three conserved proteins that span the inner membrane (ATP-binding cassette protein; ABC), the periplasmic space (membrane fusion protein; MFP) and the outer membrane (outer membrane protein; OMP). These subunits form a channel structure for the selective transport of the T1SS substrates through the bacterial envelope in a single step. The tripartite T1SS complex is assembled once the C-terminal secretion signal of the substrate protein is recognised by the ABC protein. The energy for transport is provided by ATP hydrolysis through the action of the ABC protein (reviewed in Delepelaire, 2004).

T1SS secrete a variety of substrate proteins such as haemolysins or extracellular enzymes. However, T1SS-secreted adhesins have to be attached to the bacterial envelope following secretion in order to act as an adhesin and to bridge the distance between the bacterium and the biotic or abiotic substratum. Therefore, secreted adhesins must either interact with a protein in the bacterial envelope or remain temporarily anchored to the T1SS after secretion. However, there is no experimental evidence for either model so far. Whereas BapA has been observed so far exclusively in a surface-bound form, SiiE has been detected in a released form as well as in a temporarily surface-bound version (Gerlach et al., 2007b; Latasa et al., 2005).

Cellulose and thin aggregative fimbriae are the major compounds of the biofilm matrixes formed by *S. enterica* (Austin et al., 1998; Zogaj et al., 2001). Latasa et al. (2005) set out to identify additional factors contributing to biofilm formation in *S. enterica* serovar Enteritidis. The similarity search for biofilm-associated proteins was based on the sequence of Bap (*b*iofilm *a*ssociated *p*rotein) which is a well characterised surface protein crucial for biofilm formation in *Staphylococcus aureus* (Cucarella et al., 2001). During their study, Latasa and co-workers found two proteins (BapA and SiiE) in *S.* Enteriditis that are similar to *S. aureus* Bap. Bap contains 13 identical repeats, called C-repeats, which share 29% sequence identity with the 29 B-repeats of BapA (Fig. 2.1a). The orthologous BapA in *S. enterica* serovar Typhi (sty2875), encoded on SPI9, contains 27 repeats and is therefore smaller than BapA of *S. enterica* serovar Enteriditis (Latasa et al., 2005).

BapA of *S.* Enteritidis was shown to promote pellicle and biofilm formation: a *bapA* deletion mutant lost the ability to form biofilms, whereas overproduction of

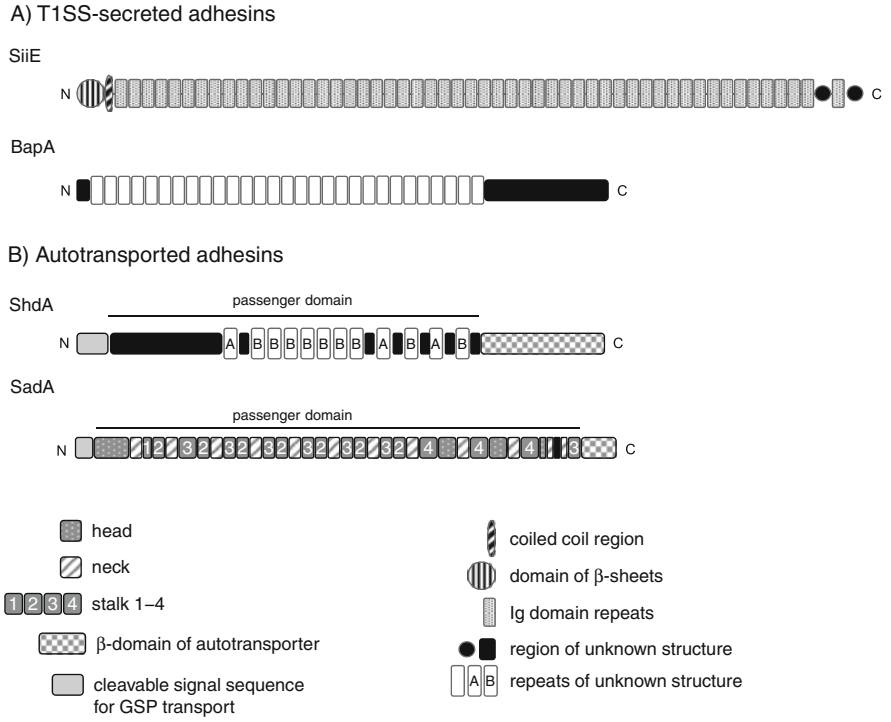

Fig. 2.1 Non-fimbrial adhesins of *Salmonella enterica*. The models show the domain organisation of large non-fimbrial adhesins secreted by type I secretion systems (T1SS) (**a**) and adhesins of the autotransporter family (**b**). The models were modified from Gerlach et al. (2007b) for SiiE, Latasa et al. (2005) for BapA, Kingsley et al. (2004a) for ShdA, and Linke et al. (2006) for SadA

BapA enhanced biofilm production. The importance of BapA in biofilm formation was also indicated by the observation that the expression of BapA was controlled by the central transcription regulator AgfD. This protein coordinates the expression of other factors involved in biofilm formation like thin aggregative fimbriae and proteins for cellulose production (Latasa et al., 2005; Römling et al., 2000, 1998b; Zogaj et al., 2001). Additionally, BapA appears to mediate homophilic interactions between different cells (Latasa et al., 2005). This interaction leads to autoaggregation of bacterial cells promoting biofilm formation. The reduced colonisation of murine ligated-ileal loops by *bapA* mutants combined with an impaired virulence in mice indicated a key role for BapA in the primary stage of infection (Latasa et al., 2005).

The second protein found by Latasa and co-workers is SiiE. In SiiE, Latasa et al. (2005) described 50 tandem repeats with 25% sequence identity to Ig repeats in the C- and B- repeats in Bap and in BapA. However, Gerlach et al. (2007b) regrouped these repeats into 53 repeats of Immunoglobulin (Ig) domains by comparison to the Ig domains of Invasin from Yersinia pseudotuberculosis (Fig. 2.1a). Latasa et al.

(2005) observed that SiiE did not contribute to biofilm formation under the conditions tested and thus considered SiiE as dispensable for biofilm formation. However, Morgan et al. (2004) proposed a role for SiiE as a host-specific colonisation factor in cattle and for intestinal infection in mice (a factor for *Salmonella i*ntestinal *i*nfection). SiiE is encoded by a gene in SPI4 which was proposed as virulence locus by Wong et al. (1998) but incorrectly annotated due to the repetitive structure of *siiE*. After sequencing the *Salmonella* genome, the formerly identified 18 ORFs in SPI4 were shown to be 6 ORFs encoding SiiE, its cognate T1SS (SiiCDF) and two accessory proteins SiiA and SiiB (Gerlach et al., 2007b; McClelland et al., 2001; Morgan et al., 2007). SiiA and SiiB are not secreted but localised in the inner membrane (Gerlach et al., 2007b). Despite the fact that SiiA and SiiB are neither required for synthesis and secretion of SiiE nor for regulation of SPI4 genes, their role seems to be crucial, as they still contribute to oral virulence in mice (Gerlach et al., 2007b; Kiss et al., 2007). These accessory proteins of T1SSs might have new functions, as described for LapD or HlyC of *Pseudomonas fluorescens* or *Escherichia coli,* respectively (Gerlach et al., 2007b; Hinsa and O'Toole, 2006; Morgan et al., 2004; Nicaud et al., 1985). Database searches did not reveal proteins similar to SiiA or SiiB and understanding their function requires further investigation.

SiiE is recognised by the T1SS via its C-terminal sequence and secreted by the T1SS formed by SiiCDF; it was found in the extracellular milieu of *Salmonella* as well as temporarily attached to the bacterial cell surface (Gerlach et al., 2007b; Morgan et al., 2007). The attachment to bacterial cell surfaces is a crucial requirement for SiiE in order to act as an adhesin (Gerlach et al., 2007b). The repetitive assembly of 53 Ig domains in SiiE is responsible for the extraordinary length (Fig. 2.1a) (Gerlach et al., 2007b). This length may allow SiiE to project beyond the O-antigen layer of the LPS in *Salmonella*: truncations of SiiE correlate with a decrease in the invasiveness, a phenotype that can be compensated by reducing the number of O-antigen repeats in the LPS (Gerlach et al., 2008).

The *sii* genes are organised in one operon in SPI4 and regulation of their expression is coordinated with that of SPI1 genes through the global regulators SirA and HilA. These regulators control *S. enterica* virulence functions in response to environmental conditions such as osmolarity, pH and oxygen availability (Ahmer et al., 1999; Bajaj et al., 1996; Gerlach et al., 2007a, b; Main-Hester et al., 2008; Morgan et al., 2007). HilA activates the expression of the SPI1-encoded transcription factor SprB, which in turn binds to the *sii* promoter in order to activate its transcription (Saini and Rao, 2010). It turned out that the concerted regulation of SPI1 and SPI4 is essential for the pathogenesis of *Salmonella* and is in line with the cooperative function of these two SPI during the infection process, where SPI4 plays a crucial role in adhesion to the apical brush border of intestinal cells (Gerlach et al., 2008). The contribution of SiiE to adhesion to host tissues has been ignored for a long time, because SiiE is dispensable for adhesion to non-polarized cell layers like HeLa cells (Gerlach et al., 2007b). However, in infection models with polarized epithelial cells, which form microvilli and tight junctions and thus more closely resemble the epithelial architecture of the intestine, SiiE exerts a crucial role in adhesion (Gerlach et al., 2007b). SiiE is required for adhesion to and invasion of the intestinal cells from the

luminal side by mediating intimate contact between *Salmonella* and the host cell to increase the efficiency of SPI1-mediated effector translocation and subsequent effacement of the brush border (Gerlach et al., 2008). Due to the absence of a brush border barrier in non-polarized epithelial cells, the barrier is missing and there is no need for SPI4-mediated adhesion to enable the SPI1-mediated effector translocation and cell invasion.

SiiE appears to play an important role for infection as SPI4 is conserved in most common serovars (Wong et al., 1998). The synthesis and secretion of SiiE was observed in various *S. enterica* serovars tested except Arizona and Typhi (Main-Hester et al., 2008). The reason for lack of SiiE in serovar Typhi is a frame-shift in *siiE* resulting in a premature stop codon that renders *siiE* a pseudo-gene (Parkhill et al., 2001). This divergence may contribute to the differences in host tropism and infections caused by serovars Typhi and Typhimurium.

2.5.2 Autotransported Adhesins

There are currently more than 800 members of the autotransporter family, also referred to as the type V secretion system (T5SS), in various Gram-negative genera. These proteins can be further categorised as monomeric proteins and trimeric autotransporter adhesins (TAA). Substrate proteins of the autotransporter pathway harbour the N-terminal signal sequence for recognition and transport through the cytoplasmic membrane by the GSP. The C-terminal segment, the β-domain, forms a β-barrel in the outer membrane and mediates the transport of the passenger domain into the extracellular space (reviewed in Dautin and Bernstein, 2007).

In *Salmonella*, three adhesins of the autotransporter family have been described. ShdA and MisL are monomeric adhesins while the putative adhesin SadA is a TAA (see Fig. 2.1b for models). SadA has similarity to YadA of *Yersinia enterocolitica*, the prototypic TAA. The members of the TAA family are exclusively adhesins. The passenger domain is composed of a stalk domain that forms a coiled-coil and defines the length of the adhesin, and a head domain. The structure appears as a trimeric lollipop-like assembly (reviewed in Linke et al., 2006). Although the conditions for the expression of *sadA* are unknown and a contribution of SadA to adhesion has not been shown so far, its structural properties clearly suggest SadA as a member of the TAA family (Hernandez Alvarez et al., 2008).

For the two monomeric autotransporter proteins of *Salmonella*, the adhesive function has been proven experimentally. ShdA is encoded by a gene within the CS54 island (Kingsley et al., 2000). Database searches revealed a 92% sequence identity to the passenger domains of other autotransporter adhesins such as AIDA of *E. coli*, MisL of *S.* Typhimurium and IcsA (VirG) involved in intracellular motility of *Shigella flexneri* (Kingsley et al., 2000). ShdA has been exclusively detected in serovars of *Salmonella enterica* subspecies I, which comprises all the mammalian and avian pathogenic serovars, whereas it was absent in serotypes of subspecies II-VII, which include the serovars isolated from cold-blooded vertebrates and *S. bongori* (Kingsley et al., 2000).

Though expression of *shdA* under standard laboratory conditions has not yet been observed, after heterologous expression ShdA was detected on the bacterial surface and shown to bind to fibronectin (Kingsley et al., 2004b, 2002). This interaction could be inhibited by heparin, as ShdA and heparin both bind to fibronectin at the same binding site, the Hep-2 domain. Thus, ShdA mimics heparin binding to fibronectin (Kingsley et al., 2004a). Furthermore, infection experiments showed that *shdA* expression is induced in the murine caecum in vivo (Kingsley et al., 2002). In addition, a *shdA* mutant showed reduced colonisation of the murine caecum and was shed from the faeces in reduced numbers and for a shorter period of time (Kingsley et al., 2003, 2000). This provides evidence that colonisation of the murine caecum mediated through ShdA is a prerequisite for the persistence of *Salmonella* in the murine intestine (Kingsley et al., 2003). However, infections of pigs with an *shdA* mutant did not indicate a role for ShdA in virulence in this model, as ShdA was not required for persistence or prolonged shedding in infected pigs. This divergence again underlines the notion that adhesins of *S. enterica* fulfil highly host-specific functions (Boyen et al., 2006).

The autotransporter adhesin MisL is encoded by a gene within SPI3 and shows very similar properties to ShdA (Blanc-Potard et al., 1999). Similar to *shdA*, expression of *misL* was not observed under standard laboratory conditions (Blanc-Potard et al., 1999; Dorsey et al., 2005), but heterologous expression resulted in the presence of MisL on the outer membrane of *S.* Typhimurium. Similar to ShdA, MisL binds to fibronectin, whereas the binding properties to other extracellular matrix proteins, like collagen IV and collagen I differ between MisL and ShdA (Dorsey et al., 2005; Kingsley et al., 2002). Expression of *misL* was activated in vitro by MarT, a SPI3-encoded transcription factor (Tükel et al., 2007). Expression of *misL* is also likely to occur in vivo, as mice infected with *S.* Typhimurium seroconvert to MisL during infection (Dorsey et al., 2005). Though in vivo infection models revealed that MisL did not contribute to lethal infections in mice, MisL was required for bacterial shedding, intestinal colonisation and persistence in mice as well as intestinal colonisation of chicken, but not of calves (Blanc-Potard et al., 1999; Dorsey et al., 2005; Morgan et al., 2004).

These observations suggest that there is a synergistic effect of ShdA and MisL, but such relation a has not been proven so far (Dorsey et al., 2005). It is remarkable that many *Salmonella* adhesins bind to extracellular matrix proteins. These interactions seem to be crucial for *Salmonella* infections and might promote their colonisation to sites of erosion of the intestinal epithelium, where extracellular matrix proteins are exposed (Dorsey et al., 2005).

The properties of MisL and ShdA have been further exploited for vaccine development. In the first attempts, MisL was used to transport heterologous passenger peptides to the extracellular space for surface display of the vaccine antigens (Ruiz-Perez et al., 2002). Through insertion of an OmpT cleavage site, the modified protein could be cleaved off and released into the extracellular environment (Luria-Perez et al., 2007; Ruiz-Olvera et al., 2003; Ruiz-Perez et al., 2002). In further applications to improve live vaccination strains, mutations were introduced into *shdA* and *misL*, resulting in reduced shedding from faeces without impairing immune response or protection (Abd El Ghany et al., 2007). This could be an advantage to reduce the

adverse side effects of vaccination with live carriers, such as faecal shedding leading to release of genetically manipulated bacteria into the environment (Abd El Ghany et al., 2007). Taken together, the adhesins ShdA and MisL are important virulence factors that could be exploited for vaccine design.

2.6 Complexity of Adhesive Mechanisms in *Salmonella enterica*

The large number of adhesive structures formed by the various serotypes of *S. enterica* is remarkable. Although the regulation of the expression of most of the adhesins and their role in the lifestyle of *Salmonella* are still unknown, the complex assortment of multiple adhesins of different classes is likely to reflect the successful adaptation of the pathogen to different niches in the host and to different host organisms. This suggestion is supported by the lack of several adhesins and the presence of pseudogenes in highly host-adapted serovars such as *S*. Typhi. The genome decay of highly adapted pathogens is a consequence of a specialised lifestyle that often requires a reduced number of adhesive structures.

In contrast, *S. enterica* serovars with broad host specificity have a very high potential to interact with surfaces both inside and outside the hosts, due to the large number of functional adhesins in combination with sequence variations in adhesin subunits leading to altered binding specificities. This is clearly an indication that the transition from planctonic, individual life to a sessile, multicellular lifestyle occurs at various occasions. It should be noted that many phases of this pathogenic lifestyle, especially the environmental stages outside a mammalian host, have not been characterised in detail so far.

2.7 Conclusions and Outlook

Cellular and molecular analysis of the virulence properties of *S. enterica* has revealed the sophisticated strategies it uses for invading mammalian cells and adapting to an intracellular lifestyle in a pathogen-containing vacuole within host cells. The various adhesins deployed by *Salmonella* are an essential prerequisite for these specialised interactions. For example, the recent characterisation of the large non-fimbrial adhesin SiiE demonstrated that host cell entry is highly dependent on the cooperation of the invasion factors with an adhesin.

Major questions regarding adhesins of *Salmonella* concern the specificity of the interaction partners and the environmental factors leading to the expression of the various structures. Here, novel experimental approaches for understanding regulation and molecular functions are required. Such approaches could be complemented by structural analyses of *Salmonella* adhesins leading to functional understanding of the adhesive properties on the atomic level. Despite our detailed knowledge of several *Salmonella* adhesins, we expect a large number of unexpected new findings to be made for the adhesion mechanisms of this versatile and successful pathogen.

Acknowledgements Work in our laboratory was supported by grants of the Deutsche Forschungsgemeinschaft (DFG) and the Staedtler-Stiftung.

References

Abd El Ghany M, Jansen A, Clare S, Hall L, Pickard D, Kingsley RA, Dougan G (2007) Candidate live, attenuated *Salmonella enterica* serotype Typhimurium vaccines with reduced fecal shedding are immunogenic and effective oral vaccines. Infect Immun 75: 1835–1842

Ahmer BM, van Reeuwijk J, Watson PR, Wallis TS, Heffron F (1999) *Salmonella* SirA is a global regulator of genes mediating enteropathogenesis. Mol Microbiol 31:971–982

Austin JW, Sanders G, Kay WW, Collinson SK (1998) Thin aggregative fimbriae enhance *Salmonella enteritidis* biofilm formation. FEMS Microbiol Lett 162:295–301

Bajaj V, Lucas RL, Hwang C, Lee CA (1996) Co-ordinate regulation of *Salmonella typhimurium* invasion genes by environmental and regulatory factors is mediated by control of *hilA* expression. Mol Microbiol 22:703–714

Barak JD, Gorski L, Naraghi-Arani P, Charkowski AO (2005) *Salmonella enterica* virulence genes are required for bacterial attachment to plant tissue. Appl Environ Microbiol 71:5685–5691

Barnhart MM, Chapman MR (2006) Curli biogenesis and function. Annu Rev Microbiol 60: 131–147

Bäumler AJ, Heffron F (1995) Identification and sequence analysis of *lpfABCDE*, a putative fimbrial operon of *Salmonella typhimurium*. J Bacteriol 177:2087–2097

Bäumler AJ, Tsolis RM, Heffron F (1996) The *lpf* fimbrial operon mediates adhesion of *Salmonella typhimurium* to murine Peyer's patches. Proc Natl Acad Sci USA 93:279–283

Blanc-Potard AB, Solomon F, Kayser J, Groisman EA (1999) The SPI-3 pathogenicity island of *Salmonella enterica*. J Bacteriol 181:998–1004

Boddicker JD, Ledeboer NA, Jagnow J, Jones BD, Clegg S (2002) Differential binding to and biofilm formation on, HEp-2 cells by *Salmonella enterica* serovar Typhimurium is dependent upon allelic variation in the *fimH* gene of the *fim* gene cluster. Mol Microbiol 45:1255–1265

Boyen F, Pasmans F, Donne E, Van Immerseel F, Morgan E, Adriaensen C, Hernalsteens JP, Wallis TS, Ducatelle R, Haesebrouck F (2006) The fibronectin binding protein ShdA is not a prerequisite for long term faecal shedding of *Salmonella typhimurium* in pigs. Vet Microbiol 115:284–290

Chessa D, Dorsey CW, Winter M, Bäumler AJ (2008) Binding specificity of *Salmonella* plasmid-encoded fimbriae assessed by glycomics. J Biol Chem 283:8118–8124

Chessa D, Winter MG, Jakomin M, Bäumler AJ (2009) *Salmonella enterica* serotype Typhimurium Std fimbriae bind terminal alpha(1,2)fucose residues in the cecal mucosa. Mol Microbiol 71:864–875

Collinson SK, Clouthier SC, Doran JL, Banser PA, Kay WW (1996) *Salmonella enteritidis* agfBAC operon encoding thin, aggregative fimbriae. J Bacteriol 178(3):662–667

Collinson SK, Doig PC, Doran JL, Clouthier S, Trust TJ, Kay WW (1993) Thin, aggregative fimbriae mediate binding of *Salmonella enteritidis* to fibronectin. J Bacteriol 175:12–18

Collinson SK, Emody L, Muller KH, Trust TJ, Kay WW (1991) Purification and characterization of thin, aggregative fimbriae from *Salmonella enteritidis*. J Bacteriol 173:4773–4781

Craig L, Li J (2008) Type IV pili: paradoxes in form and function. Curr Opin Struct Biol 18: 267–277

Crawford RW, Reeve KE, Gunn JS (2010) Flagellated but not hyperfimbriated *Salmonella enterica* serovar Typhimurium attach to and form biofilms on cholesterol-coated surfaces. J Bacteriol 192:2981–2990

Crichton PB, Yakubu DE, Old DC, Clegg S (1989) Immunological and genetical relatedness of type-1 and type-2 fimbriae in salmonellas of serotypes Gallinarum, Pullorum and Typhimurium. J Appl Bacteriol 67:283–291

Cucarella C, Solano C, Valle J, Amorena B, Lasa I, Penades JR (2001) Bap, a *Staphylococcus aureus* surface protein involved in biofilm formation. J Bacteriol 183:2888–2896

Dautin N, Bernstein HD (2007) Protein secretion in gram-negative bacteria via the autotransporter pathway. Annu Rev Microbiol 61:89–112

Delepelaire P (2004) Type I secretion in gram-negative bacteria. Biochim Biophys Acta 1694: 149–161

Dorsey CW, Laarakker MC, Humphries AD, Weening EH, Bäumler AJ (2005) *Salmonella enterica* serotype Typhimurium MisL is an intestinal colonization factor that binds fibronectin. Mol Microbiol 57:196–211

Duguid JP (1959) Fimbriae and adhesive properties in *Klebsiella* strains. J Gen Microbiol 21: 271–286

Gerlach RG, Claudio N, Rohde M, Jäckel D, Wagner C, Hensel M (2008) Cooperation of *Salmonella* pathogenicity islands 1 and 4 is required to breach epithelial barriers. Cell Microbiol 10:2364–2376

Gerlach RG, Jäckel D, Geymeier N, Hensel M (2007a) *Salmonella* pathogenicity island 4-mediated adhesion is coregulated with invasion genes in *Salmonella enterica*. Infect Immun 75: 4697–4709

Gerlach RG, Jäckel D, Stecher B, Wagner C, Lupas A, Hardt WD, Hensel M (2007b) *Salmonella* pathogenicity island 4 encodes a giant non-fimbrial adhesin and the cognate type 1 secretion system. Cell Microbiol 9:1834–1850

Gerstel U, Römling U (2001) Oxygen tension and nutrient starvation are major signals that regulate *agfD* promoter activity and expression of the multicellular morphotype in *Salmonella typhimurium*. Environ Microbiol 3:638–648

Guo A, Cao S, Tu L, Chen P, Zhang C, Jia A, Yang W, Liu Z, Chen H, Schifferli DM (2009) FimH alleles direct preferential binding of *Salmonella* to distinct mammalian cells or to avian cells. Microbiology 155:1623–1633

Hammar M, Bian Z, Normark S (1996) Nucleator-dependent intercellular assembly of adhesive curli organelles in *Escherichia coli*. Proc Natl Acad Sci USA 93:6562–6566

Hancox LS, Yeh KS, Clegg S (1997) Construction and characterization of type 1 non-fimbriate and non-adhesive mutants of *Salmonella typhimurium*. FEMS Immunol Med Microbiol 19: 289–296

Hase K, Kawano K, Nochi T, Pontes GS, Fukuda S, Ebisawa M, Kadokura K, Tobe T, Fujimura Y, Kawano S, Yabashi A, Waguri S, Nakato G, Kimura S, Murakami T, Iimura M, Hamura K, Fukuoka S, Lowe AW, Itoh K, Kiyono H, Ohno H (2009) Uptake through glycoprotein 2 of FimH(+) bacteria by M cells initiates mucosal immune response. Nature 462: 226–230

Hernandez Alvarez B, Hartmann MD, Albrecht R, Lupas AN, Zeth K, Linke D (2008) A new expression system for protein crystallization using trimeric coiled-coil adaptors. Protein Eng Des Sel 21:11–18

Hinsa SM, O'Toole GA (2006) Biofilm formation by *Pseudomonas fluorescens* WCS365: a role for LapD. Microbiology 152:1375–1383

Humphries A, Deridder S, Bäumler AJ (2005) *Salmonella enterica* serotype Typhimurium fimbrial proteins serve as antigens during infection of mice. Infect Immun 73:5329–5338

Humphries AD, Raffatellu M, Winter S, Weening EH, Kingsley RA, Droleskey R, Zhang S, Figueiredo J, Khare S, Nunes J, Adams LG, Tsolis RM, Bäumler AJ (2003) The use of flow cytometry to detect expression of subunits encoded by 11 *Salmonella enterica* serotype Typhimurium fimbrial operons. Mol Microbiol 48:1357–1376

Kingsley RA, Abi Ghanem D, Puebla-Osorio N, Keestra AM, Berghman L, Bäumler AJ (2004a) Fibronectin binding to the *Salmonella enterica* serotype Typhimurium ShdA autotransporter protein is inhibited by a monoclonal antibody recognizing the A3 repeat. J Bacteriol 186: 4931–4939

Kingsley RA, Humphries AD, Weening EH, De Zoete MR, Winter S, Papaconstantinopoulou A, Dougan G, Bäumler AJ (2003) Molecular and phenotypic analysis of the CS54 island

of *Salmonella enterica* serotype typhimurium: identification of intestinal colonization and persistence determinants. Infect Immun 71:629–640

Kingsley RA, Keestra AM, de Zoete MR, Bäumler AJ (2004b) The ShdA adhesin binds to the cationic cradle of the fibronectin 13FnIII repeat module: evidence for molecular mimicry of heparin binding. Mol Microbiol 52:345–355

Kingsley RA, Santos RL, Keestra AM, Adams LG, Bäumler AJ (2002) *Salmonella enterica* serotype Typhimurium ShdA is an outer membrane fibronectin-binding protein that is expressed in the intestine. Mol Microbiol 43:895–905

Kingsley RA, van Amsterdam K, Kramer N, Bäumler AJ (2000) The *shdA* gene is restricted to serotypes of *Salmonella enterica* subspecies I and contributes to efficient and prolonged fecal shedding. Infect Immun 68:2720–2727

Kisiela D, Laskowska A, Sapeta A, Kuczkowski M, Wieliczko A, Ugorski M (2006) Functional characterization of the FimH adhesin from *Salmonella enterica* serovar Enteritidis. Microbiology 152:1337–1346

Kisiela D, Sapeta A, Kuczkowski M, Stefaniak T, Wieliczko A, Ugorski M (2005) Characterization of FimH adhesins expressed by *Salmonella enterica* serovar Gallinarum biovars Gallinarum and Pullorum: reconstitution of mannose-binding properties by single amino acid substitution. Infect Immun 73:6187–6190

Kiss T, Morgan E, Nagy G (2007) Contribution of SPI-4 genes to the virulence of *Salmonella enterica*. FEMS Microbiol Lett 275:153–159

Korhonen TK, Lounatmaa K, Ranta H, Kuusi N (1980) Characterization of type 1 pili of *Salmonella typhimurium* LT2. J Bacteriol 144:800–805

Lara-Tejero M, Galan JE (2009) *Salmonella enterica* serovar typhimurium pathogenicity island 1-encoded type III secretion system translocases mediate intimate attachment to nonphagocytic cells. Infect Immun 77:2635–2642

Latasa C, Roux A, Toledo-Arana A, Ghigo JM, Gamazo C, Penades JR, Lasa I (2005) BapA, a large secreted protein required for biofilm formation and host colonization of *Salmonella enterica* serovar Enteritidis. Mol Microbiol 58:1322–1339

Ledeboer NA, Frye JG, McClelland M, Jones BD (2006) *Salmonella enterica* serovar Typhimurium requires the Lpf, Pef, and Tafi fimbriae for biofilm formation on HEp-2 tissue culture cells and chicken intestinal epithelium. Infect Immun 74:3156–3169

Linke D, Riess T, Autenrieth IB, Lupas A, Kempf VA (2006) Trimeric autotransporter adhesins: variable structure, common function. Trends Microbiol 14:264–270

Luria-Perez R, Cedillo-Barron L, Santos-Argumedo L, Ortiz-Navarrete VF, Ocana-Mondragon A, Gonzalez-Bonilla CR (2007) A fusogenic peptide expressed on the surface of *Salmonella enterica* elicits CTL responses to a dengue virus epitope. Vaccine 25:5071–5085

Lyczak JB, Pier GB (2002) *Salmonella enterica* serovar typhi modulates cell surface expression of its receptor, the cystic fibrosis transmembrane conductance regulator, on the intestinal epithelium. Infect Immun 70:6416–6423

Main-Hester KL, Colpitts KM, Thomas GA, Fang FC, Libby SJ (2008) Coordinate regulation of *Salmonella* pathogenicity island 1 (SPI1) and SPI4 in *Salmonella enterica* serovar Typhimurium. Infect Immun 76:1024–1035

McClelland M, Sanderson KE, Spieth J, Clifton SW, Latreille P, Courtney L, Porwollik S, Ali J, Dante M, Du F, Hou S, Layman D, Leonard S, Nguyen C, Scott K, Holmes A, Grewal N, Mulvaney E, Ryan E, Sun H, Florea L, Miller W, Stoneking T, Nhan M, Waterston R, Wilson RK (2001) Complete genome sequence of *Salmonella enterica* serovar Typhimurium LT2. Nature 413:852–856

Morgan E, Bowen AJ, Carnell SC, Wallis TS, Stevens MP (2007) SiiE is secreted by the *Salmonella enterica* serovar Typhimurium pathogenicity island 4-encoded secretion system and contributes to intestinal colonization in cattle. Infect Immun 75:1524–1533

Morgan E, Campbell JD, Rowe SC, Bispham J, Stevens MP, Bowen AJ, Barrow PA, Maskell DJ, Wallis TS (2004) Identification of host-specific colonization factors of *Salmonella enterica* serovar Typhimurium. Mol Microbiol 54:994–1010

Nevola JJ, Stocker A, Laux DC, Cohen PS (1985) Colonization of the mouse intestine by an avirulent *Salmonella typhimurium* strain and its lipopolysaccharide-defective mutants. Infet Immun 50:152–159

Nicaud JM, Mackman N, Gray L, Holland IB (1985) Characterisation of HlyC and mechanism of activation and secretion of haemolysin from *E. coli* 2001. FEBS Lett 187:339–344

Nicholson TL, Bäumler AJ (2001) *Salmonella enterica* serotype typhimurium elicits cross-immunity against a *Salmonella enterica* serotype enteritidis strain expressing LP fimbriae from the lac promoter. Infect Immun 69:204–212

Norris TL, Bäumler AJ (1999) Phase variation of the *lpf* operon is a mechanism to evade cross-immunity between *Salmonella* serotypes. Proc Natl Acad Sci USA 96:13393–13398

Norris TL, Kingsley RA, Bäumler AJ (1998) Expression and transcriptional control of the *Salmonella typhimurium Ipf* fimbrial operon by phase variation. Mol Microbiol 29:311–320

Olsen A, Arnqvist A, Hammar M, Sukupolvi S, Normark S (1993) The RpoS sigma factor relieves H-NS-mediated transcriptional repression of *csgA*, the subunit gene of fibronectin-binding curli in *Escherichia coli*. Mol Microbiol 7:523–536

Olsen A, Jonsson A, Normark S (1989) Fibronectin binding mediated by a novel class of surface organelles on *Escherichia coli*. Nature 338:652–655

Parkhill J, Dougan G, James KD, Thomson NR, Pickard D, Wain J, Churcher C, Mungall KL, Bentley SD, Holden MT, Sebaihia M, Baker S, Basham D, Brooks K, Chillingworth T, Connerton P, Cronin A, Davis P, Davies RM, Dowd L, White N, Farrar J, Feltwell T, Hamlin N, Haque A, Hien TT, Holroyd S, Jagels K, Krogh A, Larsen TS, Leather S, Moule S, O'Gaora P, Parry C, Quail M, Rutherford K, Simmonds M, Skelton J, Stevens K, Whitehead S, Barrell BG (2001) Complete genome sequence of a multiple drug resistant *Salmonella enterica* serovar Typhi CT18. Nature 413:848–852

Pier GB, Grout M, Zaidi T, Meluleni G, Mueschenborn SS, Banting G, Ratcliff R, Evans MJ, Colledge WH (1998) *Salmonella typhi* uses CFTR to enter intestinal epithelial cells. Nature 393:79–82

Ramos HC, Rumbo M, Sirard JC (2004) Bacterial flagellins: mediators of pathogenicity and host immune responses in mucosa. Trends Microbiol 12:509–517

Römling U, Bian Z, Hammar M, Sierralta WD, Normark S (1998a) Curli fibers are highly conserved between *Salmonella typhimurium* and *Escherichia coli* with respect to operon structure and regulation. J Bacteriol 180:722–731

Römling U, Rohde M, Olsen A, Normark S, Reinkoster J (2000) AgfD, the checkpoint of multicellular and aggregative behaviour in *Salmonella typhimurium* regulates at least two independent pathways. Mol Microbiol 36:10–23

Römling U, Sierralta WD, Eriksson K, Normark S (1998b) Multicellular and aggregative behaviour of *Salmonella typhimurium* strains is controlled by mutations in the *agfD* promoter. Mol Microbiol 28:249–264

Ruiz-Olvera P, Ruiz-Perez F, Sepulveda NV, Santiago-Machuca A, Maldonado-Rodriguez R, Garcia-Elorriaga G, Gonzalez-Bonilla C (2003) Display and release of the *Plasmodium falciparum* circumsporozoite protein using the autotransporter MisL of *Salmonella enterica*. Plasmid 50:12–27

Ruiz-Perez F, Leon-Kempis R, Santiago-Machuca A, Ortega-Pierres G, Barry E, Levine M, Gonzalez-Bonilla C (2002) Expression of the *Plasmodium falciparum* immunodominant epitope (NANP)(4) on the surface of *Salmonella enterica* using the autotransporter MisL. Infect Immun 70:3611–3620

Saini S, Rao CV (2010) SprB is the molecular link between *Salmonella* pathogenicity island 1 (SPI1) and SPI4. J Bacteriol 192:2459–2462

Soto GE, Hultgren SJ (1999) Bacterial adhesins: common themes and variations in architecture and assembly. J Bacteriol 181:1059–1071

Sukupolvi S, Lorenz RG, Gordon JI, Bian Z, Pfeifer JD, Normark SJ, Rhen M (1997) Expression of thin aggregative fimbriae promotes interaction of *Salmonella typhimurium* SR-11 with mouse small intestinal epithelial cells. Infect Immun 65:5320–5325

Tam CK, Morris C, Hackett J (2006) The *Salmonella enterica* serovar Typhi type IVB self-association pili are detached from the bacterial cell by the PilV minor pilus proteins. Infect Immun 74:5414–5418

Thankavel K, Shah AH, Cohen MS, Ikeda T, Lorenz RG, Curtiss R 3rd, Abraham SN (1999) Molecular basis for the enterocyte tropism exhibited by *Salmonella typhimurium* type 1 fimbriae. J Biol Chem 274:5797–5809

Townsend SM, Kramer NE, Edwards R, Baker S, Hamlin N, Simmonds M, Stevens K, Maloy S, Parkhill J, Dougan G, Baumler AJ (2001) *Salmonella enterica* serovar Typhi possesses a unique repertoire of fimbrial gene sequences. Infect Immun 69:2894–2901

Tsui IS, Yip CM, Hackett J, Morris C (2003) The type IVB pili of *Salmonella enterica* serovar Typhi bind to the cystic fibrosis transmembrane conductance regulator. Infect Immun 71: 6049–6050

Tükel C, Akcelik M, de Jong MF, Simsek O, Tsolis RM, Bäumler AJ (2007) MarT activates expression of the MisL autotransporter protein of *Salmonella enterica* serotype Typhimurium. J Bacteriol 189:3922–3926

van der Velden AW, Bäumler AJ, Tsolis RM, Heffron F (1998) Multiple fimbrial adhesins are required for full virulence of *Salmonella typhimurium* in mice. Infect Immun 66:2803–2808

Wall D, Kaiser D (1999) Type IV pili and cell motility. Mol Microbiol 32:1–10

Weening EH, Barker JD, Laarakker MC, Humphries AD, Tsolis RM, Bäumler AJ (2005) The *Salmonella enterica* serotype Typhimurium *lpf*, *bcf*, *stb*, *stc*, *std*, and *sth* fimbrial operons are required for intestinal persistence in mice. Infect Immun 73:3358–3366

White AP, Collinson SK, Banser PA, Gibson DL, Paetzel M, Strynadka NC, Kay WW (2001) Structure and characterization of AgfB from *Salmonella enteritidis* thin aggregative fimbriae. J Mol Biol 311:735–749

White AP, Gibson DL, Collinson SK, Banser PA, Kay WW (2003) Extracellular polysaccharides associated with thin aggregative fimbriae of *Salmonella enterica* serovar enteritidis. J Bacteriol 185:5398–5407

Wolfgang M, van Putten JP, Hayes SF, Dorward D, Koomey M (2000) Components and dynamics of fiber formation define a ubiquitous biogenesis pathway for bacterial pili. EMBO J 19: 6408–6418

Wong KK, McClelland M, Stillwell LC, Sisk EC, Thurston SJ, Saffer JD (1998) Identification and sequence analysis of a 27-kilobase chromosomal fragment containing a *Salmonella* pathogenicity island located at 92 minutes on the chromosome map of *Salmonella enterica* serovar typhimurium LT2. Infect Immun 66:3365–3371

Xu XF, Tan YW, Lam L, Hackett J, Zhang M, Mok YK (2004) NMR structure of a type IVb pilin from *Salmonella typhi* and its assembly into pilus. J Biol Chem 279:31599–31605

Zhang XL, Morris C, Hackett J (1997) Molecular cloning, nucleotide sequence, and function of a site-specific recombinase encoded in the major "pathogenicity island" of *Salmonella typhi*. Gene 202:139–146

Zhang XL, Tsui IS, Yip CM, Fung AW, Wong DK, Dai X, Yang Y, Hackett J, Morris C (2000) *Salmonella enterica* serovar typhi uses type IVB pili to enter human intestinal epithelial cells. Infect Immun 68:3067–3073

Zogaj X, Nimtz M, Rohde M, Bokranz W, Römling U (2001) The multicellular morphotypes of *Salmonella typhimurium* and *Escherichia coli* produce cellulose as the second component of the extracellular matrix. Mol Microbiol 39:1452–1463

Chapter 3
Adhesion Mechanisms of *Borrelia burgdorferi*

Styliani Antonara, Laura Ristow, and Jenifer Coburn

Abstract The *Borrelia* are widely distributed agents of Lyme disease and Relapsing Fever. All are vector-borne zoonotic pathogens, have segmented genomes, and enigmatic mechanisms of pathogenesis. Adhesion to mammalian and tick substrates is one pathogenic mechanism that has been widely studied. At this point, the primary focus of research in this area has been on *Borrelia burgdorferi*, one agent of Lyme disease, but many of the adhesins of *B. burgdorferi* are conserved in other Lyme disease agents, and some are conserved in the Relapsing Fever *Borrelia*. *B. burgdorferi* adhesins that mediate attachment to cell-surface molecules may influence the host response to the bacteria, while adhesins that mediate attachment to soluble proteins or extracellular matrix components may cloak the bacterial surface from recognition by the host immune system as well as facilitate colonization of tissues. While targeted mutations in the genes encoding some adhesins have been shown to affect the infectivity and pathogenicity of *B. burgdorferi*, much work remains to be done to understand the roles of the adhesins in promoting the persistent infection required to maintain the bacteria in reservoir hosts.

3.1 Introduction

The spirochetes in the genus *Borrelia* cause relapsing fever and Lyme disease. This chapter focuses on the Lyme disease agents, and primarily on a single species, *Borrelia burgdorferi*, as this organism has been the primary object of study and the focus of relatively recent advances in approaches to understanding how these organisms cause infection and, in susceptible hosts, disease. *B. burgdorferi* is normally

J. Coburn (✉)
Division of Infectious Diseases, Medical College of Wisconsin, Milwaukee, WI 53226, USA
e-mail: jcoburn@mcw.edu

D. Linke, A. Goldman (eds.), *Bacterial Adhesion*, Advances in Experimental Medicine and Biology 715, DOI 10.1007/978-94-007-0940-9_3,

maintained in mammalian reservoir hosts and tick vectors, and the mechanisms by which *B. burgdorferi* causes infection remain poorly understood. In fact, how *B. burgdorferi* causes disease has been more thoroughly characterized by manipulation of the host rather than of the bacterium. Relatively recent advances in the genetic approaches that are possible in this organism have started to turn this tide, and have been applied to understanding the in vivo significance of the numerous adhesins that have been identified through in vitro studies.

There are a few oddities of *B. burgdorferi* that warrant introduction. First, the genome is relatively small, at approximately 1.5 Mbp, but is highly segmented, as approximately one third of the annotated genes are encoded on circular and linear plasmids (Fraser et al., 1997; Casjens et al., 2000). One of the "plasmids" is better thought of as a small chromosome (Byram et al., 2004). Second, *B. burgdorferi* encodes a large repertoire of lipoproteins, with approximately 7.8% of the genome encoding known or predicted lipoproteins (Setubal et al., 2006). Some of these lipoproteins have been identified as adhesins, but not all of the adhesins are lipoproteins. Finally, given the comparatively small genome size, a relatively large number of proteins that bind to mammalian or tick cells or extracellular matrix have been identified, and some of these have additional functions that may contribute to the life style of the bacterium.

Various laboratories have shown that *Borrelia burgdorferi* binds to an array of eukaryotic cells in vitro (Coburn et al., 1993; Comstock et al., 1993; Hechemy et al., 1989; Thomas and Comstock, 1989) and to components of the extracellular matrix (Guo et al., 1995; Leong et al., 1995, 1998a, b; Isaacs, 1994). Further studies have identified receptors on the surface of mammalian cells and particular molecules of the extracellular matrix to which the bacteria attach, and the *B. burgdorferi* proteins that serve as adhesins interacting with these molecules. Table 3.1 lists *Borrelia*

Table 3.1 Known and candidate *Borrelia burgdorferi* adhesins

Adhesin (genomic locus)	Comments, references
Adhesins that bind to mammalian extracellular matrix components	
Bgp (*bb0588*)	Binds to GAGs in vitro (Parveen and Leong, 2000), mutant is infectious in mice but shows some deficiency in tissue colonization (Parveen et al., 2006; Saidac et al., 2009), may also bind cell cell-surface proteoglycans
DbpA (*bbA24*)	Binds to decorin and GAGs in vitro (Fischer et al., 2003; Guo et al., 1998), adhesion specificity is different from that of DbpB, *dbpBA* mutants are attenuated in murine infection (Blevins et al., 2008; Shi et al., 2008a; Weening et al., 2008)
DbpB (*bbA25*)	Binds to decorin and GAGs in vitro (Fischer et al., 2003; Guo et al., 1998), binding specificity is different from that of DbpA, *dbpBA* mutants are attenuated in murine infection (Blevins et al., 2008; Shi et al., 2008a; Weening et al., 2008)

Table 3.1 (continued)

Adhesin (genomic locus)	Comments, references
BBK32 (*bbK32*)	Binds to fibronectin and GAGs in vitro (Fischer et al., 2006; Probert and Johnson, 1998), these activities are important for *B. burgdorferi* interactions with the vasculature in vivo (Norman et al., 2008), *bbk32* mutants are attenuated in murine infection (Seshu et al., 2006)
RevA (*bbM27* & *bbP27*), **RevB** (*bbC10*)	Binds to fibronectin and laminin in vitro, some strains have two copies of the gene; there is a related gene (*revB*) that is present only in some *B. burgdorferi* strains (Brissette et al., 2009a)
Bmp family members A,B,C,D (*bb0382-0385*) **ErpX *(bbQ47)***	Bind to laminin in vitro (Verma et al., 2009); D was selected in vivo for adherence to vascular endothelium in living mice (Antonara et al., 2007); contributes to chronic joint infection (Pal et al., 2008) ErpX binds to laminin (Brissette et al., 2009b)
Erps: ErpA *(bbP38, bbI39)*, ErpC, ErpP *(bbN38)* **CRASPs: CRASP-1 (CspA, *bbA68)*, CRASP-2 (CspZ, *bbH06),* CRASP-3=ErpP, CRASP-4=ErpC, CRASP-5=ErpA**	Bind to factor H and/or FHR-1 (factor H related) and/or FHL (factor H-like) (Alitalo et al., 2002; Hellwage et al., 2001; Metts et al., 2003)
Adhesins that bind to mammalian cell surface receptors	
P66 (*bb0603*)	Binds to integrins $\alpha_{IIb}\beta_3$ and $\alpha_v\beta_3$ (Coburn et al., 1999), knockout mutant is severely attenuated in mice but not in ticks (Coburn lab, unpublished data)
BBB07 (*bbB07*)	Binds to β_1 integrins, stimulates proinflammatory signaling in chondrocytes (Behera et al., 2008)
Adhesins that bind to unidentified mammalian substrates (until further characterization is completed, these remain candidate adhesins)	
Lmp1 (*bb0210*)	Required for persistence and induction of disease manifestations in immunocompetent mice (Yang et al., 2009), selected in vivo for adherence to vascular endothelium in living mice (Antonara et al., 2007), host substrate(s) unknown
OspC (*bbB19*)	Essential for initiation of infection in mammals (Grimm et al., 2004b; Tilly et al., 2006, 2007) and for colonization of certain tissues (Xu et al., 2008), selected in vivo for adherence to vascular endothelium in living mice (Antonara et al., 2007), binds to cells in vitro, host substrate(s) unknown
VlsE *(bbF32)*	Required for persistent infection in mammals; (Dresser et al., 2009; Bankhead and Chaconas, 2007; Lin et al., 2009) selected in vivo for adherence to vascular endothelium in living mice (Antonara et al., 2007), binds to cells in vitro, host substrate(s) unknown

Table 3.1 (continued)

Adhesin (genomic locus)	Comments, references
OspF family members: ErpK (*bbM38*), **ErpL** (*bbO39*), **OspG** (*bbS41*), **OspF** (*bbR42*)	OspF family members, all selected in vivo for adherence to vascular endothelium in living mice (Antonara et al., 2007), host substrate(s) unknown
Adhesins that bind to tick substrates	
OspA (*bbA15*)	Binds to TROSPA (tick receptor for OspA) (Pal et al., 2004)
OspC (*bbB19*)	Binds to Salp15 (Ramamoorthi et al., 2005)

burgdorferi adhesins, both known and candidate ones, as well as additional information on their respective host cell substrates and roles in *B. burgdorferi* infection. In this section, ECM-binding proteins will be reviewed; in later sections, those that bind to molecules specifically expressed on the mammalian cell surface, and those that bind to unknown substrates, will be described.

3.2 *Borrelia burgdorferi* Proteins That Promote Interaction with the Extracellular Matrix

3.2.1 Attachment to Fibronectin

Fibronectin (Fn) is present in both soluble and insoluble extracellular matrix forms, and is targeted by many bacterial adhesins due to its ubiquity, its multiple distinct functional binding domains, and its ability to interact with multiple substrates. These may also assist bacterial pathogens in establishment of infection. In normal physiology, Fn binds to several integrins and to other extracellular matrix components including collagen, fibrinogen and some proteoglycans. It plays a major role in cell adhesion, growth, migration and differentiation, and it is important for processes such as wound healing and embryonic development (reviewed in Kadler et al., 2008).

B. burgdorferi produces several Fn-binding adhesins (Table 3.1). Early work suggesting Fn binding activity by Szczepanski et al. (1990) and Grab et al. (1998) led to the identification of the best-characterized Fn-binding adhesin of *B. burgdorferi*, BBK32 (Probert and Johnson, 1998). The Fn-binding region of BBK32 was identified as a region of 32 amino acids that was common to all *Borrelia* strains tested (Probert et al., 2001). Elegant structure-function analyses revealed that BBK32 shares a mechanism of binding to Fn with Fn-binding adhesins of the Gram-positive pathogens *Staphylocccus aureus* and *Streptococcus pyogenes* (Probert et al., 2001; Raibaud et al., 2005). It also promotes the aggregation of plasma Fn to superFn (a higher order multimer of fibronectin) (Prabhakaran et al., 2009), supporting a role for this and other specific bacterial adhesins that goes beyond simple attachment.

BBK32 is expressed by *B. burgdorferi* as the tick feeds and while the bacteria are in the mammalian host (Fikrig et al., 2000). Consistent with this pattern of expression, deletion of *bbk32* increases the ID_{50} in mice (Seshu et al., 2006), but at high dose does not significantly attenuate virulence or tick colonization (Li et al., 2006).

Given that BBK32 deficient mutant strains still bind Fn, the identification of additional Fn-binding proteins came as no surprise. In fact, three additional Fn-binding proteins have been identified (Brissette et al., 2009a). The first of these proteins, RevA, was previously studied by other groups on the basis of differential gene expression in mammalian versus tick environments (Gilmore and Mbow, 1998; Carroll et al., 2001). In some *B. burgdorferi* strains, a second copy of *revA* is present on a different plasmid. A related gene, *revB*, has also been identified and, like recombinant RevA, recombinant RevB also binds Fn. RevA binds Fn with a slightly lower affinity than BBK32, but the affinity of RevB binding to Fn has yet to be determined (Brissette et al., 2009a). Experimental evidence for RevB binding indicates a more complex interaction with Fn in contrast to the dose-dependent binding of RevA to Fn (Brissette et al., 2009a). In addition, the function of a gene annotated in the genome sequence as encoding a putative Fn-binding protein, bb0347, has not been experimentally addressed. In the future, generation of *B. burgdorferi* strains in which the genes encoding Fn-binding proteins are inactivated could illuminate the roles of all of these proteins in the life cycle of *B. burgdorferi*.

3.2.2 Attachment to Decorin

Decorin is a proteoglycan that consists of a protein core composed of leucine rich repeats, and a glycosaminoglycan (GAG) chain consisting of either chondroitin sulphate or dermatan sulphate depending on the tissue in which it is expressed (Mcewan et al., 2006). Decorin is a component of connective tissue, binds to type I collagen and Fn and plays a role in matrix assembly. In addition to playing a role in the formation of the structural components of the extracellular matrix, the decorin core protein functions as a signaling mediator by interacting with the epidermal growth factor receptor (reviewed in Seidler and Dreier, 2008).

Due to the observations by several groups that *B. burgdorferi* is frequently seen in connective tissues in infected mammals and apparently in contact with collagen fibers, early investigations focused on direct adhesion to collagen. When no direct attachment to immobilized collagen was observed, attachment of the bacteria to the collagen-associated decorin was investigated. Two decorin-binding adhesins (DbpA and DbpB) were identified; the proteins are encoded on one of the linear plasmids in a bicistronic operon (Guo et al., 1998, 1995). A *dbpAB* mutant was deficient in colonization of the skin and other tissues, even in mice lacking adaptive immunity, suggesting that DbpA and DbpB proteins help the bacteria adhere to multiple tissues and are required for successful interactions with both innate and adaptive immune mechanisms (Weening et al., 2008). Both proteins were found to be important for the virulence of *Borrelia burgdorferi* in mice, yet contribute differently to colonisation and dissemination to various tissues (Shi et al., 2008a, b). Consistent with this,

DbpA and DbpB also have distinct in vitro adhesion activities (Fischer et al., 2003). While the initial studies suggested that the Dbps require the intact proteoglycan for adhesion, subsequent studies indicated that these proteins also bind to glycosaminoglycans (GAGs) in the absence of the core protein (Fischer et al., 2003; Guo et al., 1995). Lysine residues (Lys-82, Lys-163, Lys-170) critical for decorin binding have been identified (Brown et al., 1999; Pikas et al., 2003). The decorin-binding activity is uniquely tractable to investigation from the host perspective, as decorin-deficient mice were actually the first mutants used to investigate the role of any candidate virulence factors in *B. burgdorferi*. In decorin deficient mice, there were fewer bacteria present in hind tibiotarsal joints at low doses of the bacteria, and the arthritis was less severe (Brown et al., 2001).

Later work by a different group showed that *B. burgdorferi* does, in fact, bind to type 1 collagen lattices (Zambrano et al., 2004). This work highlights the importance of the purification methods in determining whether bacterial adhesion occurs to a particular substrate. Extracellular matrix proteins have limited solubility, and the plasma forms of some of these proteins, while soluble, may behave differently. At this point, the adhesin(s) responsible for collagen binding remain unknown.

3.2.3 Attachment to Glycosaminoglycans

While decorin is a proteoglycan, additional evidence for a more generalized proteoglycan (PG) binding activity of *B. burgdorferi* was also established. Binding to PGs accounts for some, but not all, of the *B. burgdorferi* cell attachment activity, depending on the cell line and bacterial strain examined. The PG-binding activity is largely determined by recognition of glycosaminoglycan (GAG) chains (Leong et al., 1995, 1998a, b). A *Borrelia* glycosaminoglycan binding protein (Bgp) was identified by Parveen and colleagues (Parveen and Leong, 2000) and shown to be surface-exposed in intact bacteria. The recombinant protein agglutinates erythrocytes, binds to the same glycosaminoglycans as whole bacteria, and competitively inhibits binding of *B. burgdorferi* to mammalian cells. Another previously identified *B. burgdorferi* adhesin, BBK32, which binds to Fn, was also found to bind to purified preparations of dermatan sulphate and heparin (Fischer et al., 2006). The fact that exogenous heparin had no effect on the binding affinity of the BBK32-expressing bacteria to Fn suggested that BBK32 can bind to multiple molecules independently, or that binding to soluble heparin is relatively weak. Different *B. burgdorferi* strains have different cell- and GAG-binding preferences, and binding to various cell types depends in part on the GAGs they express (Parveen and Leong, 2000). Host-adapted spirochetes show enhanced binding to GAGs (Parveen et al., 2003) suggesting their importance during in vivo infection. However, Bgp, BBK32, and DbpAB mutants of *B. burgdorferi* are all infectious in mice (Seshu et al., 2006; Shi et al., 2008a; Blevins et al., 2008; Weening et al., 2008; Parveen et al., 2006) although in some cases slightly attenuated, suggesting that these different proteins may be functionally redundant.

3.2.4 Attachment to Laminin

Laminin is a trimeric glycoprotein that is a component of extracellular matrices, playing an integral role in forming structural scaffolding in almost every tissue. Attachment to laminin has been demonstrated for many bacterial pathogens, including *B. burgdorferi*. The four paralogous Bmp proteins were found to bind laminin (Verma et al., 2009), as was one of the Erps (OpsE-related proteins, see below), ErpX (Brissette et al., 2009b). The four *bmp* genes are located on the chromosome and, although they are arranged in a cluster, they are differentially regulated (Bryksin et al., 2005; Dobrikova et al., 2001). Two have been shown to contribute to the development of arthritis in the mouse model of infection (Pal et al., 2008). One of the Bmp proteins, BmpD, was selected for binding to vascular endothelium in mice by in vivo phage display (Antonara et al., 2007). Since laminin is a basement membrane protein, BmpD may also recognize additional mammalian substrates. The fragment of BmpD that was selected, however, contained sequences 3′ of the stop codon of the allele in the sequenced strain, B31. Thus it is possible that this fragment is available for binding mammalian substrates only in certain strains.

3.2.5 Erps and CRASPs: Binding to Complement-Regulatory Proteins Factor H and FHL

It has been shown that a large family of outer surface proteins, the Erps, is involved in the binding of host proteins. The Erps are encoded by a large multi-gene family, with different *erp* genes encoded on different plasmids, particularly the cp32 family of plasmids. In earlier literature in the field, these genes were known as *uhb* (upstream homology box) genes, due to the highly homologous 5′ non-coding regions (Marconi et al., 1996; Sung et al., 1998). Indeed, the Erp genes appear to be expressed in similar patterns, although there may be variations in timing and tissue-specific expression in some cases (Mcdowell et al., 2001; Stevenson, 2002). The Erp proteins can be divided into different functional categories: ErpX, which binds laminin, several that bind complement factor H and related complement regulators, and those for which adhesion activity has been demonstrated but the substrate(s) remain undefined. In general, Erp proteins are expressed during mammalian infection but are repressed during colonization of the tick (reviewed in Brissette et al., 2008).

The ErpA, ErpC and ErpP from various *Borrelia burgdorferi* strains (Alitalo et al., 2002; Hellwage et al., 2001; Metts et al., 2003) show significant affinity for factor H. Factor H is a complement regulatory protein that circulates in the human plasma and is bound to host cells, and protects host cells from attack by the complement system. Other bacteria have been shown to bind to factor H and in that way evade the complement activation which can lead to killing of the bacteria by opsonization (reviewed in Sjöberg et al., 2009). In addition, binding of factor H

can help bacteria adhere to host cells since it binds to glycosaminoglycans that are present on the surface of cells (Brissette et al., 2008).

Complement regulator acquiring surface protein (CRASP)-1 and -2 function to evade the host immune system by binding components of the host immune system, factor H-like protein 1(FHL-1) and factor H (Alitalo et al., 2001; Hellwage et al., 2001; Kraiczy et al., 2001a, b; Mcdowell et al., 2001; Wallich et al., 2005). FHL-1 is encoded by the same gene as factor H, and has redundant function in controlling the alternative pathway of complement activation within host innate immunity, but has a unique 4 amino acid extension at the C-terminus (Kraiczy et al., 2001b). Both CRASP-1 and -2 bind to a region of factor H or FHL-1 that is buried in the unbound protein, but exposed when the C-terminal region is bound. Several Erps bind the C-terminal end of factor H, and so it is possible that CRASPs and Erps act in a complementary fashion (reviewed in Brissette et al., 2008). Strains completely deficient in Erps will need to be created in order to test the function of CRASPs alone, and vice versa. Recently, CRASP-1 has been shown to bind additional host components, including Fn, laminin, plasminogen and several types of collagen (Hallstrom et al., 2010). These additional functions expand the role of CRASP-1 beyond evasion of the immune system, and potentially into aiding colonization in the mammalian host.

In addition, a distinct subset of the Erps, those belonging to the OspF subfamily, were selected by in vivo phage display as candidate adhesins to the vasculature endothelium (Antonara et al., 2007). These are BBM38 (ErpK), BBO39 (ErpL), BBK2.10 and BBS41 (OspG), and none have been shown to bind factor H. Although the Erp proteins that were selected vary in sequence, they share significant common features. A recombinant protein expressing the selected portion of ErpK, which is also common to BBK2.10 and OspG, showed specific binding to the surface of particular cell lines, suggesting that the selected sequence may be responsible for binding of members of the OspF family to the surface of mammalian cells (Antonara et al., 2007).

3.2.6 Attachment to Mammalian Cell Surface Receptors

3.2.6.1 Attachment to Integrins

Although some of the substrates for *B. burgdorferi* attachment discussed above are also associated with the mammalian cell surface, this section will cover those substrates that are specific to the cell surface and not found in the extracellular matrix or body fluids. Integrins are obligate heterodimeric cation-dependent receptors, found on the surface of all mammalian cells except erythrocytes. They consist of two distinct chains: the alpha (α) and beta (β) subunits. The specificity of each integrin depends on the combination of the α and β subunits, but some bind multiple ligands. As is the case for several other pathogens, *B. burgdorferi* binds to integrins, including $\alpha_{IIb}\beta_3$ (Coburn et al., 1993), $\alpha_v\beta_3$, $\alpha_5\beta_1$ (Coburn et al., 1998), and $\alpha_3\beta_1$ (Behera et al., 2006). Different Lyme disease *Borrelia burgdorferi* strains bind preferentially to different integrins (Coburn et al., 1998). Binding of the bacteria to $\alpha_3\beta_1$ on chondrocytes activates inflammatory responses in a TLR-independent manner.

The *B. burgdorferi* ligand for the β_3 chain integrins is an outer surface integral membrane protein, P66 (Coburn et al., 1999; Coburn and Cugini, 2003). The principal ligand for integrin $\alpha_3\beta_1$ appears to be a putative outer surface protein, BBB07. Like intact *B. burgdorferi*, BBB07 stimulates human primary chondrocytes through integrin $\alpha_3\beta_1$ to secrete proinflammatory cytokines (Behera et al., 2008). While P66 also stimulates proinflammatory responses by chondrocytes, this does not require $\alpha_3\beta_1$.

3.2.7 *Candidate Mammalian Substrate Adhesins of* B. burgdorferi

Several additional candidate *B. burgdorferi* adhesins have been identified, but not yet validated as adhesins using additional approaches; for example, the putative mammalian receptors have not yet been identified. In each case, however, other work has demonstrated the proteins to be important in *B. burgdorferi* infection in mammals, specifically. All were enriched after in vivo selection for binding to vascular endothelium in living mice, but adhesion activity has not yet been demonstrated to be critical to their importance in the life of *B. burgdorferi*. One, OspC, was shown to be critical for *B. burgdorferi* to establish disseminated infection (Grimm et al., 2004a; Tilly et al., 2006). A second, VlsE, is better known for antigenic variation during infection (Zhang and Norris, 1998a, b; Lawrenz et al., 1999; Lin et al., 2009; Dresser et al., 2009). Finally, BB0210, annotated as Lmp1, was also highly selected, and is required for persistent infection in mice (Yang et al., 2009).

3.2.8 *Interaction of* Borrelia burgdorferi *with the Arthropod Host*

As mentioned above, *Borrelia burgdorferi* spends a large portion of its life cycle in the arthropod host. It has been shown that certain genes are expressed during the mammalian life cycle, and others are expressed when the bacteria are in the tick. Some of the genes expressed in the tick portion of the life cycle encode outer surface proteins, and the roles of the corresponding proteins in the tick have been investigated. One such protein, OspA, was shown to be an adhesin for tick tissues, and to bind to the "tick receptor for OspA" (TROSPA) (Pal et al., 2004). OspA can bind specifically to recombinant TROSPA in vitro, while in vivo studies showed that disruption of TROSPA by RNA interference diminished the ability of the ticks to acquire *Borrelia burgdorferi* from infected mice (Pal et al., 2004). A small number of *B. burgdorferi* were found to still bind with TROSPA activity abolished, leaving the door open to another adhesin-receptor interaction also mediating binding to the tick midgut.

Consistent with an important role for the life of *B. burgdorferi* in the tick, *ospA*, and the other gene in the bicistronic operon, *ospB*, are expressed when the bacteria leave the mammalian host and enter the feeding tick (Schwan and Piesman, 2000). The importance of these proteins for the maintenance of the bacteria in ticks was demonstrated when *ospAB* mutant bacteria that were fully infectious in mice were acquired by ticks, but unable to persist in the tick midgut (Yang et al., 2004). More

recent work in the field has demonstrated that a primary role of OspA is protection of the bacteria already residing in the tick midgut from killing by host antibodies as the tick takes in a blood meal (Battisti et al., 2008), which would be critical for maintenance of the infection in the natural cycle between vertebrate animals and ticks.

A salivary protein of *Ixodes scapularis* ticks, Salp15, was shown to bind to a different *B. burgdorferi* protein, OspC (Ramamoorthi et al., 2005). Binding of the bacteria to Salp15, which inhibits T-cell activation, appeared to inhibit in vitro antibody mediated killing of the bacteria. Nonetheless, Salp15 does not seem to be required for *B. burgdorferi* to establish infection, since an infection can be established by needle inoculation of the bacteria into mice (Barthold et al., 1988). OspC however, is critical to the ability of *B. burgdorferi* to establish disseminated infection in mice (Grimm et al., 2004b; Tilly et al., 2006), and was selected as a candidate adhesin for the vascular endothelium in mice using in vivo phage display (Antonara et al., 2007).

3.3 Concluding Remarks

Borrelia burgdorferi expresses a number of adhesins, many with redundant functions. This redundancy suggests that these functions are critical to the ability of the bacterium to cause infection in mammals, but testing this hypothesis will require novel approaches, given the difficulties involved in the genetic manipulation of this organism. It will be especially interesting to further investigate *B. burgdorferi* interactions with the tick, which only become more complex as more is learned. It will also be interesting to see how *B. burgdorferi* adhesins interact with their host substrates at the molecular level, as many of the *B. burgdorferi* proteins have no homologs outside of the genus. With recent advances in development of genetic tool sets, the in vivo roles of the *B. burgdorferi* adhesins should be discernable within the next few years.

References

Alitalo A, Meri T, Lankinen H, Seppälä I, Lahdenne P, Hefty PS, Akins D, Meri S (2002) Complement inhibitor factor H binding to Lyme disease spirochetes is mediated by inducible expression of multiple plasmid-encoded outer surface protein E paralogs. J Immunol 169: 3847–3853

Alitalo A, Meri T, Rämö L, Jokiranta TS, Heikkilä T, Seppälä IJ, Oksi J, Viljanen M, Meri S (2001) Complement evasion by *Borrelia burgdorferi*: serum-resistant strains promote C3b inactivation. Infect Immun 69:3685–3691

Antonara S, Chafel RM, LaFrance M, Coburn J (2007) *Borrelia burgdorferi* adhesins identified using in vivo phage display. Mol Microbiol 66:262–276

Bankhead T, Chaconas G (2007) The role of VlsE antigenic variation in the Lyme disease spirochete: persistence through a mechanism that differs from other pathogens. Mol Microbiol 65:1547–1558

Barthold SW, Moody KD, Terwilliger GA, Jacoby RO, Steere AC (1988) An animal model for Lyme arthritis. Ann NY Acad Sci 539:264–273

Battisti JM, Bono JL, Rosa PA, Schrumpf ME, Schwan TG, Policastro PF (2008) Outer surface protein A protects Lyme disease spirochetes from acquired host immunity in the tick vector. Infect Immun 76:5228–5237

Behera AK, Durand E, Cugini C, Antonara S, Bourassa L, Hildebrand E, Hu LT, Coburn J (2008) *Borrelia burgdorferi BBB07* interaction with integrin α3β1 stimulates production of pro-inflammatory mediators in primary human chondrocytes. Cell Microbiol 10: 320–331

Behera AK, Hildebrand E, Uematsu S, Akira S, Coburn J, Hu LT (2006) Identification of a TLR-independent pathway for *Borrelia burgdorferi*-induced expression of matrix metalloproteinases and inflammatory mediators through binding to integrin α3β1. J Immunol 177:657–664

Blevins JS, Hagman KE, Norgard MV (2008) Assessment of decorin-binding protein A to the infectivity of *Borrelia burgdorferi* in the murine models of needle and tick infection. BMC Microbiol 8:82

Brissette CA, Bykowski T, Cooley AE, Bowman A, Stevenson B (2009a) *Borrelia burgdorferi* RevA antigen binds host fibronectin. Infect Immun 77:2802–2812

Brissette CA, Cooley AE, Burns LH, Riley SP, Verma A, Woodman ME, Bykowski T, Stevenson B (2008) Lyme borreliosis spirochete Erp proteins, their known host ligands, and potential roles in mammalian infection. Int J Med Microbiol 298(Suppl 1):257–267

Brissette CA, Verma A, Bowman A, Cooley AE, Stevenson B (2009b) The *Borrelia burgdorferi* outer-surface protein ErpX binds mammalian laminin. Microbiology 155:863–872

Brown EL, Guo BP, O'Neal P, Höök M (1999) Adherence of *Borrelia burgdorferi*. Identification of critical lysine residues in DbpA required for decorin binding. J Biol Chem 274: 26272–26278

Brown EL, Wooten RM, Johnson BJ, Iozzo RV, Smith A, Dolan MC, Guo BP, Weis JJ, Höök M (2001) Resistance to Lyme disease in decorin-deficient mice. J Clin Invest 107:845–852

Bryksin AV, Godfrey HP, Carbonaro CA, Wormser GP, Aguero-Rosenfeld ME, Cabello FC (2005) *Borrelia burgdorferi* BmpA, BmpB, and BmpD proteins are expressed in human infection and contribute to P39 immunoblot reactivity in patients with Lyme disease. Clin Diagn Lab Immunol 12:935–940

Byram R, Stewart PE, Rosa P (2004) The essential nature of the ubiquitous 26-kilobase circular replicon of *Borrelia burgdorferi*. J Bacteriol 186:3561–3569

Carroll JA, El-Hage N, Miller JC, Babb K, Stevenson B (2001) *Borrelia burgdorferi* RevA antigen is a surface-exposed outer membrane protein whose expression is regulated in response to environmental temperature and pH. Infect Immun 69:5286–5293

Casjens S, Palmer N, Van Vugt R, Huang WM, Stevenson B, Rosa P, Lathigra R, Sutton G, Peterson J, Dodson RJ, Haft D, Hickey E, Gwinn M, White O, Fraser CM (2000) A bacterial genome in flux: the twelve linear and nine circular extrachromosomal DNAs in an infectious isolate of the Lyme disease spirochete *Borrelia burgdorferi*. Mol Microbiol 35:490–516

Coburn J, Chege W, Magoun L, Bodary SC, Leong JM (1999) Characterization of a candidate *Borrelia burgdorferi* beta3-chain integrin ligand identified using a phage display library. Mol Microbiol 34:926–940

Coburn J, Cugini C (2003) Targeted mutation of the outer membrane protein P66 disrupts attachment of the Lyme disease agent, *Borrelia burgdorferi*, to integrin alphavbeta3. Proc Natl Acad Sci USA 100:7301–7306

Coburn J, Leong JM, Erban JK (1993) Integrin alpha IIb beta 3 mediates binding of the Lyme disease agent *Borrelia burgdorferi* to human platelets. Proc Natl Acad Sci USA 90:7059–7063

Coburn J, Magoun L, Bodary SC, Leong JM (1998) Integrins αvβ3 and α5β1 mediate attachment of Lyme disease spirochetes to human cells. Infect Immun 66:1946–1952

Comstock LE, Fikrig E, Shoberg RJ, Flavell RA, Thomas DD (1993) A monoclonal antibody to OspA inhibits association of *Borrelia burgdorferi* with human endothelial cells. Infect Immun 61:423–431

Dobrikova EY, Bugrysheva J, Cabello FC (2001) Two independent transcriptional units control the complex and simultaneous expression of the bmp paralogous chromosomal gene family in *Borrelia burgdorferi*. Mol Microbiol 39:370–379

Dresser AR, Hardy PO, Chaconas G (2009) Investigation of the genes involved in antigenic switching at the vlsE locus in *Borrelia burgdorferi*: an essential role for the RuvAB branch migrase. PLoS Pathog 5:e1000680

Fikrig E, Feng W, Barthold SW, Telford SR 3rd, Flavell RA (2000) Arthropod- and host-specific *Borrelia burgdorferi* bbk32 expression and the inhibition of spirochete transmission. J Immunol 164:5344–5351

Fischer JR, LeBlanc KT, Leong JM (2006) Fibronectin binding protein BBK32 of the Lyme disease spirochete promotes bacterial attachment to glycosaminoglycans. Infect Immun 74: 435–441

Fischer JR, Parveen N, Magoun L, Leong JM (2003) Decorin-binding proteins A and B confer distinct mammalian cell type-specific attachment by *Borrelia burgdorferi*, the Lyme disease spirochete. Proc Natl Acad Sci USA 100:7307–7312

Fraser CM, Casjens S, Huang WM, Sutton GG, Clayton R, Lathigra R, White O, Ketchum KA, Dodson R, Hickey EK, Gwinn M, Dougherty B, Tomb JF, Fleischmann RD, Richardson D, Peterson J, Kerlavage AR, Quackenbush J, Salzberg S, Hanson M, Van Vugt R, Palmer N, Adams MD, Gocayne J, Venter JC et al (1997) Genomic sequence of a Lyme disease spirochaete, *Borrelia burgdorferi*. Nature 390:580–586

Gilmore RD Jr, Mbow ML (1998) A monoclonal antibody generated by antigen inoculation via tick bite is reactive to the *Borrelia burgdorferi* Rev protein, a member of the 2.9 gene family locus. Infect Immun 66:980–986

Grab DJ, Givens C, Kennedy R (1998) Fibronectin-binding activity in *Borrelia burgdorferi*. Biochim Biophys Acta 1407:135–145

Grimm D, Eggers CH, Caimano MJ, Tilly K, Stewart PE, Elias AF, Radolf JD, Rosa PA (2004a) Experimental assessment of the roles of linear plasmids lp25 and lp28-1 of *Borrelia burgdorferi* throughout the infectious cycle. Infect Immun 72:5938–5946

Grimm D, Tilly K, Byram R, Stewart PE, Krum JG, Bueschel DM, Schwan TG, Policastro PF, Elias AF, Rosa PA (2004b) Outer-surface protein C of the Lyme disease spirochete: a protein induced in ticks for infection of mammals. Proc Natl Acad Sci USA 101:3142–3147

Guo BP, Brown EL, Dorward DW, Rosenberg LC, Höök M (1998) Decorin-binding adhesins from *Borrelia burgdorferi*. Mol Microbiol 30:711–723

Guo BP, Norris SJ, Rosenberg LC, Höök M (1995) Adherence of *Borrelia burgdorferi* to the proteoglycan decorin. Infect Immun 63:3467–3472

Hallström T, Haupt K, Kraiczy P, Hortschansky P, Wallich R, Skerka C, Zipfel PF (2010) Complement regulator-acquiring surface protein 1 of *Borrelia burgdorferi* binds to human bone morphogenic protein 2, several extracellular matrix proteins, and plasminogen. J Infect Dis 202:490–498

Hechemy KE, Samsonoff WA, Mckee M, Guttman JM (1989) *Borrelia burgdorferi* attachment to mammalian cells. J Infect Dis 159:805–806

Hellwage J, Meri T, Heikkilä T, Alitalo A, Panelius J, Lahdenne P, Seppälä IJ, Meri S (2001) The complement regulator factor H binds to the surface protein OspE of *Borrelia burgdorferi*. J Biol Chem 276:8427–8435

Isaacs RD (1994) *Borrelia burgdorferi* bind to epithelial cell proteoglycans. J Clin Invest 93: 809–819

Kadler KE, Hill A, Canty-Laird EG (2008) Collagen fibrillogenesis: fibronectin, integrins, and minor collagens as organizers and nucleators. Curr Opin Cell Biol 20:495–501

Kraiczy P, Skerka C, Brade V, Zipfel PF (2001a) Further characterization of complement regulator-acquiring surface proteins of *Borrelia burgdorferi*. Infect Immun 69:7800–7809

Kraiczy P, Skerka C, Kirschfink M, Brade V, Zipfel PF (2001b) Immune evasion of *Borrelia burgdorferi* by acquisition of human complement regulators FHL-1/reconectin and factor H. Eur J Immunol 31:1674–1684

Lawrenz MB, Hardham JM, Owens RT, Nowakowski J, Steere AC, Wormser GP, Norris SJ (1999) Human antibody responses to VlsE antigenic variation protein of *Borrelia burgdorferi*. J Clin Microbiol 37:3997–4004

Leong JM, Morrissey PE, Ortega-Barria E, Pereira ME, Coburn J (1995) Hemagglutination and proteoglycan binding by the Lyme disease spirochete, *Borrelia burgdorferi*. Infect Immun 63:874–883

Leong JM, Robbins D, Rosenfeld L, Lahiri B, Parveen N (1998a) Structural requirements for glycosaminoglycan recognition by the Lyme disease spirochete, *Borrelia burgdorferi*. Infect Immun 66:6045–6048

Leong JM, Wang H, Magoun L, Field JA, Morrissey PE, Robbins D, Tatro JB, Coburn J, Parveen N (1998b) Different classes of proteoglycans contribute to the attachment of *Borrelia burgdorferi* to cultured endothelial and brain cells. Infect Immun 66:994–999

Li X, Liu X, Beck DS, Kantor FS, Fikrig E (2006) *Borrelia burgdorferi* lacking BBK32, a fibronectin-binding protein, retains full pathogenicity. Infect Immun 74:3305–3313

Lin T, Gao L, Edmondson DG, Jacobs MB, Philipp MT, Norris SJ (2009) Central role of the holliday junction helicase RuvAB in vlsE recombination and infectivity of *Borrelia burgdorferi*. PLoS Pathog 5:e1000679

Marconi RT, Sung SY, Hughes CA, Carlyon JA (1996) Molecular and evolutionary analyses of a variable series of genes in *Borrelia burgdorferi* that are related to ospE and ospF, constitute a gene family, and share a common upstream homology box. J Bacteriol 178:5615–5626

McDowell JV, Sung SY, Price G, Marconi RT (2001) Demonstration of the genetic stability and temporal expression of select members of the Lyme disease spirochete OspF protein family during infection in mice. Infect Immun 69:4831–4838

McEwan PA, Scott PG, Bishop PN, Bella J (2006) Structural correlations in the family of small leucine-rich repeat proteins and proteoglycans. J Struct Biol 155:294–305

Metts MS, McDowell JV, Theisen M, Hansen PR, Marconi RT (2003) Analysis of the OspE determinants involved in binding of factor H and OspE-targeting antibodies elicited during *Borrelia burgdorferi* infection in mice. Infect Immun 71:3587–3596

Norman MU, Moriarty TJ, Dresser AR, Millen B, Kubes P, Chaconas G (2008) Molecular mechanisms involved in vascular interactions of the Lyme disease pathogen in a living host. PLoS Pathog 4:e1000169

Pal U, Li X, Wang T, Montgomery RR, Ramamoorthi N, Desilva AM, Bao F, Yang X, Pypaert M, Pradhan D, Kantor FS, Telford S, Anderson JF, Fikrig E (2004) TROSPA, an *Ixodes scapularis* receptor for *Borrelia burgdorferi*. Cell 119:457–468

Pal U, Wang P, Bao F, Yang X, Samanta S, Schoen R, Wormser GP, Schwartz I, Fikrig E (2008) *Borrelia burgdorferi* basic membrane proteins A and B participate in the genesis of Lyme arthritis. J Exp Med 205:133–141

Parveen N, Caimano M, Radolf JD, Leong JM (2003) Adaptation of the Lyme disease spirochaete to the mammalian host environment results in enhanced glycosaminoglycan and host cell binding. Mol Microbiol 47:1433–1444

Parveen N, Cornell KA, Bono JL, Chamberland C, Rosa P, Leong JM (2006) Bgp, a secreted glycosaminoglycan-binding protein of *Borrelia burgdorferi* strain N40, displays nucleosidase activity and is not essential for infection of immunodeficient mice. Infect Immun 74: 3016–3020

Parveen N, Leong JM (2000) Identification of a candidate glycosaminoglycan-binding adhesin of the Lyme disease spirochete *Borrelia burgdorferi*. Mol Microbiol 35:1220–1234

Pikas DS, Brown EL, Gurusiddappa S, Lee LY, Xu Y, Höök M (2003) Decorin-binding sites in the adhesin DbpA from *Borrelia burgdorferi*: a synthetic peptide approach. J Biol Chem 278:30920–30926

Prabhakaran S, Liang X, Skare JT, Potts JR, Höök M (2009) A novel fibronectin binding motif in MSCRAMMs targets F3 modules. PLoS One 4:e5412

Probert WS, Johnson BJ (1998) Identification of a 47 kDa fibronectin-binding protein expressed by *Borrelia burgdorferi* isolate B31. Mol Microbiol 30:1003–1015

Probert WS, Kim JH, Höök M, Johnson BJB (2001) Mapping the ligand-binding region of the *Borrelia burgdorferi* fibronectin-binding protein BBK32. Infect Immun 69:4129–4133

Raibaud S, Schwarz-Linek U, Kim JH, Jenkins HT, Baines ER, Gurusiddappa S, Höök M, Potts JR (2005) *Borrelia burgdorferi* binds fibronectin through a tandem beta-zipper, a common mechanism of fibronectin binding in staphylococci, streptococci, and spirochetes. J Biol Chem 280:18803–18809

Ramamoorthi N, Narasimhan S, Pal U, Bao F, Yang XF, Fish D, Anguita J, Norgard MV, Kantor FS, Anderson JF, Koski RA, Fikrig E (2005) The Lyme disease agent exploits a tick protein to infect the mammalian host. Nature 436:573–577

Saidac DS, Marras SA, Parveen N (2009) Detection and quantification of Lyme spirochetes using sensitive and specific molecular beacon probes. BMC Microbiol 9:43

Schwan TG, Piesman J (2000) Temporal changes in outer surface proteins A and C of the Lyme disease-associated spirochete, *Borrelia burgdorferi*, during the chain of infection in ticks and mice. J Clin Microbiol 38:382–388

Seidler DG, Dreier R (2008) Decorin and its galactosaminoglycan chain: extracellular regulator of cellular function?. IUBMB Life 60:729–733

Seshu J, Esteve-Gassent MD, Labandeira-Rey M, Kim JH, Trzeciakowski JP, Höök M, Skare JT (2006) Inactivation of the fibronectin-binding adhesin gene bbk32 significantly attenuates the infectivity potential of *Borrelia burgdorferi*. Mol Microbiol 59:1591–1601

Setubal JC, Reis M, Matsunaga J, Haake DA (2006) Lipoprotein computational prediction in spirochaetal genomes. Microbiology 152:113–121

Shi Y, Xu Q, McShan K, Liang FT (2008a) Both decorin-binding proteins A and B are critical for the overall virulence of *Borrelia burgdorferi*. Infect Immun 76:1239–1246

Shi Y, Xu Q, Seemanaplli SV, McShan K, Liang FT (2008b) Common and unique contributions of decorin-binding proteins A and B to the overall virulence of *Borrelia burgdorferi*. PLoS One 3:e3340

Sjöberg AP, Trouw LA, Blom AM (2009) Complement activation and inhibition: a delicate balance. Trends Immunol 30:83–90

Stevenson B (2002) *Borrelia burgdorferi* erp (ospE-related) gene sequences remain stable during mammalian infection. Infect Immun 70:5307–5311

Sung SY, Lavoie CP, Carlyon JA, Marconi RT (1998) Genetic divergence and evolutionary instability in ospE-related members of the upstream homology box gene family in *Borrelia burgdorferi* sensu lato complex isolates. Infect Immun 66:4656–4668

Szczepanski A, Furie MB, Benach JL, Lane BP, Fleit HB (1990) Interaction between *Borrelia burgdorferi* and endothelium in vitro. J Clin Invest 85:1637–1647

Thomas DD, Comstock LE (1989) Interaction of Lyme disease spirochetes with cultured eukaryotic cells. Infect Immun 57:1324–1326

Tilly K, Bestor A, Jewett MW, Rosa P (2007) Rapid clearance of lyme disease spirochetes lacking OspC from skin. Infect Immun 75:1517–1519

Tilly K, Krum JG, Bestor A, Jewett MW, Grimm D, Bueschel D, Byram R, Dorward D, Vanraden MJ, Stewart P, Rosa P (2006) *Borrelia burgdorferi* OspC protein required exclusively in a crucial early stage of mammalian infection. Infect Immun 74:3554–3564

Verma A, Brissette CA, Bowman A, Stevenson B (2009) *Borrelia burgdorferi* BmpA is a laminin-binding protein. Infect Immun 77:4940–4946

Wallich R, Pattathu J, Kitiratschky V, Brenner C, Zipfel PF, Brade V, Simon MM, Kraiczy P (2005) Identification and functional characterization of complement regulator-acquiring surface protein 1 of the Lyme disease spirochetes *Borrelia afzelii* and *Borrelia garinii*. Infect Immun 73:2351–2359

Weening EH, Parveen N, Trzeciakowski JP, Leong JM, Höök M, Skare JT (2008) *Borrelia burgdorferi* lacking DbpBA exhibits an early survival defect during experimental infection. Infect Immun 76:5694–5705

Xu Q, McShan K, Liang FT (2008) Verification and dissection of the ospC operator by using flaB promoter as a reporter in *Borrelia burgdorferi*. Microb Pathog 45:70–78

Yang X, Coleman AS, Anguita J, Pal U (2009) A chromosomally encoded virulence factor protects the Lyme disease pathogen against host-adaptive immunity. PLoS Pathog 5:e1000326

Yang XF, Pal U, Alani SM, Fikrig E, Norgard MV (2004) Essential role for OspA/B in the life cycle of the Lyme disease spirochete. J Exp Med 199:641–648

Zambrano MC, Beklemisheva AA, Bryksin AV, Newman SA, Cabello FC (2004) *Borrelia burgdorferi* binds to, invades, and colonizes native type I collagen lattices. Infect Immun 72:3138–3146

Zhang JR, Norris SJ (1998a) Genetic variation of the *Borrelia burgdorferi* gene vlsE involves cassette-specific, segmental gene conversion. Infect Immun 66:3698–3704

Zhang JR, Norris SJ (1998b) Kinetics and *in vivo* induction of genetic variation of vlsE in *Borrelia burgdorferi*. [erratum appears in Infect Immun 1999 67:468]. Infect Immun 66:3689–3697

Chapter 4
Adhesins of *Bartonella* spp.

Fiona O'Rourke, Thomas Schmidgen, Patrick O. Kaiser, Dirk Linke, and Volkhard A.J. Kempf

Abstract Adhesion to host cells represents the first step in the infection process and one of the decisive features in the pathogenicity of *Bartonella spp. B. henselae* and *B. quintana* are considered to be the most important human pathogenic species, responsible for cat scratch disease, bacillary angiomatosis, trench fever and other diseases. The ability to cause vasculoproliferative disorders and intraerythrocytic bacteraemia are unique features of the genus *Bartonella*. Consequently, the interaction with endothelial cells and erythrocytes is a focus in *Bartonella* research. The genus harbours a variety of trimeric autotransporter adhesins (TAAs) such as the *Bartonella* adhesin A (BadA) of *B. henselae* and the variably expressed outer-membrane proteins (Vomps) of *B. quintana,* which display remarkable variations in length and modular construction. These adhesins mediate many of the biologically-important properties of *Bartonella* spp. such as adherence to endothelial cells and extracellular matrix proteins and induction of angiogenic gene programming. There is also significant evidence that the laterally acquired Trw-conjugation systems of *Bartonella* spp. mediate host-specific adherence to erythrocytes. Other potential adhesins are the filamentous haemagglutinins and several outer membrane proteins. The exact molecular functions of these adhesins and their interplay with other pathogenicity factors (e.g., the VirB/D4 type 4 secretion system) need to be analysed in detail to understand how these pathogens adapt to their mammalian hosts.

4.1 Introduction

Reports of infections with *B. bacilliformis* date back to the Inca period (Schultz, 1968) and *B. quintana* has been identified in human tissue traced as far back as 4,000 years. *B. quintana* was also detected in the remains of soldiers from Napoleon's

V.A.J. Kempf (✉)
Institut für Medizinische Mikrobiologie und Krankenhaushygiene, Universitätsklinikum, Johann Wolfgang Goethe-Universität, 60596 Frankfurt am Main, Germany
e-mail: volkhard.kempf@kgu.de

D. Linke, A. Goldman (eds.), *Bacterial Adhesion*, Advances in Experimental Medicine and Biology 715, DOI 10.1007/978-94-007-0940-9_4,

Grand Army found in Vilinius, Lithuania (Raoult et al., 2006a) and Kassel, Hesse, Germany (von Grumbkow and Hummel, unpublished). More recently, *B. henselae* and *B. quintana* were identified as the cause of bacillary angiomatosis (Relman et al., 1990, 1991). To date, over 20 different *Bartonella* species have been identified (see Table 4.1) and the list of *Bartonella* species and corresponding hosts is growing steadily. The human pathogens *B. henselae* and *B. quintana* and the rat pathogen *B. tribocorum* have been investigated the most. Their pathogenicity and infection biology have been examined in greater detail and the genomes of these species have been sequenced (Alsmark et al., 2004; Saenz et al., 2007).

4.1.1 Cat Scratch Disease

Cat scratch disease (CSD) occurs after transmission of *B. henselae* (or sometimes *B. clarridgeiae*) by bites or scratches of infected cats. After an incubation time of 2–3 weeks, patients suffer from a unilateral lymphadenitis in the lymph draining region near the inoculation site. Immune competent individuals (mainly children) develop CSD which is primarily of self-limiting nature and such patients are usually not treated with antibiotics (Anderson and Neuman, 1997). Additional signs of CSD are headache, fever or splenomegaly. Rarely, so called "Parinaud's syndrome" (oculo-glandular involvement) may complicate the course of infection.

Cats are known as the standard reservoir host for *B. henselae* (Rolain et al., 2003). Nevertheless, a case of human osteomyelits was reported following a dog scratch (Keret et al., 1998) indicating that dogs may also serve as a reservoir for the pathogen.

There are indications for a potential role of ticks in the transmission of *B. henselae* to humans. The prevalence of *B. henselae* DNA in *Ixodes pacificus* (North America) and *I. persulcatus* (Eastern Europe) ticks, respectively (Chang et al., 2001; Hercik et al., 2007; Rar et al., 2005) and in *I. ricinus* or *Dermacentor* ticks (Central Europe) (Sanogo et al., 2003; Podsiadly et al., 2007; Angelakis et al., 2010) indicates that these arthropods may represent a newly emerged vector class. We found *B. henselae* DNA to be present in up to ~40% of tick populations in Europe (Dietrich et al., 2010). DNA of various *Bartonella* spp. was further detected in biting flies, keds and mites (Billeter et al., 2008). Recently, ticks (*I. ricinus*) were experimentally infected with *B. henselae*. A subsequent inoculation of cats with salivary glands of these ticks caused a *B. henselae* bacteraemia (Cotte et al., 2008), further strengthening the plausibility of ticks as a means of infection.

Further functional analysis of the natural course of CSD is hampered by the lack of an appropriate animal model. The subcutaneous infection of C57BL/6 or BALB/c mice appears to represent the most promising infection model: mice developed a massive lymphadenitis strongly resembling human CSD and the presence of an enhanced B-lymphocyte proliferation can be observed in both human patients and in experimentally infected mice (Kunz et al., 2008).

Table 4.1 *Bartonella* spp.: reservoirs, vectors, human diseases (modified from Dehio (2005) and Kaiser et al. (2011))

Bartonella spp.	Reservoir	Vector	Human diseases
Human-specific spp.:			
B. bacilliformis	Human	Sandfly	Carrión's disease: Oroya fever, verruga peruana
B. quintana	Human, [dog? (Kelly et al., 2006)]	Body louse [cat flea, ticks (Rolain et al., 2003)]	Trench fever, endocarditis, bacillary angiomatosis
Zoonotic spp.:			
B. alsatica	Rabbit	Unknown	Endocarditis, lymphadenitis (Raoult et al., 2006b)
B. clarridgeiae	Cat	Cat flea	Cat scratch disease
B. elizabethae	Rat	Unknown	Endocarditis, neuroretinitis
B. grahamii	Mouse, vole	Rodent flea (Bown et al., 2004)	Neuroretinitis
B. henselae	Cat, dog (Morales et al., 2007; Keret et al., 1998)	Cat flea (ticks?)	Cat scratch disease, bacillary angiomatosis, endocarditis, neuroretinitis, bacteraemia
B. koehlerae	Cat	Unknown	Endocarditis
B. rochalimae	Foxes, raccoons, coyotes (Henn et al., 2009)	Fleas (Henn et al., 2009)	Bacteraemia, fever (Eremeeva et al., 2007)
B. tamiae	Rats (?)	Mites (?)	Bacteraemia, fever (Kosoy et al., 2008)
B. vinsonii subsp. *arupensis*	Mouse	Ticks (?)	Bacteraemia, fever, endocarditis (?)
B. vinsonii subsp. *berkhoffii*	Dog	Ticks (?)	Endocarditis
B. washoensis	Ground squirrel	Unknown	Myocarditis, endocarditis (?)
Animal-specific spp.:			
B. birtlesii	Mouse	Unknown	Unknown
B. bovis (= B. weissii)	Cattle, cat	Unknown	Unknown
B. capreoli	Roe deer	Unknown	Unknown
B. chomelii	Cattle	Unknown	Unknown
B. doshiae	Vole	Unknown	Unknown

Table 4.1 (continued)

Bartonella spp.	Reservoir	Vector	Human diseases
B. peromysci	Deer, mouse	Unknown	Unknown
B. phoceensis	Rat	Unknown	Unknown
B. rattimassiliensis	Rat	Unknown	Unknown
B. schoenbuchensis	Roe deer	Unknown	Unknown
B. talpae	Vole	Unknown	Unknown
B. taylorii	Mouse, vole	Rodent flea (Bown et al., 2004)	Unknown
B. tribocorum	Rat	Unknown	Unknown
B. vinsonii subsp. *vinsonii*	Vole	Unknown	Unknown

4.1.2 Carrión's Disease

Carrión's disease is characterized by a biphasic course of infection consisting of a primary bacteremic phase ("Oroya fever") and a subsequent chronic vasculoproliferative condition ("Verruga peruana"). The infection is caused by *B. bacilliformis* and is clinically characterized by an intraerythrocytic bacteraemia often followed by fatal haemolytic anaemia (mortalilty: ~40–90%). The second chronic phase of infection (Verruga peruana) leads to vascular tumours that arise from the chronic colonization of endothelial cells with *B. bacilliformis* (Schultz, 1968). Experimentally, it has been demonstrated that *B. bacilliformis* triggers the proliferation of endothelial cells in vitro. This result has been reproduced in vivo by implanting *B. bacilliformis*-extract containing sponge discs in rats and observing the resulting neoangiogenic processes (Garcia et al., 1990). Humans seem to be the only reservoir host for this pathogen and transmission between humans occurs through sandflies (*Phlebotomus verrucarum*). The disease is endemic in the Andes (Peru, South America).

4.1.3 Trench Fever

B. quintana is the causative agent of Trench fever. Reports describing this disease date back to the time of the Napoleonic military campaign in Russia (Raoult et al., 2006a) and the disease also emerged during the First and Second World Wars (Anderson and Neuman, 1997). Blood sucking body lice (*Pediculus humanus*) transmitted the pathogen between soldiers living under the poor hygienic conditions common in trench warfare. At the end of the twentieth century, Trench fever re-emerged among homeless patients in Seattle (USA) and Marseille (France) often suffering from pediculosis (louse infestation) (Spach et al., 1995; Brouqui et al., 1999). Humans were long thought to be the exclusive host for *B. quintana*. However, it has been recently described that dogs represent a further mammalian reservoir (Kelly et al., 2006).

Following initial infection, Trench fever is characterized by a sudden onset of fever followed by subsequent periodical relapses ("five-day-fever") which are paralleled by an intraerythrocytic bacteraemia (Foucault et al., 2004). *B. quintana* was detected in erythroblasts residing in the bone marrow and these cells may serve as a possible niche for a persistent infection from where the pathogen can re-enter the bloodstream (Rolain et al., 2003a). There is also evidence that human bone marrow represents a possible niche for *B. henselae* (Mändle et al., 2005).

The *B. tribocorum* rat infection model has proved a reliable in vivo model, mimicking the course of *B. quintana* infections in humans (Schülein et al., 2001). After an intravenous infection, the pathogen is rapidly cleared from the bloodstream before a periodic relapsing bacteraemia occurs. Using a signature-tagged mutagenesis approach, the underlying pathogenicity mechanisms were elucidated in greater detail revealing a broad variety of essential pathogenicity factors [e.g., genes of VirB/D4 T4SS and others (Saenz et al., 2007)] and some of these genes are also

crucial for the intracellular persistence in endothelial cells and macrophages (Kyme et al., 2005). BadA-deficient strains of *B. tribocorum* (Saenz et al., 2007) or strains of *B. quintana* lacking the variably expressed outer-membrane proteins (Vomps) (Mackichan et al., 2008) were non-bacteraemic in the rat and macaque infection models, respectively.

4.1.4 Bacillary Angiomatosis and Peliosis Hepatis

Of all human pathogenic bacteria, only pathogens of the genus *Bartonella* are capable of inducing vasculoproliferative disorders. The earliest known example of a vasculoproliferative condition caused by *Bartonella* spp. is the chronic phase of Carrión's disease [Verruga peruana (Schultz, 1968)]. This disorder is geographically limited to endemic areas in the Andes (Peru) and is mainly of historical and local significance. Today, *B. henselae* and *B. quintana* are of more global significance as they can induce vasculoproliferative disorders in immunosuppressed patients (e.g., AIDS patients). These vasculoproliferations are designated "bacillary angiomatosis" when appearing as cutaneous manifestations or peliosis hepatis. Both bacillary angiomatosis and peliosis hepatis are histologically characterized as lobular proliferations of blood-filled capillaries and result from chronic local infections with *B. henselae* or *B. quintana* (Relman et al., 1990; 1991). Antibiotic treatment with cell-permeable compounds (e.g., macrolides) leads to eradication of the pathogen and subsequently to a complete regression of the angiomatosis.

To date, pathomechanisms operating in bacillary angiomatosis can only be analysed using cell culture infection models [including endothelial cell proliferation assays and spheroids (Kempf et al., 2001; Kirby, 2004; Garcia et al., 1990; Scheidegger et al., 2009)] as no animal model yet exists. Whereas the exposure of endothelial cells to *B. bacilliformis* leads directly to cell proliferation (Garcia et al., 1990), the induction of neoangiogenic events caused by *B. henselae* seems to be a multistep process. It can now be assumed that three separate mechanisms work synergistically: (i) triggering of endothelial cell proliferation, (ii) inhibition of endothelial cell apoptosis, and (iii) angiogenic reprogramming of infected host cells. Investigation of pathological angiogenesis in the field of cancer research provided valuable insight for examining *Bartonella*-induced angiogenesis: for example, hypoxia-inducible factor 1 (HIF-1) and vascular endothelial growth factor (VEGF) have been known for at least a decade to direct angiogenic cascades (Maxwell et al., 2001; Pugh and Ratcliffe, 2003). Such angiogenic events are also influenced by *Bartonella* spp.: here, a *B. henselae* infection drives the activation of HIF-1 and the subsequent secretion of angiogenic growth hormones (e.g. VEGF) in infected host cells (Kempf et al., 2001, 2005; Riess et al., 2004).

Interestingly, only *Bartonella* adhesin A (BadA) expressing *B. henselae* initiate a proangiogenic host response but the details of the underlying molecular mechanisms remain unclear (Kempf et al., 2001, 2005; Riess et al., 2004). Theoretically, both HIF-1 activation (dependent on BadA expression of *B. henselae*) and inhibition of endothelial cell apoptosis [dependent of the function of the VirB/D4 type 4

secretion system (T4SS) in *B. henselae*] may stimulate bacteria-induced angiogenesis in *Bartonella* infections cooperatively.

The purpose of such angiogenic stimulation may be explained from an evolutionary standpoint: as *B. henselae* grows faster in the presence of host cells than on inert cultivation media (e.g. Columbia blood agar), it appears that *Bartonella* spp. stimulates the growth of endothelial cells to ensure its own ecologically privileged environment (Kempf et al., 2000, 2002).

4.2 *Analysis of* Bartonella *spp. Pathogenicity Factors*

To date, the body of knowledge about pathogenicity factors of the genus *Bartonella* is small. Progress has been slow due to the technical difficulties in performing genetic studies on these slow growing microorganisms. Moreover, suitable animal models for in vivo pathogenicity studies exist to only a limited extent for bacteraemic diseases [e.g. the *B. tribocorum* rat infection model, the *B. birtlesii* mouse infection model (Schülein et al., 2001; Vayssier-Taussat et al., 2010)] and are completely absent for vasculoproliferative disorders. Two pathogenicity factors have been the primary focus of ongoing research: the VirB/D4 T4SS which translocates *Bartonella* effector proteins (Beps) into mammalian host cells and the family of trimeric autotransporter adhesins (TAAs) of which BadA of *B. henselae* (Riess et al., 2004) (see Fig. 4.1) and the Vomps of *B. quintana* (Zhang et al., 2004) are prominent members. More recently, the Trw T4SS system has also been implicated to play an important role in the infection process of host erythrocytes (Seubert et al., 2003; Vayssier-Taussat et al., 2010).

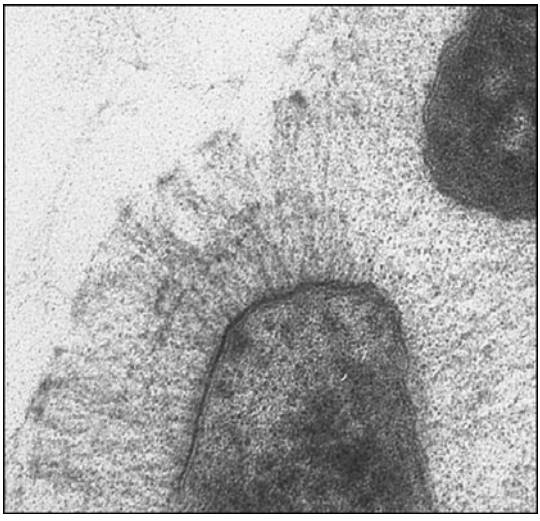

Fig. 4.1 BadA expression of *B. henselae*. Note the remarkable BadA expression forming a dense layer on the bacterial surface (length ~240 nm). Transmission electron microscopy by Heinz Schwarz (Max-Planck-Institut für Entwicklungsbiologie, Tübingen, Germany)

4.2.1 The VirB/D4 T4SS

T4SSs act like "molecular syringes" in Gram-negative bacteria and "inject" bacterial proteins or DNA either into host cells or other bacteria. Effector proteins of T4SS are secreted through a secretion channel spanning the inner and outer membrane. Originally, T4SS evolved from bacterial conjugation systems and are often essential bacterial virulence factors. Through delivery of particular bacterial effectors, host cell functions are modulated for the benefit of the pathogen (Christie et al., 2005).

The VirB T4SS of *Agrobacterium tumefaciens* is the best characterized T4SS (Chilton et al., 1977) and shows high homologies to that of *Bartonella* spp. (Padmalayam et al., 2000; Schülein and Dehio, 2002). The major function of the *B. henselae* VirB/D4 T4SS seems to be the modulation of endothelial cell functions (Schmid et al., 2004). It is responsible for (i) "invasome formation" (uptake of bacterial agglomerates formed by rearrangements of the host cell actin cytoskeleton), (ii) proinflammatory gene programming [activation of nuclear factor (NF)-κB, interleukin-8 secretion, ICAM-1 and E-selectin expression] and (iii) inhibition of apoptosis in endothelial cells. Moreover, (iv) the VirB/D4 T4SS seems to modulate the mitogenic effects of *B. henselae* on endothelial cells (Schmid et al., 2004; Schülein et al., 2005). So far, seven T4SS-dependent *Bartonella* effector proteins (Beps) have been identified (Schülein et al., 2005) of which the biological functions have been shown in greater detail for two: BepA and BepG. BepA mediates the inhibition of apoptosis in endothelial cells (Schmid et al., 2006) and is also responsible for capillary sprout formation in a more complex infection model (endothelial spheroids) whereas BepG counteracts such sprouting (Scheidegger et al., 2009). The parallel capability of *B. henselae* both to stimulate and to repress angiogenic events through the release of individual effector proteins suggests that the process of *B. henselae*-triggered neoangiogenesis is the result of a finely-balanced interaction between different bacterial effector molecules. To date, the structure and organization of the *B. henselae* VirB/D4 T4SS can only be modelled, as the protein complex has never been visualized (Pulliainen and Dehio, 2009).

4.2.2 Bartonella *Adhesin A (BadA)*

Adherence to the host is the first and most decisive step in a bacterial infection. To ensure efficient host adhesion, bacteria express surface protein complexes with the ability to bind specific molecular host components. These complexes ("adhesins") can differ greatly in their composition and may be classified as pili, fimbriae, membrane-anchored fibres and proteins attached to the cell wall (Hultgren et al., 1993; Hoiczyk et al., 2000; Niemann et al., 2004; Foster and Hook, 1998; Koretke et al., 2006). The family of trimeric autotransporter adhesins {TAAs, other designations: *n*on-*f*imbrial *a*dhesins [NFAs (Hoiczyk et al., 2000)], *o*ligomeric *c*oiled-coil *a*dhesins [Ocas (Henderson et al., 2004; Barocchi et al., 2005)]} has been defined by structure and sequence similarity (Linke et al., 2006; Szczesny and Lupas, 2008).

TAAs are present in α-, β-, and γ-proteobacteria, are clearly linked with pathogenicity and are expressed in human, animal- and plant-pathogens [e.g. *Xanthomonas* adhesin A (XadA) from *Xanthomonas oryzae* (Ray et al., 2002)]. The best examined TAA is the *Yersinia* adhesin A (YadA) of *Yersinia enterocolitica* [first identified in 1982 as "P1" protein (Bolin et al., 1982)] and it is the prototype for other TAAs such as the ubiquitous surface proteins A1 and A2 (UspA1, UspA2) of *Moraxella catarrhalis* (Hoiczyk et al., 2000) and *Neisseria* adhesin A (NadA) of *Neisseria meningitidis* (Comanducci et al., 2002).

On the bacterial surface, all TAAs assemble in a similar way best described as a trimeric "lollipop-like" structure. TAAs are constructed modularly, combining conserved elements designated as "membrane anchor", "stalk", "neck" and "head" (Linke et al., 2006) (see Fig. 4.2). TAAs are defined by their C-terminal membrane anchor domain which is responsible for the autotransport activity and is highly homologous throughout the TAA family. The C-terminal membrane anchor domains

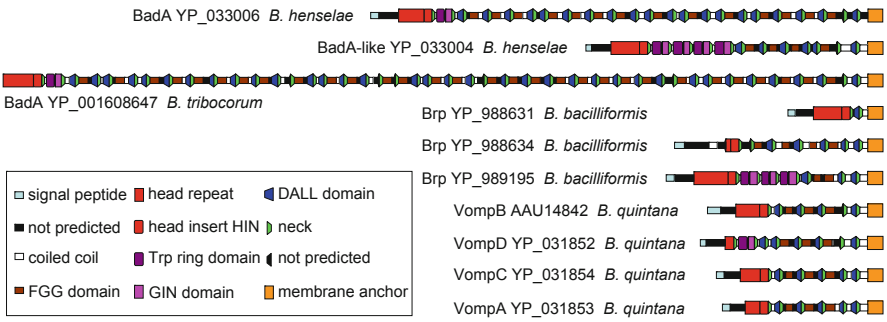

Fig. 4.2 Domain organisation of BadA homologues within the genus *Bartonella*. Homologues to BadA were found using BLAST (Altschul et al., 1997) against the sequenced genomes of *B. henselae* Houston-1, *B. quintana* Toulouse, *B. bacilliformis* KC583, and *B. tribocorum* CIP 10547. The domain composition was determined using the tool daTAA (Szczesny and Lupas, 2008). All domains are drawn to scale (sequence length). The annotation in the figure is from BadA of *B. henselae* Marseille, which harbours an intact copy of the BadA gene. In *B. henselae* Houston-1, a frame shift deletion in the membrane anchor supposedly prevents BadA expression. In addition, two incomplete TAA genes are found in the *B. henselae* Houston-1 genome (not depicted), and one shorter but intact BadA-like TAA with a long, repetitive head domain. The BadA gene of *B. tribocorum* is the longest so far observed TAA in *Bartonella*. This gene is incomplete as it lacks a signal peptide necessary for inner membrane secretion; this is possibly a sequence error as BadA has been shown to be functional in that strain (Saenz et al., 2007). Of the four Vomp genes [VompA-D; reported in (Zhang et al., 2004)], only three are found in the genome of *B. quintana* Toulouse (NC_010161.1). The annotation of VompB was made on the basis of the sequence from *B. quintana* JK31 (Zhang et al., 2004), the other Vomps were annotated from the *B. quintana* Tolouse genome (Alsmark et al., 2004). Although much shorter, VompD is related to BadA, while the other three Vomps lack the Trp-ring and the GIN domain (Szczesny et al., 2008). In *B. bacilliformis*, three Brp genes are found that differ in length and head domain structure; one of them is highly similar in its head structure to the shorter BadA-like TAA of *B. henselae*, while the others are more similar to VompA-C lacking Trp-ring and the GIN domain [reprinted in a modified format from: Kaiser et al. (2011) *Bartonella* spp.: throwing light on uncommon human infections. Int J Med Microbiol 301: 7–15]

of *Haemophilus* influenzae adhesin A (HiA) and YadA of *Y. enterocolitica* (Meng et al., 2006; Grosskinsky et al., 2007) are known to be secreted into the periplasm. Following this, they form a trimeric 12-stranded β-barrel pore in the outer membrane through which the "effector" domains are transported. Other domains (head and stalk) are present in most TAAs but may be rearranged in a variable order similar to "Lego bricks" (see Fig. 4.3).

TAAs of the genus *Bartonella* share some remarkable features which differentiate them from the TAAs of other bacteria: (i) they vary enormously in length, (ii) often more than one TAA gene variant or gene fragment is present in the genome and (iii) they are highly conserved within the genus.

The TAA of *B. henselae*, BadA, is the best understood adhesin of the genus. It was first described as a "type IV-like pilus" (Batterman et al., 1995) but further investigation revealed that it indeed represents a member of the TAA family (Riess et al., 2004). BadA is an extraordinarily large TAA (~3,000 amino acid residues resulting in a size of ~328 kDa per monomer) with a measured length

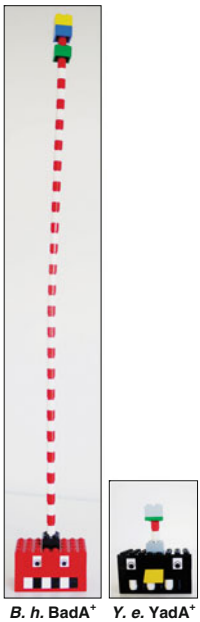

Fig. 4.3 Domain composition of BadA ("Lego brick-concept"): Model of the modular domain organisation of the TAAs *Yersinia* adhesin A (YadA) of *Y. enterocolitica* and *Bartonella* adhesin A (BadA) of *B. henselae*. In principle, certain "bricks" [membrane anchor (YadA: *grey*, BadA: *black*), neck-stalk repeats (*white-red*) and the head domain (YadA: *green*/*gray*, BadA: *green*/*red*/*blue*/*yellow*)] are present in all TAAs. Such "bricks" act as modules sharing similar functions (e.g., membrane anchor: anchoring the adhesin in the OM; neck(s): trimerization motif(s); head: adhesion to host cells). There is evidence that such "bricks" can be removed from TAAs (Kaiser et al., 2008) or even exchanged between e.g., α- and γ-proteobacteria (Schmidgen, Linke and Kempf, unpublished data)

of ~240 nm (Fig. 4.1). It was demonstrated that BadA is essential for the adhesion of *B. henselae* to host cells and extracellular matrix proteins, particularly to fibronectin, laminin and collagens. Moreover, expression of BadA is clearly linked to the capacity of *B. henselae* to trigger a proangiogenic host cell response via activation of the transcription factor HIF-1 and the secretion of angiogenic cytokines [e.g. VEGF, interleukin-8 (Kempf et al., 2001, 2005; Riess et al., 2004)]. While testing sera of patients suffering from *B. henselae* infections, it was discovered that such sera regularly (~70–80%) contained BadA-specific antibodies (Wagner et al., 2008; Riess et al., 2004). Therefore, BadA also seems to be an immunodominant protein and this finding might be used to improve current laboratory protocols for serological diagnostic approaches.

Most of the enormous length of BadA (~240 nm) is formed by multiple repeats of the neck-stalk elements, which are rich in coiled-coil structures. This repetition results in a long and fibrous BadA structure of much greater length than the prototypical YadA from *Y. enterocolitica* (~23 nm) (Hoiczyk et al., 2000). The purpose of the BadA stalk and the significance of its extreme length has not been elucidated. PCR analysis of nine *B. henselae* strains revealed surprising variations in stalk length within the species (Riess et al., 2007). Furthermore, the BadA stalk appears to be important in binding extracellular matrix proteins such as fibronectin, as experiments with a BadA mutant strain lacking almost the entire stalk impaired the fibronectin binding function (Kaiser et al., 2008). However, it is not yet clear whether the stalk of BadA contains a defined binding site for fibronectin or whether it simply represents a "spacer", separating the head at a defined distance from the bacterial cell surface.

While the length of the BadA stalk varies between different *B. henselae* strains, the head domain seems to be of conserved length and high sequence identity (Riess et al., 2007). Correspondingly, the Bad A head domain has been identified as the active element involved in most of BadA functional properties including autoagglutination, binding to extracellular matrix and host cells and triggering of proangiogenic host cell responses. Structurally, the head is composed of three subdomains: (i) an N-terminal domain, (ii) a Trp-ring and (iii) a GIN domain (Szczesny et al., 2008). The N-terminal domain of Bad A is homologous to the prototypical YadA head repeats whereas the Trp-ring and GIN domain (although arranged in opposite order) show high structural but no sequence similarity to the Hia of *H. influenzae*. Although the biological properties of the BadA head have been well analysed (Kaiser et al., 2008) it has not yet been possible to attribute specific functions to individual subdomains.

Genes encoding BadA-homolgous TAAs can be found in all other *Bartonella* species investigated so far (see Fig. 4.2) suggesting a conserved role of these adhesins in *Bartonella* pathogenicity (Zhang et al., 2004; Saenz et al., 2007; Gilmore et al., 2005). In the case of *B. quintana*, four different adhesins (Vomp A-D) are present. Although it is not clear whether all of these Vomps are expressed under natural conditions (Zhang et al., 2007), Vomp D exhibits the closest predicted structural similarity to BadA. Autoagglutination, collagen binding and VEGF secretion of host cells are attributed to Vomp expression (Zhang et al., 2004;

Schulte et al., 2006). Furthermore, Vomp-defective *B. quintana* and BadA-defective *B. tribocorum* mutants do not cause chronic bacteraemia in their respective animal models (Saenz et al., 2007; Mackichan et al., 2008).

4.2.3 Does an Interplay Between the VirB/D4 T4SS and BadA Exist?

The VirB/D4 T4SS and BadA of *Bartonella* spp. probably represent two of the most important pathogenicity factors of this genus. The functions these structures perform are crucial for infection and, in the case of *B. henselae*, both proteins may provide important elements in the multi-step process leading to neoangiogenesis. It can be hypothesized that BadA and the VirB/D4 T4SS may interact during the infection process resulting in a synergistic relationship in which BadA not only provides initial adhesion but also maintains the optimal distance between bacterium and host for effective VirB/D4 T4SS protein translocation.

Examples of such relationships already exist, for example between the type III secretion system (T3SS) and YadA of *Y. enterocolitica*. As with T4SS, the T3SS translocation systems are used by many Gram-negative bacteria for transmission of bacterial effector proteins from the bacterial cytosol into the host cell [e.g., *Yersinia* outer proteins (Yops)]. Modified from an ancestral flagellum structure, the T3SS is made up of a transmembrane basal body and a needle ("injectosome") emerging from the bacterial surface through which the effector proteins are transported. During assembly, the length of the T3SS is controlled by the "*Yersinia* size controller" (YscP), which acts as a molecular ruler alongside the growing needle machinery. Studies comparing YadA and the T3SS in *Y. enterocolitica* indicated that the YadA and T3Ss have to be the same length for effective Yop translocation in host cells (Mota et al., 2005).

One might argue that a similar relationship between the VirB/D4 T4SS and BadA of *B. henselae* is unlikely as the enormous length of BadA would imply an equally long VirB/D4 T4SS. Even though it may be difficult to imagine effective protein translocation over such a distance, T4SSs spanning such a gap are known. For example, the T-pilus of *A. tumefaciens* is even longer at ~1,400 nm (Aly and Baron, 2007). Although much is known about the functions of the VirB/D4 in *B. henselae*, the length of this structure is still unknown. Until more information exists, the plausibility of such a correlation for VirB/D4 T4SS and BadA in *B. henselae* cannot be conclusively determined.

4.2.4 Filamantous Haemagglutinin of Bartonella *spp.*

Genomic sequencing of *B. henselae* revealed the presence of multiple sequences coding for filamentous haemagglutinins (*fhaB1-8,* differing in length) and their corresponding partner secretion proteins (*fhaC/hecB*) indicating the possible existence of further adhesins in this species (Alsmark et al., 2004).

To date it is still unclear whether any of the *fha* genes of *B. henselae* play a role in pathogenicity or whether these genes are even expressed. An STM-study of *B. tribocorum* (also containing ten Fha homologues) did not reveal an obvious role for Fha in pathogenicity (Saenz et al., 2007); however, it needs to be mentioned that with such an STM-approach it is almost impossible to identify a phenotype. Theoretically it would be necessary to knock out all eight *fha* genes before an effect on pathogenicity might be observed. In fact, any kind of mutagenesis approach to this problem would be frustrated by the need to disable multiple genes simultaneously. Nevertheless, despite the technical problems they cause in analysis, the existence of so many versions of this gene may actually be an indicator of its importance: most likely, such "backup" measures against loss would be only afforded to genes of evolutionary significance.

In *B. henselae* the *fha* sequences are found on two genomic islands flanked by tRNAs and integrase genes suggesting that their presence is a result of phage interactions (Alsmark et al., 2004). Fha homologues are found in the genomes of both plant- and animal- pathogenic bacteria in the plant pathogen *Erwinia chrysanthemi* and the animal pathogen *Bordetella bronchiseptica,* Fha homologues are known to play an important role in the infection process (Rojas et al., 2002; Nicholson et al., 2009). The location of *fhaC/hecB* and *fhaB* within a genomic island of the *B. henselae* genome is consistent with the phylogenetic analysis of these homologues, which indicates horizontal transfer across species (Rojas et al., 2002).

Despite the lack of knowledge about the biological function of *B. henselae* Fha, parallels to the Fha of *Bordetella pertussis* (the pathogen causing whooping cough in humans) can be drawn. The Fha of *B. pertussis* represents the best-characterized member of the Fha protein family due to its importance in virulence and its use as a component in most acellular *B. pertussis* vaccines (Pines et al., 1999). The gene combination *fhaB* and *fhaC/hecB* represents a typical two partner secretion system in which *fhaB* codes for the Fha protein and *fhaC/hecB* for an excretion protein specifically dedicated to transport of Fha across the outer membrane. Fha of *B. pertussis* is activated through the two-component regulatory system BvgAS and is initially produced as a 367 kDa precursor protein which is extensively modified over the course of its transport to form a highly immunogenic 220-kDa hairpin-shaped protein at maturity. Transport across the cytoplasmic membrane is accomplished through a sec-signal peptide-dependent pathway followed by secretion across the OM through the Fha specific FhaC protein which forms a transmembrane β-barrel (Clantin et al., 2007). The protein reaches final maturity at the cell surface, where it is further modified and may be released in part due to interaction with the serine protease SphB1 (Mazar and Cotter, 2006; Coutte et al., 2001, 2003b).

The Fha of *B. pertussis* contains three confirmed binding domains: (i) two Arg-Gly-Asp triplets (RGD), which bind to monocytes and macrophages and to human bronchial epithelial cells via Very Late Antigen 5 (VLA-5) (Ishibashi and Nishikawa, 2002; 2003), (ii) a carbohydrate recognition domain (CRD) (Prasad et al., 1993), which binds to ciliated respiratory epithelial cells and macrophages and (iii) a heparin-binding domain, which mediates adherence to non-ciliated epithelial cells (Hannah et al., 1994). Due to the lack of suitable animal models, the biological

functions of *B. pertussis* Fha are mainly deduced from the Fha of *B. bronchiseptica*: here, Fha is crucial for tracheal colonization of rats suggesting its main role is as an adhesin (Cotter et al., 1998). Additionally, Fha is involved in autoagglutination and modulation of the inflammatory host response (Coutte et al., 2003a; McGuirk and Mills, 2000; Inatsuka et al., 2005). The length of *B. pertussis* Fha (3,590 aa; NP_880571.1) was calculated to be ~50 nm (Makhov et al., 1994). This suggests that a putative Fha of *B. henselae* (e.g., FhaB3, 2,653 aa, YP_033500.1) might be of similar length. It is not clear how *B. henselae* Fha mediates host cell interactions in the presence of BadA (~240 nm in length). However, several strains of *B. henselae* do not express BadA (Riess et al., 2007). Therefore, Fha might play an important role in the infection process when BadA is not expressed by *B. henselae*.

4.2.5 The Trw Type 4 Secretion System of Bartonella *spp.*

The function of the Trw T4SS system has been examined in several *Bartonella* species. Trw systems are assumed to have evolved from plasmid conjugation systems acquired through horizontal gene transfer from other bacterial species. Over time, co-evolution with mammalian hosts altered the original biological function from conjugation to host cell interaction leading to subsequent selection to match specific host cell structures (Nystedt et al., 2008). The first indications of the Trw system function were gained from the *B. tribocorum* rat infection model in which *trwE* mutants were characterized by a non-bactaeremic phenotype (Seubert et al., 2003). Recently, using a signature-tagged mutagenesis approach, a *B. birtlesii* mouse infection model revealed mutants impaired in establishing an intraerythrocytic bacteraemia. The corresponding genes encoded components of the Trw T4SS, demonstrating that this virulence factor is directly involved in adherence to erythrocytes. Ectopic expression of Trw of *B. tribocorum* (rat-specific) in *B. henselae* (cat-specific) or *B. quintana* (human-specific) expanded the host range for erythrocyte infection to rat, clearly demonstrating that Trw mediates host-specific erythrocyte infection (Vayssier-Taussat et al., 2010). The analysis of the exact erythrocyte binding partners of the Trw T4SS is currently ongoing (M. Vayssier-Taussat, personal communication). Cumulatively, the Trw T4SS appears to be the determining factor mediating host specific erythrocyte infections.

4.2.6 Less Characterized Adhesins of Bartonella *spp.*

Finally, several *B. henselae* outer membrane proteins (the 28, 32, 43, 52 and 58 kDa OMPs) may also act as adhesins in the course of infection, as they have been shown to bind to endothelial cells in vitro (Burgess and Anderson, 1998). ICAM-1 might be a binding partner of the 43 kDa protein which exhibits a strong affinity to endothelial cells (Burgess et al., 2000). Furthermore, exposure of endothelial cells to purified *B. henselae* outer membrane proteins resulted in NF-κB activation and increased expression of adhesion molecules (E-selectin, ICAM-1) (Fuhrmann et al., 2001).

However, detailed data for the role of these potential adhesions in the host cell infection process are still missing.

4.3 Conclusions and Outlook

Their ability of *Bartonella* spp. to cause vascularpoliferative disorders and intraerythocytic bacteraemia is unique among bacterial pathogens. The VirB/D4 T4SS and TAAs (e.g., BadA, Vomps, BrpA) represent important virulence factors which may work synergistically in host cell infection processes. Other potential adhesins are represented by the Trw-system, the filamentous haemagglutinins and several outer membrane proteins. The exact molecular functions of *Bartonella*-adhesins and their interplay with other pathogenicity factors (e.g., the VirB/D4 T4SS, the Trw T4SS or Fha) need to be analysed in greater detail.

Acknowledgments Parts of this manuscript have been reprinted in a modified form from "Kaiser, P.O., Riess, T., O'Rourke, F., Linke, D., and Kempf, V.A. (2011). *Bartonella* spp.: throwing light on uncommon human infections. Int J Med Microbiol 301: 7–15".

The work of V. Kempf is supported by grants from the Deutsche Forschungsgemeinschaft (DFG). We thank Heinz Schwarz and Jürgen Berger (Max Planck-Institut Tübingen, Germany) for providing electron microscopy of *B. henselae*.

References

Alsmark CM, Frank AC, Karlberg EO, Legault BA, Ardell DH, Canback B et al (2004) The louse-borne human pathogen *Bartonella quintana* is a genomic derivative of the zoonotic agent *Bartonella henselae*. Proc Natl Acad Sci USA 101:9716–9721

Altschul SF, Madden TL, Schaffer AA, Zhang J, Zhang Z, Miller W, Lipman DJ (1997) Gapped BLAST and PSI-BLAST: a new generation of protein database search programs. Nucleic Acids Res 25:3389–3402

Aly KA, Baron C (2007) The VirB5 protein localizes to the T-pilus tips in *Agrobacterium tumefaciens*. Microbiology 153:3766–3775

Anderson BE, Neuman MA (1997) *Bartonella* spp. as emerging human pathogens. Clin Microbiol Rev 10:203–219

Angelakis E, Pulcini C, Waton J, Imbert P, Socolovschi C, Edouard S et al (2010) Scalp eschar and neck lymphadenopathy caused by *Bartonella henselae* after Tick Bite. Clin Infect Dis 50:549–551

Barocchi MA, Masignani V, Rappuoli R (2005) Opinion: cell entry machines: a common theme in nature? Nat Rev Microbiol 3:349–358

Batterman HJ, Peek JA, Loutit JS, Falkow S, Tompkins LS (1995) *Bartonella henselae* and *Bartonella quintana* adherence to and entry into cultured human epithelial cells. Infect Immun 63:4553–4556

Billeter SA, Levy MG, Chomel BB, Breitschwerdt EB (2008) Vector transmission of *Bartonella* species with emphasis on the potential for tick transmission. Med Vet Entomol 22:1–15

Bolin I, Norlander L, Wolf-Watz H (1982) Temperature-inducible outer membrane protein of *Yersinia pseudotuberculosis* and *Yersinia enterocolitica* is associated with the virulence plasmid. Infect Immun 37:506–512

Bown KJ, Bennet M, Begon M (2004) Flea-borne *Bartonella grahamii* and *Bartonella taylorii* in bank voles. Emerg Infect Dis 10:684–687

Brouqui P, LaScola B, Roux V, Raoult D (1999) Chronic *Bartonella quintana* bacteraemia in homeless patients. N Engl J Med 340:184–189

Burgess AW, Anderson BE (1998) Outer membrane proteins of *Bartonella henselae* and their interaction with human endothelial cells. Microb Pathog 25:157–164

Burgess AW, Paquet JY, Letesson JJ, Anderson BE (2000) Isolation, sequencing and expression of *Bartonella henselae* omp43 and predicted membrane topology of the deduced protein. Microb Pathog 29:73–80

Chang CC, Chomel BB, Kasten RW, Romano V, Tietze N (2001) Molecular evidence of *Bartonella* spp. in questing adult *Ixodes pacificus* ticks in California. J Clin Microbiol 39:1221–1226

Chilton MD, Drummond MH, Merio DJ, Sciaky D, Montoya AL, Gordon MP, Nester EW (1977) Stable incorporation of plasmid DNA into higher plant cells: the molecular basis of crown gall tumorigenesis. Cell 11:263–271

Christie PJ, Atmakuri K, Krishnamoorthy V, Jakubowski S, Cascales E (2005) Biogenesis, architecture, and function of bacterial type IV secretion systems. Annu Rev Microbiol 59:451–485

Clantin B, Delattre AS, Rucktooa P, Saint N, Meli AC, Locht C et al (2007) Structure of the membrane protein FhaC: a member of the Omp85-TpsB transporter superfamily. Science 317:957–961

Comanducci M, Bambini S, Brunelli B, Adu-Bobie J, Arico B, Capecchi B et al (2002) NadA, a novel vaccine candidate of *Neisseria meningitidis*. J Exp Med 195:1445–1454

Cotte V, Bonnet S, Le RD, Le NE, Chauvin A, Boulouis HJ et al (2008) Transmission of *Bartonella henselae* by *Ixodes ricinus.* Emerg Infect Dis 14:1074–1080

Cotter PA, Yuk MH, Mattoo S, Akerley BJ, Boschwitz J, Relman DA, Miller JF (1998) Filamentous haemagglutinin of *Bordetella bronchiseptica* is required for efficient establishment of tracheal colonization. Infect Immun 66:5921–5929

Coutte L, Alonso S, Reveneau N, Willery E, Quatannens B, Locht C, Jacob-Dubuisson F (2003a) Role of adhesin release for mucosal colonization by a bacterial pathogen. J Exp Med 197: 735–742

Coutte L, Antoine R, Drobecq H, Locht C, Jacob-Dubuisson F (2001) Subtilisin-like autotransporter serves as maturation protease in a bacterial secretion pathway. EMBO J 20:5040–5048

Coutte L, Willery E, Antoine R, Drobecq H, Locht C, Jacob-Dubuisson F (2003b) Surface anchoring of bacterial subtilisin important for maturation function. Mol Microbiol 49:529–539

Dehio C (2005) *Bartonella*-host-cell interactions and vascular tumour formation. Nat Rev Microbiol 3:621–631

Dietrich F, Schmidgen T, Maggi RG, Richter D, Matuschka FR, Vonthein R et al (2010) Prevalence of *Bartonella henselae* and *Borrelia burgdorferi* sensu lato DNA in *Ixodes ricinus* ticks in Europe. Appl Environ Microbiol 76:1395–1398

Eremeeva ME, Gerns HL, Lydy SL, Goo JS, Ryan ET, Mathew SS et al (2007) Bacteraemia, fever, and splenomegaly caused by a newly recognized *Bartonella* species. N Engl J Med 356: 2381–2387

Foster TJ, Hook M (1998) Surface protein adhesins of *Staphylococcus aureus*. Trends Microbiol 6:484–488

Foucault C, Rolain JM, Raoult D, Brouqui P (2004) Detection of *Bartonella quintana* by direct immunofluorescence examination of blood smears of a patient with acute trench fever. J Clin Microbiol 42:4904–4906

Fuhrmann O, Arvand M, Gohler A, Schmid M, Krüll M, Hippenstiel S et al (2001) *Bartonella henselae* induces NF-κB-dependent upregulation of adhesion molecules in cultured human endothelial cells: possible role of outer membrane proteins as pathogenic factors. Infect Immun 69:5088–5097

Garcia FU, Wojta J, Broadley KN, Davidson JM, Hoover RL (1990) *Bartonella bacilliformis* stimulates endothelial cells *in vitro* and is angiogenic *in vivo*. Am J Pathol 136:1125–1135

Gilmore RD Jr., Bellville TM, Sviat SL, Frace M (2005) The *Bartonella vinsonii* subsp. *arupensis* immunodominant surface antigen BrpA gene, encoding a 382-kilodalton protein composed of repetitive sequences, is a member of a multigene family conserved among *Bartonella* species. Infect Immun 73:3128–3136

Grosskinsky U, Schütz M, Fritz M, Schmid Y, Lamparter MC, Szczesny P et al (2007) A conserved glycine residue of trimeric autotransporter domains plays a key role in *Yersinia* adhesin A autotransport. J Bacteriol 189:9011–9019

Hannah JH, Menozzi FD, Renauld G, Locht C, Brennan MJ (1994) Sulfated glycoconjugate receptors for the *Bordetella pertussis* adhesin filamentous haemagglutinin (FHA) and mapping of the heparin-binding domain on FHA. Infect Immun 62:5010–5019

Henderson IR, Navarro-Garcia F, Desvaux M, Fernandez RC, a'Aldeen D (2004) Type V protein secretion pathway: the autotransporter story. Microbiol Mol Biol Rev 68:692–744

Henn JB, Chomel BB, Boulouis HJ, Kasten RW, Murray WJ, Bar-Gal GK et al (2009) *Bartonella rochalimae* in raccoons, coyotes, and red foxes. Emerg Infect Dis 15:1984–1987

Hercik K, Hasova V, Janecek J, Branny P (2007) Molecular evidence of *Bartonella* DNA in ixodid ticks in Czechia. Folia Microbiol (Praha) 52:503–509

Hoiczyk E, Roggenkamp A, Reichenbecher M, Lupas A, Heesemann J (2000) Structure and sequence analysis of *Yersinia* YadA and *Moraxella* UspAs reveal a novel class of adhesins. EMBO J 19:5989–5999

Hultgren SJ, Abraham S, Caparon M, Falk P, St GJ III, Normark S (1993) Pilus and nonpilus bacterial adhesins: assembly and function in cell recognition. Cell 73:887–901

Inatsuka CS, Julio SM, Cotter PA (2005) *Bordetella* filamentous haemagglutinin plays a critical role in immunomodulation, suggesting a mechanism for host specificity. Proc Natl Acad Sci USA 102:18578–18583

Ishibashi Y, Nishikawa A (2002) *Bordetella pertussis* infection of human respiratory epithelial cells up-regulates intercellular adhesion molecule-1 expression: role of filamentous haemagglutinin and pertussis toxin. Microb Pathog 33:115–125

Ishibashi Y, Nishikawa A (2003) Role of nuclear factor-κ B in the regulation of intercellular adhesion molecule 1 after infection of human bronchial epithelial cells by *Bordetella pertussis*. Microb Pathog 35:169–177

Kaiser PO, Riess T, O'Rourke F, Linke D, Kempf VA (2011) *Bartonella* spp.: throwing light on uncommon human infections. Int J Med Microbiol 301:7–15

Kaiser PO, Riess T, Wagner CL, Linke D, Lupas AN, Schwarz H et al (2008) The head of *Bartonella* adhesin A is crucial for host cell interaction of *Bartonella henselae*. Cell Microbiol 10:2223–2234

Kelly P, Rolain JM, Maggi R, Sontakke S, Keene B, Hunter S et al (2006) *Bartonella quintana* endocarditis in dogs. Emerg Infect Dis 12:1869–1872

Kempf VA, Hitziger N, Riess T, Autenrieth IB (2002) Do plant and human pathogens have a common pathogenicity strategy? Trends Microbiol 10:269–275

Kempf VA, Lebiedziejewski M, Alitalo K, Wälzlein JH, Ehehalt U, Fiebig J et al (2005) Activation of hypoxia-inducible factor-1 in bacillary angiomatosis: evidence for a role of hypoxia-inducible factor-1 in bacterial infections. Circulation 111:1054–1062

Kempf VA, Schaller M, Behrendt S, Volkmann B, Aepfelbacher M, Cakman I, Autenrieth IB (2000) Interaction of *Bartonella henselae* with endothelial cells results in rapid bacterial rRNA synthesis and replication. Cell Microbiol 2:431–441

Kempf VA, Volkmann B, Schaller M, Sander CA, Alitalo K, Riess T, Autenrieth IB (2001) Evidence of a leading role for VEGF in *Bartonella henselae*-induced endothelial cell proliferations. Cell Microbiol 3:623–632

Keret D, Giladi M, Kletter Y, Wientroub S (1998) Cat-scratch disease osteomyelitis from a dog scratch. J Bone Joint Surg Br 80:766–767

Kirby JE (2004) *In vitro* model of *Bartonella henselae*-induced angiogenesis. Infect Immun 72:7315–7317

Koretke KK, Szczesny P, Gruber M, Lupas AN (2006) Model structure of the prototypical non-fimbrial adhesin YadA of *Yersinia enterocolitica*. J Struct Biol 155:154–161

Kosoy M, Morway C, Sheff KW, Bai Y, Colborn J, Chalcraft L et al (2008) *Bartonella tamiae* sp. nov., a newly recognized pathogen isolated from three human patients from Thailand. J Clin Microbiol 46:772–775

Kunz S, Oberle K, Sander A, Bogdan C, Schleicher U (2008) Lymphadenopathy in a novel mouse model of *Bartonella*-induced cat scratch disease results from lymphocyte immigration and proliferation and is regulated by interferon-α/β. Am J Pathol 172:1005–1018

Kyme PA, Haas A, Schaller M, Peschel A, Iredell J, Kempf VA (2005) Unusual trafficking pattern of *Bartonella henselae*-containing vacuoles in macrophages and endothelial cells. Cell Microbiol 7:1019–1034

Linke D, Riess T, Autenrieth IB, Lupas A, Kempf VA (2006) Trimeric autotransporter adhesins: variable structure, common function. Trends Microbiol 14:264–270

Mändle T, Einsele H, Schaller M, Neumann D, Vogel W, Autenrieth IB, Kempf VA (2005) Infection of human CD34+ progenitor cells with *Bartonella henselae* results in intraerythrocytic presence of *B. henselae*. Blood 106:1215–1222

Mackichan JK, Gerns HL, Chen YT, Zhang P, Koehler JE (2008) A SacB mutagenesis strategy reveals that the *Bartonella quintana* variably expressed outer membrane proteins are required for bloodstream infection of the host. Infect Immun 76:788–795

Makhov AM, Hannah JH, Brennan MJ, Trus BL, Kocsis E, Conway JF et al (1994) Filamentous haemagglutinin of *Bordetella pertussis*. A bacterial adhesin formed as a 50-nm monomeric rigid rod based on a 19-residue repeat motif rich in β strands and turns. J Mol Biol 241: 110–124

Maxwell PH, Pugh CW, Ratcliffe PJ (2001) Activation of the HIF pathway in cancer. Curr Opin Genet Dev 11:293–299

Mazar J, Cotter PA (2006) Topology and maturation of filamentous haemagglutinin suggest a new model for two-partner secretion. Mol Microbiol 62:641–654

McGuirk P, Mills KH (2000) Direct anti-inflammatory effect of a bacterial virulence factor: IL-10-dependent suppression of IL-12 production by filamentous haemagglutinin from *Bordetella pertussis*. Eur J Immunol 30:415–422

Meng G, Surana NK, St GJ III, Waksman G (2006) Structure of the outer membrane translocator domain of the *Haemophilus influenzae* Hia trimeric autotransporter. EMBO J 25:2297–2304

Morales SC, Breitschwerdt EB, Washabau RJ, Matise I, Maggi RG, Duncan AW (2007) Detection of *Bartonella henselae* DNA in two dogs with pyogranulomatous lymphadenitis. J Am Vet Med Assoc 230:681–685

Mota LJ, Journet L, Sorg I, Agrain C, Cornelis GR (2005) Bacterial injectisomes: needle length does matter. Science 307:1278

Nicholson TL, Brockmeier SL, Loving CL (2009) Contribution of *Bordetella bronchiseptica* filamentous haemagglutinin and pertactin to respiratory disease in swine. Infect Immun 77:2136–2146

Niemann HH, Schubert WD, Heinz DW (2004) Adhesins and invasins of pathogenic bacteria: a structural view. Microbes Infect 6:101–112

Nystedt B, Frank AC, Thollesson M, Andersson SG (2008) Diversifying selection and concerted evolution of a type IV secretion system in *Bartonella*. Mol Biol Evol 25:287–300

Padmalayam I, Karem K, Baumstark B, Massung R (2000) The gene encoding the 17-kDa antigen of *Bartonella henselae* is located within a cluster of genes homologous to the virB virulence operon. DNA Cell Biol 19:377–382

Pines E, Barrand M, Fabre P, Salomon H, Blondeau C, Wood SC, Hoffenbach A (1999) New acellular pertussis-containing paediatric combined vaccines. Vaccine 17:1650–1656

Podsiadly E, Chmielewski T, Sochon E, Tylewska-Wierzbanowska S (2007) *Bartonella henselae* in *Ixodes ricinus* ticks removed from dogs. Vector Borne Zoonotic Dis 7:189–192

Prasad SM, Yin Y, Rodzinski E, Tuomanen EI, Masure HR (1993) Identification of a carbohydrate recognition domain in filamentous haemagglutinin from *Bordetella pertussis*. Infect Immun 61:2780–2785

Pugh CW, Ratcliffe PJ (2003) Regulation of angiogenesis by hypoxia: role of the HIF system. Nat Med 9:677–684

Pulliainen AT, Dehio C (2009) *Bartonella henselae*: subversion of vascular endothelial cell functions by translocated bacterial effector proteins. Int J Biochem Cell Biol 41: 507–510

Raoult D, Dutour O, Houhamdi L, Jankauskas R, Fournier PE, Ardagna Y et al (2006a) Evidence for louse-transmitted diseases in soldiers of Napoleon's Grand Army in Vilnius. J Infect Dis 193:112–120

Raoult D, Roblot F, Rolain JM, Besnier JM, Loulergue J, Bastides F, Choutet P (2006b) First isolation of *Bartonella alsatica* from a valve of a patient with endocarditis. J Clin Microbiol 44:278–279

Rar VA, Fomenko NV, Dobrotvorsky AK, Livanova NN, Rudakova SA, Fedorov EG et al (2005) Tickborne pathogen detection, Western Siberia, Russia. Emerg Infect Dis 11:1708–1715

Ray SK, Rajeshwari R, Sharma Y, Sonti RV (2002) A high-molecular-weight outer membrane protein of *Xanthomonas oryzae* pv. *oryzae* exhibits similarity to non-fimbrial adhesins of animal pathogenic bacteria and is required for optimum virulence. Mol Microbiol 46:637–647

Relman DA, Falkow S, LeBoit PE, Perkocha LA, Min KW, Welch DF, Slater LN (1991) The organism causing bacillary angiomatosis, peliosis hepatis, and fever and bacteraemia in immunocompromised patients. N Engl J Med 324:1514

Relman DA, Loutit JS, Schmidt TM, Falkow S, Tompkins LS (1990) The agent of bacillary angiomatosis. An approach to the identification of uncultured pathogens. N Engl J Med 323:1573–1580

Riess T, Andersson SG, Lupas A, Schaller M, Schäfer A, Kyme P et al (2004) *Bartonella* adhesin A mediates a proangiogenic host cell response. J Exp Med 200:1267–1278

Riess T, Raddatz G, Linke D, Schäfer A, Kempf VA (2007) Analysis of *Bartonella* adhesin A expression reveals differences between various *B. henselae* strains. Infect Immun 75:35–43

Rojas CM, Ham JH, Deng WL, Doyle JJ, Collmer A (2002) HecA, a member of a class of adhesins produced by diverse pathogenic bacteria, contributes to the attachment, aggregation, epidermal cell killing, and virulence phenotypes of *Erwinia chrysanthemi* EC16 on *Nicotiana clevelandii* seedlings. Proc Natl Acad Sci USA 99:13142–13147

Rolain JM, Franc M, Davoust B, Raoult D (2003) Molecular detection of *Bartonella quintana*, *B. koehlerae*, *B. henselae*, *B. clarridgeiae*, *Rickettsia felis*, and *Wolbachia pipientis* in cat fleas, France. Emerg Infect Dis 9:338–342

Rolain JM, Foucault C, Brouqui P, Raoult D (2003) Erythroblast cells as a target for *Bartonella quintana* in homeless people. Ann N Y Acad Sci 990:485–487

Saenz HL, Engel P, Stoeckli MC, Lanz C, Raddatz G, Vayssier-Taussat M et al (2007) Genomic analysis of *Bartonella* identifies type IV secretion systems as host adaptability factors. Nat Genet 39:1469–1476

Sanogo YO, Zeaiter Z, Caruso G, Merola F, Shpynov S, Brouqui P, Raoult D (2003) *Bartonella henselae* in *Ixodes ricinus* ticks (*Acari: Ixodida*) removed from humans, Belluno province, Italy. Emerg Infect Dis 9:329–332

Scheidegger F, Ellner Y, Guye P, Rhomberg TA, Weber H, Augustin HG, Dehio C (2009) Distinct activities of *Bartonella henselae* type IV secretion effector proteins modulate capillary-like sprout formation. Cell Microbiol 11:1088–1101

Schmid MC, Scheidegger F, Dehio M, Balmelle-Devaux N, Schulein R, Guye P et al (2006) A translocated bacterial protein protects vascular endothelial cells from apoptosis. PLoS Pathog 2:e115

Schmid MC, Schülein R, Dehio M, Denecker G, Carena I, Dehio C (2004) The VirB type IV secretion system of *Bartonella henselae* mediates invasion, proinflammatory activation and antiapoptotic protection of endothelial cells. Mol Microbiol 52:81–92

Schülein R, Dehio C (2002) The VirB/VirD4 type IV secretion system of *Bartonella* is essential for establishing intraerythrocytic infection. Mol Microbiol 46:1053–1067

Schülein R, Guye P, Rhomberg TA, Schmid MC, Schroder G, Vergunst AC et al (2005) A bipartite signal mediates the transfer of type IV secretion substrates of *Bartonella henselae* into human cells. Proc Natl Acad Sci USA 102:856–861

Schülein R, Seubert A, Gille C, Lanz C, Hansmann Y, Piemont Y, Dehio C (2001) Invasion and persistent intracellular colonization of erythrocytes. A unique parasitic strategy of the emerging pathogen *Bartonella*. J Exp Med 193:1077–1086

Schulte B, Linke D, Klumpp S, Schaller M, Riess T, Autenrieth IB, Kempf VA (2006) *Bartonella quintana* variably expressed outer membrane proteins mediate vascular endothelial growth factor secretion but not host cell adherence. Infect Immun 74:5003–5013

Schultz MG (1968) A history of bartonellosis (Carrión's disease). Am J Trop Med Hyg 17:503–515

Seubert A, Hiestand R, de la CF, Dehio C (2003) A bacterial conjugation machinery recruited for pathogenesis. Mol Microbiol 49:1253–1266

Spach DH, Kanter AS, Dougherty MJ, Larson AM, Coyle MB, Brenner DJ et al (1995) *Bartonella (Rochalimaea) quintana* bacteraemia in inner-city patients with chronic alcoholism. N Engl J Med 332:424–428

Szczesny P, Linke D, Ursinus A, Bar K, Schwarz H, Riess TM et al (2008) Structure of the head of the *Bartonella* adhesin BadA. PLoS Pathog 4:e1000119

Szczesny P, Lupas A (2008) Domain annotation of trimeric autotransporter adhesins–daTAA. Bioinformatics 24:1251–1256

Vayssier-Taussat M, Le RD, Deng HK, Biville F, Cescau S, Danchin A et al (2010) The Trw type IV secretion system of *Bartonella* mediates host-specific adhesion to erythrocytes. PLoS Pathog 6:e1000946

Wagner CL, Riess T, Linke D, Eberhardt C, Schäfer A, Reutter S et al (2008) Use of *Bartonella* adhesin A (BadA) immunoblotting in the serodiagnosis of *Bartonella henselae* infections. Int J Med Microbiol 298:579–590

Zhang P, Chomel BB, Schau MK, Goo JS, Droz S, Kelminson KL et al (2004) A family of variably expressed outer-membrane proteins (Vomp) mediates adhesion and autoaggregation in *Bartonella quintana*. Proc Natl Acad Sci USA 101:13630–13635

Zhang P, Dolganov G, Gerns H, Heinemeyer E, Goo JS, Koehler JE (2007) Expression of the *Bartonella quintana* Vomp trimeric autotransporter adhesin familiy is regulated by several mechanisms. Poster presentation at the 107th General Meeting American Society of Microbiology, Toronto, Canada, 226, 21 May 2007

Chapter 5
Adhesion Mechanisms of Plant-Pathogenic *Xanthomonadaceae*

Nadia Mhedbi-Hajri, Marie-Agnès Jacques, and Ralf Koebnik

Abstract The family *Xanthomonadaceae* is a wide-spread family of bacteria belonging to the gamma subdivision of the Gram-negative proteobacteria, including the two plant-pathogenic genera *Xanthomonas* and *Xylella*, and the related genus *Stenotrophomonas*. Adhesion is a widely conserved virulence mechanism among Gram-negative bacteria, no matter whether they are human, animal or plant pathogens, since attachment to the host tissue is one of the key early steps of the bacterial infection process. Bacterial attachment to surfaces is mediated by surface structures that are anchored in the bacterial outer membrane and cover a broad group of fimbrial and non-fimbrial structures, commonly known as adhesins. In this chapter, we discuss recent findings on candidate adhesins of plant-pathogenic *Xanthomonadaceae*, including polysaccharidic (lipopolysaccharides, exopolysaccharides) and proteineous structures (chaperone/usher pili, type IV pili, autotransporters, two-partner-secreted and other outer membrane adhesins), their involvement in the formation of biofilms and their mode of regulation via quorum sensing. We then compare the arsenals of adhesins among different *Xanthomonas* strains and evaluate their mode of selection. Finally, we summarize the sparse knowledge on specific adhesin receptors in plants and the possible role of RGD motifs in binding to integrin-like plant molecules.

5.1 Introduction

The family *Xanthomonadaceae* is a wide-spread family of bacteria belonging to the gamma subdivision of the Gram-negative proteobacteria. Current taxonomy lists 22 genera, among them the two plant-pathogenic genera *Xanthomonas* and *Xylella*, and the related genus *Stenotrophomonas,* isolates of which are increasingly recognised as an important cause of hospital-acquired infections.

R. Koebnik (✉)
Laboratoire Génome et Développement des Plantes (UMR5096 Université de Perpignan–CNRS–IRD), Montpellier, France
e-mail: koebnik@gmx.de

D. Linke, A. Goldman (eds.), *Bacterial Adhesion*, Advances in Experimental Medicine and Biology 715, DOI 10.1007/978-94-007-0940-9_5,

Xanthomonas is a large genus of plant-associated bacteria, many of which cause severe diseases of crops and ornamentals, including economically important plants, such as rice, wheat, banana, beans, tomato, *Citrus* and cotton. Common diseases include vascular wilt, cankers, leaf spots, fruit spots, leaf blight and leaf streak. Strains of a certain pathovar only infect a restricted number of plant species and each strain colonizes a favoured ecological niche (tissue), some strains entering the vascular system and causing systemic disease while others stay more or less restricted to the site of infection. Several (putative) pathogenicity factors have been speculated to be responsible for this host and tissue specificity, among them the repertoire of type III effectors, presence/absence of adhesins, and/or their allelic diversity (Hajri et al., 2009; Lu et al., 2008).

Xylella fastidiosa is another important plant pathogen of the *Xanthomonadaceae* family, which is distibuted worldwide. Strains of *X. fastidiosa* cause citrus variegated chlorosis or Pierce's disease in grapevine. Other strains cause disease on shrubs and trees (e.g. oleander, almond, oak, mulberry, peach, pear), but also on alfalfa. The bacteria form biofilms which contribute to the occlusion of xylem vessels, thus leading to water stress and wilting of the host plant. Leafhoppers are the vector for this xylem-limited fastidious bacterium. The spread of the disease requires the release of the bacterium from the animal vector and its transmission into new plants (Chatterjee et al., 2008a). Four principal pathogenicity factors, most of them related to attachment, have been described for plant colonization and insect acquisition: (i) twitching motility by type IV pili, (ii) secretion of cell-wall degrading enzymes, (iii) cell-to-cell aggregation and surface attachment by fimbrial and non-fimbrial adhesins, and (iv) production of exopolysaccharides (Chatterjee et al., 2008a).

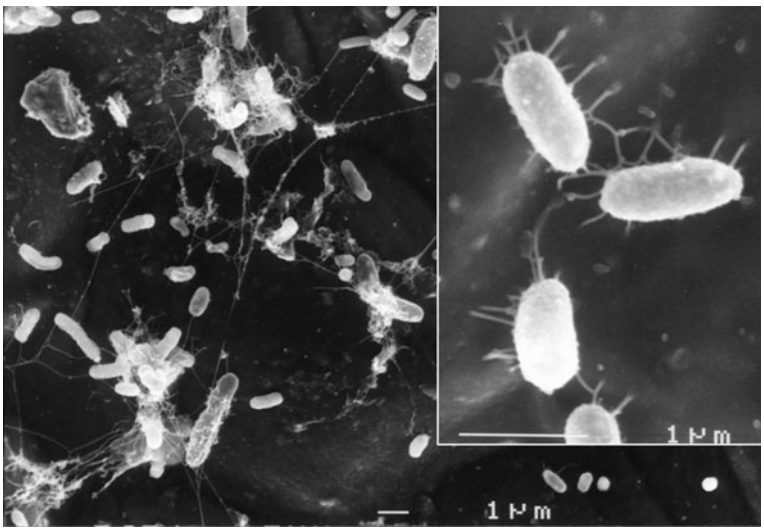

Fig. 5.1 Scanning electron micrographs of field-grown bean leaf surface colonized by seed-borne *X. axonopodis* pv. *phaseoli*. Note the various cell surface appendages used by the bacterial cells to adhere to the leaf surface

Adhesion is a widely conserved virulence mechanism among Gram-negative bacteria which is used by diverse pathogens to infect their plant, invertebrate and mammalian hosts (Amano, 2010; Cao et al., 2001; Kline et al., 2009). Attachment to a surface is also a prerequisite for aggregation in biofilms which enhance the resistance of bacteria to various biotic and abiotic stresses, favour the coordination of adapted responses to environmental changes and allow multiplication for successful colonization of host tissue (Amano, 2010; Danhorn and Fuqua, 2007). Sensing and adhesion are interconnected since biofilm formation is regulated by a chemosensory system revealing the interplay of the various systems mediating the adaptation to the environment (Dow et al., 2003). The genome sequences of plant-pathogenic *Xanthomonadaceae* contain many genes for the formation of surface adhesive structures (Moreira et al., 2004; Van Sluys et al., 2002). Electron microscopy revealed the presence of surface appendages that are assumed to be involved in attachment to abiotic and/or biotic surfaces (Fig. 5.1).

5.2 Adhesive Structures – Polysaccharides

5.2.1 Lipopolysaccharides

It is generally believed that lipopolysaccharides (LPS) play a role in adhesion, but it is difficult to ascertain whether this effect is direct or indirect (Hori and Matsumoto, 2010). Usually, LPS mutants are also affected in other traits, such as motility, production of type I pili and other adhesins, and type III secretion.

X. campestris pv. *campestris* is a vascular pathogen of cruciferous plants and enters the xylem *via* hydathodes. Analysis of *X. campestris* pv. *campestris* mutants affected in pathogenicity demonstrated that a mutation of *rfaX*, leading to an altered LPS, had the strongest impact on hydathode colonization (Hugouvieux et al., 1998). However, this effect could be due to an attachment defect or due to higher sensitivity towards the antimicrobial defense response mounted in the hydathode. Later, other virulence-reduced mutants in LPS genes were isolated in *X. campestris* pv. *campestris* (Qian et al., 2005). A loss-of-virulence screen of the non-vascular rice pathogen *X. oryzae* pv. *oryzicola* revealed a *wxocB* mutant that was assumed to be affected in the O chain assembly (Wang et al., 2007). This mutant was strongly impaired in its ability to spread in the mesophyll. Although the reasons for the reduced virulence of LPS mutants remain to be elucidated, these observations imply that an intact LPS is essential for full virulence of vascular and non-vascular xanthomonads.

5.2.2 Exopolysaccharides

Exopolysaccharide (EPS), also called xanthan gum for *Xanthomonas*, is another bacterial polysaccharide that is released as an extracellular slime (García-Ochoa et al., 2000). EPS is involved in biofilm formation (Vu et al., 2009), which in turn

mediates close association of bacteria to abiotic and biotic surfaces (Danhorn and Fuqua, 2007).

More than 10 years ago, the first EPS mutants of xanthomonads were described. A *gumD* mutant of *X. campestris* pv. *campestris* and a *gumG* mutant of *X. oryzae* pv. *oryzae* were reported to be reduced in virulence (Chou et al., 1997; Dharmapuri and Sonti, 1999). An exhaustive transposon screen of *X. campestris* pv. *campestris* revealed further mutants in EPS biosynthesis genes which were affected in provoking disease of cabbage (Lu et al., 2007; Qian et al., 2005).

A *X. axonopodis* pv. *citri gumB* mutant, not only defective in production of EPS but also in the formation of biofilms, showed reduced growth and survival on leaf surfaces and reduced disease symptoms, suggesting an important role for the formation of biofilms in the epiphytic survival of *X. axonopodis* pv. *citri* (Rigano et al., 2007). However, another xanthan-defective mutant of *X. axonopodis* pv. *citri*, mutated in *gumD*, remained fully pathogenic in citrus plants but displayed impaired survival under oxidative stress during stationary phase as well as impaired epiphytic survival on citrus leaves (Dunger et al., 2007). It was concluded that xanthan does not play an essential role in citrus canker at the initial stages of infection, but facilitates the maintenance of bacteria on the host plant, possibly improving the efficiency of colonization of distant tissue (Dunger et al., 2007).

EPS synthesis of *X. campestris* pv. *campestris* has been shown to be under control of a cell-cell signalling pathway, involving a small diffusible signal factor (DSF), the DSF synthetase RpfF and a two-component regulatory system comprising RpfC and RpfG (Fouhy et al., 2006). DSF signalling is tighly linked to the intracellular second messenger cyclic dimeric GMP (c-di-GMP) (Jenal and Malone, 2006; Ryan et al., 2006). Subsequent mutant analyses (Ryan et al., 2007; Torres et al., 2007) and microarray experiments (He et al., 2006, 2007) revealed that DSF/c-di-GMP signalling is not only finely balanced during biofilm formation but involves a hierarchical signalling network affecting many other pathogenicity-related traits, among them type III secretion, motility, extracellular hydrolytic enzymes, detoxification and resistance to oxidative stress. This way, a coordinated switch from a sessile aggregated lifestyle to motile exploratory lifestyle may be accomplished (Fouhy et al., 2006).

Cell-to-cell signalling mediated by a structurally similar diffusible signal factor is also central to the regulation of the virulence of *X. fastidiosa*. *rpfC* mutants hyperexpress *rpfF*, overproduce DSF and are deficient in virulence and movement in the xylem vessels of grape, while *rpfF* mutants deficient in DSF production have the opposite phenotypes for these traits (Chatterjee et al., 2008c). Using green fluorescent protein-labelled bacteria, the *rpfF*-deficient mutant was detected at a greater distance from the point of inoculation than the wild-type strain and attained up to 100-fold larger population sizes (Chatterjee et al., 2008b). Hence, the hypervirulence phenotype of the *rpfF* mutant is likely due to unrestrained replication and more extensive spread of bacteria within the xylem vessels, thus leading to their occlusion. It was concluded that DSF-mediated cell-to-cell signalling, which restricts movement and colonization of *X. fastidiosa*, may be an adaptation to endophytic growth of the pathogen that prevents the excessive growth of cells in vessels (Chatterjee

et al., 2008b). Interestingly, *rpfC* mutants are able to colonize the mouthparts of insect vectors but are not transmitted as efficiently as wild-type bacteria to new host plants, apparently because of their strong adhesiveness (Chatterjee et al., 2008c). Because of the opposing contributions of adhesiveness and other traits to movement within plants and transmission to new host plants, *X. fastidiosa* apparently coordinates these traits in a quorum-dependent fashion involving DSF.

5.3 Adhesive Structures – Proteins

5.3.1 Pili (Fimbriae)

Pili (fimbriae) are filamentous cell-surface appendages that have been classified by their potential to induce hemagglutination of erythrocytes, their morphology (size), their site of anchoring in the bacterium (polar *versus* omnidirectional), and by their biosynthesis. In *Xanthomonadaceae*, several types of pili have been observed or postulated to exist: chaperone/usher (CU) pili, type IV pili, and pili associated with several protein secretion systems (Büttner and Bonas, 2010). Virtually nothing is known whether or not pili of the type III, type IV and type VI protein secretion systems are specifically involved in adhesion of *Xanthomonadaceae*.

5.3.1.1 Chaperone/Usher Pili

CU pili are assembled by the relatively simple chaperone/usher pathway (Kline et al., 2010). Genes for CU pili (sometimes also called type I pili) of *Xanthomonadaceae* were first discovered in the genome sequence of *X. fastidiosa* (Bhattacharyya et al., 2002). Strain 9a5c was the first one to be completely sequenced (acc. no. NC_002488), followed by strain Temecula1 (acc. no. NC_004556). The gene cluster XF0077 to XF0083 (PD0058 to PD0062 in strain Temecula1) encodes a periplasmic chaperone, an outer membrane usher protein, and four candidate fimbrial subunits (three in strain Temecula1). The usher and chaperone proteins are almost identical among different strains of *X. fastidiosa* while the fimbrial subunits share 85–93% sequence identity among orthologs but less identity among paralogs. The predicted protein product of *fimA* (PD0062) in *X. fastidiosa* shares 23% identity with the orthologous FimA in *Escherichia coli* K–12 (Li et al., 2007); the usher (PD0060) and chaperone (PD0061) are 36 and 40% identical to their *E. coli* orthologues.

By transmission electron microscopy two length classes of fimbriae were visualized, the shorter of which (0.4–1.0 micrometer) corresponded to CU pili (Meng et al., 2005). Scanning electron microscopy revealed that fimbriae size and number, cell aggregation, and cell size were reduced in *fimA* (PD0062) or *fimF* (PD0058) mutants of *X. fastidiosa* when compared with the parental strain (Feil et al., 2003). Later, it was confirmed that a *fimA* (PD0062) mutant produced no CU pili (Li et al., 2007). Interestingly, CU pili were found to be predominantly located at only one

pole of the cell (Li et al., 2007; Meng et al., 2005). Since *X. fastidiosa* has been found to attach polarly to xylem cells (Feil et al., 2003), CU pili might therefore be involved in the polar attachment to plant cells. Mutants in *fimA* or *fimF* remained pathogenic to grapevines but exhibited significantly reduced virulence (Feil et al., 2003, 2007).

Mutants in *fimA* (PD0062), thus possessing only type IV pili, were found to be deficient in biofilm formation (Meng et al., 2005). A role of CU pili in biofilm formation was also suggested by the upregulation of *fimA* during biofilm formation (de Souza et al., 2004). Biofilm formation and adherence to surfaces might interfere with movement. Indeed, a *fimA* mutant was not only capable of moving *via* twitching motility (Meng et al., 2005), but movement was in fact enhanced, suggesting that the presence of CU pili may partially restrict cell movement (Li et al., 2007). Using a microfluidic device it was demonstrated that a *fimA* mutant moved six times faster than wild-type cells on a glass surface (De La Fuente et al., 2007a). Along with this observation, CU pili were found to mediate stronger attachment to a glass surface than type IV pili (De La Fuente et al., 2007b). Not only did *fimA* and *fimF* mutants adhere to glass surfaces less efficiently than the wild-type strain, but these cells occurred primarily as solitary cells and not as cell aggregates, unlike wild-type. In summary, CU pili of *X. fastidiosa* play an important role in cell-to-cell aggregation, biofilm formation and attachment to surfaces.

Complete genome sequencing led to the identification of a conserved gene cluster for CU pili in *Xanthomonas* (acc. no. YP_363214). This gene cluster is predicted to encode one usher protein (XCV1483), two chaperones (XCV1480, XCV1483) and two fimbrial subunits one of which is twice the size (XCV1481) of the other (XCV1484) due to a tandem duplication. The number, order and size of the genes of the CU pilus cluster of *Xanthomonas* is different to that found in *X. fastidiosa*. Moreover, the sequence similarity is very low, with less than 25% sequence identity between the chaperone and usher proteins from *Xanthomonas* and *X. fastidiosa*. *Stenotrophomonas maltophilia*, another species of the *Xanthomonadaceae*, contains two CU pilus gene clusters, one corresponding to that from *Xanthomonas* and one to that from *X. fastidiosa*. Hence, CU pili from *Xanthomonas* and from *X. fastidiosa* might play different roles.

5.3.1.2 Type IV Pili

Type IV pili are homopolymeric assemblies of a small pilin protein, called PilA in *Pseudomonas* and PilE in *Neisseria*, which are expressed by many Gram-negative bacteria, including *Xanthomonadaceae* (Craig et al., 2004). The type IV pilus assembly machinery is structurally related to the type II secretion system (Gerlach and Hensel, 2007). Once assembled, the long and flexible structure extends outward from the bacterial surface and establishes contact with host cell or abiotic surfaces. Type IV pili have the ability, once firmly attached to a surface, to retract through the bacterial cell wall, thus leading to movement of the bacterial cell – a process called twitching or gliding motility (Jarrell and McBride, 2008).

Type IV pilus-related genes are present in all sequenced strains of *Xanthomonas* and *Xylella*. The major pilin PilA (sometimes misleadingly called FimA) is

always encoded on the opposite strand close to the pilus assembly gene *pilC*. The major pilin orthologs from *Xanthomonas* display an amazing diversity which does not correlate with the phylogenetic relationships of the strains. Some pilins are more closely related to PilE from *Neisseria* while others are more similar to homologs from *Legionella*. In a few lineages of *Xanthomonas* (e.g. *X. campestris* pv. *campestris* strains ATCC33913 and 8004, *X. axonopodis* pv. *vesicatoria* strain NCPPB3240, *X. axonopodis* pv. *citri* strain 306), a tandem duplication has occurred the consequences of which are not known (i.e. whether there is an antigenic switch due to differential expression of the two genes) (Ojanen-Reuhs et al., 1997). The variability among the major pilins may be associated with specific interactions with their hosts, reminiscent of the situation in human and animal pathogens (Van Sluys et al., 2002). The genome sequences of *X. fastidiosa* also reveal a gene duplication event, which probably occurred before or along with the speciation of *X. fastidiosa*. However, compared to *Xanthomonas*, there is much less sequence variation among the six completely sequenced strains of *X. fastidiosa*.

Experiments with several *Xanthomonas* species demonstrated an important role of type IV pili in attachment and aggressiveness on their host plants. For example, immunofluorescence studies showed that purified type IV pili of *X. campestris* pv. *hyacinthi* attached to stomata of hyacinth leaves, suggesting a role for these surface structures in the first stages of yellow disease (van Doorn et al., 1994). A *fimA* (i.e. *pilA*) mutant of *X. axonopodis* pv. *vesicatoria* strain NPPPB3240 was not significantly reduced in virulence upon infiltration or spraying of bacterial suspensions onto tomato leaves (Ojanen-Reuhs et al., 1997). However, scanning electron microscopy revealed that the *fimA* mutant was affected in its ability to adhere and efficiently colonize trichomes of tomato leaves. The *fimA* mutant also was dramatically reduced in cell aggregation in laboratory cultures and on infected tomato leaves, and exhibited decreased tolerance to UV light. When the tandemly arranged paralog *fimB* (i.e. *pilB*) of strain NPPPB3240 was knocked out, compact cell aggregates similar to those formed by the wild-type strain were observed (Ojanen-Reuhs et al., 1997). Mutants in *pilB* and *pilC* of *X. campestris* pv. *campestris* were reduced in virulence upon leaf clip inoculation (Qian et al., 2005). A mutation in *pilA* of *X. axonopodis* pv. *phaseoli* decreased its aggressiveness on bean upon dip-inoculation of leaves (Darsonval et al., 2009). Moreover, PilA was found to be involved in transmission of *X. axonopodis* pv. *phaseoli* to bean seeds *via* xylem vessels (Darsonval et al., 2009).

A mutation in the *X. oryzae* pv. *oryzae pilQ* gene, which is predicted to encode the type IV pilus secretin, appeared to have no effect on leaf attachment or entry but reduces the virulence following wound inoculation and *in planta* migration (Das et al., 2009; Lim et al., 2008). These findings indicate that the type IV pilus is not only involved in initial attachment to organs of the leaf, but is also required for optimum virulence within the plant tissue, i.e. when *X. oryzae* pv. *oryzae* is multiplying or migrating within xylem vessels. This conclusion is supported by a transposon screen of *X. oryzae* pv. *oryzicola* which revealed that insertions in several *pil* genes (*pilM*, *pilQ*, *pilT*, *pilZ*, *pilY1*) reduce the colonization of rice leaves upon leaf infiltration (Wang et al., 2007). Similarly, mutation of the *pilQ* and *pilB* genes

in *X. fastidiosa* has been shown to affect colonization and upstream migration of the bacteria in xylem vessels (Meng et al., 2005). Using a microfluidic flow chamber, the speed of twitching movement of a *pilY1* mutant of *X. fastidiosa* on a glass surface against the flow of media was found to be three times slower than that of wild-type cells (De La Fuente et al., 2007a).

Type IV pili were also found to be required for optimal virulence, seed transmission, twitching motility and biofilm formation of several other Gram-negative plant pathogens, such as *Ralstonia solanacearum* and *Acidovorax avenae* subsp. *citrulli* (Bahar et al., 2009; Kang et al., 2002). In contrast, mutation of type IV pili of *Pseudomonas syringae* pv. *tomato* DC3000 had no apparent effect on pathogenicity, as judged by symptom formation upon leaf inoculation (Roine et al., 1998). Yet, type IV pili were found to play a role in fitness during foliar colonization and survival, a finding that might be related to an enhanced tolerance against environmental conditions such as exposure to UV light (Roine et al., 1998). Taken together, results from numerous studies support a role of type IV pili in attachment to certain plant surfaces, in formation of biofilms, and in colonization and migration within xylem vessels.

5.3.2 Non-Fimbrial Adhesins

Non-fimbrial adhesins are widely found in proteobacteria and contain different classes of proteins involved in attachment (Gerlach and Hensel, 2007; Pizarro-Cerdá and Cossart, 2006). Many of these proteins are presented on the cell surface upon transport via one of the three subtypes of type V secretion systems: (i) monomeric autotransporters (T5SS[a]) (Dautin and Bernstein, 2007), (ii) trimeric autotransporters or oligomeric coiled-coil adhesins (T5SS[b]) (Cotter et al., 2005; Linke et al., 2006), and (iii) two-partner secretion systems incl. filamentous hemagglutinins (T5SS[c]) (Mazar and Cotter, 2006). Other non-fimbrial adhesins are secreted via a type I secretion system (e.g. LapA from *P. fluorescens*) or represent small integral outer membrane proteins (Amano, 2010; Gerlach and Hensel, 2007).

5.3.2.1 Type V-Secreted Adhesins

Xanthomonadaceae encode type V-secreted proteins which could act as non-fimbrial adhesins (Table 5.1) (Moreira et al., 2004; Van Sluys et al., 2002). These proteins are related to the prototypic yersinial adhesins YadA and YapH and to well-studied adhesins from *Bordetella pertussis* (pertactin, filamentous hemagglutinin FHA) and *Haemophilus influenzae* (HMW1, HMW2) (Hoiczyk et al., 2000; Smith et al., 2001; St Geme 3rd and Yeo, 2009).

Comparative genomics revealed that predicted adhesion genes of some strains have frameshift mutations and/or in-frame stop codons, thus most likely leading to truncated, probably inactive protein variants (Table 5.1) (Bhattacharyya et al., 2002; Van Sluys et al., 2003). A pronounced case of DNA duplication and decay is found for the *fhaB* gene that encodes the passenger domain that is translocated

Table 5.1 Distribution of non-filamentous adhesins and accessory proteins in completely sequenced strains of *Xanthomonadaceae*

Name[a]	Prototype[b]	Annotation[c]	Pfam domains[d]	RGD[e]	Xac[f]	Xav	XooK	XooM	XooP	Xoc	XccA	Xcc8	XccB	Xca	Xal	Xf_9	Xf_T	Xf_A	Xf_D	Xf_12	Xf_23
	XCV4444	hemagglutinin-related protein	Calx_beta; He_PIG; Autotransporter	YES	Ω	+	3Ω	+	+	Ω	+	+	+	+	–	–	–	–	–	–	–
YapH	XCV2103	filamentous hemagglutinin-related protein; YapH protein	–	YES	+	+	+	2Ω	+	+	+	+	+	+	–	–	–	–	–	–	–
	XCAORF_0904	YapH protein, putative	Autotransporter	no	–	–	–	–	–	–	–	–	–	+	–	–	–	–	–	–	–
XadA1	XOO0842	adhesin-like protein	Hep-Hag; HIM	no	+	+	+	+	+	+	+	+	+	+	–	+	+	+ 2Ω	+	+	+
XadA2	XCV3672	adhesin-like protein	Hep_Hag; HIM; YadA	no	+	+	–	–	–	–	–	–	–	–	+	–	–	–	–	–	–
XadB	XOO0681	adhesin-like protein	Hep_Hag; HIM; YadA	no	–	–	+	+	+	+	–	–	–	–	–	–	–	–	–	–	–
	XALc_1305	hypothetical adhesin	Hep_Hag; HIM; YadA	YES	–	–	–	–	–	–	–	–	–	–	+	–	–	–	–	–	–
	XALc_1884	hypothetical adhesin	Hep_Hag; HIM; YadA	YES	–	–	–	–	–	–	–	–	–	–	+	–	–	–	–	–	–
	XF1981	YadA-like surface protein	Hep_Hag; HIM; YadA	no	–	–	–	–	–	–	–	–	–	–	–	+	+	2+	+	+	+
	XF1529	YadA-like surface protein	Hep_Hag; HIM; X_fast-SP_rel; YadA	no	–	–	–	–	–	–	–	–	–	–	–	+	+	2+	+	+	+

Table 5.1 (continued)

Name[a]	Prototype[b]	Annotation[c]	Pfam domains[d]	RGD[e]	Xac[f]	Xav	XooK	XooM	XooP	Xoc	XccA	Xcc8	XccB	Xca	Xal	Xf_9	Xf_T	Xf_A	Xf_D	Xf_12	Xf_23
FhaC	XAC1814	outer membrane hemolysin activator protein	POTRA_2; ShlB	/	+	+	–	–	+	+	+	+	–	+	+	+	+	2+	+	+	+
FhaB	XAC1815	filamentous hemagglutinin	Haemagg_act; Fil_haemagg	YES	+ 2Ω	2Ω	–	–	+ 3Ω	+ 4Ω	+	+ Ω	–	+ Ω	+ 7Ω	3+	2+	2+ 2Ω	3Ω	–	3+ Ω
	XAC4114	hemolysin activator protein	POTRA_2; ShlB	/	+	+	–	–	–	–	–	–	–	–	–	–	–	–	–	–	–
	XAC4113	filamentous hemagglutinin-like protein; [YapH protein]	Haemagg_act	no	+	+	Ω	–	–	Ω	–	–	–	–	–	–	–	–	–	–	–

[a] Common name given to the proteins of *Xanthomonas* spp

[b] Locus tag of the prototypical gene/protein given at http://www.ncbi.nlm.nih.gov/

[c] Common annotation of protein function at http://www.ncbi.nlm.nih.gov/

[d] Predicted protein domains at http://pfam.sanger.ac.uk/

[e] Presence of conserved RGD motifs

[f] Presence of proteins in the predicted proteome. +, presence; –, absence; Ω, protein fragments predicted from putative pseudogenes; numbers indicate numbers of paralogs or protein fragments. Xac, *X. axonopodis* pv. *citri* str. 306 (Refseq accession number [acc. no.] NC_003919); Xav, *X. axonopodis* pv. *vesicatoria* str. 85-10 (acc. no. NC_007508); XooK, *X. oryzae* pv. *oryzae* KACC10331 (acc. no. NC_006834); XooM, *X. oryzae* pv. *oryzae* MAFF 311018 (acc. no. NC_007705); XooP, *X. oryzae* pv. *oryzae* PXO99^{A} (acc. no. NC_010717); Xoc, *X. oryzae* pv. *oryzicola* BLS256 (acc. no. NZ_AAQN00000000); XccA, *X. campestris* pv. *campestris* str. ATCC 33913 (acc. no. NC_003902); Xcc8, *X. campestris* pv. *campestris* str. 8004 (acc. no. NC_007086); XccB, *X. campestris* pv. *campestris* str. B100 (acc. no. NC_010688); Xca, *X. campestris* pv. *armoraciae* 756C (available at the Comprehensive Microbial Resource http://cmr.jcvi.org/tigr-scripts/CMR/CmrHomePage.cgi); Xal, *X. albilineans* GPE PC73 (acc. no. NC_013722); Xf_9, *X. fastidiosa* 9a5c (acc. no. NC_002488); Xf_T, *X. fastidiosa* Temecula1 (acc. no. NC_004556); Xf_A, *X. fastidiosa* Ann-1 (acc. no. NZ_AAAM00000000); Xf_D, *X. fastidiosa* Dixon (acc. no. NZ_AAAL00000000); Xf_12, *X. fastidiosa* M12 (acc. no. NC_010513); Xf_23, *X. fastidiosa* M23 (acc. no. NC_010577)

across the outer membrane by the FhaC protein. Most strains appear to have a full-length *fhaB* gene, downstream of which closely related gene fragments are present. It would be interesting to study whether these fragments can serve as a genetic reservoir to evolve new adhesin gene variants. Unfortunately, such genetic variability had the side-effect of misleading genome annotation, and many predicted genes are most likely not functional. For instance, two ORFs downstream of *fhaB* [XAC1815] from *X. axonopodis* pv. *citri*, XAC1816 and XAC1818, have been annotated as hemagglutinin-like proteins but they correspond to internal protein fragments of FhaB. Since XAC1816 and XAC1818 lack the conserved two-partner secretion domain at the N terminus, these proteins (genes) are most likely not functional (Gottig et al., 2009). Similarly, *fhaB1* [XCV1860] and *fhaB2* [XCV1861] from *X. axonopodis* pv. *vesicatoria* might not be functional because these predicted genes correspond to 5′ and 3′ fragments of the full-length *fhaB* gene of *X. axonopodis* pv. *citri*. Another source of confusion comes from the annotation of several two-partner secreted proteins as YapH although they do not display any sequence homology to the yersinial YapH protein.

The first evidence that a non-fimbrial adhesin is involved in the infection process of a plant-pathogenic bacterium came from mutagenesis and expression studies of its gene (Ray et al., 2002). The *xadA1* gene of *X. oryzae* pv. *oryzae*, a homologue of the yersinial *yadA* gene, was shown to be induced in minimal medium, and *xadA1* mutants were strongly affected for virulence upon epiphytic infection, suggesting an important virulence function somewhere along the path from the leaf surface, *via* the hydathodes, into the xylem vessels (Ray et al., 2002). It should be noted that at the same time, *xadA1* mutants produced less EPS (Ray et al., 2002). Later, the role of XadA1 and, to a lesser extent, of its paralog XadB in attachment to and entry into rice leaves was elegantly confirmed by confocal fluorescence microscopy using eGFP-tagged *X. oryzae* pv. *oryzae* (Das et al., 2009). Interestingly, when *X. axonopodis* pv. *passiflorae* cells were treated with leaf extracts, the *xadA* homolog was only induced with extracts from its host plant, passion fruit, but not with extracts from a non-host plant (tomato) (Tahara et al., 2003). Darsonval and colleagues (2009) did not observe any role for XadA1 in *X. axonopodis* pv. *phaseoli* aggressiveness on bean. Instead, the paralog *xadA2* was found to be required for vascular transmission to bean seeds. Despite remaining pathogenic on grapevine, *xadA* mutants of *X. fastidiosa* also were affected in aggressiveness (Feil et al., 2007). Apparently, different paralogs play specific roles in the infection process and efficient infection and dissemination may require an intricate balance of these and other adhesins.

DNA macroarray expression studies of 279 selected genes from *X. axonopodis* pv. *citri* showed that more adhesin genes, i.e. *fhaB* and XAC4113, are induced in a minimal medium that mimics *in planta* conditions (Astua-Monge et al., 2005), and synthesis of the two-partner secreted adhesin FhaB was also found to be induced during citrus leaf colonization (Gottig et al., 2009). Mutant analysis showed that this adhesin is not only involved in epiphytic fitness, attachment to plant surfaces and colonization of citrus leaves, but also in cell-to-cell-attachment and biofilm formation. Opposite to what was observed with a *xadA1* mutant, the *fhaB* mutant secreted more EPS (Gottig et al., 2009). The homologous FhaB protein of *X. axonopodis* pv.

phaseoli is involved in attachment to seeds of beans but not to leaves (Darsonval et al., 2009). However, FhaB does not seem to be important for aggressiveness in *X. axonopodis* pv. *phaseoli*.

Conversely, the hemagglutinin-like YapH orthologue appears to limit aggressiveness of *X. axonopodis* pv. *phaseoli* on bean since a *yapH* mutant led to more severe symptoms when inoculated onto bean leaves at high concentration (Darsonval et al., 2009). Thus, *yapH* fulfills the hallmarks of an 'anti-virulence' gene, mutations of which result in a hypervirulent phenotype as measured by a lower lethal dose, a colonization advantage, reduced clearance or decreased survival time of the host (Foreman-Wykert and Miller, 2003). On the other hand, YapH is the only adhesin of *X. axonopodis* pv. *phaseoli* which was found to be required for the complete phyllosphere colonization process and for seed transmission through the vascular pathway, probably due to its requirement for adhesion to biotic and abiotic surfaces and for biofilm formation (Darsonval et al., 2009). A hypervirulent phenotype was also observed upon knockout of the haemagglutinin-like proteins HfxA (PD2118) and HxfB (PD1792) of *X. fastidiosa* strain Temecula1 (Guilhabert and Kirkpatrick, 2005). Surprisingly, Feil and colleagues reported the opposite effect when they inoculated a *hxfB* mutant of strain Temecula1 into grapevine, following the same procedure of needle inoculation at high concentration (Feil et al., 2007). The expression of adhesion genes, i.e. *fimA*, *hxfA* and *hxfB*, is much higher in *rpfC* mutants of *X. fastidiosa*, which also exhibit a hyperattachment phenotype in culture associated with their inability to migrate in xylem vessels and cause disease (Chatterjee et al., 2008c). Conversely, *rpfF* mutants synthesize less FimA, HxfA, and HxfB and are hypervirulent, thus looking like phenocopies of *hxfA* and *hxfB* mutants.

5.3.2.2 Other Outer Membrane Adhesins

Beside type V-secreted proteins, other integral outer membrane proteins have been identified as adhesins in human and animal pathogens. These proteins are embedded in the outer membrane as antiparallel beta-barrels (Koebnik et al., 2000). The eight-stranded OmpA of *E. coli* is the archetype of this class of proteins and has been shown to function as an adhesin (Smith et al., 2007). Despite the presence of similar small beta-barrel proteins in phytopathogenic bacteria, it is unknown whether or not they are involved in attachment to plant cells. Given the thick plant cell wall, such a mechanism seems unlikely to be exploited by plant pathogens. However, bacterial plant pathogens, such as *Xanthomonas* spp., secrete a plethora of cell-wall degrading enzymes that might help the bacteria to approach the plant cell plasma membrane (Moreira et al., 2004; Van Sluys et al., 2002).

5.4 Adhesin Repertoires and Diversifying Selection

Recently, repertoires of genes involved in early stages of interaction between host and pathogenic bacteria were characterized in a large collection of *Xanthomonas* strains (Mhedbi-Hajri et al., 2011). Three categories of adhesin genes were

described: (i) ubiquitous genes that are widespread among different pathovars and genetic lineages (type IV pilus genes *pilL*, *pilS*, *pilU* and *pilA*); (ii) less conserved genes that were not detected in several strains (e.g. XCV2103, *fhaB* [XAC1815] and XAC1816); and (iii) species-specific genes that were detected only in *X. axonopodis* (e.g. *xadA2*, *fhaB1* [XCV1860] and *fhaB2* [XCV1861]). For instance, XAC1816 is present in ten pathovars of *X. axonopodis* and is also present in non-pathogenic strains of *X. campestris* whereas *fhaB1* and *fhaB2* were only detected in six pathovars of *X. axonopodis* (Mhedbi-Hajri et al., 2011).

Using the McDonald-Kreitman test, Mhedbi-Hajri and colleagues analyzed adhesin genes from three strains of *X. axonopodis* (pathovars *vesicatoria, citri* and *phaseoli*) and from three strains of *X. campestris* pv. *campestris* for molecular signatures of selection pressure (Mhedbi-Hajri et al., 2011). Adaptive divergence by diversifying selection was found to affect *xadA1* and *fhaB*, particularly within the *X. axonopodis* clade. It was concluded that adhesion should be considered as a selective step for settlement of bacteria on plant tissue (Mhedbi-Hajri et al., 2011).

5.5 Adhesin Receptors

Adhesins are thought to interact with a variety of host components, either nonspecifically via hydrophobic or electrostatic interactions, or by binding to specific host cell receptor moieties (Hori and Matsumoto, 2010). Adhesion-binding may trigger the activation of complex signal-transduction cascades in host cells, thus inducing innate defense responses which can be either harmful or beneficial to the bacteria (Amano, 2010).

A few examples may illustrate the diversity of adhesin-receptor interactions that have been discovered for human pathogens (Amano, 2010; Gerlach and Hensel, 2007; Kline et al., 2009). Tip adhesins of type I pili have been found to interact with glycolipids and glycoprotein receptors while type IV PAK pili from *Pseudomonas aeruginosa* bind to gangliosides. Nonfimbrial adhesins recognize many different elements on host cell surfaces, including components of the extracellular matrix (ECM). For instance, the prototypic trimeric autotransporter YadA from *Yersinia* spp. mediates adhesion to several ECM proteins, such as collagen, laminin, and fibronectin (Nummelin et al., 2004). Other outer membrane-associated adhesins (e.g. neisserial Opa proteins) bind to integral host cell membrane receptors, such as integrins, cadherins, selectins, and carcinoembryonic antigen-related cell adhesion molecules (CEACAM). In contrast to these examples, nothing is known for plant-pathogenic *Xanthomonadaceae*.

Type V-secreted adhesins, such as the *E. coli* antigen 43 and pertactin from *B. pertussis*, bind to integrins via conserved RGD motifs (Junker et al., 2006; Takagi 2004; van der Woude and Henderson, 2008). Similar to their role in animal tissue, integrin-like molecules of plants have been found to be involved in connecting the plant cell wall to the plasma membrane (Lü et al., 2007), and this

interaction could be disrupted by treatment with RGD-containing peptides (Canut et al., 1998; Lü et al., 2007; Schindler et al., 1989). Candidate integrin-like RGD-binding receptors have been identified by immunolabelling with integrin-specific antisera, by cross-linking of iodinated RGD-heptapeptides and by affinity chromatography using immobilized RGD-containing peptides (Faik et al., 1998; Labouré et al., 1999; Senchou et al., 2004).

The plant-pathogenic oomycete *Phytophthora infestans* secretes an RGD-containing protein which might bind to a specific receptor protein of *Arabidopsis thaliana*, thus enabling/promoting the infection process via a loosened cellular organization (Senchou et al., 2004). Subsequently, a RGD-reactive receptor-like kinase with a lectin-like extracellular domain was identified, and it was speculated that RGD-dependent protein-protein interactions could play a structural and signalling role at the plant cell surface (Gouget et al., 2006). Whether bacterial plant pathogens take advantage of RGD motifs for binding to plant cells is still unknown. However, conserved RGD motifs have been found in the monomeric autotransporters XCV2103 and XCV4444 but not in the trimeric autotransporters XadA or XadB. RGD motifs are also present in the FhaB homologs. Even if RGD-mediated binding to integrin-like proteins is involved in attachment to host cells, it is not clear whether these bacterial proteins determine host specificity due to the evolution of new binding specificities. Rather, diversifying selection might lead to host adaptation via escape from detection by the plant's immune system, and these adhesins would thus constitute a further class of pathogen-associated molecular patterns (PAMPs) (Postel and Kemmerling, 2009; Silipo et al., 2010).

5.6 Concluding Remarks

Our current knowledge about the adhesion process and the involved molecular structures of *Xanthomonadaceae* resembles a kaleidoscope but how all the different components interact synergistically or antagonistically is still very much unknown. In recent years, phytopathologists have mainly used genetics and genomics to gain insight into the initial steps of the pathogen-host interaction. They often relied on genetic screens, which were not well-suited to elucidate the individual roles of candidate adhesion molecules. New assays, mimicking the infection process and using in situ fluorescence microscopy (Das et al., 2009; Newman et al., 2003), will allow a better understanding of the adaptive phase of infection of vascular and non-vascular pathogens, i.e. attraction and attachment. Moreover, structural biology, biochemistry and biophysics are expected to provide detailed insights into specific molecular interactions between pathogen-derived adhesins and their host cell receptors.

Acknowledgments We are grateful to Maurice Lesourd and Robert Filmon from the Service Commun d'Imagerie et d'Analyses Microscopiques, Faculté de Médecine, Université d'Angers, France, for help with scanning electron microscopy.

References

Amano A (2010) Bacterial adhesins to host components in periodontitis. Periodontol 2000(52): 12–37

Astua-Monge G, Freitas-Astua J, Bacocina G, Roncoletta J, Carvalho SA, Machado MA (2005) Expression profiling of virulence and pathogenicity genes of *Xanthomonas axonopodis* pv. *citri*. J Bacteriol 187:1201–1205

Bahar O, Goffer T, Burdman S (2009) Type IV Pili are required for virulence, twitching motility, and biofilm formation of *Acidovorax avenae* subsp. *citrulli*. Mol Plant Microbe Interact 22: 909–920

Bhattacharyya A, Stilwagen S, Ivanova N, D'Souza M, Bernal A, Lykidis A, Kapatral V, Anderson I, Larsen N, Los T, Reznik G, Selkov Jr E, Walunas TE, Feil H, Feil WS, Purcell A, Lassez JL, Hawkins TL, Haselkorn R, Overbeek R, Predki PF, Kyrpides NC (2002) Whole-genome comparative analysis of three phytopathogenic *Xylella fastidiosa* strains. Proc Natl Acad Sci USA 99:12403–12408

Büttner D, Bonas U (2010) Regulation and secretion of *Xanthomonas* virulence factors. FEMS Microbiol Rev 34:107–133

Canut H, Carrasco A, Galaud JP, Cassan C, Bouyssou H, Vita N, Ferrara P, Pont-Lezica R (1998) High affinity RGD-binding sites at the plasma membrane of *Arabidopsis thaliana* links the cell wall. Plant J 16:63–71

Cao H, Baldini RL, Rahme LG (2001) Common mechanisms for pathogens of plants and animals. Annu Rev Phytopathol 39:259–284

Chatterjee S, Almeida RP, Lindow SE (2008a) Living in two worlds: the plant and insect lifestyles of *Xylella fastidiosa*. Annu Rev Phytopathol 46:243–271

Chatterjee S, Newman KL, Lindow SE (2008b) Cell-to-cell signaling in *Xylella fastidiosa* suppresses movement and xylem vessel colonization in grape. Mol Plant Microbe Interact 21:1309–1315

Chatterjee S, Wistrom C, Lindow SE (2008c) A cell-cell signaling sensor is required for virulence and insect transmission of *Xylella fastidiosa*. Proc Natl Acad Sci USA 105: 2670–2675

Chou FL, Chou HC, Lin YS, Yang BY, Lin NT, Weng SF, Tseng YH (1997) The *Xanthomonas campestris gumD* gene required for synthesis of xanthan gum is involved in normal pigmentation and virulence in causing black rot. Biochem Biophys Res Commun 233: 265–269

Cotter SE, Surana NK, Geme 3rd JW (2005) Trimeric autotransporters: a distinct subfamily of autotransporter proteins. Trends Microbiol 13:199–205

Craig L, Pique ME, Tainer JA (2004) Type IV pilus structure and bacterial pathogenicity. Nat Rev Microbiol 2:363–378

Danhorn T, Fuqua C (2007) Biofilm formation by plant-associated bacteria. Annu Rev Microbiol 61:401–422

Darsonval A, Darrasse A, Durand K, Bureau C, Cesbron S, Jacques MA (2009) Adhesion and fitness in the bean phyllosphere and transmission to seed of *Xanthomonas fuscans* subsp. *fuscans*. Mol Plant Microbe Interact 22:747–757

Das A, Rangaraj N, Sonti RV (2009) Multiple adhesin-like functions of *Xanthomonas oryzae* pv. *oryzae* are involved in promoting leaf attachment, entry, and virulence on rice. Mol Plant Microbe Interact 22:73–85

Dautin N, Bernstein HD (2007) Protein secretion in gram-negative bacteria via the autotransporter pathway. Annu Rev Microbiol 61:89–112

De La Fuente L, Burr TJ, Hoch HC (2007a) Mutations in type I and type IV pilus biosynthetic genes affect twitching motility rates in *Xylella fastidiosa*. J Bacteriol 189:7507–7510

De La Fuente L, Montanes E, Meng Y, Li Y, Burr TJ, Hoch HC, Wu M (2007b) Assessing adhesion forces of type I and type IV pili of *Xylella fastidiosa* bacteria by use of a microfluidic flow chamber. Appl Environ Microbiol 73:2690–2696

de Souza AA, Takita MA, Coletta-Filho HD, Caldana C, Yanai GM, Muto MH, de Oliveira RC, Nunes LR, Machado MA (2004) Gene expression profile of the plant pathogen *Xylella fastidiosa* during biofilm formation in vitro. FEMS Microbiol Lett 237:341–353

Dharmapuri S, Sonti RV (1999) A transposon insertion in the *gumG* homologue of *Xanthomonas oryzae* pv. *oryzae* causes loss of extracellular polysaccharide production and virulence. FEMS Microbiol Lett 179:53–59

Dow JM, Crossman L, Findlay K, He YQ, Feng JX, Tang JL (2003) Biofilm dispersal in *Xanthomonas campestris* is controlled by cell-cell signaling and is required for full virulence to plants. Proc Natl Acad Sci USA 100:10995–11000

Dunger G, Relling VM, Tondo ML, Barreras M, Ielpi L, Orellano EG, Ottado J (2007) Xanthan is not essential for pathogenicity in citrus canker but contributes to *Xanthomonas* epiphytic survival. Arch Microbiol 188:127–135

Faik A, Labouré AM, Gulino D, Mandaron P, Falconet D (1998) A plant surface protein sharing structural properties with animal integrins. Eur J Biochem 253:552–559

Feil H, Feil WS, Detter JC, Purcell AH, Lindow SE (2003) Site-directed disruption of the *fimA* and *fimF* fimbrial genes of *Xylella fastidiosa*. Phytopathology 93:675–682

Feil H, Feil WS, Lindow SE (2007) Contribution of fimbrial and afimbrial adhesins of *Xylella fastidiosa* to attachment to surfaces and virulence to grape. Phytopathology 97:318–324

Foreman-Wykert AK, Miller JF (2003) Hypervirulence and pathogen fitness. Trends Microbiol 11:105–108

Fouhy Y, Lucey JF, Ryan RP, Dow JM (2006) Cell-cell signaling, cyclic di-GMP turnover and regulation of virulence in *Xanthomonas campestris*. Res Microbiol 157:899–904

García-Ochoa F, Santos VE, Casas JE, Gómez E (2000) Xanthan gum: production, recovery, and properties. Biotechnol Adv 18:549–579

Gerlach RG, Hensel M (2007) Protein secretion systems and adhesins: the molecular armory of Gram-negative pathogens. Int J Med Microbiol 297:401–415

Gottig N, Garavaglia BS, Garofalo C, Orellano EG, Ottado J (2009) A filamentous hemagglutinin-like protein of *Xanthomonas axonopodis* pv. *citri,* the phytopathogen responsible for citrus canker, is involved in bacterial virulence. PLoS One 4:e4358

Gouget A, Senchou V, Govers F, Sanson A, Barre A, Rougé P, Pont-Lezica R, Canut H (2006) Lectin receptor kinases participate in protein-protein interactions to mediate plasma membrane-cell wall adhesions in *Arabidopsis*. Plant Physiol 140:81–90

Guilhabert MR, Kirkpatrick BC (2005) Identification of *Xylella fastidiosa* antivirulence genes: hemagglutinin adhesins contribute to *X. fastidiosa* biofilm maturation and colonization and attenuate virulence. Mol Plant Microbe Interact 18:856–868

Hajri A, Brin C, Hunault G, Lardeux F, Lemaire C, Manceau C, Boureau T, Poussier S (2009) A "repertoire for repertoire" hypothesis: repertoires of type three effectors are candidate determinants of host specificity in *Xanthomonas*. PLoS One 4:e6632

He YW, Ng AY, Xu M, Lin K, Wang LH, Dong YH, Zhang LH (2007) *Xanthomonas campestris* cell-cell communication involves a putative nucleotide receptor protein Clp and a hierarchical signalling network. Mol Microbiol 64:281–292

He YW, Xu M, Lin K, Ng YJ, Wen CM, Wang LH, Liu ZD, Zhang HB, Dong YH, Dow JM, Zhang LH (2006) Genome scale analysis of diffusible signal factor regulon in *Xanthomonas campestris* pv. *campestris*: identification of novel cell-cell communication-dependent genes and functions. Mol Microbiol 59:610–622

Hoiczyk E, Roggenkamp A, Reichenbecher M, Lupas A, Heesemann J (2000) Structure and sequence analysis of *Yersinia* YadA and Moraxella UspAs reveal a novel class of adhesins. EMBO J 19:5989–5999

Hori K, Matsumoto S (2010) Bacterial adhesion: From mechanism to control. Biochem Eng J 48:424–434

Hugouvieux V, Barber CE, Daniels MJ (1998) Entry of *Xanthomonas campestris* pv. *campestris* into hydathodes of *Arabidopsis thaliana* leaves: a system for studying early infection events in bacterial pathogenesis. Mol Plant Microbe Interact 11:537–543

Jarrell KF, McBride MJ (2008) The surprisingly diverse ways that prokaryotes move. Nat Rev Microbiol 6:466–476

Jenal U, Malone J (2006) Mechanisms of cyclic-di-GMP signaling in bacteria. Annu Rev Genet 40:385–407

Junker M, Schuster CC, McDonnell AV, Sorg KA, Finn MC, Berger B, Clark PL (2006) Pertactin β-helix folding mechanism suggests common themes for the secretion and folding of autotransporter proteins. Proc Natl Acad Sci USA 103:4918–4923

Kang Y, Liu H, Genin S, Schell MA, Denny TP (2002) *Ralstonia solanacearum* requires type 4 pili to adhere to multiple surfaces and for natural transformation and virulence. Mol Microbiol 46:427–437

Kline KA, Dodson KW, Caparon MG, Hultgren SJ (2010) A tale of two pili: assembly and function of pili in bacteria. Trends Microbiol 18:224–232

Kline KA, Fälker S, Dahlberg S, Normark S, Henriques-Normark B (2009) Bacterial adhesins in host-microbe interactions. Cell Host Microbe 5:580–592

Koebnik R, Locher KP, Van Gelder P (2000) Structure and function of bacterial outer membrane proteins: barrels in a nutshell. Mol Microbiol 37:239–253

Labouré AM, Faik A, Mandaron P, Falconet D (1999) RGD-dependent growth of maize calluses and immunodetection of an integrin-like protein. FEBS Lett 442:123–128

Li Y, Hao G, Galvani CD, Meng Y, De La Fuente L, Hoch HC, Burr TJ (2007) Type I and type IV pili of *Xylella fastidiosa* affect twitching motility, biofilm formation and cell-cell aggregation. Microbiology 153:719–726

Lim SH, So BH, Wang JC, Song ES, Park YJ, Lee BM, Kang HW (2008) Functional analysis of pilQ gene in *Xanthomonas oryzae* pv. *oryzae*, bacterial blight pathogen of rice. J Microbiol 46:214–220

Linke D, Riess T, Autenrieth IB, Lupas A, Kempf VA (2006) Trimeric autotransporter adhesins: variable structure, common function. Trends Microbiol 14:264–270

Lu GT, Ma ZF, Hu JR, Tang DJ, He YQ, Feng JX, Tang JL (2007) A novel locus involved in extracellular polysaccharide production and virulence of *Xanthomonas campestris* pathovar *campestris*. Microbiology 153:737–746

Lu H, Patil P, Van Sluys MA, White FF, Ryan RP, Dow JM, Rabinowicz J, Salzberg SL, Leach JE, Sonti R, Brendel V, Bogdanove AJ (2008) Acquisition and evolution of plant pathogenesis-associated gene clusters and candidate determinants of tissue-specificity in *Xanthomonas*. PLoS One 3:e3828

Lü B, Chen F, Gong ZH, Xie H, Zhang JH, Liang JS (2007) Intracellular localization of integrin-like protein and its roles in osmotic stress-induced abscisic acid biosynthesis in *Zea mays*. Protoplasma 232:35–43

Mazar J, Cotter PA (2006) Topology and maturation of filamentous haemagglutinin suggest a new model for two-partner secretion. Mol Microbiol 62:641–654

Meng Y, Li Y, Galvani CD, Hao G, Turner JN, Burr TJ, Hoch HC (2005) Upstream migration of *Xylella fastidiosa* via pilus-driven twitching motility. J Bacteriol 187:5560–5567

Mhedbi-Hajri N, Darrasse A, Pigné S, Durand K, Fouteau S, Barbe V, Manceau C, Lemaire C, Jacques MA (2011) Sensing and adhesion are adaptive functions in the plant pathogenic xanthomonads. BMC Evol Biol (in press)

Moreira LM, de Souza RF, Almeida Jr NF, Setubal JC, Oliveira JC, Furlan LR, Ferro JA, da Silva AC (2004) Comparative genomics analyses of citrus-associated bacteria. Annu Rev Phytopathol 42:163–184

Newman KL, Almeida RP, Purcell AH, Lindow SE (2003) Use of a green fluorescent strain for analysis of *Xylella fastidiosa* colonization of *Vitis vinifera*. Appl Environ Microbiol 69: 7319–7327

Nummelin H, Merckel MC, Leo JC, Lankinen H, Skurnik M, Goldman A (2004) The *Yersinia* adhesin YadA collagen-binding domain structure is a novel left-handed parallel beta-roll. EMBO J 23:701–711

Ojanen-Reuhs T, Kalkkinen N, Westerlund-Wikström B, van Doorn J, Haahtela K, Nurmiaho-Lassila EL, Wengelnik K, Bonas U, Korhonen TK (1997) Characterization of the *fimA* gene encoding bundle-forming fimbriae of the plant pathogen *Xanthomonas campestris* pv. *vesicatoria*. J Bacteriol 179:1280–1290

Pizarro-Cerdá J, Cossart P (2006) Bacterial adhesion and entry into host cells. Cell 124:715–727

Postel S, Kemmerling B (2009) Plant systems for recognition of pathogen-associated molecular patterns. Semin Cell Dev Biol 20:1025–1031

Qian W, Jia Y, Ren SX, He YQ, Feng JX, Lu LF, Sun Q, Ying G, Tang DJ, Tang H, Wu W, Hao P, Wang L, Jiang BL, Zeng S, Gu WY, Lu G, Rong L, Tian Y, Yao Z, Fu G, Chen B, Fang R, Qiang B, Chen Z, Zhao GP, Tang JL, He C (2005) Comparative and functional genomic analyses of the pathogenicity of phytopathogen *Xanthomonas campestris* pv. *campestris*. Genome Res 15:757–767

Ray SK, Rajeshwari R, Sharma Y, Sonti RV (2002) A high-molecular-weight outer membrane protein of *Xanthomonas oryzae* pv. *oryzae* exhibits similarity to non-fimbrial adhesins of animal pathogenic bacteria and is required for optimum virulence. Mol Microbiol 46: 637–647

Rigano LA, Siciliano F, Enrique R, Sendín L, Filippone P, Torres PS, Qüesta J, Dow JM, Castagnaro AP, Vojnov AA, Marano MR (2007) Biofilm formation, epiphytic fitness, and canker development in *Xanthomonas axonopodis* pv. *citri*. Mol Plant Microbe Interact 20: 1222–1230

Roine E, Raineri DM, Romantschuk M, Wilson M, Nunn DN (1998) Characterization of type IV pilus genes in *Pseudomonas syringae* pv. *tomato* DC3000. Mol Plant Microbe Interact 11:1048–1056

Ryan RP, Fouhy Y, Lucey JF, Crossman LC, Spiro S, He YW, Zhang LH, Heeb S, Cámara M, Williams P, Dow JM (2006) Cell-cell signaling in *Xanthomonas campestris* involves an HD-GYP domain protein that functions in cyclic di-GMP turnover. Proc Natl Acad Sci USA 103:6712–6717

Ryan RP, Fouhy Y, Lucey JF, Jiang BL, He YQ, Feng JX, Tang JL, Dow JM (2007) Cyclic di-GMP signalling in the virulence and environmental adaptation of *Xanthomonas campestris*. Mol Microbiol 63:429–442

Schindler M, Meiners S, Cheresh DA (1989) RGD-dependent linkage between plant cell wall and plasma membrane: consequences for growth. J Cell Biol 108:1955–1965

Senchou V, Weide R, Carrasco A, Bouyssou H, Pont-Lezica R, Govers F, Canut H (2004) High affinity recognition of a *Phytophthora* protein by *Arabidopsis* via an RGD motif. Cell Mol Life Sci 61:502–509

Silipo A, Erbs G, Shinya T, Dow JM, Parrilli M, Lanzetta R, Shibuya N, Newman MA, Molinaro A (2010) Glyco-conjugates as elicitors or suppressors of plant innate immunity. Glycobiology 20:406–419

Smith AM, Guzmán CA, Walker MJ (2001) The virulence factors of *Bordetella pertussis*: a matter of control. FEMS Microbiol Rev 25:309–333

Smith SG, Mahon V, Lambert MA, Fagan RP (2007) A molecular Swiss army knife: OmpA structure, function and expression. FEMS Microbiol Lett 273:1–11

St. Geme 3rd JW, Yeo HJ (2009) A prototype two-partner secretion pathway: the *Haemophilus influenzae* HMW1 and HMW2 adhesin systems. Trends Microbiol 17:355–360

Tahara ST, Mehta A, Rosato YB (2003) Proteins induced by *Xanthomonas axonopodis* pv. *passiflorae* with leaf extract of the host plant (*Passiflorae edulis*). Proteomics 3:95–102

Takagi I (2004) Structural basis for ligand recognition by RGD (Arg-Gly-Asp)-dependent integrins. Biochem Soc Trans 32:403–406

Torres PS, Malamud F, Rigano LA, Russo DM, Marano MR, Castagnaro AP, Zorreguieta A, Bouarab K, Dow JM, Vojnov AA (2007) Controlled synthesis of the DSF cell-cell signal is

required for biofilm formation and virulence in *Xanthomonas campestris*. Environ Microbiol 9:2101–2109

van Doorn J, Boonekamp PM, Oudega B (1994) Partial characterization of fimbriae of *Xanthomonas campestris* pv. *hyacinthi*. Mol Plant Microbe Interact 7:334–344

Van Sluys MA, Monteiro-Vitorello CB, Camargo LEA, Menck CFM, da Silva ACR, Ferro JA, Oliveira MC, Setubal JC, Kitajima JP, Simpson AJ (2002) Comparative genomic analysis of plant-associated bacteria. Annu Rev Phytopathol 40:169–189

Van Sluys MA, de Oliveira MC, Monteiro-Vitorello CB, Miyaki CY, Furlan LR et al (2003) Comparative analyses of the complete genome sequences of Pierce's disease and citrus variegated chlorosis strains of *Xylella fastidiosa*. J Bacteriol 185:1018–1026

van der Woude MW, Henderson IR (2008) Regulation and function of Ag43 (flu). Annu Rev Microbiol 62:153–169

Vu B, Chen M, Crawford RJ, Ivanova EP (2009) Bacterial extracellular polysaccharides involved in biofilm formation. Molecules 14:2535–2554

Wang L, Makino S, Subedee A, Bogdanove AJ (2007) Novel candidate virulence factors in rice pathogen *Xanthomonas oryzae* pv. *oryzicola* as revealed by mutational analysis. Appl Environ Microbiol 73:8023–8027

Chapter 6
Adhesion by Pathogenic Corynebacteria

Elizabeth A. Rogers, Asis Das, and Hung Ton-That

Abstract Pathogenic members of the genus *Corynebacterium* cause a wide range of serious infections in humans including diphtheria. Adhesion to host cells is a crucial step during infection. In *Corynebacterium diphtheriae*, adhesion is mediated primarily by filamentous structures called pili or fimbriae that are covalently attached to the bacterial cell wall. *C. diphtheriae* produces three distinct pilus structures, SpaA-, SpaD- and SpaH-type pili. Similar to other types, the prototype SpaA pilus consists of SpaA forming the pilus shaft and two minor pilins SpaB and SpaC located at the base and at the tip, respectively. The minor pilins SpaB/SpaC are critical for bacterial binding to human pharyngeal cells, and thus represent the major adhesins of corynebacteria. Like pili of many other gram-positive microbes, the assembly of corynebacterial pili occurs by a two-step mechanism, whereby pilins are covalently polymerized by a transpeptidase enzyme named pilin-specific sortase and the generated pilus polymer is subsequently anchored to the cell wall peptidoglycan via the base pilin by the housekeeping sortase or a non-polymerizing sortase. This chapter reviews the current knowledge of corynebacterial adhesion, with a specific focus on pilus structures, their assembly, and the mechanism of adhesion mediated by pili.

6.1 Introduction

Pathogenic corynebacteria cause a number of debilitating and life threatening diseases in humans (Coyle and Lipsky, 1990) (for a partial list, see Table 6.1). These organisms are from the genus *Corynebacterium* with more than 110 validated species, all of which are rod shaped, aerobic, non-motile, and non-spore forming

H. Ton-That (✉)
Department of Microbiology and Molecular Genetics, The University of Texas Medical School at Houston, Houston, TX 77030, USA
e-mail: Ton-That.Hung@uth.tmc.edu

D. Linke, A. Goldman (eds.), *Bacterial Adhesion*, Advances in Experimental Medicine and Biology 715, DOI 10.1007/978-94-007-0940-9_6,

Table 6.1 Select *Corynebacterium* species, associated diseases, and pilus gene clusters

Organism	Associated disease	Pilus gene clusters
C. diphtheriae (toxigenic)	Respiratory diphtheria, Cutaneous diphtheria, Pharyngitis	SpaA-type SpaD-type and SpaH-type
C. diphtheriae (nontoxigenic)	Endocarditis	Not known
C. ulcerans	Respiratory diphtheria Zoonotic infections	Not known
C. jeikeium	Septicemia, endocarditis, Wound infections Catheter/shunt infections	SpaH-type
C. amycolatum	Septicemia Respiratory tract infections Urinary tract infections Wound infections Catheter/shunt infections	SpaD-type
C. urealyticum	Urinary tract infections (pyelonephritis, cystitis) Wound infections Septicemia, endocarditis	SpaD-type
C. pseudotuberculosis	Abscess formation Lymphadenitis Ulcerative lymphangitis	Not known

gram-positive bacteria with high levels of mycolic acid in the cell wall. While most *Corynebacterium* species are innocuous (such as *Corynebacterium glutamicum*, which is used in the food industry), quite a few are medically relevant (Funke et al., 1997). The most well known among these is *Corynebacterium diphtheriae*, which secretes an extremely potent toxin and thereby causes cutaneous and pharyngeal diphtheria. Diphtheria is also linked to *Corynebacterium ulcerans* and *Corynebacterium pseudotuberculosis,* which share a zoonotic mode of transmission (Bonmarin et al., 2009). The other significant human diseases caused by pathogenic corynebacteria include endocarditis, septicemia, urinary tract infections, wound infections and infections on abiotic surfaces such as catheters and shunts (Table 6.1). Specific corynebacterial species are also associated with infections in immunocompromised patients; these include *Corynebacterium jeikeium*, *Corynebacterium striatum*, and *Corynebacterium amycolatum* (Adderson et al., 2008; Otsuka et al., 2006; Schiffl et al., 2004).

C. diphtheriae is one of the most extensively investigated bacterial pathogens and provided key evidence for Koch's postulates on the germ theory. Likewise, the diphtheria toxin (DT) produced by toxigenic corynebacteria is an archetypal exotoxin. It not only served as a major paradigm for toxin research, but also helped to advance molecular immunology and the development of vaccines (Collier, 2001; Holmes, 2000; Popovic et al., 2000). Importantly, the genomic sequences of more and more

corynebacterial species are becoming available, starting with the publication of the *C. diphtheriae* NCTC13129 genome in 2003 (Cerdeno-Tarraga et al., 2003), thus providing a facile new path of molecular investigations of these pathogens. In fact, a major outcome from genome sequencing was the discovery of the pilus gene clusters in *C. diphtheriae* (Ton-That and Schneewind, 2003) that now serve as a major experimental model for the assembly and function of the gram-positive pili (Mandlik et al., 2008b). In this chapter, we first outline the clinical and molecular aspects of *C. diphtheriae* and diphtheria, followed by an account of the relatively little that is known to date about the molecular mechanisms of corynebacterial adherence with an emphasis on pili.

6.2 Corynebacterium Diphtheriae and Clinical Disease

C. diphtheriae was designated as the type species of the genus *Corynebacterium* (Barksdale, 1970). A club-shaped bacillus, its cell wall contains arabinose, galactose, manose, and a muramyl peptide made of L-Ala-D-Glu-meso α, ε-diaminopimelic acid (DAP)-D-Ala. The peptide subunits of the murein are crosslinked via D-Ala-meso-DAP bridges. Mycolic and mycolenic acids are also part of corynebacterial cell walls. Based on the morphology of corynebacterial colonies and the severity of infections, three distinct types of *C. diphtheriae* have been identified: *mitis* (smooth colonies causing mild infections), *gravis* (semirough colonies causing severe disease) and *intermedius* (dwarf smooth colonies associated with infections of intermediate severity). The sequenced strain NCTC13129 belongs to the *gravis* biotype, and the genome of this strain contains an integrated prophage called corynephage beta (36.5 kb), which encodes the diphtheria toxin. *C. diphtheriae* is known to confer toxigenicity by lysogenic conversion (Barksdale, 1970).

C. diphtheriae is transmitted by direct contact with infected persons or bodily fluids. The pathogen causes two forms of diphtheria: pharyngeal diphtheria (infection of the upper respiratory tract), which is common, and cutaneous diphtheria (infection of skin), which is much less frequent. Diphtheria is characterized by the formation of a pseudomembrane at the site of infection due to bacterial colonization and growth, toxin production, tissue damage and host immune response (Love and Murphy, 2006). Respiratory diphtheria presents as a sore throat with a low-grade fever. Left untreated, the developing pseudomembrane can cause complete airway obstruction, leading to suffocation and death (Hadfield et al., 2000).

Diphtheria toxin (DT) is a prototype A-B toxin composed of two subunits. The A subunit is the active toxin, whose uptake and release in the host cell cytoplasm is aided by the B subunit. The B subunit binds to the heparin-binding EGF-like growth factor (HB-EGF) on human epithelial cells (Naglich et al., 1992), and facilitates toxin uptake by endocytosis. As the pH of the endocytic vesicle drops, the A subunit is released in the cytoplasm. There, the toxin obliterates protein synthesis by ADP-ribosylating translation elongation factor 2 (EF-2), ultimately causing host cell death

(Mitamura et al., 1995; Naglich et al., 1992). The systemic effects of DT are most commonly manifested in the heart and nerves, leading to myocarditis, acute cardiac failure, and severe neuropathy (Hadfield et al., 2000).

6.3 History of Diphtheria

The earliest clinical description of diphtheria is found in writings of the ancient Greek physician Hippocrates during the fourth century C.E. (Shulman, 2004). During the modern era, the first recorded outbreak of diphtheria occurred in 1659 in Roxbury, MA. Episodic outbreaks occurred in 1686 in Virginia and in 1689 in Connecticut (Shulman, 2004). Decades later, between 1735 and 1740, a severe outbreak in New England killed nearly 40% of children under the age of 10. Records reveal that this epidemic took an estimated 5000 lives (2.5% of the total population at that time), sometimes wiping out entire families (English, 1985).

Bretonneau, who described the disease in great detail in 1826 (Semple, 1859), is credited with naming the bacterium diphtherite from a "Greek root [meaning] skin or hide, because the pharyngeal membrane in diphtheria often looked like a piece of leather" (English, 1985). Bretonneau also made the astonishing association of the organism releasing a "blood poison," similar to that found in jequirity seeds (Pappenheimer, 1984). This diphtheria-associated toxin was eventually isolated by Emile Roux and Alexander Yersin (Roux and Yersin, 1888), soon after Friedrich Loeffler demonstrated the etiological agent of diphtheria by growing it in pure culture (Kwantes, 1984; Loeffler, 1884). Interestingly, the diphtheria toxin works by a mechanism similar to the toxin found in jequirity seeds, abrin. Both toxins are AB-type toxins that block protein synthesis in human cells.

During this remarkable era in the history of modern medicine, Emil Adolf von Behring used antitoxin from a horse to successfully treat a human case of diphtheria. von Behring received the first ever Nobel prize in Medicine in 1901 "for his work on serum therapy and especially for its use against diphtheria, with which he opened up a new path in the field of medical science and gave the physician a powerful weapon with which to combat disease and death" (Winau and Winau, 2002), In 1913, von Behring developed the vaccine against DT, with widespread vaccinations beginning in 1920.

6.4 Epidemiology of Diphtheria

Before the development of the antitoxin and vaccination, there were more than 40 deaths per 100,000 people in the United States every year (Linder and Grove, 1947). By 1920, when vaccination began, that number had already been reduced to around 15 deaths per 100,000 with the use of the antitoxin alone. By 1950, the combination

of vaccination and antitoxin therapy had reduced the number of deaths to less than 1 per 100,000 (Grove and Hetzel, 1968). By 1980, there were less than 1 in 50 million cases, and since 2004, there have been no reported cases of diphtheria in the US (Wagner et al., 2009).

However, diphtheria outbreaks still occur in other regions of the world. The largest recent outbreak was in the independent states of the former Soviet Union, with more than 140,000 cases and a large number of deaths between 1991 and 1997 (Mattos-Guaraldi et al., 2003; Vitek and Wharton, 1998). More recently, the World Health Organization (WHO) reported an outbreak in a refugee camp in Afghanistan in 2003 where 6% of the infected population died.

Globally, there were over 7,000 cases of diphtheria reported to the WHO in 2008 (Papaioannou et al., 2009). Importantly, some of these have occurred in regions where greater than 95% of the population has been vaccinated. Cases are being reported worldwide where the infecting strains were non-toxigenic, i.e. those lacking the corynephage that encodes the diphtheria toxin. The fact that the vaccine is against the toxin and that the vaccinated population is at risk for infection by non-toxigenic strains of *C. diphtheriae* has led to a renewed interest in the mechanisms of pathogenesis of *C. diphtheriae*, as well as a systematic investigation of the virulence factors that mediate adherence, colonization and invasion (Mandlik et al., 2008b; Mattos-Guaraldi et al., 2000). A better understanding of the pathogenic mechanisms and the underlying virulence factors of corynebacterial infection would certainly provide the new therapeutic strategies required to combat not only diphtheria but also many other important diseases caused by *Corynebacterium* species (Table 6.1).

6.5 Adherence Factors of Corynebacteria

Compared to our knowledge of some bacterial pathogens, relatively little is known about corynebacterial adherence. Early studies of adhesion used various strains of *Corynebacterium* to test for autoagglutination, haemagglutination, neuraminidase activity, and trans-sialidase activity (reviewed by Mattos-Guaraldi et al., 2000); however, the mechanisms or proteins responsible for these phenotypes were never established. Similarly, many studies have examined the ability of various clinical isolates to adhere to epithelial cells (Colombo et al., 2001; Deacock et al., 1983; Hirata, et al., 2004; Honda and Yanagawa, 1975; Marty et al., 1991; Moreira et al., 2003; Silva De Souza et al., 2003), but the surface molecule involved remained unknown. One specific surface component of *C. diphtheriae* that may be involved in adhesion is a lipoglycan called CdiLAM. A recent study found that the *C. diphtheriae* cell surface contains CdiLAM, and that preincubation of bacteria with anti-CdiLAM significantly inhibited adherence to HEp-2 cells (Moreira et al., 2008). Another adhesive component identified in *C. diphtheriae* is a cell surface protein, DIP1281. Mutants lacking DIP1281 show over 3-fold reduction in

adherence to human pharyngeal cells compared to their isogenic parental strains (Bensing and Sullam, 2002). Importantly, the DIP1281 mutant was also defective in invasion.

6.5.1 Cell-Wall-Anchored Surface Proteins

Surface proteins are key virulence factors of most bacterial pathogens (Isberg, 1991). Gram-positive pathogens use a variety of surface proteins to bind to host tissues, evade the innate and acquired immune systems, and invade host epithelial and immune cells (Navarre and Schneewind, 1999). Many, but not all, surface proteins in gram-positive bacteria are covalently anchored to the cell wall peptidoglycan by a novel mechanism that is catalyzed by a sortase enzyme (Cossart and Jonquieres, 2000). The cell-wall-linked surface proteins contain a cell wall sorting signal (CWSS) with a conserved LPXTG motif at the carboxyl terminus. Sortases are transpeptidase enzymes that cleave the surface protein LPXTG motif between the threonine and glycine residues and tether the threonine-carboxyl group to the amino group of cell wall cross bridge within the lipid II peptidoglycan precursor (Mazmanian et al., 2001; Ton-That et al., 1999). First discovered in *Staphylococcus aureus* and named SrtA for surface protein sorting A (Mazmanian et al., 1999), sortases are ubiquitous in gram-positive bacteria. By comparative genomic analysis (Comfort and Clubb, 2004; Dramsi et al., 2005), sortase homologs have been classified into four groups based on primary sequence and putative function: class A (with *S. aureus* SrtA as the prototype), class B (*S. aureus* SrtB for iron acquisition), class C (pilin-specific sortases; see below) and class D (includes the housekeeping sortase SrtF of *C. diphtheriae*).

A homolog of the class A sortase is found in all corynebacterial genomes sequenced to date. This sortase catalyzes cell wall anchoring of surface proteins that contain the cell wall sorting signal with the LPXTG motif (see Ton-That et al., 2004a for the detailed mechanism of cell wall sorting). In *C. diphtheriae* strain NCTC13129, there are 17 genes encoding proteins with the LPXTG motif (Boekhorst et al., 2005) nine clustered at three genetic loci that are now known to encode the various pilus proteins (see below). The other LPXTG-containing proteins, scattered throughout the chromosome, are likely anchored to the cell wall as monomers and involved in host interactions based on their sequence features. This remains to be investigated.

During colonization, tissue-specific adhesion may involve bacterial cell surface carbohydrates that bind specific host cell surface lectins, and conversely, bacterial surface proteins that bind specific host cell surface carbohydrates or proteins. However, prior to colonization, the initial bacterial attachment is likely mediated by proteinaceous fibers (fimbriae or pili) that extend from the cell surface. Although these structures were first observed on the surface of *Corynebacterium renale* in 1968 by Yanagawa et al (Fig. 6.1a), the nature and mechanism of pilus assembly in corynebacteria, and in gram-positive bacteria in general, was not elucidated until 2003 (Ton-That and Schneewind, 2003). As described below, these

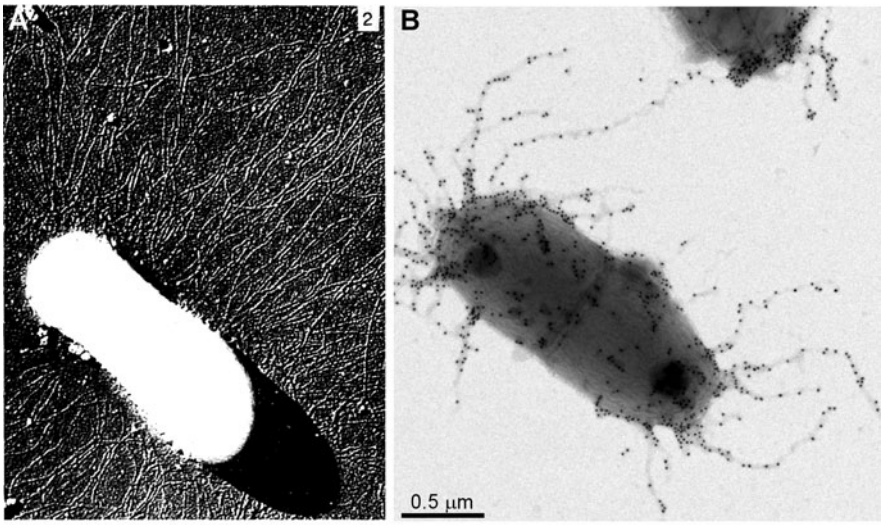

Fig. 6.1 Electron microscopy of corynebacterial pili. *Panel A* shows the first published image of corynebacterial pilus structures, reported by Yanagawa and colleagues in *Corynebacterium renale* (Yanagawa et al., 1968) (reprint with permission). *Panel B* shows *Corynebacterium diphtheriae* pili by immuno-electron microscopy. *C. diphtheriae* cells were incubated with a specific antiserum against SpaA, followed by 18 nm gold particles conjugated with IgG and 1% uranyl acetate (Courtesy of Chungyu Chang)

pili are covalent polymers of a distinct set of pilin proteins that are joined by pilus-specific sortases and ultimately attached to the cell wall by a non-polymerizing sortase.

6.5.2 *Sortase-Mediated Pilus Assembly in* Corynebacterium Diphtheriae

As mentioned, *C. diphtheriae* harbours three pilus gene clusters that encode a total of nine pilus proteins, named SpaA through SpaI (Spa for sortase-mediated pilus assembly), each containing the LPXTG motif. The three pilus loci also encode a total of five class C sortases, named SrtA through SrtE (Ton-That and Schneewind, 2004). The sixth sortase of *C. diphtheriae* (SrtF) is a class D sortase homolog (Dramsi et al., 2005), located at a different region of the chromosome, and is now referred to as the housekeeping sortase. The evidence that each pilus gene cluster encodes a distinct pilus structure was obtained by generating antibodies against individual pilins and using the antibodies in immunogold labeling and electron microscopy experiments (Fig. 6.1b), which revealed three distinct types of pili on the surface of *C. diphtheriae*. Consequently, these pili were named the SpaA-, SpaD-, and SpaH-type pili after the major pilin subunit from each pilus type (Gaspar

and Ton-That, 2006; Swierczynski and Ton-That, 2006; Ton-That and Schneewind, 2003). Electron microscopy and biochemical experiments established that each pilus is composed of three proteins, a major pilin subunit, which forms the shaft of the pilus, and two minor pilin subunits, which are located at the pilus tip and base. In the case of the SpaA-type pilus, SpaA forms the shaft, SpaC is the tip protein, and SpaB is found along the shaft and at the base (Mandlik et al., 2008a; Ton-That and Schneewind, 2003). Corynebacterial pili, as well as other gram-positive pili, remain intact upon treatment with formic acid or boiling in SDS, indicative of covalent linkage of pilus polymers (Mandlik et al., 2008b; Scott and Zahner, 2006; Telford et al., 2006).

The mechanism of sortase-mediated polymerization of pilus polymers was elucidated largely from an investigation of the SpaA-type pilus as the prototype. The SpaA pilus is produced from the gene cluster *spaA-srtA-spaB-spaC* (Fig. 6.2). In addition to the cell wall sorting signal, SpaA (and the other major pilin subunits, SpaD and SpaH) contains a pilin motif with the consensus sequence of WxxxVxVYPKN (Ton-That et al., 2004b). It was proposed that the pilin motif lends the conserved lysine residue to join two pilin subunits through a threonine-lysine isopeptide bond. Indeed, mutation of either the lysine or the threonine residue obliterates pilus assembly. According to the current model, the pilin-specific sortase,

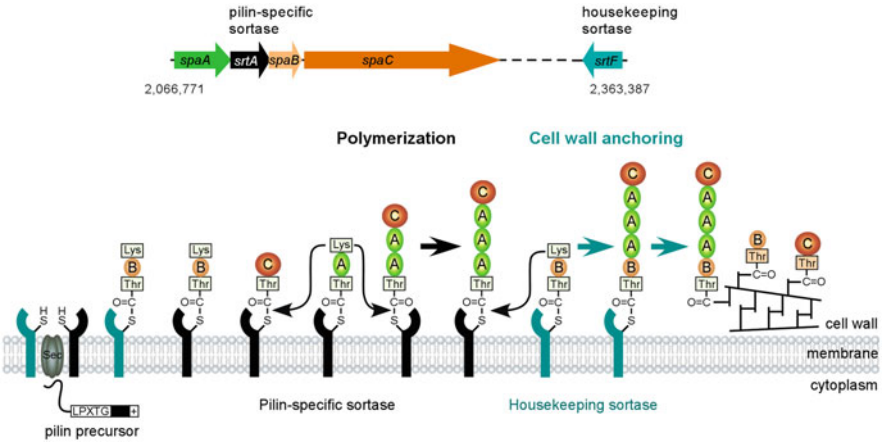

Fig. 6.2 Biphasic model of pilus assembly in *Corynebacterium diphtheriae*. This figure depicts the biphasic mechanism of pilus assembly in gram-positive bacteria, derived from studies of the archetype SpaA-type pili, encoded by the gene locus *spaA-srtA-spaB-spaC* (*top*). The model outlines the basic steps of pilus polymerization followed by the cell wall anchoring step. As shown, Spa pilin precursors are synthesized in the cytoplasm, translocated across the cytoplasmic membrane by the secretion system (Sec), and inserted into the membrane by the cell wall sorting signal. Membrane-bound sortase enzymes cleave the LPXTG motif of the CWSS and form acyl-enzyme intermediates. Pilus polymerization occurs via lysine-mediated transpeptidation reactions catalyzed by the pilin-specific sortase, SrtA (*black*). Polymerization ends by the incorporation of the base pilin SpaB via lysine-mediated transpeptidation. The housekeeping sortase, SrtF (*teal*), catalyzes anchoring of the resulting polymer to the cell wall peptidoglycan. *Curved arrows* indicate direction of nucleophilic attack. Modified from (Mandlik et al., 2008a) with permission

SrtA, cleaves the SpaA LPXTG motif between threonine and glycine and forms an acyl-enzyme intermediate with the substrate (Fig. 6.2). An acyl-enzyme SrtA-SpaC intermediate is also formed this way. Incorporation of SpaC at the tip occurs when the lysine residue of the SpaA pilin motif resolves the SrtA-SpaC intermediate by nucleophilic attack, leading to the formation of a SpaC-SpaA linkage (Fig. 6.2). Pilus extension or polymerization begins when additional SrtA-SpaA intermediates feed additional SpaA monomers to the growing SpaC-SpaA pilus *via* a lysine-mediated transpeptidation reaction. The existence of SrtA-Spa intermediates with varying polymer lengths has now been documented (Guttilla et al., 2009), and overproduction of the major pilin subunit has been shown to increase pilus length (Swierczynski and Ton-That, 2006). Pilus length is also increased when the minor pilin SpaB is absent; however, the resulting polymers are largely secreted into the culture medium (Mandlik et al., 2008a). Conversely, pilus length is shortened when SpaB is overproduced. These results led to the realisation of the biphasic mechanism of pilus assembly: pilus polymerization ends when SpaB is incorporated to the pilus base by a transpeptidation reaction that utilizes a lysine residue of SpaB (Mandlik et al., 2008a) and transfers the pilus from SrtA to SrtF (Fig. 6.2). SrtF then catalyzes the joining of the SpaB-terminated pilus polymer to the cell wall peptidoglycan *via* the lipid II molecule, similar to that of monomeric cell surface proteins (Swaminathan et al., 2007). There is evidence that SpaC and SpaB pilins are also anchored to the cell wall as monomers, especially if SpaA is absent (Mandlik et al., 2007) (Fig. 6.2).

6.5.3 Corynebacterial Pili as Adhesins

The first observation that corynebacterial pili may mediate host cell interactions was proposed in early studies with *C. renale* pili, which were shown to agglutinate trypsinized sheep red blood cells (Honda and Yanagawa, 1974). Over 30 years later, Mandlik et al. identified the minor pilins SpaB and SpaC of *C. diphtheriae* as specific adhesins that mediate efficient corynebacterial adherence to host pharyngeal cells (Mandlik et al., 2007). Wild type *C. diphtheriae* cells were shown to bind to human lung epithelial, laryngeal, and pharyngeal cells. However, mutants that lacked SrtA (and thus did not polymerize SpaA-type pili) showed over a 90% reduction in the ability to adhere to human pharyngeal cells. Surprisingly, mutants that lacked only the major pilin subunit, SpaA, showed a modest 10% reduction in adherence to these cells. This is in contrast to mutants that lacked either of the minor pilin subunits, SpaB or SpaC, which showed a 70–75% reduction in adherence. Additionally, latex beads coated with only SpaB or SpaC were sufficient to adhere to host pharyngeal cells, while beads coated with SpaA showed no binding. As mentioned above, SpaB and SpaC anchor to the cell wall as monomers independent of pilus structures. It is speculated that the long pili mediate initial attachment, whereas monomeric pilins on the bacterial surface may help to create an intimate zone of adhesion that allows for efficient delivery of toxin and other virulence factors, and may even play a significant role in host cell signaling.

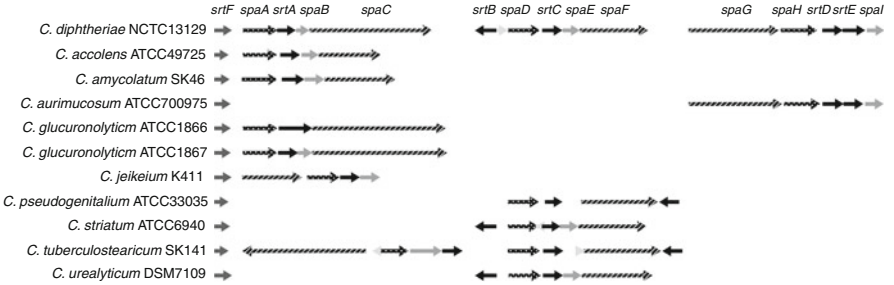

Fig. 6.3 Pilus gene clusters in pathogenic *Corynebacterium* species. The genome of *C. diphtheriae* NCTC13129 contains three pilus gene clusters, which encode for the SpaA-type pili (*spaA-srtA-spaB-spaC*), the SpaD-type pili (*srtB-spaD-srtC-spaE-spaF*) and the SpaH-type pili (*spaG-spaH-srtD-srtE-spaI*). The housekeeping sortase, *srtF*, is located elsewhere on the chromosome. Similar pilus gene clusters and the housekeeping sortase gene are found in many pathogenic species of the genus *Corynebacterium*. Shown in dots, hatches, and *grey* are genes encoding pilus shaft, tip protein and pilus base, respectively, based on *C. diphtheriae* pilus systems. Sortase genes are shown in *black* and *dark grey*, and other unknown genes are shown in *light grey*. All *arrows* are drawn to scale

Importantly, the host cell receptor(s) targeted by SpaB and SpaC have yet to be identified as well as the specific functions of the SpaD- and SpaH-type pili. Such studies are likely to be rewarding because some important corynebacterial pathogens do not contain the SpaA-type pilus but harbor only the SpaD-type or the SpaH-type pilus (Fig. 6.3).

6.6 Concluding Remarks

Pili serve as major adhesins in bacterial pathogens. Corynebacteria will continue to serve as a major paradigm to understand the mechanism of gram-positive pilus assembly and function in pathogenesis. One or more pilus gene clusters with specific types of pilins and pilus-specific sortases are found in the genomes of many different *Corynebacterium* species sequenced to date. It will be important to determine whether these gene clusters encode pilus structures, like the ones described in *C. diphtheriae*, and whether they are instrumental to bacterial interactions with specific host tissues. The well-developed genetics and biochemistry of the *C. diphtheriae* pilus system should provide the key methodology and experimental approaches to seed studies of the various pili in the different *Corynebacterium* species.

Acknowledgments We thank Anjali Mandlik, Anu Swaminathan, Andrew Gasper and Arlene Swierczynski, Arunima Mishra, Chenggang Wu and Chungyu Chang for their invaluable contributions to the studies of pili; supported by grants AI061381 and DE017382 from the NIH to HTT.

References

Adderson EE, Boudreaux JW, Hayden RT (2008) Infections caused by coryneform bacteria in pediatric oncology patients. Pediatr Infect Dis J 27:136–141

Barksdale L (1970) *Corynebacterium diphtheriae* and its relatives. Bacteriol Rev 34:378–422

Bensing BA, Sullam PM (2002) An accessory sec locus of *Streptococcus gordonii* is required for export of the surface protein GspB and for normal levels of binding to human platelets. Mol Microbiol 44:1081–1094

Boekhorst J, de Been MW, Kleerebezem M, Siezen RJ (2005) Genome-wide detection and analysis of cell wall-bound proteins with LPxTG-like sorting motifs. J Bacteriol 187:4928–4934

Bonmarin I, Guiso N, Le Fleche-Mateos A, Patey O, Patrick AD, Levy-Bruhl D (2009) Diphtheria: a zoonotic disease in France? Vaccine 27:4196–4200

Cerdeno-Tarraga AM, Efstratiou A, Dover LG, Holden MT, Pallen M, Bentley SD, Besra GS, Churcher C, James KD, De Zoysa A, Chillingworth T, Cronin A, Dowd L, Feltwell T, Hamlin N, Holroyd S, Jagels K, Moule S, Quail MA, Rabbinowitsch E, Rutherford KM, Thomson NR, Unwin L, Whitehead S, Barrell BG, Parkhill J (2003) The complete genome sequence and analysis of *Corynebacterium diphtheriae* NCTC13129. Nucleic Acids Res 31: 6516–6523

Collier RJ (2001) Understanding the mode of action of diphtheria toxin: a perspective on progress during the 20th century. Toxicon 39:1793–1803

Colombo AV, Hirata Júnior R, Rocha de Souza CM, Monteiro-Leal LH, Previato JO, Formiga LC, Andrade AF, Mattos-Guaraldi AL (2001) *Corynebacterium diphtheriae* surface proteins as adhesins to human erythrocytes. FEMS Microbiol Lett 197:235–239

Comfort D, Clubb RT (2004) A comparative genome analysis identifies distinct sorting pathways in gram-positive bacteria. Infect Immun 72:2710–2722

Cossart P, Jonquieres R (2000) Sortase, a universal target for therapeutic agents against gram-positive bacteria? Proc Natl Acad Sci USA 97:5013–5015

Coyle MB, Lipsky BA (1990) Coryneform bacteria in infectious diseases: clinical and laboratory aspects. Clin Microbiol Rev 3:227–246

Deacock SJ, Steward KA, Carne HR (1983) The role of adherence in determining the site of infection by *Corynebacterium diphtheriae*. J Hyg (Lond) 90:415–424

Dramsi S, Trieu-Cuot P, Bierne H (2005) Sorting sortases: a nomenclature proposal for the various sortases of Gram-positive bacteria. Res Microbiol 156:289–297

English PC (1985) Diphtheria and theories of infectious disease: centennial appreciation of the critical role of diphtheria in the history of medicine. Pediatrics 76:1–9

Funke G, von Graevenitz A, Clarridge JE 3rd, Bernard KA (1997) Clinical microbiology of coryneform bacteria. Clin Microbiol Rev 10:125–159

Gaspar AH, Ton-That H (2006) Assembly of distinct pilus structures on the surface of *Corynebacterium diphtheriae*. J Bacteriol 188:1526–1533

Grove RD, Hetzel AM (1968) Vital statistics rates in the United States 1940–1960. In: E. U.S. Department of Health E, and Welfare (ed) National Center for Health Statistics, Washington, DC, Amo Press, New York, NY, pp 587–596

Guttilla IK, Gaspar AH, Swierczynski A, Swaminathan A, Dwivedi P, Das A, Ton-That H (2009) Acyl enzyme intermediates in sortase-catalyzed pilus morphogenesis in gram-positive bacteria. J Bacteriol 191:5603–5612

Hadfield TL, McEvoy P, Polotsky Y, Tzinserling VA, Yakovlev AA (2000) The pathology of diphtheria. J Infect Dis 181(Suppl 1):S116–S120

Hirata Júnior R, Souza SMS, Rocha desouza CM, Andrade AF, Monteiro-Leal LH, Formiga LC, Mattos-Guaraldi AL (2004) Patterns of adherence to HEp-2 cells and actin polymerisation by toxigenic *Corynebacterium diphtheriae* strains. Microb Pathog 36:125–130

Holmes RK (2000) Biology and molecular epidemiology of diphtheria toxin and the tox gene. J Infect Dis 181(Suppl 1):S156–S167

Honda E, Yanagawa R (1974) Agglutination of trypsinized sheep erythrocytes by the pili of *Corynebacterium renale*. Infect Immun 10:1426–1432

Honda E, Yanagawa R (1975) Attachment of *Corynebacterium renale* to tissue culture cells by the pili. Am J Vet Res 36:1663–1666

Isberg RR (1991) Discrimination between intracellular uptake and surface adhesion of bacterial pathogens. Science 252:934–938

Kwantes W (1984) Diphtheria in Europe. J Hyg (Lond) 93:433–437

Linder FE, Grove RD (1947) Vital statistics rates in the United States 1900–1940. In: E. U.S. Department of Health E, and Welfare (ed). National Center for Health Statistics, Washington, DC, Amo Press, New York, NY, pp 559–578

Loeffler F (1884) Untersuchungen über die Bedeutung der Mikroorganismen für die Enstehung der Diphtherie beim Menschen, bei der Taube und beim Kalbe. Mitt Klin Gesundheitsamte Berlin 2:421–499

Love JF, Murphy JR (2006) Corynebacterium diphtheriae: iron-mediated activation of DtxR and regulation of diphtheria toxin expression. In: Fischetti VA, Novick RP, Ferretti JJ, Portnoy DA, Rood JI (eds) Gram-positive pathogens. ASM Press, Washington, DC, pp 726–737

Mandlik A, Das A, Ton-That H (2008a) The molecular switch that activates the cell wall anchoring step of pilus assembly in gram-positive bacteria. Proc Natl Acad Sci USA 105:14147–14152

Mandlik A, Swierczynski A, Das A, Ton-That H (2007) *Corynebacterium diphtheriae* employs specific minor pilins to target human pharyngeal epithelial cells. Mol Microbiol 64:111–124

Mandlik A, Swierczynski A, Das A, Ton-That H (2008b) Pili in gram-positive bacteria: assembly, involvement in colonization and biofilm development. Trends Microbiol 16:33–40

Marty N, Agueda L, Lapchine L, Clave D, Henry-Ferry S, Chabanon G (1991) Adherence and hemagglutination of *Corynebacterium* group D2. Eur J Clin Microbiol Infect Dis 10:20–24

Mattos-Guaraldi AL, Duarte Formiga LC, Pereira GA (2000) Cell surface components and adhesion in *Corynebacterium diphtheriae*. Microbes Infect 2:1507–1512

Mattos-Guaraldi AL, Moreira LO, Damasco PV, Hirata Júnior R (2003) Diphtheria remains a threat to health in the developing world–an overview. Mem Inst Oswaldo Cruz 98:987–993

Mazmanian SK, Liu G, Ton-That H, Schneewind O (1999) *Staphylococcus aureus* sortase, an enzyme that anchors surface proteins to the cell wall. Science 285:760–763

Mazmanian SK, Ton-That H, Schneewind O (2001) Sortase-catalysed anchoring of surface proteins to the cell wall of *Staphylococcus aureus*. Mol Microbiol 40:1049–1057

Mitamura T, Higashiyama S, Taniguchi N, Klagsbrun M, Mekada E (1995) Diphtheria toxin binds to the epidermal growth factor (EGF)-like domain of human heparin-binding EGF-like growth factor/diphtheria toxin receptor and inhibits specifically its mitogenic activity. J Biol Chem 270:1015–1019

Moreira LO, Andrade AF, Vale MD, Souza SMS, Hirata Júnior R, Asad LM, Asad NR, Monteiro-Leal LH, Previato JO, Mattos-Guaraldi AL (2003) Effects of iron limitation on adherence and cell surface carbohydrates of *Corynebacterium diphtheriae* strains. Appl Environ Microbiol 69:5907–5913

Moreira LO, Mattos-Guaraldi AL, Andrade AF (2008) Novel lipoarabinomannan-like lipoglycan (CdiLAM) contributes to the adherence of *Corynebacterium diphtheriae* to epithelial cells. Arch Microbiol 190:521–530

Naglich JG, Metherall JE, Russell DW, Eidels L (1992) Expression cloning of a diphtheria toxin receptor: identity with a heparin-binding EGF-like growth factor precursor. Cell 69: 1051–1061

Navarre WW, Schneewind O (1999) Surface proteins of gram-positive bacteria and mechanisms of their targeting to the cell wall envelope. Microbiol Mol Biol Rev 63:174–229

Otsuka Y, Ohkusu K, Kawamura Y, Baba S, Ezaki T, Kimura S (2006) Emergence of multidrug-resistant *Corynebacterium striatum* as a nosocomial pathogen in long-term hospitalized patients with underlying diseases. Diagn Microbiol Infect Dis 54:109–114

Papaioannou W, Gizani S, Haffajee AD, Quirynen M, Mamai-Homata E, Papagiannoulis L (2009) The microbiota on different oral surfaces in healthy children. Oral Microbiol Immunol 24: 183–189

Pappenheimer AM Jr (1984) The diphtheria bacillus and its toxin: a model system. J Hyg (Lond) 93:397–404

Popovic T, Mazurova IK, Efstratiou A, Vuopio-Varkila J, Reeves MW, De Zoysa A, Glushkevich T, Grimont P (2000) Molecular epidemiology of diphtheria. J Infect Dis 181(Suppl 1):S168–S177

Roux E, Yersin A (1888) Contribution à l'étude de la diphtérie. Annales de l'Institut Pasteur 2: 629–661

Schiffl H, Mucke C, Lang SM (2004) Exit-site infections by non-diphtheria corynebacteria in CAPD. Perit Dial Int 24:454–459

Scott JR, Zahner D (2006) Pili with strong attachments: gram-positive bacteria do it differently. Mol Microbiol 62:320–330

Semple RH (1859) Memoirs on Diphtheria: from the writings of Bretonneau, P., Guersant, Trousseau, Bouchut, Empis, and Daviot. The New Sydenham Society, London

Shulman ST (2004) The history of pediatric infectious diseases. Pediatr Res 55:163–176

Silva De Souza SM, Hirata Júnior R, Moreira LO, Gomes ML, Braga De Andrade AF, Bernardo-Filho M, Mattos-Guaraldi AL (2003) Influence of stannous chloride on the adhesive properties of *Corynebacterium diphtheriae* strains. Int J Mol Med 12:657–661

Swaminathan A, Mandlik A, Swierczynski A, Gaspar A, Das A, Ton-That H (2007) Housekeeping sortase facilitates the cell wall anchoring of pilus polymers in *Corynebacterium diphtheriae*. Mol Microbiol 66:961–974

Swierczynski A, Ton-That H (2006) Type III pilus of corynebacteria: Pilus length is determined by the level of its major pilin subunit. J Bacteriol 188:6318–6325

Telford JL, Barocchi MA, Margarit I, Rappuoli R, Grandi G (2006) Pili in Gram-positive pathogens. Nat Rev Microbiol 4:509–519

Ton-That H, Liu G, Mazmanian SK, Faull KF, Schneewind O (1999) Purification and characterization of sortase, the transpeptidase that cleaves surface proteins of *Staphylococcus aureus* at the LPXTG motif. Proc Natl Acad Sci USA 96:12424–12429

Ton-That H, Marraffini LA, Schneewind O (2004a) Protein sorting to the cell wall envelope of Gram-positive bacteria. Biochim Biophys Acta 1694:269–278

Ton-That H, Marraffini LA, Schneewind O (2004b) Sortases and pilin elements involved in pilus assembly of *Corynebacterium diphtheriae*. Mol Microbiol 53:251–261

Ton-That H, Schneewind O (2003) Assembly of pili on the surface of *Corynebacterium diphtheriae*. Mol Microbiol 50:1429–1438

Ton-That H, Schneewind O (2004) Assembly of pili in Gram-positive bacteria. Trends Microbiol 12:228–234

Vitek CR, Wharton M (1998) Diphtheria in the former Soviet Union: reemergence of a pandemic disease. Emerg Infect Dis 4:539–550

Wagner KS, Stickings P, White JM, Neal S, Crowcroft NS, Sesardic D, Efstratiou A (2009) A review of the international issues surrounding the availability and demand for diphtheria antitoxin for therapeutic use. Vaccine 28:14–20

Winau F, Winau R (2002) Emil von Behring and serum therapy. Microbes Infect 4:185–188

Yanagawa R, Otsuki K, Tokui, T (1968) Electron microscopy of fine structure of *Corynebacterium renale* with special reference to pili. Jpn J Vet Res 16:31–37

Chapter 7
Adhesion Mechanisms of Staphylococci

Christine Heilmann

Abstract Staphylococcal adherence to an either biotic or abiotic surface is the critical first event in the establishment of an infection with these serious pathogens. Especially *Staphylococcus aureus* harbours a variety of proteinaceous and non-proteinaceous adhesins that mediate attachment to a multitude of host factors, such as extracellular matrix and plasma proteins and human host cells, or intercellular adhesion, which is essential for biofilm accumulation. Proteinaceous adhesins may be classified in covalently surface-anchored proteins of the MSCRAMM (microbial surface components recognizing adhesive matrix molecules) family or in proteins that are surface-associated by different means, such as ionic or hydrophobic interactions. Non-covalently surface-associated proteins include the autolysin/adhesins, proteins of the SERAM (secretable expanded repertoire adhesive molecules) family, or membrane-spanning proteins. Non-proteinaceous adhesins comprise the polysaccharide PIA (polysaccharide intercellular adhesin) and wall teichoic and lipoteichoic acids. The features and functions of surface and surface-associated protein adhesins as well as of non-proteinaceous adhesins are discussed.

7.1 Introduction

Besides being harmless inhabitants of the human skin and mucous membranes, the Gram-positive staphylococci belong to the most important pathogens causing diseases ranging from mild skin infections to serious and life-threatening syndromes, such as endocarditis, osteomyelitis, pneumonia, and sepsis (Ziebuhr, 2001). The coagulase-positive species *Staphylococcus aureus* usually causes more acute infections associated with the colonization of the host tissue, but is also a common cause of foreign body-associated infections and known to cause persisting and relapsing infections (Lentino, 2003). Infections due to coagulase-negative species

C. Heilmann (✉)
Institute for Medical Microbiology, University Hospital of Münster, 48149 Münster, Germany
e-mail: heilmac@uni-muenster.de

D. Linke, A. Goldman (eds.), *Bacterial Adhesion*, Advances in Experimental Medicine and Biology 715, DOI 10.1007/978-94-007-0940-9_7,

typically are more subacute or even chronic and usually require a predisposed or immunocompromised host, for example patients with indwelling medical devices. *Staphylococcus epidermidis* is the most frequent coagulase-negative species isolated from medical device-associated infections, such as prosthetic heart valves and orthopaedic implants (Lentino, 2003). The fact that *S. aureus* is more virulent is reflected by its production of numerous virulence factors, i.e. a variety of adhesins, extracellular enzymes, and toxins. In contrast, the capacity of *S. epidermidis* to produce adhesins and especially to secrete extracellular enzymes and toxins is much less pronounced.

To become a pathogen, staphylococci have to gain access to the human host usually by adhering to biotic surfaces, such as components of the extracellular matrix or host tissue, or to abiotic surfaces, such as those of medical devices. Upon adherence, the bacteria proliferate and colonize the respective biotic or abiotic surface by forming a biofilm. The formation of a biofilm can be differentiated in two phases: the primary adherence phase, followed by the accumulation phase. The latter requires intercellular adherence to form the multilayered biofilm. Intercellular adherence may be mediated by polysaccharide- or protein-factors. Within the biofilms, the staphylococci are embedded in a polysaccharide and/or proteinaceous matrix with wall teichoic acids, host factors and extracellular DNA in addition. All these protect the bacteria against the host immune system as well as antibiotic treatment (Heilmann and Götz, 2010). As a consequence, removal of the medical device is frequently necessary to eradicate the infection in implant-associated infections. Some staphylococcal adhesins are not only involved in adherence and colonization, but also in internalization by human host cells. Internalized staphylococci are protected against the human immune system as they "hide" within the host cells representing a potential reservoir for recurrent infections.

Compared to *S. aureus*, much less is known about adhesins and adhesive mechanisms in coagulase-negative staphylococci except for some aspects of *S. epidermidis* biofilm formation. Therefore, this chapter mainly deals with the presentation of *S. aureus* adherence mechanisms. The adhesive mechanisms involved in *S. aureus* biofilm formation on abiotic or biotic surfaces are summarized in Fig. 7.1.

7.2 Surface Adhesion Proteins of *Staphylococcus aureus*

S. aureus is able to directly adhere to host tissue, such as the host epithelium or endothelium and binds to a multitude of components of the extracellular matrix, such as fibronectin (Fn), fibrinogen (Fg), vitronectin (Vn), thrombospondin, bone-sialoprotein, elastin, collagen, and von Willebrand factor. Moreover, implanted material rapidly becomes coated with plasma and extracellular matrix proteins or platelets. Thus, all these host factors could serve as specific receptors for colonizing bacteria. Proteinaceous surface adhesins of *S. aureus* can either be covalently linked to the cell wall peptidoglycan or surface-associated by different means, such as ionic or hydrophobic interactions (summarized in Table 7.1).

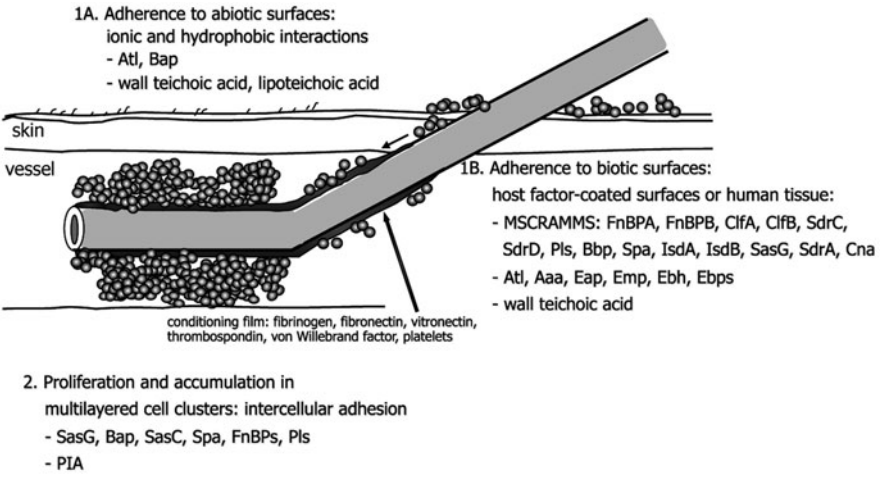

Fig. 7.1 Overview on the complex adhesive mechanisms involved in the different phases of *S. aureus* biofilm formation. *S. aureus* factors involved in the colonization of a catheter surface or host tissue, such as the extracellular matrix and the human endothelium or epithelium are given

7.2.1 Covalently-Linked Cell Surface Proteins (MSCRAMMs)

Most *S. aureus* surface adhesins are covalently linked to the cell wall peptidoglycan and belong to the MSCRAMM (microbial surface components recognizing adhesive matrix molecules) protein family (Clarke and Foster, 2006). Covalently-linked MSCRAMMs have a common overall organization including an N-terminal signal peptide, an exposed ligand-binding domain, which is often followed or interrupted by direct repeated sequences, a characteristic hydrophobic cell wall- and membrane-spanning domain, a C-terminal LPXTG motif responsible for cell-wall anchorage, and a positively charged tail. In most cases, cell-wall anchorage is mediated by a membrane-bound transpeptidase, called sortase (SrtA) that cleaves the peptide bond between the threonine and glycin of the LPXTG motif and covalently links the carboxyl group of threonine with the amino group of peptidoglycan cross-bridges (Schneewind et al., 1993). *S. aureus* genomes contain more than 20 genes encoding surface-anchored adhesins. In contrast, there are only 12 genes encoding covalently-linked MSCRAMMs in the *S. epidermidis* RP62A genome. MSCRAMMs can bind to one or more host extracellular matrix and plasma protein and a given host factor can be bound by more than one staphylococcal adhesin. However, not the ligands or functions of all MSCRAMMs have been identified yet.

7.2.1.1 Fibronectin-Binding Proteins (FnBPA and FnBPB)

S. aureus produces two closely related covalently-linked Fn-binding MSCRAMMs, FnBPA and FnBPB, which are encoded by *fnbA* and *fnbB*, respectively (Jönsson

Table 7.1 Surface and surface-associated proteins of *S. aureus*

Gene	Product	Ligand specificity/Function	Reference
Covalently-linked surface proteins			
bbp	Bbp	Bone sialoprotein	Tung et al. (2000)
bap	Bap	Attachment to polystyrene; intercellular adhesion; prevents binding to Fg, Fn, and host tissue and internalization	Cucarella et al. (2002)
clfA	ClfA	Fg; platelet aggregation	McDevitt et al. (1997), O'Brien et al. (2002a)
clfB	ClfB	Fg, cytokeratin 10, desquamated nasal epithelial cells; platelet aggregation	Corrigan et al., (2009), Ni Eidhin et al. (1998), O'Brien et al. (2002a, b)
cna	Cna	collagen	Patti et al. (1995)
fnbA	FnBPA	Fn, Fg, elastin; intercellular adhesion	Signas et al. (1989), Roche et al. (2004), Wann et al. (2000), Vergara-Irigaray et al. (2009)
fnbB	FnBPB	Fn, elastin; intercellular adhesion	Jönsson et al. (1991), Roche et al. (2004), Vergara-Irigaray et al. (2009)
isdA	IsdA	Fg, Fn, fetuin, haemoglobin, transferrin, haemin, desquamated nasal epithelial cells	Clarke and Foster (2006), Mazmanian et al. (2003)
isdB	IsdB	haemoglobin, haemin, platelet integrin GPIIb/IIIa	Mazmanian et al. (2003), Miajlovic et al. (2010)
isdC	IsdC	Haemin	Mazmanian et al. (2003)
isdH	IsdH	Haptoglobulin, haptoglobulin-haemoglobin complex	Dryla et al. (2003)
sasA (*sraP*)	SasA (SraP)	Binding to platelets	Siboo et al. (2008)
sasB	SasB	unknown	Roche et al. (2003a)
sasC	SasC	Attachment to polystyrene; intercellular adhesion	Schroeder et al. (2009)
sasD	SasD	unknown	Roche et al. (2003a)
sasF	SasF	unknown	Roche et al. (2003a)

Table 7.1 (continued)

Gene	Product	Ligand specificity/Function	Reference
sasG	SasG	Binding to nasal epithelial cells; intercellular adhesion; prevents binding to Fg, Fn, cytokeratin 10, IgG	Corrigan et al. (2007), Roche et al. (2003b)
sasK	SasK	unknown	Roche et al. (2003a)
sasH	SasH	unknown	Roche et al. (2003a)
sdrC	SdrC	Binding to nasal epithelial cells and β-neurexin	Barbu et al. (2010), Corrigan et al. (2009)
sdrD	SdrD	Binding to nasal epithelial cells	Corrigan et al. (2009)
sdrE	SdrE	Platelet aggregation	O'Brien et al. (2002a)
spa	Protein A (Spa)	IgG, IgM, von Willebrand Factor, platelet receptor gC1qR; bacterial cell aggregation	Chavakis et al. (2005), Nguyen et al. (2000), Merino et al. (2009)
pls	Pls	Promotes binding to nasal epithelial cells, glycolipids; intercellular adhesion; prevents binding to IgG and Fn and internalization	Huesca et al. (2002), Roche et al. (2003b), Hussain et al. (2009)
Non covalently-linked surface-associated proteins			
atl	Atl	Attachment to polystyrene, Fg, Fn, Vn, endothelial cells	Hirschhausen et al. (2010)
aaa	Aaa	Fg, Fn, Vn	Heilmann et al. (2005)
eap	Eap (Map, P70)	Fg, Fn, Vn, collagen, ICAM-1, eukaryotic cell surfaces, staphylococcal cells; promotes uptake of *S. aureus* by eukaryotic cells	Chavakis et al. (2005)
emp	Emp	Fg, Fn, Vn, collagen	Chavakis et al. (2005)
ebh	Ebh	Fn	Clarke and Foster (2006)
ebps	Ebps	Elastin	Downer et al. (2002)

et al., 1991; Signas et al., 1989). The Fn-binding activity of both proteins has been localized to a C-terminally located and highly conserved repeat domain (D repeats) that is composed of an approximately 40-amino acid unit repeated four times (D1 to D4) with the repeat D4 being incomplete (shown for FnBPA in Fig. 7.2). A fifth repeat (Du) is located approximately 100 residues N-terminal to D1. Only the *fnbA/fnbB* double-knockout mutant of *S. aureus* 8325-4 showed strongly reduced

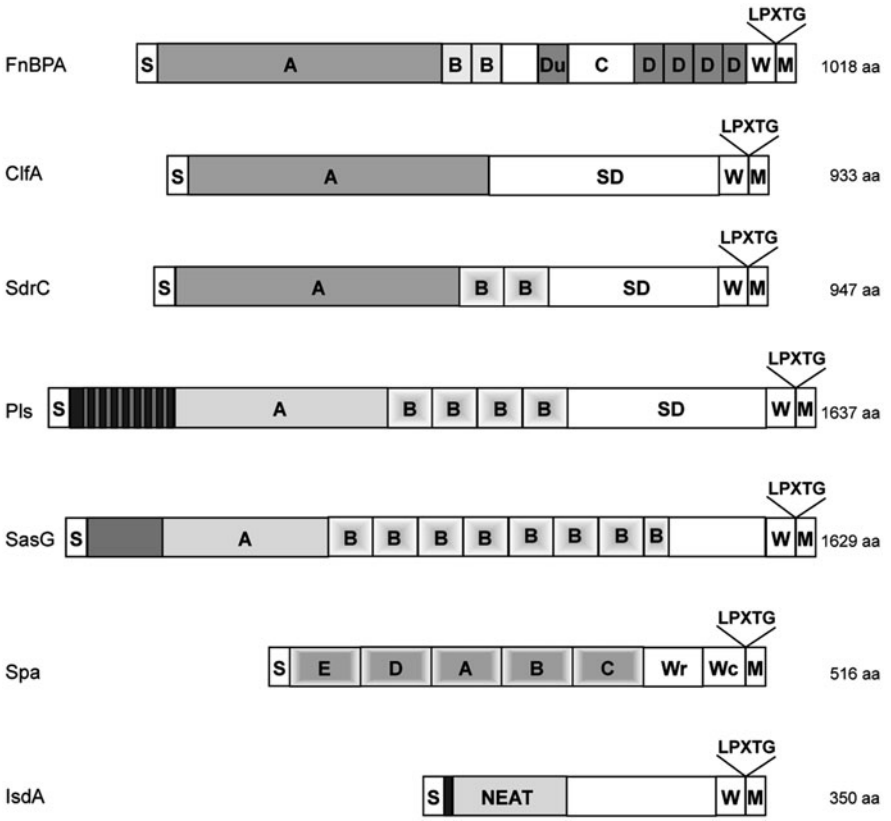

Fig. 7.2 Schematic model of selected *S. aureus* MSCRAMMs. The positions of the signal sequences (S), the ligand-binding A domains (A), the B repeats (B), the serine-aspartate (SD) dipeptide repeats (or region R), the wall (W) and membrane (M)-spanning regions including positively charged residues, and the LPXTG motifs are shown. The domains are defined in the text. The A domains of FnBPA, ClfA, and SdrC are homologous. Moreover, the A domains of Pls and SasG as well as the B repeats of SdrC, Pls, and SasG are homologous. The sizes of the proteins may vary among different *S. aureus* strains. FnBPA: D, Fn-binding D repeats. C, non-repeated region with unknown function. Spa: E, D, A, B, C, IgG-binding domains; Wr is composed of an octapeptide repeat, and Wc is a non-repeated region. IsdA: ligand-binding NEAT (near iron transporters) domain

Fn-binding activity (Greene et al., 1995). Complementation of the *fnbA/fnbB* double mutant with either plasmid-encoded *fnbA* or *fnbB* was able to fully restore the Fn-binding activity. This indicates that both proteins are expressed in *S. aureus* and contribute to the ability of strain 8325-4 to adhere to Fn-coated surfaces. The approximately 500-residue N-terminal domains (A domain) of FnBPA and FnBPB share only 40% sequence identity. The A domain of FnBPA exhibits substantial sequence identity to the A domains of the Fg-binding proteins ClfA and ClfB, and like them has been shown to contain Fg-binding activity (Wann et al., 2000). Recombinant FnBPA seems to bind to the same binding site in the γ-chain of Fg like ClfA and can compete with ClfA for binding to both immobilized and soluble Fg. Moreover, the A domains of both FnBPA and FnBPB can bind to immobilized elastin (Roche et al., 2004). Recently, the structural organization of FnBPA has been revised with the Fn-binding domain consisting of 11 tandem repeats. Each repeat is predicted to interact with Fn by a tandem β-zipper mechanism (Schwarz-Linek et al., 2003).

Most *S. aureus* strains carry both *fnb* genes, but there seems to be no difference in Fn-binding activity between the strains carrying one or two *fnb* genes (Greene et al., 1995). However, a study analysing a larger collection of isolates from infected patients indicated that *S. aureus* strains associated with invasive disease were more likely to encode both *fnb* genes (Peacock et al., 2000).

Besides being multifunctional adhesins, the FnBPs are efficient mediators of *S. aureus* internalization. Classically, staphylococci have been regarded as extracellular pathogens. However, it is now widely accepted that *S. aureus* can also be internalized by human host cells and replicate intracellularly. The FnBP-mediated mechanism of *S. aureus* internalization requires Fn as bridging molecule and the $\alpha_5\beta_1$ integrins as the host cell receptor resulting in signal transduction, tyrosine kinase activity, and cytosceletal rearrangements (Chavakis et al., 2005).

There have been contrasting results regarding the importance of the FnBPs in virulence (Clarke and Foster, 2006). Previous results suggested that the FnBPs do not play a significant role in infection, i.e. in the induction and/or propagation of endocarditis or in the development of septic arthritis by *S. aureus*. In a rat model of pneumonia, an *fnbA*/*fnbB* mutant even showed increased virulence compared to its wild-type strain. However, expression of *fnbA* or *fnbB* in the non-pathogenic *Staphylococcus carnosus* significantly increased adherence to intact endothelium in vivo and *Lactococcus lactis* cells expressing *fnbA* revealed a considerably higher infectivity in an experimental rat endocarditis model in comparison with *L. lactis* cells harbouring an empty vector. The latter findings were further supported by the observation that FnBPA and FnBPB mediate adherence to platelets and induce platelet activation (Chavakis et al., 2005). Moreover, the FnBPs were found to play an important role in the induction of systemic inflammation (Clarke and Foster, 2006). Most recently, increased efficiency of host cell invasion and virulence in a murine sepsis model mediated by FnBPA has been associated with an increased number of the 11 Fn-binding tandem repeats (Edwards et al., 2010).

7.2.1.2 Fibrinogen-Binding Proteins (ClfA and ClfB) and the Sdr Protein Family

Fibrinogen-Binding Proteins: ClfA and ClfB

S. aureus produces several proteins that can specifically bind to Fg. Two of them are the covalently-linked Fg-binding MSCRAMMs, clumping factors A and B (ClfA and ClfB), which are encoded by *clfA* and *clfB*, respectively (McDevitt et al., 1997, Ni Eidhin et al., 1998). The Fg-receptor was first recognized as a factor that mediates cell clumping in the presence of human plasma and therefore was named clumping factor. *clfA* mutants not only failed to form clumps in soluble Fg, but also adhered poorly to surface-immobilized Fg. Additionally to the common features of all MSCRAMMs, ClfA and ClfB are characterized by the region R that consists of repeating serine-aspartate (SD) dipeptides and is located between the wall-spanning domain and the ligand-binding domain A (shown for ClfA in Fig. 7.2) Thus, ClfA and ClfB are members of an MSCRAMM subfamily, the SD repeat-containing (Sdr) protein family.

The predicted 92 kDa ClfA has significant sequence similarity with the FnBPs, especially in the N-terminal region A. The Fg-binding activity of ClfA was mapped to a 218-residue domain within the ~500-residue region A (332–550). In a later study, the adjacent residues Glu^{526} and Val^{527} were identified as being important for the Fg-binding activity (Hartford et al., 2001). Despite similar functions and structural organization, the A domains of ClfA and ClfB are only 26% identical. ClfA exclusively binds to the Fg γ-chain with the binding site for ClfA located within the C-terminus of the γ-chain. In contrast, ClfB binds to the α- and β-chains of Fg (McDevitt et al., 1997, Ni Eidhin et al., 1998). A recombinantly expressed truncated ClfA protein comprising residues 221–550 inhibits ADP-induced, Fg-dependent platelet aggregation in a concentration-dependent manner and moreover competes for platelet adhesion to immobilized Fg under shear stress indicating that the platelet receptor and ClfA binding sites on Fg overlap. A later study indicated that ClfA also mediates direct binding to platelets by interacting with a 118 kDa platelet membrane receptor (Siboo et al., 2001). Furthermore, ClfA as well as ClfB are able to aggregate platelets, which is thought to play a role in the establishment of experimental endocarditis (O'Brien et al., 2002a). Platelet aggregation mediated by ClfA and ClfB occurs in a Fg-dependent manner. However, ClfA as well as ClfB can cause platelet aggregation in a Fg-independent manner that requires IgG and complement deposition (Loughman et al., 2005, Miajlovic et al., 2007).

ClfB binds also to human desquamated nasal epithelial cells and to cytokeratin 10, which was shown to be present on the surface of these cells, suggesting that ClfB may be an important factor in *S. aureus* nasal colonization (O'Brien et al., 2002b). A remarkable difference between ClfA and ClfB is their expression pattern, with ClfB being only detectable on cells grown to the early exponential phase, but absent from cells from late exponential phase or stationary phase cultures.

The binding of ClfA as well as ClfB to Fg is regulated by the divalent cations Ca^{2+} and Mn^{2+} (Clarke and Foster, 2006). Both cations inhibit ClfA-mediated clumping of *S. aureus* in the presence of soluble Fg as well as the interaction of a

recombinant ClfA subdomain with a peptide resembling the C-terminal Fg γ-chain. In agreement with this, ClfA harbours a putative EF-hand motif within the A region (310–321) that mediates both regulation by Ca^{2+} and ligand binding.

The ClfA region A is composed of three domains (N1, N2, and N3). The crystal structure of the Fg-binding segment (residues 221–559), which contains two of the domains (N2N3) demonstrates that each domain adopts an IgG-like fold (Deivanayagam et al., 2002).

Consistent with its platelet-binding and -aggregation function, ClfA has been shown to be a virulence factor in a rabbit and rat infective endocarditis model as well as in a mouse model of septic arthritis. Moreover, active and passive immunization studies suggested ClfA as a suitable vaccine compound and novel anti-staphylococcal agents have been proposed based on a structural model of the ClfA-Fg interaction (Clarke and Foster, 2006, Ganesh et al., 2008).

Sdr protein Family: SdrC, SdrD, and SdrE

Other members of the *S. aureus* Sdr-protein family are SdrC, SdrD, and SdrE (Clarke and Foster, 2006). The Sdr proteins are predicted to have a similar structural organization like ClfA and ClfB. Additionally, they contain two (SdrC), five (SdrD), or three (SdrE) B repeats with 110–129 residues per repeat, which interconnect the regions A and R (shown for SdrC in Fig. 7.2). Like ClfA and ClfB, SdrE induces platelet aggregation while SdrC and SdrD play a role in adherence to human desquamated nasal epithelial cells (O'Brien et al., 2002a, Corrigan et al., 2009). Moreover, by using the phage display technique, the N2N3 domain of SdrC was recently found to bind to β-neurexin (Barbu et al., 2010).

Sdr protein Family: Pls

Pls "plasmin sensitive" contains short N-terminal repeats and four B repeats (Fig. 7.2). It has a surprisingly divergent function. On the one hand, Pls binds to cellular lipids and glycolipids and promotes bacterial cell-cell interaction as well as adherence to nasal epithelial cells (Huesca et al., 2002, Roche et al., 2003b). On the other hand, Pls prevents binding of *S. aureus* to immunoglobulin (Ig) G, soluble and immobilized Fn, as well as internalization by human host cells probably by steric hindrance (Hussain et al., 2009).

Sdr protein Family: Bbp

The 97 kDa bone sialoprotein-binding protein Bbp has similarity with SdrC, SdrD, and SdrE (Tung et al., 2000). Bbp was identified from *S. aureus* strains associated with bone and joint infections and found to specifically interact with bone sialoprotein, which is a glycoprotein of bone and dentine extracellular matrix. Further studies indicated that Bbp is immunogenic and expressed during infection suggesting an important role in the pathogenesis of osteomyelitis.

7.2.1.3 Protein A (Spa)

Protein A (Spa) was the first *S. aureus* protein identified and has been used as the model system to study sortase-mediated cell wall anchoring (Schneewind et al., 1993). Protein A contains five N-terminally located approximately 60-residue long tandem repeats (designated E, D, A, B, and C), which bind to the Fc portion of immunoglobulins (Ig) G, leading to reduced antibody-mediated opsonisation. Consequently, the inhibition of phagocytosis has been proposed to be the basic contribution of protein A to virulence. However, it is now clear that its function in pathogenesis is more complex than previously thought. Protein A also binds to both soluble and immobilized vWF, a large multimeric glycoprotein that mediates platelet adhesion at sites of endothelial damage, which is thought to play a role in endovascular infection (Chavakis et al., 2005). Spa has also been identified to directly interact with platelets via binding to the platelet receptor gC1qR/p33 (Nguyen et al., 2000). Moreover, protein A can bind to TNFR1, which is a receptor for tumour-necrosis factor-α (TNF-α) widely distributed on the airway epithelium and stimulate an inflammatory response in airway epithelial cells. Thus, the protein A-TNFR1 signalling pathway is thought to have a central function in the pathogenesis of staphylococcal pneumonia (Gomez et al., 2004).

7.2.1.4 Iron-Regulated Surface Determinants (IsdA, IsdB, IsdC, IsdH)

The iron-regulated surface determinants include IsdA, IsdB, IsdC, and IsdH. The transcription of *isdA*, *isdB*, *isdC*, and *isdH* is regulated by environmental iron and the iron-responsive regulator Fur (Clarke and Foster, 2006). Each of the Isd proteins contains one to three NEAT (near iron transporters) domains and bind to one or more iron-containing proteins, such as transferrin, haemin, or haemoglobin. Thus, these proteins have been suggested to have a role in iron acquisition, but this has not yet been proven. The NEAT domains in IsdA and IsdH are responsible for the binding to their ligands. IsdA binds to a wide range of host products, among them Fg, Fn, and human desquamated nasal epithelial cells (Clarke and Foster, 2006, Corrigan et al., 2009). However, physiologically relevant binding of IsdA to Fg and Fn can only be observed when *S. aureus* is grown under iron-limited conditions, such as in vitro in serum or in vivo, which favours the expression of IsdA. Moreover recently, IsdA was found to bind to proteins of the cornified envelope of human desquamated epithelial cells, such as involucrin, loricrin, cytokeratin 10, which are thought to be the predominant ligands in the ecological niche of *S. aureus*, further delineating the importance of IsdA in nasal colonization (Clarke et al., 2009). IsdH binds to haptoglobin and haptoglobin-haemoglobin complexes (Dryla et al., 2003). Differences in the ligand-binding specificity of IsdA and IsdH might be due to the pronounced sequence differences among their NEAT domains. Immunization with purified IsdA and IsdH resulted in reduced nasal colonization by *S. aureus* in the cotton rat model.

IsdB was found to be involved in platelet adhesion and aggregation: when *S. aureus* was grown under iron-limited conditions, mutants deficient in IsdB, but

not IsdA or IsdH were unable to adhere to or aggregate platelets. The platelet integrin GPIIb/IIIa was identified as the platelet receptor for IsdB and the direct interaction of these proteins could be demonstrated by surface plasmon resonance (Miajlovic et al., 2010). Immunization with IsdB protects against staphylococcal sepsis in different animal models.

7.2.1.5 Biofilm-Associated Proteins

In recent years, several *S. aureus* surface-anchored proteins have been associated with the formation of biofilm, especially with the accumulation phase and intercellular adherence. However, the first protein reported to be involved in the accumulative growth during biofilm formation was the 220 kDa accumulation-associated protein Aap from *S. epidermidis*. Aap is highly homologous to the *S. aureus* surface protein SasG (Fig. 7.2), which also mediates biofilm accumulation (Heilmann and Götz, 2010). The function of Aap in the accumulation process was speculated to be the anchoring of PIA (polysaccharide intercellular adhesin) to the cell surface. However recently, it was shown that Aap is able to mediate intercellular adhesion and biofilm accumulation in a completely PIA-independent background. A repeat domain B, which becomes active only after proteolytic cleavage of the N-terminal A-domain, mediates intercellular adhesion. Recently, the B repeats of Aap (also known as G5 domains) were found to be zinc-dependent adhesion modules and a "zinc zipper" mechanism was suggested for G5 domain-based intercellular adhesion in Aap- or SasG-mediated biofilm accumulation. A zinc-dependent dimerisation of recombinant B repeats was also observed with SasG (Geoghegan et al., 2010). SasG not only mediates bacterial intercellular adhesion, but also promotes binding to nasal epithelial cells (Roche et al., 2003b). Moreover as with Pls, which has sequence similarities with SasG and Aap, the expression of SasG masked the ability of the *S. aureus* cells to adhere to Fg, Fn, cytokeratin 10, and IgG. SasG-mediated binding to nasal epithelial cells was proposed to compensate for masking the ability of ClfB to bind to cytokeratin 10. While intercellular adhesion is mediated by the SasG B repeats with at least five of the eight repeats being required, binding to the nasal epithelial cells is carried out by the N-terminal region A. The functions of SasG and Aap might be explained by their fibrillar structure, which was recently observed by transmission electron microscopy (Corrigan et al., 2007).

The 239 kDa biofilm-associated protein Bap was the first protein reported to be involved in *S. aureus* biofilm formation. Bap mediates *S. aureus* attachment to a polystyrene surface and intercellular adhesion leading to biofilm accumulation. Moreover, Bap was found to prevent adherence to Fg, Fn, and host tissue (sheep mammary glands) as well as cellular internalization (Cucarella et al., 2002). The clinical significance of Bap is not clear, because it is apparently present in only 5% of 350 bovine mastitis and absent from all human clinical *S. aureus* isolates tested so far. However, a gene encoding a Bap-homologous protein, the 258 kDa Bhp, is present in the human clinical strain *S. epidermidis* RP62A.

Recently, we reported that the *S. aureus* surface protein C (SasC) mediates attachment to polystyrene and biofilm accumulation, but not adherence to Fg,

thrombospondin-1, von Willebrand factor, or platelets. Intercellular adhesion is conferred by the N-terminal domain of SasC (Schroeder et al., 2009).

Furthermore, a function for the multifactorial virulence factor protein A in biofilm development was detected, when expressed at high levels due to a mutation in the accessory gene regulator *agr* (Merino et al., 2009). A role for Spa in the development of biofilm-associated infections was suggested in a murine model of subcutaneous catheter infection.

Additionally, FnBPA and FnBPB were found to be important for biofilm accumulation of methicillin-resistant *S. aureus* (MRSA) strains with the A domain of FnBPA, but not the Fn-binding domain, being responsible for biofilm accumulation. Accordingly, the FnBPs play a significant role in a catheter-associated murine infection model (O'Neill et al., 2008, Vergara-Irigaray et al., 2009).

7.2.1.6 Other Covalently-Linked Surface Proteins

Further MSCRAMMs of *S. aureus* include the collagen-binding protein Cna and the serine-rich adhesin for platelets (SraP, also called SasA) (Patti et al., 1995, Siboo et al., 2008). The collagen-binding site within the 133 kDa Cna is located in a region between residues Asp^{209} and Tyr^{233}. Based on crystal structures from the subdomains N1 and N2 of Cna, each of them adopting an IgG-like fold, and in complex with a synthetic collagen-like triple helical peptide, a "collagen hug" model was proposed for the interaction of the multidomain Cna with its extended rope-like ligand (Zong et al., 2005). In a rabbit model of soft contact lens-associated bacterial keratitis, Cna has been found to be a virulence factor (Rhem et al., 2000).

SraP is a glycoprotein with a calculated molecular mass of 227 kDa that is involved in adherence to platelets (Siboo et al., 2008). It contains an unusually long N-terminal signal peptide and two serine-rich repeat regions (srr1 and srr2) separated by a nonrepeat region. A recombinant fragment of SraP consisting of the N-terminally located Srr1 and the nonrepeat region was shown to directly bind to platelets, a trait that is thought to be an important pathogenicity factor in the development of infective endocarditis. Consistently, in a rabbit model of endocarditis, an *sraP* mutant strain had significant lower bacterial counts within vegetations than the wild-type strain. Recently, the accessory Sec system that is encoded downstream of the *sraP* structural gene has been found to be required for the export of SraP.

7.2.2 Non Covalently-Linked Surface-Associated Proteins

7.2.2.1 Autolysin/Adhesins

Another class of staphylococcal adhesins is represented by the autolysin/adhesins first described by us and others (Hirschhausen et al., 2010). These non-covalently bound proteins are associated with the surface by ionic or hydrophobic interactions and have both enzymatic (peptidoglycan-hydrolytic) and adhesive functions. In general, peptidoglycan hydrolases or autolysins are thought to play important roles in

cell-wall turnover, cell division, cell separation, and antibiotic-induced lysis of bacteria. Using transposon mutagenesis, the 148 kDa autolysin AtlE of *S. epidermidis* was identified as a surface-associated component, which mediates attachment to polystyrene, biofilm formation, and adherence to Vn. In a rat central venous catheter infection model, the *atlE* mutant was attenuated compared to the wild type. The homologous 137 kDa autolysin Atl from *S. aureus* also mediates attachment to polystyrene and biofilm formation (Biswas et al., 2006).

AtlE and Atl show the same structural organization and are proteolytically cleaved into two bacteriolytically active domains, an N-terminal amidase and a C-terminal glucosaminidase. The bacteriolytically active domains are interconnected by three direct repeated sequences (R1, R2, and R3), which are involved in binding to peptidoglycan. Each repeat consists of approximately 170 residues with two glycine-tryptophane (GW)-dipeptide motifs. GW-containing repeats have been previously characterized from surface proteins of *Listeria monocytogenes* that mediate adherence to and uptake by eukaryotic cells.

Recently, we found that Atl also binds to Fg, Fn, Vn, and human endothelial cells (Hirschhausen et al., 2010). Moreover, Atl/AtlE also functions in staphylococcal internalization by endothelial cells by using the 70 kDa heat shock cognate protein Hsc70 as the host cell receptor. While this novel Atl- or AtlE-mediated internalization mechanism may represent a "backup"-mechanism in *S. aureus* internalization, it may also be the major or even sole mechanism involved in the internalization of coagulase-negative staphylococci.

Further multifunctional autolysin/adhesins include the Aaa from *S. aureus* and the homologous Aae from *S. epidermidis*. Aaa and Aae both have bacteriolytic activities and bind to Fg, Fn, and Vn in a dose-dependent and saturable fashion and with high affinity (Heilmann et al., 2005).

7.2.2.2 SERAMs (Eap/Map/P70 and Emp)

Further examples of non-covalently associated surface proteins of *S. aureus* are secreted proteins that bind back to the bacterial cell surface by so far unknown mechanisms and have a broad binding spectrum; therefore they were termed SERAMs (Secretable expanded repertoire adhesive molecules) (Chavakis et al., 2005). Among the SERAMs are the 60–72 kDa extracellular adherence protein Eap (also designated as Map, "MHC class II analogous protein" or P70) and the 40 kDa extracellular matrix and plasma binding protein Emp, both of which bind to various components of the extracellular matrix, such as Fg, Fn, or Vn. Map/Eap contains six repeated domains of 110 residues each, with a subdomain of 31 residues sharing significant homology to a segment in the peptide binding groove of the β-chain of the major histocompatibility complex (MHC) class II proteins from different mammalian species. *S. aureus* strains that do not express Eap were less able to colonize and invade host tissue and mutants defective in *emp* showed reduced attachment to immobilized Fg and Fn (Chavakis et al., 2005).

The SERAMs are thought to play a role in endovascular infection, like infective endocarditis. The pathogenesis of infective endocarditis is characterized by a serious

of events, such as endocardial damage, exposure of the subendothelial matrix, deposition of activated platelets and extracellular matrix and plasma proteins that serve as binding foci for adhering bacteria. Thus, Eap and Emp can mediate binding to these vegetations as well as to the surface of endothelial cells most likely via plasma proteins as bridging molecules. Moreover, binding of Eap to endothelial cells via Fn may enhance the staphylococcal uptake by the eukaryotic cell. Additional functions of Eap include the direct interaction with the host adhesive protein intercellular adhesion molecule 1 (ICAM-1), inhibition of neutrophil binding to and transmigration through the endothelium and the decrease in phagocytic activity (Chavakis et al., 2005). Thus, Eap is a potent anti-inflammatory factor. More recently, another function for Eap as a potent angiostatic agent was described (Sobke et al., 2006).

No homologues of the *S. aureus* extracellular matrix and plasma binding protein Emp and the extracellular adherence protein Eap could be detected in *S. epidermidis*.

7.2.2.3 Membrane-Spanning Proteins (Ebh and Ebps)

Further non-covalently anchored cell surface proteins include the giant 1.1 mDa Fn-binding protein Ebh (extracellular matrix-binding protein homologue) of *S. aureus* and the homologous Embp of *S. epidermidis* (Clarke and Foster, 2006, Williams et al., 2002), whose genes are by far the largest of the *S. aureus* and *S. epidermidis* genomes, respectively. The Fn-binding sites of Ebh and Embp seem to be unrelated to those of the *S. aureus* FnBPs. Ebh appears to be anchored to the cell surface by a C-terminally located membrane-spanning domain that is followed by a repeat region containing positively charged residues, which is predicted to be located intracellularly. Furthermore, Embp was recently demonstrated to mediate biofilm accumulation (Christner et al., 2010).

EbpS is another protein with a membrane anchor that binds elastin, which is a major component of the extracellular matrix (Downer et al., 2002).

7.3 Non-proteinaceous Staphylococcal Adhesins

7.3.1 Polysaccharide Intercellular Adhesin (PIA)

S. epidermidis transposon mutants not able to accumulate in multilayered cell clusters lack a specific polysaccharide antigen referred to as polysaccharide intercellular adhesin (PIA) (Götz, 2002, Heilmann and Götz, 2010), also designated as poly-N-acetylglucosamine (PNAG). Purification and structural analysis of PIA revealed that it is a linear β-1,6-linked N-acetylglucosaminoglycan with 15–20% of the N-acetylglucosaminyl residues being non-N-acetylated. Thus, the designation as PNAG is certainly not correct. Later, it was found that PIA is also produced by *S. aureus*. It has been published that the *N*-acetylglucosamine residues of PIA

from *S. aureus* are completely succinylated, which led to its designation as poly-*N*-succinyl β-1,6-glucosamine (PNSG). However, it is now clear that the succinyl groups were an artefact.

The partial deacetylation of 15–20% of the N-acetylglucosaminyl residues renders the polysaccharide positively charged, which determines its biological activity (Götz, 2002). Possibly, it functions as an intercellular adhesin by electrostatically attracting the negatively charged teichoic acid to the bacterial cell surface. The structure of PIA so far is unique. However, PIA-mediated biofilm formation might represent a common principle, because PIA-related structures have also been identified to play a role in the biofilm formation of pathogenic Gram-negative bacteria.

PIA is produced by the gene products encoded by the *icaADBC* operon. The *icaADBC* operon was first identified in *S. epidermidis* and is also present in *S. aureus* and other staphylococcal species. The *N*-acetylglucosaminyltransferase activity is carried out by IcaA, which requires IcaD for full activity. With its transmembrane helices, IcaC very likely is an integral membrane protein that putatively transports the *N*-acetylglucosamine oligomers across the membrane. IcaB is mainly found in the culture supernatant and deacetylates PIA (Heilmann and Götz, 2010).

The importance of PIA as a pathogenicity factor has been confirmed in various foreign-body animal infection models with different *S. epidermidis icaADBC* mutants. However in *S. aureus*, conflicting results were obtained: PIA production did not increase the capacity to induce persistent infections in a tissue cage model (Kristian et al., 2004). A study investigating the pathogenic properties of *S. epidermidis* strains obtained from polymer-associated septicemic disease compared with saprophytic skin and mucosal isolates demonstrated a strong correlation of biofilm formation and presence of the *ica* gene cluster essentially associated with disease isolates (Ziebuhr et al., 1997).

7.3.2 Wall Teichoic Acid (WTA) and Lipoteichoic Acid (LTA)

S. aureus teichoic acids are highly charged cell wall polymers, composed of alternating phosphate and ribitol (wall teichoic acid; WTA) or glycerol (lipoteichoic acid; LTA) groups, which are substituted with D-alanine and N-acetylglucosamine. While the WTA is covalently linked to the peptidoglycan, the LTA is anchored in the outer leaflet of the cytoplasmic membrane via a glycolipid. The *S. aureus* colonization of abiotic surfaces depends on the charge of its teichoic acid. A *dltA* mutant lacks D-alanine in its WTA rendering it higher negatively charged. The *dltA* mutant has a biofilm-negative phenotype due to a decreased initial attachment to polystyrene or glass, which is hydrophobic or negatively charged, respectively (Götz, 2002). WTA also mediates adherence to human nasal epithelial cells and is involved in nasal colonization, which is considered a major risk factor for serious *S. aureus* infections. Moreover, a WTA-deficient mutant (Δ*tagO*) showed decreased adherence to human endothelial cells especially under flow conditions and was attenuated in a rabbit model of infective endocarditis (Weidenmaier et al., 2005).

The glycolipid synthase YpfP is involved in the biosynthesis of LTA. An *S. aureus* SA113 *ypfP* mutant, which showed a markedly decreased production of LTA, revealed altered physicochemical properties and a reduced capacity to form a biofilm on a polystyrene surface (Fedtke et al., 2007). Thus, LTA and its biosynthetic enzymes were proposed as potential targets in the development of novel anti-biofilm measurements.

In *S. epidermidis*, the cell wall teichoic acid is involved in adherence to Fn (Hussain et al., 2001).

7.4 Conclusion

In conclusion, *S. aureus* harbours a variety of proteinaceous and non-proteinaceous adhesins that can mediate adherence to an abiotic surface or a multitude of host factors, such as extracellular matrix and plasma proteins and human host cells. Upon adherence, the bacteria may proliferate and accumulate into multilayered cell clusters, which requires intercellular adhesion and finally leads to the formation of a biofilm. Alternatively upon adherence, the bacteria may be internalized by the human host cell and "hide" within the host cell. Both, the formation of a biofilm as well as the intracellular environment seem to protect the bacteria against the host immune system and antibiotic therapy. Therefore, understanding *S. aureus* adhesive mechanisms represents a necessary first step to developing strategies to prevent or combat infections with this serious pathogen.

References

Barbu EM, Ganesh VK, Gurusiddappa S, Mackenzie RC, Foster TJ, Sudhof TC, Höök M (2010) β-Neurexin is a ligand for the *Staphylococcus aureus* MSCRAMM SdrC. PLoS Pathog 6:e1000726

Biswas R, Voggu L, Simon UK, Hentschel P, Thumm G, Götz F (2006) Activity of the major staphylococcal autolysin Atl. FEMS Microbiol Lett 259:260–268

Chavakis T, Wiechmann K, Preissner KT, Herrmann M (2005) *Staphylococcus aureus* interactions with the endothelium: the role of bacterial "secretable expanded repertoire adhesive molecules" (SERAM) in disturbing host defense systems. Thromb Haemost 94:278–285

Christner M, Franke G, Schommer N, Wendt U, Wegert K, Pehle P, Kroll G, Schulze C, Buck F, Mack D, Aepfelbacher M, Rohde H (2010) The giant extracellular matrix binding protein of *Staphylococcus epidermidis* mediates biofilm accumulation and attachment to fibronectin. Mol Microbiol 75:187–207

Clarke SR, Andre G, Walsh EJ, Dufrene YF, Foster TJ, Foster SJ (2009) Iron-regulated surface determinant protein A mediates adhesion of *Staphylococcus aureus* to human corneocyte envelope proteins. Infect Immun 77:2408–2416

Clarke SR, Foster SJ (2006) Surface adhesins of *Staphylococcus aureus*. Adv Microb Physiol 51:187–224

Corrigan RM, Miajlovic H, Foster TJ (2009) Surface proteins that promote adherence of *Staphylococcus aureus* to human desquamated nasal epithelial cells. BMC Microbiol 9:22

Corrigan RM, Rigby D, Handley P, Foster TJ (2007) The role of *Staphylococcus aureus* surface protein SasG in adherence and biofilm formation. Microbiology 153:2435–2446

Cucarella C, Tormo MA, Knecht E, Amorena B, Lasa I, Foster TJ, Penadés JR (2002) Expression of the biofilm-associated protein interferes with host protein receptors of *Staphylococcus aureus* and alters the infective process. Infect Immun 70:3180–3186

Deivanayagam CC, Wann ER, Chen W, Carson M, Rajashankar KR, Höök M, Narayana SV (2002) A novel variant of the immunoglobulin fold in surface adhesins of *Staphylococcus aureus*: crystal structure of the fibrinogen-binding MSCRAMM, clumping factor A. EMBO J 21: 6660–6672

Downer R, Roche F, Park PW, Mecham RP, Foster TJ (2002) The elastin-binding protein of *Staphylococcus aureus* (EbpS) is expressed at the cell surface as an integral membrane protein and not as a cell wall-associated protein. J Biol Chem 277:243–250

Dryla A, Gelbmann D, von Gabain A, Nagy E (2003) Identification of a novel iron regulated staphylococcal surface protein with haptoglobin-haemoglobin binding activity. Mol Microbiol 49:37–53

Edwards AM, Potts JR, Josefsson E, Massey RC (2010) *Staphylococcus aureus* host cell invasion and virulence in sepsis is facilitated by the multiple repeats within FnBPA. PLoS Pathog 6:e1000964

Fedtke I, Mader D, Kohler T, Moll H, Nicholson G, Biswas R, Henseler K, Götz F, Zähringer U, Peschel A (2007) A *Staphylococcus aureus ypfP* mutant with strongly reduced lipoteichoic acid (LTA) content: LTA governs bacterial surface properties and autolysin activity. Mol Microbiol 65:1078–1091

Ganesh VK, Rivera JJ, Smeds E, Ko YP, Bowden MG, Wann ER, Gurusiddappa S, Fitzgerald JR, Höök M (2008) A structural model of the *Staphylococcus aureus* ClfA-fibrinogen interaction opens new avenues for the design of anti-staphylococcal therapeutics. PLoS Pathog 4:e1000226

Geoghegan JA, Corrigan RM, Gruszka DT, Speziale P, O'Gara JP, Potts JR, Foster TJ (2010) The role of surface protein SasG in biofilm formation by *Staphylococcus aureus*. J Bacteriol 192:5663–5673

Gomez MI, Lee A, Reddy B, Muir A, Soong G, Pitt A, Cheung A, Prince A (2004) *Staphylococcus aureus* protein A induces airway epithelial inflammatory responses by activating TNFR1. Nat Med 10:842–848

Götz F (2002) *Staphylococcus* and biofilms. Mol Microbiol 43:1367–1378

Greene C, McDevitt D, Francois P, Vaudaux PE, Lew DP, Foster TJ (1995) Adhesion properties of mutants of *Staphylococcus aureus* defective in fibronectin-binding proteins and studies on the expression of *fnb* genes. Mol Microbiol 17:1143–1152

Hartford OM, Wann ER, Höök M, Foster TJ (2001) Identification of residues in the *Staphylococcus aureus* fibrinogen-binding MSCRAMM clumping factor A (ClfA) that are important for ligand binding. J Biol Chem 276:2466–2473

Heilmann C, Götz F (2010) Cell-cell communication and biofilm formation in gram-positive bacteria. In: Krämer R, Jung K (eds) Bacterial signaling. Wiley-VCH Verlag GmbH & Co. KGaA, Weinheim, pp 7–17

Heilmann C, Hartleib J, Hussain M, Peters G (2005) The multifunctional *Staphylococcus aureus* autolysin Aaa mediates adherence to immobilized fibrinogen and fibronectin. Infect Immun 73:4793–4802

Hirschhausen N, Schlesier T, Schmidt MA, Götz F, Peters G, Heilmann C (2010) A novel staphylococcal internalization mechanism involves the major autolysin Atl and heat shock cognate protein Hsc70 as host cell receptor. Cell Microbiol 12:1746–1764

Huesca M, Peralta R, Sauder DN, Simor AE, McGavin MJ (2002) Adhesion and virulence properties of epidemic Canadian methicillin-resistant *Staphylococcus aureus* strain 1: identification of novel adhesion functions associated with plasmin-sensitive surface protein. J Infect Dis 185:1285–1296

Hussain M, Heilmann C, Peters G, Herrmann M (2001) Teichoic acid enhances adhesion of *Staphylococcus epidermidis* to immobilized fibronectin. Microb Pathog 31:261–270

Hussain M, Schafer D, Juuti KM, Peters G, Haslinger-Löffler B, Kuusela PI, Sinha B (2009) Expression of Pls (plasmin sensitive) in *Staphylococcus aureus* negative for pls reduces adherence and cellular invasion and acts by steric hindrance. J Infect Dis 200:107–117

Jönsson K, Signas C, Müller HP, Lindberg M (1991) Two different genes encode fibronectin binding proteins in *Staphylococcus aureus*. The complete nucleotide sequence and characterization of the second gene. Eur J Biochem 202:1041–1048

Kristian SA, Golda T, Ferracin F, Cramton SE, Neumeister B, Peschel A, Götz F, Landmann R (2004) The ability of biofilm formation does not influence virulence of *Staphylococcus aureus* and host response in a mouse tissue cage infection model. Microb Pathog 36:237–245

Lentino JR (2003) Prosthetic joint infections: bane of orthopedists, challenge for infectious disease specialists. Clin Infect Dis 36:1157–1161

Loughman A, Fitzgerald JR, Brennan MP, Higgins J, Downer R, Cox D, Foster TJ (2005) Roles for fibrinogen, immunoglobulin and complement in platelet activation promoted by *Staphylococcus aureus* clumping factor A. Mol Microbiol 57:804–818

Mazmanian SK, Skaar EP, Gaspar AH, Humayun M, Gornicki P, Jelenska J, Joachmiak A, Missiakas DM, Schneewind O (2003) Passage of heme-iron across the envelope of *Staphylococcus aureus*. Science 299:906–909

McDevitt D, Nanavaty T, House-Pompeo K, Bell E, Turner N, McIntire L, Foster T, Höök M (1997) Characterization of the interaction between the *Staphylococcus aureus* clumping factor (ClfA) and fibrinogen. Eur J Biochem 247:416–424

Merino N, Toledo-Arana A, Vergara-Irigaray M, Valle J, Solano C, Calvo E, Lopez JA, Foster TJ, Penadés JR, Lasa I (2009) Protein A-mediated multicellular behavior in *Staphylococcus aureus*. J Bacteriol 191:832–843

Miajlovic H, Loughman A, Brennan M, Cox D, Foster TJ (2007) Both complement- and fibrinogen-dependent mechanisms contribute to platelet aggregation mediated by *Staphylococcus aureus* clumping factor B. Infect Immun 75:3335–3343

Miajlovic H, Zapotoczna M, Geoghegan JA, Kerrigan SW, Speziale P, Foster TJ (2010) Direct interaction of iron-regulated surface determinant IsdB of *Staphylococcus aureus* with the GPIIb/IIIa receptor on platelets. Microbiology 156:920–928

Nguyen T, Ghebrehiwet B, Peerschke EIB (2000) *Staphylococcus aureus* Protein A recognizes platelet gC1qR/p33: a novel mechanism for staphylococcal interactions with platelets. Infect Immun 68:2061–2068

Ni Eidhin D, Perkins S, Francois P, Vaudaux P, Höök M, Foster TJ (1998) Clumping factor B (ClfB), a new surface-located fibrinogen-binding adhesin of *Staphylococcus aureus*. Mol Microbiol 30:245–257

O'Brien L, Kerrigan SW, Kaw G, Hogan M, Penadés J, Litt D, Fitzgerald DJ, Foster TJ, Cox D (2002a) Multiple mechanisms for the activation of human platelet aggregation by *Staphylococcus aureus*: roles for the clumping factors ClfA and ClfB, the serine-aspartate repeat protein SdrE and protein A. Mol Microbiol 44:1033–1044

O'Brien LM, Walsh EJ, Massey RC, Peacock SJ, Foster TJ (2002b) *Staphylococcus aureus* clumping factor B (ClfB) promotes adherence to human type I cytokeratin 10: implications for nasal colonization. Cell Microbiol 4:759–770

O'Neill E, Pozzi C, Houston P, Humphreys H, Robinson DA, Loughman A, Foster TJ, O'Gara JP (2008) A novel *Staphylococcus aureus* biofilm phenotype mediated by the fibronectin-binding proteins, FnBPA and FnBPB. J Bacteriol 190:3835–3850

Patti JM, House-Pompeo K, Boles JO, Garza N, Gurusiddappa S, Höök M (1995) Critical residues in the ligand-binding site of the *Staphylococcus aureus* collagen-binding adhesin (MSCRAMM. J Biol Chem 270:12005–12011

Peacock SJ, Day NP, Thomas MG, Berendt AR, Foster TJ (2000) Clinical isolates of *Staphylococcus aureus* exhibit diversity in *fnb* genes and adhesion to human fibronectin. J Infect 41:23–31

Rhem MN, Lech EM, Patti JM, McDevitt D, Höök M, Jones DB, Wilhelmus KR (2000) The collagen-binding adhesin is a virulence factor in *Staphylococcus aureus* keratitis. Infect Immun 68:3776–3779

Roche FM, Downer R, Keane F, Speziale P, Park PW, Foster TJ (2004) The N-terminal A domain of fibronectin-binding proteins A and B promotes adhesion of *Staphylococcus aureus* to elastin. J Biol Chem 279:38433–38440

Roche FM, Massey R, Peacock SJ, Day NP, Visai L, Speziale P, Lam A, Pallen M, Foster TJ (2003a) Characterization of novel LPXTG-containing proteins of *Staphylococcus aureus* identified from genome sequences. Microbiology 149:643–654

Roche FM, Meehan M, Foster TJ (2003b) The *Staphylococcus aureus* surface protein SasG and its homologues promote bacterial adherence to human desquamated nasal epithelial cells. Microbiology 149:2759–2767

Schneewind O, Mihaylova-Petkov D, Model P (1993) Cell wall sorting signals in surface proteins of gram-positive bacteria. EMBO J 12:4803–4811

Schroeder K, Jularic M, Horsburgh SM, Hirschhausen N, Neumann C, Bertling A, Schulte A, Foster S, Kehrel BE, Peters G, Heilmann C (2009) Molecular characterization of a novel *Staphylococcus aureus* surface protein (SasC) involved in cell aggregation and biofilm accumulation. PLoS One 4:e7567

Schwarz-Linek U, Werner JM, Pickford AR, Gurusiddappa S, Kim JH, Pilka ES, Briggs JA, Gough TS, Höök M, Campbell ID, Potts JR (2003) Pathogenic bacteria attach to human fibronectin through a tandem β-zipper. Nature 423:177–181

Siboo IR, Chaffin DO, Rubens CE, Sullam PM (2008) Characterization of the accessory Sec system of *Staphylococcus aureus*. J Bacteriol 190:6188–6196

Siboo IR, Cheung AL, Bayer AS, Sullam PM (2001) Clumping Factor A Mediates Binding of *Staphylococcus aureus* to Human Platelets. Infect Immun 69:3120–3127

Signas C, Raucci G, Jönsson K, Lindgren PE, Anantharamaiah GM, Höök M, Lindberg M (1989) Nucleotide sequence of the gene for a fibronectin-binding protein from *Staphylococcus aureus*: use of this peptide sequence in the synthesis of biologically active peptides. Proc Natl Acad Sci USA 86:699–703

Sobke AC, Selimovic D, Orlova V, Hassan M, Chavakis T, Athanasopoulos AN, Schubert U, Hussain M, Thiel G, Preissner KT, Herrmann M (2006) The extracellular adherence protein from *Staphylococcus aureus* abrogates angiogenic responses of endothelial cells by blocking Ras activation. FASEB J 20:2621–2623

Tung H, Guss B, Hellman U, Persson L, Rubin K, Ryden C (2000) A bone sialoprotein-binding protein from *Staphylococcus aureus*: a member of the staphylococcal Sdr family. Biochem J 345(Pt 3):611–619

Vergara-Irigaray M, Valle J, Merino N, Latasa C, García B, Ruiz De LosMozos I, Solano C, Toledo-Arana A, Penadés JR, Lasa I (2009) Relevant role of fibronectin-binding proteins in *Staphylococcus aureus* biofilm-associated foreign-body infections. Infect Immun 77:3978–3991

Wann ER, Gurusiddappa S, Höök M (2000) The fibronectin-binding MSCRAMM FnbpA of *Staphylococcus aureus* is a bifunctional protein that also binds to fibrinogen. J Biol Chem 275:13863–13871

Weidenmaier C, Peschel A, Xiong YQ, Kristian SA, Dietz K, Yeaman MR, Bayer AS (2005) Lack of wall teichoic acids in *Staphylococcus aureus* leads to reduced interactions with endothelial cells and to attenuated virulence in a rabbit model of endocarditis. J Infect Dis 191:1771–1777

Williams RJ, Henderson B, Sharp LJ, Nair SP (2002) Identification of a fibronectin-binding protein from *Staphylococcus epidermidis*. Infect Immun 70:6805–6810

Ziebuhr W (2001) *Staphylococcus aureus* and *Staphylococcus epidermidis*: emerging pathogens in nosocomial infections. Contrib Microbiol 8:102–107

Ziebuhr W, Heilmann C, Götz F, Meyer P, Wilms K, Straube E, Hacker J (1997) Detection of the intercellular adhesion gene cluster (*ica*) and phase variation in *Staphylococcus epidermidis* blood culture strains and mucosal isolates. Infect Immun 65:890–896

Zong Y, Xu Y, Liang X, Keene DR, Höök A, Gurusiddappa S, Höök M, Narayana SV (2005) A 'Collagen Hug' model for *Staphylococcus aureus* CNA binding to collagen. EMBO J 24: 4224–4236

Chapter 8
Protein Folding in Bacterial Adhesion: Secretion and Folding of Classical Monomeric Autotransporters

Peter van Ulsen

Abstract Bacterial adhesins mediate the attachment of bacteria to their niches, such as the tissue of an infected host. Adhesins have to be transported across the cell envelope to become active and during this secretion process they fold into their final conformation. This chapter focuses on the biogenesis of the classical monomeric autotransporter proteins, which are the most ubiquitous class of secreted proteins in Gram-negative bacteria. They may function as adhesins, but other functions are also known. Autotransporter proteins have a modular structure and consist of an N-terminal signal peptide and a C-terminal translocator domain with in between the secreted passenger domain that harbours the functions. The signal peptide directs the transport across the inner membrane to the periplasm via the Sec machinery. The translocator domain inserts into the outer membrane and facilitates the transport of the passenger to the cell surface. In this chapter, I will review our current knowledge of the secretion of classical monomeric autotransporters and the methods that have been used to assess their folding during the translocation, both in vitro and in vivo.

8.1 Introduction

Bacterial adhesins can be classified into multi-component and long cellular extensions like the pili, and single-molecule adhesins involved in tight adherence. They position the bacteria at different distances from target host cells and often act concertedly during the colonisation of host tissues. This is illustrated by the adherence pattern of the human pathogen *Neisseria meningitidis*, which first attaches to the epithelial cells of the upper respiratory tract through type IV pili, followed

P. van Ulsen (✉)
Section Molecular Microbiology, Department of Molecular Cell Biology, VU University Amsterdam, De Boelelaan 1085, 1081 HV, Amsterdam, The Netherlands
e-mail: peter.van.ulsen@falw.vu.nl

D. Linke, A. Goldman (eds.), *Bacterial Adhesion*, Advances in Experimental Medicine and Biology 715, DOI 10.1007/978-94-007-0940-9_8,

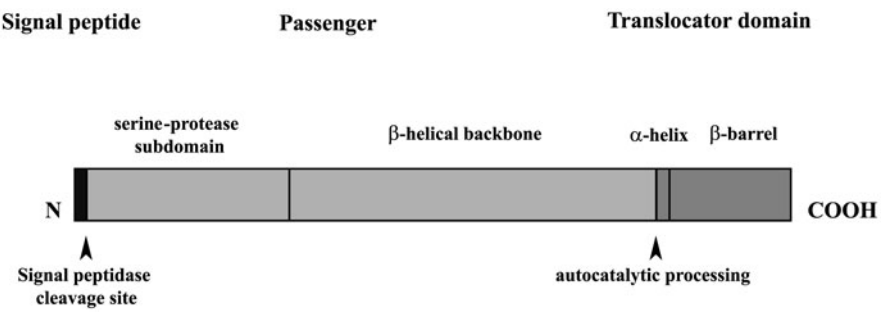

Fig. 8.1 Autotransporter domains. Tripartite domain organisation of monomeric autotransporters with the signal peptide in *black*, the passenger in *light gray* and the translocator domain in *dark gray*. Subdomains that are discussed in the text are indicated and *boxed*. *Arrowheads* indicate the sites of proteolytic cleavage

by a phase of tight adherence mediated by various single-molecule adhesins, like outer membrane proteins and autotransporters (Virji, 2009). Adhesins have to be transported across the cell envelope to become active, during or after which they fold into their final conformation. Here, I will focus on the autotransporter proteins, which are the most ubiquitous class of secreted proteins in Gram-negative bacteria. These modular proteins consist of an N-terminal signal peptide and a C-terminal translocator domain with the secreted passenger domain that harbours the functions in between (Henderson et al., 1998; Jacob-Dubuisson et al., 2004) (Fig. 8.1). The signal peptide directs the transport across the inner membrane to the periplasm via the Sec machinery. The translocator domain inserts into the outer membrane and facilitates the transport of the passenger to the cell surface. Autotransporter passengers can be involved in adherence, but also in a host of other processes. They often are processed by proteolytic cleavage, but may remain associated with the cell surface. In this chapter, I will review our current knowledge of the secretion of classical monomeric autotransporters and the methods that have been used to assess their folding in vitro and in vivo.

8.2 Autotransporters Are a Branch of the Type V Secretion Pathway

The cell envelope of Gram-negative bacteria consists of the inner and outer membranes separated by the periplasmic space that contains the peptidoglycan layer. The Type V Secretion Pathway comprises the most wide-spread and simplest secretion systems employed to pass this barrier (Kajava and Steven, 2006). It is subdivided into three branches; i.e. the classical autotransporters (Type Va), the trimeric autotransporters (Type Vc) and the two-partner secretion pathway (Type Vb; the sub-numbering reflects the order of description) (Jacob-Dubuisson et al., 2004).

Type V secretion systems pass across the cell envelope in two consecutive steps. The classical autotransporters are single-protein secretion systems that use the existing machinery of the cell. The protein crosses the inner membrane via the Sec machinery, which is targeted by the N-terminal signal peptide (Fig. 8.1). The C-terminal translocator domain then inserts into the outer membrane to facilitate the transport of the passenger to the cell surface. This step involves the Bam protein complex: the general protein machinery that inserts integral outer membrane proteins into the outer membrane (see below). Trimeric and classical autotransporters share the tripartite domain organisation, as well as the structural features of their translocator domains, but the structure of the passengers is rather different. The structures of trimeric autotransporters are discussed in Chapter 9 of this volume. However, the specific requirements for transport across the cell envelope have mostly been studied for classical autotransporters.

Two-partner secretion (TPS) systems consist of two proteins instead of one; i.e. a secreted protein, generically designated TpsA, and a transporter protein in the outer membrane, named TpsB (Jacob-Dubuisson et al., 2004). The TpsB transports the TpsA across the outer membrane and is targeted via a TPS targeting domain in TpsA (Jacob-Dubuisson et al., 2004). The TPS system is usually organised in one operon, although exceptions exist (e.g. van Ulsen et al., 2008). They include several adhesins that, after secretion, remain non-covalently attached to the cell surface (Jacob-Dubuisson et al., 2004); e.g. the filamentous haemagglutinin of *Bordetella pertussis* and the HMW adhesin of *Haemophilus influenzae*.

The TpsB transporter and the autotransporter translocator domains are structurally and functionally very different (Jacob-Dubuisson et al., 2004). Nevertheless, the secreted lipolytic enzyme PlpD of *Pseudomonas aeruginosa* was recently shown to be an autotransporter-like monomeric protein, but with a TpsB-like C-terminal domain (Salacha et al., 2010). This remarkable protein may provide a conceptual link between the TPS and autotransporter secretion systems and, at the least, underscores their relatedness.

8.3 Functions of Monomeric Autotransporters

The secreted passenger domains carry the functions of autotransporters. They are characterised by a β-helical stem structure that serves as a backbone from which functional subdomains extend (Fig. 8.2). Two major subclasses of passenger domains can be discriminated. The first contains a globular serine-protease subdomain at the passenger N terminus. This subclass includes IgA1 protease of *N. gonorrhoeae*, the first autotransporter protein described (Pohlner et al., 1987). IgA1 proteases cleave human IgA type 1 molecules (Plaut et al., 1975), as well as other human proteins including the lysosomal marker Lamp-1 (Lin et al., 1997; Hauck and Meyer, 1997). The protein also appears to have a role in the passage by *N. gonorrhoeae* across layers of cultured epithelial cells (Lin et al., 1997). The autotransporter Hap of *H. influenzae* also contains a serine protease domain. Hap

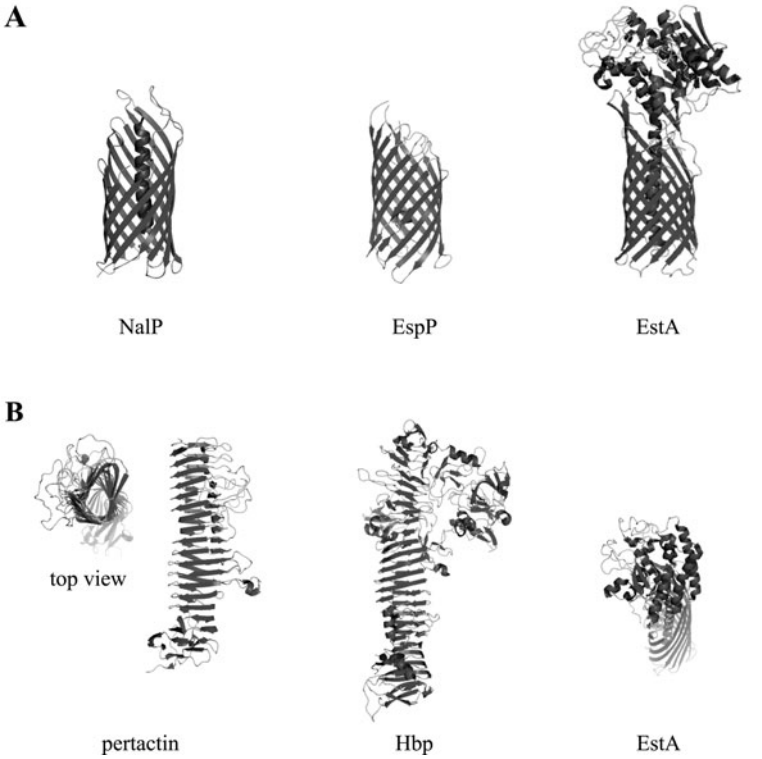

Fig. 8.2 Crystal structures of autotransporter domains. (**a**) Structures of translocator domains of NalP (1UYN) and EspP (2QOM), as well as of the passenger-translocator domain fusion of EstA (3KVN). (**b**) Structures of the passenger domains of pertactin (1DAB), Hbp (1WXR) and EstA. On the left, a top-view of pertactin shows the triangular structure of the β-helical backbone. The image of EstA was made by tilting the molecule that is depicted in (**a**). The images were generated using Pymol

mediates attachment to airway epithelial cells, as well as to purified extracellular matrix proteins (Hendrixson and St. Geme III, 1998; Fink et al., 2002). The homologous App protein of *N. meningitidis* is an adhesin as well (Serruto et al., 2003), which is expressed during infection (van Ulsen et al., 2001), whereas the serine-protease autotransporter AusI (or MspA) mediates adherence to a subset of human cell lines (Turner et al., 2006; van Ulsen et al., 2006a). The serine-protease autotransporters of *Enterobacteriaceae* (also called SPATEs) are a diverse group of virulence factors that function as haemagglutinins and adhesins (e.g. Tsh (Stathopoulos et al., 1999)), cytotoxins (e.g. Pet Eslava et al., 1998), or proteolytically active proteins, including the haemoglobin protease Hbp (Otto et al., 2005) and the mucinase Pic (Henderson et al., 1999).

The second major subclass of passenger domains also contains the β-helical backbone, but lacks a protease subdomain. The first studied example is the adhesin

pertactin of the human pathogens *B. pertussis*, *B. parapertussis* and *B. bronchiseptica*. Pertactin-mediated adhesion has been shown using several cultured cell lines (Leininger et al., 1991) and explanted ciliated airway epithelia (Edwards et al., 2005). *Escherichia coli* adhesins of this subclass are AIDA-I, TibA and Ag43, which mediate the adherence to and invasion of various human and non-human cell types (Benz and Schmidt, 1992; Sherlock et al., 2004; Lindenthal and Elsinghorst, 2001; Fexby et al., 2007). All three also induce autoaggregation of *E. coli* cell cultures and are implicated in biofilm formation (Klemm et al., 2004). Furthermore, AIDA-I and TibA are glycosylated by dedicated glycosyl transferases in the cytoplasm (Benz and Schmidt, 2001; Lindenthal and Elsinghorst, 2001), which is required for binding to human cells (Lindenthal and Elsinghorst, 2001), although the reduced binding of the non-glycosylated proteins may be due to their reduced stability (Charbonneau and Mourez, 2008).

The autotransporters EstA of *P. aeruginosa* (Wilhelm et al., 1999) and McaP of *Moraxella catarrhalis* (Lipski et al., 2007) are members of a third subclass. Their passenger domains are rather small and lack the β-helical stem structure, as shown by the crystal structure of EstA (van den Berg, 2010). Apart from the lipolytic activity, the McaP passenger also mediates adherence to cultured human epithelial cells (Lipski et al., 2007).

8.4 Proteolytic Processing of Passenger Domains at the Cell Surface

In most classical autotransporters, the passenger domain is released from the translocator domain by a proteolytic cleavage. For example, the adhesins pertactin, AIDA-I and Ag43 are proteolytically cleaved, but they remain attached to the cell surface via non-covalent interactions. These can be released by a relatively mild heat-treatment (Benz and Schmidt, 1992). Several different cleavage mechanisms have evolved. IcsA of *Shigella flexneri* is released by a dedicated protease, SopA, present in the outer membrane to ensure polar localization of the passenger domain at the cell surface (Fukuda et al., 1995). The N-terminal serine protease subdomain of passenger domains can be used for intermolecular autocatalytic release, as exemplified by Hap (Fink et al., 2001). It requires interaction of two Hap monomers and a threshold number of molecules to be present at the cell surface. A similar autocatalytic release of App and IgA protease of *N. meningitidis* occurs in competition with an intermolecular cleavage by another autotransporter, NalP (van Ulsen et al., 2003). In contrast, the N-terminal serine protease subdomain of the SPATE passenger domains is not involved in their release. Instead, they are released by a proteolytic cleavage that occurs intramolecularly and within the hydrophilic channel of the translocator domain (see below) (Barnard et al., 2007). The catalytic residues are conserved within the SPATEs and also found in pertactin. The AIDA adhesin is cleaved autocatalytically and intramolecularly as well, but the catalytic residues are located in the region that links the passenger and translocation domain (Charbonneau et al., 2009).

Proteolytic release appears counterintuitive for an adhesin, but the different mechanisms that have evolved suggest that it is functionally relevant. It appears not to be absolutely required, since a non-cleavable AIDA mutant mediates adherence like wild type (Charbonneau et al., 2006), while the Hap-mediated adherence increases when proteolytic processing is blocked (Hendrixson and St. Geme III, 1998), although it is already detectable at normal secretion levels (Fink et al., 2002). On the other hand, a more loose association like the non-covalently attached pertactin and AIDA may yield an interaction that is detachable and temporary, which may benefit colonisation in vivo. For example, *B. pertussis* infection of mice requires the release of the filamentous haemagglutinin adhesin from the cell surface through the proteolytic activity of the autotransporter SphB1 (Coutte et al., 2003).

8.5 Structural Biology and In Vitro Folding of Classical Autotransporters

The crystal structures of several autotransporter domains have been solved (Fig. 8.2). On the sequence level, homology between these domains is hard to prove, but secondary structure predictions indicated similarities that were confirmed by the solved structures. The similarities also suggest a general secretion mechanism, with constraints that derive from the shared conformations although the actual folding mechanisms have been studied for only a few autotransporters.

8.5.1 The Translocator Domain

The C-terminal translocator domain is a 25- to 35-kDa domain that is essential for the transport of the attached passenger domain across the outer membrane. It was proposed to adopt a conformation similar to other outer membrane proteins (Loveless and Saier, 1997). The latter are β-barrels consisting of amphipathic β-strands with hydrophobic residues that face the membrane lipids and hydrophilic residues that form a hydrophilic central channel (Bos et al., 2007). The β-strands are connected by relatively long and variable extracellular loops, while the periplasmic turns are short. The strands have a high number of aromatic amino acid residues that align the barrel with the hydrophilic headgroups of the membrane lipids. Translocator domains also comply with these general rules (Loveless and Saier, 1997).

The folding of an outer membrane protein into its β-barrel conformation can be assessed by its “heat-modifiability”; i.e. the heat-denatured form of a β-barrel protein shows a different electrophoretic mobility than the non-heated folded form when run on a polyacrylamide gel with low SDS (van Ulsen et al., 2006b; Burgess et al., 2008). Translocator domains also show heat-modifiability, as has been shown for AIDA-I (Konieczny et al., 2001), NalP (Oomen et al., 2004), Tsh (Hritonenko et al., 2006), EspP (Barnard et al., 2007) and SphB1 (Dé et al., 2008). Purifying

the considerable amounts of a fully-folded membrane protein needed for structural and functional assays can be difficult and in vitro folding is a relatively easy alternative (Buchanan, 1999; van Ulsen et al., 2006b). It involves overproduction of the desired protein in *E. coli* without a signal peptide to prevent Sec-mediated transport across the inner membrane. The large amounts of insoluble inclusion bodies that accumulate in the cytoplasm can be isolated by breaking the cells. Subsequently, the proteins are denatured by solubilising the inclusion bodies in 7–8 M urea or 6 M guanadinium–HCl and folded in vitro by rapid dilution into a buffer containing detergents that mimic the membrane environment. Heat-modifiability is used to assess whether in vitro folding yielded a β-barrel conformation (de Jonge et al., 2002; Oomen et al., 2004; van Ulsen et al., 2006b). The specific conditions, e.g. the detergent used or the buffer condition, are subject to trial and error and may differ between proteins. However, in vitro folding of the translocator domains of NalP of *N. meningitidis* and Hbp of *E. coli* succeeded using rather similar conditions and the same detergent (Roussel-Jazédé et al., 2011). Subsequent analysis of the conformational status of the heat-modifiable protein involves analytical techniques like circular dichroism (Oomen et al., 2004; Dé et al., 2008). Ideally, also a functional assay is included in the analysis. In vitro folding of the Opa adhesin of *N. meningitidis*, which is a β-barrel outer membrane protein, yielded a heat-modifiable protein that bound its human receptor, whereas the unfolded protein did not (de Jonge et al., 2002). Unfortunately, there is no functional assay for translocator domains.

The first crystal structure of a translocator domain was obtained using the in vitro folded domain of NalP (Oomen et al., 2004) (Fig. 8.2). To date, three other structures of monomeric translocator domains have been solved: EspP and Hbp of *E. coli* (Barnard et al., 2007; Tajima et al., 2010), and EstA of *P. aeruginosa* (van den Berg, 2010), solved as a full-length protein (passenger-translocator). Furthermore, the structure of the translocator domain of the trimeric autotransporter Hia has also been solved (Meng et al., 2006). These four structures were obtained by purifying recombinant proteins from solubilised outer membranes using detergents and affinity tags. Nevertheless, they showed a great similarity to the NalP structure. All translocator domains are 12-stranded β-barrels with a hydrophilic channel that is occupied by an α-helix (or three in case of the trimeric autotransporters), and all have quite similar dimensions (van den Berg, 2010). The structure of the EspP translocator domain revealed a very small and tilted α-helix (Fig. 8.2), which results from the intra-channel cleavage that releases the passenger domain from the cell surface (Barnard et al., 2007). The Hbp translocator domain structure shows a mutant in which that cleavage is prevented (Tajima et al., 2010). The structure contains the tilted α-helix, suggesting that it is present prior to cleavage.

The pore-forming activity of the translocator domains of NalP, IgA protease, Hbp (a close homologue of EspP), and SphB1 has been monitored on proteins reconstituted in planar lipid bilayers (Oomen et al., 2004; Dé et al., 2008; Roussel-Jazédé et al., 2011). A voltage is applied over the lipid bilayer and the current flowing through the pores of single molecules is measured (Van Gelder et al., 2000). These electrophysiological experiments revealed pores with two types of channels: frequently observed small channels with a conductance of 0.15 nS that and, rarely,

larger channels with a conductance of 1.3 nS. The calculated pore-sizes match with the channels observed in the crystal structures (Oomen et al., 2004; Roussel-Jazédé et al., 2011) and may represent closed and open pores, respectively, the closure being effected by the α-helix. The α-helices of the EstA and NalP translocator domains are superimposable and both slightly off-centre (van den Berg, 2010), which leaves a small channel through which water molecules could diffuse. Indeed, removing the α-helices in the translocator domains of SphB1, NalP and Hbp resulted in measurements of only the larger channels (Dé et al., 2008; Roussel-Jazédé et al., 2011). The measured channels were very variable, which suggested a role for the α-helix in barrel stability. This function was also suggested by molecular dynamics simulations (Khalid and Sansom, 2006) and confirmed by the chemical denaturation curves of translocator domains with and without α-helices obtained by diluting the proteins in increasing concentrations of guanadine hydrochloride and measuring the Trp fluoresence (Roussel-Jazédé et al., 2011). Apparently, the α-helix both stabilizes the barrel structure and closes the translocator domain channel once the passenger domain is secreted.

8.5.2 The Passenger Domain

To date, crystal structures of five passenger domains have been solved (Fig. 8.2); i.e. adhesin pertactin (Emsley et al., 1996), haemoglobin protease Hbp (Otto et al., 2005), vacuolating cytotoxin VacA of *Helicobacter pylori* (Gangwer et al., 2007), IgA protease of *H. influenzae* (Johnson et al., 2009) and lipolytic esterase EstA (van den Berg, 2010). These structures are derived from secreted proteins that were isolated from the culture medium of (heterologous) cells producing the autotransporter, except for EstA that was isolated intact from the outer membrane.

The pertactin structure was the first solved and shows a rigid and protease-resistant domain with a helix of β-strands that are connected by short loops and constitute a triangular structure of three β-sheets (Emsley et al., 1996; Kajava and Steven, 2006). A similar β-helical stem was identified in Hbp, VacA and IgA protease, but not in EstA (see below). Functional subdomains extend from the stem, such as the loop involved in binding to epithelial cells in pertactin (Emsley et al., 1996). Hbp and IgA protease have a similar structure with a globular trypsin-like protease domain at the N terminus, while other domains of unknown function extend from the β-helical backbone (Otto et al., 2005; Johnson et al., 2009). The short β-strands of 6 amino acid residues that form the rungs of the helical structure often contain repeats of alternating polar and apolar residues, of which the apolar residues constitute the interior of the β-helical structure (Kajava and Steven, 2006).

Furthermore, arrays of repeated residues run along the β-helix axis, like the array of Asn on the Hbp passenger domain (Otto et al., 2005). The repeats are a weak, but conserved and general feature of passengers and can be used to identify them in database searches (Oomen et al., 2004; Junker et al., 2006; Kajava and Steven, 2006). In fact, the autotransporter motifs in the pfam database (e.g. Pfam PF03212) are based upon these repeats. Nevertheless, not all passenger domains

are predicted to contain a β-helical subdomain, as is illustrated by EstA (van den Berg, 2010). Instead, the EstA passenger shows the characteristic conformation of lipolytic serine esterases, with a four-stranded parallel β-sheet sandwiched between α-helices. Apparently, the β-helical conformation is not a prerequisite for autotransporter secretion, which is also illustrated by the heterologous passengers that may lack a β-helical fold but are exposed on the cell surface (e.g. Veiga et al., 2004).

The in vitro folding of a passenger domain has been assessed using the adhesin pertactin and the cytotoxin Pet, which is a SPATE related to Hbp and EspP (Junker et al., 2006; Renn and Clark, 2008; Junker and Clark 2010). Pertactin was folded by dissolving inclusion bodies in 6M guanidine hydrochloride, followed by stepwise dilution in a folding buffer (Junker et al., 2006). Pet was purified from the medium of an *E. coli* culture and subsequently unfolded and re-folded (Renn and Clark, 2008). Unfolding in guanidine hydrochloride was monitored by measuring the tryptophan fluorescence or circular dichroism and indicated that the passenger domains unfold in two steps. Limited proteolyis by proteinase K revealed that the C-terminal region of the β-helical stem showed increased stability. Refolding of the protein by lowering the guanidine hydrochloride concentration was extremely slow, but not prone to aggregation and without a molten-globule intermediate. This slow refolding is remarkable and not in line with the observed fast secretion across the outer membrane (Skillman et al., 2005) and the speed of cell division. Detailed analysis using site-directed fluorescent labeling of pertactin mutants containing single cysteine residues showed that the β-strands of the passenger domain fold in multiple steps in a concerted manner, whereby there is no difference in the speed of folding of the C- and N-terminal parts of the β-helical stem (Junker and Clark, 2010). It suggests that the stable C terminus is not the starting point for folding per se. Nevertheless, the C-terminal region of a passenger is the first part that emerges from the outer membrane during secretion (Junker et al., 2009) and the folding of the β-helical part of the passenger domain is believed to drive translocation through the outer membrane (Jacob-Dubuisson et al., 2004).

8.6 Folding of Classical Autotransporters During Passage Through the Cell Envelope

The autotransporter domain organisation with the N-terminal signal peptide and the C-terminal outer-membrane-protein-like translocator domain suggested a fairly simple secretion route. N-terminal signal peptides direct proteins to the Sec machinery, whereas outer membrane β-barrel proteins have a central hydrophilic channel that could act as a pore. Subsequently, the secretion mechanism appeared straightforward and was hypothesised to include Sec-mediated passage of the inner membrane and secretion across the outer membrane through the pore in the translocator domain (Henderson et al., 1998; Jacob-Dubuisson et al., 2004). It also led to the name "autotransporter", although it rather reflects the absence of a dedicated secretion machinery than that no other proteins are involved in secretion (Fig. 8.3).

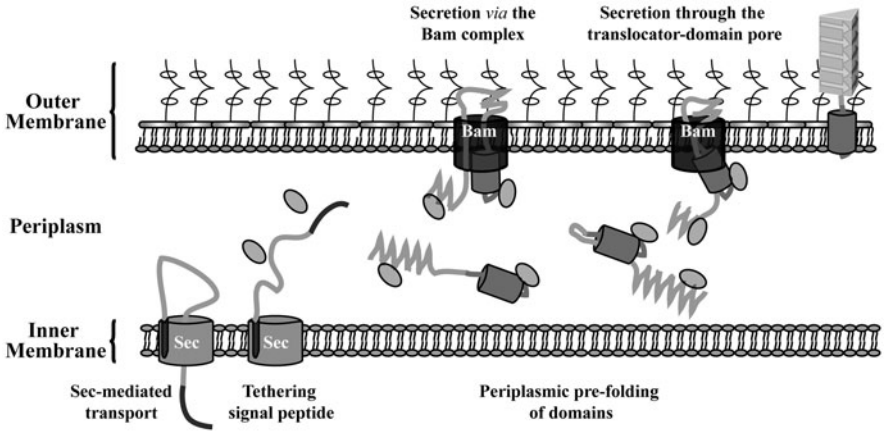

Fig. 8.3 Schematic overview of autotransporter secretion. Depicted from left to right: translocation across the inner membrane through the Sec machinery in an unfolded form; tethering to the Sec machinery via the extended signal peptide; pre-folding in the periplasm in presence of chaperones (*spheres*), with either an α-helix (*left*) or a hairpin (*right*) in the channel of the translocator domain; translocation across the outer membrane via the Bam complex, with the passenger domain going via the multi-protein Bam complex (*left*) or through the pore of the translocator domain (*right*); full insertion of the translocator domain in the outer membrane and full folding of the passenger at the cell surface

8.6.1 Passage Through the Inner Membrane

Most autotransporters carry fairly normal signal peptides (Desvaux et al., 2006). A few autotransporters carry a lipoprotein signal peptide with a lipobox [LA(A/G)C] that is acylated at the cysteine residue (van Ulsen et al., 2003). However, ~10% of the autotransporters, mostly found in the β- and γ-*proteobacteriae*, have rather long signal peptides of over 45 residues that contain an N-terminal extension of around 20–25 amino acid residues of which some are conserved (i.e. M^1,N^2,Y^5,Y^9 and E^{21}) (Henderson et al., 1998; Desvaux et al., 2006). Such extended signal peptides are found among all branches of the Type V secretion pathway.

Sec transports protein in an unfolded conformation to the periplasm. Two targeting routes exist. Hydrophobic inner membrane proteins target the Sec machinery cotranslationally via the signal recognition particle (SRP) route, while periplasmic and outer membrane proteins follow the posttranslational SecB pathway. Strikingly, however, in vitro cross-linking studies showed that nascent chains of Hbp and EspP, both containing an N-terminal extension, interact with components of the SRP pathway (Sijbrandi et al., 2003; Jong and Luirink, 2008; Zhang et al., 2010). However, the secretion did not appear to depend on either pathway, since it was not impaired in mutant strains lacking them (Sijbrandi et al., 2003; Brandon et al., 2003; Peterson et al., 2006). It was proposed that the N-terminal extension would act as a SRP-avoidance signal (Peterson et al., 2006), but its deletion did not alter the cross-linking or binding to the SRP particle (Jong and Luirink, 2008; Zhang et al.,

2010), nor did it change the facultative use of either pathway (Szabady et al., 2005; Peterson et al., 2006). The extension did seem to be important for later steps in the secretion process. In its absence the secretion of EspP was very inefficient and the folding of the passenger and translocator domain was impaired, as judged by the reduced heat-modifiability of the mutant (Szabady et al., 2005). Deleting the extension also prevented cell-surface exposure of the EspP passenger, since it became insensitive to extracellularly added proteases. Furthermore, overexpression of proteins that contained the full-length EspP signal peptide appeared to jam the Sec machinery. These observations led to a model in which the extension in the signal peptide keeps the autotransporters tethered to the Sec machinery longer to ensure the correct order of the later secretion steps (Fig. 8.3). Whether similar processes also occur during the secretion of autotransporters that carry non-extended signal peptides remains to be shown. However, the fusion of various types of signal peptides to NalP, including an extended one, resulted in some periplasmic degradation (V. Roussel-Jazédé, J. Tommassen, P. van Ulsen, unpublished results). Apparently, the passage of the cell envelope involves a tight interplay between the signal peptide and the other autotransporter domains, as well as the periplasmic factors that bind them (see below).

8.6.2 Passage Through the Outer Membrane

The first likely model for transport across the outer membrane was the hairpin model (Oomen et al., 2004; Jacob-Dubuisson et al., 2004). In this model, the translocator domain folds into a β-barrel that inserts into the outer membrane having in its lumen a hairpin containing the passenger C-terminus. The extracellular folding of the β-helical structure, starting from the hairpin, would thread the passenger domain through the channel. Epitopes inserted in the C-terminal region of the pertactin passenger appear first at the cell surface during secretion (Junker et al., 2009), which is in line with the C- to N-terminal folding sequence of the model. The folding could also provide the energy for secretion.

The crystal structures of the translocator domains clearly represent the end-stage of the secretion process, but also pose a problem for the hairpin model. The dimensions of the channels in the crystal structures are only just wide enough to accommodate the passage of two unfolded polypeptide chains, but not of a bulky tertiary-structure element. Therefore, transport would require a completely unfolded passenger domain; and initial experiments, in which the cholera toxin B subunit was fused as an artificial passenger to the translocator domain of IgA protease, indicated that formation of disulfide bridges blocked outer-membrane passage (Klauser et al., 1990). However, many natural passenger domains contain pairs of cysteines that potentially form a disulfide bridge. In Gram-negative bacteria these are formed by the Dsb enzymes in the periplasm; i.e. before transport – as indeed has been shown for a disulfide bridge in the IcsA passenger (Brandon and Goldberg, 2001). Similarly, an immunoglobulin fragment containing a disulfide-bridge was used as an artificial passenger domain; it, too, was found to be surface exposed (Veiga et al.,

2004). However, there seems to be a size limit. Pairs of cysteine residues were introduced into the Hbp and pertactin passengers to form smaller and larger loops (Jong et al., 2007; Junker et al., 2009). The larger loops blocked secretion, while smaller loops did not. Furthermore, when a small subdomain that extends from the β-helical backbone of Hbp was replaced by calmodulin, which adopts a bulky and rigid conformation in the presence of calcium but remains more flexible when it is absent, the mutant was only secreted when the calcium was depleted from the medium by adding EDTA (Jong et al., 2007). Overall, the results indicate that a certain degree of folding is tolerated for secretion.

Despite their name, autotransporters do require other proteins to be transported across the outer membrane. Absence of the multi-protein Bam complex, which assembles and inserts β-barrel outer membrane proteins into the outer membrane (Bos et al., 2007), impairs the secretion of IgA protease in *N. meningitidis* (Voulhoux et al., 2003) and IcsA when expressed in *E. coli* (Jain and Goldberg, 2007). The involvement of this complex may be restricted to the insertion of translocator domains into the outer membrane, but, in view of the size of the translocator domain channels, it was also proposed to have a more direct role in the secretion of passenger domains (Oomen et al., 2004) (Fig. 8.3). There is some experimental evidence that supports this model. The passenger of the secretion-incompetent Hbp disulfide-bridge mutant is exposed on the cell surface (Jong et al., 2007), even before its translocator domain is inserted into the outer membrane, since it did not display the characteristic heat-modifiability (Sauri et al., 2009). Similarly, the secretion-stalled mutants of pertactin and EspP were exposed on the cell surface before the translocator domains were inserted in the outer membrane (Junker et al., 2009; Ieva and Bernstein, 2009). Chemical cross-linking experiments, indeed, indicated an interaction between the stalled mutants of Hbp and EspP and the Bam complex (Sauri et al., 2009; Ieva and Bernstein, 2009). These interactions appear transient, since they could not be detected when the wild-type autotransporters were used. In EspP, the interactions mapped to both the passenger and the translocator domain (Ieva and Bernstein, 2009). The data indicate that the Bam complex might directly be involved in the secretion of the passenger domain across the outer membrane, while inserting the translocator domain. The complex might still harbour the passenger domain in a hairpin-like configuration as a starting point for secretion, as suggested by its C- to N-terminal appearance at the cell surface (Junker et al., 2009).

Not only does the passenger domain appear to adopt a partly folded conformation in the periplasm (Veiga et al., 2004; Jong et al., 2007; Junker et al., 2009); the translocator domain may also fold to some extent. Mutants of EspP that contained a protease recognition site within the α-helix that occupies the β-barrel channel were not accessible for that protease during periplasmic transit, since they were not cleaved when the protease was added to spheroplasts (Ieva et al., 2008). The protected fragment appeared to be in an α-helical conformation and not in an extended hairpin, since single-cysteine mutants in the region were not accessible for labelling, which would be expected for the latter. The β-barrel, apparently, folds around the α-helix before it inserts into the outer membrane.

8.6.3 Periplasmic and Extra-Cellular Folding of Autotransporter Domains

The periplasmic transit and folding of outer membrane proteins is governed by chaperones. These include the general chaperone Skp, folding catalysts like the disulphide-bridge-forming Dsb proteins, the cis/trans peptidyl prolyl isomerases (PPIases) SurA, Fkp and PpiA and D and the proteases DegP and DegQ, which function in the removal of misfolded proteins, while DegP also acts as a folding chaperone. Periplasmic chaperones appear redundant for outer membrane protein biogenesis, but the absence of two is lethal (Sklar et al., 2007). Chaperones are also involved in autotransporter secretion (Fig. 8.3), although again none appears essential. Nevertheless, the absence of chaperones Skp, SurA and DegP led to decreased secretion of IcsA and EspP (Purdy et al., 2007; Wagner et al., 2009; Ruiz-Pérez et al., 2009). Furthermore, the secretion-stalled mutants of Hbp and EspP cross-linked to the SurA chaperone (Sauri et al., 2009; Ieva and Bernstein, 2009). For outer membrane proteins, two routes appear to exist to the Bam complex (Sklar et al., 2007). The bulk of the outer membrane proteins interact with SurA, while the Skp/DegP route serves as a back-up system, which either rescues or degrades misfolded proteins not interacting with SurA (Sklar et al., 2007). Autotransporters appear to follow the same routes. Binding of SurA and Skp to the translocator domains of EspP and NalP has been shown by techniques like surface plasma resonance, yeast two-hybrid association and fluorescence spectroscopy (Qu et al., 2007; Ruiz-Pérez et al., 2009), while the DegP protease was found to be involved in the degradation of stalled mutants of Hbp (Jong et al., 2007). Interactions not only mapped to the translocator domain, but also involved the passenger domain (Ieva and Bernstein, 2009; Ruiz-Pérez et al., 2009), most likely via the aromatic residues in those domains since deletion of those residues in the EspP passenger abolished binding (Ruiz-Pérez et al., 2009).

Folding of the passenger domain at the cell surface would provide the energy for outer membrane translocation and the chaperones in the periplasm may prevent formation of fully-folded passengers. Mutations in the region that links the translocator domain β-barrel to the passenger domain were found to interfere with passenger stability and secretion (Ohnishi et al., 1994; Velarde and Nataro, 2004; Kostakioti and Stathopoulos, 2006). However, when the C-terminal part of the predicted β-helical stem of the BrkA autotransporter of *B. pertussis* was deleted, the protein was transported to cell surface, but the exposed passenger was unstable and prone to proteolytic degradation (Oliver et al., 2003). Apparently, the secretion is not blocked per se when a passenger can not attain its fully-folded conformation. The chaperone-binding sites in the EspP passenger mapped outside of this C-terminal autochaperone-like domain (Ruiz-Pérez et al., 2009). If, indeed, the passenger can be secreted without a folding step at the cell surface, it would exclude that a hairpin is the starting point for extra-cellular folding, although the sensitivity to proteases does not exclude the possibility of partial folding to a level that would suffice for secretion.

8.7 Concluding Remarks

It is now clear that the secretion route of autotransporters is grafted onto the biogenesis route of outer membrane proteins (Fig. 8.3). However, it remains to be seen to what extent the autotransporter domains fold in the periplasm versus at the cell surface and what their conformation is during the intermediate secretion steps, for example during the interaction with the Bam complex. Furthermore, the influence of the periplasmic chaperones on folding is still not resolved, nor is the difference between in vivo and in vitro folding efficiency. These types of data will be very important for a full understanding of the mechanism of autotransporter secretion.

References

Barnard TJ, Dautin N, Lukacik P, Bernstein HD, Buchanan SK (2007) Autotransporter structure reveals intra-barrel cleavage followed by conformational changes. Nat Struct Mol Biol 14:1214–1220

Benz I, Schmidt MA (1992) Isolation and serologic characterization of AIDA-I, the adhesin mediating the diffuse adherence phenotype of the diarrhea-associated *Escherichia coli* strain 2787, O126-H27. Infect Immun 60:13–18

Benz I, Schmidt MA (2001) Glycosylation with heptose residues mediated by the aah gene product is essential for adherence of the AIDA-I adhesin. Mol Microbiol 40:1403–1413

Bos MP, Robert V, Tommassen J (2007) Biogenesis of the Gram-negative bacterial outer membrane. Annu Rev Microbiol 61:191–214

Brandon LD, Goldberg MB (2001) Periplasmic transit and disulfide bond formation of the autotransported *Shigella* protein IcsA. J Bacteriol 183:951–958

Brandon LD, Goehring N, Janakiraman A, Yan AW, Wu T, Beckwith J, Goldberg MB (2003) IcsA, a polarly localized autotransporter with an atypical signal peptide, uses the sec apparatus for secretion, although the sec apparatus is circumferentially distributed. Mol Microbiol 50:45–60

Buchanan SK (1999) β-barrel proteins from bacterial outer membranes: structure, function and refolding. Curr Opin Struct Biol 9:455–461

Burgess NK, Dao TP, Stanley AM, Fleming KG (2008) β-barrel proteins that reside in the *Escherichia coli* outer membrane in vivo demonstrate varied folding behavior in vitro. J Biol Chem 283:26748–26758

Charbonneau ME, Berthiaume F, Mourez M (2006) Proteolytic processing is not essential for multiple functions of the Escherichia coli autotransporter adhesin involved in diffuse adherence, AIDA-I. J Bacteriol 188:8504–8512

Charbonneau ME, Janvore J, Mourez M (2009) Autoprocessing of the *Escherichia coli* AIDA-I autotransporter a new mechanism involving acidic residues in the junction region. J Biol Chem 284:17340–17351

Charbonneau ME, Mourez M (2008) The *Escherichia coli* AIDA-I autotransporter undergoes cytoplasmic glycosylation independently of export. Res Microbiol 159:537–544

Coutte L, Alonso S, Reveneau N, Willery E, Quatannens B, Locht C, Jacob-Dubisson F (2003) Role of adhesin release for mucosal colonization by a bacterial pathogen. J Exp Med 197: 735–742

de Jonge MI, Bos MP, Hamstra HJ, Jiskoot W, van Ulsen P, Tommassen J, van Alphen L, van der Ley P (2002) Conformational analysis of opacity proteins from *Neisseria meningitidis*. Eur J Biochem 269:5215–5223

Dé E, Saint N, Glinel K, Meli AC, Lévy D, Jacob-Dubuisson F (2008) Influence of the passenger domain of a model autotransporter on the properties of its translocator domain. Mol Membr Biol 25:192–U14

Desvaux M, Cooper LM, Filenko NA, Scott-Tucker A, Turner SM, Cole JA, Henderson IR (2006) The unusual extended signal peptide region of the type V secretion system is phylogenetically restricted. FEMS Microbiol Lett 264:22–30

Edwards JA, Groathouse NA, Boitano S (2005) *Bordetella bronchiseptica* adherence to cilia is mediated by multiple adhesin factors and blocked by surfactant protein A. Infect Immun 73:3618–3626

Emsley P, Charles IG, Fairweather NF, Isaacs NW (1996) Structure of *Bordetella pertussis* virulence factor P.69 pertactin. Nature 381:90–92

Eslava C, Navarro-Garcia F, Czeczulin JR, Henderson IR, Cravioto A, Nataro JP (1998) Pet, an autotransporter enterotoxin from enteroaggregative *Escherichia coli*. Infect Immun 66: 3155–3163

Fexby S, Bjarnsholt T, Jensen PO, Roos V, Høiby N, Givskov M, Klemm P (2007) Biological trojan horse: antigen 43 provides specific bacterial uptake and survival in human neutrophils. Infect Immun 75:30–34

Fink DL, Cope LD, Hansen EJ, St. Geme JW III (2001) The *Hemophilus influenzae* Hap autotransporter is a chymotrypsin clan serine protease and undergoes autoproteolysis via an intermolecular mechanism. J Biol Chem 276:39492–39500

Fink DL, Green BA, St Geme JW III (2002) The *Haemophilus influenzae* Hap autotransporter binds to fibronectin, laminin, and collagen IV. Infect Immun 70:4902–4907

Fukuda I, Suzuki T, Munakata H, Hayashi N, Katayama E, Yoshikawa M, Sasakawa C (1995) Cleavage of *Shigella* surface protein VirG occurs at a specific site, but the secretion is not essential for intracellular spreading. J Bacteriol 177:1719–1726

Gangwer KA, Mushrush DJ, Stauff DL, Spiller B, McClain MS, Cover TL, Lacy DB (2007) Crystal structure of the *Helicobacter pylori* vacuolating toxin p55 domain. Proc Natl Acad Sci USA 104:16293–16298

Hauck CR, Meyer TF (1997) The lysosomal/phagosomal membrane protein h-Lamp-1 is a target of the IgA1 protease of *Neisseria gonorrhoeae*. FEBS Lett 405:86–90

Henderson IR, Czeczulin J, Eslava C, Noriega F, Nataro JP (1999) Characterization of pic, a secreted protease of shigella flexneri and enteroaggregative *Escherichia coli*. Infect Immun 67:5587–5596

Henderson IR, Navarro-Garcia F, Nataro JP (1998) The great escape: structure and function of the autotransporter proteins. Trends Microbiol 6:370–378

Hendrixson DR, St Geme IIIJW (1998) The *Haemophilus influenzae* Hap serine protease promotes adherence and microcolony formation, potentiated by a soluble host protein. Mol Cell 2: 841–850

Hritonenko V, Kostakioti M, Stathopoulos C (2006) Quaternary structure of a SPATE autotransporter protein. Mol Membr Biol 23:466–474

Ieva R, Bernstein HD (2009) Interaction of an autotransporter passenger domain with bama during its translocation across the bacterial outer membrane. Proc Natl Acad Sci USA 106: 19120–19125

Ieva R, Skillman KM, Bernstein HD (2008) Incorporation of a polypeptide segment into the β-domain pore during the assembly of a bacterial autotransporter. Mol Microbiol 67: 188–201

Jacob-Dubuisson F, Fernandez R, Coutte L (2004) Protein secretion through autotransporter and two-partner pathways. Biochim Biophys Acta 1694:235–257

Jain S, Goldberg MB (2007) Requirement for yaet in the outer membrane assembly of autotransporter proteins. J Bacteriol 189:5393–5398

Johnson TA, Qiu JZ, Plaut AG, Holyoak T (2009) Active-site gating regulates substrate selectivity in a chymotrypsin-like serine protease: the structure of *Haemophilus influenzae* Immunoglobulin A1 protease. J Mol Biol 389:559–574

Jong WSP, Luirink J (2008) The conserved extension of the Hbp autotransporter signal peptide does not determine targeting pathway specificity. Biochem Biophys Res Comm 368: 522–527

Jong WSP, ten Hagen-Jongman CM, den Blaauwen T, Slotboom DJ, Tame JRH, Wickström D, de Gier JW, Otto BR, Luirink J (2007) Limited tolerance towards folded elements during secretion of the autotransporter Hbp. Mol Microbiol 63:1524–1536

Junker M, Besingi RN, Clark PL (2009) Vectorial transport and folding of an autotransporter virulence protein during outer membrane secretion. Mol Microbiol 71:1323–1332

Junker M, Clark PL (2010) Slow formation of aggregation-resistant β-sheet folding intermediates. Proteins 78:812–824

Junker M, Schuster CC, McDonnell AV, Sorg KA, Finn MC, Berger B, Clark PL (2006) Pertactin β-helix folding mechanism suggests common themes for the secretion and folding of autotransporter proteins. Proc Natl Acad Sci USA 103:4918–4923

Kajava AV, Steven AC (2006) The turn of the screw: variations of the abundant β-solenoid motif in passenger domains of type V secretory proteins. J Struct Biol 155:306–315

Khalid S, Sansom MSP (2006) Molecular dynamics simulations of a bacterial autotransporter: NalP from *Neisseria meningitidis*. Mol Membr Biol 23:499–508

Klauser T, Pohlner J, Meyer TF (1990) Extracellular transport of cholera-toxin B-subunit using *Neisseria* IgA protease β-domain – conformation-dependent outer-membrane translocation. EMBO J 9:1991–1999

Klemm P, Hjerrild L, Gjermansen M, Schembri MA (2004) Structure-function analysis of the self-recognizing antigen 43 autotransporter protein from *Escherichia coli*. Mol Microbiol 51: 283–296

Konieczny MPJ, Benz I, Hollinderbäumer B, Beinke C, Niederweis M, Schmidt MA (2001) Modular organization of the AIDA autotransporter translocator: the N-terminal β(1)-domain is surface-exposed and stabilizes the transmembrane β(2)-domain. Antonie Van Leeuwenhoek 80:19–34

Kostakioti M, Stathopoulos C (2006) Role of the α-helical linker of the C-terminal translocator in the biogenesis of the serine protease subfamily of autotransporters. Infect Immun 74: 4961–4969

Leininger E, Roberts M, Kenimer JG, Charles IG, Fairweather N, Novotny P, Brennan MJ (1991) Pertactin, an arg-gly-asp-containing *Bordetella pertussis* surface protein that promotes adherence of mammalian cells. Proc Natl Acad Sci USA 88:345–349

Lin L, Ayala P, Larson J, Mulks M, Fukuda M, Carlsson SR, Enns C, So M (1997) The *Neisseria* type-2 IgA1 protease cleaves lamp1 and promotes survival of bacteria within epithelial cells. Mol Microbiol 24:1083–1094

Lindenthal C, Elsinghorst EA (2001) Enterotoxigenic *Escherichia coli* TibA glycoprotein adheres to human intestine epithelial cells. Infect Immun 69:52–57

Lipski SL, Akimana C, Timpe JM, Wooten RM, Lafontaine ER (2007) The *Moraxella catarrhalis* autotransporter McaP is a conserved surface protein that mediates adherence to human epithelial cells through its N-terminal passenger domain. Infect Immun 75:314–324

Loveless BJ, Saier MH (1997) A novel family of channel-forming, autotransporting, bacterial virulence factors. Mol Membr Biol 14:113–123

Meng GY, Surana NK, St Geme IIIJW, Waksman G (2006) Structure of the outer membrane translocator domain of the *Haemophilus influenzae* Hia trimeric autotransporter. EMBO J 25:2297–2304

Ohnishi Y, Nishiyama M, Horinouchi S, Beppu T (1994) Involvement of the COOH-terminal prosequence of *Serratia marcescens* serine-protease in the folding of the mature enzyme. J Biol Chem 269:32800–32806

Oliver DC, Huang G, Nodel E, Pleasance S, Fernandez RC (2003) A conserved region within the *Bordetella pertussis* autotransporter BrkA is necessary for folding of its passenger domain. Mol Microbiol 47:1367–1383

Oomen CJ, van Ulsen P, Van Gelder P, Feijen M, Tommassen J, Gros P (2004) Structure of the translocator domain of a bacterial autotransporter. EMBO J 23:1257–1266

Otto BR, Sijbrandi R, Luirink J, Oudega B, Heddle JG, Mizutani K, Park SY, Tame JRH (2005) Crystal structure of hemoglobin protease, a heme binding autotransporter protein from pathogenic *Escherichia coli*. J Biol Chem 280:17339–17345

Peterson JH, Szabady RL, Bernstein HD (2006) An unusual signal peptide extension inhibits the binding of bacterial presecretory proteins to the signal recognition particle, trigger factor, and the SecYEG complex. J Biol Chem 281:9038–9048

Plaut AG, Gilbert JV, Artenstein MS, Capra JD (1975) *Neisseria gonorrhoeae* and *Neisseria meningitidis* extracellular enzyme cleaves human Immunoglobulin A. Science 190:1103–1105

Pohlner J, Halter R, Beyreuther K, Meyer TF (1987) Gene structure and extracellular secretion of *Neisseria gonorrhoeae* IgA protease. Nature 325:458–462

Purdy GE, Fisher CR, Payne SM (2007) Icsa surface presentation in *Shigella flexneri* requires the periplasmic chaperones DegP, Skp, and SurA. J Bacteriol 189:5566–5573

Qu J, Mayer C, Behrens S, Holst O, Kleinschmidt JH (2007) The trimeric periplasmic chaperone Skp of *Escherichia coli* forms 1:1 complexes with outer membrane proteins via hydrophobic and electrostatic interactions. J Mol Biol 374:91–105

Renn JP, Clark PL (2008) A conserved stable core structure in the passenger domain α-helix of autotransporter virulence proteins. Biopolymers 89:420–427

Roussel-Jazédé V, Van Gelder P, Sijbrandi R, Rutten L, Otto BR, Luirink J, Gros P, Tommassen J, van Ulsen P (2011) Channel properties of the translocator domain of the autotransporter Hbp of Escherichia coli. Mol Membr Biol in press, doi:10.3109/09687688.2010.550328, appeared online 14 Feb 2011

Ruiz-Pérez F, Henderson IR, Leyton DL, Rossiter AE, Zhang YH, Nataro JP (2009) Roles of periplasmic chaperone proteins in the biogenesis of serine protease autotransporters of *Enterobacteriaceae*. J Bacteriol 191:6571–6583

Salacha R, Kovačić F, Brochier-Armanet C, Wilhelm S, Tommassen J, Filloux A, Voulhoux R, Bleves S (2010) The *Pseudomonas aeruginosa* patatin-like protein PlpD is the archetype of a novel type V secretion system. Environ Microbiol 12:1498–1512

Sauri A, Soprova Z, Wickström D, de Gier JW, Van der Schors RC, Smit AB, Jong WSP, Luirink J (2009) The Bam, Omp85, complex is involved in secretion of the autotransporter haemoglobin protease. Microbiology 155:3982–3991

Serruto D, Adu-Bobie J, Scarselli M, Veggi D, Pizza M, Rappuoli R, Aricò B (2003) *Neisseria meningitidis* App, a new adhesin with autocatalytic serine protease activity. Mol Microbiol 48:323–334

Sherlock O, Schembri MA, Reisner A, Klemm P (2004) Novel roles for the AIDA adhesin from diarrheagenic *Escherichia coli*: cell aggregation and biofilm formation. J Bacteriol 186: 8058–8065

Sijbrandi R, Urbanus ML, ten Hagen-Jongman CM, Bernstein HD, Oudega B, Otto BR, Luirink J (2003) Signal recognition particle (SRP)-mediated targeting and sec-dependent translocation of an extracellular *Escherichia coli* protein. J Biol Chem 278:4654–4659

Skillman KM, Barnard TJ, Peterson JH, Ghirlando R, Bernstein HD (2005) Efficient secretion of a folded protein domain by a monomeric bacterial autotransporter. Mol Microbiol 58:945–958

Sklar JG, Wu T, Kahne D, Silhavy TJ (2007) Defining the roles of the periplasmic chaperones SurA, Skp and DegP in *Escherichia coli*. Genes Dev 21:2473–2484

Stathopoulos C, Provence DL, Curtiss R (1999) Characterization of the avian pathogenic *Escherichia coli* hemagglutinin Tsh, a member of the immunoglobulin A protease-type family of autotransporters. Infect Immun 67:772–781

Szabady RL, Peterson JH, Skillman KM, Bernstein HD (2005) An unusual signal peptide facilitates late steps in the biogenesis of a bacterial autotransporter. Proc Natl Acad Sci USA 102: 221–226

Tajima N, Kawai F, Park SY, Tame JRH (2010) A novel Intein-like autoproteolytic mechanism in autotransporter proteins. J Mol Biol 402:645–656

Turner DPJ, Marietou AG, Johnston L, Ho KKL, Rogers AJ, Wooldridge KG, Ala'Aldeen DAA (2006) Characterization of MspA, an immunogenic autotransporter protein that mediates adhesion to epithelial and endothelial cells in *Neisseria meningitidis*. Infect Immun 74:2957–2964

van den Berg B (2010) Crystal structure of a full-length autotransporter. J Mol Biol 396:627–633

Van Gelder P, Dumas F, Winterhalter M (2000) Understanding the function of bacterial outer membrane channels by reconstitution into black lipid membranes. Biophys Chem 85:153–167

van Ulsen P, Adler B, Fassler P, Gilbert M, van Schilfgaarde M, van der Ley P, van Alphen L, Tommassen J (2006a) A novel phase-variable autotransporter serine protease, AusI, of Nei*sseria meningitidis*. Microbes Infect 8:2088–2097

van Ulsen P, Gros P, Tommassen J (2006b) Structure and function of the translocator domain of bacterial autotransporters. In: Grisshammer R, Buchannan SK (eds) Structural biology of membrane proteins. Royal Society of Chemistry, Cambridge, pp 270–287

van Ulsen P, Rutten L, Feller M, Tommassen J, van der Ende A (2008) Two-partner secretion systems of *Neisseria meningitidis* associated with invasive clonal complexes. Infect Immun 76:4649–4658

van Ulsen P, van Alphen L, Hopman CTP, van der Ende A, Tommassen J (2001) In vivo expression of *Neisseria meningitidis* proteins homologous to the *Haemophilus influenzae* Hap and Hia autotransporters. FEMS Immunol Med Microbiol 32:53–64

van Ulsen P, van Alphen L, ten Hove J, Fransen F, van der Ley P, Tommassen J (2003) A neisserial autotransporter NalP modulating the processing of other autotransporters. Mol Microbiol 50:1017–1030

Veiga E, de Lorenzo V, Fernández LA (2004) Structural tolerance of bacterial autotransporters for folded passenger protein domains. Mol Microbiol 52:1069–1080

Velarde JJ, Nataro JP (2004) Hydrophobic residues of the autotransporter EspP linker domain are important for outer membrane translocation of its passenger. J Biol Chem 279:31495–31504

Virji M (2009) Pathogenic *Neisseriae*: surface modulation, pathogenesis and infection control. Nat Rev Microbiol 7:274–286

Voulhoux R, Bos MP, Geurtsen J, Mols M, Tommassen J (2003) Role of a highly conserved bacterial protein in outer membrane protein assembly. Science 299:262–265

Wagner JK, Heindl JE, Gray AN, Jain S, Goldberg MB (2009) Contribution of the periplasmic chaperone Skp to efficient presentation of the autotransporter icsa on the surface of *Shigella flexneri*. J Bacteriol 191:815–821

Wilhelm S, Tommassen J, Jaeger KE (1999) A novel lipolytic enzyme located in the outer membrane of *Pseudomonas aeruginosa*. J Bacteriol 181:6977–6986

Zhang X, Rashid R, Wang K, Shan SO (2010) Sequential checkpoints govern substrate selection during cotranslational protein targeting. Science 328:757–760

Chapter 9
Structure and Biology of Trimeric Autotransporter Adhesins

Andrzej Łyskowski, Jack C. Leo, and Adrian Goldman

Abstract Trimeric autotransporter adhesins (TAAs) are a family of secreted Gram-negative bacterial outer membrane (OM) proteins. These obligate homotrimeric proteins share a common molecular organisation, consisting of a N-terminal "passenger" domain followed by a C-terminal translocation unit/membrane anchor. All described TAAs act as adhesins. The passenger domain is responsible for specific adhesive and other activities of the protein and has a modular architecture. Its globular head domain(s), where ligands often bind, are projected away from the bacterial surface by an extended triple α-helical coiled coil stalk attached to the β-barrel anchor. The head domains appear to be constructed from a limited set of subdomains. The β-barrel anchor is the only part of the protein strictly conserved between family members. It appears that the extracellular export of the passenger does not require an external energy source or auxiliary proteins, though recent data indicate that an OM complex (the Bam complex) is involved in passenger domain secretion. The ability to bind to a variety of host molecules such as collagen, fibronectin, laminin or cell surface receptors via a structurally diverse elements suggests that TAAs have evolved a unique mechanism which closely links structure to folding and function.

9.1 Introduction

Although the vast majority of symbiotic bacteria are either harmless or beneficial to their (human) hosts, one of the most evident, negative results of human interaction with the surrounding ocean of microbial life is the occurrence of diseases, some life-threatening. Gram-negative infectious bacteria have caused very high levels of morbidity and mortality, such as *Yersinia pestis*, the causative agent of

A. Goldman (✉)
Institute of Biotechnology, Viikinkaari 1, University of Helsinki, FIN-00014 Helsinki, Finland
e-mail: adrian.goldman@helsinki.fi

D. Linke, A. Goldman (eds.), *Bacterial Adhesion*, Advances in Experimental Medicine and Biology 715, DOI 10.1007/978-94-007-0940-9_9,

bubonic plague, which eradicated up to 40% of the population of Europe in the fourteenth century (Perry and Fetherston, 1997). Even today, septicemic melioidosis, caused by *Burkholderia pseudomallei* which is endemic in Southeast Asia, has a greater than 10% mortality rate even with treatment (e.g. Warner et al., 2007). The introduction of effective antibiotics in the twentieth century, starting with the discovery of penicillin in 1928 (Fleming, 1929), resulted in a huge decrease in mortality due to bacterial infections. However, the emergence of multiply antibiotic-resistant bacterial strains and the steadily growing threat of bioterrorism have increased interest in what were only recently considered defeated diseases.

To successfully colonize the host, bacteria need to establish and maintain an association with host tissues. Various secreted virulence factors facilitate forming such connections during infection. Trimeric autotransorter adhesins (TAAs) comprise a group of virulence-related proteins in Gram-negative bacteria (Linke et al., 2006). These obligate homotrimeric proteins are embedded in the outer membrane (OM) and act primarily as adhesins. Members of the family bind to diverse molecules, such as cell surface receptors, components of the extracellular matrix (ECM) such as collagen and laminin, and each other (i.e. they act as autoagglutinins). Furthermore, they often protect the bacterium from host immune responses by binding modulators of both the antibody-mediated and innate pathways of complement, such as Factor H, antibodies, or C4b binding protein (Kirjavainen et al., 2008).

TAAs are obligate homotrimeric proteins with a common modular organisation, consisting of an N-terminal "passenger" domain followed by a C-terminal translocation unit/membrane anchor. The N-terminal part, the passenger domain, is responsible for binding. The highly conserved C-terminal domain, the translocation unit, transports the passenger across the outer membrane (OM) into the extracellular space. The β-barrel is the only part of the protein strictly conserved between family members in terms of sequence and structure. The translocation process seems to be independent of any external source of free energy, such as adenosine triphosphate (ATP), ion gradients, or other proteins; hence the name autotransporter (Henderson et al., 2004). However, recent data indicates that an OM complex (the Bam complex) is involved in passenger domain secretion. Overall, the available data suggest that folding, function and structure are very closely linked in TAAs.

The prototypical trimeric autotransporter is the *Yersinia* adhesin A (YadA), found in two enteropathogenic species, *Y. enterocolitica* and *Y. pseudotuberculosis*. Other TAAs have been characterized (Table 9.1), and genomic sequencing has shown that they are common in a variety of pathogenic, commensal and environmental Gram-negative species (Szczesny and Lupas, 2008). The sizes of TAAs vary not only between bacterial species but also between strains of the same species. For instance, *Y. enterocolitica* YadA can be between 422 and 455 amino acids long (El Tahir and Skurnik, 2001). Among the well-studied TAAs, the size range is from 340 residues (the putative TAA from *Fusobacterium nucleatum*) to 3082 residues (*Bartonella* adhesin A, BadA) (Szczesny and Lupas, 2008; Szczesny et al., 2008).

Table 9.1 Selected characterized trimeric autotransporter adhesins. STEC = Shiga toxin-producing *E. coli,* UPEC = uropathogenic *E. coli*

Protein	Organism(S)	Disease	Functions
AhsA	*Mannheimia haemolytica*	Bovine pneumonic pateurellosis	Collagen binding
BadA	*Bartonella henselae*	Cat scratch disease	Collagen binding, binding to epithelial cells, phagocytosis resistance, proangiogenic factor
BimA	*Burkholderia pseudomallei*	Melioidosis	Actin binding, polymerisation and actin-based motility
Cha	*Haemophilus* sp.	Maternal urogenital and neonatal respiratory infections	Binding to epithelial cells
DsrA	*Haemophilus ducreyi*	Chancroid	Serum resistance, keratinocyte binding, ecm binding
EibA, EibE	*E. coli*	–	IgG binding, serum resistance
EibC, EibD, EibF	*E. coli*	–	IgA and IgG binding, serum resistance
EibG	STEC	Gastroenteritis	Binding IgA and IgG, chain-like adhesion to mammalian cells
EmaA	*Aggregatibacter actino-mycetemcomi-tans*	Periodontal disease	Collagen binding
HadA	*H. influenzae*	Otitis media, sinusitis, conjunctivitis, pneumonia	Autoagglutination, ECM binding, epithelial cell binding and invasion
Hia, Hsf	*H. influenzae*	Otitis media, sinusitis, conjunctivitis, pneumonia	Epithelial cell binding
MID	*Moraxella catarrhalis*	Otitis media, bronchitis, sinusitis, laryngitis	IgD binding, adhesion to lung and middle ear epithelial cells, biofilm formation
NadA	*Neisseria meningitidis*	Meningitis	Adhesion to and invasion of epithelial cells
NhhA	*Neisseria meningitidis*	Meningitis	ECM binding, binding to epithelial cells, serum and phagocytosis resistance
Saa	STEC	Gastroenteritis	Autoagglutination, binding to epithelial cells
UpaG	UPEC	Urinary tract infections	ECM binding, biofilm formation, autoagglutination
UspA1, UspA2	*M. catarrhalis*	Otitis media, bronchitis, sinusitis, laryngitis	ECM and epithelial cell binding, serum resistance, biofilm formation
VompA, VompC	*B. quintata*	Trench fever	Collagen binding, autoagglutination

Table 9.1 (continued)

Protein	Organism(S)	Disease	Functions
XadA	*Xanthomonas oryzae* pv. *Oryzae*	Rice blight	Leaf attachment and entry
YadA	*Yersinia enterocolitica*, *Y. pseudotuberculosis*	Gastroenteritis, mesenteric lymphadenitis	ECM binding, serum and phagocytosis resistance, autoagglutination, binding to epithelial cells and neutrophils
YadB, YadC	*Yersinia pestis*	Plague	Epithelial cell invasion

9.2 TAA Secretion and Folding

In Gram-negative bacteria, secreted proteins must successfully traverse two membranes. To facilitate this, Gram-negative bacteria have evolved several specialised secretion systems. The type V secretion system includes autotransportation and two-partner secretion. Type V secretion is a two-step process: the proteins contain a signal peptide that directs them to the Sec machinery (the general secretion pathway; Dautin and Bernstein, 2007) to cross the inner membrane. Once in the periplasm, there are three distinct subsystems for crossing the OM. Type Va is the classical autotransportation pathway; type Vb refers to two-partner secretion; and type Vc refers to TAAs (see Chapter 8, this volume). In all three, transport of the extracellular passenger domain through the OM depends on an integral β-barrel membrane component. In Type Va and type Vc, a single gene appears to encode all the components required for transportation. For type Vc (TAAs), three identical copies of the resulting polypeptide chain are required to allow secretion and to form the functional protein (Dautin and Bernstein, 2007). Separate genes encode the secreted passenger domain and the translocation unit in the two-partner secretion system (Hodak and Jacob-Dubuisson, 2007).

IgA1 protease from *Neisseria gonorrheae* was the first example of a classical autotransporter (Pohlner et al., 1987). Classical autotransporters are composed of a single polypeptide chain with three distinct regions: an N-terminal signal peptide, a central large passenger domain, encoding the biological function of the autotransporter, and the C-terminal β-barrel domain or translocation unit. Secretion and folding are proposed to occur thus: the N-terminal signal peptide is recognized by the Sec machinery, which translocates the protein across the inner membrane. Afterwards, the C-terminal β-barrel inserts into the OM to form a pore. The passenger domain is then transported through this pore into the extracellular space. Folding of the extracellular passenger domain into its native conformation appears to be concurrent with translocation. In some cases, the mature passenger is cleaved from the surface resulting in soluble protein (Henderson et al., 2004).

This is in contrast to TAAs (see below). There are a limited number of domain structures of classical autotransporters in the protein data bank (PDB); for a review see (Nishimura et al., 2010).

Two-partner secretion (type Vb) is similar to type Va in that there are two separate components: a secreted passenger domain and a translocation unit. However, these components are encoded by two separate genes, referred to as TspA (the passenger domain) and TspB (the membrane embedded translocation unit). The TspB seems to dedicated to secreting only its associated TspA partner. As for classical autotransporters, many members of the two-partner secretion system are released into medium. However, some remain attached to the OM (Hodak and Jacob-Dubuisson, 2007).

TAAs constitute the third class of the type V secretion system (type Vc). Members of this group are, as the name implies, obligate homotrimers and trimerisation is required for activity (Cotter et al., 2006). In contrast to classical autotransporters, all passenger domains of TAAs studied so far remain covalently attached to the β-barrel membrane anchor; they are not cleaved following secretion (Linke et al., 2006). The prototypical members of the family are YadA (El Tahir and Skurnik, 2001; Koretke et al., 2006) and the *Haemophilus influenzae* adhesion protein Hia (St. Geme and Cutter, 2000). Originally, YadA was described as a non-pilus-associated adhesin in order to differentiate it from fimbriae and pili. Due to the presence of the extended coiled coil content in characterized members of the family, a second name, oligomeric coiled-coil adhesin or Oca was used (Roggenkamp et al., 2003). Finally, trimeric autotransporter adhesins (TAAs) was established to emphasize the trimeric nature of the proteins, translocation mechanism through the OM and their main function (Linke et al., 2006).

The mechanism of autotransport is generally assumed to be the same for both classical autotransporters and TAAs, the principal difference being how many chains are translocated. Three models have been proposed to explain the autotransportation mechanism.

The single-chain model predicts that the C-terminal β-barrel folds into the outer membrane first while the passenger domain remains in a transport-competent (unfolded) state in the periplasm, possibly due to slow release from the Sec machinery (Szabady et al., 2005) and/or the participation of chaperones (Hagan et al., 2010). Once the functional β-barrel is formed, the most probable translocation sequence would require formation of a β-hairpin at the C-terminus of the passenger domain and insertion of this hairpin into the pore of the β-barrel. The rest of the polypeptide chain would then pass through the pore with C-to-N-terminal polarity (Fig. 9.1).

In a variant of this model, the passenger domain is threaded from the N-terminus first, as this forms the membrane-distal structure in the folded protein. This seems unlikely, for several reasons. First, deletions and modifications of the N-terminal part of autotransporters do not inhibit translocation, so it is unlikely that a pore targeting sequence exists at the N-terminus of the passenger domain (Bernstein, 2007; Hoiczyk et al., 2000). Second, the sheer length of some of the passenger domains makes it unlikely that three could be folded through the pore in register. Third, passage of the N-terminus first is inconsistent with the requirement for slow

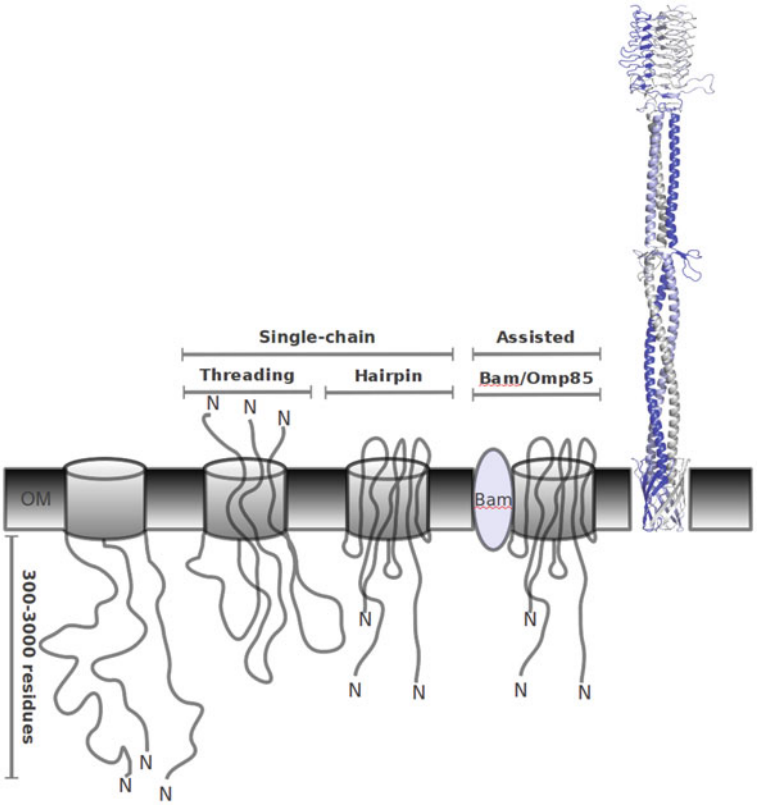

Fig. 9.1 Models for the autotransport mechanism. In the "single-chain" models all elements required for the autotransport are contained within the polypeptide chain. Specifically, the passenger domain inserts through the pore of the translocation unit β-barrel in an unfolded state and folds on the outside of the cell. There are two possible ways in which this can be achieved: N-terminus first (threading model) or C-terminus first (hairpin model). In the assisted model, Bam machinery is involved in initial biogenesis of the translocation unit and assists in passenger secretion (see Chapter 8, this volume). *Right*: theoretical model of EibD

release from the Sec machinery (Szabady et al., 2005). In either case, folding of the passenger domain would be concurrent with it crossing the membrane pore, and the free energy released upon folding presumably provides the driving force required for translocation. The resulting topology makes the process essentially irreversible (Klauser et al., 1990).

In the multimeric model, translocation is a joint effort. The passenger domain is presumed to be secreted by a macrostructure formed by several translocation domains. The central pore generated by the oligomeric structure would be sufficiently large to allow passage of even folded proteins (Veiga et al., 2002). A central problem with this model is topological. Once the passenger domain has been transported through the putative central pore, it must be passed into the centre of the

β-barrel. The folded passenger domain is interwound and attaches to the β-barrel in three different places, at the beginning of strands 1, 5 and 9. Passing the passenger domain into the core of the barrel would thus require not only unwinding it at least slightly but also opening the barrel in three separate places. Such opening is at the very least inconsistent with the fact that the barrel is the most stable part of a TAA.

The third model suggests that auxiliary outer membrane proteins are required to assist in translocation. The Bam complex (formerly Omp85 or YaeT), which is required for the biogenesis of outer membrane β-barrel proteins (Voulhoux et al., 2003), could assist during translocation either by providing a temporary channel through which the passenger is transported or by acting as an assembly scaffold by stabilizing the membrane pore (Bernstein, 2007). Recent evidence suggests that the Bam complex interacts with the passenger domains of classical autotransporters, and it is reasonable to assume this would be the case for TAAs as well (Sauri et al., 2009; Ieva and Bernstein, 2009).

For TAAs, the most probable model is a combination of the single-chain model and Bam-assisted transportation. For example, the Bam complex could assist in the initial biogenesis of the membrane pore, with the final translocation occurring by the single-chain mechanism. However, it has to be emphasized that even though the general mechanism is probably similar between classical autotransporters and TAAs, differences must exist. Due to their multimeric nature, TAAs must have evolved a unique way to deal with the synchronized transport and folding of multicomponent passenger domains.

9.3 Structural Organisation

TAAs show a simple head-stalk-anchor organization. The head mediates host-specific binding properties, the stalk projects the head beyond the membrane, and the membrane anchor secretes both previous components. Bacteria have evolved a wide array of head domains, and the structural mismatch between the globular head domains and the fibre-like stalk domain requires the presence of an additional class of "neck" elements acting as connectors. These provide a smooth transition to and from the stalk.

Detailed electron microscopy studies on the expression of YadA of *Yersinia enterrocolitica* and UspA1 of *Moraxella catarrhalis* provided the first information on the structural organization of TAAs. Electron micrographs of *Yersinia* YadA and *Moraxella* UspA1 revealed "lollipop"-like projections on the surface of the bacteria (Hoiczyk et al., 2000). In the case of YadA, projections approximately 23 nm long were observed. These pillar-like projections consisted of two distinct elements: a *ca*. 18 nm long stem-like part (the stalk) and a bulky head domain *ca*. 5 nm long. The identity of these structural elements was verified by mutagenesis and deletion studies. Four YadA constructs were studied (Hoiczyk et al., 2000). The N-terminal deletion mutant $YadA_{\Delta 29–81}$ showed a ~50% decrease in size of

the head domain in comparison to wild-type YadA. Similarly, various deletions in the stalk domain resulted in a reduction in stalk length proportional to the size of the deletion.

Sequence analysis combined with the electron micrograph data suggested that the YadA stalk was most likely formed by an extended coiled coil, a structure with two or more α-helices packed either parallel or antiparallel with respect to each other (Moutevelis and Woolfson, 2009). A search for repetitive patterns in YadA by Fourier analysis revealed a strong 15-residue periodicity. Further analysis suggested that the whole region should form a strongly amphipathic α-helix. However, the calculated periodicity of 3.75 residue/turn was significantly larger then the 3.5/3.6-residue periodicity expected for a typical left-handed coiled coil. A right-handed coiled coil *ca*. 17.5 nm long was found to be most compatible with the experimental data.

This was surprising. The coiled coils in TAAs are perforce trimeric, and typical trimeric coiled coils are left-handed (see below). The sequence motif encoding a coiled coil is composed of hydrophobic (H) residues separated by three and four polar (P) residues [$(HPPHPPP)_{n\geq 3}$]: the positions in the heptad repeat are designated *abcdefg*. The crossing angle between the helices in a coiled coil is close to zero, and the packing follows a "knobs-into-holes" arrangement (Crick, 1953), where the knobs formed by hydrophobic residues in positions *a* and *d* pack into cavities formed by residues on a neighbouring helix (Lupas and Gruber, 2005). In TAAs, the three helices are wound in register around each other, so all of the *a* residues are at the same height, as are the *b*s and so on. Position *a* favours β-branched side-chains (Ile, Val, Thr), while residues in position *d* are closer together and so unbranched residues are favoured (Lupas and Gruber, 2005).

Identifying and classifying the TAA coiled coils is thus important. Lupas and coworkers have thus developed the Domain Annotation in Trimeric Autotransporter Adhesins (daTAA, http://toolkit.tuebingen.mpg.de/dataa) server to assist in annotation of TAAs and to provide detailed information on their modular structure (Szczesny and Lupas, 2008). TAAs are hard to annotate because they are modular and trimeric; the domains are too small to be properly identified when only the monomer is considered. The daTAA server addresses the above issues and, with the help of a knowledge-based approach and manually curated TAA sequence profiles, it provides a unique tool for TAA domain analysis. Below we discuss the structurally solved TAA domains, as annotated in the daTAA server (Fig. 9.2).

9.3.1 YadA-Like Head Domain (YLhead)

The YadA head domain from *Y. enterocolitica* was the first structure containing this fold to be solved. Short β-strands form layers of a left-handed parallel β-roll (LPBR) fold with a right-handed superhelical twist (Nummelin et al., 2004). The YadA β-roll has a number of unique features. It is one of the most compact β-roll structures known. It is composed of a canonical 14-residue repeat motif, of the form Turn 1 – three-residue inner strand – Turn 2 – three-residue outer strand. The repeat

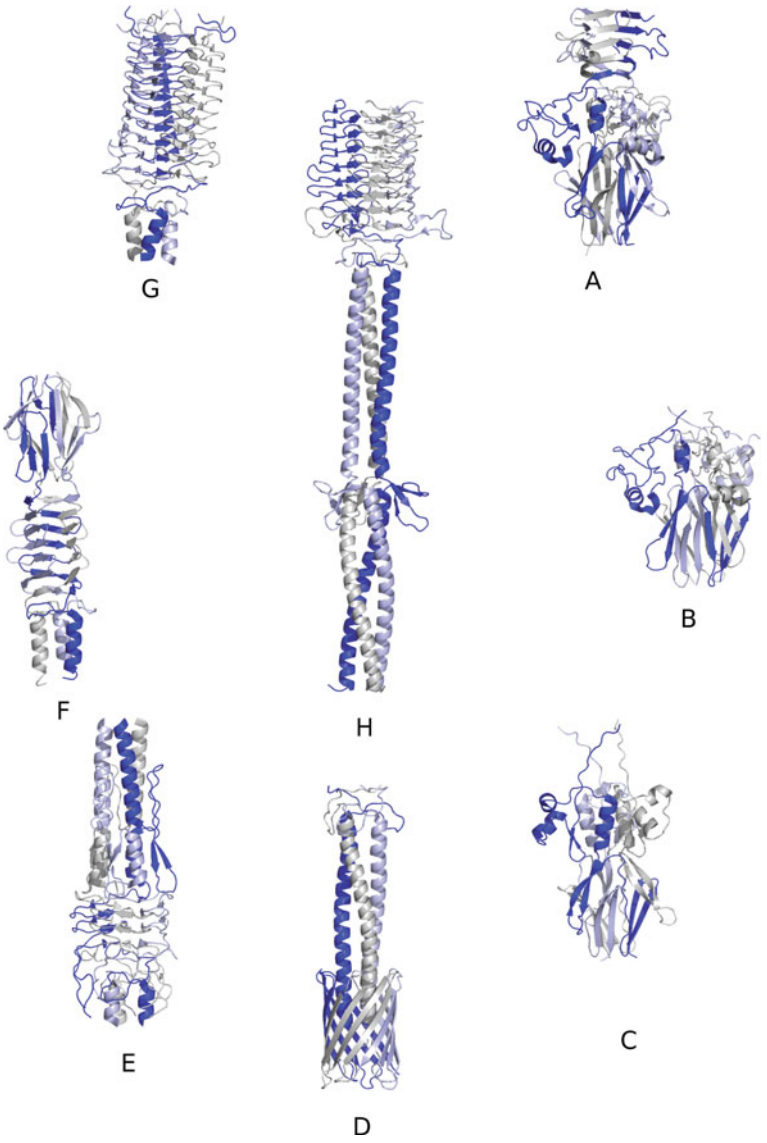

Fig. 9.2 Cartoon representation of selected experimentally determined domain structures of TAAs, all scaled to the same size. The structures are identified by their PDB ID codes where available. (**a**) 1s7m: structure of *Haemophilus* HiaBD1; (**b**) 3emf: structure of *Haemophilus* HiaDB2; (**c**) 3emi: structure of *Haemophilus* Hia 307–442 non-adhesive domain; (**d**) 3emo: structure of transmembrane domain of *Haemophilus* Hia 973–1098; (**e**) 3la9: structure of *Burkholderia* BpaA; (**f**) 3dx9: structure of the head of the *Bartonella adhesin* BadA; (**g**) 1p9h: structure of the collagen binding domain of *Yersinia* YadA; (**h**) 2xqh: structure of the head domain of *E. coli* EibD

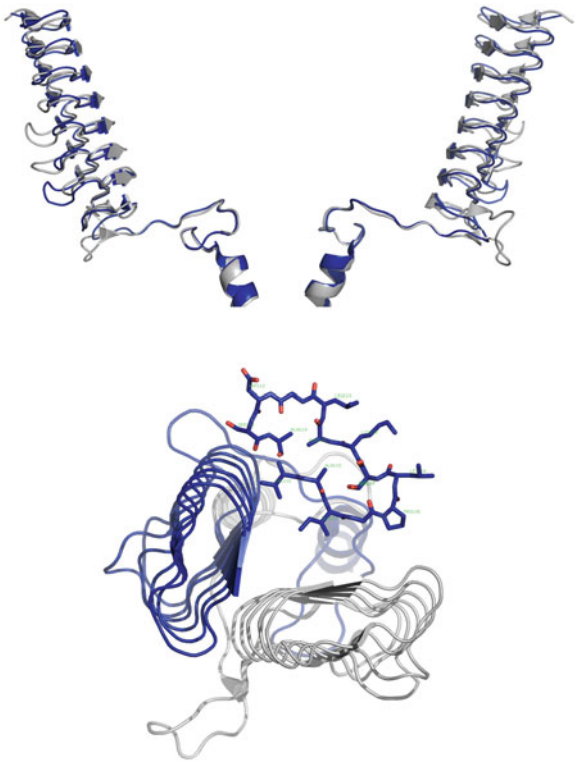

Fig. 9.3 YadA like head domain characteristics. *Top*: YadA (*blue*) and EibD (*silver*) head monomer overlay in two different orientations, showing the longer loops in the EibD head. *Bottom*: The left-handed parallel β-roll (LPBR) viewed from above along the three-fold axis. The colour scheme is as in the top panel. In the top right, a single layer of the YadA LPBR, showing a conserved NSVAIG motif. The residues are coloured in atom colour and labeled

varies in YadA from 13 to 16 residues, due to insertions in the outer strand, with the longest one at the C-terminus of the LPBR. Longer insertions are found in other TAAs (Fig. 9.3). The trimeric domain is formed from a total of nine repeats with the consensus sequence of NSVAIGXXS and binds diverse proteins of the extracellular matrix. The hydrophobic interior of the trimer is formed by the conserved Val and Ile, while small hydrophobic residues, typically Ala, pack in the monomer interior. Both turns in YLhead are type II turns, with a left-handed α-helical residue at position one. This position is always Gly in Turn 2 due to steric hindrance from neighbouring monomers, but Gly occurs only 3/9 times in the equivalent position in Turn 1. In both turns, the conformation is often stabilized by hydrogen bonding between the carbonyl oxygen at position one and the Ser at position four (Fig. 9.3).

9.3.2 Trp ring, GIN and KG Head Domains

The secondmost frequent TAA head domain after the YLhead is the Trp ring domain, which was observed in all of the Hia head domain structures. The name

comes from a distinctive feature of this domain, a ring of highly conserved Trp residues in the C-terminal part of the domain. These residues are located at the interface between the preceding coiled coil and the domain's β-meander. A GIN domain frequently neighbours Trp ring domains. The GIN domain is named after a characteristic Gly-Ile-Asn motif, which allows it to be identified in TAAs by sequence alone. Like many of the head domains, it is an all-β domain. It is formed by five antiparallel β-sheets arranged to form a motif shaped like the letter N: two pairs of antiparallel β-sheets are connected by a diagonally running extended β-sheet. In the functional trimer, the sheets are tightly intertwined to form a β-prism in which each wall is composed of a complete set of five β-strands.

The KG domain is another type of head domain. Observed in various species, this domain is structurally similar to the ISneck domain (discussed below), but the structural elements are arranged with a different topology. KG domains have a mixed α/β-fold where helical elements are localized at the edge of the domain. Head domains can also be interrupted by head insert motifs, such as "HIN2", which forms an extended loop protruding from the otherwise smooth YLhead domain in a fragment of *Burkholderia pseudomallei* BpaA (Edwards et al., 2010).

9.3.3 Neck and ISneck Domains

The head domains are always wider than the coiled-coil stalks, and have their own superhelical, right-handed, twist (Fig. 9.3). This can be best seen in YLhead domains, where the monomers twist counterclockwise when viewed from the N-terminus. As a result, TAAs have a number of connector "neck" domains whose function appears to be to adapt the diameter and twist of the head domains to the diameter and twist of the stalks.

Neck domains are never found next to each other; they always connect head domains to coiled coils in an N-to-C direction. The classic neck domain occurs in two variations, differing by insertion/deletion of only three amino acids in the central part. Despite its small length, it is very conserved. Structurally, it is a stretch of residues from one of the monomers that runs below the inner sheet of the adjacent monomer in a clockwise direction when viewed from the N-terminus. The connection between the domains thus always involves a 120° rotation such that the helix from monomer A starts under the head of monomer B, from monomer B under monomer C, and so on. This does not appear to be structurally necessary as the hydrophobic residues of the neck continue the hydrophobic core of the head. However, the arrangement leads to a conserved, multivalent ion network that may be important in stabilising the structure of the TAA or, possibly, in relieving strain during folding (see Future Directions). Another variant of the neck domain, the ISneck, also occurs in two types. ISneck is a neck motif interrupted by an insertion. The insertion can take form of either folded (ISneck 1) or much shorter, unfolded (ISneck 2) perturbation.

9.3.4 Stalk Domain

The TAA stalk consists of coiled-coil regions with different structural characteristics. Many TAA stalks are unusual in that they switch from right-handed to left-handed supercoiling. Detailed sequence analysis of the YadA stalk suggested that the right-handed N-terminal part (Fig. 9.3) is followed by a C-terminal left-handed part (Hernandez Alvarez et al., 2010). The N-terminal right-handed part was predicted to contain between seven and nine repeats with 15/4 (3.75) periodicity and a single element with 19/5 (3.8) periodicity. The left-handed part of the stalk apparently contained four repeats with the classical 3.5 residues/turn. This is indeed observed in experimental structures; the transition between the two twist directions is achieved by a local supercoiling over about 14 residues (Hernandez Alvarez et al., 2010).

Very recently, it has been shown that certain TAA coiled coils sequester ions in their hydrophobic core, as initially observed in UspA1 (Conners et al., 2008). This occurs when positions *a* and *d* are occupied by polar residues like Asn and His, rather than Ala, Ile or Val. Both phosphate (UspA1) and chloride ions (UspA1, SadA, EibD) have been found, and they are associated with Asn in position *d* to such an extent that they can be identified in the daTAA database (Hartmann et al., 2009).

Finally, TAAs coiled coils may be interrupted by small and unique domains of as yet unknown function. They may increase stalk flexibility by adding extra degrees of freedom; or they may increase rigidity, as they are thicker than the surrounding stalk; or they may be involved in releasing the strain caused by local superhelical stalk twisting. Two structures are known: the FGG domain in BpaA (Edwards et al., 2010) and the saddle domain in EibD. In both cases, these minidomains rotate the otherwise continuous α-helix by 120°. The FGG domain is formed by an elongated loop with two short stretches of β-sheet running parallel to the trimer axis. It facilitates a 120° counter-clockwise rotation when viewed from the N-terminus of the stalk. The EibD saddle is only 22 residues long and consists of three anti-parallel β-sheets, and the rotation introduced by the saddle is also counter-clockwise – *i. e.* in the opposite direction to the neck domains. As in the neck, the saddle is stabilized at the exit and re-entry points in the stalk by a well-defined ion network composed of the amino acids from all three monomers.

9.3.5 C-Terminal Translocation Domain

There are currently three essentially identical structures of a single TAA translocation domain, that of Hia, differing only in the lengths of N-terminal stalk. Proceeding from the C-terminal end, the structure is formed by a four-stranded β-sheet followed by the N-terminal α-helix, which forms the end of the coiled-coil stalk. The functional trimeric membrane anchor is created by side-by-side placement of the monomers. The trimer then contains three α-helices running approximately parallel to the trimer axis surrounded by a total of 12 β-sheets, which

create a β-barrel. The barrel is 29 Å in diameter and 36 Å deep. The barrel pore is approximately 18 Å in diameter, just large enough to accommodate all three helices (Meng et al., 2006). The stalk helices are packed against the inner face of the β-sheets. The part of the helices inside the β-barrel is not superhelically coiled whereas the part outside is.

The translocation unit is the most conserved part in the TAA family and allows efficient identification of TAAs from sequence databases. The anchor contains a nearly invariant Gly residue that faces the pore lumen. In YadA, mutating this residue to larger amino acids decreases the level of expression and stability of YadA as a function of increasing side chain size. The mutations, however, do not impair YadA-mediated adhesion to collagen and to host cells (Grosskinsky et al., 2007), suggesting that the effect is on YadA translocation efficiency and subsequent passenger domain folding.

9.4 Structure-Function Relationships

The major ligand for YadA from *Y. enterocolitica* is collagen. The collagen-binding activity of YadA maps to the head domain (El Tahir and Skurnik, 2001). Mutagenesis studies identified more then 15 surface residues with small but quantifiable effects on the YadA collagen-binding activity (Nummelin et al., 2004). Using these data, a collagen-mimicking peptide could be docked diagonally onto the YadA surface. The peptide makes contact with residues from more than one monomer. The angle between YadA and the collagen peptide is about 30 degrees, which implies that the rigid 10–300 nm long collagen fibril would collide with the bacterial surface roughly 25 nm away from the head domain. YadA must therefore bend to allow collagen to bind. Bending would also allow many heads to come in contact with the same collagen fibril, consistent with the fact that the overall avidity of YadA presented on the pathogen surface for collagen is much higher than that of isolated YadA heads (Nummelin et al., 2004). Additionally, being able to expose different combinations of binding surfaces could also explain how YadA can interact with different ECM molecules. Other YadA adhesin properties mediated by the head domain include autoagglutination, binding to other ECM molecules, neutrophil binding and epithelial cell binding (see Chapter 1, this volume). In contrast, the serum resistance properties of YadA mapped to the stalk (El Tahir and Skurnik, 2001; Hoiczyk et al., 2000).

Bending was also suggested for the interaction of UspA1 with its cellular receptor, carcinoembryonic antigen-related adhesion molecule 1 (CEACAM1). While the atomic structure of the complex is not available, small-angle X-ray scattering studies and modelling revealed that in solution the stalk domain bends in order to accommodate the CEACAM1 molecule. The estimated angle of 30–60 degrees from the linear form resulted in a boomerang shape.

In contrast to YadA, no biological function other than folding has been ascribed to the YLhead of EibD. The non-immune IgG and IgA-binding activity of EibD has

been mapped to the stalk, and no biological function has been ascribed to the head domain so far other than folding (Leo et al., in press). The binding site for IgA is located in the N-terminal, right-handed coiled-coil part of the stalk, while the IgG binding site is located in the C-terminal left-handed coiled-coil region, just above the outer membrane. They are separated from each other by the saddle mini-domain (see Section 9.3.4).

Of the three subdomains forming the high-affinity binding domain in the original Hia structure (HiaBD1) only subdomains two and three (ISneck and Trp ring) are essential for receptor binding. In the overall structure of HiaBD1, these two domains create the top of the unique mushroom-like structure. The β-sheets of the subdomain preceding the ISneck, the stem, interact with strands from neighbouring monomers and, while not essential for binding, this sub-domain does contribute to the overall stability. It is also the essential structural difference between the HiaBD1 and HiaBD2, a lower-affinity binding domain located in the N-terminal part of Hia. HiaBD1 and HiaBD2 have a similar binding pocket. The resulting groove was identified as the surface responsible for the binding activity. Mutations in this region abolish the adhesive activity of Hia. Residues located at the edge of the "mushroom" rim, N617, E668 and E678, also form the rim of the binding pocket. Comparison of the binding grooves revealed that the essential difference in binding affinity can be pinpointed to a single amino acid: Asp618 residue in HiaBD1, corresponding to Gln83 in HiaBD2 (Yeo et al., 2004).

9.5 Future Directions

TAAs form a remarkable family of proteins. Its members exhibit unique binding properties as well as astonishing structural diversity. However, while the function of a number of them is known, three major research areas can be identified.

First, it should be possible to construct complete homology models of TAAs from parts. The daTAA server lists more than 20 structural domains identified by sequence similarity. Only a handful have been determined experimentally, and a few more than once. To be able to efficiently build model structures of TAAs, the domain dictionary must be completed, preferably with more than a single representative of each.

Second is the folding mechanism of TAAs. So far, a number of models have been proposed (Bernstein, 2007). These include different variants of the passenger domain threading through the initially established β-barrel pore, as well as the Bam-assisted model. So far none of the models have been proven experimentally, due to the lack of a tractable experimental system. However, very recent work has shown that the Bam complex is capable of in vitro folding of the outer membrane protein OmpT (Hagan et al., 2010), which offers a new and promising way of studying the folding mechanism of TAAs.

Finally, studying TAA-ligand interactions structurally has medical importance. Binding sites or surfaces have been identified using mutational and biochemical

studies for YadA, Hia, EibD and UspA1, but no complex structure is yet available. There are crude models of YadA interacting with collagen (Nummelin et al., 2004), UspA1 with CEACAM1 (Conners et al., 2008) and EibD with IgG (Leo et al., in prep.), but they do not provide accurate enough information required for advanced structural studies. Only an atomic-resolution complex structure can be reliably used in the design of novel drugs. For instance, drugs interfering with TAA folding/structure would be specific to and universal for TAA-utilizing pathogens.

References

Bernstein HD (2007) Are bacterial 'autotransporters' really transporters? Trends Microbiol 15:441–447

Conners R, Hill DJ, Borodina E, Agnew C, Daniell SJ, Burton NM, Sessions RB (2008) The *Moraxella* adhesin UspA1 binds to its human CEACAM1 receptor by a deformable trimeric coiled-coil. EMBO J 27:1779–1789

Cotter SE, Surana NK, Grass S, St. Geme III JW (2006) Trimeric autotransporters require trimerization of the passenger domain for stability and adhesive activity. J Bacteriol 188:5400–5407

Crick FHC (1953) The packing of α-helices: simple coiled-coils. Acta Crystallogr 6:689–697

Dautin N, Bernstein HD (2007) Protein secretion in gram-negative bacteria *via* the autotransporter pathway. Ann Rev Microbiol 61:89–112

Edwards TE, Phan I, Abendroth J, Dieterich SH, Masoudi A, Guo W, Hewitt SN, Kelley A, Leibly D, Brittnacher MJ, Staker BL, Miller SI, Van Voorhis WC, Myler PJ, Stewart LJ (2010) Structure of a *Burkholderia pseudomallei* trimeric autotransporter adhesin head. PLoS One 5:e12803. doi:101371

El Tahir Y, Skurnik M (2001) YadA, the multifaceted *Yersinia* adhesin. Int J Med Microbiol 291:209–218

Fleming A (1929) On the antibacterial action of cultures of a penicillium with special reference to their use in the isolation of *B influenzae*. Br J Exp Pathol 10:226–236

Grosskinsky U, Schütz M, Fritz M, Schmid Y, Lamparter MC, Szczesny P, Lupas AN, Autenrieth IB, Linke D (2007) A conserved glycine residue of trimeric autotransporter domains plays a key role in *Yersinia* adhesin A. Autotransport J Bacteriol 189:9011–9019

Hagan CL, Kim S, Kahne D (2010) Reconstitution of outer membrane protein assembly from purified components. Science 328:890–892

Hartmann MD, Ridderbusch O, Zeth K, Albrecht R, Testa O, Woolfson DN, Sauer G, Dunin-Horkawicz S, Lupas AN, Hernandez Alvarez B (2009) A coiled-coil motif that sequesters ions to the hydrophobic core. Proc Natl Acad Sci USA 106:16950–16955

Henderson IR, Navarro-Garcia F, Desvaux M, Fernandez RC, Ala'Aldeen D (2004) Type V protein secretion pathway: the autotransporter story. Microbiol Mol Biol Rev 68:692–744

Hernandez Alvarez B, Gruber M, Ursinus A, Dunin-Horkawicz S, Lupas AN, Zeth K (2010) A transition from strong right-handed to canonical left-handed supercoiling in a conserved coiled-coil segment of trimeric autotransporter adhesions. J Struct Biol 170:236–245

Hodak H, Jacob-Dubuisson F (2007) Current challenges in autotransport and two-partner protein secretion pathways. Res Microbiol 158:631–637

Hoiczyk E, Roggenkamp A, Reichenbecher M, Lupas A, Heesemann J (2000) Structure and sequence analysis of *Yersinia* YadA and *Moraxella* UspAs reveal a novel class of adhesins. EMBO J 19:5989–5999

Ieva R, Bernstein HD (2009) Interaction of an autotransporter passenger domain with BamA during its translocation across the bacterial outer membrane. Proc Natl Acad Sci USA 106: 19120–19125

Kirjavainen V, Jarva H, Biedzka-Sarek M, Blom AM, Skurnik M, Meri S (2008) *Yersinia enterocolitica* serum resistance proteins YadA and ail bind the complement regulator C4b-binding protein. PLoS Pathog 4(8):e1000140

Klauser T, Pohlner J, Meyer TF (1990) Extracellular transport of cholera toxin B subunit using *Neisseria* IgA protease β-domain: conformation-dependent outer membrane translocation. EMBO J 9:1991–1999

Koretke KK, Szczesny P, Gruber M, Lupas AN (2006) Model structure of the prototypical non-fimbrial adhesin YadA of *Yersinia enterocolitica*. J Struct Biol 155:154–161

Leo JC, Lyskowski A, Hattula K, Hartmann MD, Schwarz H, Butcher SJ, Linke D, Lupas AN, Goldman A (2011) The structure of *E. coli* IgG-binding protein D suggests a general model for bending and binding in trimeric autotransporter adhesins Structure 19: (in press)

Linke D, Riess T, Autenrieth IB, Lupas A, Kempf VAJ (2006) Trimeric autotransporter adhesins: variable structure common function. Trends Microbiol 14:264–270

Lupas AN, Gruber M (2005) The structure of α-helical coiled coils. Adv Prot Chem 70:37–78

Meng G, Surana NK, St Geme III JW, Waksman G (2006) Structure of the outer membrane translocator domain of the *Haemophilus influenzae* Hia trimeric autotransporter. EMBO J 25:2297–2304

Moutevelis E, Woolfson DN (2009) A periodic table of coiled-coil protein structures. J Mol Biol 385:726–732

Nishimura K, Tajima N, Yoon Y-H, Park S-Y, Tame J (2010) Autotransporter passenger proteins: virulence factors with common structural themes. J Mol Med 88:451–458

Nummelin H, Merckel MC, Leo JC, Lankinen H, Skurnik M, Goldman A (2004) The *Yersinia* adhesin YadA collagen-binding domain structure is a novel left-handed parallel β-roll. EMBO J 23:701–711

Perry RD, Fetherston JD (1997) *Yersinia pestis*–etiologic agent of plague. Clin Microbiol Rev 10:35–66

Pohlner J, Halter R, Beyreuther K, Meyer TF (1987) Gene structure and extracellular secretion of *Neisseria gonorrhoeae* IgA protease. Nature 325:458–462

Roggenkamp A, Ackermann N, Jacobi CA, Truelzsch K, Hoffmann H, Heesemann J (2003) Molecular analysis of transport and Oligomerization of the *Yersinia enterocolitica* Adhesin YadA. J Bacteriol 185:3735–3744

Sauri A, Soprova Z, Wickström D, de Gier J-W, Van der Schors RC, Smit AB, Jong WSP, Luirink J (2009) The Bam (Omp85) complex is involved in secretion of the autotransporter haemoglobin protease. Microbiology 155:3982–3991

St. Geme III JW, Cutter D (2000) The *Haemophilus influenzae* Hia Adhesin Is an Autotransporter Protein That Remains Uncleaved at the C Terminus and Fully Cell Associated. J Bacteriol 182:6005–6013

Szabady RL, Peterson JH, Skillman KM, Bernstein HD (2005) An unusual signal peptide facilitates late steps in the biogenesis of a bacterial autotransporter. Proc Natl Acad Sci USA 102:221–226

Szczesny P, Linke D, Ursinus A, Bär K, Schwarz H, Riess TM, Kempf VAJ, Lupas AN, Martin J, Zeth K (2008) Structure of the head of the *Bartonella* Adhesin BadA. PLoS Pathog 4:e1000119

Szczesny P, Lupas A (2008) Domain annotation of trimeric autotransporter adhesins – daTAA. Bioinformatics 24:1251–1256

Veiga E, Sugawara E, Nikaido H, de Lorenzo V, Fernández LA (2002) Export of autotransported proteins proceeds through an oligomeric ring shaped by C-terminal domains. EMBO J 21:2122–2131

Voulhoux R, Bos MP, Geurtsen J, Mols M, Tommassen J (2003) Role of a highly conserved bacterial protein in outer membrane protein assembly. Science 299:262–265

Warner JM, Pelowa DB, Currie BJ, Hirst RG (2007) Melioidosis in a rural community of Western Province Papua New Guinea. Trans R Soc Trop Med Hyg 101:809–813

Yeo H-J, Cotter SE, Laarmann S, Juehne T, St Geme III JW, Waksman G (2004) Structural basis for host recognition by the *Haemophilus influenzae* Hia autotransporter. EMBO J 23:1245–1256

Chapter 10
Crystallography and Electron Microscopy of Chaperone/Usher Pilus Systems

Sebastian Geibel and Gabriel Waksman

Abstract Among bacteria, the chaperone-usher (CU) pathway is a widespread conserved assembly and translocation system for adhesive protein fibres, called pili or fimbriae. Pili are large linear polymers that protrude from the outer bacterial surface and consist of several subunits. Pili contain adhesin proteins at the tip that are used by pathogenic bacteria to mediate attachment to host cells and initiate infections. Well studied examples of CU pili are P and type 1 pili of uropathogenic *Escherichia coli* (UPEC), which are responsible for kidney and bladder infections, respectively. Upon secretion into the periplasm, pilus subunits are stabilized by periplasmic chaperones and the resulting chaperone:subunit complexes are guided to the usher located in the outer membrane. The usher catalyzes the ordered assembly of pilus subunits while releasing the chaperones and translocating the growing pilus stepwise to the outer surface. Here we review the structural biology of the chaperone-usher pathway that has helped to understand the mechanisms by which biogenesis of an important class of bacterial organelles occurs.

10.1 Introduction

Gram-negative uropathogenic *Escherichia coli* (UPEC) is the leading causative agent of human urinary tract infections (Hooton et al., 1996). UPEC expresses adhesive, hair-like protein polymers termed pili or fimbriae, which protrude from the bacterial surface. Their ability to recognize and adhere to specific structures on host cells makes pili an indispensible tool for UPEC to colonize the urinary tract. The onset of cystitis or pyelonephritis is closely associated with two different types of pili expressed by UPEC. P pili (P abbreviation for pyelonephritis) are used by UPEC

G. Waksman (✉)
Institute of Structural Molecular Biology, Birkbeck and University College London, London, UK
e-mail: g.waksman@bbk.ac.uk

D. Linke, A. Goldman (eds.), *Bacterial Adhesion*, Advances in Experimental Medicine and Biology 715, DOI 10.1007/978-94-007-0940-9_10,

to bind to renal tissue and proceed to infection of the kidney (Roberts et al., 1994). Type 1 pili are used to bind to and invade urothelial cells in order to cause cystitis (Martinez et al., 2000; Mulvey et al., 1998). Specific attachment of piliated bacteria to receptors on host cells is mediated by specialized proteins on the pilus tip termed adhesins. For example, type 1 pili exhibit the adhesin FimH on their tip for the specific recognition of mannosylated receptors of the bladder epithelium cells (Krogfelt et al., 1990; Mulvey et al., 1998), whilst P pilus adhesin PapG recognizes specifically Gal-α(1–4)-Gal-containing glycolipid receptors on the kidney epithelium of the host (Lund et al., 1987).

10.2 Classification and Morphology of P and Type 1 Pili

P and type 1 pili are assembled by a specific pathway of biogenesis called the "chaperone-usher (CU) pathway". The CU pathway of pilus biogenesis is widespread among pathogenic Gram-negative bacteria. The superfamily of CU systems comprises 189 members and can be classified into six major clades termed α,β,γ(1–4),κ,π and σ based on amino acid sequence comparisons (Nuccio and Baumler, 2007). CU pili are linear hair-like protein fibres consisting of hundreds to thousands of pilus subunits of molecular weights between ∼12–20 kDa. The morphology of CU pili varies from thin fibre- to rod-like helical shapes with a thin fibrillum on the top of the rod. Typical rod-like shaped pili are found within the α, γ and π clades. P pili and type 1 pili of UPEC belong to π and γ1 fimbrial clades, respectively, and are paradigms for pili assembled by the CU pathway because these two pili types are biochemically and structurally very well studied.

The P pilus exhibits a rod-like shape. The P pilus rod has a diameter of 6.8 nm and is connected to a flexible fibrillum termed the "tip fibrillum", which is located on the top of the rod and is 2.0 nm in diameter (Jones et al., 1995; Kuehn et al., 1992). The P pilus is assembled by six different subunits termed PapA, PapE, PapF, PapG, PapK and PapH (Fig. 10.1). PapH, located at the base of the pilus, anchors the P pilus in the cell wall (Baga et al., 1987; Verger et al., 2006). The P pilus rod protrudes out from the bacterial surface and is composed of >1000 copies of subunit PapA, forming a right-handed helix with a 2.5 nm pitch and 3.3 PapA molecules per turn (Bullitt and Makowski, 1995; Gong and Makowski, 1992). The tip fibrillum on the top of the rod contains 5–10 copies of PapE followed by one copy each of PapF and PapG (Kuehn et al., 1992). The adaptor subunit PapK links the PapA rod to the PapE:F:G tip fibrillum.

The tip fibrillum of the type 1 pilus is shorter than that of the P pilus, because it is composed of only one copy of subunits FimG and FimH (Hahn et al., 2002). The pilus adaptor subunit FimF links the fibrillum with the rod, which consists of approximately 1000 FimA subunits. The adhesin FimH of type 1 pilus is displayed at the distal end of the fibrillum (Jones et al., 1995) (Fig. 10.1).

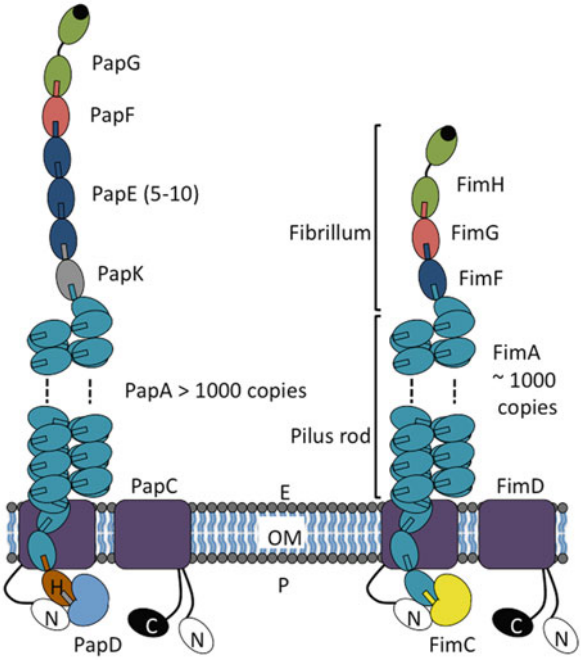

Fig. 10.1 Architecture of P and type 1 pili. A schematic of P and type 1 pili is presented. *Left side*: P pilus. *Right side*: type 1 pilus. Usher dimers FimD and PapC are shown as *rectangles* spanning the outer membrane (OM). The N- (*white*) and C-terminal (*black*) domains of the usher and P and type 1 pilus subunits are drawn as *oval shapes*. Chaperones FimC and PapD are marked. Extracellular space (E), periplasm (P)

10.3 Principles of Pilus Assembly by the Chaperone Usher Pathway

Two accessory proteins are needed to assemble CU pili: an usher and a periplasmic chaperone. Ushers FimD and PapC are dimeric translocation pores in the outer bacterial membrane where they catalyse the polymerisation of type 1 pili subunits and P pilus subunits, respectively (see Section 10.4). In the periplasm, chaperones FimC and PapD recruit type 1 and P pilus subunits, respectively, at the exit of the SecYEG translocon (Jones et al., 1997) and guide them to their cognate ushers FimD and PapC at the outer membrane for pilus assembly.

10.3.1 Donor Strand Complementation

CU chaperones play four roles: (i) folding of subunits (see below), (ii) prevention of premature polymerization in the periplasm (Kuehn et al., 1991), (iii) priming of subunit for polymerization at the usher (see Section 10.3.3), and (iv) targeting of subunits to the usher (see Section 10.4.1).

The mechanism of chaperone function leading to correct folding of pilus subunits and induction of a polymerisation competent state of the pilus subunits is termed

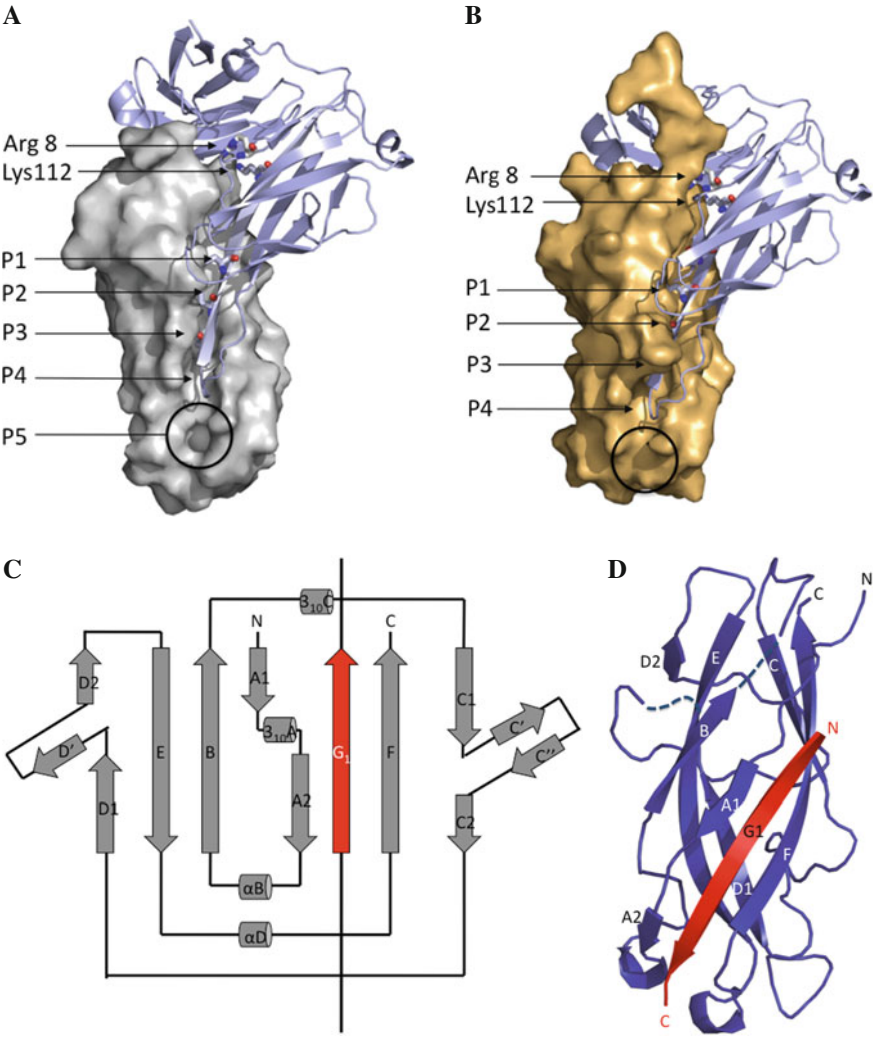

Fig. 10.2 Principles of chaperone-usher catalysed pilus assembly: Donor strand complementation and Donor strand exchange. (**a**) Crystal structure of P pilus adaptor subunit PapK in complex with chaperone PapD. PapK is presented as grey surface model and PapD as light *blue ribbon* model. Structurally conserved residues Arg-8 and Lys-112 and P1–P4 of PapD are drawn as *grey stick* models. Pocket P5 of PapK is indicated with a black open circle. (**b**) Crystal structure of P pilus termination- and anchor subunit PapH in complex with chaperone PapD. PapG is shown as light brown surface model and PapD as light *blue ribbon* model. Structurally conserved residues Arg-8 and Lys-112 and P1–P4 of PapD are drawn as *grey stick* models. The missing pocket P5 of PapG is indicated with a *black open circle*. (**c**) Topology diagram of P pilus adaptor subunit PapK (*grey*) with the Nte of chaperone PapD bound (*red*). (**d**) Crystal structure of P pilus subunit PapE in complex with Nte of the preceding subunit PapK after DSE. PapE (*blue*) and Nte of PapK (*red*) are drawn as ribbon models. (**e**) Topology diagram of P pilus subunit PapE (*blue*) with the Nte of the following P pilus subunit PapD (*red*)

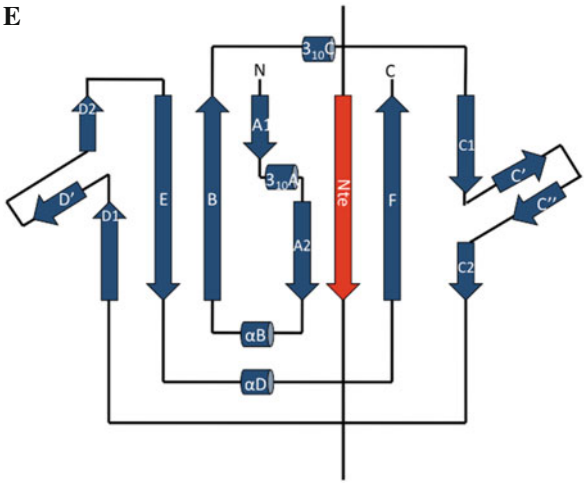

Fig. 10.2 (continued)

donor strand complementation (DSC) and was deduced from crystal structures of the chaperone-pilus subunit complexes FimC:FimH and PapD:PapK (Choudhury et al., 1999; Sauer et al., 1999). Chaperones FimC and PapD (each ~25 kDa) share a boomerang-like shape consisting of two immunoglobulin-like (Ig-like) domains (Holmgren and Brändén, 1989; Kuehn et al., 1993; Pellecchia et al., 1998) and interact with pilus subunits by their β-strands A1 and G1 of their N-terminal domain and two structurally conserved basic residues (Arg 8 and Lys 112, PapD numbering), which are found in a cleft between the two Ig-like domains (Kuehn et al., 1993) (Figs. 10.2a,b).

Pilus subunits cannot fold correctly in the absence of the chaperone (Barnhart et al., 2000; Vetsch et al., 2004) because pilus subunits have an incomplete Ig-like fold, which consists of six β-strands (A–F) and lacks a seventh C-terminal β-strand (G) (Choudhury et al., 1999; Sauer et al., 1999). The lack of a β-strands creates a hydrophobic groove where the missing strand G would be. The chaperone enables the correct folding of the pilus subunit because it provides in trans the missing seventh β-strand to complement the Ig-like fold of the subunit. In the crystal structures of FimC:FimH and PapD:PapG, the chaperone inserts its β-strand G1 (strand G of the chaperone's N-terminal Ig-like domain 1) into the hydrophobic groove of the pilus subunit (Fig. 10.2a) (Choudhury et al., 1999; Sauer et al., 1999). A motif of four alternating hydrophobic residues P1–P4 on the G1 β-strand occupies four of five hydrophobic acceptor pockets in the groove of the pilus subunit, which are termed "P1–P5 pockets" (Fig. 10.2a). The fifth hydrophobic pocket P5 remains accessible, which is crucial for pilus subunit polymerisation (see Section 10.3.1). PapH is an exception as it is the only Pap subunit that does not possess a P5 pocket (Fig. 10.2b, see Section 10.7). The chaperone-complemented Ig-like fold of the pilus

subunit is atypical, because the donor β-strand G1 of the chaperone runs parallel to the subunit's F β-strand (Fig. 10.2c). In a regular Ig-like fold the seventh G β-strand runs antiparallel to the F strand. Because the chaperone donates in trans the missing β-strand to complement the incomplete Ig-like fold of the pilus subunit, the reaction of pilus subunit stabilisation by the chaperone is termed donor strand complementation (DSC) (Choudhury et al., 1999; Sauer et al., 1999). After DSC stable binary chaperone-pilus subunit complexes are formed, which are used for pilus assembly by the usher.

10.3.2 Donor Strand Exchange

The reaction underlying pilus subunit polymerisation is termed "donor strand exchange (DSE)" and occurs at the usher. During pilus assembly the usher adds pilus subunits to the growing pilus one at a time to catalyse non-covalent interactions between the subunit assembled last and the incoming subunit.

Pilus subunits exhibit a disordered 10–20 amino acids long N-terminal extension peptide (Nte), which is crucial for polymerisation with other subunits. The Nte of pilus subunits is not part of their Ig-like fold and contains a motif of four alternating hydrophobic residues termed "P2–P5 residues" (Sauer et al., 1999). For polymerisation the Nte of an incoming pilus subunit replaces the donor β-strand G1 of the chaperone in the groove of the previously assembled subunit of the growing pilus (Sauer et al., 2002) (Fig. 10.2d). After DSE, residues P2–P5 of the incoming pilus subunit's Nte occupy pockets P2–P5 of the acceptor subunit groove (the "acceptor" subunit being the previously assembled subunit), whilst pocket P1 of the acceptor subunit remains empty. Residue P4 of the Nte of the pilus subunit is a Gly and is conserved among all pilus subunits. Gly P4 lies on top of the P4 pocket in the subunit groove, which contains a bulk formed by an aromatic residue. Gly is the only residue that is small enough to adapt to this bulk. Therefore, the interaction of P4 Gly with the bulk works as a control for the correct positioning of the incoming Nte in the acceptor groove. After DSE the complemented pilus subunit exhibits a canonical Ig-fold because the Nte of the incoming pilus subunit runs anti-parallel to β-strand F of the acceptor subunit (Fig. 10.2e).

DSE is initiated by insertion of residue P5 of the incoming subunit's Nte into the P5 pocket of the previously assembled pilus subunit. Further insertion of the Nte into the groove proceeds from pockets P5–P1 of the acceptor subunit and progressively displaces the donor strand of the chaperone. The first evidence for this mechanism was the observation of a ternary chaperone-subunit-Nte complex of *Salmonella* pilus subunit SafA by non-denaturing mass spectrometry (Remaut et al., 2006). The formation of ternary chaperone-subunit-Nte complexes was dependent on the accessibility of pocket P5 of the subunit. Sequential mutagenesis of amino acids P5, P4 and P3 of the Nte of the (incoming) pilus subunit correlated with decreasing DSE rates. A "zip-in zip-out" mechanism was proposed, in which the Nte of the incoming subunit-chaperone complex replaces the G1 donor β-strand of the chaperone step by step moving from pocket P5–P1.

10.3.3 Pilus Subunit Ordering is Dependent on DSE Rates

The order of subunits in the P pilus was elucidated by biochemical and electron microscopy studies (Jacob-Dubuisson et al., 1993; Kuehn et al., 1992; Lindberg et al., 1987). Pilus subunit ordering of P pilus is affected by affinity of the subunits to each other (Rose et al., 2008) and by the ability of the usher to selectively catalyse DSE between the subunits (Nishiyama and Glockshuber 2010). In vitro measured DSE rates of Pap chaperone-subunit complexes and isolated Nte peptides of cognate and non-cognate pilus subunits showed highest DSE rate for subunits and their cognate Nte peptides ("cognate" here refers to the natural order of subunits in the pilus) (Fig. 10.1) (Rose et al., 2008) and indicated that affinity of subunits to each other determines their order in the pilus. The usher also affects pilus subunit ordering. A recent study demonstrated that the usher FimD of type 1 pili selectively catalyses DSE between pairs of subunits (Nishiyama and Glockshuber, 2010).

The DSE rate is dependent on accessibility and flexibility of the P5 pocket of pilus subunits. The more flexible and accessible the region around the P5 pocket, the faster the DSE rate is (Verger et al., 2008). The crystal structures of P pilus subunits PapA and PapK show well-defined P5 pockets. DSE of PapA and PapK occurs with similar rates. The region around pocket P5 of pilus subunit PapE is more flexible compared to those of PapA and PapK. As a result, PapE is the subunit that undergoes DSE with the highest rate among the Pap subunits. In contrast, the P5 pockets of PapH and PapF are blocked (Thr 52 in PapH and Pro 32 in PapF). Consequently, PapH is unable to undergo DSE whilst PapF undergoes DSE only slowly compared to the other Pap subunits. Structure-guided mutagenesis and molecular dynamics studies in combination with DSE experiments indicated that the obstructed P5 pocket of PapF becomes accessible periodically and thus DSE of PapF is still possible. This is not the case for PapH.

10.4 Structure of the Usher

In vitro DSE occurs spontaneously but only at very slow rates in absence of the usher. DSE rates of type 1 pili are increased significantly by addition of the usher FimD. Thus the usher catalyses DSE for pilus assembly (Nishiyama et al., 2008). Usher-catalysed polymerisation of pilus subunit is thermodynamically driven and independent from intracellular energy (Jacob-Dubuisson et al., 1994). The required energy for pilus subunit polymerisation is stored in the fold of the chaperone-subunit intermediates and released upon DSE (Sauer et al., 2002).

Electron microscopy studies of the P pilus usher PapC reconstituted in *E. coli* lipids demonstrated that PapC forms a homodimeric channel and complementation studies with PapC loss of function mutants showed that the usher functions at least as a dimer in vivo (Li et al., 2004; So and Thanassi, 2006), although an usher monomer may also be sufficient for pilus assembly in vitro (Huang et al., 2009).

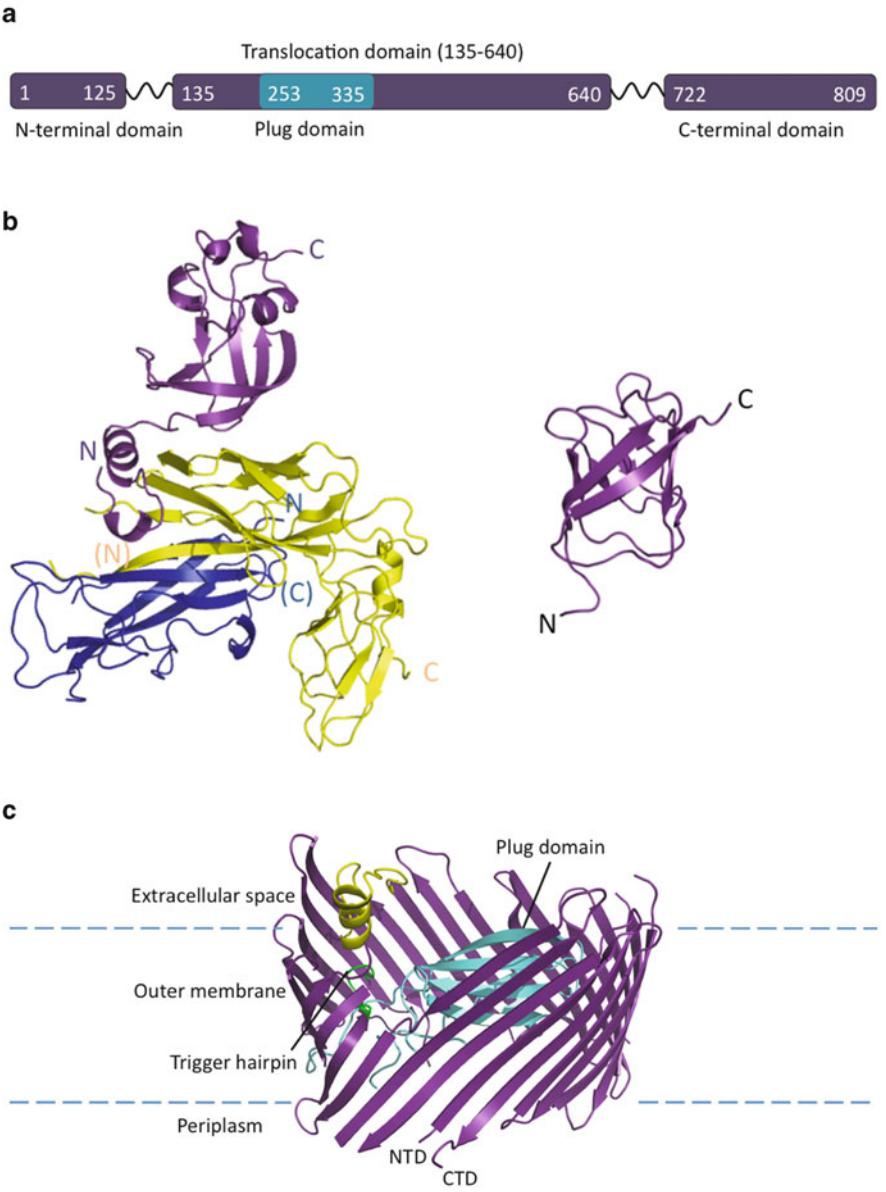

Fig. 10.3 Structures of the usher: The P and type 1 pilus assembly platform. (**a**) The domain architecture of usher PapC. N-terminal (residues 1–125) and C-terminal (residues 722–809) domains (both *purple*) are connected with unstructured amino acid linkers to the translocation domain (residues 135–640, purple) which is interrupted by the plug domain (residues 235–335, cyan). (**b**) Left panel: The crystal structure of the N-terminal domain of FimD (*purple*) in complex with chaperone FimC (*yellow*) and a fragment of subunit FimF (*blue*) as ribbon representation. Right panel: The crystal structure of the C-terminal domain of usher PapC (*purple*) as ribbon model. (**c**) The crystal structure of usher PapC. The PapC dimer is shown as ribbon model (*purple*).

The usher is a 90 kDa protein consisting of about 800 residues and four functional domains: (i) an N-terminal periplasmic domain (~125 residues), (ii) a central translocation pore domain: (~500 residues) in the bacterial outer membrane, (iii) a plug domain (~110 residues), found within the translocation pore, and (iv) a C-terminal, periplasmic domain (~170 residues) (Fig. 10.3a) (Capitani et al., 2006; Nishiyama et al., 2003; Remaut et al., 2008; Thanassi et al., 2002).

10.4.1 The N-terminal Usher Domain Binds Chaperone-Subunit Complexes

The N-terminal domain (NTD) of the usher FimD exhibits high affinity for chaperone-subunit complexes and is likely to be the main platform for recruitment of chaperone-subunit complexes (Ng et al., 2004; Nishiyama et al., 2005). The crystal structures of the NTD of the usher FimD in complex with chaperone FimC and adhesin FimH or subunit FimF showed that the NTD of the usher FimD interacts with with both the chaperone and the subunit (Fig. 10.3b) (Eidam et al., 2008; Nishiyama et al., 2005). The largest part of the binding interface between FimD NTD and chaperone-subunit complexes is between a conserved hydrophobic patch on the chaperone FimC and the NTD of the usher FimD and is structurally conserved; only a small part of the binding interface is subunit-specific. Specific interactions are observed between the flexible N-terminus of FimD NTD and subunits FimF and FimH and can explain how the N-terminal domain of FimD is able to discriminate between different chaperone-subunit complexes.

10.4.2 The C-terminal Domain of Usher PapC Supports Subunit Binding

Truncations and substitution mutants of the C-terminal domain of usher PapC demonstrated that the C-terminal domain is required for proper binding of chaperone-subunit complexes to the usher and supports pilus assembly (Huang et al., 2009; So and Thanassi, 2006). A fragment of the C-terminal region of usher PapC shows a β-sandwich fold similar to the plug domain of PapC (Fig. 10.3b) (Ford et al., 2010). Due to the structural similarity of plug and C-terminal domain, it was suggested that both domains could exert similar functions but at different stages of pilus assembly.

Fig. 10.3 (continued) The view to the PapC dimer is from the periplasmic side (*top*) and extracellular side (*bottom*). The Plug domain is coloured cyan, the β-barrel of the translocation pore purple, the trigger hairpin green and a single α-helix inside the β-barrel yellow. N- and C-terminal domains of PapC are indicated by NTD and CTD

10.4.3 The Translocation Pore of Usher PapC

The translocation pore domain of usher PapC folds into a β-barrel, which is composed of 24 β-strands and is interrupted by the plug domain between β-strands six and seven. The diameter of the pore is ~45 × 25 Å and is big enough to extrude the growing pilus in a folded state (Fig. 10.3c) (Remaut et al., 2008).

10.4.4 The Plug Domain of the Usher PapC

In vitro studies demonstrated that the plug domain of the usher PapC is required for pilus assembly because PapC is unable to assemble pili without it (Huang et al., 2009). The crystal structure of the translocation pore of PapC showed that the plug domain exhibits a β-sandwich fold similar to the C-terminal domain of the usher and obstructs the translocation pore (Remaut et al., 2008) (Fig. 10.3c).

10.4.5 Activation of the Usher FimD

Upon binding of adhesin FimH, the susceptibility of the usher FimD to trypsin changes, indicating a conformational change of the usher (Munera et al., 2007; 2008; Saulino et al., 1998). The adhesin-induced conformational change of FimD is a crucial activation step in type 1 pilus biogenesis as it significantly increases the pilus subunit assembly rate of the usher (Nishiyama et al., 2008). The conformational change of FimD requires moving the plug domain aside within the translocation pore or outwards away from the pore into the periplasm to allow the translocation of a growing pilus through the pore.

10.5 Intermediate FimD2:C:F:G:H (Tip Assembly)

Electron microscopy images provided snapshots of a type 1 pilus intermediate which consists of dimeric usher FimD, the chaperone FimC and the adhesin FimH, and the subunits FimG and FimF (Fig. 10.4a) (Remaut et al., 2008). Pilus subunits FimH, FimG and FimF compose the tip fibrillum of the type 1 pilus. Surprisingly, it was observed that only a single usher pore in the usher dimer is used for secretion of the growing pilus. The second usher pore was supposed to be in a non-activated

Fig. 10.4 (continued) drawn as oval shapes and labelled N1 (NTD of FimD1) and N2 (NTD of FimD2) respectively. C-terminal and plug domains of the FimD dimer are left out for clarity. All pilus subunits have oval shapes. Chaperone FimC (*yellow*) has heart shape. The protruding rectangles from the subunits and FimC indicate Nte's (except for FimH). Colours of pilus subunits are: FimA (*cyan*) FimF (*blue*), FimG (*red*), FimH (*green*). *Black closed circle* on adhesin FimH represents its α-D mannose binding site. E (extracellular), OM (outer membrane), P (periplasm). Arrows indicate interaction between molecules

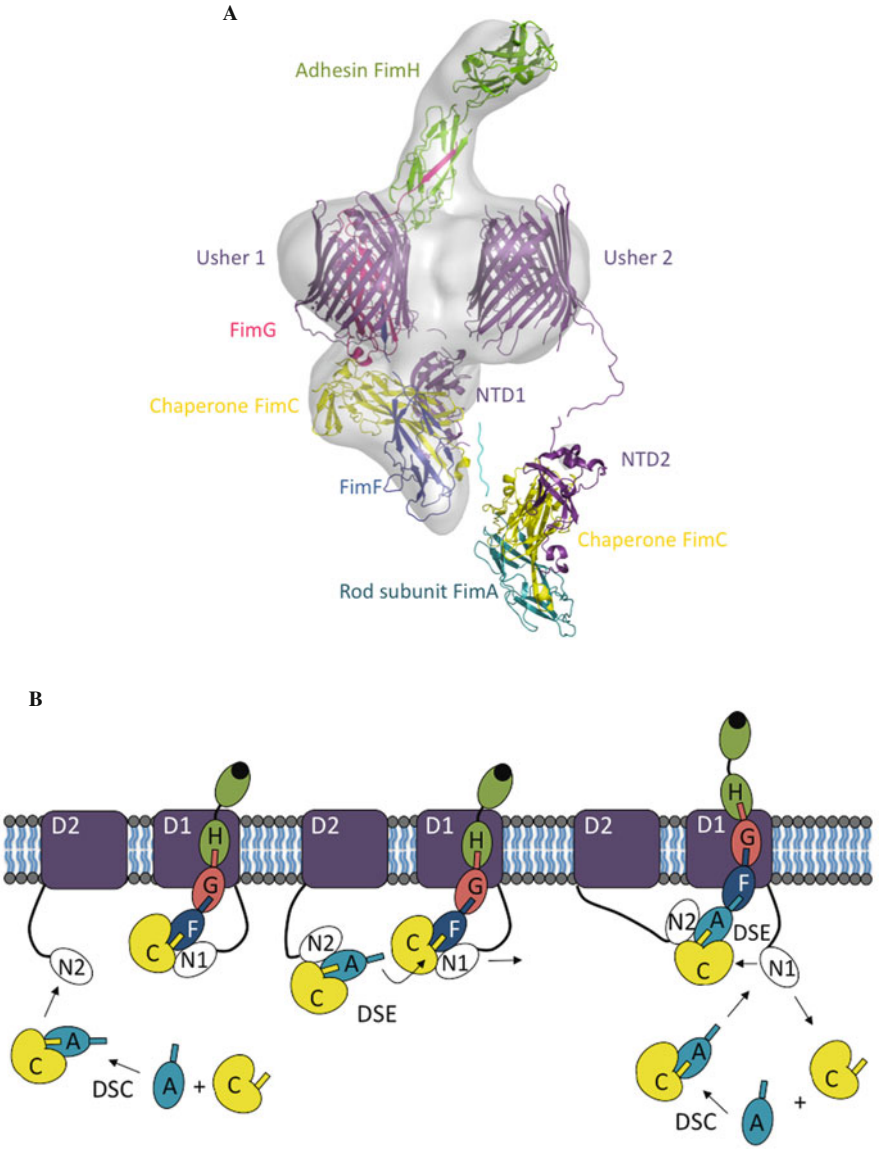

Fig. 10.4 Pilus subunit assembly by the chaperone-usher pathway. (**a**) Cryo electron microscopy structure of a type 1 pilus intermediate consisting of chaperone FimC (*yellow*), usher dimer FimD (*purple*) and subunits FimF (*blue*), FimG (*red*) and FimH (*green*). The pilus intermediate is shown as *ribbon* representation. The plug and C-terminal domains of the usher are not modelled. The crystal structure of homologues usher PapC was used for modelling usher FimD since the three dimensional structure of FimD is unknown. A model of rod subunit FimA (*cyan*) in complex with chaperone FimC (*yellow*) and N-terminal domain of the second usher (*purple*) is also shown, which is not covered by experimental data. (**b**) Model for subunit assembly of type 1 pili. Each monomer of the FimD dimer is shown as purple square and labelled D1 and D2 respectively (FimD1 and FimD2 in the main text respectively). The two N-terminal domains (NTD) of the usher dimer are

state and to adopt a closed form. A model was provided for the need of a second usher, which suggests that the second usher functions as a second recruitment platform for chaperone-subunit complexes but not for translocation of the growing pilus. The N-terminal domains of each of the two ushers could alternately recruit the chaperone-subunit complexes. This model is in agreement with in vivo data indicating that more than a single usher molecule is essential for pilus assembly (So and Thanassi, 2006). In contrast, in vitro experiments indicated that the usher can function as a monomer (Huang et al., 2009).

10.6 Model for Pilus Subunit Incorporation Cycle

Based on the EM reconstructed $FimD_2$:C:F:G:H intermediate structure a model for incorporation of the pilus subunit FimA was presented in which subunit FimA is recruited by the N-terminal domain of the second usher (Usher2 in Fig. 10.4a). Its N-terminal domain (NTD2 in Fig. 10.4a) is attached by a flexible linker to the usher's translocation pore (Fig. 10.4a). It could bind to a FimC:FimA complex, bring it to Usher1 (the secretion pore), close to the already engaged FimC:FimF complex and into a position such that the P5 residue of the incoming FimA subunit can engage in the P5 pocket of the acceptor FimF subunit, thereby initiating DSE of FimA with FimF (Fig. 10.4a). Upon DSE, the chaperone FimC is released, FimF enters the translocation pore as part of the growing pilus and the N-terminal domain of Usher1 is free to recruit the next FimC:FimA chaperone-subunit complex and bring it near the previously assembled FimC:FimA complex for DSE (Fig. 10.4b). Unbound FimC lacks affinity to the usher (Nishiyama et al., 2003; Saulino et al., 1998) and would be ready to pick up new pilus subunits (Fig. 10.4b). The cycle of chaperone-subunit recruitment, subunit polymerisation and translocation of the pilus fibre is repeated until the pilus is completed.

10.7 Termination of Pilus Biogenesis

Growth of P pilus is terminated by incorporation of termination-and anchor subunit PapH (Baga et al., 1987), because PapH is unable to undergo DSE. The crystal structure of chaperone-subunit complex PapD:PapH reveals that PapH lacks the P5 pocket required for DSE (Verger et al., 2006). The termination process for type-1 pili is still unknown since no corresponding termination subunit has been found (Fig. 10.2b).

10.8 Adhesin-Receptor Interactions

Bacterial attachment to host cell surfaces is accomplished by specific binding of the adhesin molecule of the pilus tip to a host receptor. Type 1 pili are essential for UPEC to cause cystitis (Martinez et al., 2000; Mulvey et al., 1998) and are

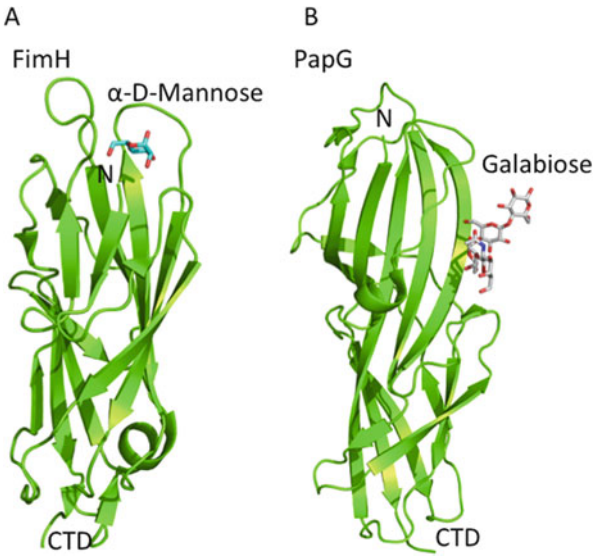

Fig. 10.5 Adhesin receptor interactions. Proteins molecules are shown as ribbon representation and bound molecules as stick models. CTD, C-terminal domain. (**a**) Crystal structure of adhesin receptor domain FimH in complex with α-D-Mannose. (**b**) Crystal structure of adhesin PapG bound to GalNAc β 1–3Gal α 1–4Gal β 1–4Glc (Galabiose)

also involved in later stages of cystitis where type 1 pili ensure formation of intracellular bacterial communities (Justice et al., 2006; Wright et al., 2007). Binding and invasion of type 1 piliated UPEC to human bladder cells was demonstrated to be dependent on adhesin FimH, which binds α-D mannose residues (Hung et al., 2002).

Crystal structures of several adhesin molecules are available, including FimH from enterotoxigenic *E. coli* (ETEC) and from UPEC, the P Pilus adhesin PapG from UPEC, adhesin GafD in G-fimbriae from UPEC and adhesin F17-G in F17 fimbriae from ETEC. All adhesin structures share a similar β-barrel jelly-roll fold (Buts et al., 2003; Dodson et al., 2001; Hung et al., 2002; Merckel et al., 2003), but their receptor binding sites differ noticeably and are found in different parts of the structures. In the crystal structure of FimH bound to D-Mannopyranoside, mannose is bound in a deep negatively charged pocket at the tip of the receptor-binding domain (Fig. 10.5a). The crystal structure of PapGII (class II of three different PapG classes binding different globoseries of glycolipids) shows that Gal(α1–4)Gal is bound in a shallow pocket, which is formed by three β-strands and a loop located on the side of the molecule (Fig. 10.5b). The interaction between tip adhesin PapGII and Gal(α1–4)Gal is crucial for pyelophrenetic strains of P piliated *E. coli* to bind renal tissue and to cause kidney disease (Roberts et al., 1994).

10.9 Conclusion

Our understanding of the molecular basis of pilus biogenesis and adhesion by CU pili has increased dramatically in the last decade starting with the elucidation of DSC and DSE as the fundamental mechanisms of chaperone and usher

functions. This knowledge is being exploited in the design of inhibitors of pilus biogenesis. One recent success has been the design of the first active "pilicides", small molecules capable of disrupting the interaction between the usher and the chaperone-subunit complexes (Pinkner et al., 2006). Future work will aim to elucidate further the interactions between the translocation pore and the subunits as they pass through the pore. There is no doubt that future unravelling of the usher system will yield new targets for antibiotics design. In this era of increased antibiotics resistance, targeting virulence factors rather then killing the bacteria (good or bad) is an approach well worth pursuing and thus, we anticipate research on pilicides to benefit greatly from further fundamental insights into the processes described in this review.

References

Baga M, Norgren M, Normark S (1987) Biogenesis of *E. coli* pap pili: papH, a minor pilin subunit involved in cell anchoring and length modulation. Cell 49:241–251

Barnhart MM, Pinkner JS, Soto GE, Sauer FG, Langermann S, Waksman G, Frieden C, Hultgren SJ (2000) PapD-like chaperones provide the missing information for folding of pilin proteins. Proc Natl Acad Sci USA 97:7709–7714

Bullitt E, Makowski L (1995) Structural polymorphism of bacterial adhesion pili. Nature 373: 164–167

Buts L, Bouckaert J, De Genst E, Loris R, Oscarson S, Lahmann M, Messens J, Brosens E, Wyns L, De Greve H (2003) The fimbrial adhesin F17-G of enterotoxigenic *Escherichia coli* has an immunoglobulin-like lectin domain that binds N-acetylglucosamine. Mol Microbiol 49: 705–715

Capitani G, Eidam O, Grütter MG (2006) Evidence for a novel domain of bacterial outer membrane ushers. Proteins 65:816–823

Choudhury D, Thompson A, Stojanoff V, Langermann S, Pinkner J, Hultgren SJ, Knight SD (1999) X-ray structure of the FimC-FimH chaperone-adhesin complex from uropathogenic *Escherichia coli*. Science 285:1061–1066

Dodson KW, Pinkner JS, Rose T, Magnusson G, Hultgren SJ, Waksman G (2001) Structural basis of the interaction of the pyelonephritic *E. coli* adhesin to its human kidney receptor. Cell 105:733–743

Eidam O, Dworkowski FS, Glockshuber R, Grütter MG, Capitani G (2008) Crystal structure of the ternary FimC-FimF(t)-FimD(N) complex indicates conserved pilus chaperone-subunit complex recognition by the usher FimD. FEBS Lett 582:651–655

Ford B, Rego AT, Ragan TJ, Pinkner J, Dodson K, Driscoll PC, Hultgren S, Waksman G (2010) Structural homology between the C-terminal domain of the Papc usher and its plug. J Bacteriol 192:1824–1831

Gong M, Makowski L (1992) Helical structure of P pili from *Escherichia coli*. Evidence from X-ray fiber diffraction and scanning transmission electron microscopy. J Mol Biol 228: 735–742

Hahn E, Wild P, Hermanns U, Sebbel P, Glockshuber R, Haner M, Taschner N, Burkhard P, Aebi U, Müller SA (2002) Exploring the 3D molecular architecture of *Escherichia coli* type 1 pili. J Mol Biol 323:845–857

Holmgren A, Brändén C-I (1989) Crystal structure of chaperone protein PapD reveals an immunoglobulin fold. Nature 342:248–251

Hooton TM, Scholes D, Hughes JP, Winter C, Roberts PL, Stapleton AE, Stergachis A, Stamm WE (1996) A prospective study of risk factors for symptomatic urinary tract infection in young women. N Engl J Med 335:468–474

Huang Y, Smith BS, Chen LX, Baxter RH, Deisenhofer J (2009) Insights into pilus assembly and secretion from the structure and functional characterization of usher PapC. Proc Natl Acad Sci USA 106:7403–7407

Hung CS, Bouckaert J, Hung D, Pinkner J, Widberg C, DeFusco A, Auguste CG, Strouse R, Langermann S, Waksman G, Hultgren SJ (2002) Structural basis of tropism of *Escherichia coli* to the bladder during urinary tract infection. Mol Microbiol 44:903–915

Jacob-Dubuisson F, Heuser J, Dodson K, Normark S, Hultgren S (1993) Initiation of assembly and association of the structural elements of a bacterial pilus depend on two specialized tip proteins. EMBO J 12:837–847

Jacob-Dubuisson F, Striker R, Hultgren SJ (1994) Chaperone-assisted self-assembly of pili independent of cellular energy. J Biol Chem 269:12447–12455

Jones CH, Danese PN, Pinkner JS, Silhavy TJ, Hultgren SJ (1997) The chaperone-assisted membrane release and folding pathway is sensed by two signal transduction systems. EMBO J 16:6394–6406

Jones CH, Pinkner JS, Roth R, Heuser J, Nicholes AV, Abraham SN, Hultgren SJ (1995) FimH adhesin of type 1 pili is assembled into a fibrillar tip structure in the enterobacteriaceae. Proc Natl Acad Sci USA 92:2081–2085

Justice SS, Hunstad DA, Seed PC, Hultgren SJ (2006) Filamentation by *Escherichia coli* subverts innate defenses during urinary tract infection. Proc Natl Acad Sci USA 103:19884–19889

Krogfelt KA, Bergmans H, Klemm P (1990) Direct evidence that the FimH protein is the mannose-specific adhesin of *Escherichia coli* type 1 fimbriae. Infect Immun 58: 1995–1998

Kuehn MJ, Heuser J, Normark S, Hultgren SJ (1992) P pili in uropathogenic *E. coli* are composite fibres with distinct fibrillar adhesive tips. Nature 356:252–255

Kuehn MJ, Normark S, Hultgren SJ (1991) Immunoglobulin-like PapD chaperone caps and uncaps interactive surfaces of nascently translocated pilus subunits. Proc Natl Acad Sci USA 88:10586–10590

Kuehn MJ, Ogg DJ, Kihlberg J, Slonim LN, Flemmer K, Bergfors T, Hultgren SJ (1993) Structural basis of pilus subunit recognition by the PapD chaperone. Science 262:1234–1241

Li H, Qian L, Chen Z, Thibault D, Liu G, Liu T, Thanassi DG (2004) The outer membrane usher forms a twin-pore secretion complex. J Mol Biol 344:1397–1407

Lindberg F, Lund B, Johansson L, Normark S (1987) Localization of the receptor-binding protein adhesin at the tip of the bacterial pilus. Nature 328:84–87

Lund B, Lindberg F, Marklund BI, Normark S (1987) The PapG protein is the alpha-D-galactopyranosyl-(1—4)-beta-D-galactopyranose-binding adhesin of uropathogenic *Escherichia coli*. Proc Natl Acad Sci USA 84:5898–5902

Martinez JJ, Mulvey MA, Schilling JD, Pinkner JS, Hultgren SJ (2000) Type 1 pilus-mediated bacterial invasion of bladder epithelial cells. EMBO J 19:2803–2812

Merckel MC, Tanskanen J, Edelman S, Westerlund-Wikström B, Korhonen TK, Goldman A (2003) The structural basis of receptor-binding by *Escherichia coli* associated with diarrhea and septicemia. J Mol Biol 331:897–905

Mulvey MA, Lopez-Boado YS, Wilson CL, Roth R, Parks WC, Heuser J, Hultgren SJ (1998) Induction and evasion of host defenses by type 1-piliated uropathogenic *Escherichia coli*. Science 282:1494–1497

Munera D, Hultgren S, Fernandez LA (2007) Recognition of the N-terminal lectin domain of FimH adhesin by the usher FimD is required for type 1 pilus biogenesis. Mol Microbiol 64: 333–346

Munera D, Palomino C, Fernandez LA (2008) Specific residues in the N-terminal domain of FimH stimulate type 1 fimbriae assembly in *Escherichia coli* following the initial binding of the adhesin to FimD usher. Mol Microbiol 69:911–925

Ng TW, Akman L, Osisami M, Thanassi DG (2004) The usher N terminus is the initial targeting site for chaperone-subunit complexes and participates in subsequent pilus biogenesis events. J Bacteriol 186:5321–5331

Nishiyama M, Glockshuber R (2010) The outer membrane usher guarantees the formation of functional pili by selectively catalyzing donor-strand exchange between subunits that are adjacent in the mature pilus. J Mol Biol 396:1–8

Nishiyama M, Horst R, Eidam O, Herrmann T, Ignatov O, Vetsch M, Bettendorff P, Jelesarov I, Grütter MG, Wüthrich K, Glockshuber R, Capitani G (2005) Structural basis of chaperone-subunit complex recognition by the type 1 pilus assembly platform FimD. EMBO J 24: 2075–2086

Nishiyama M, Ishikawa T, Rechsteiner H, Glockshuber R (2008) Reconstitution of pilus assembly reveals a bacterial outer membrane catalyst. Science 320:376–379

Nishiyama M, Vetsch M, Puorger C, Jelesarov I, Glockshuber R (2003) Identification and characterization of the chaperone-subunit complex-binding domain from the type 1 pilus assembly platform FimD. J Mol Biol 330:513–525

Nuccio SP, Baumler AJ (2007) Evolution of the chaperone/usher assembly pathway: fimbrial classification goes Greek. Microbiol Mol Biol Rev 71:551–575

Pellecchia M, Guntert P, Glockshuber R, Wüthrich K (1998) NMR solution structure of the periplasmic chaperone FimC. Nat Struct Biol 5:885–890

Pinkner JS, Remaut H, Buelens F, Miller E, Aberg V, Pemberton N, Hedenstrom M, Larsson A, Seed P, Waksman G, Hultgren SJ, Almqvist F (2006) Rationally designed small compounds inhibit pilus biogenesis in uropathogenic bacteria. Proc Natl Acad Sci USA 103:17897–17902

Remaut H, Rose RJ, Hannan TJ, Hultgren SJ, Radford SE, Ashcroft AE, Waksman G (2006) Donor-strand exchange in chaperone-assisted pilus assembly proceeds through a concerted βstrand displacement mechanism. Mol Cell 22:831–842

Remaut H, Tang C, Henderson NS, Pinkner JS, Wang T, Hultgren SJ, Thanassi DG, Waksman G, Li H (2008) Fiber formation across the bacterial outer membrane by the chaperone/usher pathway. Cell 133:640–652

Roberts JA, Marklund BI, Ilver D, Haslam D, Kaack MB, Baskin G, Louis M, Mollby R, Winberg J, Normark S (1994) The Gal(ά 1–4)Gal-specific tip adhesin of *Escherichia coli* P-fimbriae is needed for pyelonephritis to occur in the normal urinary tract. Proc Natl Acad Sci USA 91:11889–11893

Rose RJ, Verger D, Daviter T, Remaut H, Paci E, Waksman G, Ashcroft AE, Radford SE (2008) Unraveling the molecular basis of subunit specificity in P pilus assembly by mass spectrometry. Proc Natl Acad Sci USA 105:12873–12878

Sauer FG, Futterer K, Pinkner JS, Dodson KW, Hultgren SJ, Waksman G (1999) Structural basis of chaperone function and pilus biogenesis. Science 285:1058–1061

Sauer FG, Pinkner JS, Waksman G, Hultgren SJ (2002) Chaperone priming of pilus subunits facilitates a topological transition that drives fiber formation. Cell 111:543–551

Saulino ET, Thanassi DG, Pinkner JS, Hultgren SJ (1998) Ramifications of kinetic partitioning on usher-mediated pilus biogenesis. EMBO J 17:2177–2185

So SS, Thanassi DG (2006) Analysis of the requirements for pilus biogenesis at the outer membrane usher and the function of the usher C-terminus. Mol Microbiol 60:364–375

Thanassi DG, Stathopoulos C, Dodson K, Geiger D, Hultgren SJ (2002) Bacterial outer membrane ushers contain distinct targeting and assembly domains for pilus biogenesis. J Bacteriol 184:6260–6269

Verger D, Miller E, Remaut H, Waksman G, Hultgren S (2006) Molecular mechanism of P pilus termination in uropathogenic *Escherichia coli*. EMBO Rep 7:1228–1232

Verger D, Rose RJ, Paci E, Costakes G, Daviter T, Hultgren S, Remaut H, Ashcroft AE, Radford SE, Waksman G (2008) Structural determinants of polymerization reactivity of the P pilus adaptor subunit PapF. Structure 16:1724–1731

Vetsch M, Puorger C, Spirig T, Grauschopf U, Weber-Ban EU, Glockshuber R (2004) Pilus chaperones represent a new type of protein-folding catalyst. Nature 431:329–333

Wright KJ, Seed PC, Hultgren SJ (2007) Development of intracellular bacterial communities of uropathogenic *Escherichia coli* depends on type 1 pili. Cell Microbiol 9:2230–2241

Chapter 11
Crystallography of Gram-Positive Bacterial Adhesins

Vengadesan Krishnan and Sthanam V.L. Narayana

Abstract Both Gram-negative and Gram-positive pathogens display a multitude of proteins and protein assemblies (pili or fimbriae) on their cell surfaces, which are often used for adherence and initiate colonization and pathogenesis. Adhesive proteins known as MSCRAMMs (microbial surface components recognizing adhesive matrix molecules), anchored by a specific enzyme called sortase in Gram-positive bacteria, target the host's extracellular matrix proteins (ECM) like collagen, fibrinogen and fibronectin. In the past decade, structural analysis by X-ray crystallography has enhanced our understanding of the interactions between MSCRAMMs and the host ECM by revealing several novel structural features that dictate surface protein assembly and the mode of their adhesion to host tissue. The latest focus is on the recently discovered Gram-positive bacterial pili, assembly of which is assisted by yet another specific sortase. Novel features like inter- and intra-molecular isopeptide bonds that facilitate the stability of the pilins, and intra-molecular donor strand complementation to stabilize the adhesin-target interactions are specific to Gram-positive bacteria. This chapter describes and discusses the common structural details between surface proteins and pilins of Gram-positive bacteria and biological implications emanating from these structures.

11.1 Introduction

Adhesion to host tissue is the first critical step for bacterial pathogenesis, and both Gram-positive and Gram-negative bacteria use a multitude of proteins and protein assemblies (pili or fimbriae) that are associated with their cell walls for adhesion. A subfamily of adhesive proteins covalently linked to the Gram-positive

S.V.L. Narayana (✉)
Center for Biophysical Sciences and Engineering, University of Alabama at Birmingham, Birmingham, AL 35294, USA
e-mail: narayana@uab.edu

D. Linke, A. Goldman (eds.), *Bacterial Adhesion*, Advances in Experimental Medicine and Biology 715, DOI 10.1007/978-94-007-0940-9_11,

cell wall peptidoglycans is called MSCRAMMs (microbial surface components recognizing adhesive matrix molecules) (Patti et al., 1994b), and some of the extracellular matrix proteins targeted by the MSCRAMMs of *Staphylococcus aureus* include fibrinogen (Hawiger et al., 1982), fibronectin (Kuusela, 1978), and collagen (Speziale et al., 1986).

The net repulsive forces caused by the negative charges present on the host and guest cell surfaces is a general problem that the bacterium faces during adhesion, and one of the ways the pathogen overcomes this is with the help of hair-like, filamentous cell surface organelles known as pili or fimbriae that are anchored to the cell wall. These organelles are assembled using two or more distinct proteins (pilins) (Navarre and Schneewind, 1999), which are stabilized by non-covalent and hydrophobic interactions in Gram-negative bacteria and with the help of covalent linkages in Gram-positive bacteria. The main extended pilus segment, also known as the fimbrial rod or pilus shaft, is composed of several small subunits or major pilins assembled in a head-to-tail manner (Choudhury et al., 1999; Hahn et al., 2002; Hilleringmann et al., 2009; Kang et al., 2007). In some cases, the minor pilins are decorated along the pilus shaft and also at the tip. Chaperone mediated pili assembly in Gram-negative bacteria has been extensively investigated and is well understood (Sauer et al., 2000b; Waksman and Hultgren, 2009), where the individual pilins are held together by an interesting and exquisite "donor strand complementation" technique (Choudhury et al., 1999; Remaut et al., 2006; Sauer et al., 2000a). However, the pili in Gram-positive bacteria, a relatively recent discovery (Scott and Zahner, 2006; Telford et al., 2006; Ton-That and Schneewind, 2004), are assembled by a distinct mechanism catalyzed by a transpeptidase, called a sortase (Ton-That and Schneewind, 2003; 2004). Sortase mediated pili assembly is still a nascent field of investigation and much of the story is still evolving.

There has been a sustained push for the structure determination of Gram-positive surface adhesins during the past decade, mainly to understand their interactions with host tissue. Presently, many crystal structures of Gram-positive bacterial surface proteins and their complexes with host ligands are available (Table 11.1) and the recent focus is on visualizing the individual pilin components and their associations leading to the formation of the adhesive pili. The Gram-positive bacterial surface proteins (MSCRAMMs) and the individual pilin components have similar structural motifs (Fig. 11.1a) to facilitate their transport from the cytoplasm through the Sec system and target them for incorporation into the cell wall. The cell wall sorting motifs include a canonical LPXTG sequence at the C-terminus, where X is any of the 20 amino acids, followed by a hydrophobic stretch of residues and ending with a short positively charged segment, and these three motifs are sufficient and essential for anchoring to the cell wall (Schneewind et al., 1992). Besides that, MSCRAMMs are modular proteins with individual domains for specific functions such as binding to host proteins, extending their binding sites away from the bacterial surface etc., and there are few domains of unknown function. The N-terminal half of most MSCRAMMs carry ligand binding domains (A regions) (Fig. 11.1b) that target host extracellular matrix proteins (ECM) such as collagen, fibrinogen, and fibronectin, while other structural domains that facilitate the extension of A-regions

Table 11.1 Available crystal structures of Gram-positive adhesins

Organism	Surface/pilins	Receptors	Fragment	PDB code	Refs
S. aureus	MSCRAMMS	Collagen	CNA A-region (N2 domain)	1AMX	Symersky et al. (1997)
S. aureus	MSCRAMMS	Collagen	CNA A-region (N1 & N2 domains)	2F68 (apo) 2F6A (complex)	Zong et al. (2005)
S. aureus	MSCRAMMS	–	CNA B-repeats	1D2O (B1) 1D2P (B1B2)	Deivanayagam et al. (2000)
E. faecalis	MSCRAMMS	Collagen	ACE (N2 domain)	2OKM	Ponnuraj and Narayana (2007)
E. faecalis	MSCRAMMS	Collagen	ACE (N1 & N2 domain)	2Z1P	Liu et al. (2007)
S. aureus	MSCRAMMS	Fibrinogen	ClfA (N2 & N3 domains)	1N67	Deivanayagam et al. (2002)
S. aureus	MSCRAMMS	Fibrinogen	ClfA (N2 & N3 domains)	2VR3 (complex)	Ganesh et al. (2008)
S. epidermidis	MSCRAMMS	Fibrinogen	SdrG (N2 & N3 domains)	1R19 (apo) 1R17 (complex)	Ponnuraj et al. (2003)
S. epidermidis	MSCRAMMS	Fibrinogen	SdrG (N2 & N3 mutant)	2RAL(E381C/P595C)	Bowden et al. (2008)
S. aureus	MSCRAMMS	Fibronectin	FnBPA-1/$^{2-3}$F1	2RKZ (FnBPA-1/$^{2-3}$F1) 2RKY (FnBPA-1/$^{4-5}$F1) 3CAL (FnBPA-5/$^{2-3}$F1) 2RL0 (FnBPA-1/$^{2-3}$F1)	Bingham et al. (2008)
S. agalactiae	Minor pilin	–	GBS52	2PZ4	Krishnan et al. (2007)
S. pyogenes	Major pilin	–	Spy0128	3B2M	Kang et al. (2007)
S. pyogenes	Major pilin	–	Spy0128 mutant	3GLD (E177A) 3GLE (N168A)	Kang and Baker (2009)
C. diphtheriae	Major pilin	–	SpaA	3HR6/3HTL	Kang et al. (2009)
S. pneumoniae	Minor pilin	–	RrgA	2WW8	Izoré et al. (2010)
B. cereus	Major pilin	–	BcPA*	3KPT	Budik et al. (2009)

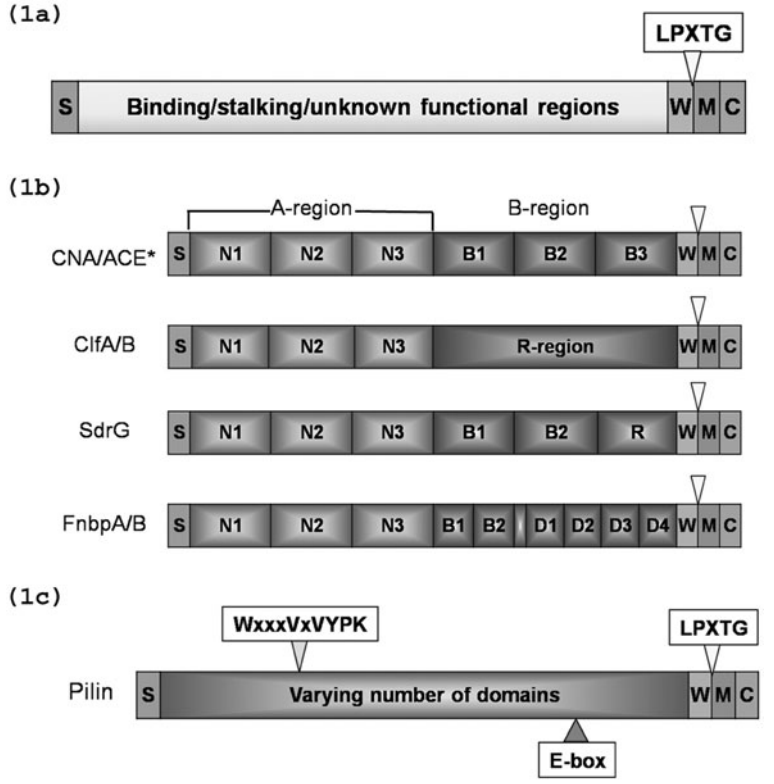

Fig. 11.1 The domain organization for Gram-positive adhesins. (**a**) Common structural motifs present in the MSCRAMMS and Pilin components. A N-terminal signal sequence (S) followed by varying number of non-repetitive and repetitive regions suitable for various functions (ligand binding, projecting binding region/stalking, etc.) and C-terminal region for cell wall anchoring that includes a cell wall sorting region (W) containing the LPXTG motif, membrane-spanning hydrophobic domain (M) and cytoplasmic positively charged C-terminus tail (C). (**b**) The organization of three distinct MSCRAMMS**:** Collagen-binding (CNA/ACE), Fibrinogen-binding (ClfA/B, SdrG) and Fibronectin-binding (FnbpA/B) MSCRAMMs. In addition to common structural motifs (S, W, M and C), most adhesins carry the ligand binding domains (N1, N2, N3,. . .) in the N-terminal half (A-region) and other structural domains that facilitate the extension of A-regions away from cell surface and unknown functions in the C-terminal half (B-region). Exceptions to this rule are the bifunctional FnbpA/B that display fibronectin binding activity at the C-terminal repeats (D1-D4) and fibrinogen binding activity in the N-terminal half. CNA and ACE are highly homologous; however, the ACE is made of only two subdomains (N1 and N2) but exhibits equal affinity to the N1 + N2 domains of CNA. (**c**) The organization of pilins. In addition to common structural motifs (S, W, M and C), the pilins carry varying numbers of domains that make up the pilus shaft and are used for adhesion. The major pilins contain an E-box (YxLxETxAPxGY) and conserved pilin motif (WxxxVxVYPK) suitable for minor pilin incorporation and for covalent polymerization that is catalyzed by an enzyme sortase, respectively

away from cell surface are in the C-terminal half. Interestingly, *S. aureus* strains like 8325-4, Newman and P1 carry two fibronectin binding proteins FnbpA and FnbpB (Flock et al., 1987; Froman et al., 1987), which display fibronectin binding activity that is localized to four 40-residue repeat domains (D1-D4) in the C-terminal half. However, FnbpA and FnbpB are also bifunctional, exhibiting binding sites for fibrinogen in the N-terminal half as well (Wann et al., 2000).

Similar to the surface proteins (MSCRAMMS), the Gram-positive pilus components (pilins) also carry an N-terminal signal peptide and a C-terminal LPXTG sorting signal followed by a hydrophobic domain and a positively charged tail (Fig. 11.1c). In addition, the major pilins contain a conserved element called the pilin motif (WxxxVxVYPK). The side chain amide group of the Lys residue from

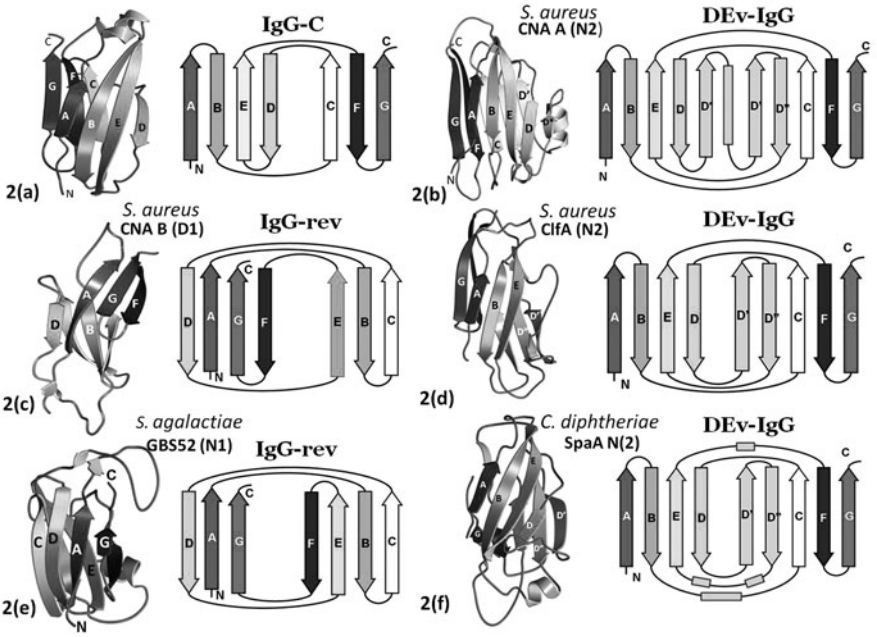

Fig. 11.2 IgG fold variants in Gram-positive adhesions. Ribbon cartoons and topology diagrams of some representative adhesin domains are shown. The core β-strands are labeled A to G (All the ribbon and surface diagrams were prepared with CCP4MG version 2.4.). **(a)** The ubiquitous IgG-constant domain. The IgG constant domain (IgG-C) has a four-stranded β sheet I (A, B, E, D) on one side of the barrel and a three-stranded β sheet II (C, F, G) on the other side. **(b)** DEv-IgG fold of *S. aureus* CNAN2 domain. The additional strands, compared to that of conventional IgG-C fold (Fig. 11.2a) are labeled D*, D' and D" between strands D and E. **(c)** IgG-rev fold of *S. aureus* CNA B-repeats. The IgG-rev fold resembles four and three stranded IgG-C fold (Fig. 11.2a) but differ in topology i.e. the order of β-strands and their linking segments. **(d)** DEv-IgG fold of *S. aureus* ClfAN2. The additional strands between the strands D and E are labeled D' and D". **(e)** The IgG-rev fold of *S. agalactiae* minor pilin GBS52. The fold observed in GBS52 is similar to the IgG-rev fold observed in CNA B repeats (Fig. 11.2c) but strand F is shifted to β-sheet II. **(f)** DEv-IgG fold of *C. diphtheriae* major pilin SpaA (middle) domain (N2)

this region is linked to a Thr residue carbonyl of another pilin and many repeats of the same linkage lead to covalent polymerization of major pilins. This intermolecular cross-linking is catalyzed by a specific enzyme called sortase, SrtC, as demonstrated for *Corynebacterium diphtheriae* pilus assembly (Ton-That and Schneewind, 2003; 2004). To date, crystal structures are available for many individual pilins (Budzik et al., 2009; Izoré et al., 2010; Kang et al., 2009; Krishnan et al., 2007) but, unlike the surface proteins, the ligands they target and their binding mode are still not clear.

One important commonality between these adhesins is the presence of the IgG-constant domain fold and its variants, which are different from the widely observed V-, C-, H- and I-type folds of the immunoglobulin superfamily (Bork et al., 1994; Harpaz and Chothia, 1994). The IgG constant domain has a four-stranded β sheet (I), ABED on one side of the barrel and a three stranded β sheet (II) CFG on the other side (Fig. 11.2). As we discuss later, this motif and its variants are seen across all the Gram-positive surface adhesins and the manifestation of such a common fold suggests that enrichment of these bacterial receptors with IgG-like domains is critical for their adhesion activity. The following sections discuss the structural details of surface proteins and pilins of Gram-positive bacteria and biological implications of these structures.

11.2 Gram-Positive Adhesins

11.2.1 Collagen-Binding MSCRAMMs

Collagens are the most abundant structural proteins in vertebrates and both eukaryotes and prokaryotes express collagen-binding adhesins. They are the major structural component of the extracellular matrix (ECM) and participate in many cellular processes such as cell attachment, differentiation, and migration. Collagen fibers are thin, long and rope-like right-handed triple helical structures composed of three parallel, left-handed polypeptide strands coiled about each other. Each polypeptide strand is made of a repeating Gly-X-Y sequence where X and Y can be any amino acid, but are usually Proline (Pro) and Hydroxyproline (Hyp) (Shoulders and Raines, 2009). The triple helical structure of collagen creates significant structural limitations on the complementarity of the binding domains of interacting proteins. The only crystal structure of eukaryotic collagen-bound protein complex available to date is the I-domain of integrin α2, in complex with a collagen-derived peptide ligand (Emsley et al., 2000). A metal ion (Mg^{2+}) present in the I-domain facilitates the protein-ligand interactions, and a Glu residue of the ligand collagen completes the I-domain metal coordination and stabilizes the complex. There are many collagen-binding adhesins (MSCRAMMs) in Gram-positive bacteria but they do not share sequence and structural homology with the collagen binding I-domain and do not require metal ion for collagen binding.

11.2.1.1 The Ligand Binding A-Region

CNA, the collagen binding MSCRAMM of *S. aureus,* binds collagen with moderate affinity (House-Pompeo et al., 1994) and was shown to be a virulence factor in different animal models of staphylococcal infections including arthritis, endocarditis, osteomyelitis, mastitis and keratitis, suggesting that its ability to interact with collagen provides a general advantage to the bacteria in pathogenesis. As shown in Fig. 11.1b, it has an N-terminal 55 kDa non-repetitive collagen binding A region, followed by C-terminal 23 kDa repetitive B regions. Similar to the fibrinogen–binding protein ClfA (Deivanayagam et al., 2002) of *S. aureus* and SdrG of *S. epidermidis* (Ponnuraj et al., 2003), the A-region of CNA is made of N1 (31-140), N2 (141–344) and N3 (345–531) subdomains. The crystal structure of the 19 kDa N2 domain (CNA 151–318), the minimal collagen binding region denoted as CBD19 (Patti et al., 1995), provided the first structural insight (Symersky et al., 1997) into Gram-positive bacterial adhesins. It revealed a single domain with a novel variant of the IgG-like fold that had a jelly-roll topological pattern (Richardson, 1981). This was later named the DEv-IgG fold (see below; Deivanayagam et al., 2002). CBD19 is composed of two β-sheets (I and II) that are parallel to each other with a largely hydrophobic interior. Each sheet consists of five anti-parallel β-strands: β-sheet I (A,B,E,D,D*) and β-sheet II (D',D",C,F,G). A two turn α-helix between the D* and D' strands and a single α-helical turn between E and D" (Figs. 11.2b and 11.3a) are also observed. The molecular surface of CBD19 revealed an apparent groove of 1–5 Å depth and 10–15 Å width on β-sheet I, indicating a putative collagen-binding region. The binding interface along the groove, suggested by the docking of a triple helical collagen model (Fig. 11.3a) containing four repeats of Gly-Pro-Hyp or Gly-Pro-Pro per chain onto the CBD19 structure, had considerable geometrical and chemical complementarity to the collagen (Symersky et al., 1997). Site directed mutagenesis of residues in this putative collagen binding grove and the measured ligand binding affinities of CBD19 and full length CBD55 mutants supported both the docking model and the earlier observations of CNA specificity for the triple-helical structures (Speziale et al., 1986). A similar model was proposed for ACE (Ponnuraj and Narayana, 2007), the collagen binding MSCRAMM of *Enterococcus faecalis*, where the ACE19 subdomain exhibits 95% sequence identity with CBD19. However, ACE is made of only two subdomains N1 and N2 and has the same affinity towards collagen as CBD35 (the N1 and N2 construct of CNA) (Liu et al., 2007).

CBD19 and ACE19 have 10-fold lower affinity for collagen than their respective full length proteins, suggesting that the other domains of the A-region participate significantly in the interactions with collagen (Patti et al., 1993; Xu et al., 2004). However, the CNA CBD35 construct binds collagen with an affinity that is equivalent to or more than that of full length CBD55 (Patti et al., 1993). The crystal structure of CBD35 was determined as an apo-structure and in complex with a synthetic, collagen-like triple-helical peptide (Zong et al., 2005). Both structures displayed two distinct N1 (31–163) and N2 (174–329) domains. The N1 domain exhibits a DEv-IgG fold (Deivanayagam et al., 2002), which contains three

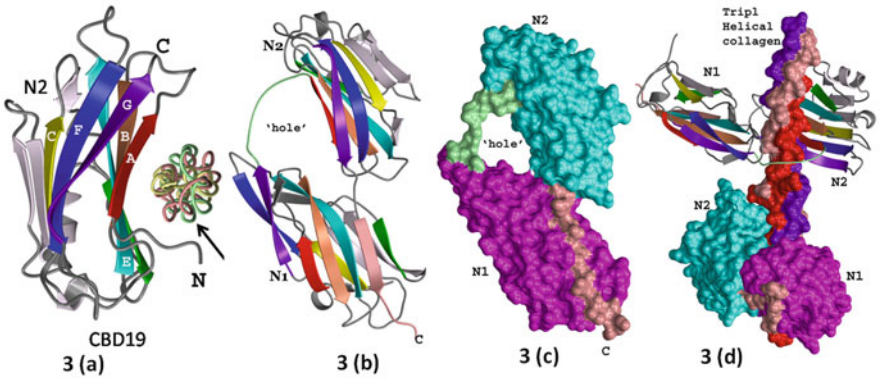

Fig. 11.3 Structure of domains of CNA alone and complexed with collagen peptide. (**a**) Ribbon representation of the Collagen-binding domain (N2) of CNA. The N2 domains display the DEv-IgG fold (Fig. 11.2b). The collagen-binding groove on β-sheet I is shown by *arrow* with docked collagen peptide. **(b)** Ribbon representation of the Collagen-binding domains (N1 and N2) of CNA. The N1 and N2 domains display a DEv-IgG fold (Fig. 11.2b). A long flexible linker (in *light green*) connects the N1 and N2 domain. The C-terminus of the N2 domain extends toward and into the N1 domain and forms a β-strand (in *pink*) that complements one of the β-sheets of N1 domain. **(c)** Surface representation of CBD35N1N2 of CNA. N1 and N2 domains are shown in *magenta* and *cyan* colors, respectively. The N1-N2 linker is in *light green* and the C-terminal extension of N2 domain is in *pink*. **(d)** Structure of CBD35N1N2 in complex with collagen-like triple helical peptide. The three chains of collagen peptide (in surface representation) are leading (L) (*purple*), middle (M) (*pink*), and trailing (T) (*red*) as viewed from their N-termini. Two CNA molecules (one in ribbon as in Fig. 11.3b, and another in surface mode, colored as in (Fig. 11.3c) interact with the collagen peptide in an identical manner. The leading and trailing chains interact with the N2 domain and the middle chain with N1. The N1-N2 linker covers the leading and trailing chains, and holds the rope-like ligand in place

additional strands D*, D' and D" between the D and E strands of β-sheet I compared to the conventional IgG-C fold. The N2 domain is very similar to the CBD19 structure (Symersky et al., 1997), but the N-terminal part of β-strand D is converted into a short β-strand and a α-helical turn. The N1 and N2 domains are connected by a long flexible linker (164–173), which creates a distinct hole between the two domains (Fig. 11.3b and 3c). Surprisingly, the C-terminus of the N2 domain extends toward and into the N1 domain and forms a β-strand that complements one of its β-sheets (Fig. 11.3b and 3c). This intra-molecular donor strand observed in the apo-CBD35 is analogous to the "latch" observed in the structure of ligand-bound SdrGN2N3 complex (Ponnuraj et al., 2003), where the C-terminus of N3 domain extends into the solvent for apo- SdrGN2N3 and is redirected and latched into a trench present in its N2 domain, after ligand-binding (Bowden et al., 2008).

11.2.1.2 The Ligand Bound A-Region

The CBD35-Collagen peptide complex, presented by Zong et al. (2005), was only the second collagen-bound protein complex crystal structure available in the Protein Data Bank. The collagen and cell surface receptor interactions are very much

different between the two available complex structures, which are metal mediated in eukaryotic I-domain bound collagen complex, while hydrophobic interactions dominate the CBD35-Collagen peptide complex formation. In the CBD35-collagen peptide [$(GPO)_4GPRGRT(GPO)_4$) complex structure (Zong et al., 2005), the collagen triple helix is seen penetrated through the hole between the N1 and N2 domains of two CNA molecules in such a way that one CNA molecule is present at each end of the triple helix, resulting in a dumbbell shaped molecular complex (Fig. 11.3d). The inter-domain "hole" is about 12 to 15 Å in diameter (Fig. 11.3b and 3c) into which the GPO repeating units of the collagen peptide fit precisely leaving no extra space to accommodate any other larger side chain for X and Y amino acids, suggesting high specificity. The CNA molecules at either end of the collagen peptide exhibit identical interactions, which are primarily hydrophobic and in addition to few hydrogen bonds and van der Walls contacts. Looking down the helical axis, one can see two CBD35 molecules associated with the triple helical collagen peptide by adopting its "pitch" and twist. The adhesins recognize the collagen peptide only in one direction as most of the interactions are lost if the triple helical peptide has the opposite orientation.

The three chains of the collagen peptide are named as leading, middle and trailing when viewed from their N-termini (Emsley et al., 2004; 2000). The leading and trailing chains (L and T) of the ligand interact with the N2 domain trench region, while the middle chain (M) interacts with the N1 domain that acts as a cover. The inter-domain linker region, which is essential for the confinement of collagen (Symersky et al., 1997), covers the leading chain of the bound peptide and has no specific contacts with the other two chains. Significantly, the Val172 residue from the linker and Tyr175 from the N2 domain sandwich the same Pro11L of the leading chain. The electron density was missing for Val172 in the apo-CNA structure and present in the complex, possibly indicating its role in sequestering the collagen chain. The hydrophobic Tyr175, Phe191 and Tyr233 and polar Asn193, Asn223 and Asn278 residues present in the N2 domain trench region, identified previously by molecular modeling and site-directed mutagenesis studies (Symersky et al., 1997) as important for collagen-adhesin interactions, are observed as predicted (Zong et al., 2005). The hydrophobic residues of the N2 trench region are seen stacked parallel to Pro11L, Pro8L and Pro5T residues, respectively and the polar residues hydrogen bond to Hyp6T and Hyp9T side chain hydroxyls. There are slight variations (5–10°) in the inter-domain association angle between the two CNA molecules, possibly due to the helical twist flexibility of the binding sites in collagen. A single 3_{10} helix (138–148) observed in the apo-CBD35 structure adjacent to the inter domain linker (164–173), was transformed into a β-strand upon ligand binding. This newly formed β-strand facilitates the shortening and tightening of the linker around the bound ligand. These conformational changes result in shrinkage of the inter-domain hole snugly around the bound ligand (Zong et al., 2005).

11.2.1.3 The C-Terminal B-Region of CNA

The B-region of CNA in *S. aureus* (strain FDA574) contains three 23 kDA repeat units (B_1, B_2 and B_3) (Fig. 11.1b), which neither bind collagen nor influence the

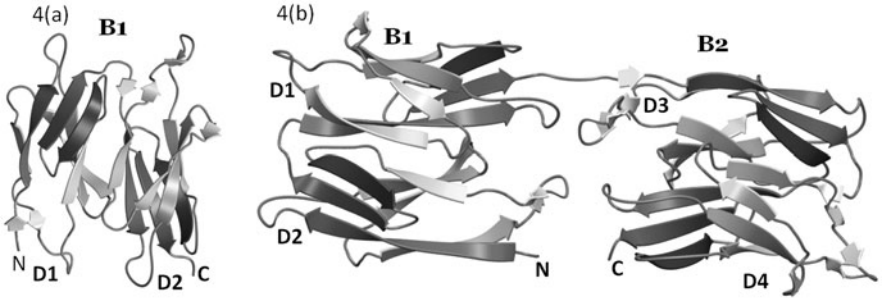

Fig. 11.4 Structure of B repeats of CNA. (**a**) Ribbon representation of B1. B1 has two similar domains (D_1 and D_2) side by side. Both have the IgG-rev fold (Fig. 11.2c). **(b)** Ribbon representation of two individual repeat units B1 and B2. The B1 and B2 domain structures are very similar. The loop (KYTPGET) connecting D_1 to D_2 and D_3 to D_4 in B repeats is flexible with a Gly residue and forms a β-turn, which places the domains side by side; however, the loop (KYTPET) connecting the B repeats (D_2 to D_3) without the Gly has reduced flexibility

A-region's collagen-binding activity (Rich et al., 1998). The B-region repeats have been proposed to serve as a "stalk" that projects the A-region away from the bacterial cell surface and positions it for binding collagen (Rich et al., 1998). The crystal structures of the B_1 and B_1B_2 repeats (Deivanayagam et al., 2000) (Fig. 11.4a and 4b) revealed them to be IgG-like, with variations in β-strand arrangement. Each of the two similar domains in B1, D_1 and D_2, displays a four and three-strand arrangement similar to the IgG domain but with different topology, i.e. the order of β-strands and their linking segments (Fig. 11.2c). We named this the IgG-rev fold. In the B1B2 structure, the B1 (D_1 and D_2) and B2 (D_3 and D_4) domain structures are the same (Fig. 11.4b) and have almost identical primary sequence (99.5%). A Gly residue present in the D_1-D_2 and D_3–D_4 linkers provides the needed flexibility between the D subdomains of B repeats, while the linker joining B1 and B2 repeats (D_2–D_3), without such a Gly residue, have restricted flexibility.

11.2.1.4 The Collagen Hug Model

The closed conformation of *E. faecalis* ACE40, stabilized by engineering a disulphide link between the latch sequence (C-terminal extension of N2 domain) and the bottom of the N1 domain, did not bind type I collagen, proving that only an open conformation of ACE (and CNA) is capable of binding collagen (Liu et al., 2007). In addition, as collagens are long (~200 Å) rope like structures that exhibit side chains of different sizes, shapes and polarity for amino acids at the X and Y positions, and hence could not be "threaded" through the tight "hole" seen between the N1 and N2 domains of apo-CNA35 structure, we proposed a multistep "Collagen Hug" model. In this model, CNA exists in equilibrium between open and closed conformations and may be extended away from the bacterial surface to seek the ligand. Upon ligand binding, initiated by low-affinity (hydrophobic and polar) interactions between the residues present in the shallow "trench" of N2 domain and the ligand,

the inter-domain linker wraps around the triple helical ligand and repositions the N1 domain to cover the bound ligand. Then the inter-domain "hole" shrinks like a clamp, triggered by some specific conformational changes and fits CNA snugly around the bound collagen. The N2 domain's C-terminal extension (connected to N3 domain in CNA) occupies the "latch" space available in the N1 domain β-sheet I to further secure the ligand (Liu et al., 2007). This multistep "Collagen Hug" is conceptually similar but mechanistically different to that of the Dock, lock and Latch (DLL, discussed below) mechanism used for binding linear peptides by MSCRAMMs. The "Collagen Hug" model also suggests that CNA can only bind to monomeric forms of collagen, which either occur naturally or are generated through tissue injury (Kehrel, 1995; Liotta et al., 1980).

11.2.2 Fibrinogen (Fg) -binding MSCRAMMs

Fibrinogen (Fg), a 340 kDa glycoprotein found in blood plasma, plays key roles in hemostatis and coagulation (Herrick et al., 1999). Fg is composed of six polypeptide chains (two α-, two β- and two γ-chains) arranged in a symmetrical dimeric complex structure. The C-terminus of the Fg γ-chain is targeted by the pathogen *Staphylococcus aureus*, resulting in Fg-dependent cell clumping and tissue adherence (Hawiger et al., 1982) and the same Fg γ-chain region also interacts with the platelet integrin $\alpha_{II}\beta_3$ during Fg-dependent platelet adherence and aggregation (Kloczewiak et al., 1984). Clumping factor A (ClfA) of *S. aureus* was the first MSCRAMM identified targeting the γ-chain of Fg and ClfB was identified later that binds specifically to the Fg α-chain (Patti et al., 1994a). Both ClfA and ClfB contain a Ser-Asp repeat region (R region) in the C-terminal part of the protein, in addition to all other common features observed in a typical MSCRAMM. The Fg-binding activity of ClfA is affected by the divalent cations Ca^{2+} and Mn^{2+}, analogous to $\alpha_{II}\beta_3$ integrin (D'Souza et al., 1994; Smith et al., 1994). Higher concentrations of both cations inhibit Fg-dependent bacterial clumping and binding of the recombinant ClfA to isolated Fg.

11.2.2.1 The Crystal Structure of ClfAN2N3

The crystal structure of the proteolytically stable minimum Fg-binding truncation of ClfA (221-559) (Deivanayagam et al., 2002) revealed two compact domains (N2 and N3) with an Ig-like fold similar to the C-type IgG fold ((Fig. 11.2, 11.5a), but displaying variations between its D and E strands, and thus named the DEv-IgG fold (DE-variant fold), and also occurs in CNAN2 (see above). The DEv-IgG fold was also predicted for the ligand binding regions of other *S. aureus* MSCRAMMs ClfB, FnbpA and FnbpB, CNA etc. Three metal ions with octahedral coordination geometry were observed in the ClfA N2N3 structure and they are predominantly coordinated through main-chain carbonyl oxygen atoms and waters. The recombinant ClfA N1 and N2 domains fail to bind Fg when expressed independently, suggesting a cooperative ligand binding role for both domains (Deivanayagam et al., 2002).

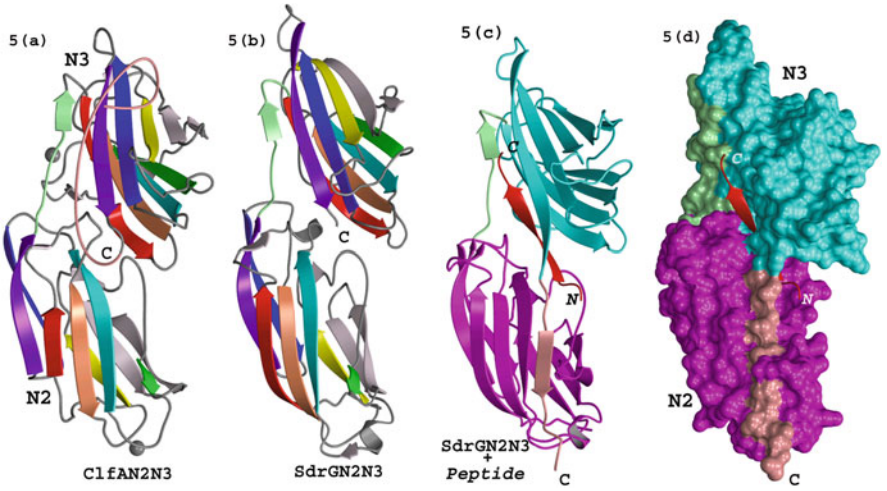

Fig. 11.5 Structures of ClfAN2N3 and of SdrGN2N3 as apo- and in complex with Fibrinogen peptide. **(a)** Ribbon representation of Fg-binding domains (N2 and N3) of apo-ClfAN2N3. The N2 and N3 domain linker is short, in contrast to the CNA inter-domain linker. The C-terminus of the N3 domain (shown in *pink*) turns back and interacts with G strand of N3 domain, occupying the space where the ligand peptide is observed in ClfAN2N3-Fg peptide complex crystal structure (Fig. 11.5c). **(b)** Ribbon representation of N2 and N3 domains of SdrG. N2 and N3 domains are shown in *rainbow* colours. The N2-N3 linker is represented in *light green* and the C-terminus is flexible (no electron density present). **(c)** Ribbon representation of SdrGN2N3 in complex with fibrinogen peptide. The N2 and N3 domains are in magenta and cyan. The interdomain linker and C-terminal latch region are in *light green* and *pink*. The fibrinogen peptide (in red) forms an anti-parallel β-strand with the G strand of the N3 domain. **(d)** Surface representation of SdrGN2N3 in complex with fibrinogen peptide as in Fig. 11.5c

11.2.2.2 The "Dock, Lock and Latch" Model

The crystal structures of Fg-binding A region N2N3 segment of *Staphylococcus epidermidis* SdrG (Ponnuraj et al., 2003), determined as apo- and in complex with a synthetic peptide similar to the N-terminal 6–20 of human Fg β-chain (Ponnuraj et al., 2003) (Fig. 11.5b and 5c), revealed the topology of both N2 and N3 domains to be the same as the DEv-IgG fold. A similar DEv-IgG fold arrangement is also seen in the recently determined peptide bound ClfAN2N3 complex structure (Ganesh et al., 2008). The Fg-derived peptides in both ClfA and SdrG complexes are in an extended conformation and fit snugly into a cleft (~30 Å in length) present between the respective N2 and N3 domains. The topologies and relative orientations of the N2 and N3 domains in the apo- and peptide bound complexes of SdrG and ClfA are similar. However, with the C-terminus of N3 domain directed into the solvent, the apo-SdrGN2N3 and apo-ClfaN2N3 crystal structures exhibit an unoccupied space in the respective N2 domain β-sheet I, sufficient for an extra β-stand between respective D and E strands. However, in the complex structure, once the ligand peptide is positioned in the "cleft" region and stabilized by hydrogen bonds and hydrophobic interactions, the N3 C-terminus is redirected and forms a regular

β-strand that is inserted between the D and E strands of the above mentioned N2 domain β-sheet that has "unoccupied space" (Fig. 11.5c). Based on these observed conformational changes, a "dock, lock and latch (DLL)" model was proposed for SdrG ligand binding. In this model, the ligand binding takes place in multiple steps: the ligand peptide docks into the cleft followed by structural rearrangement at the C-terminus, which crosses over the binding "cleft" and locks the bound peptide in place. The resulting hydrogen bonds between the peptide and adhesin secure the ligand in the binding pocket and the final step is latching, which stabilizes the complex by the insertion of the N3 C-terminus as a strand between the D and E strands of N2 domain, completing the intra-molecular β-strand complementation. This is conceptually similar, but physically different from the inter-molecular donor strand complementation observed in Gram-negative pili assembly (Choudhury et al., 1999; Remaut et al., 2006; Sauer et al., 2000a). The TYTFTDYVD-like motif present in the back of the latching cleft is conserved across MSCRAMMs such as ClfA, ClfB, CNA and ACE, etc. suggesting that all Gram-positive bacterial adhesins use a similar ligand-binding mechanism. In addition, the SdrG-peptide complex structure explained how the thrombin cleavage site is blocked and fibrinopeptide B release is inhibited. Interestingly, the staphylococci express proteins that bind Fg and prevent the release of chemotactic elements such as fibrinopeptide B, thus reducing the influx of phagocytic neutrophils, which possibly enhances bacterial survival at the infection site.

The comparison of the SdrG-peptide and ClfA-peptide complex crystal structures reveals some significant similarities but also differences. The two ligand peptides, snugly docked in the "cleft" region and held in place by the respective reoriented N3 domain C-terminal regions display opposite directionality. The N-terminal Fg β chain (9-18) residues in the SdrG complex form an anti-parallel β-sheet complementary to strand G of the N3 domain. However, Fg γ-chain C-terminal (395–411) residues form a parallel β-sheet with the same G strand in the ClfA complex. Significantly, a stabilized closed conformation of SdrG (locked in closed conformation by an engineered disulfide link) does not bind to Fg, whereas similarly engineered ClfA does bind the ligand (Ganesh et al., 2008), suggesting that an open conformation is required for the initial docking of the ligand peptide for SdrG but not for ClfA. Significantly, the ClfAN2N3 in closed conformation bound ligand with higher affinity compared to the wild-type ClfAN2N3, and this observation raises the possibility that Fg peptide binding to ClfA involves a different mechanism or a variation of DLL.

11.2.3 Fibronectin (Fn) -Binding Proteins (FnBPs)

Fibronectin (Fn) is a ~440 kDa glycoprotein found in the ECM and body fluids of vertebrates and is involved in many cellular processes including cell adhesion, growth, migration, tissue repair and blood clotting. Many MSCRAMMs of staphylococci and streptococci target Fn using the D repeats in their C-terminal region. The

MSCRAMM binding site present in the N-terminal domain (NTD) of Fn contains five sequential type I repeats ($^{1–5}$F1). An NMR structure of $^{1–2}$F1 module pair complexed with FnBP peptide (B3) from *Streptococcus dysgalactiae* was determined and a tandem β-zipper model was proposed for such binding, where the ^{1}F1 and ^{2}F1 – binding motif in B3 forms an additional antiparallel β-strand on sequential F1 modules (Schwarz-Linek et al., 2006; 2004; Schwarz-Linek et al., 2003).

11.2.3.1 Tandem β-zipper Model

Two Fn-binding MSCRAMMs (FnBPA and FnBPB) were identified in *S. aureus (*Jonsson et al., 1991) that contain multiple Fn binding repeats (FnBRs) in the C-terminal region, six of which bind the Fn NTD with high-affinity. The crystal structures of FnBPA–1 and FnBPA–5 peptides (STAFF1 and STATT5) with F1 module pairs ($^{2–3}$F1, $^{4–5}$F1) were solved as ($^{2–3}$F1-STATT1, $^{4–5}$F1-STAFF1, $^{2–3}$F1-STATT5, and $^{4–5}$F1-STAFF5) complexes (Bingham et al., 2008). The FnBP peptide, with four short conserved motifs, binds Fn by adding an antiparallel strand to the three-stranded β-sheet of the four sequential F1 modules (Schwarz-Linek et al., 2003). These structures also suggest that other Fn-binding sites in FnbpA may also follow the same β-zipper binding mechanism. The B3 peptide-bound F1 module structures are very similar to peptide free-forms. The FnBRs in the intact bacterial protein are likely to have less flexible N and C-termini, which possibly influences their interactions with F1 modules. The FnBPA-1/Fn NTD and FnBPA-5/Fn NTD interactions are dominated by hydrophobic and electrostatic interactions with large buried surface area (~4,300 Å^2). Interestingly, FnBPA also binds to Fg *via* its N-terminal A-region, and this bi-functionality of FnBPA may facilitate the disease progression by synergistic and/or cumulative adhesion (Wann et al., 2000) to the host ECM.

11.3 Gram-Positive Pilins

Pili in Gram-positive bacteria were identified first on *Corynebacterium renale (*Yanagawa et al., 1968) and followed by others such as *Actinomyces, Ruminococcus, Enterococcus, Clostridia,* and species of *Streptococcus* (reviews (Mandlik et al., 2007; Proft and Baker, 2009; Telford et al., 2006; Ton-That and Schneewind, 2004)). The structural study of Gram-positive pili is an emerging field and their target tissues in the host are not yet well defined. Therefore, the classification of pili and their components based on their receptors/targets, as done for the surface MSCRAMMs, is not available. Here we present a short description of the available individual pilin structures and conserved folding patterns among them. Interestingly, Gram-positive pilins harbor intra-molecular isopeptide bonds, a covalent bond between the side chains of Lys and Asn, which are mostly present on two neighboring β-strands and such bond formation is catalyzed by a proximal Asp or Glu residue (Kang et al., 2007). Mutations that abrogate the formation of such isopeptide bonds affect the thermal stability of pilins and decrease their resistance to proteases (Kang and Baker, 2009; Kang et al., 2009).

11.3.1 *Streptococcus agalactiae* Minor Pilin GBS52

S. agalactiae or group B Streptococcus (GBS) is the major cause of sepsis, meningitis and pneumonia leading to significant morbidity and mortality in the United States and Europe (Baker and Edward, 2001). Genomic analysis showed the presence of two similar pilus islands (PIs) that encode number of LPXTG motif-bearing proteins and associated sortase enzymes (Dramsi et al., 2006; Lauer et al., 2005; Rosini et al., 2006). EM and biochemical studies revealed that the PI-1 in strain 2603 V/R encodes pilus components, in which a major pilin GBS80 forms the pilus shaft while two minor (associated) pilins GBS52 and GBS104 are also incorporated at various positions in the pilus fiber. GBS minor pilins have recently been shown to be adhesins (Dramsi et al., 2006; Krishnan et al., 2007) and the deletion of minor pilins (GBS52 and GBS104) significantly reduced bacterial adherence to pulmonary epithelial cells while the deletion of major pilin (GBS80) resulted in pilus-deficient, but fully adhesive bacterial cells, suggesting that the minor pilins anchored as surface proteins act as adhesins independent of the pilus structure. The structure of GBS52, the first crystal structure of a Gram-positive bacterial pilin, revealed the presence of two IgG-like domains (N1 and N2) each with IgG-rev topology, respectively (Fig. 11.6a and 11.2e). Significant features are an extended Pro-rich hydrophobic C-terminus in the N2 domain and a predominantly hydrophobic interface between the structurally homologous N1 and N2 domains, which are linked head-to-tail. Biochemical studies revealed that the N2 domain alone of GBS52 is necessary and sufficient for GBS adhesion to lung epithelial cells (Krishnan et al., 2007).

11.3.2 *Streptococcus pyogenes* Major Pilin Spy0128

S. pyogenes or group A streptococcus (GAS), often found in the throat and on the skin, is implicated in impetigo, cellulites, necrotizing fasciitis and streptococcal toxic shock syndrome. The pili of GAS are assembled from three pilins (strain SF370): a major pilin Spy0128 and two minor pilins Spy0125 and Spy0130. The structure of Spy0128 (Kang et al., 2007) revealed the presence of two IgG-like domains (Fig. 11.6b), with one intra-molecular (intra-domain) isopeptide bond between proximal Lys and Asn side chains. Each isopeptide bond is surrounded by many aromatic residues, and a conserved glutamate residue is seen associated with it forming hydrogen bonds to the isopeptide C=O and NH groups (Kang et al., 2007). Kang et al. (2007) also analyzed the previously reported crystal structures of Gram-positive adhesins and revealed the presence of many undetected intra-molecular isopeptide bonds. Interestingly, the predicted inter-molecular isopeptide bonds catalyzed by Sortases have yet to be observed, as no crystal structure of isopeptide linked multiple pilins is available. Even though no structural proof is available, similar inter-molecular isopeptide bonds are known to exist, such as that observed during ubiquitination (Pickart, 2001) and transglutamination (Greenberg et al., 1991) dictating the stability of the participants.

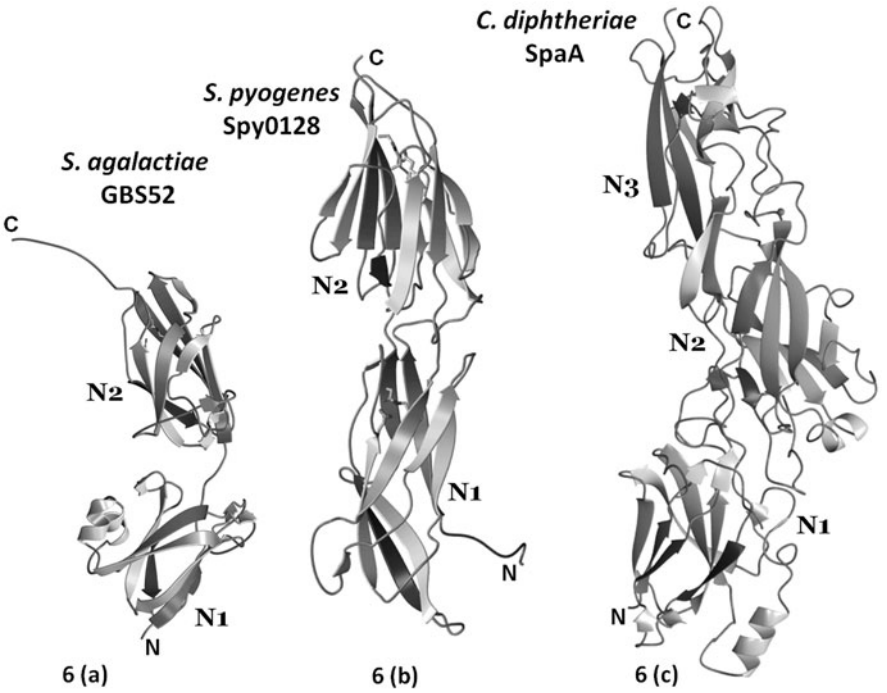

Fig. 11.6 Structures of some Gram-positive Pilins. **(a)** Ribbon representation of minor pilin, GBS52 of group B *Streptococcus*. GBS52 has two domains (N1 and N2) that display IgG-rev fold, but with strand F shifted to β-sheet II. The isopeptide bond between the Lys and Asn residues and the conserved proximal Glu residue are shown as sticks. **(b)** Ribbon representation of major pilin spy0128 of group A *Streptococcus*. The Spy0128 shows two IgG-like domains and each domain hosts an isopeptide bond. **(c)** Ribbon representation of major pilin SpaA of *Corynebacterium diphtheriae*. The SpaA shows three domains (N1, N2 and N3). Both N2 and N3 domains host a single isopeptide bond. The N1 and N3 domains exhibit IgG-rev fold, while the middle N2 domain exhibits DEv-IgG fold

11.3.3 Corynebacterium diphtheriae Major Pilin SpaA

C. diphtheriae, the causative agent of pharyngeal diphtheria, was one of the earliest organisms in which the presence of pili was described (Yanagawa et al., 1968) and best described (Gaspar and Ton-That, 2006; Swierczynski and Ton-That, 2006; Ton-That and Schneewind, 2003). *C. diphtheriae* display three types of pili, which are named according to their respective major pilins and are products of sortase-mediated pilus assembly (Spa), SpaA-, SpaD- and SpaH-type. In the SpaA-type pilus, the major pilin SpaA builds the pilus shaft while SpaB decorates the shaft and SpaC sits at the tip of pilus. The crystal structure of SpaA revealed the presence of three (N1, N2 and N3) domains, arranged in tandem, each domain exhibiting an IgG-like fold (Fig. 11.6c). Both N2 and N3 domains have a single isopeptide bond. Interestingly, the N1 and N3 domains have the IgG-rev fold observed in the CNA

B-region subdomains; and the N2 domain is a DEv-IgG fold similar to that in the ligand binding A-region of CNA. The pilin motif is located on the last strand of the N1-domain and the critical Lys, whose mutation abrogates the polymerization of SpaA molecules during pilus shaft formation, is located close to the N1 and N2 domain interface. A high affinity Ca^{2+} binding site is observed in the N2 domain, but its role is not certain.

11.4 Conclusions

Host colonization by a microbe happens only when the latter is successful in establishing a "beachhead" in the host, and pathogens utilize a multitude of adhesins and adhesin complexes toward their successful campaign. Understanding the mode of adhesion and the structural biology of bacterial tools used for invasion and colonization will facilitate the design of new classes of antimicrobials, whose necessity is obvious in light of prevailing antibiotic resistance. The structural biology of Gram-positive bacterial adhesins is an emerging field and has made considerable progress in a relatively short time; and protein crystallography has made significant contributions toward this journey. Starting from the crystal structure of the minimum collagen binding domain of CNA, CBD19 (Symersky et al., 1997), a steady stream of crystal structures of adhesins (Table 11.1) and their complexes with target host proteins have broadened our perspective of bacterial adhesion. By employing the topologically simple immunoglobulin IgG constant domain, which is observed in numerous proteins encoded all across human genome, for adhesion to host proteins of varied shape and topology, the microbes have gained a tactical advantage and are steps ahead of the human immune arsenal. The observed versatility could be evidence for convergent evolution, possibly by simple lateral or horizontal gene transfer from higher organisms. The microbes have perfected the utilization of IgG domains for adhesion and improved their adaptability by employing a "donor strand complementation" technique, inter-molecular in Gram-negative bacteria and intramolecular in Gram-positive bacteria for pilus assembly and ligand adhesion, respectively.

References

Baker C, Edward M (2001) Group B streptococcal infections. In: Remington JS, Klein JO (eds) Infectious diseases of the fetus and newborn infant. WB Saunders, Philadelphia: PA, pp 1091–1156

Bingham RJ, Rudino-Pinera E, Meenan NA, Schwarz-Linek U, Turkenburg JP, Höök M, Garman EF, Potts JR (2008) Crystal structures of fibronectin-binding sites from *Staphylococcus aureus* FnBPA in complex with fibronectin domains. Proc Natl Acad Sci USA 105:12254–12258

Bork P, Holm L, Sander C (1994) The immunoglobulin fold. Structural classification, sequence patterns and common core. J Mol Biol 242:309–320

Bowden MG, Heuck AP, Ponnuraj K, Kolosova E, Choe D, Gurusiddappa S, Narayana SV, Johnson AE, Höök M (2008) Evidence for the "dock, lock, and latch" ligand binding mechanism

of the staphylococcal microbial surface component recognizing adhesive matrix molecules (MSCRAMM) SdrG. J Biol Chem 283:638–647

Budzik JM, Poor CB, Faull KF, Whitelegge JP, He C, Schneewind O (2009) Intramolecular amide bonds stabilize pili on the surface of bacilli. Proc Natl Acad Sci USA 106:19992–19997

Choudhury D, Thompson A, Stojanoff V, Langermann S, Pinkner J, Hultgren SJ, Knight SD (1999) X-ray structure of the FimC-FimH chaperone-adhesin complex from uropathogenic *Escherichia coli*. Science 285:1061–1066

Deivanayagam CC, Rich RL, Carson M, Owens RT, Danthuluri S, Bice T, Höök M, Narayana SV (2000) Novel fold and assembly of the repetitive B region of the *Staphylococcus aureus* collagen-binding surface protein. Structure 8:67–78

Deivanayagam CC, Wann ER, Chen W, Carson M, Rajashankar KR, Höök M, Narayana SV (2002) A novel variant of the immunoglobulin fold in surface adhesins of *Staphylococcus aureus*: crystal structure of the fibrinogen-binding MSCRAMM, clumping factor A. EMBO J 21: 6660–6672

Dramsi S, Caliot E, Bonne I, Guadagnini S, Prevost MC, Kojadinovic M, Lalioui L, Poyart C, Trieu-Cuot P (2006) Assembly and role of pili in group B streptococci. Mol Microbiol 60:1401–1413

D'Souza SE, Haas TA, Piotrowicz RS, Byers-Ward V, McGrath DE, Soule HR, Cierniewski C, Plow EF, Smith JW (1994) Ligand and cation binding are dual functions of a discrete segment of the integrin β3 subunit: cation displacement is involved in ligand binding. Cell 79: 659–667

Emsley J, Knight CG, Farndale RW, Barnes MJ (2004) Structure of the integrin α2β1-binding collagen peptide. J Mol Biol 335:1019–1028

Emsley J, Knight CG, Farndale RW, Barnes MJ, Liddington RC (2000) Structural basis of collagen recognition by integrin α2β1. Cell 101:47–56

Flock JI, Froman G, Jonsson K, Guss B, Signas C, Nilsson B, Raucci G, Höök M, Wadstrom T, Lindberg M (1987) Cloning and expression of the gene for a fibronectin-binding protein from *Staphylococcus aureus*. EMBO J 6:2351–2357

Froman G, Switalski LM, Speziale P, Höök M (1987) Isolation and characterization of a fibronectin receptor from *Staphylococcus aureus*. J Biol Chem 262:6564–6571

Ganesh VK, Rivera JJ, Smeds E, Ko YP, Bowden MG, Wann ER, Gurusiddappa S, Fitzgerald JR, Höök M (2008) A structural model of the *Staphylococcus aureus* ClfA-fibrinogen interaction opens new avenues for the design of anti-staphylococcal therapeutics. PLoS Pathog 4:e1000226

Gaspar AH, Ton-That H (2006) Assembly of distinct pilus structures on the surface of *Corynebacterium diphtheriae*. J Bacteriol 188:1526–1533

Greenberg CS, Birckbichler PJ, Rice RH (1991) Transglutaminases: multifunctional cross-linking enzymes that stabilize tissues. FASEB J 5:3071–3077

Hahn E, Wild P, Hermanns U, Sebbel P, Glockshuber R, Häner M, Taschner N, Burkhard P, Aebi U, Müller SA (2002) Exploring the 3D molecular architecture of *Escherichia coli* type 1 pili. J Mol Biol 323:845–857

Harpaz Y, Chothia C (1994) Many of the immunoglobulin superfamily domains in cell adhesion molecules and surface receptors belong to a new structural set which is close to that containing variable domains. J Mol Biol 238:528–539

Hawiger J, Timmons S, Strong DD, Cottrell BA, Riley M, Doolittle RF (1982) Identification of a region of human fibrinogen interacting with staphylococcal clumping factor. Biochemistry 21:1407–1413

Herrick S, Blanc-Brude O, Gray A, Laurent G (1999) Fibrinogen. Int J Biochem Cell Biol 31: 741–746

Hilleringmann M, Ringler P, Müller SA, De Angelis G, Rappuoli R, Ferlenghi I, Engel A (2009) Molecular architecture of *Streptococcus pneumoniae* TIGR4 pili. EMBO J 28:3921–3930

House-Pompeo K, Boles JO, Höök M (1994) Characterization of bacterial adhesin interactions with extracellular matrix components utilizing biosensor technology. Methods: Companion Method Enzymol 6:134–142

Izoré T, Contreras-Martel C, El Mortaji L, Manzano C, Terrasse R, Vernet T, Di Guilmi AM, Dessen A (2010) Structural basis of host cell recognition by the pilus adhesin from *Streptococcus pneumoniae*. Structure 18:106–115

Jonsson K, Signas C, Müller HP, Lindberg M (1991) Two different genes encode fibronectin binding proteins in *Staphylococcus aureus*. The complete nucleotide sequence and characterization of the second gene. Eur J Biochem 202:1041–1048

Kang HJ, Baker EN (2009) Intramolecular isopeptide bonds give thermodynamic and proteolytic stability to the major pilin protein of *Streptococcus pyogenes*. J Biol Chem 284: 20729–20737

Kang HJ, Coulibaly F, Clow F, Proft T, Baker EN (2007) Stabilizing isopeptide bonds revealed in Gram-positive bacterial pilus structure. Science 318:1625–1628

Kang HJ, Paterson NG, Gaspar AH, Ton-That H, Baker EN (2009) The *Corynebacterium diphtheriae* shaft pilin SpaA is built of tandem Ig-like modules with stabilizing isopeptide and disulfide bonds. Proc Natl Acad Sci USA 106:16967–16971

Kehrel B (1995) Platelet-collagen interactions. Semin Thromb Hemost 21:123–129

Kloczewiak M, Timmons S, Lukas TJ, Hawiger J (1984) Platelet receptor recognition site on human fibrinogen. Synthesis and structure-function relationship of peptides corresponding to the carboxy-terminal segment of the γ chain. Biochemistry 23:1767–1774

Krishnan V, Gaspar AH, Ye N, Mandlik A, Ton-That H, Narayana SV (2007) An IgG-like domain in the minor pilin GBS52 of *Streptococcus agalactiae* mediates lung epithelial cell adhesion. Structure 15:893–903

Kuusela P (1978) Fibronectin binds to *Staphylococcus aureus*. Nature 276:718–720

Lauer P, Rinaudo CD, Soriani M, Margarit I, Maione D, Rosini R, Taddei AR, Mora M, Rappuoli R, Grandi G, Telford JL (2005) Genome analysis reveals pili in *Group B Streptococcus*. Science 309:105

Liotta LA, Tryggvason K, Garbisa S, Hart I, Foltz CM, Shafie S (1980) Metastatic potential correlates with enzymatic degradation of basement membrane collagen. Nature 284:67–68

Liu Q, Ponnuraj K, Xu Y, Ganesh VK, Sillanpää J, Murray BE, Narayana SV, Höök M (2007) The *Enterococcus faecalis* MSCRAMM ACE binds its ligand by the collagen hug model. J Biol Chem 282:19629–19637

Mandlik A, Swierczynski A, Das A, Ton-That H (2007) *Corynebacterium diphtheriae* employs specific minor pilins to target human pharyngeal epithelial cells. Mol Microbiol 64:111–124

Navarre WW, Schneewind O (1999) Surface proteins of Gram-positive bacteria and mechanisms of their targeting to the cell wall envelope. Microbiol Mol Biol Rev 63:174–229

Patti JM, Allen BL, McGavin MJ, Höök M (1994a) MSCRAMM-mediated adherence of microorganisms to host tissues. Annu Rev Microbiol 48:585–617

Patti JM, Boles JO, Höök M (1993) Identification and biochemical characterization of the ligand binding domain of the collagen adhesin from *Staphylococcus aureus*. Biochemistry 32: 11428–11435

Patti JM, Bremell T, Krajewska-Pietrasik D, Abdelnour A, Tarkowski A, Ryden C, Höök M (1994b) The *Staphylococcus aureus* collagen adhesin is a virulence determinant in experimental septic arthritis. Infect Immun 62:152–161

Patti JM, House-Pompeo K, Boles JO, Garza N, Gurusiddappa S, Höök M (1995) Critical residues in the ligand-binding site of the *Staphylococcus aureus* collagen-binding adhesin (MSCRAMM). J Biol Chem 270:12005–12011

Pickart CM (2001) Mechanisms underlying ubiquitination. Annu Rev Biochem 70:503–533

Ponnuraj K, Bowden MG, Davis S, Gurusiddappa S, Moore D, Choe D, Xu Y, Höök M, Narayana SV (2003) A "dock, lock, and latch" structural model for a staphylococcal adhesin binding to fibrinogen. Cell 115:217–228

Ponnuraj K, Narayana SV (2007) Crystal structure of ACE19, the collagen binding subdomain of *Enterococus faecalis* surface protein ACE. Proteins 69:199–203

Proft T, Baker EN (2009) Pili in Gram-negative and Gram-positive bacteria – structure, assembly and their role in disease. Cell Mol Life Sci 66:613–635

Remaut H, Rose RJ, Hannan TJ, Hultgren SJ, Radford SE, Ashcroft AE, Waksman G (2006) Donor-strand exchange in chaperone-assisted pilus assembly proceeds through a concerted β strand displacement mechanism. Mol Cell 22:831–842

Rich RL, Demeler B, Ashby K, Deivanayagam CC, Petrich JW, Patti JM, Narayana SV, Höök M (1998) Domain structure of the *Staphylococcus aureus* collagen adhesin. Biochemistry 37:15423–15433

Richardson JS (1981) The anatomy and taxonomy of protein structure. Adv Prot Chem 34: 167–399

Rosini R, Rinaudo CD, Soriani M, Lauer P, Mora M, Maione D, Taddei A, Santi I, Ghezzo C, Brettoni C, Buccato S, Margarit I, Grandi G, Telford JL (2006) Identification of novel genomic islands coding for antigenic pilus-like structures in *Streptococcus agalactiae*. Mol Microbiol 61:126–141

Sauer FG, Knight SD, Waksman Gj, Hultgren SJ (2000a) PapD-like chaperones and pilus biogenesis. Semin Cell Dev Biol 11:27–34

Sauer FG, Mulvey MA, Schilling JD, Martinez JJ, Hultgren SJ (2000b) Bacterial pili: molecular mechanisms of pathogenesis. Curr Opin Microbiol 3:65–72

Schneewind O, Model P, Fischetti VA (1992) Sorting of protein A to the staphylococcal cell wall. Cell 70:267–281

Schwarz-Linek U, Höök M, Potts JR (2006) Fibronectin-binding proteins of Gram-positive cocci. Microbes Infect 8:2291–2298

Schwarz-Linek U, Pilka ES, Pickford AR, Kim JH, Höök M, Campbell ID, Potts JR (2004) High affinity streptococcal binding to human fibronectin requires specific recognition of sequential F1 modules. J Biol Chem 279:39017–39025

Schwarz-Linek U, Werner JM, Pickford AR, Gurusiddappa S, Kim JH, Pilka ES, Briggs JA, Gough TS, Höök M, Campbell ID, Potts JR (2003) Pathogenic bacteria attach to human fibronectin through a tandem β-zipper. Nature 423:177–181

Scott JR, Zahner D (2006) Pili with strong attachments: Gram-positive bacteria do it differently. Mol Microbiol 62:320–330

Shoulders MD, Raines RT (2009) Collagen structure and stability. Annu Rev Biochem 78: 929–958

Smith JW, Piotrowicz RS, Mathis D (1994) A mechanism for divalent cation regulation of β 3-integrins. J Biol Chem 269:960–967

Speziale P, Raucci G, Visai L, Switalski LM, Timpl R, Höök M (1986) Binding of collagen to *Staphylococcus aureus* Cowan 1. J Bacteriol 167:77–81

Swierczynski A, Ton-That H (2006) Type III pilus of corynebacteria: pilus length is determined by the level of its major pilin subunit. J Bacteriol 188:6318–6325

Symersky J, Patti JM, Carson M, House-Pompeo K, Teale M, Moore D, Jin L, Schneider A, DeLucas LJ, Höök M, Narayana SV (1997) Structure of the collagen-binding domain from a *Staphylococcus aureus* adhesin. Nat Struct Biol 4:833–838

Telford JL, Barocchi MA, Margarit I, Rappuoli R, Grandi G (2006) Pili in Gram-positive pathogens. Nat Rev Microbiol 4:509–519

Ton-That H, Schneewind O (2003) Assembly of pili on the surface of *Corynebacterium diphtheriae*. Mol Microbiol 50:1429–1438

Ton-That H, Schneewind O (2004) Assembly of pili in Gram-positive bacteria. Trends Microbiol 12:228–234

Waksman G, Hultgren SJ (2009) Structural biology of the chaperone-usher pathway of pilus biogenesis. Nat Rev Microbiol 7:765–774

Wann ER, Gurusiddappa S, Höök M (2000) The fibronectin-binding MSCRAMM FnbpA of *Staphylococcus aureus* is a bifunctional protein that also binds to fibrinogen. J Biol Chem 275:13863–13871

Xu Y, Liang X, Chen Y, Koehler TM, Höök M (2004) Identification and biochemical characterization of two novel collagen binding MSCRAMMs of *Bacillus anthracis*. J Biol Chem 279:51760–51768

Yanagawa R, Otsuki K, Tokui T (1968) Electron microscopy of fine structure of *Corynebacterium renale* with special reference to pili. Jpn J Vet Res 16:31–37

Zong Y, Xu Y, Liang X, Keene DR, Höök A, Gurusiddappa S, Höök M, Narayana SV (2005) A "collagen hug" model for *Staphylococcus aureus* CNA binding to collagen. EMBO J 24: 4224–4236

Chapter 12
The Nonideal Coiled Coil of M Protein and Its Multifarious Functions in Pathogenesis

Partho Ghosh

Abstract The M protein is a major virulence factor of *Streptococcus pyogenes* (group A *Streptococcus*, GAS). This gram-positive bacterial pathogen is responsible for mild infections, such as pharyngitis, and severe invasive disease, like streptococcal toxic shock syndrome. M protein contributes to GAS virulence in multifarious ways, including blocking deposition of antibodies and complement, helping formation of microcolonies, neutralizing antimicrobial peptides, and triggering a proinflammatory and procoagulatory state. These functions are specified by interactions between M protein and many host components, especially C4BP and fibrinogen. The former interaction is conserved among many antigenically variant M protein types but occurs in a strikingly sequence-independent manner, and the latter is associated in the M1 protein type with severe invasive disease. Remarkably for a protein of such diverse interactions, the M protein has a relatively simple but nonideal α-helical coiled coil sequence. This sequence nonideality is a crucial feature of M protein. Nonideal residues give rise to specific irregularities in its coiled-coil structure, which are essential for interactions with fibrinogen and establishment of a proinflammatory state. In addition, these structural irregularities are reminiscent of those in myosin and tropomyosin, which are targets for crossreactive antibodies in patients suffering from autoimmune sequelae of GAS infection.

12.1 Introduction

The M protein is a central virulence factor of the widespread, gram-positive bacterial pathogen *Streptococcus pyogenes* (group A *Streptococcus,* GAS) (Cunningham, 2000). Extending ~500 Å outwards from the GAS surface in the form of hair-like

P. Ghosh (✉)
Department of Chemistry and Biochemistry, University of California, San Diego, CA 92093-0375, USA
e-mail: pghosh@ucsd.edu

D. Linke, A. Goldman (eds.), *Bacterial Adhesion*, Advances in Experimental Medicine and Biology 715, DOI 10.1007/978-94-007-0940-9_12,

fimbriae (Fischetti, 1989), the M protein is in a prime location to interact with host components and guide the course of infection. GAS is responsible for both mild infections, such as pharyngitis ("strep throat"), as well as severe invasive diseases having high mortality rates (~30%), such as necrotizing fasciitis and streptococcal toxic shock syndrome (STSS) (O'Loughlin et al., 2007). GAS infection, especially if untreated, can also lead to delayed autoimmune diseases, such as acute rheumatic fever (Steer et al., 2009).

M protein contributes to GAS infection in a number of different ways. Most well recognized is the capacity of M protein to block antibodies and complement from being deposited onto the surface of *S. pyogenes*. This enables GAS to evade phagocytic destruction by leukocytes and survive in whole blood (Carlsson et al., 2003). M protein is also involved in the adhesion of GAS to host cells (Okada et al., 1995), intracellular invasion of host cells (Cue et al., 2000), formation of GAS aggregates that enhance phagocytic resistance and host cell adhesion (Frick et al., 2000), neutralization of antimicrobial peptides (Nilsson et al., 2008; Lauth et al., 2009), and assembly of GAS biofilms (Cho and Caparon, 2005). A growing body of evidence indicates that M protein evokes a proinflammatory and procoagulatory state that causes severe tissue damage reminiscent of the symptoms of STSS (Herwald et al., 2004). M protein is also involved in eliciting crossreactive antibodies in autoimmune sequelae of GAS infection (Cunningham, 2000). The multifarious functions of M protein depend on its interaction with a sizeable number of host components. Curiously for a protein of such diverse interactions, the M protein has a seemingly simple α-helical coiled-coil sequence, albeit one that is nonideal and one that is just beginning to be understood in the light of the first atomic-resolution structure of M protein (McNamara et al., 2008).

12.2 Antigenic Variation and M Types

The M protein was first described as a type-specific substance that could be extracted by acid from virulent strains of GAS (Lancefield, 1928). The type-specificity refers to the antigenic variation of M protein, which has served as the basis for the Lancefield serological typing of GAS strains. M types are now defined genotypically by the first 160 bases of the mature protein, which encode the hypervariable region (HVR) (Fig. 12.1) (Facklam et al., 2002). While greater than 100 M types have been identified, only a few are prevalent in the human population (Steer et al., 2009).

The M1 protein type is especially notable not only for being the most prevalent M type but also for being strongly associated with invasive GAS infection and for having proinflammatory properties (Herwald et al., 2004; O'Loughlin et al., 2007). A subclone of the M1T1 serotype has been the leading cause of severe invasive GAS infection worldwide for the past 30 years (Aziz and Kotb, 2008). The M12 and M3

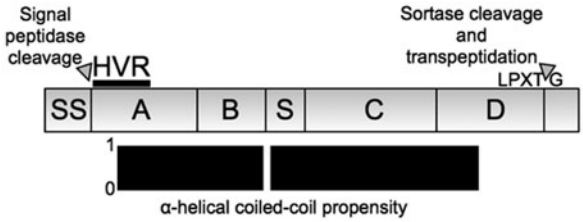

Fig. 12.1 Regions of M protein. *Top*, the M1 protein type is used as an example to delineate regions. The signal sequence (SS) is removed proteolytically, and the C-terminal "LPXTG" motif is cleaved and covalently attached to the peptidoglycan. Mature M1 is constituted by the A-region, which contains the 50-residue long hypervariable region (HVR); the B-repeats, which consist of ~2.2 imperfect repeats of a 28-residue sequence; the S-region, which is unique to M1; the C-repeats, which consist of 3 imperfect repeats of a 42-residue sequence; and the D-region. *Bottom*, most of mature M1 has a high propensity for forming an α-helical coiled coil, with a slight break at the end of the B-repeats

types are also strongly associated with severe invasive disease (O'Loughlin et al., 2007), but less is known about the proinflammatory or procoagulatory properties of these M protein types.

12.3 Bacterial Surface and Released Forms of M Protein

M protein is synthesized in immature form with an N-terminal signal sequence and a C-terminal site for processing by sortase (Fig. 12.1). The N-terminal signal sequence of ~40 residues directs secretion of M protein to the bacterial division septum (Carlsson et al., 2006), and is removed by signal peptidase. The signal sequence is well conserved among M protein types, suggesting a functional importance to secretion at the division septum. Once secreted across the bacterial membrane, M protein is processed by sortase, which cleaves between the Thr and Gly residues in an "LPXTG" motif located close to the C-terminus. Sortase then carries out a transpeptidation reaction in which the Thr residue is covalently attached to the peptidoglycan precursor lipid II, and eventually to the peptidoglycan itself (Navarre and Schneewind, 1999). With the removal of these N- and C-terminal regions, the mature form of M protein contains ~300–400 residues.

M protein is found not only attached to the GAS surface but also as a released molecule. Release may occur through cleavage by the streptococcal cysteine protease SpeB (Berge and Bjorck, 1995). For severe invasive strains which have little or no SpeB expression (Kansal et al., 2000), M protein is released during infection by the action of neutrophil proteases (Herwald et al., 2004). In fact, the greater part of M1 protein in patient samples occurs as released rather than bacterial surface-attached protein (Kahn et al., 2008). Significantly, the released form of M1 retains

its proinflammatory and procoagulatory properties (Herwald et al., 2004; Shannon et al., 2007; Kahn et al., 2008; Nilsson et al., 2008).

12.4 Repeats and Nonideal Coiled-Coil Sequences

Two features distinguish the sequence of mature M protein. This is true for both the highly divergent N-terminal half of the protein as well as the more well conserved C-terminal half. The first distinguishing feature is the presence of imperfect repeats in the sequence. Repeats in the sequence divergent N-terminal half are designated A-repeats and B–repeats (Fig. 12.1), but somewhat confusingly, the repeats of two different M types need not be closely related in sequence. A case in point is the B-repeats of M1 and M5, which both bind fibrinogen (Carlsson et al., 2005). The M1 and M5 B-repeats have no obvious relationship to one another (~14% identity), and consistent with this divergence, bind fibrinogen noncompetitively (Ringdahl et al., 2000). In contrast, in the sequence conserved C-terminal half, the 42-residue long C-repeats of different M types are ~70–95% identical. These are followed by a ~90-residue D-region, which has up to ~90% identity between M types. While the D-region is covalently attached to the peptidoglycan and likely buried within it, the C-repeats are exposed and bind host components (Sandin et al., 2006). Why M protein has such a preponderance of repeat sequences is not yet clear.

The second distinguishing feature of the M protein sequence is the presence of an α-helical coiled-coil heptad periodicity (Manjula and Fischetti, 1980). This is true for the divergent N-terminal half, except for the first ~20 residues of the HVR, as well as the conserved C-terminal half, except for the last ~50-residues of the D-region. The heptad periodicity is marked by the recurrence of small hydrophobic residues at the *a* and *d* positions. These small hydrophobic residues form the hydrophobic core of the coiled coil through "knobs-into-holes" packing (Fig. 12.2a). Parallel as well as anti-parallel associations of α-helices are possible in coiled coils (Fig. 12.2a), as are homotypic and heterotypic associations. In addition, a number of stoichiometries have been observed for coiled coils.

M protein forms a dimeric, parallel α-helical coiled coil structure as directly shown by the crystal structure of a physiologically relevant fragment of M1 protein encompassing the A-region and B-repeats, called $M1^{AB}$ (McNamara et al., 2008). The structure also reveals a substantial number of structural irregularities in the coiled coil (Figs. 12.2b and 12.2c). These structural irregularities stem from a sequence that is far from ideal at the core *a* and *d* positions (Nilson et al., 1995; McNamara et al., 2008). The ideal residues for a dimeric, parallel coiled coil at the *a* and *d* positions are Val and Leu, respectively (Wagschal et al., 1999; Tripet et al., 2000). Destabilizing residues at *a* positions are Ala, Gln, His, Lys, Ser, Glu, Arg, and Gly; and at *d* positions Ala, Trp, Asn, His, Thr, Lys, Asp, Ser, Glu, Arg, and Gly. M protein, regardless of type, has a substantial number of these nonideal residues at predicted *a* and *d* positions throughout its length (Nilson et al., 1995; McNamara et al., 2008).

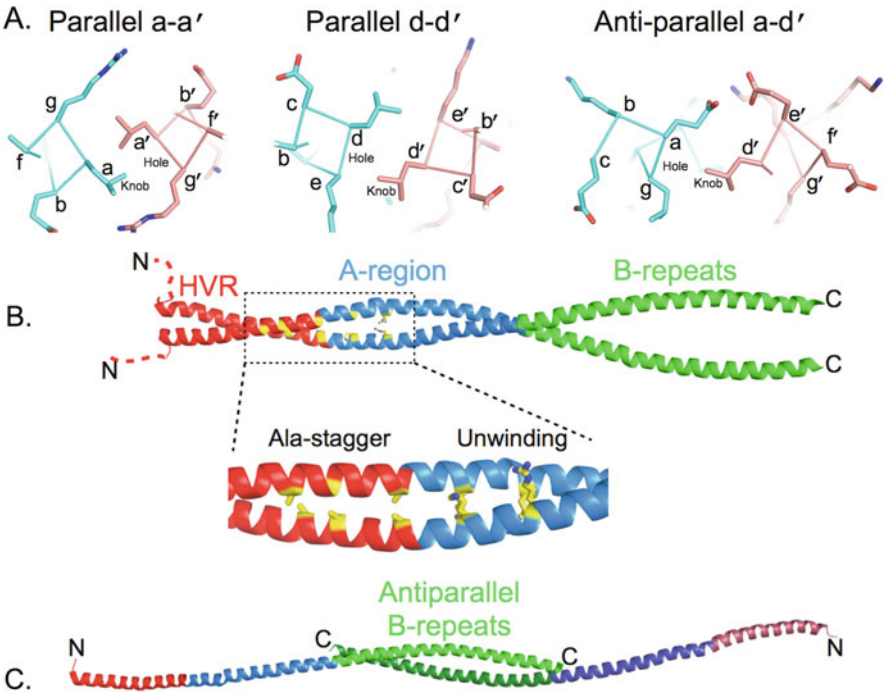

Fig. 12.2 Crystal structure of M protein. **(a)** Knobs-into-hole packing of residues in the *a* and *d* positions, *left* and *middle*, respectively, in a dimeric, parallel α-helical coiled coil. Both *a* and *d* positions in this example are occupied by Leu, and examples of "knobs" and "holes" are labelled. *Right*, knobs-into-hole packing of an Asp at the *a* position with a Leu in the *d* position in a dimeric, anti-parallel α-helical coiled coil. This and other molecular figures were generated with PyMol (http://www.pymol.org). (**b**) Structure of the $M1^{AB}$ α-helical coiled-coil dimer. The HVR is in red (with its ~15 initial residues disordered and shown in an arbitrary position as dashed lines), the rest of the A-region in blue, and the B-repeats in green. In yellow, residues that form the Ala-stagger and cause unwinding due to large positively charged residues at *a* positions. This region is *boxed* and *expanded* below. (**c**) The B-repeats of the $M1^{AB}$ dimer splay apart and engage in an anti-parallel α-helical coiled-coil with the B-repeats of a neighbouring molecule. This anti-parallel interaction between two neighbouring $M1^{AB}$ dimers is shown, with one α-helix of each dimer omitted for clarity

12.5 Structural Irregularities

The consequences of sequence nonidealities in M protein were recently revealed by the crystal structure of $M1^{AB}$ (McNamara et al., 2008). $M1^{AB}$ forms a parallel, dimeric α-helical coiled coil through the A-region, while the B-repeats splay apart and engage in an anti-parallel coiled coil with the B-repeats of an adjoining $M1^{AB}$ molecule in the crystal (Figs. 12.2b and 12.2c). Only two short stretches in $M1^{AB}$ have regular structure. Each of these short segments consists of ~2 heptads (residues 63–79 in the HVR and residues 106–119 of the A-region). The rest of the structure is irregular. These structural irregularities consist of an Ala-stagger due to a cluster of

poorly packed Ala residues at contiguous *a* and *d* positions in the HVR, superhelical unwinding due to large positively charged residues at consecutive *a* positions in the A-region, and splaying apart of the entire B-repeats.

Each of these specific structural features has been seen in the α-helical coiled coil portions of myosin, tropomyosin, or both (Brown et al., 2001; Li et al., 2003; Brown et al., 2005; Blankenfeldt et al., 2006). This is notable as patients with acute rheumatic fever have crossreactive antibodies directed against myosin, tropomyosin, and other host α-helical coiled coil proteins (e.g. laminin, keratin, and vimentin) (Cunningham, 2000). This raises the possibility that specific structural irregularities shared between M1, myosin, and tropomyosin are being recognized by crossreactive antibodies rather than the generic "coiled coil-ness" of the structure. In support of this notion, sequence idealization of the B-repeats of M1, in which *a* and *d* positions of the B-repeats were substituted with Val and Leu, respectively, resulted in decreased recognition by the crossreactive antibody 36.2.2 (McNamara et al., 2008), noted for its cytoxicity against heart cells (Cunningham et al., 1992). This B-repeat idealized version of M1 retained the capacity to elicit protective immunity (McNamara et al., 2008), suggesting that sequence idealization may be applicable to vaccine design.

While the splaying apart of the B-repeats is indicative of the instability of the coiled coil in this region, it is also possible that the anti-parallel coiled coil reflects a physiologically relevant state in promoting GAS aggregation (Fig. 12.3a). GAS aggregation is involved in the evasion of phagocytosis as well as the formation of microcolonies that adhere better to epithelial cells than single bacterial cells (Caparon et al., 1991; Frick et al., 2000). Evidence exists that M protein dimers dynamically dissociate and reassociate (Akerstrom et al., 1992; Cedervall et al., 1995; Nilson et al., 1995; McNamara et al., 2008), making it possible for M proteins from abutting bacterial cells to associate in anti-parallel form. For the B-repeats and perhaps for other portions of the M protein, the anti-parallel coil form may be more favourable than the parallel one (Nilson et al., 1995; McNamara et al., 2008). This is because the packing in an anti-parallel coiled coil is between *a*-*d*′ and *d*-*a*′ positions (the prime referring to the residue in the opposing helix) as opposed to the *a*-*a*′ and *d*-*d*′ packing in a parallel coiled coil (Fig. 12.2a). Anti-parallel packing in the B-repeats of M1 avoids several *a*-*a*′ charge-charge clashes that would occur in the parallel conformation. Electron micrographs suggest that this sort of interaction occurs (Phillips et al., 1981), and the importance of M protein to GAS aggregation has been reported (Caparon et al., 1991).

For myosin and tropomyosin, structural irregularities in the coiled coil are correlated with function. The same appears to be the case for M protein. Idealization of the *a* and *d* positions in the B-repeats of M1 was seen to impart greater stability to the molecule but also reduced its affinity for fibrinogen (McNamara et al., 2008). The regularity of a coiled coil, while structurally elegant, appears not to be conducive to conferring specific recognition or conformational flexibility. These features require nonideal sequences and structural irregularity, with the cost of this being a diminution in protein stability. This explains a puzzling feature of M protein, its instability at 37°C (Akerstrom et al., 1992; Cedervall et al.,

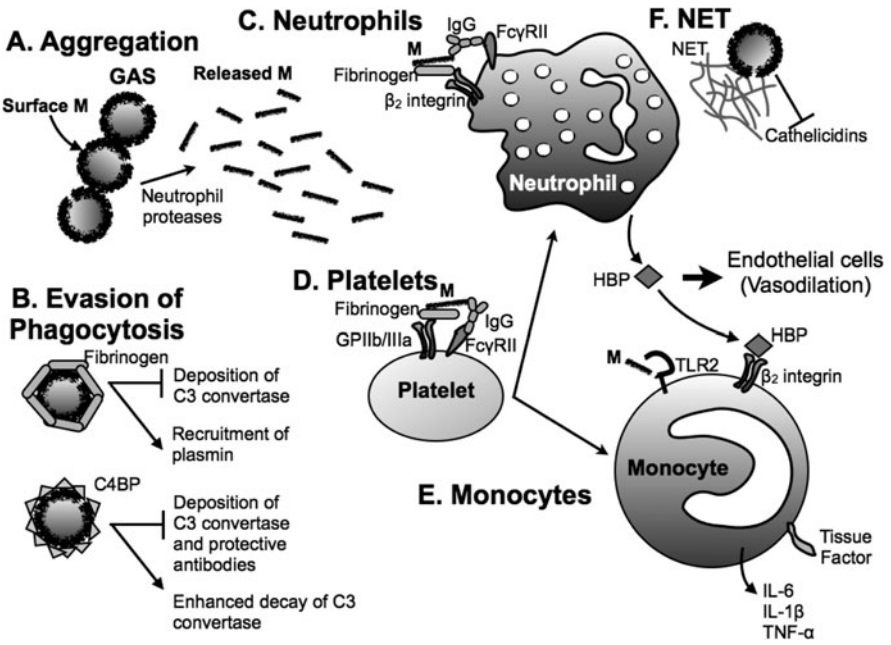

Fig. 12.3 Functional interactions of M protein. Bacterial surface-bound M protein contributes to (**a**) GAS aggregation through homotypic interactions, and (**b**) evasion of phagocytosis through recruitment of fibrinogen or C4BP to the bacterial surface. Bound fibrinogen is also responsible for recruiting plasmin to the GAS surface, which is associated with a transition from localized to invasive infection. (**c**) M protein released by neutrophil proteases from the bacterial surface interacts with fibrinogen, and M-fibrinogen complexes activate neutrophils via β_2 integrins along with IgGs that bind to M protein and interact with FcγRII. Activated neutrophils release the vasodilator heparin binding protein (HBP). (**d**) M-fibrinogen complexes also activate platelets. This occurs through interaction of these complexes with the integrin GPIIb/IIIa along with IgGs that bind to M protein and interact with FcγRII. Activated platelets in turn lead to further activation of neutrophils and monocytes. (**e**) M protein synergizes in a TLR2-dependent manner with HBP to activate monocytes, which then secrete proinflammatory cytokines and upregulate the procoagulatory protein tissue factor. (**f**) M protein is also responsible for neutralizing the antimicrobial effects of cathelicidins in neutrophil extracellular traps (NET)

1995; Nilson et al., 1995; Cedervall et al., 1997; Gubbe et al., 1997; McNamara et al., 2008).

12.6 B-Repeats and Proinflammatory Effects

The B-repeats of several M protein types are crucial to the evasion of phagocytosis through the recruitment of fibrinogen to the GAS surface (Ringdahl et al., 2000; Carlsson et al., 2005). Bound fibrinogen substantially interferes with the formation and deposition of the classical complement pathway C3 convertase, C4bC2a, (even

in the absence of immune conditions) on the GAS surface (Fig. 12.3b) (Carlsson et al., 2005). Fibrinogen is also responsible for recruiting plasmin to the GAS surface, which is essential for the transition of an infection from localized to invasive (Sun et al., 2004; Cole et al., 2006). The B-repeats are also immunodominant, although the antibodies elicited by this region are nonopsonic and do not provide protection (Fischetti and Windels, 1988; Huber et al., 1994; Stalhammar-Carlemalm et al., 2007).

A separate role for the B-repeats of released M1 protein in septic shock has been uncovered in recent years (Herwald et al., 2004). Released M1 binds fibrinogen through the B-repeats (Herwald et al., 2004; McNamara et al., 2008), and the resulting M1-fibrinogen complex interacts with β_2 integrins (i.e. CD11b/CD18) on the surface of neutrophils (Fig. 12.3c). This brings about neutrophil activation, as seen by an increase of several cell surface markers (e.g. CD11b) and the release of soluble granule components, including heparin binding protein (HBP), the antimicrobial peptide LL-37, MMP-9 (gelatinase), and albumin (Herwald et al., 2004; Soehnlein et al., 2008). This activation event requires both M1 protein and fibrinogen (Herwald et al., 2004; McNamara et al., 2008; Soehnlein et al., 2008), and likely occurs through crosslinking of β_2 integrins on the neutrophil surface as deduced from the observation that antibody crosslinking of β_2 integrins has the same effects as M1-fibrinogen complexes (Gautam et al., 2000; Herwald et al., 2004; Soehnlein et al., 2008). Neutrophil activation, as monitored by the release of HBP, is substantially enhanced by binding of IgG antibodies directed to the S-region of M1 (between the B-repeats and C-repeats) (Figs. 12.1 and 12.3) (Kahn et al., 2008). These antibodies act through the FcγRII receptor (Kahn et al., 2008). Neutrophil activation is also promoted by the binding of M1-fibrinogen complexes to the low-affinity integrin GPIIb/IIIa on the surface of platelets, in concert with the binding of IgGs directed against M1 to FcγRII (Fig. 12.3d) (Shannon et al., 2007). These interactions lead to platelet activation, aggregation, and generation of thrombi, and activated platelets in turn stimulate neutrophils and monocytes.

The most damaging substance released by activated neutrophils is HBP (also called azurocidin and CAP37). HBP is an inactive serine protease and a member of the serprocidin family of neutrophil cationic proteins (Gautam et al., 2001; Herwald et al., 2004), and is stored in azurophilic granules and secretory vesicles (Tapper et al., 2002). Once released, HBP acts on endothelial cells to cause Ca^{2+}-dependent cytoskeletal rearrangements and intercellular gap formation (Gautam et al., 2001). These events lead in vivo to vasodilation, haemorrhage, and acute pulmonary damage resembling the symptoms of STSS (Herwald et al., 2004; Soehnlein et al., 2008). In agreement with these findings, high plasma levels of HBP in patients have been found to be a strong indicator for the onset of sepsis and circulatory failure (Linder et al., 2009).

HBP also synergizes with M1 protein in bringing about the secretion of the proinflammatory cytokines IL-6, IL-1β, and TNF-α from monocytes (Fig. 12.3e) (Pahlman et al., 2006). HBP acts on β_2 integrins on the surface of monocytes, and M1 acts in a TLR2-dependent manner on monocytes (Pahlman et al., 2006). In fact, M1 binds preferentially to monocytes as compared to neutrophils and lymphocytes,

and M1 and TLR2 appear to colocalize on the surface of monocytes (Pahlman et al., 2006). Whether this interaction is direct and which portions of M1 protein are involved are not known. M1, as well as some other M protein types, upregulate tissue factor on monocytes to produce a procoagulatory state (Pahlman et al., 2007). The time to clot formation is decreased by these M protein types, with C-terminal portions of M1 (S-region through the C-repeats) being required for this effect (Pahlman et al., 2007).

Lastly and somewhat surprisingly, M1 also acts as a superantigen. M1 stimulates T cell proliferation and causes the release of Th1 type cytokines (TNF-β and IFN-γ). This effect is dependent on class II MHC and shows a preference for certain T cell receptor (TCR) Vβ chains, which is the case for other superantigens (Pahlman et al., 2008). Presumably, M1 crosslinks class II MHC molecules on antigen presenting cells with particular TCRs, but this has not been shown directly and, again, which portions of M1 are involved is not yet known.

The M1 protein type has been intensively studied for proinflammatory and procoagulatory properties due to the prevalence of the M1 type among strains causing invasive disease. Other M protein types have been documented to evoke responses from host cells similar to that of M1. For example, M3, M5, and M49 have also been found to stimulate the release of IL-6 from monocytes (Pahlman et al., 2006). More comparative work will be required to determine whether M1 is especially virulent compared to other M types.

12.7 Hypervariable Region

The very N-terminus of M protein, the HVR (Fig. 12.1), has intriguing functional properties. Within a particular M type, the HVR sequence is quite stable (Facklam et al., 2002). While the HVR is non-immunodominant (Stalhammar-Carlemalm et al., 2007), it specifically elicits protective (i.e. opsonic) antibody responses (Dale et al., 1983; Fischetti and Windels, 1988; Jones and Fischetti, 1988; Persson et al., 2006; Sandin et al., 2006). Due to this protective feature, a multivalent vaccine composed of portions of the HVRs of 26 prevalent M types has been tested and shown to be promising (Dale et al., 2005). The sequence stability of the HVR in the face of immune pressure suggests a functional importance to this region.

Consistent with the HVR having functional significance, deletion of the M5 HVR resulted in a ~50-fold lower competitive index in the liver and spleen of mice (Waldemarsson et al., 2009). The functional basis for the importance of the M5 HVR is unknown. While the M5 HVR binds factor H-like protein 1 (FHL-1) (Johnsson et al., 1998), an alternative splice variant of the complement regulatory protein factor H, the interaction with FHL-1 lacks functional significance (Kotarsky et al., 2001). In contrast to the deletion of the entire HVR, a smaller deletion of residues 3–22 of the M5 HVR had no effect on colonization of the upper respiratory tract of mice (Penfound et al., 2010). This smaller deletion did, however, lead to decreased binding of lipotechoic acid (LTA) to M5 and decreased GAS adherence to epithelial cells

(Penfound et al., 2010). LTA displayed on M protein acts as an adhesin (Beachey and Ofek, 1976).

No studies on the virulence of M1 protein lacking its HVR have been carried out, but a functionally important interaction of the M1 HVR with a host component has been identified (Lauth et al., 2009). The M1 HVR provides protection against cathelicidin antimicrobial peptides (i.e. LL-37 and mCRAMP), which kill GAS upon entrapment in neutrophil or mast cell extracellular traps (Fig. 12.3f) (Lauth et al., 2009). The effect is direct as incubation of an M1 fragment containing the HVR results in a dose-dependent decrease of LL-37 in solution. At this point, the structure of the M1 HVR provides little direction in understanding how cathelicidins are recognized. The first ~15 residues of the M1 HVR are disordered (Fig. 12.2b). The following ~4 residues are in random coil conformation, after which the HVR forms an α-helix. This α-helix makes one turn and then engages in a parallel, dimeric coiled coil, at the end of which is the Ala-stagger (Fig. 12.2b). M1 also inhibits a second antimicrobial peptide, this one derived from β_2 glycoprotein I, but the region of M1 responsible for this activity has not yet been mapped (Nilsson et al., 2008).

Perhaps the most remarkable feature uncovered for the HVR is the astonishing number of sequence unrelated HVRs that bind the regulatory complement component C4b-binding protein (C4BP) (Morfeldt et al., 2001; Persson et al., 2006). The soluble glycoprotein C4BP increases the rate of dissociation of the C3 convertase and increases the activity of the regulatory complement component factor I (Gigli et al., 1979), which cleaves C3b. The C4BP-binding HVRs, although lacking sequence identity, all bind to the same site on the α chain of C4BP (Accardo et al., 1996; Jenkins et al., 2006). Recruitment of C4BP to the GAS surface by the HVR of M protein is crucial for inhibiting phagocytosis through the interference with deposition of the classical pathway C3 convertase as well as degradation of the C3 convertase, presumably mediated by factor I (Fig. 12.3b) (Carlsson et al., 2003). Furthermore, C4BP competes with opsonising antibodies targeted to the HVR (Berggard et al., 2001; Carlsson et al., 2003).

Sequence analysis has revealed that C4BP-binding HVRs have only four residues that are well conserved, two Glu residues at predicted outward-facing *g* positions of the heptad and two Leu residues at predicted inward-facing *d* positions (Fig. 12.2a) (Persson et al., 2006). Individual substitutions of these glutamates in the M22 HVR with Ala had no effect on binding to C4BP, while individual substitutions of the leucines in the M22 HVR with Ala did (Persson et al., 2006). These Glu and Leu residues occur in the ordered coiled-coil portion of the HVR as determined from nuclear magnetic resonance (NMR) spectroscopy evidence; by comparison, the N-terminus is unstructured as it is in the M1 HVR (Andre et al., 2006). Not enough information is available from the NMR data to indicate whether the coiled coil in the C4BP-binding HVRs of M4 and M22 are structurally irregular (Andre et al., 2006). Of note, the predicted coiled-coil register of the M22 HVR and other C4BP-binding HVRs contain several nonideal residues at *a* and *d* positions. While C4BP binding is maintained even when the putatively surface-exposed *g* position glutamates are substituted by Ala, recognition by antibodies is compromised (Persson et al., 2006). This suggests that small variations in the HVR that enable escape from immune

pressure are possible without destroying essential functions. The structural basis for the relatively sequence-independent interaction between the HVR and C4BP is currently unknown.

12.8 Concluding Remarks

The M protein is remarkable for the number of different functions in GAS virulence that are specified by its relatively simple, albeit nonideal, α-helical coiled coil sequence. These functions depend on interactions between M protein and a diverse set of host proteins, prominent among these being regulators of the complement system and the blood clotting protein fibrinogen. Deeper knowledge of how the sequence nonideality of M protein relates to its multifarious functions is beginning to be gained. Recent work has shown that sequence nonidealities in M1 result in structural irregularities, and that these structural irregularities are essential for binding fibrinogen and eliciting proinflammatory effects. They also appear to be involved in antibody crossreactivity. A number of important questions remain to be addressed. For example, a detailed accounting of how structural irregularities beget specific recognition and function remains to be furnished. It also remains to be determined whether structural irregularities in M protein are necessary for recognition of other host components, such as C4BP. It will also be important to understand whether the M1 protein type has special proinflammatory and procoagulatory properties that distinguish it from other M protein types. The convergence of structural, biochemical, genetic, and in vivo studies promises to shed light on these questions in the coming years.

References

Accardo P, Sánchez-Corral P, Criado O, García E, Rodriguez de Córdoba S (1996) Binding of human complement component C4b-binding protein (C4BP) to *Streptococcus pyogenes* involves the C4b-binding site. J Immunol 157:4935–4939

Åkerström B, Lindahl G, Björck L, Lindqvist A (1992) Protein Arp and protein H from group A streptococci. Ig binding and dimerization are regulated by temperature. J Immunol 148: 3238–3243

André I, Persson J, Blom AM, Nilsson H, Drakenberg T, Lindahl G, Linse S (2006) Streptococcal M protein: structural studies of the hypervariable region, free and bound to human C4BP. Biochemistry 45:4559–4568

Aziz RK, Kotb M (2008) Rise and persistence of global M1T1 clone of *Streptococcus pyogenes*. Emerg Infect Dis 14:1511–1517

Beachey EH, Ofek I (1976) Epithelial cell binding of group A streptococci by lipoteichoic acid on fimbriae denuded of M protein. J Exp Med 143:759–771

Berge A, Björck L (1995) Streptococcal cysteine proteinase releases biologically active fragments of streptococcal surface proteins. J Biol Chem 270:9862–9867

Berggård K, Johnsson E, Morfeldt E, Persson J, Stalhammar-Carlemalm M, Lindahl G (2001) Binding of human C4BP to the hypervariable region of M protein: a molecular mechanism of phagocytosis resistance in *Streptococcus pyogenes*. Mol Microbiol 42:539–551

Blankenfeldt W, Thomä NH, Wray JS, Gautel M, Schlichting I (2006) Crystal structures of human cardiac β-myosin II S2-Δ provide insight into the functional role of the S2 subfragment. Proc Natl Acad Sci USA 103:17713–17717

Brown JH, Kim KH, Jun G, Greenfield NJ, Dominguez R, Volkmann N, Hitchcock-DeGregori SE, Cohen C (2001) Deciphering the design of the tropomyosin molecule. Proc Natl Acad Sci USA 98:8496–8501

Brown JH, Zhou Z, Reshetnikova L, Robinson H, Yammani RD, Tobacman LS, Cohen C (2005) Structure of the mid-region of tropomyosin: bending and binding sites for actin. Proc Natl Acad Sci USA 102:18878–18883

Caparon MG, Stephens DS, Olsén A, Scott JR (1991) Role of M protein in adherence of group A streptococci. Infect Immun 59:1811–1817

Carlsson F, Berggård K, Stålhammar-Carlemalm M, Lindahl G (2003) Evasion of phagocytosis through cooperation between two ligand-binding regions in *Streptococcus pyogenes* M protein. J Exp Med 198:1057–1068

Carlsson F, Sandin C, Lindahl G (2005) Human fibrinogen bound to *Streptococcus pyogenes* M protein inhibits complement deposition *via* the classical pathway. Mol Microbiol 56: 28–39

Carlsson F, Stålhammar-Carlemalm M, Flärdh K, Sandin C, Carlemalm E, Lindahl G (2006) Signal sequence directs localized secretion of bacterial surface proteins. Nature 442:943–946

Cedervall T, Åkesson P, Stenberg L, Herrmann A, Åkerström B (1995) Allosteric and temperature effects on the plasma protein binding by streptococcal M protein family members. Scand J Immunol 42:433–441

Cedervall T, Johansson MU, Åkerström B (1997) Coiled-coil structure of group A streptococcal M proteins. Different temperature stability of class A and C proteins by hydrophobic-nonhydrophobic amino acid substitutions at heptad positions a and d. Biochemistry 36: 4987–4994

Cho KH, Caparon MG (2005) Patterns of virulence gene expression differ between biofilm and tissue communities of *Streptococcus pyogenes*. Mol Microbiol 57:1545–1556

Cole JN, McArthur JD, McKay FC, Sanderson-Smith ML, Cork AJ, Ranson M, Rohde M, Itzek A, Sun H, Ginsburg D, Kotb M, Nizet V, Chhatwal GS, Walker MJ (2006) Trigger for group A streptococcal M1T1 invasive disease. FASEB J 20:1745–1747

Cue D, Southern SO, Southern PJ, Prabhakar J, Lorelli W, Smallheer JM, Mousa SA, Cleary PP (2000) A nonpeptide integrin antagonist can inhibit epithelial cell ingestion of *Streptococcus pyogenes* by blocking formation of integrin α5β1-fibronectin-M1 protein complexes. Proc Natl Acad Sci USA 97:2858–2863

Cunningham MW (2000) Pathogenesis of group A streptococcal infections. Clin Microbiol Rev 13:470–511

Cunningham MW, Antone SM, Gulizia JM, McManus BM, Fischetti VA, Gauntt CJ (1992) Cytotoxic and viral neutralizing antibodies crossreact with streptococcal M protein, enteroviruses, and human cardiac myosin. Proc Natl Acad Sci USA 89:1320–1324

Dale JB, Penfound T, Chiang EY, Long V, Shulman ST, Beall B (2005) Multivalent group A streptococcal vaccine elicits bactericidal antibodies against variant M subtypes. Clin Diagn Lab Immunol 12:833–836

Dale JB, Seyer JM, Beachey EH (1983) Type-specific immunogenicity of a chemically synthesized peptide fragment of type 5 streptococcal M protein. J Exp Med 158:1727–1732

Facklam RF, Martin DR, Lovgren M, Johnson DR, Efstratiou A, Thompson TA, Gowan S, Kriz P, Tyrrell GJ, Kaplan E, Beall B (2002) Extension of the Lancefield classification for group A streptococci by addition of 22 new M protein gene sequence types from clinical isolates: emm103 to emm124. Clin Infect Dis 34:28–38

Fischetti VA (1989) Streptococcal M protein: molecular design and biological behavior. Clin Microbiol Rev 2:285–314

Fischetti VA, Windels M (1988) Mapping the immunodeterminants of the complete streptococcal M6 protein molecule. Identification of an immunodominant region. J Immunol 141:3592–3599

Frick IM, Mörgelin M, Björck L (2000) Virulent aggregates of *Streptococcus pyogenes* are generated by homophilic protein-protein interactions. Mol Microbiol 37:1232–1247

Gautam N, Herwald H, Hedqvist P, Lindbom L (2000) Signaling *via* β_2 integrins triggers neutrophil-dependent alteration in endothelial barrier function. J Exp Med 191:1829–1839

Gautam N, Olofsson AM, Herwald H, Iversen LF, Lundgren-Akerlund E, Hedqvist P, Arfors KE, Flodgaard H, Lindbom L (2001) Heparin-binding protein (HBP/CAP37): a missing link in neutrophil-evoked alteration of vascular permeability. Nat Med 7:1123–1127

Gigli I, Fujita T, Nussenzweig V (1979) Modulation of the classical pathway C3 convertase by plasma proteins C4 binding protein and C3b inactivator. Proc Natl Acad Sci USA 76: 6596–6600

Gubbe K, Misselwitz R, Welfle K, Reichardt W, Schmidt KH, Welfle H (1997) C repeats of the streptococcal M1 protein achieve the human serum albumin binding ability by flanking regions which stabilize the coiled-coil conformation. Biochemistry 36:8107–8113

Herwald H, Cramer H, Mörgelin M, Russell W, Sollenberg U, Norrby-Teglund A, Flodgaard H, Lindbom L, Björck L (2004) M protein, a classical bacterial virulence determinant, forms complexes with fibrinogen that induce vascular leakage. Cell 116:367–379

Huber SA, Moraska A, Cunningham M (1994) Alterations in major histocompatibility complex association of myocarditis induced by coxsackievirus B3 mutants selected with monoclonal antibodies to group A streptococci. Proc Natl Acad Sci USA 91:5543–5547

Jenkins HT, Mark L, Ball G, Persson J, Lindahl G, Uhrin D, Blom AM, Barlow PN (2006) Human C4b-binding protein, structural basis for interaction with streptococcal M protein, a major bacterial virulence factor. J Biol Chem 281:3690–3697

Johnsson E, Berggård K, Kotarsky H, Hellwage J, Zipfel PF, Sjöbring U, Lindahl G (1998) Role of the hypervariable region in streptococcal M proteins: binding of a human complement inhibitor. J Immunol 161:4894–4901

Jones KF, Fischetti VA (1988) The importance of the location of antibody binding on the M6 protein for opsonization and phagocytosis of group A M6 streptococci. J Exp Med 167: 1114–1123

Kahn F, Mörgelin M, Shannon O, Norrby-Teglund A, Herwald H, Olin AI, Björck L (2008) Antibodies against a surface protein of *Streptococcus pyogenes* promote a pathological inflammatory response. PLoS Pathog 4:e1000149

Kansal RG, McGeer A, Low DE, Norrby-Teglund A, Kotb M (2000) Inverse relation between disease severity and expression of the streptococcal cysteine protease, SpeB, among clonal M1T1 isolates recovered from invasive group A streptococcal infection cases. Infect Immun 68:6362–6369

Kotarsky H, Gustafsson M, Svensson HG, Zipfel PF, Truedsson L, Sjöbring U (2001) Group A streptococcal phagocytosis resistance is independent of complement factor H and factor H-like protein 1 binding. Mol Microbiol 41:817–826

Lancefield RC (1928) The antigenic complex of streptococcus haemolyticus: I. Demonstration of a Type-Specific Substance in Extracts of Streptococcus Haemolyticus. J Exp Med 47:91–103

Lauth X, von Köckritz-Blickwede M, McNamara CW, Myskowski S, Zinkernagel AS, Beall B, Ghosh P, Gallo RL, Nizet V (2009) M1 protein allows group A streptococcal survival in phagocyte extracellular traps through cathelicidin inhibition. J Innate Immun 1:202–214

Li Y, Brown JH, Reshetnikova L, Blazsek A, Farkas L, Nyitray L, Cohen C (2003) Visualization of an unstable coiled coil from the scallop myosin rod. Nature 424:341–345

Linder A, Christensson B, Herwald H, Björck L, Åkesson P (2009) Heparin-binding protein: an early marker of circulatory failure in sepsis. Clin Infect Dis 49:1044–1050

Manjula BN, Fischetti VA (1980) Tropomyosin-like seven residue periodicity in three immunologically distinct streptococal M proteins and its implications for the antiphagocytic property of the molecule. J Exp Med 151:695–708

McNamara C, Zinkernagel AS, Macheboeuf P, Cunningham MW, Nizet V, Ghosh P (2008) Coiled-coil irregularities and instabilities in group A *Streptococcus* M1 are required for virulence. Science 319:1405–1408

Morfeldt E, Berggård K, Persson J, Drakenberg T, Johnsson E, Lindahl E, Linse S, Lindahl G (2001) Isolated hypervariable regions derived from streptococcal M proteins specifically bind human C4b-binding protein: implications for antigenic variation. J Immunol 167:3870–3877

Navarre WW, Schneewind O (1999) Surface proteins of gram-positive bacteria and mechanisms of their targeting to the cell wall envelope. Microbiol Mol Biol Rev 63:174–229

Nilson BH, Frick IM, Åkesson P, Forsén S, Björck L, Åkerström B, Wikström M (1995) Structure and stability of protein H and the M1 protein from *Streptococcus pyogenes*. Implications for other surface proteins of gram-positive bacteria. Biochemistry 34:13688–13698

Nilsson M, Wasylik S, Mörgelin M, Olin AI, Meijers JC, Derksen RH, de Groot PG, Herwald H (2008) The antibacterial activity of peptides derived from human β-2 glycoprotein I is inhibited by protein H and M1 protein from *Streptococcus pyogenes*. Mol Microbiol 67:482–492

Okada N, Liszewski MK, Atkinson JP, Caparon M (1995) Membrane cofactor protein (CD46) is a keratinocyte receptor for the M protein of the group A streptococcus. Proc Natl Acad Sci USA 92:2489–2493

O'Loughlin RE, Roberson A, Cieslak PR, Lynfield R, Gershman K, Craig A, Albanese BA, Farley MM, Barrett NL, Spina NL, Beall B, Harrison LH, Reingold A, Van Beneden C (2007) Active Bacterial Core Surveillance T. The epidemiology of invasive group A streptococcal infection and potential vaccine implications: United States, 2000–2004. Clin Infect Dis 45:853–862

Påhlman LI, Malmström E, Mörgelin M, Herwald H (2007) M protein from *Streptococcus pyogenes* induces tissue factor expression and pro-coagulant activity in human monocytes. Microbiology 153:2458–2464

Påhlman LI, Mörgelin M, Eckert J, Johansson L, Russell W, Riesbeck K, Soehnlein O, Lindbom L, Norrby-Teglund A, Schumann RR, Björck L, Herwald H (2006) Streptococcal M protein: a multipotent and powerful inducer of inflammation. J Immunol 177:1221–1228

Påhlman LI, Olin AI, Darenberg J, Mörgelin M, Kotb M, Herwald H, Norrby-Teglund A (2008) Soluble M1 protein of *Streptococcus pyogenes* triggers potent T cell activation. Cell Microbiol 10:404–414

Penfound TA, Ofek I, Courtney HS, Hasty DL, Dale JB (2010) The NH(2)-Terminal region of *Streptococcus pyogenes* M5 protein confers protection against degradation by proteases and enhances mucosal colonization of mice. J Infect Dis 201:1580–1588

Persson J, Beall B, Linse S, Lindahl G (2006) Extreme sequence divergence but conserved ligand-binding specificity in *Streptococcus pyogenes* M protein. PLoS Pathog 2:e47

Phillips GN Jr, Flicker PF, Cohen C, Manjula BN, Fischetti VA (1981) Streptococcal M protein: α-helical coiled-coil structure and arrangement on the cell surface. Proc Natl Acad Sci USA 78:4689–4693

Ringdahl U, Svensson HG, Kotarsky H, Gustafsson M, Weineisen M, Sjöbring U (2000) A role for the fibrinogen-binding regions of streptococcal M proteins in phagocytosis resistance. Mol Microbiol 37:1318–1326

Sandin C, Carlsson F, Lindahl G (2006) Binding of human plasma proteins to *Streptococcus pyogenes* M protein determines the location of opsonic and non-opsonic epitopes. Mol Microbiol 59:20–30

Shannon O, Hertzén E, Norrby-Teglund A, Mörgelin M, Sjöbring U, Björck L (2007) Severe streptococcal infection is associated with M protein-induced platelet activation and thrombus formation. Mol Microbiol 65:1147–1157

Soehnlein O, Oehmcke S, Ma X, Rothfuchs AG, Frithiof R, van Rooijen N, Mörgelin M, Herwald H, Lindbom L (2008) Neutrophil degranulation mediates severe lung damage triggered by streptococcal M1 protein. Eur Respir J 32:405–412

Stålhammar-Carlemalm M, Waldemarsson J, Johnsson E, Areschoug T, Lindahl G (2007) Nonimmunodominant regions are effective as building blocks in a streptococcal fusion protein vaccine. Cell Host Microbe 2:427–434

Steer AC, Law I, Matatolu L, Beall BW, Carapetis JR (2009) Global emm type distribution of group A streptococci: systematic review and implications for vaccine development. Lancet Infect Dis 9:611–616

Sun H, Ringdahl U, Homeister JW, Fay WP, Engleberg NC, Yang AY, Rozek LS, Wang X, Sjobring U, Ginsburg D (2004) Plasminogen is a critical host pathogenicity factor for group A streptococcal infection. Science 305:1283–1286

Tapper H, Karlsson A, Mörgelin M, Flodgaard H, Herwald H (2002) Secretion of heparin-binding protein from human neutrophils is determined by its localization in azurophilic granules and secretory vesicles. Blood 99:1785–1793

Tripet B, Wagschal K, Lavigne P, Mant CT, Hodges RS (2000) Effects of side-chain characteristics on stability and oligomerization state of a de novo-designed model coiled-coil: 20 amino acid substitutions in position "d". J Mol Biol 300:377–402

Wagschal K, Tripet B, Lavigne P, Mant C, Hodges RS (1999) The role of position a in determining the stability and oligomerization state of α-helical coiled coils: 20 amino acid stability coefficients in the hydrophobic core of proteins. Protein Sci 8:2312–2329

Waldemarsson J, Stålhammar-Carlemalm M, Sandin C, Castellino FJ, Lindahl G (2009) Functional dissection of *Streptococcus pyogenes* M5 protein: the hypervariable region is essential for virulence. PLoS One 4:e7279

Chapter 13
Bacterial Extracellular Polysaccharides

Kateryna Bazaka, Russell J. Crawford, Evgeny L. Nazarenko, and Elena P. Ivanova

Abstract Extracellular polysaccharides are as structurally and functionally diverse as the bacteria that synthesise them. They can be present in many forms, including cell-bound capsular polysaccharides, unbound "slime", and as O-antigen component of lipopolysaccharide, with an equally wide range of biological functions. These include resistance to desiccation, protection against nonspecific and specific host immunity, and adherence. Unsurprisingly then, much effort has been made to catalogue the enormous structural complexity of the extracellular polysaccharides made possible by the wide assortment of available monosaccharide combinations, non-carbohydrate residues, and linkage types, and to elucidate their biosynthesis and export. In addition, the work is driven by the commercial potential of these microbial substances in food, pharmaceutics and biomedical industries. Most recently, bacteria-mediated environmental restoration and bioleaching have been attracting much attention owing to their potential to remediate environmental effluents produced by the mining and metallurgy industries. In spite of technological advances in chemistry, molecular biology and imaging techniques that allowed for considerable expansion of knowledge pertaining to the bacterial surface polysaccharides, current understanding of the mechanisms of synthesis and regulation of extracellular polysaccharides is yet to fully explain their structural intricacy and functional variability.

13.1 Introduction

Bacteria secrete an intricate assortment of extracellular polymeric substances, including polysaccharides, proteins, and nucleic acids, that vary in molecular mass and structural properties (Jayaratne et al., 1993). Extracellular polysaccharides

E.P. Ivanova (✉)
Faculty of Life and Social Sciences, Swinburne University of Technology, Hawthorn, VIC 3122, Australia
e-mail: EIvanova@swin.edu.au

D. Linke, A. Goldman (eds.), *Bacterial Adhesion*, Advances in Experimental Medicine and Biology 715, DOI 10.1007/978-94-007-0940-9_13,

(EPSs) are produced by a broad range of bacterial species. They can be present in many forms, including that of capsular polysaccharides, which are also referred to as "cell-bound extracellular polymeric substances". These are located on the outermost surface of a wide range of bacteria. The EPS can also be found in its unbound form, or "free EPS" (Dong et al., 2006; Roberts, 1996). In contrast to free EPS (otherwise known as slime), which maintains only limited association with the surface of the bacterial cells, capsular polysaccharides remain connected to cell surfaces by means of a covalent attachment to phospholipid or lipid A molecules present at the bacterial surface (Deng et al., 2000; Sørensen et al., 1990; Whitfield and Valvano, 1993). However, using the extent of attachment as a means to differentiate between capsular and free EPS can be complicated, since capsular polysaccharides may themselves be released into the growth medium (i.e. become "free") as a consequence of the low stability of the phosphodiester linkage between the polysaccharide and the phospholipid membrane anchor. Moreover, certain free EPS molecules can also remain in close proximity to the cell surfaces in the absence of a detectable membrane anchoring mechanism (Roberts, 1996; Troy et al., 1971). These tightly attached capsular polysaccharides form a distinct structural layer (the capsule) which encloses the cell and serves as a protective layer. This layer acts as a shield, protecting the cell from major bacterial pathogens (Dong et al., 2006).

The commonly described biological functions of bacterial EPS include resistance to desiccation (Roberson and Firestone, 1992), protection against nonspecific and specific host immunity, and adherence. Capsular polysaccharides are major determinants of virulence for many pathogenic bacteria as they may act to inhibit the complement-mediated bactericidal activity of human serum. They may also impede antibody opsonization and phagocytosis, promote colonisation of tissues and surfaces, and induce inflammation and aberrant complement activation that can be damaging to host tissues. In addition, the presence of the capsule may significantly increase the survival of a pathogen in the environment by acting as a permeability barrier that facilitates selective transportation of nutrients, whilst at the same time providing a protective barrier that excludes harmful substances such as antimicrobial agents. Most significantly, EPS play a major role in mediating the bacterial colonization of surfaces, biotic and abiotic, by enabling cell adhesion and co-aggregation via dipole interactions, covalent or ionic bonding, steric interactions, and hydrophobic association (Beveridge and Fyfe, 1985; Beveridge and Graham, 1991; Bruno and Yves, 2002; Decho, 1990; Flemming, 1995). Components of free EPS can be released onto surfaces that might otherwise be considered unfriendly for bacterial settlement, such as mineral surfaces. These pre-condition the target surface by adsorbing to it hence making it more attractive for bacterial attachment. In Gram-negative bacteria, lipopolysaccharides represent a significant component of the outer leaflet of the outer membrane. As a result, these lipopolysaccharides are also likely to have a profound influence over the adhesive behaviour of the microorganism (Fletcher, 1996). In *Escherichia coli*, the lipopolysaccharide core and O-antigen have been identified as key components that mediate bacterial binding with inorganic surfaces. Hydrogen bonding is an important factor in controlling O-antigen adhesion to inorganic molecules such as Si_3N_4, TiO_2, SiO_2, and Al_2O_3 (Strauss

et al., 2009), and they also facilitate aggregation with other cells (Sheng et al., 2008). The length and heterogeneity of the O-antigen may also contribute to the adhesive interactions between the microorganism and its environment (Abu-Lail and Camesano, 2003; Strauss et al., 2009). Equally, the ability of a bacterium to attach and adhere to biotic targets such as host tissues and other microorganisms is also strongly influenced by the secretion of EPS. The temperature, solution pH, electrolyte and macromolecule concentration, and adsorbent surface chemistry will directly influence the chemical composition and structure of the EPS substances that are responsible for the surface conditioning (Cheng et al., 1994; Ong et al., 1994).

13.2 Bacterial Polysaccharides Chemistry and Structures

Bacterial polysaccharides are composed of repeating monosaccharide units that are joined by glycosidic linkages. They can take form of homo- or heteropolymers, with heteropolysaccharides generally comprised of oligosaccharide repeating units. Bacterial cell surface polysaccharides, such as lipopolysaccharides and capsular polysaccharides, are characterised by enormous structural complexity. The efforts to understand their biosynthesis and export are driven by their importance in host–bacteria interface biology, their strong association with bacterial pathogenicity, and their important role in microorganism adhesion and biofilm formation (Woodward et al., 2010). Such factors as the solution chemistry, abundance of nutrients, and the cell growth phase exert a significant effect on the nature and the distribution of the bacterial polysaccharides (Omoike and Chorover, 2004).

Bacterial capsular polysaccharides are generally linear and comprised of regularly repeating subunits of one to six monosaccharides. Their molecular weight ranges between 100 and 1000 kDa. Lipopolysaccharides are comprised of the lipid A which is embedded into the bacterial membrane, a core oligosaccharide, and a polysaccharide, otherwise known as O-antigen, with repeating units of two to greater than 100 (Strauss et al., 2009). The chemical structure of lipid A is highly conserved, with the classical backbone of lipid A comprising of a β-1',6-linked disaccharide of 2-amino-2-deoxy-D-glucose (D-glucosamine, D-GlcN) to which fatty acids, typically 3-hydroxyalkanoic acids, are bound *via* ester or amide linkages. More variable compared to the lipid moiety, the inner region of the core oligosaccharide is typically constructed from 3-deoxy-D-*manno*-oct-2-ulosonic acid (Kdo) and L-*glycero*-D-*manno*-heptose (LD-Hep). Kdo and phosphate, and less frequently hexuronic and other sugar acid residues, contribute to the anionic nature of both the inner core region and of lipid A. The phosphate groups frequently act as a bridge to an amino alcohol (ethanolamine, Et_3N), to 4-amino-4-deoxy-L-arabinose (L-Ara4N), or to other amino sugar residues.

The O-antigenic side chains consist of polymerized oligosaccharide units, and are highly variable in terms of their chemical structure and composition. In addition to the vast potential for complexity and diversity available with the common hexoses alone, the scope of variation within extracellular polysaccharides is often further enhanced by the presence of less common enantiomers, other stereoisomers,

monosaccharides of different chain length (C_5–C_{10}), ketoses, aldoses and branched monosaccharides (Caroff and Karibian, 2003). In addition, the diversity of these polysaccharides is further enhanced by other structural modifications (e.g. positional and cumulative permutations of deoxy, amino and carboxyl functions; esterification, etherification and amidation) and the presence of non-carbohydrate residues (e.g. polyols, carboxylic and amino acids). Furthermore, a wide variety of configurations may be adopted between any two structural units due to the high number of hydroxyl groups in each monosaccharide, each of which may form a glycoside bond. The configuration of O-antigen is flexible and depends on the immediate environment of the bacterium. The preferred conformation of lipopolysaccharides seems to have the O-antigen positioned flat on top of the saturated fats and phospholipids of the lipid A, and possibly on the non-polar sites of the cell surface (Fletcher, 1996).

Since the presence of certain terminal sugars within the structure of the O-specific side chain confers immunological specificity of the antigen, the degree of O-chain polymerisation can be used to define biologically distinct serotypes within a species. Depending on the degree of the O-antigen attenuation, a species with a complete O-antigen is classified as smooth (S-type), whereas loss of the O-specific region by mutation renders the strain rough (R-type), or deep-rough (core-defective R-type) if the core oligosaccharide is incomplete. In addition to having a direct effect on the virulence of the strain and its susceptibility to various chemicals, such mutations also significantly influence the surface properties of the microorganism, and hence the nature of the bacterium-host and bacterium-abiotic target interactions.

13.3 Biological Specificity of Extracellular Polysaccharides

Extracellular polysaccharides are highly hydrated, generally containing more than 95% water (Costerton et al., 1981). The biosynthesis of extracellular polysaccharides is hierarchical, with the biological repeating unit polymerised from an already-assembled oligosaccharide. In most structural studies, only the “chemical” repeating unit has been determined, whereas the “biological” repeating unit may be any cyclic permutation of that structure (Jansson, 1999; Kenne and Lindberg, 1983). Biological specificity is achieved through chemical diversity, through variations in composition and structure. Hence, it is not surprising that bacterial populations within the same species can express distinctly dissimilar capsular polysaccharides. For instance, over 80 distinct capsular serotypes have been indentified for *E. coli* (Nesper et al., 2003), 91 capsular serotypes indentified for *Streptococcus pneumonia* (Weinberger et al., 2009), and 78 for *Klebsiella pneumonia* (Pan et al., 2008). On the other hand, chemically identical capsular polysaccharides have been identified in a taxonomically diverse range of bacterial species, including the group B capsule of *Neisseria meningitidis* homopolymer of α2,8-linked N-acetylneuraminic acid (NeuNAc), which is identical to the K1 capsule of *E. coli* (Grados and Ewing, 1970), while *Pasteurella multocida* type D repeating disaccharides of glucuronic acid linked to N-acetylglucosamine are identical to the *E. coli* K5 antigen (DeAngelis and White, 2002).

13.4 Factors Influencing Bacterial Interactions with Surfaces

Extracellular polysaccharides play a crucial role in the bacterial colonization of surfaces by facilitating cell adhesion to biotic (i.e. epithelial and endothelial cells) and abiotic surfaces (i.e. mineral surfaces or medical implants), and to each other (Beveridge and Graham, 1991; Bruno and Yves, 2002; Decho, 1990; Flemming, 1995). Adhesion of the cells to solid surfaces involves a combination of electrostatic interactions, hydrogen bonds, and London dispersion forces. This may result in the formation of biofilms and EPS-mediated interspecies co-aggregation within biofilms that can boost their individual potential for colonisation of various ecological niches (Costerton et al., 1987; Mayer et al., 1999). For bacterial cells, the biofilm can also act as a defence mechanism against predation by phagocytic protozoa, and can serve as a permeability barrier against antimicrobial agents (Costerton et al., 1999). It also confers certain nutritional advantages over the planktonic state, which can be essential for the survival of bacterial populations, by acting as a sorptive sponge that binds and concentrates organic molecules and ions close to the cells (Decho, 2000). A biofilm can comprise bacteria, algae, fungi and protozoa embedded in a dynamic aggregation of polymeric compounds, mostly polysaccharides, with the addition of proteins, nucleic acids, lipids, and humic substances. The composition and quantity of the extracellular polymeric materials that form the matrix of the biofilm will change with the type of microorganism, the age of the biofilm and the environmental circumstances – viz the level of oxygen and nitrogen, the extent of desiccation, temperature, pH, and availability of nutrients (Mayer et al., 1999). This highlights how bacteria can respond to their rapidly changing environment by adapting their capsular polysaccharides (Ahimou et al., 2007). It also explains how bacteria can successfully occupy a diverse range of ecological niches (Costerton et al., 1987). The degree of colonization and the stability of the attachment to an abiotic surface vary with the properties of that surface. Adhesion and settlement improve with surface roughness due to the associated increase in surface area available for colonisation. In addition, the "valleys" on the surface supply the microorganisms with a protected habitat, with reduced shear forces (Donlan, 2002). Factors influencing the rate and degree of attachment to the surface include the surface energy of the structure, the hydrophobicity of the bacterial cell, the presence of fimbriae and flagella, the degree of EPS production and the type of polymeric materials being produced by the cell (Donlan, 2002). Bacterial cells attach more favourably and rapidly to hydrophobic, non-polar rather than hydrophilic surfaces (Flemming and Wingender, 2001). Certain polysaccharide–surface combinations result in irreversible attachment. In these instances, the binding forces between the individual cell and the abiotic surface improve the overall stability of the biofilm matrix (Romaní et al., 2008). Charged non-carbohydrate components such as uronic acids or ketal-linked pyruvates present in the EPS further enhance the anionic nature of the surface polysaccharides of Gram-negative bacteria, thus allowing the association of divalent cations (i.e. calcium, magnesium) to increase the binding forces within biofilm (Sutherland, 2001). These non-carbohydrate components also strongly influence the tertiary structure and the physical properties of EPS.

13.5 Role of Extracellular Polymeric Substances in Adhesion and Biofilm Formation

Capsular polysaccharides and free EPS are present in the outermost layer of a cell. As a result, they form an additional barrier between the membrane of the bacterium and its environment. They have a significant role in the bacterial colonization of surfaces by facilitating cell adhesion to host cells, other surfaces, and each other (Camesano and Logan, 2000; Cescutti et al., 2010). Mineral surfaces and other harsh environments can be pre-conditioned for settlement by the bacterial cell using components of free EPS that adsorb to the target surface, making it more suitable for attachment. The nature of the polymeric substances involved in the conditioning step will be dependent on such environmental factors as temperature, solution pH, electrolyte and macromolecule concentration, and adsorbent surface chemistry (Cheng et al., 1994; Ong et al., 1994). In cell suspensions, EPS are distributed between the cell surface (i.e. capsular polysaccharides), the aqueous phase (i.e. free EPS), or a hydrated matrix in biofilm (biofilm EPS) (Omoike and Chorover, 2004). The distribution of the extracellular polymeric substances is also influenced to a great extent by the nature of the cells' ambient conditions, such as solution chemistry, abundance of nutrients, and the growth phase of the cells.

13.5.1 Extracellular Polysaccharides of Clinically Relevant Microorganisms

For pathogenic bacteria, cell adhesion to host tissues is strongly associated with the presence of extracellular polysaccharides, particularly capsular polysaccharides. For many years, capsular serotyping was the primary method used to classify strains of many encapsulated pathogenic bacteria, since their pathogenicity is affed significantly by the type of capsular polysaccharide. During invasive infection, the interactions between the host and the bacteria are directly mediated by extracellular polymeric substances (Tomlinson, 1993). For example, in *S. pneumonia*, the capsular serotype is closely associated with its propensity to cause diseases such as otitis media, pneumonia, bacteraemia, and meningitis, or to be carried by the host asymptomatically (Bogaert et al., 2004; Lipsitch and O'Hagan, 2007). Capsular polysaccharides of *S. pneumonia* are often a primary target of the immune system (Janeway et al., 2001). Consequently, they are used for vaccination (Black et al., 2000) and passive immunization. There is considerable diversity in the types of capsular polysaccharides that exist, thereby assisting the pathogen to elude host immune mechanisms (Shu et al., 2009).

Similarly, capsular polysaccharides present on the surface of *N. meningitidis* have been shown to be a key virulence factor (Caugant et al., 2007), as almost all strains that cause meningococcal disease are encapsulated (Dolan-Livengood et al., 2003; Yazdankhah and Caugant, 2004). Along with averting detection and recognition by immune mechanisms of the host, the capsule may help meningococcal shedding from mucosal surfaces in the host, thus enhancing transmission of the bacteria from

one individual to another (Dolan-Livengood et al., 2003). The presence of the highly hydrated capsule and "slime" provides protection against desiccation, which ensures host to host transmission and survival of encapsulated bacteria under harsh environmental conditions. Mucoid strains of *E. coli, Acinetobacter calcoaceticus*, and *Erwinia stewartii* have higher levels of resistance to desiccation than their corresponding isogenic acapsular mutants, with survival rates decreased from 35 to 5% in mucoid and nonmucoid cells, respectively (Ophir and Gutnick, 1994). Reduced humidity affects the osmolarity in the cells' immediate environment, as shown by induction of β-galactosidase in a genetic fusion experiment (Ophir and Gutnick, 1994). The expression of capsular polysaccharides in alginate EPS of *Pseudomonas aeruginosa* and *Salmonella typhi* also increases with increased osmolarity in the environment (Berry et al., 1989; Pickard et al., 1994).

Streptococcus pyogenes (or GAS) is the cause of many important clinical infections, ranging from mild superficial skin infections to systemic diseases such as acute rheumatic fever, streptococcal pharyngitis, streptococcal toxic shock syndrome, and necrotizing fasciitis (Hoge et al., 1993; Kaul et al., 1997). Apart from being a vital stage in the life cycle of *S. pyogenes*, colonisation of the pharynx by these cells also functions as a reservoir for strains of GAS associated with such infections as necrotizing fasciitis and pharyngitis. Several studies have demonstrated the importance of the hyaluronic acid capsule in the colonisation of the pharynx keratinocytes in vivo (Cywes et al., 2000). CD44, a hyaluronic acid-binding protein that mediates human cell-cell– and cell-extracellular matrix–binding interactions, acts as a receptor for attachment (Ashbaugh et al., 2000). Wessels and Bronze (1994) demonstrated that GAS capsule confers a powerful selective advantage in this environmental niche by injecting mice with an acapsular mutant of the strain that reverted to its encapsulated state at a low frequency ($<10^{-4}$). Mice inoculated with the revertible mutant yielded a high number of encapsulated revertants, with mortality levels similar to those caused by the parental strain. The attached GAS cells induced lamellipodia formation in keratinocytes, similar to some Gram-negative pathogens (i.e. *Shigella flexneri*), with subsequent internalization of the bacterial cell taking place by fusion of the lamellipodia. Significant cytoskeletal rearrangements and cell signalling events triggered by the direct contact between the pathogen and host cell allow bacteria to move in an intracellular fashion, infecting the adjacent host cells and disseminating the infection across the epithelium (Van Nhieu et al., 2003).

The internalization mechanism triggered by *Klebsiella pneumoniae*, however, is notably different. The acapsular mutant of *K. pneumoniae* has been demonstrated to hinder the initial attachment of the pathogen to the host cell by increasing the surface levels of ICAM-1, causing the release of IL-8 (Regueiro et al., 2006). The capsule-defective mutant demonstrated a greater level of adhesion to epithelial cell lines compared to its wild-type strain counterpart, with the aggregative pattern being maintained, indicating that the capsule was not related to the adhesion phenotype (Favre-Bonte et al., 1999). However, the encapsulated isolates of the same *K. pneumoniae* strain attached more efficiently to a mucus-producing cell line than an acapsular mutant, indicating that for certain pathogens, capsular polysaccharides

may help in early colonisation of the mucus layer. Subsequent interaction with the underlying epithelial layer is inhibited by the presence of a capsule, most probably due to the masking of bacterial functions required for specific interaction with the epithelial surface (Moranta et al., 2009; Roberts, 1996). The level of encapsulation in the wild type stain depended on the growth phase, peaking at the lag and early log phases, with the level of adhesin modulated by the presence of the capsule (Favre-Bonte et al., 1999).

13.5.2 Functions of Polysaccharides in Bacterial Attachment

Capsular polysaccharides mitigate the effects of the changing environment upon the bacteria. Any spatial or temporal variations in the location of the bacteria may directly or indirectly select for certain capsular polysaccharides.. Local variation within the same host may favour particular genetic or phenotypic variability, as demonstrated by Briles and co-workers (2005). To facilitate survival and adaptation to its current or potential host environments, bacterial pathogens also take advantage of localized hypermutation, through the polymerase slippage of simple sequence repeats, to generate phenotypic variations that are better equipped for a given habitat and so lead to enhanced population fitness (Moxon et al., 2006).

13.6 Commercial Applications for Extracellular Polysaccharides

As a result of their ability to adjust to varied environmental conditions, marine bacteria from different classes of *Proteobacteria* have recently gained attention due to their potential to decontaminate polluted sites (Head et al., 2006). A number of strategies involving marine bacteria of different species, both planktonic and biofilm-forming, have been developed to remediate environmental effluents produced by the mining and metallurgy industries (Gadd, 2010; Rawlings and Johnson, 2007; Valenzuela et al., 2006) and to lessen the amount of toxic waste entering both aquatic and terrestrial systems (Liu et al., 2008). Biofilm-mediated environmental restoration is thought to be more effective compared with bioremediation with planktonic bacteria since the EPS matrix of the biofilm acts as a mediator between cells and their ambient environment, thus increasing the chances of the bacteria to survive by adapting to rapidly changing external pressures (Costerton et al., 2003; Singh and Cameotra, 2004).

Bioremediation can be targeted at pollutants like heavy metals, BTEX hydrocarbons, petroleum, polycyclic aromatic hydrocarbons, microaromatics, polychlorinated biphenyls, chlorinated phenols and aliphatics (James and Andrew, 2005). In addition to significant efficiency and associated economic advantages (Pal and Paul, 2008), bacteria-mediated remediation offers significant environmental benefits compared to traditional chemical and physical treatment methods. Capsular polysaccharides and free EPS play a vital role in biosorption as the electrostatic interactions between the metal ligands and negatively charged EPS lead to

formation of stable complexes. EPS also plays a significant role in determining whether bacteria have the ability to flocculate (Pal and Paul, 2008). Marine sulphate reducing bacteria have been demonstrated to be highly efficient in biosorption of Mo(VI), Ni(II) and Cr(III) and anaerobic degradation of many organic pollutants (Singh and Cameotra, 2004). A number of *Shewanella* spp. have been shown to be capable of dissimilatory reduction of a wide range of electron acceptors, including metal oxides (e.g. Fe(III) and Mn(IV)) and organic pollutants. The photosynthetic bacterium *Rhodovulum* sp. PS88 has been found suitable for wastewater treatment of soybean curd and sugar cane manufacturing, and for the environmental restoration of polluted sea water discharged from the fishery industries (Watanabe et al., 1998). *Pseudoalteromonas haloplanktis* TAC125 has been shown to possess valuable degradative properties, efficiently converting several aromatic compounds into their corresponding catechols over a wide range of temperatures, making the strain appropriate for the bioremediation of chemically contaminated marine environments and/or cold effluents (Papa et al., 2009). A deep-sea, mesophilic and heterotrophic bacterium *Alteromonas macleodii* subsp. *fijiensis* binds Pb(II), Cd(II) and Zn(II) to form stable non-toxic complexes (Rougeaux et al., 1998). Another economically significant application of the ability of bacteria to bind metal ions is bioleaching, a process of recovering metals from low-grade mineral ores using microorganisms capable of oxidizing solid compounds into soluble and extractable elements (Rohwerder et al., 2003). *Hyphomonas adhaerens* MHS-3 possesses the unusual capacity to sequester gold and to concentrate it to very high levels, with the gold-binding site being specifically located on the polysaccharide capsule of the microorganism (Quintero et al., 2001). Marine acidophilic thiobacillus, *Thiobacillus prosperus*, is a halotolerant metal-mobilizing bacterium known to use sulfidic ores, elemental sulfur or ferrous iron as energy sources and hence can be utilized for metal recovery from sulfide minerals (Robertson and Kuenen, 2006).

13.7 Concluding Remarks

As extracellular polysaccharides are very important in baterial adhesion and other processes, a greater understanding of these complex structures would be very valuable. The carbohydrate structures are commonly elucidated using either sugar and methylation analyses, or NMR spectroscopy. However, differentiating between capsular polysaccharides, unbound EPS, and O-antigens is challenging due to the sensitivity limitations of currently available detection and analytical techniques (Ørskov and Ørskov, 1991; Wagner et al., 2009). Advanced microscopy and spectroscopy techniques, atomic force microscopy (AFM), confocal laser scanning microscopy (CLSM), infrared spectroscopy, nuclear magnetic resonance imaging (NMRI), Raman spectroscopy (RM) and scanning electron microscopy (SEM) can assist in the surface and structure analysis of bacterial extracellular polysaccharide (Denkhaus et al., 2007; Wolf et al., 2002). For instance, a combination of CLSM and RM techniques allows for improved in-situ resolution and chemical classification of polysaccharides and other EPS constituents (Haisch and Niessner, 2007;

Pradhan et al., 2008; Schmid et al., 2008). AFM is capable of imaging the surface morphology with sub-nanometer resolution under hydrated conditions and in aqueous solutions, without the need for staining (unlike CLSM) or coating (unlike SEM) (Mangold et al., 2008; Pradhan et al., 2008). Simultaneous application of AFM and RM techniques facilitates high resolution dynamic visualization of the macromolecules as they assemble as a response to different stress factors or in the course of attachment to surfaces (Pradhan et al., 2008). Optical coherence tomography can further enhance the resolution of the image and assist visualization of EPS structures under a range of environmental conditions (Xi et al., 2006). Sum-frequency-generation spectroscopy is a highly surface sensitive technique particularly applicable to situations where probing structure under a layer of live cells is desired (Howell et al., 2008).

References

Abu-Lail NI, Camesano TA (2003) Role of lipopolysaccharides in the adhesion, retention, and transport of *Escherichia coli* JM109. Env Sci Technol 37:2173–2183

Ahimou F, Semmens MJ, Haugstad G, Novak PJ (2007) Effect of protein, polysaccharide, and oxygen concentration profiles on biofilm cohesiveness. Appl Environ Microbiol 73:2905–2910

Ashbaugh CD, Moser TJ, Shearer MH, White GL, Kennedy RC, Wessels MR (2000) Bacterial determinants of persistent throat colonization and the associated immune response in a primate model of human group a streptococcal pharyngeal infection. Cell Microbiol 2:283–292

Berry A, Devault JD, Chakrabarty AM (1989) High osmolarity is a signal for enhanced ALGD transcription in mucoid and nonmucoid *Pseudomonas aeruginosa* strains. J Bacteriol 171:2312–2317

Beveridge TJ, Fyfe WS (1985) Metal fixation by bacterial cell walls. Can J Earth Sci 22:1893–1898

Beveridge TJ, Graham LL (1991) Surface layers of bacteria. Microbiol Mol Biol Rev 55:684–705

Black S, Shinefield H, Fireman B, Lewis E, Ray P, Hansen JR, Elvin L, Ensor KM, Hackell J, Siber G, Malinoski F, Madore D, Chang I, Kohberger R, Watson W, Austrian R, Edwards K (2000) Efficacy, safety and immunogenicity of heptavalent pneumococcal conjugate vaccine in children. Pediatr Infect Dis J 19:187–195

Bogaert D, de Groot R, Hermans PWM (2004) *Streptococcus pneumoniae* colonisation: the key to pneumococcal disease. Lancet Infect Dis 4:144–154

Briles DE, Novak L, Hotomi M, van Ginkel FW, King J (2005) Nasal colonization with *Streptococcus pneumoniae* includes subpopulations of surface and invasive pneumococci. Infect Immun 73:6945–6951

Bruno C, Yves F (2002) In situ characterization of bacterial extracellular polymeric substances by AFM. Colloids Surf B: Biointerfaces 23:173–182

Camesano TA, Logan BE (2000) Probing bacterial electrosteric interactions using atomic force microscopy. Env Sci Technol 34:3354–3362

Caroff M, Karibian D (2003) Structure of bacterial lipopolysaccharides. Carbohydr Res 338: 2431–2447

Caugant DA, Tzanakaki G, Kriz P (2007) Lessons from meningococcal carriage studies. FEMS Microbiol Rev 31:52–63

Cescutti P, Otto H, Patrick JB, Mark von I (2010) Bacterial capsular polysaccharides and exopolysaccharides. Microbial glycobiology. Academic, San Diego, CA, pp 93–108

Cheng SS, Chittur KK, Sukenik CN, Culp LA, Lawrence K (1994) The Conformation of fibronectin on self-assembled monolayers with different surface composition:an FTIR/ATR study. J Colloid Interf Sci 162:135–143

Costerton JW, Cheng KJ, Geesey GG, Ladd TI, Nickel JC, Dasgupta M, Marrie TJ (1987) Bacterial biofilms in nature and disease. Ann Rev Microbiol 41:435–464
Costerton JW, Irvin RT, Cheng KJ (1981) The bacterial glycocalyx in nature and disease. Ann Rev Microbiol 35:299–324
Costerton JW, Lewandowski Z, Caldwell DE, Korber DR, Lappin-Scott HM (2003) Microbial biofilms. Ann Rev Microbiol 49:711–745
Costerton JW, Stewart PS, Greenberg EP (1999) Bacterial biofilms: a common cause of persistent infections. Science 284:1318–1322
Cywes C, Stamenkovic I, Wessels MR (2000) CD44 as a receptor for colonization of the pharynx by group A *Streptococcus*. J Clin Invest 106:995–1002
DeAngelis PL, White CL (2002) Identification and molecular cloning of a heparosan synthase from *Pasteurella multocida* type D. J Biol Chem 277:7209–7213
Decho AW (1990) Microbial cxopolymcr secretions in ocean environments: their role(s) in food webs and marine processes. Oceanogr Marine Biol Ann Rev 28:73–153
Decho AW (2000) Microbial biofilms in intertidal systems: an overview. Continent Shelf Res 20:1257–1273
Deng L, Kasper DL, Krick TP, Wessels MR (2000) Characterization of the linkage between the type III capsular polysaccharide and the bacterial cell wall of group B *Streptococcus*. J Biol Chem 275:7497–7504
Denkhaus E, Meisen S, Telgheder U, Wingender J (2007) Chemical and physical methods for characterisation of biofilms. Mikrochim Acta 158:1–27
Dolan-Livengood JM, Miller YK, Martin LE, Urwin R, Stephens DS (2003) Genetic basis for nongroupable *Neisseria meningitidis*. J Infect Dis 187:1616–1628
Dong C, Beis K, Nesper J, Brunkan-LaMontagne AL, Clarke BR, Whitfield C, Naismith JH (2006) Wza the translocon for *E. coli* capsular polysaccharides defines a new class of membrane protein. Nature 444:226–229
Donlan RM (2002) Biofilms: microbial life on surfaces. Emerg Infect Dis 8:881–890
Favre-Bonte S, Joly B, Forestier C (1999) Consequences of reduction of *Klebsiella pneumoniae* capsule expression on interactions of this bacterium with epithelial cells. Infect Immun 67: 554–561
Flemming HC (1995) Biofouling und biokorrosion – die folgen unerwünschter biofilme. Chem Ingnieur Technik 67:1425–1430
Flemming HC, Wingender J (2001) Relevance of microbial extracellular polymeric substances (EPSs) – part I: structural and ecological aspects. Water Sci Technol 43:1–8
Fletcher M (1996) Bacterial attachment in aquatic environments: a diversity of surfaces and adhesion strategies. In: Fletcher M (ed) Bacterial adhesion: molecular and ecological diversity. Wiley-Liss, New York, NY, pp 1–24
Gadd GM (2010) Metals, minerals and microbes: geomicrobiology and bioremediation. Microbiology 156:609–643
Grados O, Ewing W (1970) Antigenic relationship between *Escherichia coli* and *Neisseria meningitidis*. J Infect Dis 122:100–103
Haisch C, Niessner R (2007) Visualisation of transient processes in biofilms by optical coherence tomography. Water Res 41:2467–2472
Head IM, Jones DM, Roling WFM (2006) Marine microorganisms make a meal of oil. Nat Rev Micro 4:173–182
Hoge CW, Schwartz B, Talkington DF, Breiman RF, Macneill EM, Englender SJ (1993) The changing epidemiology of invasive group-A Streptococcal infections and the emergence of Streptococcal toxic shock-like syndrome – a retrospective population-based study. JAMA 269:1638–1638
Howell C, Diesner M-O, Grunze M, Koelsch P (2008) Probing the extracellular matrix with sum-frequency-generation spectroscopy. Langmuir 24:13819–13821
James ML, Andrew JM (2005) Bioremediation: prospects for the future application of innovative applied biological research. Ann Appl Biol 146:217–221

Janeway CA, Travers P, Walport MS (eds) (2001) Immunobiology. Garland, New York, NY
Jansson P-E (1999) The chemistry of the polysaccharide chains in bacterial lipopolysaccharides. In: Brade H, Opal SM, Vogel SM, Morrison DC (eds) Endotoxin in health and disease. Marcel Dekker, New York, NY, pp 155–178
Jayaratne P, Keenleyside WJ, MacLachlan PR, Dodgson C, Whitfield C (1993) Characterization of rcsB and rcsC from *Escherichia coli* O9:K30:H12 and examination of the role of the rcs regulatory system in expression of group I capsular polysaccharides. J Bacteriol 175: 5384–5394
Kaul R, McGeer A, Low DE, Green K, Schwartz B, Simor AE (1997) Population-based surveillance for group A streptococcal necrotizing fascitis: clinical features, prognostic indicators, and microbiologic analysis of seventy-seven cases. Am J Med 103:18–24
Kenne L, Lindberg B (1983) Bacterial polysaccharides. Academic, New York, NY
Lipsitch M, O'Hagan JJ (2007) Patterns of antigenic diversity and the mechanisms that maintain them. J Royal Soc Interf 4:787–802
Liu Y-G, Zhou M, Zeng G-M, Wang X, Li X, Fan T, Xu W-H (2008) Bioleaching of heavy metals from mine tailings by indigenous sulfur-oxidizing bacteria: effects of substrate concentration. Bioresour Technol 99:4124–4129
Mangold S, Harneit K, Rohwerder T, Claus G, Sand W (2008) Novel Combination of atomic force microscopy and epifluorescence microscopy for visualization of leaching bacteria on pyrite. Appl Environ Microbiol 74:410–415
Mayer C, Moritz R, Kirschner C, Borchard W, Maibaum R, Wingender J, Flemming H-C (1999) The role of intermolecular interactions: studies on model systems for bacterial biofilms. Int J Biol Macromol 26:3–16
Moranta D, Regueiro V, March C, Llobet E, Margareto J, Larrate E, Garmendia J, Bengoechea JA (2009) *Klebsiella pneumoniae* capsule polysaccharide impedes the expression of β-defensins by airway epithelial cells. Infect Immun 78:1135–1146
Moxon R, Bayliss C, Hood D (2006) Bacterial contingency loci: the role of simple sequence DNA repeats in bacterial adaptation. Ann Rev Genet 40:307–333
Nesper J, Hill CMD, Paiment A, Harauz G, Beis K, Naismith JH, Whitfield C (2003) Translocation of group 1 capsular polysaccharide in *Escherichia coli* serotype K30. J Biol Chem 278: 49763–49772
Omoike A, Chorover J (2004) Spectroscopic study of extracellular polymeric substances from *Bacillus subtilis*: aqueous chemistry and adsorption effects. Biomacromolecules 5:1219–1230
Ong JL, Chittur KK, Lucas LC (1994) Dissolution/reprecipitation and protein adsorption studies of calcium phosphate coatings by FT-IR/ATR techniques. J Biomed Mater Res 28:1337–1346
Ophir T, Gutnick DL (1994) A role for exopolysaccharides in the protection of microorganisms from desiccation. Appl Environ Microbiol 60:740–745
Ørskov F, Ørskov I (1991) Complex formation between *Escherichia coli* lipopolysaccharide O antigen and capsular K antigen as detected by immunoelectrophoresis. APMIS 99:615–619
Pal A, Paul A (2008) Microbial extracellular polymeric substances: central elements in heavy metal bioremediation. Ind J Microbiol 48:49–64
Pan YJ, Fang HC, Yang HC, Lin TL, Hsieh PF, Tsai FC, Keynan Y, Wang JT (2008) Capsular polysaccharide synthesis regions in *Klebsiella pneumoniae* serotype K57 and a new capsular serotype. J Clin Microbiol 46:2231–2240
Papa R, Parrilli E, Sannia G (2009) Engineered marine antarctic bacterium *Pseudoalteromonas haloplanktis* TAC125: a promising micro-organism for the bioremediation of aromatic compounds. J Appl Microbiol 106:49–56
Pickard D, Li JL, Roberts M, Maskell D, Hone D, Levine M, Dougan G, Chatfield S (1994) Characterization of defined OMPR mutants of *Salmonella* Typhi-OMPR is involved in the regulation of VI polysaccharide expression. Infect Immun 62:3984–3993
Pradhan N, Pradhan SK, Nayak BB, Mukherjee PS, Sukla LB, Mishra BK (2008) Micro-Raman analysis and AFM imaging of *Acidithiobacillus ferrooxidans* biofilm grown on uranium ore. Res Microbiol 159:557–561

Quintero EJ, Langille SE, Weiner RM (2001) The polar polysaccharide capsule of *Hyphomonas adhaerens* MHS-3 has a strong affinity for gold. J Ind Microbiol Biotechnol 27:1–4

Rawlings DE, Johnson DB (2007) The microbiology of biomining: development and optimization of mineral-oxidizing microbial consortia. Microbiology 153:315–324

Regueiro V, Campos MA, Pons J, Alberti S, Bengoechea JA (2006) The uptake of a klebsiella pneumoniae capsule polysaccharide mutant triggers an inflammatory response by human airway epithelial cells. Microbiology 152:555–566

Roberson EB, Firestone MK (1992) Relationship between desiccation and exopolysaccharide production in a soil *Pseudomonas sp*. Appl Environ Microbiol 58:1284–1291

Roberts IS (1996) The biochemistry and genetics of capsular polysaccharide production in bacteria. Ann Rev Microbiol 50:285–315

Robertson L, Kuenen J (2006) The genus *Thiobacillus*. In: Dworkin M, Falkow S, Rosenberg E, Schleifer K-H, Stackebrandt E (eds) The Prokaryotes. Springer, New York, pp 812–827

Rohwerder T, Gehrke T, Kinzler K, Sand W (2003) Bioleaching review part A. Appl Microbiol Biotechnol 63:239–248

Romaní A, Fund K, Artigas J, Schwartz T, Sabater S, Obst U (2008) Relevance of polymeric matrix enzymes during biofilm formation. Microb Ecol 56:427–436

Rougeaux H, Talaga P, Carlson RW, Guezennec J (1998) Structural studies of an exopolysaccharide produced by *Alteromonas macleodii subsp. fijiensis* originating from a deep-sea hydrothermal vent. Carbohydr Res 312:53–59

Schmid T, Burkhard J, Yeo B-S, Zhang W, Zenobi R (2008) Towards chemical analysis of nanostructures in biofilms I: imaging of biological nanostructures. Anal Bioanal Chem 391:1899–1905

Sheng H, Lim JY, Watkins MK, Minnich SA, Hovde CJ (2008) Characterization of an *Escherichia coli* O157:H7 O-Antigen deletion mutant and effect of the deletion on bacterial persistence in the mouse intestine and colonization at the bovine terminal rectal mucosa. Appl Environ Microbiol 74:5015–5022

Shu HY, Fung CP, Liu YM, Wu KM, Chen YT, Li LH, Liu TT, Kirby R, Tsai SF (2009) Genetic diversity of capsular polysaccharide biosynthesis in *Klebsiella pneumoniae* clinical isolates. Microbiology 155:4170–4183

Singh P, Cameotra SS (2004) Enhancement of metal bioremediation by use of microbial surfactants. Biochem Biophys Res Comm 319:291–297

Sørensen UBS, Henrichsen J, Chen H-C, Szu SC (1990) Covalent linkage between the capsular polysaccharide and the cell wall peptidoglycan of *Streptococcus pneumoniae* revealed by immunochemical methods. Microb Pathog 8:325–334

Strauss J, Burnham NA, Camesano TA (2009) Atomic force microscopy study of the role of LPS O-antigen on adhesion of *E. coli*. J Mol Recogn 22:347–355

Sutherland IW (2001) Biofilm exopolysaccharides: a strong and sticky framework. Microbiology 147:3–9

Tomlinson S (1993) Complement defense mechanisms. Curr Opin Immunol 5:83–89

Troy FA, Frerman FE, Heath EC (1971) Biosynthesis of capsular polysaccharide in *Aerobacter aerogenes*. J Biol Chem 246:118–133

Valenzuela L, Chi A, Beard S, Orell A, Guiliani N, Shabanowitz J, Hunt DF, Jerez CA (2006) Genomics, metagenomics and proteomics in biomining microorganisms. Biotechnol Adv 24:197–211

Van Nhieu GT, Clair C, Bruzzone R, Mesnil M, Sansonetti P, Combettes L (2003) Connexin-dependent inter-cellular communication increases invasion and dissemination of *Shigella* in epithelial cells. Nat Cell Biol 5:720–726

Wagner M, Ivleva NP, Haisch C, Niessner R, Horn H (2009) Combined use of confocal laser scanning microscopy (CLSM) and Raman microscopy (RM): investigations on EPS – matrix. Water Res 43:63–76

Watanabe M, Shiba H, Sasaki K, Nakashimada Y, Nishio N (1998) Promotion of growth and flocculation of a marine photosynthetic bacterium, *Rhodovulum sp*. by metal cations. Biotechnol Lett 20:1109–1112

Weinberger DM, Trzcinski K, Lu YJ, Bogaert D, Brandes A, Galagan J, Anderson PW, Malley R, Lipsitch M (2009) Pneumococcal capsular polysaccharide structure predicts serotype prevalence. Plos Pathog 5:e1000476

Wessels MR, Bronze MS (1994) Critical role of the group A streptococcal capsule in pharyngeal colonization and infection in mice. Proc Natl Acad Sci USA 91:12238–12242

Whitfield C, Valvano MA (1993) Biosynthesis and expression of cell-surface polysaccharides in Gram-negative bacteria. Adv Microb Physiol 35:135–246

Wolf G, Crespo JG, Reis MAM (2002) Optical and spectroscopic methods for biofilm examination and monitoring. Re Environ Sci Biotechnol 1:227–251

Woodward R, Yi W, Li L, Zhao G, Eguchi H, Sridhar PR, Guo H, Song JK, Motari E, Cai L, Kelleher P, Liu X, Han W, Zhang W, Ding Y, Li M, Wang PG (2010) *In vitro* bacterial polysaccharide biosynthesis: defining the functions of Wzy and Wzz. Nat Chem Biol 6:418–423

Xi C, Marks D, Schlachter S, Luo W, Boppart SA (2006) High-resolution three-dimensional imaging of biofilm development using optical coherence tomography. J Biomed Opt 11:034001–034006

Yazdankhah SP, Caugant DA (2004) *Neisseria meningitidis*: an overview of the carriage state. J Med Microbiol 53:821–832

Chapter 14
Carbohydrate Mediated Bacterial Adhesion

Roland J. Pieters

Abstract In the process of adhesion, bacteria often carry proteins on their surface, adhesins, that bind to specific components of tissue cells or the extracellular matrix. In many cases these components are carbohydrate structures. The carbohydrate binding specificities of many bacteria have been uncovered over the years. The design and synthesis of inhibitors of bacterial adhesion has the potential to create new therapeutics for the prevention and possibly treatment of bacterial infections. Unfortunately, the carbohydrate structures often bind only weakly to the adhesion proteins, although drug design approaches can improve the situation. Furthermore, in some cases linking carbohydrates covalently together, to create so-called multivalent systems, can also significantly enhance the inhibitory potency. Besides adhesion inhibition as a potential therapeutic strategy, the adhesion proteins can also be used for detection. Novel methods to do this are being developed. These include the use of microarrays and glyconanoparticles. New developments in these areas are discussed.

14.1 Introduction

In the process of adhesion, bacteria often carry proteins on their surface, adhesins, that bind to specific components of tissue cells or the extracellular matrix. In many cases they bind to carbohydrate structures on the cell surface that are part of the glycoproteins or glycolipids. The specific recognition is often required for bacterial infection or invasion to take place (Fig. 14.1). Recognition is also the cause of the preference of certain pathogens for selected tissues, a phenomenon called tissue tropism. Similarly, pathogens are often species specific because of this recognition. The specificities of many bacteria have been uncovered over the years and the use

R.J. Pieters (✉)
Department of Medicinal Chemistry and Chemical Biology, Utrecht Institute for Pharmaceutical Sciences, Utrecht University, Utrecht, The Netherlands
e-mail: R.J.Pieters@pharm.uu.nl

D. Linke, A. Goldman (eds.), *Bacterial Adhesion*, Advances in Experimental Medicine and Biology 715, DOI 10.1007/978-94-007-0940-9_14,

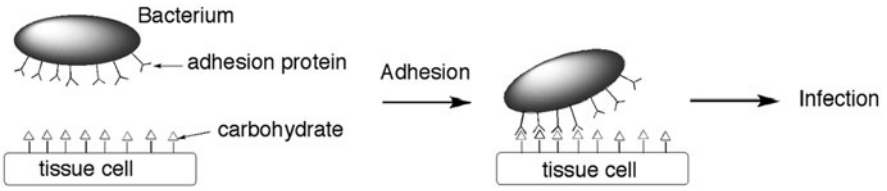

Fig. 14.1 The principle of bacterial adhesion as a prelude to infection

of carbohydrate microarrays has accelerated this process. The design and synthesis of inhibitors of bacterial adhesion has the potential to create new therapeutics for the prevention and possibly treatment of infections. Unfortunately, inhibition by simple carbohydrates requires high sugar concentrations due to the low affinity of the sugars. In some cases linking carbohydrates covalently together, i.e. the generation of multivalent carbohydrates, significantly enhanced the inhibitory potency. More inhibitor design at the mono and multivalent level is needed in order to create therapeutics.

Besides the potency for interference, the adhesion proteins can also be used for detection. Since the adhesion specificity for one or more carbohydrate sequences is specific, the specific binding pattern of a pathogen could serve as a profiling identification tool. In addition, as functional adhesins are often virulence factors, a positive identification may yield important diagnostic information. Novel methods to do this are being developed. These include the use of microarrays and glyconanoparticles. Specific binding patterns of bacteria to carbohydrate microarrays have been observed. The glyconanoparticles have a large surface area and bind tightly to the bacteria, that can subsequently be detected using several methods. In this chapter several important binding specificities of relevant pathogens are shown. Furthermore, I describe selected examples of adhesion inhibitors and the latest developments in adhesion-based detection. Finally, some examples are shown where the bacterial binding does not involve adhesin proteins, but carbohydrates, on the bacteria. Such cases may involve protein carbohydrate interactions, but carbohydrate–carbohydrate interactions have also been observed.

14.2 Adhesins

Several adhesins of *E. coli* are well-studied, especially those associated with urinary tract infections. These are typically displayed on pili or fimbriae, which are hair-like appendages on the surface of the bacterial cells and include the type 1, P, S, and F1C fimbriae. They contain adhesion proteins (Fig. 14.2) that exhibit affinity for α-linked mannosides (**1**), Galα1-4Gal (galabiose) (**2**) (Fig. 14.3), sialylated galactose ligands such as **3** and GalNAcβ1-4Gal (**4**) epitopes, respectively (Korhonen et al., 1984; Moch et al., 1987; Khan et al., 2000ab, Khan and Hacker, 2000). The type I mannose-specific fimbriae are the most studied and contain the FimH adhesin (Fig. 14.2a) (Krogfelt et al., 1990; Choudhury et al., 1999). This adhesin contains

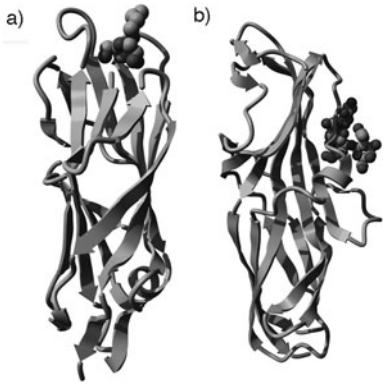

Fig. 14.2 X-ray structures of carbohydrate binding adhesins. (**a**) structure of the *E. coli* adhesin FimH bound to butyl α-D mannoside (pdb 1TR7); (**b**) structure of the PapGII adhesin of *E. coli* in complex with GalNAcβ1-4Galα1-4Galβ1-4Glc (pdb 1J8R)

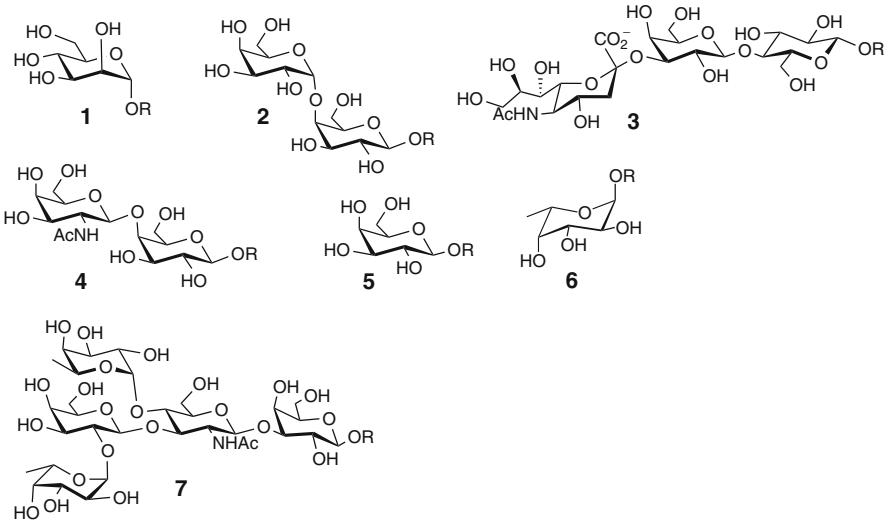

Fig. 14.3 Bacterial adhesins bind to these structures: D-mannose (**1**), galabiose (**2**), 2-3 sialyllactose (**3**), GalNAcβ1-4Gal (**4**), D-galactose (**5**), L-fucose (**6**), Lewis b antigen (**7**)

a single binding site for α-linked mannose derivatives, is present and functional at the fimbrial tip and seemingly also along the fimbrial shaft at roughly 100–150 nm intervals, based on visualization with gold nanoparticles by transmission electron microscopy (Lin et al., 2002). The P fimbriae contain the galabiose specific-PapG adhesin, which is linked to pyelonephritis, a serious urinary tract disease involving kidney infection. The three types of the adhesin, PapGI, PapGII and PapGIII, all bind to glycolipids of the Globo series sharing affinity for the galabiose epitope (**2**), with subtle differences. There is an X-ray structure (Dodson et al., 2001) of the PapGII adhesin bound to a galabiose-containing ligand (Fig. 14.2b) as well as an NMR structure (Sung et al., 2001). Less is known of the adhesins of the other two *E. coli* fimbriae.

Pulmonary pathogens such as those typically infecting cystic fibrosis (CF) patients, *Pseudomonas aeruginosa* (but also *Haemophilus influenzae*, *Staphylococcus aureus*, *Streptococcus pneumoniae* and *Klebsiella pneumoniae*) bind to GalNAcβ1-4Gal (**4**) as their minimal adhesion sequence (Krivan et al., 1988). Interestingly, the GalNAcβ1-4Gal sequence is present in lung tissue as part of the ganglioside asialo-GM-1, i.e. the glycosphingolipid with a sugar part of Galβ1-3GalNAcβ1-4Galβ1-4Glc. Asialo-GM-1 is present in higher abundance on CF-affected lung epithelia, which may enhance the degree of colonization of the lungs by these respiratory pathogens (Imundo et al., 1995). More recently, *Legionella pneumophila*, which causes Legionnaires' disease, and *Yersinia pestis* were shown to be inhibited by this disaccharide (Thomas and Brooks, 2004a,b). The binding of *Pseudomonas aeruginosa* to GalNAcβ1-4Gal was studied in more detail (Sheth et al., 1994) and the structure of the adhesin, part of the type IV pilin, was solved, suggesting that it interacts mostly with the oligosaccharide through the main chain (Hazes et al., 2000). Besides the type IV pili, *P. aeruginosa* uses additional adhesion factors, the two related soluble lectins LecA (or PA-IL) and LecB (or PA-IIL), with specificities for galactosides (**5**) and fucosides (**6**) respectively. These lectins are found on the bacterial outer membrane and play a role in biofilm formation.

The stomach bacterium *Helicobacter pylori,* which causes gastric ulcers and cancer, is well-studied with respect to its adhesion profile. Details of the fine specificity of *H. pylori* for the various gangliosides continue to emerge (Miller-Podraza et al., 2004, 2005; Roche et al., 2004; Walz et al., 2005). Carbohydrates recognized by the pathogen include the Lewis b antigen (**7**), neolacto structures, ganglio structures and some sulphated structures (Miller-Podraza et al., 2009). Three adhesins have been characterized: the Lewis-b binding BabA and two sialic-acid binding proteins SabA (Mahdavi et al., 2002) and HP0721 (Bennett and Roberts, 2005). A recent study showed that if the glycosyl transferase (a fucosyl transferase) responsible for building up the BabA target structures was not present in a mouse model, *H. pylori* adhesion was greatly reduced (Magalhães et al., 2009).

The Gram-positive bacteria *Streptococcus suis* can cause meningitis, septicemia, and pneumonia in pigs and meningitis in humans (Arends and Zanen, 1988; Staats et al., 1997). The pathogen recognizes the galabiose epitope (**2**) (Haataja et al., 1993). Two galabiose-binding subtypes of *S. suis* designated as P_N and P_O exist that showed subtle differences in their binding specificities (Haataja et al., 1994, 1999).

14.3 Inhibition

Inhibition of bacterial adhesion has therapeutic potential, since the adhesion step is often crucial for the subsequent steps towards disease. For this reason, adhesion inhibitors have been designed and synthesized. Early on, high concentrations of mannose were shown to prevent the adhesion of type I fimbriated *E. coli* to

tissue (Firon et al., 1987). More recently it was found that a lipophilic aglycone part such as a heptyl group can enhance binding by a factor of 440-fold compared to methyl α-D-mannoside. A hydrophobic ridge outside the mannose binding pocket was deemed responsible for the enhanced binding based on an X-ray structure of the protein (Bouckaert et al., 2005.). Further optimization efforts resulted in compound **8** (Fig. 14.4), which is almost 7000-fold more potent than methyl α-D-mannoside (Sperling et al., 2006). Recently, more insights into the binding specificity were obtained from bacterial binding studies to mannose derivatives conjugated to a polylysin matrix attached to a surface (Barth et al., 2008). Interestingly, of all the derivatives tested, ranging from the monosaccharide mannose up to the full branched high mannose core structure Man_9, the monosaccharide linked to a propyl spacer **12** and the trisaccharide **13** bound the most bacteria (Fig. 14.5). Also, the adhesion profile changed as a function of shear stress, as determined using flow conditions.

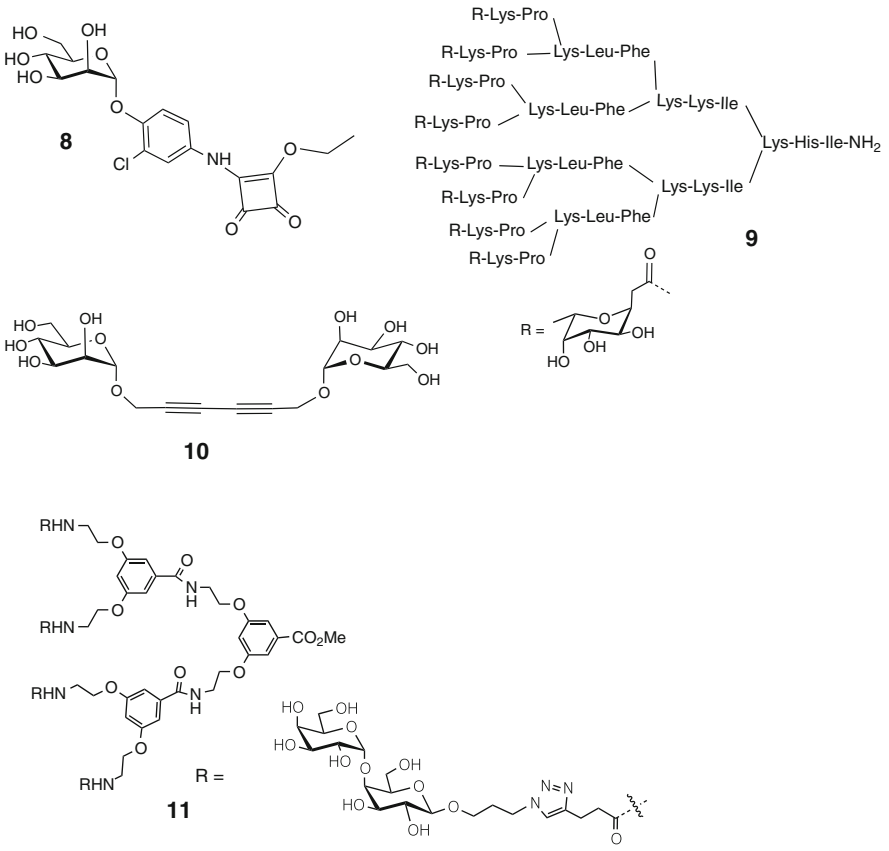

Fig. 14.4 Inhibitors of the adhesion of type 1 fimbriated *E. coli* (**8**), *P.aeruginosa* lectin lecB (**9**), *Burkholderia cenocepacia* lectin BC2L-A (**10**) and *Streptococcus suis* (**11**)

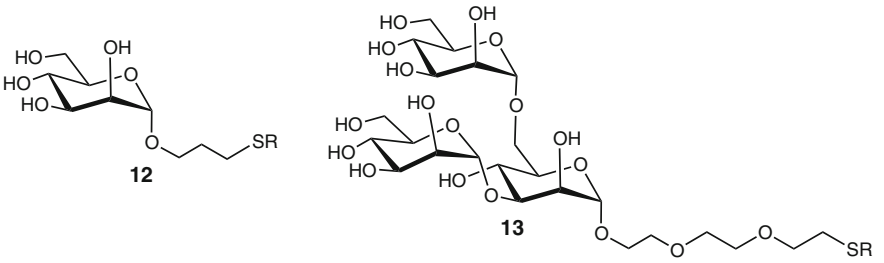

Fig. 14.5 Favoured ligands for type 1 fimbriated *E. coli* found by screening a series of mannosides linked to a surface

In order to find inhibitors for LecB, the Reymond group screened a solid-phase peptide dendrimer library in which each of the arms terminated in a fucose moiety, hoping to find inhibitors with significantly enhanced potency when compared to the corresponding monosaccharides. The search and also some further optimization yielded multivalent inhibitors that were up to 30-fold more potent (compound **9**, Fig. 14.4) per sugar than a monovalent glycopeptide reference compound in an enzyme-linked lectin assay. Interestingly, the inhibitors were also able to inhibit the formation of a biofilm of the bacteria (Johansson et al., 2008; Kolomiets et al., 2009). Related to this, LecA and LecB have recently been shown to cause significant injury by themselves, because they are cytotoxic and increase the permeability of the alveolar barrier. In animal studies, blocking the lectins with monosaccharides (Me-α-Fuc, Me-α-Gal and GalNAc) or by mutation reduced both the effects and the bacterial load in the lungs, and thus the subsequent bacterial dissemination. The results clearly indicate the therapeutic potential of potent adhesion inhibitors. A microarray screening of over 200 carbohydrate sequences with LecA revealed that the sequence Galα1,4Gal bound most strongly. Surprisingly the Galα1,3Gal isomer bound as strongly in a microcalorimetry experiment (Blanchard et al., 2008). The binding data were rationalized with docking data in conjunction with an X-ray structure of the lectin bound to Galα1,3Galβ1,4Glc. The opportunistic pathogen *Burkholderia cenocepacia* produces lectins related to LecB (Lameignere et al., 2010). One of these, BC2L-A, bound mannose derivatives with a preference for the divalent compound **10** (Fig. 14.4), which probably leads to the formation of a linear array of the dimeric lectin. Finally, the pig pathogen and emerging human pathogen *Streptococcus suis* can be blocked by the disaccharide galabiose (Galα1,4Gal). However, the binding of the bacterium can more effectively be blocked by the use of multivalent versions of the galabiose moiety, as was shown for compound **11** (Fig. 14.4) with an IC_{50} in a haemagglutination assay as low as 2.3 nM, compared to 400 nM for a monovalent galabiose derivative (Joosten et al., 2004; Branderhorst et al., 2008). Inhibitors of bacterial adhesion are also being sought among natural carbohydrate sources (Wittschier et al., 2007). High molecular weight fractions of carbohydrates mostly from plants were screened for their ability to block the adhesion of *H. pylori*, *Campylobacter jejeuni,* the oral pathogen *Porphyromonas*

gingivalis and *Candida albicans* to relevant tissue samples. Glucuronic acid rich fractions from okra fruits had a strong effect on the adhesion of *H. pylori, C. jejeuni* and *P. gingivalis.* No potent inhibitors against *C. albicans* adhesion were found. Pectic oligosaccharides were also tested for their ability to block the adhesion and invasion of Caco-2 cells by *C. jejeuni*. In this case, bacterial adhesion was not affected but the oligosaccharides significantly inhibited bacterial invasion (Ganan et al., 2010).

14.4 Detection

The binding specificity of bacteria can be used as a sensitive and specific detection and characterization handle for bacterial pathogens and as a way to remove unwanted industrial bacterial contaminants. Rapid and accurate detection assays could become a practical alternative to time-consuming bacterial cell culture, which would greatly speed up the development of a treatment plan in the case of a serious infection. For this purpose glycopolymers and carbohydrate arrays have been explored, but currently the focus is mostly on the use of glyconanoparticles, and ideally magnetic ones. Most studies have focused on the detection of type 1 fimbriated uropathogenic *E. coli* since its binding to mannosides is very well established (*vide supra*). A complete detection system has not yet been developed in all cases, but the capture of the bacteria by microscopic techniques has been demonstrated. The fluorescent polymer poly(*p*-phenylene ethynylene) linked to mannose units **14** (Fig. 14.6) was able to bind to bacteria which could be detected after removing the excess polymer by centrifugation and resuspending the (now fluorescent) bacteria (Fig. 14.6). The degree of binding was detected by fluorescence microscopy. Using this method it was possible to detect 10^4 bacteria per mL (Disney et al., 2004). In another approach, a microarray displaying various monosaccharides was used (Disney and Seeberger, 2004). The bacteria were made fluorescent with a cell-permeable fluorescent dye that stains nucleic acids. Incubation resulted in fluorescent mannose displaying spots, leaving the others dark. The detection limit in this case was around 10^5 bacteria per mL. Silica coated magnetic glyconanoparticles **15** (Fig. 14.6) were also used for bacterial detection. These particles have an average diameter of 10 nm and contained about 300 mannosides, which allows numerous particles to bind to a single bacterium. The advantage of using magnetic particles is that, after incubation of the particles with the *E. coli* bacteria, the bound bacteria can be separated from the unbound ones simply by a magnet. In this study the bacteria were fluorescently stained. 10^4 bacteria per mL were detectable by fluorescent microscopy (El-Boubbou et al., 2007). Interestingly, most of the bacteria were captured from the fluids (up to 88%) indicating the potential of the magnetic nanoparticles to remove unwanted bacteria from fluids, i.e. decontamination. In a related study, much larger (2.8 μm diameter) magnetic particles **16** conjugated via a streptavidin monolayer were incubated with a mannose derivative linked to biotin (Hatch et al., 2008). The resulting particles were also used to detect *E. coli.* After

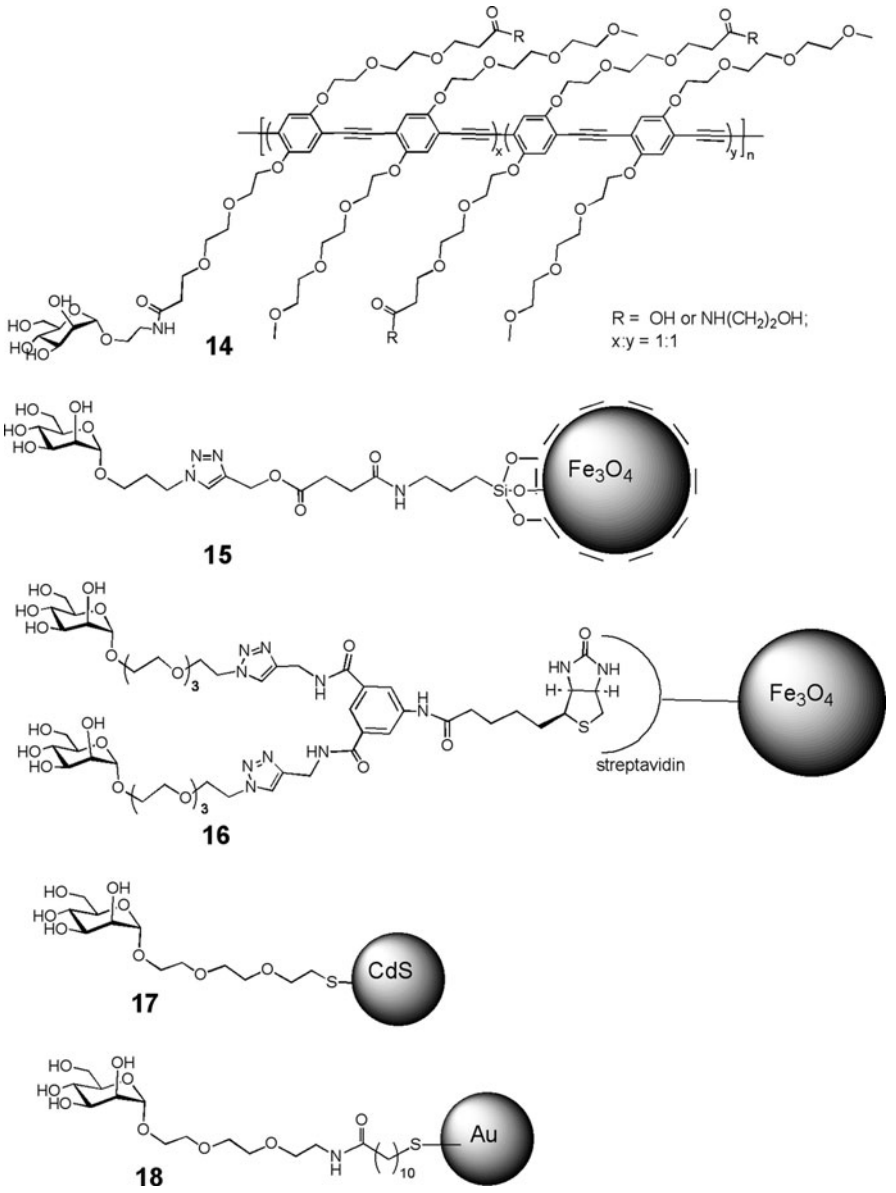

Fig. 14.6 Selected conjugated ligands for detection of type 1 fimbriated uropathogenic *E. coli*

magnetic capture and washing, the attached bacteria were quantified by a luminescence assay that determines the amount of ATP in the bacterial cells. The overall method is simple and convenient and has a detection limit of 10^5 bacteria per mL. The method was shown to be more sensitive than when the same particles were used displaying specific antibodies.

E. coli was also recognized with the aid of a Quartz Crystal Microbalance (QCM) (Shen et al., 2007). A gold surface was decorated with a monolayer displaying mannose moieties. However, only a small signal was observed due to the flexible nature of the pili-based bacterial binding. Interestingly, when a small amount of the mannose and glucose specific lectin Concanavalin A was added, the signal was much stronger. This enhancement was attributed to the bridging function of the lectin, which has four binding sites. On the one side it binds to suitable carbohydrate moieties of the bacterial LPS and on the other side to the mannosides of the monolayer. This bridging increases the contact area to the sensor surface, resulting in a strong signal. With this method 7.5×10^2 bacterial cells/mL could be detected.

Recently non-magnetic particles such as quantum dots (Mukhopadhyay et al., 2009) and gold nanoparticles (Huang et al., 2009), were also used to detect type 1 fimbriated *E. coli*. Quantum dots **17** (Fig. 14.6) with an average diameter of 15 nm were prepared and incubated with the bacterial cells. Detection by fluorescence microscopy was possible down to 10^4 cells/mL after removing unbound particles by centrifugation. The gold nanodots **18** worked in a similar manner. Their diameter was just 1.8 nm and they were strongly fluorescent. As for the quantum dots, the labelled bacteria were purified by centrifugation, but in this case excess soluble mannose was added afterwards to liberate the particles from the bacterial aggregate and quantify them by conventional fluorescence spectroscopy.

In my laboratory we explored the detection of the zoonotic *Streptococcus suis*, which has a specificity for the galabiose disaccharide (Galα1-4Gal). For this purpose, we used magnetic particles with a diameter of 250 nm that were decorated with streptavidin units. The particles were first incubated with the galabiose-linked biotin **19**, washed and then incubated with the bacteria (Fig. 14.7). After capturing

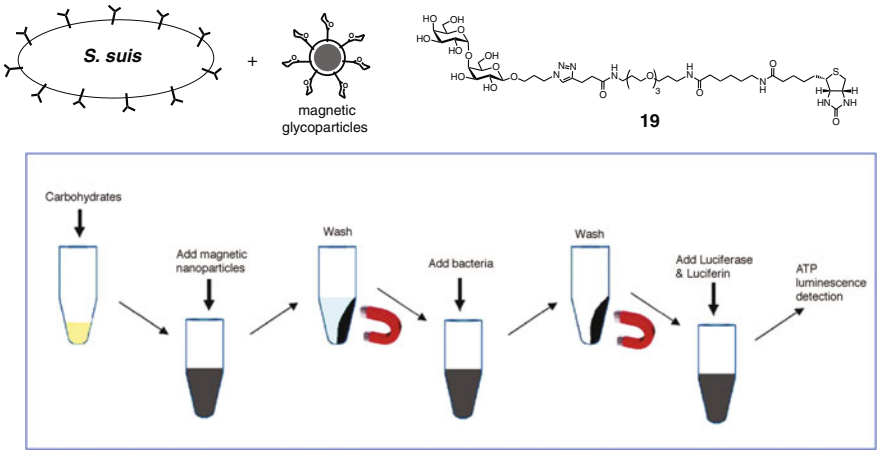

Fig. 14.7 (**a**) Detection of *Streptococcus suis* by magnetic glycoparticles assembled from streptavidine coated particles linked to **19**. (**b**) Actual protocol of particle preparation and detection

the particles containing the bound bacteria with a magnet; we quantified the bacterial ATP by luminescence. This simple method gave a detection limit of 10^4 bacteria/mL.

14.5 Cases Where Other Molecules Are Involved in the Adhesion

Bacterial adhesion does not only involve the bacterium binding to the tissue carbohydrate structures. There are numerous other ways. For example, an industrially relevant bacterium, *Deinococcus geothermalis*, which produces biofilms in paper machines, uses type IV pili (Saarimaa et al., 2006). Interestingly these pili were shown to be glycosylated with structures such as Galβ1,3GalNAc that are involved in the adhesion process. Another case is the adhesion mechanism of *Entereococcus faecalis*, which is of great interest because it causes bloodstream infections. The interactions of *Entereococcus faecalis* with Caco2 cells were studied (Sava et al., 2009). Interestingly, two sugar components, one on the bacterium and one on the tissue surface, are responsible for the adhesion. There is polysulfated heparin or heparan sulphate (**20**, Fig. 14.8) on the tissue cell surface and the glycolipid DGlc-DAG **21** on the bacterium. Surface plasmon resonance experiments showed that these components interact directly. This is unusual and, considering the location of the glycolipids on the cell membrane of the Gram-positive bacterium, the interaction mechanism is not fully understood.

The carbohydrates on the bacterial surface are also of importance in the infection process and/or the subsequent immune response. Such sugars are part of LPS (lipopolysaccharide) or part of capsular polysaccharides (CPS), and their structural variation results in many different pathogen serotypes (Sahly et al., 2008). Furthermore, using a lectin microarray (Hsu and Mahal, 2006a, b) the sugars can be used for characterization of the pathogens as mentioned before for the reverse case involving adhesin specificities. This was done with an array of 21 lectins. Bacteria were fluorescently labelled and their specific binding pattern was uncovered by the microarray. Specific recognition was validated by adding competing soluble sugars such as lactose or GlcNAc and the appropriate spots were observed to disappear. The method also provided an insight into the dynamic changes in the display of the

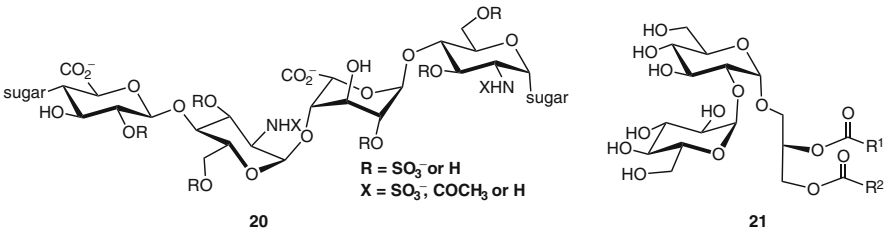

Fig. 14.8 Components of the Caco cell surface (**20**) and *Entereococcus faecalis* (**21**) involved in bacterial adhesion

carbohydrate structures due to phase variation. An *E. coli* strain showed significant changes in binding profile as a function of its growth density.

Carbohydrates on bacteria can also be involved in binding to surfaces as was shown in a study of the adhesion and subsequent biofilm formation of the oral bacterium *Streptococcus mutans,* which causes dental caries. In a recent study, the role of various plant lectins from edible sources on initial bacterial adhesion was tested (Islam et al., 2009). The lectins chosen had binding specificities for mannose, glucose, GlcNAc and GalNAc. In all cases a sizeable reduction of both adhesion and biofim formation was observed. The adhesion inhibition ranged from 20 to 60% in the presence of 0.2–500 μg/mL sugar, i.e. full inhibition was not reached, indicating the presence of additional adhesion mechanisms.

References

Arends JP, Zanen HC (1988) Meningitis caused by *Streptococcus suis* in humans. Rev Infect Dis 10:131–137

Barth KA, Coullerez G, Nilsson LM, Castelli R, Seeberger PH, Vogel V, Textor M (2008) An engineered mannoside presenting platform: *Escherichia coli* adhesion under static and dynamic conditions. Adv Funct Mater 18:1459–1469

Bennett HJ, Roberts IS (2005) Identification of a new sialic acid-binding protein in *Helicobacter pylori*. FEMS Immunol Med Microbiol 44:163–169

Blanchard B, Nurisso A, Hollville E, Tétaud C, Wiels J, Pokorná M, Wimmerová M, Varrot A, Imberty A (2008) Structural basis of the preferential binding for globo-series glycosphingolipids displayed by *Pseudomonas aeruginosa* lectin I. J Mol Biol 383:837–853

Bouckaert J, Berglund J, Schembri M, De Genst E, Cools L, Wuhrer M, Hung CS, Pinkner J, Slättegård R, Zavialov A, Choudhury D, Langermann S, Hultgren SJ, Wyns L, Klemm P, Oscarson S, Knight SD, De Greve H (2005) Receptor binding studies disclose a novel class of high-affinity inhibitors of the *Escherichia coli* FimH adhesin. Mol Microbiol 55:441–455

Branderhorst HM, Kooij R, Salminen A, Jongeneel LH, Arnusch CJ, Liskamp RMJ, Finne J, Pieters RJ (2008) Synthesis of multivalent *Streptococcus suis* adhesion inhibitors by enzymatic cleavage of polygalacturonic acid and "click" conjugation. Org Biomol Chem 6:1425–1434

Choudhury D, Thompson A, Stojanoff V, Langermann S, Pinkner J, Hultgren SJ, Knight SD (1999) X-ray structure of the FimC-FimH chaperone-adhesin complex from uropathogenic *Escherichia coli*. Science 285:1061–1066

Disney MD, Seeberger PH (2004) The use of carbohydrate microarrays to study carbohydrate-cell interactions and to detect pathogens. Chem Biol 11:1701–1707

Disney MD, Zheng J, Swager TM, Seeberger PH (2004) Detection of bacteria with carbohydrate-functionalized fluorescent polymers. J Am Chem Soc 126:13343–13346

Dodson KW, Pinkner JS, Rose T, Magnusson G, Hultgren SJ, Waksman G (2001) Structural basis of the interaction of the pyelonephritic *E. coli* adhesin to its human kidney receptor. Cell 105:733–743

El-Boubbou K, Gruden C, Huang X (2007) Magnetic glyco-nanoparticles: a unique tool for rapid pathogen detection, decontamination, and strain differentiation. J Am Chem Soc 129:13392–13393

Firon N, Ashkenazi S, Mirelman D, Ofek I, Sharon N (1987) Aromatic a-glycosides of mannose are powerful inhibitors of the adherence of type 1 fimbritated *Escherichia coli* to teast and intestinal epithelial cells. Infect Immun 55:472–476

Ganan M, Collins M, Rastall R, Hotchkiss AT, Chau HK, Carrascosa AV, Martinez-Rodriguez AJ (2010) Inhibition by pectic oligosaccharides of the invasion of undifferentiated and differentiated Caco-2 cells by *Campylobacter jejuni*. Int J Food Microbiol 137:181–185

Haataja S, Tikkanen K, Liukkonen J, François-Gerard C, Finne J (1993) Characterization of a novel bacterial adhesion specificity of *Streptococcus suis* recognizing blood group P receptor oligosaccharides. J Biol Chem 268:4311–4317

Haataja S, Tikkanen K, Nilsson U, Magnusson G, Karlsson KA, Finne J (1994) Oligosaccharide-receptor interaction of the Gal-α1-4Gal binding adhesin of *Streptococcus suis*. Combining site architecture and characterization of two variant adhesion specificities. J Biol Chem 269:27466–27472

Haataja S, Zhang Z, Tikkanen K, Magnusson G, Finne J (1999) Determination of the cell adhesion specificity of *Streptococcus suis* with the complete set of monodeoxy analogues of globotriose. Glycoconj J 16:67–71

Hatch DM, Weiss AA, Kale RR, Iyer SS (2008) Biotinylated bi- and tetra-antennary glycoconjugates for *Escherichia coli* detection. ChemBioChem 9:2433–2442

Hazes B, Sastry PA, Hayakawa K, Read RJ, Irvin RT (2000) Crystal structure of *Pseudomonas aeruginosa* PAK pilin suggests a main-chain-dominated mode of receptor binding. J Mol Biol 299:1005–1017

Hsu KL, Mahal LK (2006a) A lectin microarray approach for the rapid analysis of bacterial glycans. Nat Protocol 1:543–549

Hsu KL, Pilobello KT, Mahal LK (2006b) Analyzing the dynamic bacterial glycome with a lectin microarray approach. Nat Chem Biol 2:153–157

Huang CC, Chen CT, Shiang YC, Lin ZH, Chang HT (2009) Synthesis of fluorescent carbohydrate-protected Au nanodots for detection of Concanavalin A and *Escherichia coli*. Anal Chem 81:875–882

Imundo L, Barasch J, Prince A, Al-Awqati Q (1995) Cystic fibrosis epithelial cells have a receptor for pathogenic bacteria on their apical surface. Proc Natl Acad Sci USA 92:3019–3023

Islam B, Khan SN, Naeem A, Sharma V, Khan AU (2009) Novel effect of plant lectins on the inhibition of *Streptococcus mutans* biofilm formation on saliva-coated surface. J Appl Microbiol 106:1682–1689

Johansson EMV, Crusz SA, Kolomiets E, Buts L, Kadam RU, Cacciarini M, Bartels K-M, Diggle SP, Camara M, Williams P, Loris R, Nativi C, Rosenau F, Jaeger K-E, Darbre T, Reymond J-L (2008) Inhibition and dispersion of *Pseudomonas aeruginosa* biofilms by glycopeptide dendrimers targeting the fucose-specific lectin LecB. Chem Biol 15:1249–1257

Joosten JAF, Loimaranta V, Appeldoorn CCM, Haataja S, El Maate FA, Liskamp RMJ, Finne J, Pieters RJ (2004) Inhibition of *Streptococcus suis* adhesion by dendritic galabiose compounds at low nanomolar concentration. J Med Chem 47:6499–6508

Khan AS, Hacker J (2000) Glycolipid receptors of F1C fimbrial adhesin of uropathogenic *Escherichia coli*. Adv Exp Med Biol 485:213–217

Khan AS, Kniep B, Oelschlaeger TA, Van Die I, Korhonen T, Hacker J (2000b) Receptor structure for F1C fimbriae of uropathogenic *Escherichia coli*. Infect Immun 68:3541–3547

Khan AS, Mühldorfer I, Demuth V, Wallner U, Korhonen TK, Hacker J (2000a) Functional analysis of the minor subunits of S fimbrial adhesin (Sfal) in pathogenic *Escherichia coli*. Mol Gen Genet 263:96–105

Kolomiets E, Swiderska MA, Kadam RU, Johansson EMV, Jaeger K-E, Darbre T, Reymond J-L (2009) Glycopeptide dendrimers with high affinity for the fucose-binding lectin LecB from *Pseudomonas aeruginosa*. ChemMedChem 4:562–569

Korhonen TK, Väisänen-Rhen V, Rhen M, Pere A, Parkkinen J, Finne J (1984) *Escherichia Coli* fimbriae recogninzing sialyl galactosides. J Bacteriol 159:762–766

Krivan HC, Roberts DD, Ginsburg V (1988) Many pulmonary pathogenic bacteria bind specifically to the carbohydrate sequence GalNAcβ-1-4Gal found in some glycolipids. Proc Natl Acad Sci USA 85:6157–6161

Krogfelt KA, Bergmans H, Klemm P (1990) Direct evidence that the FimH protein is the mannose-specific adhesion of *Escherichia coli* type 1 fimbriae. Infect Immun 58:1995–1998

Lameignere E, Shiao TC, Roy R, Wimmerova M, Dubreuil F, Varrot A, Imberty A (2010) Structural basis of the affinity for oligomannosides and analogs displayed by BC2L-A, a *Burkholderia cenocepacia* soluble lectin. Glycobiology 20:87–98

Lin C-C, Yeh Y-C, Yang C-Y, Chen C-L, Chen G-F, Chen C-C, Wu Y-C (2002) Selective binding of mannose-encapsulated gold nanoparticles to type 1 pili in *Escherichia coli*. J Am Chem Soc 124:3508–3509

Magalhães A, Gomes J, Ismail MN, Haslam SM, Mendes N, Osório H, David L, Le Pendu J, Haas R, Dell A, Borén T, Reis CA (2009) Fut2-null mice display an altered glycosylation profile and impaired BabA-mediated *Helicobacter pylori* adhesion to gastric mucosa. Glycobiology 19:1525–1536

Mahdavi J, Sonden B, Hurtig M, Olfat FO, Forsberg L, Roche N, Angström J, Larsson T, Teneberg S, Karlsson KA, Altraja S, Wadstrom T, Kersulyte D, Berg DE, Dubois A, Petersson C, Magnusson KE, Norberg T, Lindh F, Lundskog BB, Arnqvist A, Hammarstrom L, Borén T (2002) *Helicobacter pylori* sabA adhesin in persistent infection and chronic inflammation. Science 297:573–578

Miller-Podraza H, Johansson P, Ångström J, Larsson T, Longard M, Karlsson K-A (2004) Studies on gangliosides with affinity for *Helicobacter plyori*: binding to natural and chemically modified structures. Glycobiology 14:205–217

Miller-Podraza H, Lanne B, Ångström J, Teneberg S, Milh MA, Jovall PA, Karlsson H, Karlsson K-A (2005) Novel binding epitope for *Helicobacfer pylori* found in neolacto carbohydrate chains: structure and cross-binding properties. J Biol Chem 280:19695–19703

Miller-Podraza H, Weikkolainen K, Larsson T, Linde P, Helin J, Natunen J, Karlsson K-A (2009) *Helicobacter pylori* binding to new glycans based on N-acetyllactosamine. Glycobiology 19:399–407

Moch T, Hoschützky H, Hacker J, Kröncke K-D, Jann K (1987) Isolation and characterization of the α–sialyl-β-2,3-galactosyl-specific adhesin from fimbriated *Escherichia coli*. Proc Natl Acad Sci USA 84:3462–3466

Mukhopadhyay B, Martins MB, Karamanska R, Russell DA, Field RA (2009) Bacterial detection using carbohydrate-functionalised CdS quantum dots: a model study exploiting E.coli recognition of mannnosidees. Tetrahedron Lett 50:886–889

Roche N, Ångström J, Hurtig M, Larsson T, Borén T, Teneberg S (2004) *Helicobacter pylori* and complex gangliosides. Infect Immun 72:1519–1529

Saarimaa C, Peltola M, Raulio M, Neu TR, Salkinoja-Salonen MS, Neubauer P (2006) Characterization of adhesion threads of *Deinococcus geothermalis* as type IV pili. J Bacteriol 188:7016–7021

Sahly H, Keisari Y, Crouch E, Sharon N, Ofek I (2008) Recognition of bacterial surface polysaccharides by lectins of the innate immune system and its contribution to defense against infection: the case of pulmonary pathogens. Infect Immun 76:1322–1332

Sava IG, Zhang F, Toma I, Theilacker C, Li B, Baumert TF, Holst O, Linhardt RJ, Huebner J (2009) Novel interactions of glycosaminoglycans and bacterial glycolipids mediate binding of enterococci to human cells. J Biol Chem 284:18194–18201

Shen Z, Huang M, Xiao C, Zhang Y, Zeng X, Wang PG (2007) Nonlabeled quartz crystal microbalance biosensor for bacterial detection using carbohydrate and lectin recognitions. Anal Chem 79:2312–2319

Sheth HB, Lee KK, Wong WY, Srivastava G, Hindsgaul O, Hodges RS, Paranchych W, Irvin RT (1994) The pili of *Pseudomonas aeruginosa* strains PAK and PAO bind specifically to the carbohydrate sequence β-GalNAc(1-4)β-Gal found in glycosphingolipids asialo-GM1 and asialo-GM2. Mol Microbiol 11:715–723

Sperling O, Fuchs A, Lindhorst TK (2006) Evaluation of the carbohydrate recognition domain of the bacterial adhesin FimH: design, synthesis and binding properties of mannoside ligands. Org Biomol Chem 4:3913–3922

Staats JJ, Feder I, Okwumabua O, Chengappa MM (1997) *Streptococcus suis*: past and present. Vet Res Commun 21:381–407

Sung M-A, Fleming K, Chen HA, Matthews S (2001) The solution structure of PapGII from uropathogenic *Escherichia coli* and its recognition of glycolipid receptors. EMBO Rep 2:621–627

Thomas RJ, Brooks T (2004a) Common oligosaccharide moieties inhibit the adherence of typical and atypical respiratory pathogens. J Med Microbiol 53:833–840
Thomas RJ, Brooks TJ (2004b) Oligosaccharide receptor mimics inhibit *Legionella pneumophila* attachment to human respiratory epithelial cells. Microb Pathog 36:83–92
Walz A, Odenbreit S, Mahdavi J, Borén T, Ruhl S (2005) Identification and characterization of binding properties of *Helicobacter pylori* by glycoconjugate arrays. Glycobiology 15:700–708
Wittschier N, Lengsfeld C, Vorthems S, Stratmann U, Ernst JF, Verspohl EJ, Hensel A (2007) Large molecules as anti-adhesive compounds against pathogens. J Pharm Pharmacol 59:777–786

Chapter 15
The Application of NMR Techniques to Bacterial Adhesins

Frank Shewmaker

Abstract Abstract Extracellular adhesins frequently compose large, highly-ordered structural assemblies that project away from the bacterial surface. These assemblies, known as pili or fimbriae, are rod-like polymeric structures that in some cases can extend up to several micrometers from the cell surface. Because these adhesin structures are critical to bacterial colonization of host cell surfaces, there is an incentive to understand their structure, assembly and mechanism of host cell attachment. Various methods in Nuclear Magnetic Resonance (NMR) spectroscopy have been used to address these topics, yielding structural information at the atomic level. Also, new methods in solid-state NMR spectroscopy have thus far been under-utilized in the study of large adhesin structures and offer a powerful approach to overcoming problems with crystallization to better understand the structures of these complexes. The following is a brief overview of the contributions of NMR to the study of bacterial adhesins with an emphasis on the future potential of solid-state NMR.

15.1 Introduction

Nuclear Magnetic Resonance (NMR) spectroscopy is an important method for the determination of molecular structures at the atomic level. In the study of protein adhesins, multi-dimensional NMR can provide structural and functional information that can both complement and sometimes exceed the information derived from x-ray crystallography. NMR is an obvious alternative when proteins fail to crystallize, but NMR is also especially suited for studying natively unfolded domains and domains that fold upon interaction with other components. Such domains when

F. Shewmaker (✉)
Department of Pharmacology, Uniformed Services University of the Health Sciences, Bethesda, MD 20814, USA
e-mail: frank.shewmaker@usuhs.mil

D. Linke, A. Goldman (eds.), *Bacterial Adhesion*, Advances in Experimental Medicine and Biology 715, DOI 10.1007/978-94-007-0940-9_15,

incorporated into a crystal may be in conformations imposed by the crystal lattice or remain invisible to diffraction methods due to their disorder. Methods in NMR also enable the study of dynamic protein–protein and protein–ligand interactions. As adhesins are surface exposed and potentially interact with many proteins in the extracellular milieu, techniques in NMR offer the opportunity to study an array of binding interactions with other adhesins and various host receptors in solution.

One traditional drawback of NMR spectroscopy, relative to x-ray crystallography, is that larger proteins and protein complexes can exceed the resolution limits of the technique. In general, it can be challenging to assign structure to proteins that are several hundred amino acids in length. Also, large macromolecular complexes that tumble slowly in solution diminish the resolution of NMR spectroscopy. In the case of adhesin structures that are composed of thousands of subunits, such as surface pili, this would seem especially true. However, developments in solid-state NMR have proved successful in the study of high molecular weight amyloid fibres and many of the same methods could also be adapted to the study of large filamentous adhesin structures. As pili/fimbriae are not easily amenable to crystallization (Craig et al., 2003; Forest, 2005), solid-state NMR offers a potential alternative to determining high-resolution structural information.

15.1.1 Structure Determination by NMR

A primary objective of using multi-dimensional NMR techniques for adhesins, or any protein, is the elucidation of a high-resolution structure. An advantage of using NMR over x-ray crystallography is the sample does not require crystallization and can be maintained in an aqueous, native-like environment. The preparation of protein samples for NMR is generally no different than preparing protein from bacteria for other biophysical techniques, with the exception that protein samples must be enriched for ^{13}C and ^{15}N, nuclei that are visible by NMR spectroscopy. This is easily performed by growing the bacteria in defined media that contain either carbon or nitrogen sources enriched for these isotopes. In the case of solid-state NMR, protein samples are frequently harvested by high-speed centrifugation and loaded into sample rotors as either hydrated or lyophilized solids.

The specifics of structural determination of proteins by multi-dimensional NMR spectroscopy are well beyond the scope of this review. However, in principle there are two basic requirements for determining an NMR protein structure: the ability to assign cross-peaks in the NMR spectra and the collection of sufficient distance and angle restraints for structure building. Assignment of cross-peaks in NMR spectroscopy is essentially the matching of specific amino acids within a protein with their corresponding chemical shifts in the NMR spectra. A reason larger proteins can be challenging for structure determination is simply because there are more nuclei and thus more cross-peaks in the spectrum, so it becomes much harder to make individual assignments due to signal overlap. Distance restraints are specific inter-atomic distances that can be estimated by various NMR techniques. With

enough known distances between the identified nuclei in the protein sample, a high-resolution model can be built that satisfies the restrictions imposed by these restraints. Several examples of adhesin solution structures solved by NMR are listed in Table 15.1.

15.1.2 Solid-State NMR

Solid-state NMR offers an alternative for structural elucidation when there are sample problems with solubility, crystallization or size. In the case of adhesins, solid-state NMR offers the possibility of studying fimbrial structures in their native state without artificially manipulating the proteins to remain as soluble monomers. Solid-state NMR does not require that the samples have any long-range order like in crystal assemblies, nor are particular sample orientations with respect to the magnetic field required (although some techniques employ this). Also, as "solids", samples can be nearly all protein, only depending on the level of hydration. As a result, sample volumes are small and only a few milligrams of labeled protein can be sufficient for experimentation.

In principle structure assignment by solid-state NMR is the same as solution NMR; however signal line widths are much broader for samples in the solid state and can render chemical shift assignment nearly impossible. The broadening of nuclear chemical shifts is a consequence of limited sample motion. In solution NMR, the rapid isotropic tumbling of molecules averages out dipole–dipole couplings and chemical shift anisotropy, which results in very narrow chemical shift line widths. In solid-state NMR the problem of broad line widths is overcome by Magic Angle Spinning (MAS) (reviewed in Tycko, 2006). MAS is the rapid rotation of the sample around an axis that lies at an angle of $\sim 55°$ ($\cos^{-1}(1/\sqrt{3})$) with the external magnetic field of the NMR spectrometer. As a result, dipole–dipole couplings and chemical shift anisotropy are averaged out and the signal line widths are dramatically narrower.

A drawback to solid-state NMR is that ^{1}H sensitivity is relatively low due to signal broadening that results from strong ^{1}H–^{1}H dipolar couplings. As a consequence, most methods rely on ^{13}C and ^{15}N signals. Also, sample size limits are still a major concern. Existing solid-state NMR protein structures are mostly restricted to small proteins and polypeptides. However, the technology is rapidly advancing to the point that the typical size of fimbrial adhesins should fall within the limits of solid-state NMR (see below).

15.1.3 Chemical Shift Perturbation and Mapping

The assignment of multi-dimensional spectra mentioned above can be especially important for downstream applications for studies of adhesin binding. Beyond structure elucidation, there are several examples of the use of NMR to study

Table 15.1 Representative NMR experiments on bacterial adhesins

Protein & function	Organism	NMR experimental results
Type 1 and P-pili/fimbiae, chaperone-usher pathway		
AfaD (AfaD-III): Invasin cap of Afa adhesin fimbriae; mediates bacteria internalization	*E. coli*	Solution structure of self-complementing, monomeric protein (AfaD-dsc; see text); archetypal immunoglobulin-like pilin fold (Cota et al., 2006). NMR titration used to show donor strand exchange between AfaE and AfaD (Anderson et al., 2004).
AfaDE (Afa tip complex): Synthetically-fused invasin and adhesin fimbrial tip complex	*E. coli*	Solution structure of fused, functional AfaDE synthetic tip complex (see text); extended domain arrangement with interdomain flexibility (Cota et al., 2006).
AfaE (AfaE-III): Structural subunit of fimbriae	*E. coli*	Solution structure of self-complementing, monomeric protein (AfaE-dsc; see text) with archetypal pilin fold; high-resolution support for donor strand exchange and fimbrial polymerization. Receptor binding site identified by chemical shift mapping (Anderson et al., 2004). Chemical shift mapping of CEA receptor binding region of AfaE-dsc; revealed CEA and DAF receptor binding sites are exclusive. High-resolution model for AfaE-dsc in complex with N-terminal CEA receptor (Korotkova et al., 2006; 2008).
Dispersin (Aap): Facilitates disperse, erect Aggregative Adherence Fimbriae (AAF)	*E. coli* (EAEC strain 042)	Solution structure; novel β-sandwich fold (Velarde et al., 2007).
DraE: Dr adhesin fimbrial subunit	*E. coli*	Chemical shift mapping of chloramphenicol binding site; structural interpretation of ligand specificity differences with AfaE (Pettigrew et al., 2004).
FimC: Periplasmic chaperone for type I pilus assembly	*E. coli*	Solution structure of complete protein; revealed distinctions with PapD P-pili chaperone (Pellecchia et al., 1998). Identification of FimH-binding site on N-terminal domain by chemical shift mapping (Pellecchia et al., 1999). Pilicide binding sites also identified by chemical shift mapping (Hedenstrom et al., 2005).
FimD: Outer membrane pili assembly protein	*E. coli*	Solution structure for $FimD^{25–125/139}$; N-terminal domain undergoes order transition upon binding adhesin-chaperone complex (Nishiyama et al., 2005).

Table 15.1 (continued)

Protein & function	Organism	NMR experimental results
FimF: Structural subunit of type I pilus tip fibrillum	*E. coli*	Solution structure of self-complementing form ($FimF_F$; see text) reveals Ig-like fold with natively-disordered N-terminal donor strand; donor strand forms "molecular zipper" with next adhesin subunit (Gossert et al., 2008, 2007).
PapG (class II): P pili adhesin tip, glycan receptor binding	*E. coli* (UPEC)	Solution structure of adhesin domain ($PapG^{21–219}$), elongated β sandwich fold; chemical shift mapping of receptor-binding site (Sung et al., 2001a, (2001b).
Type IV Pili, general secretion pathway		
Bundlin (BfpA): Structural subunit of bundle-forming pili	*E. coli* (EPEC)	Solution structure of Type IVb pilus head domain used for high-resolution model of filament structure (Ramboarina et al., 2004, 2005).
PilA: Structural subunit of pilus	*Pseudomonas aeruginosa* (K122-4)	Solution structure of $PilA^{29–150}$ used to propose novel left-handed pilus helix based on complementary charged surfaces Keizer et al., 2001).
PilP: Lipoprotein that facilitates pilus biogenesis	*Neisseria meningitidis*	Solution structure: $PilP^{(69–181)}$ forms novel β-sandwich fold. Amino-terminal domain (residues 20–84) is natively disordered (Golovanov et al., 2006a, 2006b).
PilS: Structural subunit of pilus	*Salmonella typhi*	First solution structure of Type IVb pilus head domain ($PilS^{25–181}$); structure used as basis for pilus assembly model (Xu et al., 2004).
Pseudopili, type II secretion pathway		
XcpT: Potential pseudopilin structural subunit	*Pseudomonas aeruginosa*	Solution structure with αβ-Roll fold; similar to Type IV pilus subunits (Alphonse et al., 2009).
Curli, nucleation-precipitation pathway		
CsgA: Major structural component of curli fibres	*E. coli*	Solid-state NMR suggests functional amyloid based on β-solenoid fold (Shewmaker et al., 2009b).
Intimins, auto-transporter secretion pathway		
Intimin: Outer membrane protein, binds Translocated intimin receptor (Tir)	*E. coli*	Solution structure of C-terminal Tir-binding domain; chemical shift mapping of Tir-binding interface (Batchelor et al., 2000; Kelly et al., 1999).

adhesion–protein and adhesion–ligand interactions. The amino acid assignment of protein NMR spectra matches specific cross-peaks in the spectra with specific amino acids of the protein. This facilitates the method of chemical shift mapping, which is the interpretation of binding sites based on chemical shift perturbations. Frequently, [^{1}H, ^{15}N]-HSQC (Heteronuclear Single Quantum Coherence) NMR spectra will be generated, which yield one cross-peak for each backbone amide and are thus easily interpreted. When the local environment of an amino acid changes, such as occurs during the direct interaction with another protein, there can be a corresponding perturbation in the chemical shifts of the nuclei of that amino acid. Thus through the displacement of various cross-peaks the perturbed amino can be identified, yielding information about ligand-binding sites or protein-binding interfaces. Some examples of chemical shift mapping applied to bacterial adhesins are listed in Table 15.1. Observing perturbations can also yield information about binding stoichiometry, affinity and conformational switching.

15.2 Application of NMR to Adhesins

Considering the breadth of the bacterial adhesin field, NMR spectroscopic studies of adhesins are relatively underrepresented, especially solid-state NMR. Nonetheless, there are several excellent examples of the application of NMR in the study of adhesins. Most NMR studies have focused on adhesins of Gram-negative bacteria and many representative examples are listed in Table 15.1. The table is not intended to be all-inclusive, but does include many of the important contributions made to the study of bacterial adhesins by NMR spectroscopy over approximately the past decade. A few of the studies and their significance are discussed in greater detail below with emphasis on the information that was gained specifically through NMR techniques.

15.2.1 NMR Studies of Type I Pili

Several interesting NMR studies have looked at components of Type I pili of *E. coli*. These pili are primarily composed of the structural subunit FimA. Secretion of FimA, and the adhesin tip proteins (FimF, FimG and FimH), occurs via a chaperone-usher pathway that employs FimC to deliver adhesin subunits to the membrane usher protein FimD for the final secretion and assembly step (reviewed in Waksman and Hultgren, 2009).

Periplasmic adhesin chaperones like FimC differ from the standard chaperone paradigm in that their adhesin substrates are not bound in unfolded conformations. Instead, the substrates are essentially in their functionally folded state, but with an incomplete β sheet. The adhesin chaperone supplies a β strand (G1) to complete the sheet in a process known as donor-strand complementation (DSC)

(Barnhart et al., 2000; Choudhury et al., 1999; Sauer et al., 1999; Zavialov et al., 2003). A conceptually identical process known as donor-strand exchange (DSE) is the basis for polymerization of fimbrial adhesins. The fimbrial subunits each supply an N-terminal strand to the next subunit, thus forming a chain of molecules. The first high-resolution structure of FimC was determined by NMR spectroscopy (Pellecchia et al., 1998). Interestingly, the sequence at the beginning of the G1 strand was observed to be intrinsically disordered; this is consistent with the fact that the G1 peptide strand has to reversibly interact with several different substrates. The FimC NMR assignments were also used for chemical shift mapping, which confirmed that the N-terminal domain of FimC is the substrate-recognition domain (Pellecchia et al., 1999).

In order to isolate soluble and stable Type I pili subunits for biophysical studies, donor strands can be added in *cis*. FimF is a component of the tip fibrillum of Type 1 pili. A self-donating form ($FimF_F$) was created for study by solution NMR (Gossert et al., 2008). $FimF_F$ has a C-terminal extension that consists of a short linker followed by a peptide identical to the first 15 residues of its N-terminus. This extension can self-complement, resulting in a stable and monomeric protein suitable for solution NMR techniques. Characterization of $FimF_F$ by NMR showed it to have an archetypal immunoglobulin-like pilin fold, with the donor strand forming a "molecular zipper" by intercalating into an acceptor cleft. Alternatively, the N-terminus, lacking an acceptor cleft of another adhesin, was stuck in a natively disordered state. $FimF_F$ binary complexes were formed with $FimG_T$ and $FimF_T$ (the $_T$ indicates that the proteins are truncated of their N-termini). Intermolecular restraints indicated that the binary complexes have a linear head-to-tail mode of binding while maintaining inter-domain flexibility, supporting the hypothesis that the tip fibrillum is extended and articulated.

The outer membrane usher FimD has a periplasmic domain that facilitates recognition of the chaperone-adhesin complex (Nishiyama et al., 2003). Nishiyama and coworkers solved solution structures for this domain ($FimD^{25–125}$ and $FimD^{25–139}$) by NMR spectroscopy, revealing a novel protein fold (Nishiyama et al., 2005). Interestingly, the NMR data indicated that the amino-terminal domain (residues 1–24) is natively disordered in solution (negative ([^{15}N,^{1}H] Nuclear Overhauser Effects; NOEs), but it undergoes a structural transition into an ordered conformation concomitant with recognition of the chaperone-adhesin complex (Nishiyama et al., 2005). These amino-terminal residues are essential for FimD to recognize the chaperone-substrate complex; X-ray crystallography alone would not have revealed the plasticity in this substrate-recognition domain. Chemical shift mapping, comparing $FimD^{1–139}$ alone or with the adhesion-chaperone complex FimC-$FimH^{158–279}$, indicated a potential mechanism for discrimination and secretion of substrate by FimD. The residues affected by formation of the ternary complex indicated that the FimD periplasmic domain could be cycling between open and closed states in a manner that depends on the delivery of the properly-loaded chaperone-adhesin complex.

15.2.2 NMR Studies of Afa/Dr Adhesins

AfaE and AfaD are members of the *E. coli* Afa/Dr adhesin family, which is associated with diarrhea and urinary tract infections. Members of this family target the host cell receptor Decay-Accelerating Factor (DAF). Anderson and coworkers (2004) created a self-donating variant of AfaE (AfaE-*dsc*) that is functional, soluble and does not form heterogeneous oligomers. They solved a solution structure showing that AfaE assumes an archetypal pilin fold. NMR titration data suggested donor strand complementation between AfaE and AfaD. The authors concluded that AfaE, like other adhesins, polymerizes into fine, flexible fibres through DSE. They further used chemical shift perturbation assays to map the DAF binding surface of AfaE-*dsc*.

AfaD is an invasin that lacks an N-terminal extension, and is thus reasoned to be the tip subunit of AfaE fimbriae. This idea was further advanced with the solving of the NMR solution structure of AfaD-*dsc* and an AfaDE fusion that mimics the Dr/Afa invasive tip complex (Cota et al., 2006). The solution structures of both constructs confirmed DSE for these adhesins, and that AfaD has a typical immunoglobulin-like topology.

Some members of the Dr family bind Carcinoembryonic Antigen (CEA)-related host receptor molecules. The CEA family, which can serve as binding targets for pathogenic bacteria, includes highly glycosylated proteins that are expressed on the surface of epithelial, endothelial and other cells. Korotkova and coworkers (2006) used chemical shift mapping to identify the binding surface of AfaE that recognizes the N-terminal domain of CEA. Strikingly, it is distinct from the DAF-binding surface, suggesting that both receptors could be bound simultaneously. In continuation of this work, the same group used a combination of crystallographic, NMR structure and chemical shift mapping data to build a structural model for the AfaE-CEA complex (Korotkova et al., 2008). This was an elegant application of NMR for model building because all previous attempts at Dr adhesin-CEA receptor co-crystallization had failed.

15.2.3 NMR Studies of Type IV Adhesins

Multi-dimensional solution NMR has been used to solve several Type IV major pilin structures. *Pseudomonas aeruginosa* Type IV pilus is composed of a single pilin subunit, PilA. A solution NMR structure was determined for an amino-terminal truncation variant that remains soluble while retaining its biologically relevant structure (Keizer et al., 2001). The pilin has an αβ-fold composed of four curved anti-parallel β-strands that form a sheet surrounding an amino-terminal α-helix, a fold similar to other Type IV pilin subunits (Audette et al., 2004; Craig et al., 2003; Hazes et al., 2000; Parge et al., 1995). The highly conserved first 22 amino acids likely form an α-helix and were used to build a model for pilin assembly that is based on helical bundles of the amino-terminal α-helices, forming a left-handed helix. Complementary electrostatic interactions stabilize the pilin fibre.

Two Type IVb pilin proteins, PilS of *Salmonella Typhi* and BFP of *E. coli*, have also been solved by NMR spectroscopy (Ramboarina et al., 2005; Xu et al., 2004). Interestingly, the Type IVb pilin solution structures have a different topology and larger head domain than Type IVa structures, yet still produce morphologically and functionally similar pili.

15.3 The Possibilities of Solid-State NMR for Studying Fimbrial Adhesins

The impetus for using solid-state NMR for studying fimbrial adhesins is that it offers a way to elucidate high-resolution structural information while the adhesin is in its native, high-molecular weight assembly. As mentioned above, polypeptide size is still a major obstacle for structure elucidation with solid-state NMR. However, this is a technology in transition and the upper size limits are nearing the sizes of typical fimbrial subunits. Some recent examples of structure determination using solid-state NMR include: the 62-residue α-spectrin Src-homology 3 (SH3) domain (Castellani et al., 2002, 2003), the 76-residue human ubiquitin (Zech et al., 2005), the 56-residue α1 immunoglobulin binding domain of protein G (GB1) (Franks et al., 2005), a 38-residue scorpion toxin (kaliotoxin) (Korukottu et al., 2008) and an 85-residue catabolite-repression protein (Crh) (Loquet et al., 2008). Most recently complete assignments were made for the 189-residue disulfide bond-forming enzyme DsbA (Sperling et al., 2010); this puts a huge number of biologically-relevant proteins within the potential size limit of this method.

15.3.1 Solid-State NMR and Pathological Amyloids

Determining atomic-level structures of amyloid has been a driving force in the development of solid-state NMR techniques. Amyloid is a highly-ordered filamentous protein aggregate that is rich in cross-β secondary structure and relatively resistant to proteases and denaturant. Cross β means that the protein monomers of the amyloid are arranged such that their β strands lie perpendicular to the fibre axis. Amyloid fibres are generally on the order of 2–20 nm in diameter and can be up to many micrometers in length (dimensions similar to many extracellular adhesin structures). The accumulation of amyloid in various tissues is associated with many human diseases that frequently have late age onset and poor prognoses, such as Alzheimer's and Parkinson's diseases. Because amyloid aggregates are intrinsically non-crystalline they are not amenable to x-ray crystallography, so solid-state NMR has been the most powerful method for gaining structural information.

Much work has focused on amyloid-beta (Aβ) peptide associated with Alzheimer's disease. Solid-state NMR studies of high molecular-weight amyloid fibres composed of either the 40 or 42-residue Aβ peptide reveal that individual peptides form β arches that stack and hydrogen bond in parallel and in register,

forming long β sheets that run the length of the fibre (Luhrs et al., 2005; Petkova et al., 2002, 2006). The benefit of working with a 40-residue peptide is that samples can be synthesized with very specific isotope labelling that facilitates NMR experimentation. Full-length proteins are usually produced as recombinant proteins from bacteria and thus they are more limited in the isotope labelling options. Solid-state NMR experiments with longer amyloid-forming polypeptides have generally been successful in determining structural characteristics of the amyloid, but do not necessarily yield atomic-level resolution. Solid-state NMR experiments with fibres of α-synuclein (residues 30–110), an amyloid-forming protein associated with Parkinson's disease, indicated that the amyloid is also based on in-register, parallel β-sheet stacking of polypeptides, but there were too few assignments and distance restraints to determine a high-resolution structure (Vilar et al., 2008).

Lastly, a typical problem with amyloid is that there is a high degree of structural heterogeneity within samples, resulting in spectra that are difficult to interpret. This is believed to be at least partly a consequence of the amyloid being composed of many different structural variants. Solid-state NMR techniques have been applied to several different yeast prion amyloids (Baxa et al., 2007; Shewmaker et al., 2009a, 2006; Wickner et al., 2008), but the resolution is thus far not sufficient for atomic-level model building. However, since filamentous adhesin structures are not the consequence of misfolding, they may not have the structural heterogeneity typical of many amyloid samples.

15.3.2 Application of Solid-State NMR to Curli

Curli of *Enterobacteriaceae* are a type of adhesin that assembles into long curly fibres that share the characteristics of amyloid. Since many human diseases are associated with amyloid accumulation in tissue, it has traditionally been considered an aberrant phenomenon. Curli however belong to a small but growing class of functional amyloids (for a review see Epstein and Chapman, 2008; Fowler et al., 2007), which are proteins that are amyloid in their native state. Curli of *E. coli* are essentially homopolymers of the secreted protein CsgA. (Another protein, CsgB, is necessary for initial fibre seeding and cell attachment (Hammer et al., 2007), but is a minor component of the mature fibre).

The structural basis of CsgA polymerization into fibres is largely unknown. It is not obviously through a mechanism of donor strand exchange because deletion of any region of the protein does not abolish fibre formation in vitro (Wang et al., 2008); even individual repeats can polymerize into amyloid fibres. Because the CsgA protein is so prone to amyloid formation, it is not clear that any small change or truncation could trap the protein in a folded monomeric and soluble state that resembles the individual monomer structure in the functional amyloid. As a result, the protein is not amenable to x-ray crystallography nor to solution NMR methods.

Solid-state NMR was recently used to characterize the structure of CsgA in the amyloid state (Shewmaker et al., 2009b). It was hypothesized that functional

amyloids would yield higher quality NMR data because they would lack the structural variation observed in pathological amyloids (see HET-s below). However, uniformly ^{15}N, ^{13}C-lableled CsgA amyloid did not yield sufficiently sharp line widths in the NMR spectra for structure assignment. This could be an artefact from using spontaneously-formed amyloid after removing CsgA from denaturant. It is possible that natively-assembled CsgA, purified from curliated *E. coli*, would maintain a more homogeneous structure. Nevertheless, the solid-state NMR data provided distance information between specific amino acid groups, leading the authors to conclude that individual CsgA monomers are likely to fold as β solenoids within the larger fibre structure.

Like CsgA, TasA of the Gram-positive bacterium *Bacillus subtilis* was recently shown to form an extracellular, functional amyloid (Romero et al., 2010). These fibres are 10–15 nm in diameter and are a core component of the bacterial biofilm. TasA and other functional amyloids of biofilms are likely interesting candidates for applying the current techniques of solid-state NMR.

15.3.3 HET-s Prion Amyloid Structure

Structural studies of the prion protein HET-s offer perhaps the best example of the possibilities of using solid-state NMR on bacterial adhesins. The HET-s protein of the fungus *Podospora anserina* is a naturally-occurring prion (Coustou et al., 1997) that adopts a self-propagating amyloid conformation when in the prion state (Balguerie et al., 2003). The conformational state of HET-s influences heterokaryon compatibility, a natural cell-fusion process in filamentous fungi. HET-s is 289 amino acids in length, but only a segment in the C-terminus is necessary for its prion capability. The HET-$s^{218–289}$ truncation fragment is sufficient to propagate the prion in vivo, and incubation of recombinant HET-$s^{218–289}$ in vitro results in the formation of infectious filamentous structures (Fig. 15.1, left panel). These structures are morphologically similar to fimbrial adhesins; they are both non-covalent linear assemblies with comparable dimensions.

Solid-state NMR has been used effectively to elucidate the basis of the HET-s prion amyloid. Ritter et al. were the first to show by solid-state NMR that each HET-s polypeptide is arranged as a two-turn β solenoid in the fibril structure (Ritter et al., 2005). Further work from the same group developed a high-resolution structure for the amyloid core, including inter-subunit interactions that revealed how the monomers pack to form a filamentous structure (Wasmer et al., 2008). Each monomer has a triangular-shaped hydrophobic core formed by the wrapping of three β strands (Fig. 15.1, middle panel). The β strands stack in parallel, forming a left-handed solenoid structure and each monomer stacks linearly with the next monomer, creating a filament with parallel β sheets running the length of the fibre (Fig. 15.1, right panel).

The elucidation of HET-s subunit structure in the context of large insoluble amyloid fibres is a huge step forward for the application of solid-state NMR. Moreover,

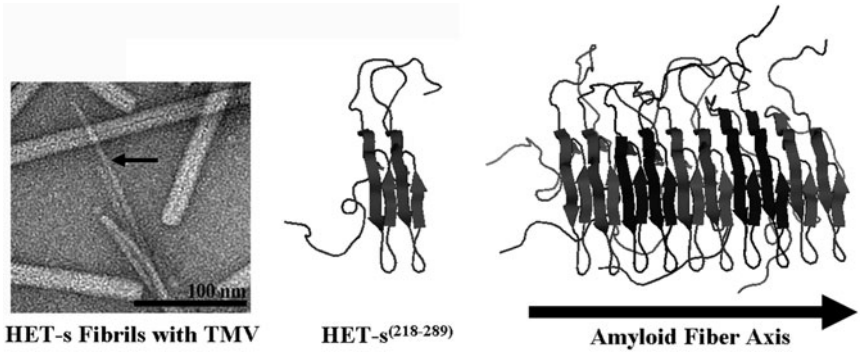

Fig. 15.1 The prion HET-s forms fibrils composed of repeating β-solenoid subunits. The panel on the left is an electron micrograph of the infectious fibrils (indicated with *arrow*) formed by the prion domain of HET-s (residues 218–289). The *middle panel* shows a ribbon cartoon of the structure of the HET-s prion domain that was solved using solid-state NMR (Wasmer et al., 2008). Each monomer forms a β solenoid composed of two helical turns of the polypeptide, with strands aligning in parallel β sheets. (PDB: 2RNM). The *right panel* shows how the amyloid is formed by the stacking of the individual β solenoids

the structural basis for fibre assembly was discerned based on inter-subunit distance restraints. A possible reason that solving the HET-s structure preceded the elucidation of some other amyloid structures may be because HET-s is a functional amyloid and does not appear to have the structural heterogeneity that is observed in aberrant amyloids. This would result in narrower line widths and more easily interpreted NMR spectra. In the case of bacterial fimbrial structures, they are composed of regularly folded subunits and likely will not display the structural heterogeneity that is problematic with some amyloid structures. HET-s monomers are nearly half the size of major fimbrial subunits like FimA and PapA. However, complete chemical shift assignments were recently achieved for the 189-residue periplasmic DsbA protein using solid-state NMR (Sperling et al., 2010), thus putting many fimbrial proteins within the applicable range of solid-state NMR.

15.4 Concluding Remarks

As listed above, there are many examples of NMR techniques applied to the study of bacterial adhesins. NMR offers an obvious alternative for structure determination when there are problems with crystallization, but also offers a straightforward method for studying binding interfaces with ligands and receptors in solution. There is also the added benefit of avoiding crystallization artefacts. For example, in an attempt to form crystals of a short, trimeric AfaE-III complex, a non-linear cyclic arrangement was observed (Pettigrew et al., 2004), which possessed non-native intra- and inter-domain contacts.

There are several good examples of pilus/fimbria models in the literature (Craig et al., 2003). For example, the major pilin subunit CfaB of enterotoxigenic *E. coli* (ETEC) polymerizes into fimbriae used for attachment to epithelial cells. Elegant CfaB fibre models have been constructed by using electron microscopy and image reconstruction (Mu et al., 2008), and models can be further supplemented with x-ray diffraction data (Li et al., 2009). Similarly, electron microscopy and image reconstruction have created models for the P pilus formed by PapA (Mu and Bullitt, 2006; Mu et al., 2005). These models are very informative, but can still lack important atomic-level information of the subunits in their native environments. While x-ray crystal data may not lack in atomic-level information, in many cases the data are collected on artificially truncated or fused proteins. Likewise, solution NMR has similar disadvantages of requiring many adhesin proteins to be truncated in order that they stay soluble. Solid-state NMR will offer an approach to obtain atomic-level information of protein subunits in the context of their native fibres. Due to the latest technical advances, polymeric adhesins that form fimbrial structures should be within the reach of solid-state NMR techniques, which are poised to play an important role in the study of bacterial adhesins.

References

Alphonse S, Durand E, Douzi B, Waegele B, Darbon H, Filloux A, Voulhoux R, Bernard C (2009) Structure of the *Pseudomonas aeruginosa* XcpT pseudopilin, a major component of the type II secretion system. J Struct Biol 169:75–80

Anderson KL, Billington J, Pettigrew D, Cota E, Simpson P, Roversi P, Chen HA, Urvil P, du Merle L, Barlow PN, Medof ME, Smith RA, Nowicki B, Le Bouguénec C, Lea SM, Matthews S (2004) An atomic resolution model for assembly, architecture, and function of the Dr adhesins. Mol Cell 15:647–657

Audette GF, Irvin RT, Hazes B (2004) Crystallographic analysis of the *Pseudomonas aeruginosa* strain K122-4 monomeric pilin reveals a conserved receptor-binding architecture. Biochemistry 43:11427–11435

Balguerie A, Dos Reis S, Ritter C, Chaignepain S, Coulary-Salin B, Forge V, Bathany K, Lascu I, Schmitter JM, Riek R, Saupe SJ (2003) Domain organization and structure-function relationship of the HET-s prion protein of *Podospora anserina*. EMBO J 22:2071–2081

Barnhart MM, Pinkner JS, Soto GE, Sauer FG, Langermann S, Waksman G, Frieden C, Hultgren SJ (2000) PapD-like chaperones provide the missing information for folding of pilin proteins. Proc Natl Acad Sci USA 97:7709–7714

Batchelor M, Prasannan S, Daniell S, Reece S, Connerton I, Bloomberg G, Dougan G, Frankel G, Matthews S (2000) Structural basis for recognition of the translocated intimin receptor (Tir) by intimin from enteropathogenic *Escherichia coli*. EMBO J 19:2452–2464

Baxa U, Wickner RB, Steven AC, Anderson DE, Marekov LN, Yau WM, Tycko R (2007) Characterization of β-sheet structure in Ure2p1-89 yeast prion fibrils by solid-state nuclear magnetic resonance. Biochemistry 46:13149–13162

Castellani F, van Rossum BJ, Diehl A, Rehbein K, Oschkinat H (2003) Determination of solid-state NMR structures of proteins by means of three-dimensional ^{15}N-^{13}C-^{13}C dipolar correlation spectroscopy and chemical shift analysis. Biochemistry 42:11476–11483

Castellani F, van Rossum B, Diehl A, Schubert M, Rehbein K, Oschkinat H (2002) Structure of a protein determined by solid-state magic-angle-spinning NMR spectroscopy. Nature 420: 98–102

Choudhury D, Thompson A, Stojanoff V, Langermann S, Pinkner J, Hultgren SJ, Knight SD (1999) X-ray structure of the FimC-FimH chaperone-adhesin complex from uropathogenic *Escherichia coli*. Science 285:1061–1066

Cota E, Jones C, Simpson P, Altroff H, Anderson KL, du Merle L, Guignot J, Servin A, Le Bouguénec C, Mardon H, Matthews S (2006) The solution structure of the invasive tip complex from Afa/Dr fibrils. Mol Microbiol 62:356–366

Coustou V, Deleu C, Saupe S, Begueret J (1997) The protein product of the het-s heterokaryon incompatibility gene of the fungus *Podospora anserina* behaves as a prion analog. Proc Natl Acad Sci USA 94:9773–9778

Craig L, Taylor RK, Pique ME, Adair BD, Arvai AS, Singh M, Lloyd SJ, Shin DS, Getzoff ED, Yeager M, Forest KT, Tainer JA (2003) Type IV pilin structure and assembly: x-ray and EM analyses of *Vibrio cholerae* toxin-coregulated pilus and *Pseudomonas aeruginosa* PAK pilin. Mol Cell 11:1139–1150

Epstein EA, Chapman MR (2008) Polymerizing the fibre between bacteria and host cells: the biogenesis of functional amyloid fibres. Cell Microbiol 10:1413–1420

Forest KT (2005) Structure and assembly of type IV pilins. In: Waksman G, Caparon M, Hultgren S (eds) Structural biology of bacterial pathogenesis. ASM Press, Washington, DC, pp 81–100

Fowler DM, Koulov AV, Balch WE, Kelly JW (2007) Functional amyloid – from bacteria to humans. Trends Biochem Sci 32:217–224

Franks WT, Zhou DH, Wylie BJ, Money BG, Graesser DT, Frericks HL, Sahota G, Rienstra CM (2005) Magic-angle spinning solid-state NMR spectroscopy of the beta1 immunoglobulin binding domain of protein G (GB1): ^{15}N and ^{13}C chemical shift assignments and conformational analysis. J Am Chem Soc 127:12291–12305

Golovanov AP, Balasingham S, Tzitzilonis C, Goult BT, Lian LY, Homberset H, Tonjum T, Derrick JP (2006a) Assignment of ^{1}H, ^{13}C, and ^{15}N resonances for the PilP pilot protein from *Neisseria meningitidis*. J Biomol NMR 36(Suppl 1):68

Golovanov AP, Balasingham S, Tzitzilonis C, Goult BT, Lian LY, Homberset H, Tonjum T, Derrick JP (2006b) The solution structure of a domain from the Neisseria meningitidis lipoprotein PilP reveals a new β-sandwich fold. J Mol Biol 364: 186–195

Gossert AD, Bettendorff P, Puorger C, Vetsch M, Herrmann T, Glockshuber R, Wüthrich K (2008) NMR structure of the *Escherichia coli* type 1 pilus subunit FimF and its interactions with other pilus subunits. J Mol Biol 375:752–763

Gossert AD, Hiller S, Fiorito F, Wüthrich K (2007) NMR assignment of the *E. coli* type 1 pilus protein FimF. J Biomol NMR 38:195

Hammer ND, Schmidt JC, Chapman MR (2007) The curli nucleator protein, CsgB, contains an amyloidogenic domain that directs CsgA polymerization. Proc Natl Acad Sci USA 104: 12494–12499

Hazes B, Sastry PA, Hayakawa K, Read RJ, Irvin RT (2000) Crystal structure of *Pseudomonas aeruginosa* PAK pilin suggests a main-chain-dominated mode of receptor binding. J Mol Biol 299:1005–1017

Hedenstrom M, Emtenäs H, Pemberton N, Aberg V, Hultgren SJ, Pinkner JS, Tegman V, Almqvist F, Sethson I, Kihlberg J (2005) NMR studies of interactions between periplasmic chaperones from uropathogenic *E. coli* and pilicides that interfere with chaperone function and pilus assembly. Org Biomol Chem 3:4193–4200

Keizer DW, Slupsky CM, Kalisiak M, Campbell AP, Crump MP, Sastry PA, Hazes B, Irvin RT, Sykes BD (2001) Structure of a pilin monomer from *Pseudomonas aeruginosa*: implications for the assembly of pili. J Biol Chem 276:24186–24193

Kelly G, Prasannan S, Daniell S, Fleming K, Frankel G, Dougan G, Connerton I, Matthews S (1999) Structure of the cell-adhesion fragment of intimin from enteropathogenic *Escherichia coli*. Nat Struct Biol 6:313–318

Korotkova N, Cota E, Lebedin Y, Monpouet S, Guignot J, Servin AL, Matthews S, Moseley SL (2006) A subfamily of Dr adhesins of *Escherichia coli* bind independently to decay-accelerating factor and the N-domain of carcinoembryonic antigen. J Biol Chem 281: 29120–29130

Korotkova N, Yang Y, Le Trong I, Cota E, Demeler B, Marchant J, Thomas WE, Stenkamp RE, Moseley SL, Matthews S (2008) Binding of Dr adhesins of *Escherichia coli* to carcinoembryonic antigen triggers receptor dissociation. Mol Microbiol 67:420–434

Korukottu J, Schneider R, Vijayan V, Lange A, Pongs O, Becker S, Baldus M, Zweckstetter M (2008) High-resolution 3D structure determination of kaliotoxin by solid-state NMR spectroscopy. PLoS One 3:e2359

Li YF, Poole S, Nishio K, Jang K, Rasulova F, McVeigh A, Savarino SJ, Xia D, Bullitt E (2009) Structure of CFA/I fimbriae from enterotoxigenic *Escherichia coli*. Proc Natl Acad Sci USA 106:10793–10798

Loquet A, Bardiaux B, Gardiennet C, Blanchet C, Baldus M, Nilges M, Malliavin T, Böckmann A (2008) 3D structure determination of the Crh protein from highly ambiguous solid-state NMR restraints. J Am Chem Soc 130:3579–3589

Luhrs T, Ritter C, Adrian M, Riek-Loher D, Bohrmann B, Dobeli H, Schubert D, Riek R (2005) 3D structure of Alzheimer's amyloid-β(1–42) fibrils. Proc Natl Acad Sci USA 102:17342–17347

Mu XQ, Bullitt E (2006) Structure and assembly of P-pili: a protruding hinge region used for assembly of a bacterial adhesion filament. Proc Natl Acad Sci USA 103:9861–9866

Mu XQ, Jiang ZG, Bullitt E (2005) Localization of a critical interface for helical rod formation of bacterial adhesion P-pili. J Mol Biol 346:13–20

Mu XQ, Savarino SJ, Bullitt E (2008) The three-dimensional structure of CFA/I adhesion pili: traveler's diarrhea bacteria hang on by a spring. J Mol Biol 376:614–620

Nishiyama M, Horst R, Eidam O, Herrmann T, Ignatov O, Vetsch M, Bettendorff P, Jelesarov I, Grütter MG, Wüthrich K, Glockshuber R, Capitani G (2005) Structural basis of chaperone-subunit complex recognition by the type 1 pilus assembly platform FimD. EMBO J 24: 2075–2086

Nishiyama M, Vetsch M, Puorger C, Jelesarov I, Glockshuber R (2003) Identification and characterization of the chaperone-subunit complex-binding domain from the type 1 pilus assembly platform FimD. J Mol Biol 330:513–525

Parge HE, Forest KT, Hickey MJ, Christensen DA, Getzoff ED, Tainer JA (1995) Structure of the fibre-forming protein pilin at 26 A resolution. Nature 378:32–38

Pellecchia M, Guntert P, Glockshuber R, Wüthrich K (1998) NMR solution structure of the periplasmic chaperone FimC. Nat Struct Biol 5:885–890

Pellecchia M, Sebbel P, Hermanns U, Wüthrich K, Glockshuber R (1999) Pilus chaperone FimC-adhesin FimH interactions mapped by TROSY-NMR. Nat Struct Biol 6:336–339

Petkova AT, Ishii Y, Balbach JJ, Antzutkin ON, Leapman RD, Delaglio F, Tycko R (2002) A structural model for Alzheimer's β-amyloid fibrils based on experimental constraints from solid state NMR. Proc Natl Acad Sci USA 99:16742–16747

Petkova AT, Yau WM, Tycko R (2006) Experimental constraints on quaternary structure in Alzheimer's β-amyloid fibrils. Biochemistry 45:498–512

Pettigrew D, Anderson KL, Billington J, Cota E, Simpson P, Urvil P, Rabuzin F, Roversi P, Nowicki B, du Merle L, Le Bouguénec C, Matthews S, Lea SM (2004) High resolution studies of the Afa/Dr adhesin DraE and its interaction with chloramphenicol. J Biol Chem 279:46851–46857

Ramboarina S, Fernandes PJ, Daniell S, Islam S, Simpson P, Frankel G, Booy F, Donnenberg MS, Matthews S (2005) Structure of the bundle-forming pilus from enteropathogenic *Escherichia coli*. J Biol Chem 280:40252–40260

Ramboarina S, Fernandes P, Simpson P, Frankel G, Donnenberg M, Matthews S (2004) Complete resonance assignments of bundlin (BfpA) from the bundle-forming pilus of enteropathogenic *Escherichia coli*. J Biomol NMR 29:427–428

Ritter C, Maddelein ML, Siemer AB, Luhrs T, Ernst M, Meier BH, Saupe SJ, Riek R (2005) Correlation of structural elements and infectivity of the HET-s prion. Nature 435:844–848

Romero D, Aguilar C, Losick R, Kolter R (2010) Amyloid fibers provide structural integrity to *Bacillus subtilis* biofilms. Proc Natl Acad Sci USA 107:2230–2234

Sauer FG, Fütterer K, Pinkner JS, Dodson KW, Hultgren SJ, Waksman G (1999) Structural basis of chaperone function and pilus biogenesis. Science 285:1058–1061

Shewmaker F, Kryndushkin D, Chen B, Tycko R, Wickner RB (2009a) Two prion variants of Sup35p have in-register parallel β-sheet structures, independent of hydration. Biochemistry 48:5074–5082

Shewmaker F, McGlinchey RP, Thurber KR, McPhie P, Dyda F, Tycko R, Wickner RB (2009b) The functional curli amyloid is not based on in-register parallel β-sheet structure. J Biol Chem 284:25065–25076

Shewmaker F, Wickner RB, Tycko R (2006) Amyloid of the prion domain of Sup35p has an in-register parallel β-sheet structure. Proc Natl Acad Sci USA 103:19754–19759

Sperling LJ, Berthold DA, Sasser TL, Jeisy-Scott V, Rienstra CM (2010) Assignment strategies for large proteins by magic-angle spinning NMR: the 21-kDa disulfide-bond-forming enzyme DsbA. J Mol Biol 399:268–282

Sung MA, Chen HA, Matthews S (2001a) Sequential assignment and secondary structure of the triple-labelled carbohydrate-binding domain of papG from uropathogenic *E. coli*. J Biomol NMR 19:197–198

Sung MA, Fleming K, Chen HA, Matthews S (2001b) The solution structure of PapGII from uropathogenic *Escherichia coli* and its recognition of glycolipid receptors. EMBO Rep 2: 621–627

Tycko R (2006) Molecular structure of amyloid fibrils: insights from solid-state NMR. Q Rev Biophys 39:1–55

Velarde JJ, Varney KM, Inman KG, Farfan M, Dudley E, Fletcher J, Weber DJ, Nataro JP (2007) Solution structure of the novel dispersin protein of enteroaggregative *Escherichia coli*. Mol Microbiol 66:1123–1135

Vilar M, Chou HT, Luhrs T, Maji SK, Riek-Loher D, Verel R, Manning G, Stahlberg H, Riek R (2008) The fold of β-synuclein fibrils. Proc Natl Acad Sci USA 105:8637–8642

Waksman G, Hultgren SJ (2009) Structural biology of the chaperone-usher pathway of pilus biogenesis. Nat Rev Microbiol 7:765–774

Wang X, Hammer ND, Chapman MR (2008) The molecular basis of functional bacterial amyloid polymerization and nucleation. J Biol Chem 283:21530–21539

Wasmer C, Lange A, Van Melckebeke H, Siemer AB, Riek R, Meier BH (2008) Amyloid fibrils of the HET-s(218–289) prion form a β solenoid with a triangular hydrophobic core. Science 319:1523–1526

Wickner RB, Dyda F, Tycko R (2008) Amyloid of Rnq1p, the basis of the [PIN+] prion, has a parallel in-register β-sheet structure. Proc Natl Acad Sci USA 105:2403–2408

Xu XF, Tan YW, Lam L, Hackett J, Zhang M, Mok YK (2004) NMR structure of a type IVb pilin from *Salmonella typhi* and its assembly into pilus. J Biol Chem 279:31599–31605

Zavialov AV, Berglund J, Pudney AF, Fooks LJ, Ibrahim TM, MacIntyre S, Knight SD (2003) Structure and biogenesis of the capsular F1 antigen from *Yersinia pestis*: preserved folding energy drives fiber formation. Cell 113:587–596

Zech SG, Wand AJ, McDermott AE (2005) Protein structure determination by high-resolution solid-state NMR spectroscopy: application to microcrystalline ubiquitin. J Am Chem Soc 127:8618–8626

Chapter 16
Electron Microscopy Techniques to Study Bacterial Adhesion

Iwan Grin, Heinz Schwarz, and Dirk Linke

Abstract Since its introduction 70 years ago electron microscopy has become an invaluable tool for microbiology and the study of bacterial interaction. Technological development over the past decades has enabled researchers to resolve smaller and smaller details in bacterial samples, while new preparation techniques like cryo preparation now allow to investigate bacteria even closer to their natural state. In this chapter we give a brief overview of electron microscopy techniques suitable for the investigation of bacterial adhesion at molecular as well as cellular level and a short outlook on future technologies relevant to the field.

16.1 Introduction

Since the days of natural philosophy, new technologies have revolutionized our view of biology by enabling researchers to gain new insights into the inner workings of nature. Nowhere is this more apparent than in the field of microscopy. When the first light microscopes were developed in the 16th century, the discovery of bacteria opened a vast new field of research – microbiology. Centuries later, the light microscope was instrumental in the discoveries of Koch and coworkers, who found bacteria to be the causative agent of many diseases and ailments.

Still there were some cases where the infectious principle was not visible under even the best light microscopes. After the transmission electron microscope (TEM) was introduced in 1931 by Ernst Ruska, the first images of bacteria (von Borries et al. 1938) and of bacterial flagella (Piekarski and Ruska, 1939) were published. In parallel, scanning electron microscopy (SEM) was pioneered by von Ardenne (1940); however, commercial SEM systems were only introduced in the 1960s. This

D. Linke (✉)
Department of Protein Evolution, Max Planck Institute for Developmental Biology, 72076 Tübingen, Germany
e-mail: dirk.linke@tuebingen.mpg.de

D. Linke, A. Goldman (eds.), *Bacterial Adhesion*, Advances in Experimental Medicine and Biology 715, DOI 10.1007/978-94-007-0940-9_16,

new and detailed structural information again changed the view of biology, and specifically of cell biology and microbiology, dramatically.

Further development of electron microscopy technology and also of sample preparation techniques over the past 70 years allowed researchers to push the resolution limit further and further. Today, the resolution of electron microscopes has reached sub-nanometer scale. Still, some physical limitations of the method that is based on the use of electrons for imaging cannot be overcome. The low mass of the electrons leads to scattering and absorption in air, and therefore the electron beam can only be propagated in a vacuum. Moreover, for transmission electron microscopy the samples must be sufficiently thin, while for scanning electron microscopy, imaging is restricted to the surface of the sample.

For the study of bacterial adhesion, a broad spectrum of preparation methods is available (Knutton, 1995; Pilhofer et al., 2010). In this chapter, we describe the imaging of isolated adhesion molecules, of bacterial appendages on the surface of bacterial cells, and of the interaction of bacteria with their eukaryotic host cells. We show which preparation methods are suitable for use with the different EM imaging techniques.

16.2 Overview of Imaging Methods

SEM is very well suited to provide a quick overview of the sample, as well as capturing surface details of the specimens. While the electrons are not able to penetrate deep into the sample by themselves, fracturing and etching techniques have been developed to expose the interior of cells as a surface, which can then be imaged by SEM. SEM is also compatible with immunolabelling techniques to label specific features on the surface of cells.

TEM excels at resolving structural details in a two-dimensional plane, but gives only very limited depth information. If the specimens are thin enough, as is the case with many bacteria, it is possible to image them as whole-mount. Naturally, the interior of the cell is too dense to resolve details, but surface appendages, filaments and extracellular material can be visualized around the cells. Information on the interior structure of the cells can be gained by sectioning cells and examining the sections. As a section contains a very thin slice of the bacterial surface, it may be difficult to visualize membrane-bound or extracellular objects, e.g. flagella, especially if these are not aligned in the plane of the section. Both whole-mount and sectioning techniques are compatible with immunolabelling.

16.3 Scanning Electron Microscopy

As SEM visualizes surfaces directly, it is very well suited to observe the structures and interactions relevant in bacterial adhesion. The resulting images can be interpreted intuitively as they contain three-dimensional information just as a

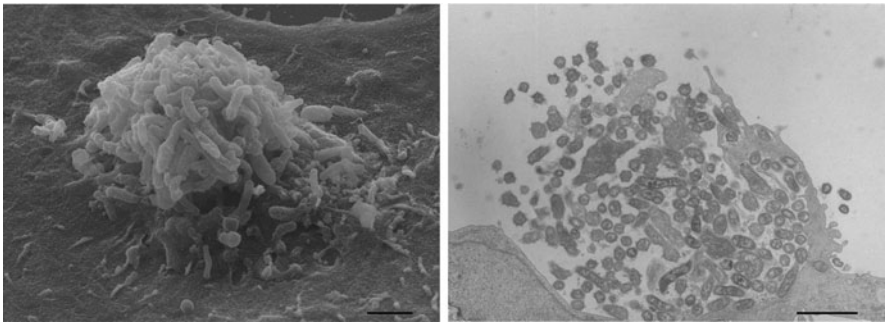

Fig. 16.1 Aggregation of *Bartonella henselae* on the surface of a human umbilical vein endothelial cell in SEM (*left panel*) and as seen in a thin section in TEM (*right panel*). Cells provided by Christoph Dehio, micrographs by Jürgen Berger and Heinz Schwarz. Bars: 2 μm. See also Dehio et al. (1997)

conventional photograph. In contrast to TEM, large objects can be imaged as a whole, limited only by the size of the sample chamber of the microscope. In the context of bacterial adhesion SEM can be used to investigate bacterial cells attached to artificial surfaces like medical implants and devices or to host cells. Furthermore, interactions of bacteria e.g. in biofilms or even appendages of single cells can be studied (Fig. 16.1).

In routine SEM samples are fixed, dehydrated and sputter-coated with a thin metal layer to create a conductive surface and to increase the signal. This signal is provided by the amount of secondary electrons released from the outer shell of the atoms hit by the primary beam of electrons. It correlates with their atomic number. Moreover, electrons of the illuminating beam can also be reflected by the nuclei of the atoms and are then detected separately as back-scattered electrons.

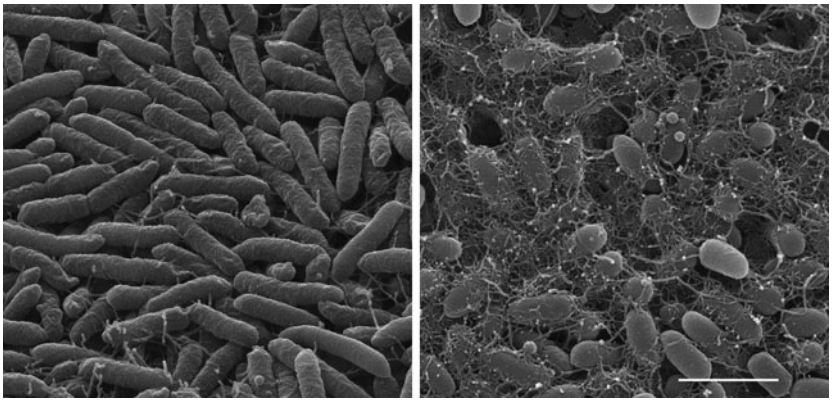

Fig. 16.2 Biofilms of *E. coli* 5K strain in SEM. Wild-type bacteria (*left*) and a mutant (*right*) producing more extracellular matrix (Picture by D. Röhrich). Bar 2 μm

It should be noted that the metal film is the major factor limiting the achievable resolution of SEM. In addition, the surface of interest can be obscured e.g. by cell debris from the culture medium or by particles precipitated onto the surface during fixation and preparation steps. While the first can be remedied by washing the sample under physiological conditions prior to fixation, the latter can be avoided by briefly centrifuging all solutions before use (Fig. 16.2).

For cryo-SEM, the best approach is actually to image freeze-fractured samples or freshly prepared surfaces of cryosectioned samples (block faces) with backscattered electrons at temperatures below 140 K after coating with a thin metal layer and a backing carbon layer (Walther et al., 1995). The use of block faces avoids the major drawbacks of inspecting cryosections, such as compression or crevasses. In addition the specimen is less radiation sensitive (Walther and Müller, 1999).

16.4 Transmission Electron Microscopy

The power of TEM, as became apparent soon after its discovery, is the ability to visualize details of objects down to the level of molecules. Here, viruses (pox virus, tobacco mosaic virus (TMV), bacteriophages) and bacterial appendages like flagella were visualized for the first time. These objects were very well suited for observation due to their thickness, which was thin enough to "see through" yet electron dense enough to give sufficient contrast. Nevertheless, the generally low contrast of biological samples has driven the development of staining techniques to improve contrast as described below. Thick objects, starting from bacteria, are too dense to image internal details directly. Therefore they must be embedded and sectioned for subsequent imaging of their interior.

Historically, the first contrasting methods developed were OsO_4 vapor fixation and much more importantly metal shadowing using platinum (Fig. 16.3).

This enhanced the visualization of thin structures such as flagella or other surface appendages of bacteria. However, internal details are obscured by the metal covering the surface. Moreover the underlying biological material reduces the achievable

Fig. 16.3 *Proteus mirabilis* after filtration on collodium film on top of agar plate and subsequent shadowing with platinum. TEM image (taken 1966) provided by Hermann Frank, formerly Max Planck Institute for Virus Research, Tübingen

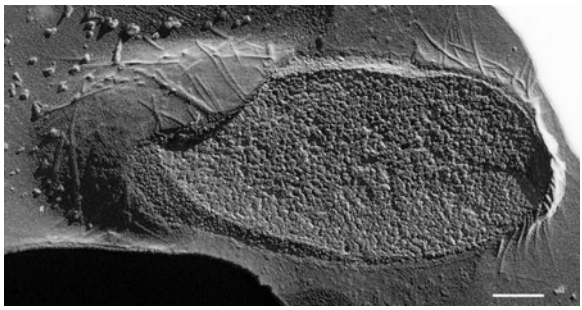

Fig. 16.4 TEM image of fimbriae on the surface of a freeze-fractured and freeze-etched *E. coli* bacterium. Bar 200 nm

resolution due to a high total thickness of the sample. Removal of the biological material by acid or detergent treatment produces a metal replica of the sample surface which results in improved resolution and contrast. This effect is particularly prominent in the case of freeze-fracture replicas. As cells fracture preferentially in the lipid layer of the membranes, a subsequent etching or freeze-drying step is required to expose the molecules on the cell surface (Fig. 16.4).

Internal details of thin objects such as viruses, but also molecular complexes (flagella, antibodies, proteasome), can be visualized using the negative staining method (Brenner and Horne, 1959). This method is particularly powerful with uniform (purified) material, where image processing and single particle analysis can be applied (See Chapter 17). Potential drawbacks are the superimposition of structural information which may complicate image interpretation. Furthermore structures binding heavy metal in similar amounts as the surrounding negative stain cannot be distinguished (Fig. 16.5).

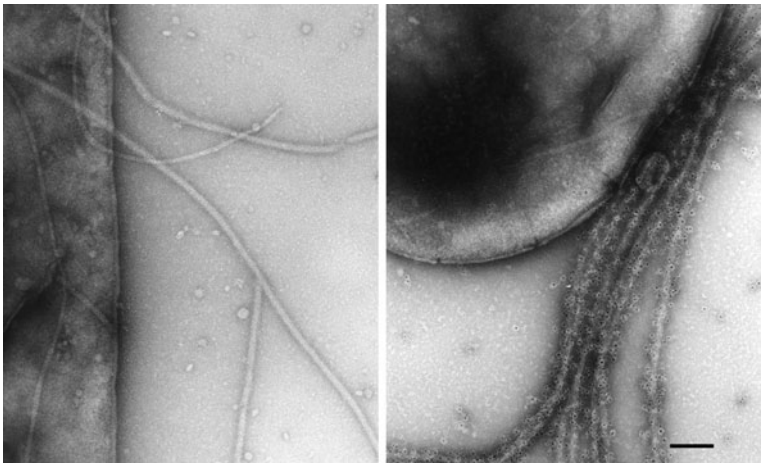

Fig. 16.5 *E. coli* cells negatively stained with phosphor tungstic acid. Bacteria before (*left*) and after labelling with a fimbriae-specific antibody and colloidal gold complexes (*right*). Micrographs provided by Hans Gelderblom. Bar 100 nm. For details see Beutin et al. (2005)

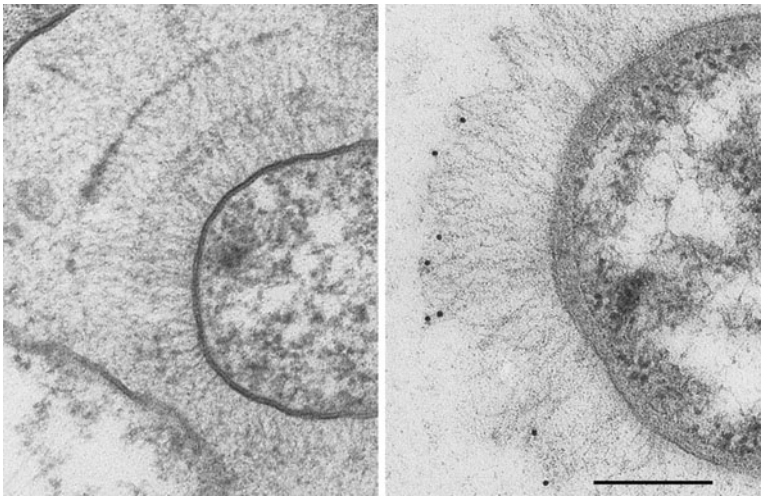

Fig. 16.6 Thin sections of *Bartonella henselae* embedded in EPON showing the 240 nm long BadA adhesion molecules (*left*). On methacrylate Lowicryl HM20 sections (*right*), the head region of BadA is labelled with an antibody raised against the C-terminal head fragment in combination with colloidal gold complexes. Bar 200 nm. See also Szczesny et al. (2008)

The inspection of thin sections of embedded material allows in situ imaging of biological molecules. In the case of standard resin embedding, the structures of interest have to be selectively stained with heavy metals to provide contrast against the resin. If this is not possible because the target molecules do not bind the metal, visualization can only be achieved by indirect methods like immunolabelling or histochemical staining (Fig. 16.6).

The requirement of ultra-thin sections for TEM makes the technique unsuitable for direct investigation of thick samples. As a consequence, the sectioning hinders the observation of flexible appendages (flagella etc.) or surface features of cells, because the observed space is inherently limited to two-dimensional sections. Unlike SEM, the visualization of three-dimensional structure in TEM requires additional procedures. For molecules, single particle analysis methods have been successfully established (Frank, 2006). For bulk material either images of serial sections or of tilt series of thick sections must be used for computer-aided 3D-reconstruction (Koster et al., 1997; Geerts et al., 2008). Cryo TEM allows the visualisation of biological structures in a life-like frozen state without any chemical treatment, just by phase contrast imaging. Striking results were obtained with this approach for molecular complexes and complete viruses (Dubochet et al., 1988; Yamaguchi et al., 2008). Finally, electron crystallography can produce outstanding high resolution data. In cases where high quality two-dimensional crystals are available, it is possible to reach atomic resolution, as demonstrated e.g. for aquaporins, where a 1.9 Å structure is available (Gonen et al., 2005). Details of this technology are reviewed in Schenk et al. (2010).

16.5 Overview of Preparation Methods

For obvious reasons, the inspection of samples in vacuum does not allow imaging of living samples. The major component of all biological samples, water, must either be removed or frozen. In practice, samples are either fixed and dehydrated for inspection at ambient temperatures, or inspected in a frozen state in the microscope. Moreover, the light elements prevalent in biological systems do not scatter electrons sufficiently, requiring contrast enhancing measures like heavy metal staining or phase contrast imaging.

There is no one-size-fits-all electron microscopy method that can be applied to all questions and systems. This is partly due to the inherent differences in the information that can be gained by between SEM and TEM, but more importantly due to the characteristics of the underlying biological systems and the specifics of the question asked. Therefore the sample preparation protocol has to be adapted and optimized for every new experiment. It cannot be stressed enough, however, that the quality of the images critically depends on the quality of the biological sample itself (i.e. its "freshness" and purity), even more than on the quality of the sample preparation described in this chapter.

Generally, the choice between room temperature and cryogenic methods depends on the compatibility of the biological material with the preparation steps (desiccation, resin embedding) and may be limited by availability of the instrumentation. Figure 16.7 shows a representative selection of possible preparation methods for the

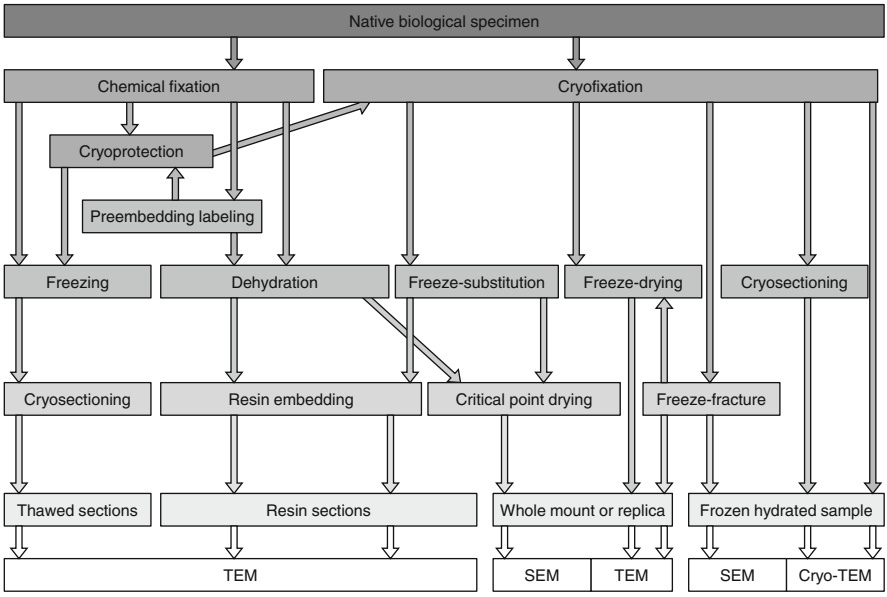

Fig. 16.7 Flow chart of possible preparation methods for the different microscopy techniques

different microscopy techniques. The choice of the right technique for an experiment is crucial for the desired outcome.

The first preparation step in biological electron microscopy is always the fixation of the object. This serves two main purposes: to arrest the samples in a distinct physiological state and to protect the biological structures from damage during subsequent preparation and imaging steps. It is of utmost importance to perform the fixation as close to the desired physiological conditions as possible. Particularly, the time between sample collection and fixation should be minimized.

The two fundamentally different ways of fixing samples are either chemical fixation or cryofixation. Chemical fixation is a routine method due to the low technical requirements in equipment and handling. Moreover, it is the only reliable way to inactivate infectious material for imaging. An intrinsic drawback is that the method is dependent on the diffusion of the fixative into the sample. Therefore the fixation process is not homogenous, particularly in larger samples.

In contrast, cryofixation allows immediate and simultaneous arrest of all biological processes – but it requires sophisticated equipment and is drastically limited by the thickness of the sample. While chemical fixation is intrinsically selective based on the chemistry of the fixative, cryofixation allows for a complete and indiscriminate (non-selective) arrest of all components in the sample.

16.6 Ambient Temperature Preparation Methods

Imaging rather stable structures such as molecular complexes, viruses and cell appendages (flagella or fimbriae) in TEM is straightforward as often demanding fixation and dehydration can be omitted. In the simplest case the sample is adsorbed as a rather diluted solution (e.g. 10–100 ng/ml) to hydrophilic support films mounted on grids, which are prepared freshly by glow-discharge. The sample is then air-dried. For efficient processing of bacterial cell suspensions, either embedding in agarose or gelatine, or filling into cellulose capillary tubes (Hohenberg et al., 1994) is useful.

SEM samples which already have a solid support, such as cells grown in a culture dish or bacteria attached to a medical device can be processed directly. In the case of bacterial cell suspensions, the cells must be immobilized on a surface e.g. on poly-L-lysine coated coverslips.

16.7 Chemical Fixation

There is a wealth of different protocols for chemical fixation in the literature, e.g. (Griffiths, 1993; Hayat, 1981, 2000). As any protocol needs to be adapted to the specific biological question, this chapter can only provide some general rules and

guidelines. The concept behind chemical fixation is the arrest of biological processes and the stabilization of structures via cross-linking of chemical groups in the sample. Typically, aldehydes are used to crosslink primary amines, mostly arginine and lysine moieties in proteins. In addition, OsO_4 reacts with C=C bonds and cross-links proteins and unsaturated fatty acids; however, OsO_4 shows proteolytic activity, particular at room or higher temperatures. Uranyl salts mainly cross-link phosphate groups in lipids and nucleic acids.

Suitable fixatives must react under the pH and temperature conditions given by the sample. As an example, the reaction of aldehydes with primary amino groups is strongly pH dependent and will not work under acidic conditions where the amines are protonated. The fixative of choice should specifically react with the sample and not with the buffer. Classical mistakes are the use of primary amino group-containing buffers such as Tris which completely and rapidly inactivates aldehyde fixatives, or phosphate based buffers which form insoluble precipitates with many heavy metal salts. Note also that sufficient time must be allowed for the fixative to penetrate the entire sample. This is primarily dependent on the sample thickness, but also on the permeability of the biological material for the fixative and the sample temperature.

16.8 Dehydration, Embedding and Sectioning for TEM

Typically, the water of bulk material is removed in a graded series of solvents like ethanol or acetone for the further processing steps such as embedding in resin for TEM or critical-point drying for SEM. However, proteins may be denatured and lipids are dissolved by the solvent. This effect can be reduced by dehydration of the samples at progressively lower temperatures (PLT method), e.g. by starting with 30% ethanol at 273 K, and later switching to 70–100% steps at 243 K and by the use of DMF (dimethylformamide) as solvent (Bayer et al., 1985) (Fig. 16.8).

For embedding, epoxy resins which are heat polymerized are routinely used. They show perfect sectioning properties as the resin monomers cross-link the biological material, which unfortunately often coincides with the loss of antigenicity for subsequent on-section labelling. In such cases, the use of methacrylates may be indicated as they react poorly with the biological material. Moreover, methacrylates can be polymerized by increased temperature or by UV even at low temperature (e.g. Lowicryl HM20 or K11M at 223 K).

In this context, the method of Tokuyasu (1973) should be mentioned. He infiltrated chemically fixed samples with 2.3 M sucrose, omitting the detrimental step of dehydration with solvents. Such samples are then frozen in liquid nitrogen. Sucrose acts as a cryoprotectant, preventing ice crystal growth, and as an embedding medium for subsequent cryosectioning at about 170 K. Thawed sections are mounted on grids for possible immunolabelling, always followed by a final embedding in a thin

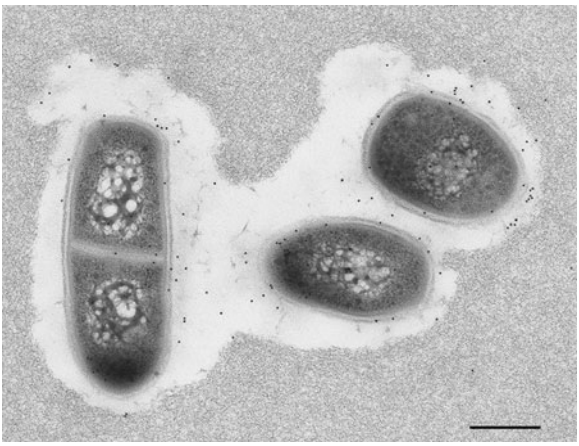

Fig. 16.8 The capsule of gelatine-embedded Rhodococcus bacteria can be visualized by using DMF (dimethylformamide) as a solvent during dehydration at progressively lower temperatures followed by low temperature embedding in Lowicryl K4M. On-section immunolabelling was performed using a monoclonal antibody against capsular polysaccharides in combination with colloidal gold complexes. Cells provided by Thomas Neu and Karl Poralla. Bar 500 nm. See also Neu and Poralla (1988)

layer of methyl cellulose containing uranyl acetate to stabilize structures and to create negative contrast (Tokuyasu, 1997).

16.9 Dehydration and Critical Point Drying for SEM

In addition to the general processing steps described above, samples for SEM inspection at ambient temperature must be critical point dried to remove organic solvents: fixed samples are dehydrated and the organic solvent is exchanged by liquid carbon dioxide in a pressure chamber above the critical point of carbon dioxide. Using this method, drying artifacts occurring at the transition of the liquid-gas phase boundary are avoided. As a final step a thin metal film is sputter-coated onto the sample to create a conductive surface and increase secondary electron emission. For structural studies, platinum or gold alloys are used. For the detection of gold particles in SEM by backscattered electrons immuno-labelled samples are coated with chromium.

16.10 Affinity Labelling

Molecules can be detected by affinity labelled antibodies, lectins or other probes which are typically visualized indirectly with the help of secondary antibodies bound to colloidal gold complexes. If the epitopes are accessible at the sample

surface, pre-embedding labelling is a valuable tool, especially when the embedding procedure abolishes the epitopes for antibody recognition. Epitopes within structures may be visualized by pre-embedding labelling of permeabilized samples or by post-embedding labelling of thawed cryosections (Tokuyasu, 1997) or thin plastic (in particular methacrylate) sections (Schwarz and Humbel, 2008). In all cases, the sections can be finally stained with uranium and lead salt solutions to enhance the structural contrast.

16.11 Cryopreparation Methods

Ice crystal growth during freezing and all subsequent preparation steps and even during imaging is a major problem in cryo-electron microscopy. Thin layers of material with a maximal thickness of 10 μm can be vitrified by plunge freezing in liquid ethane or propane at about 90 K. Thicker layers up to 200 μm must be frozen under high pressure (2100 bar) to avoid ice crystal formation. Special attention must be paid to adequate freezing at the exterior of bacterial cells: here, segregation patterns due to ice crystal growth can easily occur and alter the native structure of surface layers. In the worst cases, the use of non-osmotic cryoprotectants such as dextran or bovine serum albumin may be indicated.

Thin biological samples can be directly imaged in frozen-hydrated state in a cryo electron microscope at temperatures below 140 K, whereas thicker material has to be sectioned. Cryosectioning of native material is prone to cutting artifacts like compression, ruptures and crevices due to the rigid structure of frozen water. Nevertheless it is the only method available to visualize biological structures in their native state.

A useful compromise is the combination of cryofixation with subsequent freeze-substitution and resin embedding: here, the vitrified water is substituted by an organic solvent at low temperatures, where the biological structure is preserved and less organic material is extracted compared to room temperature dehydration. Fixatives can be added to the organic solvent, and will react and stabilize the sample, while still at subzero temperatures. The polymerization of the resins is the final step, and is done either with UV or heat activation as described above. The resin-embedded samples can then be sectioned and imaged at ambient temperature.

16.12 Recent Developments and Future Perspectives

Even today, electron microscopy technology improves, and will probably allow us to observe biological phenomena at even higher resolution very soon. Electron crystallography has already been mentioned in this context. Alternatively, the use of better phase contrast imaging conditions in TEM with the introduction of phase plates (Danev and Nagayama, 2010; Hosogi et al., 2011) and Cs-corrected lenses (Haider

et al., 2008) will certainly improve the achievable resolution for biological specimen and subsequent tomographic reconstructions.

Another encouraging development is X-ray microscopy using synchrotron radiation, mainly pioneered by the group of Schmahl (in Berlin) and of Larabell (in Berkeley) (Larabell and Nugent, 2010). In soft X-ray tomography, cells are imaged using photons from a region of the spectrum known as the "water window". This results in quantitative, high-contrast images of intact, fully hydrated frozen cells without the need to use contrast-enhancing agents. Using soft X-ray microscopy, projection images can be collected in less than 20 min. The actual achieved resolution of the tomograms is in the range of 20–50 nm. The object can be mounted in a capillary and therefore rotated freely without angular limitation. This is a big advantage over tilt series of thick sections in TEM tomography where the variable path length for the electrons under different tilt angles limits the maximum tilt to +/– 70 degrees and so reduces the practical resolution of the EM tomograms (McDermott et al., 2009).

References

Bayer ME, Carlemalm E, Kellenberger E (1985) Capsule of *Escherichia coli* K29: ultrastructural preservation and immunoelectron microscopy. J Bacteriol 162:985–991

Beutin L, Strauch E, Zimmermann S, Kaulfuss S, Schaudinn C, Männel A, Gelderblom HR (2005) Genetical and functional investigation of fliC genes encoding flagellar serotype H4 in wildtype strains of Escherichia coli and in a laboratory E. coli K-12 strain expressing flagellar antigen type H48. BMC Microbiol 5:4

Brenner S, Horne RW (1959) A negative staining method for high resolution eclectron microscopy of viruses. Biochim Biophys Acta 14:103–110

Danev R, Nagayama K (2010) Phase plates for transmission electron microscopy. Methods Enzymol 481:343–369

Dehio C, Meyer M, Berger J, Schwarz H, Lanz C (1997) Interaction of *Bartonella henselae* with endothelial cells results in bacterial accumulation and aggregation on the cell surface and the subsequent engulfment and internalisation of the bacterial aggregate by a well-defined structure, the invasome. J Cell Sci 110:2141–2154

Dubochet J, Adrian M, Chang JJ, Homo JC, Lepault J, McDowall AW, Schultz P (1988) Cryo-electron microscopy of vitrified specimens. Q Rev Biophys 21:129–228

Frank J (2006) Three-dimensional electron microscopy of macromolecular assemblies: visualization of biological molecules in their native state. Oxford University Press, Oxford

Geerts WJC, Humbel BM, Verkleij AJ (2008) 3-D electron tomography of cells and organelles. In: Cavalier A, Spehner D, Humbel BM (eds) Handbook of cryo-preparation methods for electron microscopy, chapter 21. CRC Press, Boca Raton, FL, pp 537–565

Gonen T, Cheng Y, Sliz P, Hiroaki Y, Fujiyoshi Y, Harrison SC, Walz T (2005) Lipid-protein interactions in double-layered two-dimensional AQP0 crystals. Nature 438:633–638

Griffiths G (1993) Fine structure immuno-cytochemistry. Springer, Berlin

Haider M, Müller H, Uhlemann S, Zach J, Loebau U, Hoeschen R (2008) Prerequisites for a Cc/Cs corrected ultrahigh resolution TEM. Ultramicroscopy 108:167–178

Hayat MA (1981) Fixation for biological electron microscopy. Academic, New York, NY

Hayat MA (2000) Principles and techniques of electron microscopy. Biological applications. Cambridge University Press, Cambridge

Hohenberg H, Mannweiler K, Müller M (1994) High-pressure freezing of cell suspensions in cellulose capillary tubes. J Microsc 175:34–43

Hosogi N, Shigematsu H, Terashima H, Homma M, Nagayama K (2011) Zernike phase contrast cryo-electron tomography of sodium-driven flagellar hook-basal bodies from *Vibrio alginolyticus*. J Struct Biol 173:67–76

Knutton S (1995) Electron microscopical methods in adhesion. Meth Enzymol 253:145–158

Koster AJ, Grimm R, Typke D, Hegerl R, Stoschek A, Walz J, Baumeister W (1997) Perspectives of molecular and cellular electron tomography. J Struct Biol 120:276–308

Larabell CA, Nugent KA (2010) Imaging cellular architecture with X-rays. Curr Opin Struct Biol 20:623-631

McDermott G, Le Gros MA, Knoechel CG, Uchida M, Larabell CA (2009) Soft X-ray tomography and cryogenic light microscopy: the cool combination in cellular imaging. Trends Cell Biol 19:587–595

Neu TR, Poralla K (1988) An amphiphilic polysaccharide from an adhesive Rhodococcus strain. FEMS Microbiol Lett 49:389–392

Piekarski G, Ruska H (1939) Übermikroskopische Darstellung von Bakteriengeisseln. Klin Wschr 18:383–386

Pilhofer M, Ladinski MS, McDowall AW, Jensen GJ (2010) Bacterial TEM: new insights from cryo-microscopy. Meth Cell Biol 96:21–45

Schenk AD, Hite RK, Engel A, Fujiyoshi Y, Walz T (2010) Electron crystallography and aquaporins. Methods Enzymol 483:91–119

Schwarz H, Humbel BM (2008) Correlative light and electron microscopy. In: Cavalier A, Spehner D, Humbel BM (eds) Handbook of cryo-preparation methods for electron microscopy, chapter 21. CRC Press, Boca Raton, FL, pp 537–565

Szczesny P, Linke D, Ursinus A, Bär K, Schwarz H, Riess TM, Kempf VA, Lupas AN, Martin J, Zeth K (2008) Structure of the head of the Bartonella adhesin BadA. PLoS Pathog 4(8):e1000119

Tokuyasu KT (1973) A technique for ultracryotomy of cell suspensions and tissues. J Cell Biol 57:551–565

Tokuyasu KT (1997) Immunocytochemistry on Ultrathin Cryosections. In: Spector DL, Goldman RD, Leinwand LA (eds) Cells – A Laboratory Manual, Chapter 131, Cold Spring Harbor Laboratory Press, pp 1–27

von Ardenne M (1940) Elektronen-Übermikroskopie. Springer, Berlin

von Borries B, Ruska E, Ruska H (1938) Bakterien und Virus in übermikroskopischer Aufnahme. Klin Wschr 17:921–925

Walther P, Müller M (1999) Biological ultrastructure as revealed by high resolution cyro-SEM by block faces after cryosectioning. J Microsc 196:279–287

Walther P, Wehrli E, Hermann R, Müller M (1995) Double layer coating for high resolution low temperature SEM. J Microsc 179:229–237

Yamaguchi M, Danev R, Nishiyama K, Sugawara K, Nagayama K (2008) Zernike phase contrast electron microscopy of ice-embedded influenza A virus. J Struct Biol 162:271–276

Chapter 17
EM Reconstruction of Adhesins: Future Prospects

Ferlenghi Ilaria and Fabiola Giusti

Abstract Both Gram-negative and Gram-positive pathogenic bacteria present a remarkable number of surface-exposed organelles and secreted toxins that allow them to control the primary stages of infection, bacterial attachment to host cell receptors and colonization. The mediators of these processes, called adhesins, form a heterogeneous group that varies in architecture, domain content and mechanism of binding. A full understanding of how adhesins mediate cellular adhesion and colonization requires quantitative functional assays to evaluate the strength of the binding interactions, as well as determination of the high-resolution three-dimensional structures of the molecules to provide the atomic details of the interactions. The combination of classical imaging techniques like X-ray crystallography and Nuclear Magnetic Resonance (NMR) with the emerging technique of single-particle electron cryomicroscopy has become a tremendously helpful tool to understand the three-dimensional structure at near atomic-level resolution of newly discovered adhesins and their complexes. A detailed study of the structure of these molecules, both isolated and expressed on bacterial surface is a fundamental requirement for understanding the adhesion mechanism to host cells. This chapter will focus on the structure determination of such surface-exposed protein structures in both Gram-negative and Gram-positive bacterial adhesins.

17.1 Introduction

17.1.1 Adhesins

Bacteria are among the most diverse living organisms and have adapted to a great variety of ecological environments, including the human body. Pathogenic bacteria, both Gram-negative and Gram-positive, present a remarkable number of

F. Ilaria (✉)
Novartis Vaccines and Diagnostics srl, 53100 Siena, Italy
e-mail: ilaria.ferlenghi@novartis.com

D. Linke, A. Goldman (eds.), *Bacterial Adhesion*, Advances in Experimental Medicine and Biology 715, DOI 10.1007/978-94-007-0940-9_17,

surface-exposed adhesins and secreted toxins that allow them to control many different niches throughout the course of infection. Adherence to the host is a key event in bacterial pathogenesis. The mediators of this process, called adhesins, form a heterogeneous group that varies in architecture, domain content and mechanism of binding. The complexity of the bacterial tools used for cell adhesion and invasion ranges from single monomeric proteins to intricate multimeric macromolecules that perform highly sophisticated functions.

A full understanding of how adhesins mediate cellular adhesion requires quantitative functional assays to evaluate the strength of the binding interactions, as well as high-resolution three-dimensional structures to provide the atomic details of the interactions. High-resolution structures of adhesins, by using the currently advanced procedures from the observation of biological structure and for image processing combined with 3D reconstruction, help elucidate their role in pathogenicity. A detailed study of the structure of these molecules, both isolated and expressed on the bacterial surface is a fundamental requirement for understanding the adhesion mechanism to host cells. This chapter will focus on structure determination using electron microscopy of such surface-exposed protein structures in both Gram-negative and Gram-positive bacteria.

17.2 Pili and Fimbriae

Non-flagellar appendages were first observed in bacteria in the early 1950s, when the outer–membrane surface of Gram-negative pathogens was scanned with the electron microscope (Houwink and Iterson, 1950; Duguid et al., 1955). Pili are 1 to 3 μm-long hair-like bacterial appendages with diameters ranging from 2 to 8 nm and are built by protein subunits called fimbrins or pilins. Pili can be classified on the basis of physical properties, antigenic determinants, adhesion characteristics, characteristics of the major protein subunits, or assembly pathways. In the post-genomic era, it has now become clear that Gram-negative bacteria have four major classes of pili, based on their biosynthetic pathways: a) pili assembled by the chaperone-usher pathway (CU pili); c) Type III secretion needle; b) Type IV pili; and d) Type IV secretion pili (not discussed below). Historically the best characterised of these cell-surface organelles are CU pili (Duguid and Campbell, 1969; Martinez et al., 2000) expressed by *E. coli*, *Pseudomonas* and *Neisseria* species (Olsen et al., 1989; Kikuchi et al., 2005).

Under the electron microscope, CU pili appear as rigid, rod-like structures extending in all directions from the bacterium. They are 1–2 μm in length with a visibly flexible tip that is involved in bacterial interaction with receptors on the host cell surface (Hahn et al., 2002; Kuehn et al., 1994; Saulino et al., 2000). Type IV pili are similar in length but differ from CU pili in that they appear to be more flexible and often form bundles at the pole (Craig et al., 2004; Strom and Lory, 1993). Type III secretion-system pili were first observed in *Salmonella* Typhimurium as needle-like surface appendages responsible for bacterial entry into epithelial cells (Schraidt et al., 2010). Curli are, as their name suggests, coiled structures synthesized by the

CU pathway as linear multi subunit pili. They are mainly found in *Pseudomonas, Haemophilus, Bordetella* and *Acinetobacter* species (Sauer et al., 2004). All four types are formed by non-covalent association of pilin subunits into regular polymeric structures. Pilus assembly in Gram-negative bacteria has been well studied and involves the Sec-dependent secretion system (Wu and Fives-Taylor, 2001). A common feature of Gram-negative pili is their role in adhesion to eukaryotic cells: bacteria use these structures to form an initial association with host cells, which is then followed by a more intimate attachment that brings the bacterium close to the host-cell surface. Pili are known to adhere to components of the extracellular matrix (ECM) (Amano, 2003), as well as to carbohydrate moieties present on glycoprotein or glycolipid receptors (Sung et al., 2001; Schweizer et al., 1998). Receptor specificity might be important in determining the specificity and tropism of bacteria for particular host cells (Telford et al., 2006).

So far only a few adhesin structures have been determined by three-dimensional electron microscopy (3DEM). They are prototypes for various types of assembly: P-pili, type I pilus and Saf pilus (CU pili), *S.* Typhimurium "pilus" (type III secretion system pili), and *Neisseria gonorrhoeae* pilus (type IV pilus).

17.3 Structures Exported by Chaperone/Usher Pathway: P-Pili, Type I Pili

The chaperone/usher pathway is used by a wide range of Gram-negative bacteria to expose pili on their outer surface (Hung et al., 1996). Pilus biogenesis involves a periplasmic chaperone and an outer membrane protein called the usher (Thanassi et al., 1998). The periplasmic chaperone aids pilus subunit folding in the periplasm and maintains subunits in polymerization-competent folding state (Bann and Frieden, 2004). The usher recruits chaperone-subunit complexes to the outer membrane, facilitates their ordered polymerization by proximal addition of pilin subunits and is responsible for pilus translocation to the outer surface.

CU pili, including P-pili, type I pili, and Hib pili are all helical structures 7–8 nm in diameter, with an axial hole of 2.0–2.5 nm in diameter, and comprising 3.0–3.5 subunits per turn of the helix. Clear depictions of the assembly and the architecture of macromolecular complexes have been achieved by the integration of the three-dimensional (3D) reconstructions derived from cryo-electron microscopy (cryo-EM) with atomic resolution subunit models derived from X-ray crystallography and NMR.

FGS-chaperone assembled pili, exemplified by the type I and P-pili found in uropathogenic *Escherichia coli* (UPEC), are typically rigid, rod-shaped pili with a complex quaternary organisation made up of multiple subunit types. Type I and P-pili are composed of two distinct subassemblies: a rigid helically wound rod of 6.8-nm diameter composed of over 1000 copies of the FimA or PapA subunits, respectively, and a distal tip fibrillum measuring 2 nm in diameter. The tip fibrillum is composed of a distally located adhesin (FimH in type I and PapG in P-pili, respectively) and the FimG and FimF subunits or the PapF, PapE (∼5–10 copies) and PapK

subunits in type I and P-pili, respectively. These pili, also referred to as "typical CU pili", are readily observable as individual fibres, radiating out of the bacterial surface in all directions (Hahn et al., 2002; Jones et al., 1995).

17.3.1 P-Pili

One of the first and best-characterised fimbria is the pyelonephritis-associated (P) pilus, expressed by UPEC strains that colonise the urinary tract and infect the kidney. At the outer membrane the pilins are translocated through a pore-forming usher and assembled into the pilus by proximal addition to the growing helical filament. The pore is large enough to accommodate a single pilin subunit in its native conformation. P-pili are the appendages that pyelonephritic *E. coli* uses to colonise and infect host tissues. Clear depictions of the assembly and architecture of macromolecular complexes have been achieved by the integration of 3D reconstructions (Fig. 17.1A) from cryo-electron microscopy (cryoEM) with atomic resolution subunit models from X-ray crystallography. The three-dimensional structure of P-pili obtained at 9.8 Å resolution from material preserved in vitreous ice and using iterative helical real space reconstruction method (IHRSR) (Egelman, 2000; Mu and Bullit, 2006) show the P-pilus to be an elongated filament with an external diameter of 82 Å. It has an axial channel of 25 Å in diameter running straight up the center of the helix axis with openings that extend to the pilus surface. The P-pilus shell contains 3.28 subunits per turn of the helix turn and a 7.54 Å rise per subunit. Surface protrusions that extend 7 Å from the filament surface with a height of 17 Å have been also observed A homology-based model of PapA was constructed using the known structure of the minor P-pilin, PapK (protein Data Bank ID code 1PDK) (Sauer et al., 1999) as a template based on its 26% sequence identity with PapA. Fitting of the modelled PapA subunit into the cryo-electron microscopy data provided a detailed view of these pilins within the supramolecular architecture of the pilus filament. A structural hinge in the N-terminal region of the subunit is located at the site of electron density that protrudes from the pilus surface. The structural flexibility provided by this hinge is necessary for assembly of P-pili, illustrating one solution to the construction of large macromolecular complexes from small repeating units. These data support the hypothesis that domain-swapped pilin subunits transit the outer cell membrane vertically and rotate about the hinge for final positioning into the pilus filament.

17.3.2 Type I Pili

The structure of Type I pilus was determined in 1969 by Brinton, who used electron microscopy, crystallography and X-ray diffraction. More recent electron microscopy and three dimensional reconstruction studies by Hahn et al. (2002) showed that the adhesive organelle has a composite structure based on a 6.9 nm thick and 1–2 μm long helical rod. Briefly, an integrated approach combining information gained by

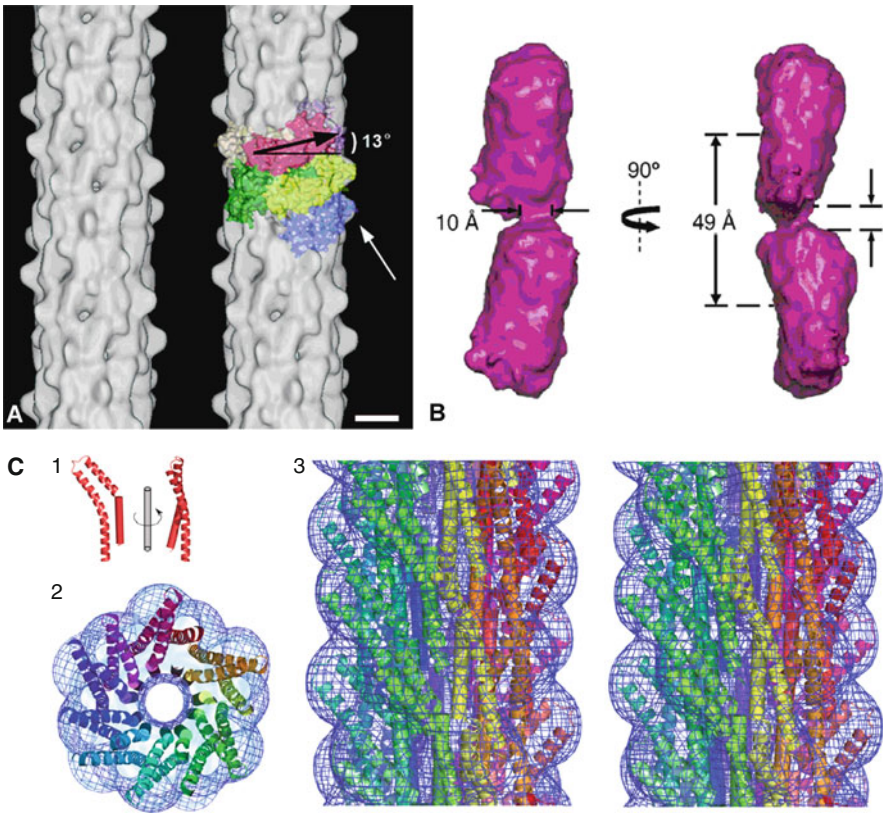

Fig. 17.1 (**a**) Cryo-EM density map (Mu and Bullit, 2006) of P-pili. The helical reconstruction (*left hand* figure) shows a filament structure 82 Å in diameter, with surface protrusions that extend 7 Å from the filament surface, for 17 Å along the helical axis (*white arrow*). PapA subunits fitting into the 3D P-pilus electron density map are visualized in different colours (*right hand* figure). The subunits are inclined by an angle of 13° from horizontal (*black arrow*). (**b**) Three-dimensional reconstruction of the type A Saf pilus (Salih et al., 2008). Each reconstruction is contoured at the molecular mass expected for two SafA subunits (28.8 kDa). Structures are viewed from two orthogonal directions and show two subunits connected by a narrower stretch of density. (**c**) Docking of the atomic model of MxiH into the EM density of the *Shigella* T3SS needle (Deane et al., 2006). (1) Molecule A of MxiH (*ribbon*). (2) End-on view of a 40-Å-thick section of the assembled needle. (3) Stereo diagram of the *side view* of the assembled needle

Fourier transformation, linear Markham superposition (real space) and mass-per-length measurement by scanning transmission electron microscopy was used to analyze the helical structure of the rod-like type I pili expressed by UPEC. The three-dimensional reconstruction showed the pili to be 6.9 nm wide, right-handed helical tubes with a 19.31(±0.34) nm long helical repeat comprising 27 FimA monomers associated head-to-tail in eight turns of the one-start helix. Adjacent turns of the helix are connected via three binding sites making the pilus rod rather stiff. In situ immuno-electron microscopy experiments showed that the minor subunit

(FimH) mediating pilus adhesion to bladder epithelial cells was the distal protein of the pilus tip, which had a spring-like appearance at higher magnification. The subunits FimG and FimF connect FimH to the FimA rod, the sequential orientation being FimA–FimF–FimG–FimH. The electron density map calculated at 18 Å resolution from an atomic model of the pilus rod built using the pilin domain FimH together with the G1 strand of FimC as a template for FimA and applying the optimal helical parameters described above was practically identical to the actual three-dimensional reconstruction (Hahn et al., 2002; Choudhury et al., 1999).

17.3.3 Saf Pilus

In contrast to the well-established quaternary structure of typical chaperone/usher pili, little was known about the supramolecular organisation in atypical/FGL-chaperone assembled fimbriae. Salih and co-workers (2008) used negative stain electron microscopy and single-particle image analysis to determine the three-dimensional structure of the *Salmonella* Typhimurium Saf pilus (Fig. 17.1B). Their results show atypical/FGL-chaperone assembled fimbriae are composed of highly flexible linear multi-subunit fibres that are formed by globular subunits connected to each other by short links giving a "beads on a string"-like appearance. Quantitative fitting of the atomic structure of the SafA pilus subunit into the electron density maps (Salih et al., 2008), in combination with linker modelling and energy minimisation, has enabled analysis of subunit arrangement and intersubunit interactions in the Saf pilus. Short intersubunit linker regions provide the molecular basis for flexibility of the Saf pilus by acting as molecular hinges allowing a large range of movement between consecutive subunits in the fibre.

17.4 Type III Secretion-System Pili

Besides pili, enteropathogenic *E. coli* (EPEC) and enterohaemorrhagic *E. coli* (EHEC) have another bacterial adhesion system (Type III secretion-related pili) in which the bacteria provide both the ligand and the receptor with a mechanism known as "attaching and effacing". Type III secretion-related appendages were first observed in *S.* Typhimurium as needle-like surface structures responsible for bacterial entry into cultured epithelial cells (Roine et al., 1997; Kubori et al., 1998). The assembly of these structures depends on systems now known to form a flagellum-like secretion nanomachine known as the type III secretion system (T3SS). T3SS assembles a complex injectisome designed to secrete effector proteins across the bacterial and host cell envelopes. Injectisome assembly involves over 20 proteins (Cornelis, 2006). The injectisome basal structure is a large cylindrical heterocomplex with two double rings spanning the inner and outer membranes that are linked by a hollow structure that crosses the intermediate periplasmic space (Kubori et al., 1998). On the cytoplasmic side, the basal body interacts with ATPases

and accessory proteins responsible for driving and ordering protein secretion and filament assembly (Woestyn et al., 1994; Akeda and Galan, 2005; Müller et al., 2006). On the outer surface, the basal body forms a hollow filamentous structure. The basic extracellular structure, as first identified in the *Salmonella* SPI-1 T3SS (Kubori et al., 1998) and later observed in detail from purified *Shigella* injectisomes (Tamano et al., 2000; Blocker et al., 2001), is a short rigid hollow "needle" about 60 nm in length with an inner diameter of 2–3 nm. The basic needle is composed of a homopolymer of 100 subunits with a RMM of 9 kDa each (PrgJ, MxiH, YscF and Escf in *Salmonella, Shigella, Yersinia* and EPEC, respectively). These subunits reveal a helix-loop-helix structure similar to the D0 portion of flagellin (Deane et al., 2006).

Similar to flagellin, needle subunits polymerise into a hollow superhelical structure (Fig. 17.1C). The distal end of the needle carries a distinct tip complex. In *Yersinia*, it is composed of the protein LcrV, one of the three translocators involved in pore formation in the target cytoplasmic membrane (Mueller et al., 2005). LcrV forms a dumbbell-shaped structure that has been modelled as a pentameric complex at the tip of the needle and is thought to provide the scaffold for the additional two translocator proteins, assembled upon contact with the target membrane (YopB and YopD) (Derewenda et al., 2004; Deane et al., 2006). In EPEC, this needle base is extended by a longer flexible "filament" up to 600 nm in length (Knutton et al., 1998; Sekiya et al., 2001) and composed of an EspA homopolymer. In plant pathogens, the needles are replaced altogether by a long flexible "pilus", the Hrp pilus (Roine et al., 1997; Li et al., 2002). In the *Salmonella* SPI-1 T3SS, a different mechanism for needle length control has been suggested based on the 3DEM reconstruction at 17 Å resolution. Purified *Salmonella* injectisomes indicate the presence of an inner rod structure, possibly composed of a specialised subunit, PrgJ, inside the basal body of the secretion system. In the model, secretion of rod and needle subunits (PrgJ and PrgI, respectively) occurs simultaneously. Completion of the inner rod assembly signals a halt in secretion of rod and needle subunits, thereby controlling needle length (Marlovits et al., 2006).

17.5 Type IV Pili

Much current interest is focused in the study of type IV pili, another category of polymeric adhesive surface structures expressed by many Gram-negative bacteria including pathogens such as EPEC, EHEC, *Neisseria gonorrhoeae* and *Neisseria meningitidis*. These helical arrays of thousands of copies of a single pilin subunit such as PilA (Parge et al., 1995) and PilE (Craig et al., 2003) are extremely thin and flexible but remarkably strong, and they have several different physiological functions. Type IV pili are essential for host colonization and virulence for many Gram-negative bacteria, and may also play a role in pathogenesis for some Gram-positive bacteria. High resolution structures of pilin subunits have been determined by X-ray crystallography and nuclear magnetic resonance spectroscopy both as full length proteins and as soluble fragments (Parge et al., 1995; Craig et al., 2003).

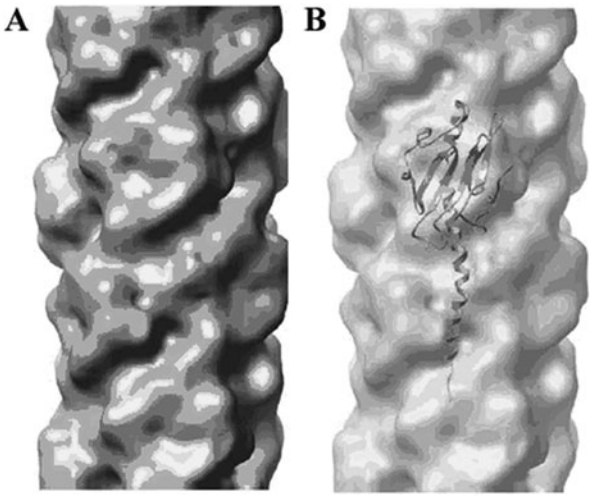

Fig. 17.2 Cryo-EM and 3D Reconstruction of the GC Pilus at 12.5 Å (Craig et al., 2006) (**a**) Filament density map for GC-T4P (**b**) Pilin subunit match to cryo-EM density map

These structures have been used to generate computational models of pilus filament assemblies, guided by biophysical parameters extracted from fibre diffraction data and electron microscopy image analysis, and by the extensive biological data. Most recently, cryo-electron microscopy has provided an intermediate resolution (12.5 Å) structure of a pilus filament (Fig. 17.2) showing its helical organization (Craig et al., 2006). The pilin structures and filament models have been instrumental in advancing our understanding of the molecular mechanisms driving pilus assembly and the role of Type IV pili in key bacterial functions such as immune evasion, microcolony formation and DNA uptake. In very general terms the structural data point to a shared subunit structure and filament architecture for all Type IV pili, but a comprehensive, atomic-level understanding of these filaments and their biological processes will require additional higher resolution filament structures as well as new structural, genetic and biochemical data on the many components of the pilus assembly apparatus.

17.6 Pili in Gram-Positive Bacteria

While many Gram-negative pili have been studied in detail over the last decades (Fronzes et al., 2008), the majority of Gram-positive pili have been discovered only recently and their study, initiated by Schneewind and co-workers on *Corynebacterium diphteriae* (Ton-That and Schneewind, 2003; Ton-That et al., 2004), it is still at its infancy. Pilus-like structures on the surface of Gram-positive bacteria were first detected in *Corynebacterium renale* by electron microscopy (Yanagawa et al., 1968; Yanagawa and Otsuki, 1970). In the recent past pili have also been characterized in all three of the principal streptococcal pathogens that cause invasive disease in humans: Group A *Streptococcus* (GAS) (Mora et al., 2005), Group B *Streptococcus* (GBS) (Lauer et al., 2005; Rosini et al., 2006) and *Streptococcus pneumoniae*, a very important human pathogen (Barocchi et al.,

2006). In all cases, the pili have been shown to play a key role in adhesion and invasion and in pathogenesis. Until a few years ago, only two types of pilus-like structures had been identified by electron microscopy in Gram-positive bacteria. Certain Gram-positive bacteria, like *Streptococcus gordonii* and *Streptococcus oralis*, appear to be decorated with short, thin rods or fibrils that extend between 70 and 500 nm from the bacterial surface (McNab et al., 1999; Willcox and Drucker, 1989). Much longer (up to 3 μm) pilus-like structures that appear as flexible rods have been described in the oral pathogenic *Corynebacterium* species and in pathogenic streptococci (Yanagawa et al., 1968; Yanagawa and Otsuki, 1970; Ton-That and Schneewind, 2003; Mora et al., 2005; Thanassi et al., 2005; Rosini et al., 2006; Barocchi et al., 2006; Jameson et al., 1995). Ton-That and Schneewind were the first to characterize the long rod-like pili in *C. diptheriae* (Ton-That and Schneewind, 2003). The general feature of these rod-like pili, as well as the rod-like pili that have been identified in GAS (Mora et al., 2005), GBS (Lauer et al., 2005) and *S. pneumoniae* (Barocchi et al., 2006), is that they have three covalently linked protein subunits, each of which contains an LPXTG amino-acid motif or a variant of it, which is the target of specific sortase enzymes. During pilus formation, specific sortases catalyse the covalent attachment of the pilin subunits to each other and to the peptidoglycan cell wall (Ton-That and Schneewind, 2003).

The molecular architecture of pilus-1 of *S. pneumoniae* is the only structure of a Gram-positive pilus known so far (Hilleringmann et al., 2009). One major (RrgB) and two minor components (RrgA and RrgC) assemble into the pilus. TEM and scanning transmission electron microscopy (STEM) show that the native pili are approximately 6 nm wide, flexible filaments that can be over 1 μm long. They are formed by a single string of RrgB monomers, which give a polarity to the pilus defined by a nose-like protrusion (Fig. 17.3). These protrusions correlate to the

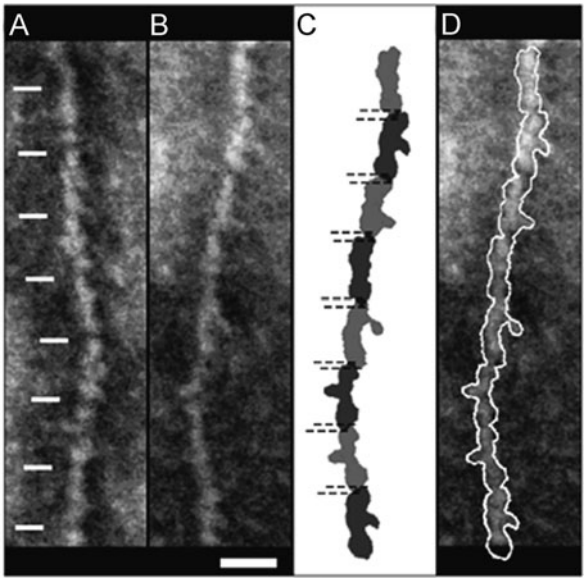

Fig. 17.3 STEM analysis of isolated TIGR4 pili (Hilleringmann et al., 2009). (**a, b**) Contrast-reversed STEM *dark-field* images from negatively stained TIGR4. A nose-like protrusion is present at irregular intervals. Subunit boundaries are indicated by *white lines* in panel a. (**c**) Highly contoured TEM images of RrgB–His monomers; (**d**) Pilus outer contours. Scale bar: panel A, 10 nm

shape of monomeric RrgB-His, which, like RrgA-His and RrgC-His, has an elongated, multidomain structure. RrgA and RrgC are present at opposite ends of the pilus shaft, compatible with their putative roles as adhesin and anchor to the cell wall surface, respectively. This is the first experimental evidence that the native *S. pneumoniae* pilus shaft is composed exclusively of covalently linked monomeric RrgB subunits oriented head-to-tail.

17.7 Perspectives

The past few years have witnessed an incredible number of new discoveries. They have not only enhanced our understanding of how adhesin structures are assembled at the atomic and molecular level, but have also dramatically widened the number of species known to possess adhesive structures. Thus adhesins have been found on Gram-positive pathogens such as *Streptococcus pneumoniae*, the Group A and B *streptococci*, and *Staphylococcus aureus*, complementing the wide range of Gram-negative organisms that have long been known to express adhesins. Much has also been learned about adhesin structure and assembly: the donor-strand complementation mechanism used in the chaperone-usher assembly pathway; the assembly of Type IV pilin subunits into complete pilus fibres; and most recently the first structure for a Gram-positive major pilin and the structural architecture of a whole Gram-positive pilus.

Whereas much is known about the structure and assembly of many of the adhesion machines, many questions still surround their modes of adhesion to host cells. It is generally assumed that adhesion capability resides at the most exposed domains of these macromolecular assembly, but this is not necessarily true for all adhesins; there is much evidence that the pilus shaft also plays some role in adhesion in some Gram-negative bacteria. For Gram-positive pili, for example, so-called minor pilin subunits are necessary for binding to host cells, but it is not known how or where these are attached to the shaft. Likewise, whereas some adhesion domains, such as the FimH domain of Type I pili, are known to bind host-cell glycans, the molecular targets for other pili and pili-like structures are not known, and may involve extracellular matrix components such as collagen or fibronectin.

Determination of all protein structures and their macromolecular assemblies at high resolution is a key modern target for biological electron microscopy, representing one of the most important goals in biology and medicine. In the past two decades, significant methodological advances have occurred in ultrastructural analysis by electron microscopy: the high resolution analysis of biological material has been taken to a new level by the development of cryo-EM and of new efficient strategies for image processing and 3D rendering of biological structures. After being overshadowed by the rapid advances in biochemistry, genetics, and light microscopy, in the 1970s and 1980s, TEM has now re-attracted attention as a crucial tool to bridge the data gained by the aforementioned techniques.

The three-dimensional methods developed to solve the different biological problems and the different adhesion structures are based on two main groups

of strategies: electron tomography and single particle analysis. Cryo-electron microscopy is a powerful tool in the study of macromolecular assemblies, especially in single particle form. Technical improvements including computer controlled microscopes equipped with field emission guns, improved specimen stages, CCD cameras, as well as energy filters, combined with increased computational power and improvements of image processing software, are making cryo-electron microscopy almost routine. The popularity of this technique stems from the ability to record the structure of radiation sensitive specimens in their native state thereby eliminating the deleterious effects of negative stains and fixatives that mask the high resolution components of the structure. Finally emerging methods combining cryo-electron microscopy with X-ray crystallography and NMR allow the determination of three-dimensional structures at the atomic level for entire adhesin complexes.

References

Akeda Y, Galan JE (2005) Chaperone release and unfolding of substrates in type III secretion. Nature 437:911–915

Amano A (2003) Molecular interaction of *Porphyromonas gingivalis* with host cells: implication for the microbial pathogenesis of periodontal disease. J Periodontol 74:90–96

Bann JG, Frieden C (2004) Folding and domain-domain interactions of the chaperone PapD measured by ^{19}F NMR. Biochemistry 43:13775–13786

Barocchi MA, Ries J, Zogaj X, Hemsley C, Albiger B, Kanth A, Dahlberg S, Fernebro J, Moschioni M, Masignani V, Hultenby K, Taddei AR, Beiter K, Wartha F, von Euler A, Covacci A, Holden DW, Normark S, Rappuoli R, Henriques-Normark B (2006) A pneumococcal pilus influences virulence and host inflammatory responses. Proc Natl Acad Sci USA 103:2857–2862

Blocker A, Jouihri N, Larquet E, Gounon P, Ebel F, Parsot C, Sansonetti P, Allaoui A (2001) Structure and composition of the *Shigella flexneri* "needle complex", a part of its type III secretion. Mol Microbiol 39:652–663

Choudhury D, Thompson A, Stojanoff V, Langermann S, Pinkner J, Hultgren SJ, Knight SD (1999) X-ray structure of the FimC-FimH chaperone-adhesin complex from uropathogenic *Escherichia coli*. Science 285:1061–1066

Cornelis GR (2006) The type III secretion injectisome. Nat Rev Microbiol 4:811–825

Craig L, Pique ME, Tainer JA (2004) Type IV pilus structure and bacterial pathogenicity. Nat Rev Microbiol 2:363–378

Craig L, Taylor RK, Pique ME, Adair BD, Arvai AS, Singh M, Lloyd SJ, Shin DS, Getzoff ED, Yeager M, Forest KT, Tainer JA (2003) Type IV pilin structure and assembly: X-ray and EM analyses of *Vibrio cholerae* toxin-coregulated pilus and *Pseudomonas aeruginosa* PAK pilin. Mol Cell 11:1139–1150

Craig L, Volkmann N, Arvai AS, Pique ME, Yeager M, Egelman EH, Tainer JA (2006) Type IV pilus structure by cryo-electron microscopy and crystallography: implications for pilus assembly and functions. Mol Cell 23:651–662

Deane JE, Roversi P, Cordes FS, Johnson S, Kenjale R, Daniell S, Booy F, Picking WD, Picking WL, Blocker AJ, Lea SM (2006) Molecular model of a type III secretion system needle: implications for host-cell sensing. Proc Natl Acad Sci USA 103:12529–12533

Derewenda U, Mateja A, Devedjiev Y, Routzahn KM, Evdokimov AG, Derewenda ZS, Waugh DS (2004) The structure of *Yersinia pestis* V-antigen, an essential virulence factor and mediator of immunity against plague. Structure 12:301–306

Duguid JP, Campbell I (1969) Antigens of the type I fimbriae of *Salmonella* and other Enterobacteria. J Med Microbiol 2:535–553

Duguid JP, Smith IW, Dempster G, Edmund SPN (1955) Non-flagellar filamentous appendages ("fimbriae") and haemagglutinating activity in *Bacterium coli*. J Path Bact 70:335–348

Egelman EH (2000) A Robust algorithm for the reconstruction of helical filaments using single-particle methods. Ultramicroscopy 85:225–234

Fronzes R, Remaut H, Waksman G (2008) Architectures and biogenesis of non-flagellar protein appendages in gram-negative bacteria. EMBO J 27:2271–2280

Hahn E, Wild P, Hermanns U, Sebbel P, Glockshuber R, Häner M, Taschner N, Burkhard P, Aebi U, Müller SA (2002) Exploring the 3D molecular architecture of *Escherichia coli* type I pili. J Mol Biol 323:845–857

Hilleringmann M, Ringler P, Müller SA, De Angelis G, Rappuoli R, Ferlenghi I, Engel A (2009) Molecular architecture of *Streptococcus pneumoniae* TIGR4 pili. EMBO J 28:3921–3930

Houwink AL, Iterson W (1950) Electron microscopical observations on bacterial cytology. II. A study on flagellation. Biochim Biophys Acta 5:10–44

Hung DL, Knight SD, Woods RM, Pinkner JS, Hultgren SJ (1996) Molecular basis of two subfamilies of immunoglobulin-like chaperones. EMBO J 15:3792–3805

Jameson MW, Jenkinson HF, Parnell K, Handley PS (1995) Polypeptides associated with tufts of cell-surface fibrils in an oral *Streptococcus*. Microbiology 141:2729–2738

Jones CH, Pinkner JS, Roth R, Heuser J, Nicholes AV, Abraham SN, Hultgren SJ (1995) FimH adhesin of type I pili is assembled into a fibrillar tip structure in the Enterobacteriaceae. Proc Natl Acad Sci USA 92:2081–2085

Kikuchi T, Mizunoe Y, Takade A, Naito S, Yoshida S (2005) Curli fibers are required for development of biofilm architecture in *Escherichia coli* K-12 and enhance bacterial adherence to human uroepithelial cells. Microbiol Immunol 49:875–884

Knutton S, Rosenshine I, Pallen MJ, Nisan I, Neves BC, Bain C, Wolff C, Dougan G, Frankel G (1998) A novel EspA-associated surface organelle of enteropathogenic *Escherichia coli* involved in protein translocation into epithelial cells. EMBO J 17:2166–2176

Kubori T, Matsushima Y, Nakamura D, Uralil J, Lara-Tejero M, Sukhan A, Galan JE, Aizawa SI (1998) Supramolecular structure of the *Salmonella typhimurium* type III protein secretion system. Science 280:602–605

Kuehn MJ, Jacob-Dubuisson F, Dodson K, Slonim L, Striker R, Hultgren SJ (1994) Genetic, biochemical, and structural studies of biogenesis of adhesive pili in bacteria. Methods Enzymol 236:282–306

Lauer P, Rinaudo CD, Soriani M, Margarit I, Maione D, Rosini R, Taddei AR, Mora M, Rappuoli R, Grandi G, Telford JL (2005) Genome analysis reveals pili in Group B *Streptococcus*. Science 309:105

Li CM, Brown I, Mansfield J, Steven C, Boureau T, Romantschuk M, Taira S (2002) The Hrp pilus of *Pseudomonas syringae* elongates from its tip and acts as a conduit for translocation. EMBO J 21:1909–1915

Marlovits TC, Kubori T, Lara-Tejero M, Thomas D, Unger VM, Galan JE (2006) Assembly of the inner rod determines needle length in the type III secretion injectisome. Nature 441:637–640

Martinez JJ, Mulvey MA, Schilling JD, Pinkner JS, Hultgren SJ (2000) Type I pilus-mediated bacterial invasion of bladder epithelial cells. EMBO J 19:2803–2812

McNab R, Forbes H, Handley PS, Loach DM, Tannock GW, Jenkinson HF (1999) Cell wall-anchored CshA polypeptide (259 kilodaltons) in *Streptococcus gordonii* forms surface fibrils that confer hydrophobic and adhesive properties. J Bacteriol 181:3087–3095

Mora M, Bensi G, Capo S, Falugi F, Zingaretti C, Manetti AGO, Maggi T, Taddei AR, Grandi G, Telford JL (2005) Group A *Streptococcus* produce piluslike structures containing protective antigens and Lancefield T antigens. Proc Natl Acad Sci USA 102:15641–15646

Mu XQ, Bullitt E (2006) Structure and assembly of P-pili: a protruding hinge region used for assembly of a bacterial adhesion filament. Proc Natl Acad Sci USA 103:9861–9866

Mueller CA, Broz P, Müller SA, Ringler P, Erne-Brand F, Sorg I, Kuhn M, Engel A, Cornelis GR (2005) The V-antigen of *Yersinia* forms a distinct structure at the tip of injectisome needles. Science 310:674–676

Müller SA, Pozidis C, Stone R, Meesters C, Chami M, Engel A, Economou A, Stahlberg H (2006) Double hexameric ring assembly of the type III protein translocase ATPase HrcN. Mol Microbiol 61:119–125

Olsén A, Jonsson A, Normark S (1989) Fibronectin binding mediated by a novel class of surface organelles on *Escherichia coli*. Nature 338:652–655

Parge HE, Forest KT, Hickey MJ, Christensen DA, Getzoff ED, Tainer JA (1995) Structure of the fibre-forming protein pilin at 2.6 Å resolution. Nature 378:32–38

Roine E, Wei W, Yuan J, Nurmiaho-Lassila EL, Kalkkinen N, Romantschuk M, He SY (1997) Hrp pilus: an hrp-dependent bacterial surface appendage produced by *Pseudomonas syringae* pv. tomato DC3000. Proc Natl Acad Sci USA 94:3459–3464

Rosini R, Rinaudo CD, Soriani M, Lauer P, Mora M, Maione D, Taddei A, Santi I, Ghezzo C, Brettoni C, Buccato S, Margarit I, Grandi G, Telford JL (2006) Identification of novel genomic islands coding for antigenic pilus-like structures in *Streptococcus agalactiae*. Mol Microbiol 61:126–141

Salih O, Remaut H, Waksman G, Orlova EV (2008) Structural analysis of the Saf Pilus by electron microscopy and image processing. J Mol Biol 379:174–187

Sauer F, Fütterer K, Pinkner JS, Dodson K, Hultgren SJ, Waksman G (1999) Structural basis of chaperone function and pilus biogenesis. Science 285:1058–1061

Sauer FG, Remaut H, Hultgren SJ, Waksman G (2004) Fiber assembly by the chaperone–usher pathway. Biochim Biophys Acta 1694:259–267

Saulino ET, Bullitt E, Hultgren SJ (2000) Snapshots of usher-mediated protein secretion and ordered pilus assembly. Proc Natl Acad Sci USA 97:9240–9245

Schraidt O, Lefebre MD, Brunner MJ, Schmied WH, Schmidt A, Radics J, Mechtler K, Galán JE, Marlovits TC (2010) Topology and organization of the *Salmonella typhimurium* Type III secretion needle complex components. PLoS Pathog 6:e1000824

Schweizer F, Jiao H, Hindsgaul O, Wong WY, Irvin RT (1998) Interaction between the pili of *Pseudomonas aeruginosa* PAK and its carbohydrate receptor beta-D-GalNAc(1->4) beta-D-Gal analogs. Can J Microbiol 44:307–311

Sekiya K, Ohishi M, Ogino T, Tamano K, Sasakawa C, Abe A (2001) Supermolecular structure of the enteropathogenic *Escherichia coli* type III secretion system and its direct interaction with the EspA-sheath-like structure. Proc Natl Acad Sci USA 98:11638–11643

Strom MS, Lory S (1993) Structure-function and biogenesis of the type IV pili. Annu Rev Microbiol 47:565–596

Sung M, Fleming K, Chen HA, Matthews S (2001) The solution structure of PapGII from uropathogenic *Escherichia coli* and its recognition of glycolipid receptors. EMBO Rep 2:621–627

Tamano K, Aizawa S, Katayama E, Nonaka T, Imajoh-Ohmi S, Kuwae A, Nagai S, Sasakawa C (2000) Supramolecular structure of the *Shigella* type III secretion machinery: the needle part is changeable in length and essential for delivery of effectors. EMBO J 19:3876–3887

Telford JL, Barocchi MA, Margarit I, Rappuoli R, Grandi G (2006) Pili in gram-positive pathogens. Nat Rev Microbiol 4:509–519

Thanassi DG, Saulino ET, Lombardo MJ, Roth R, Heuser J, Hultgren SJ (1998) The PapC usher forms an oligomeric channel: implications for pilus biogenesis across the outer membrane. Proc Natl Acad Sci USA 95:3146–3151

Thanassi DG, Stathopoulos C, Dodson K, Lauer P (2005) Genome analysis reveals pili in group B *Streptococcus*. Science 309:105

Ton-That H, Marraffini LA, Schneewind O (2004) Protein sorting to the cell wall envelope of gram-positive bacteria. Biochim Biophys Acta 1694:269–278

Ton-That H, Schneewind O (2003) Assembly of pili on the surface of *Corynebacterium diphtheriae*. Mol Microbiol 50:1429–1438

Willcox MD, Drucker DB (1989) Surface structures, co-aggregation and adherence phenomena of *Streptococcus oralis* and related species. Microbios 59:19–29

Woestyn S, Allaoui A, Wattiau P, Cornelis GR (1994) YscN, the putative energizer of the *Yersinia* Yop secretion machinery. J Bacteriol 176:1561–1569

Wu H, Fives-Taylor PM (2001) Molecular strategies for fimbrial expression and assembly. Crit Rev Oral Biol Med 12:101–115

Yanagawa R, Otsuki K (1970) Some properties of the pili of *Corynebacterium renale*. J Bacteriol 101:1063–1069

Yanagawa R, Otsuki K, Tokui T (1968) Electron microscopy of fine structure of *Corynebacterium renale* with special reference to pili. Jpn Vet Res 16:31–37

Chapter 18
Atomic Force Microscopy to Study Intermolecular Forces and Bonds Associated with Bacteria

Steven K. Lower

Abstract Atomic force microscopy (AFM) operates on a very different principle than other forms of microscopy, such as optical microscopy or electron microscopy. The key component of an AFM is a cantilever that bends in response to forces that it experiences as it touches another surface. Forces as small as a few picoNewtons can be detected and probed with AFM. AFM has become very useful in biological sciences because it can be used on living cells that are immersed in water. AFM is particularly useful when the cantilever is modified with chemical groups (e.g. amine or carboxylic groups), small beads (e.g. glass or latex), or even a bacterium. This chapter describes how AFM can be used to measure forces and bonds between a bacterium and another surface. This paper also provides an example of the use of AFM on *Staphylococcus aureus*, a Gram-positive bacterium that is often associated with biofilms in humans.

18.1 Introduction to AFM

In most microbiology laboratories, students are taught how to culture bacteria in enclosed vessels that contain nutrient broth. The growth cycle of a bacteria population is determined by measuring the optical density of cell suspensions. However, most bacteria do not naturally live as suspended entities within a solution. In nature, most bacteria live attached to or in contact with a solid surface (Parsek and Fuqua, 2004; Watnick and Kolter, 2000; Whitman et al., 1998). The planktonic mode of life is simply a means to move from one surface to another.

What forces allow a bacterium to make contact with an inorganic surface? How does a bacterium form a bond with a protein-coated material? It wasn't until very recently that we were able to directly probe the interface between a mineral or

S.K. Lower (✉)
Ohio State University, Columbus, OH 43210, USA
e-mail: lower.9@osu.edu

D. Linke, A. Goldman (eds.), *Bacterial Adhesion*, Advances in Experimental Medicine and Biology 715, DOI 10.1007/978-94-007-0940-9_18,

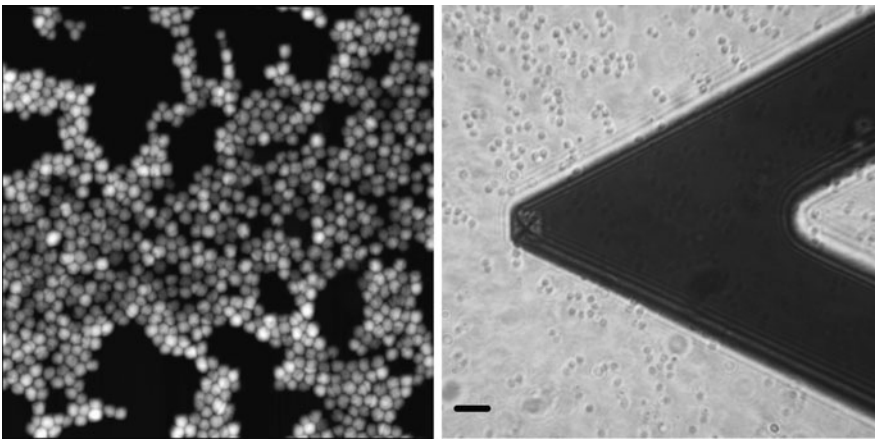

Fig. 18.1 (*Left*) Image of living *Staphylococcus aureus* on a glass slide immersed in a saline buffer. This image was collected with an AFM. The image size is 25 μm × 25 μm. (*Right*) Optical micrograph that shows the positions of the AFM cantilever and tip (square pyramid near end of cantilever) as well as cocci-shaped *S. aureus* cells on the glass slide. The bacteria are blurred because the plane of focus is on the AFM tip. Scale bar is approximately 10 μm

material and a living bacterium. The invention of the atomic force microscope (AFM) (Binnig et al., 1986) opened the door to investigations into the fundamental forces and bonds that control how a bacterium interacts with a solid surface.

Figure 18.1 shows the Gram-positive bacteria *Staphylococcus aureus* on a silica surface, that is, a glass slide. This image was collected by scanning a relatively sharp AFM tip over the *S. aureus* cells (see right image in Fig. 18.1). Images like this AFM micrograph provide a visual depiction of a bacterium in contact with another surface. However, the actual interface is hidden from view. One would need to probe under the bacterium to reveal the true region of interest.

Intermolecular forces, such as van der Waals, electrostatic, solvation, and steric interactions (Leckband and Israelachvili, 2001), control how a bacterium's cell wall physically interacts with another surface. The small magnitude of these forces and the small length scale over which they operate make it a challenge to probe these forces. AFM has the force- and space-sensitivity to accomplish this task. The first papers describing the use of AFM to study adhesion forces of bacteria began to appear in the literature about a decade ago (Camesano and Logan, 2000; Lower et al., 1999, 2000; Razatos et al., 1998). Since then, AFM has been used countless times to study the fundamental forces that direct adhesion and biofilm formation.

This chapter provides readers with a brief overview of AFM. For a more extensive review of AFM the reader is referred to the following publications: (Cappella and Dietler, 1999; Kendall and Lower, 2004; Yongsunthon and Lower, 2006). This chapter also provides examples to illustrate how AFM can be used to study (i) forces as a bacterium approaches a surface, and (ii) bonds that may rupture as a bacterium is pulled away from the surface. These examples will draw primarily upon my knowledge and experience with *S. aureus*.

18.2 The Main Components of AFM

AFM is a scanning probe microscopy instrument that consists of a force-sensing cantilever, a piezoelectric scanner, and a photodiode detector (Fig. 18.2). The cantilever bends upwards due to repulsive forces, or downwards due to attractive forces, between a sample (e.g. a bacterium) and a small tip that is an integrated part of the end of the cantilever. The deflection of the cantilever is monitored by reflecting a laser off the top of the free-end of the cantilever and into the photodetector.

The cantilever behaves like a spring such that the force (F in Newtons) acting on the cantilever tip is given by Hooke's Law $F = -(K_{sp})(x)$, where K_{sp} is the cantilever spring constant (N m^{-1}) and x is the deflection of the free-end of the lever (in m). The piezoelectric scanner moves the fixed-end of the cantilever towards and away from the sample (see Fig. 18.2), or in some systems the sample moves towards or away from the cantilever. In essence, the piezoelectric scanner allows one to precisely control the formation and subsequent destruction of a contact event between two surfaces. Simultaneously, the optical lever detection system of the AFM allows the quantitative measure of forces between the two surfaces.

This chapter will focus primarily on the one-dimension "force curves" that are generated as a cantilever tip is brought into contact with a bacterium and then pulled away from the bacterium. It is important to note that AFM can also be used to create a three-dimensional topographic image like the one shown in Fig. 18.1. This

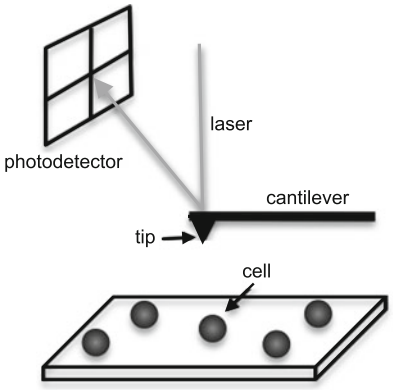

Fig. 18.2 Schematic diagram showing the key components of an AFM. A piezoelectric scanner (not shown) moves the "fixed end" of the cantilever relative to the sample (cell or substrate). Forces between the sample and tip cause the "free end" of the cantilever to deflect or bend. The behaviour of the cantilever is monitored by tracking a laser beam reflected off the top side of the cantilever and onto a photodetector. One can use this setup to measure forces as the tip approaches, makes contact with, and is subsequently retracted from the sample. A topographic image of the sample can also be collected by laterally scanning the tip across the sample while measuring the deflection of the cantilever

is accomplished by monitoring the vertical deflection of the cantilever as the tip is scanned laterally across the sample.

18.2.1 Modification of AFM Cantilever and Tip for Biological Experiments

Commercially available force-transducing cantilevers may be V-shaped silicon nitride levers or single beam silicon levers (Albrecht et al., 1990; Tortonese, 1997). However, these materials may not be the most interesting substrates for microbiological investigations. Therefore, the cantilever (or tip) is often modified prior to use. For example, the tip may be functionalised with various chemical groups (Noy et al., 1997). Small (2–10 μm radius) beads may be glued to the end of an AFM cantilever (Ducker et al., 1991, 1992). Living cells can even be linked to the end of an AFM cantilever (Lower et al., 2000, 2001b).

Figure 18.3 shows a glass bead, approximately 10 μm in diameter, on the end of the AFM cantilever. The tip is still visible in this image, although its size (~4 μm) means that a sample will interact with the bead rather than the tip. Figure 18.3 also shows a bacteria-coated bead on the end of an AFM cantilever. These cells on the end of the cantilever are living (Lower et al., 2000). A single bacterium can also be attached to an AFM tip (Jericho et al., 2004; Lower et al., 2001b).

It is important to note that a cantilever's nominal spring constant (N m^{-1}), as quoted by the manufacturer, can vary significantly from the actual value (Senden and Ducker, 1994). Therefore, one should always calibrate the spring constant of a cantilever. There are a number of methods including the Cleveland method (Cleveland et al., 1993), the hydrodynamic drag method (Craig and Neto, 2001), and the resonant frequency method (Hutter and Bechhoefer, 1993).

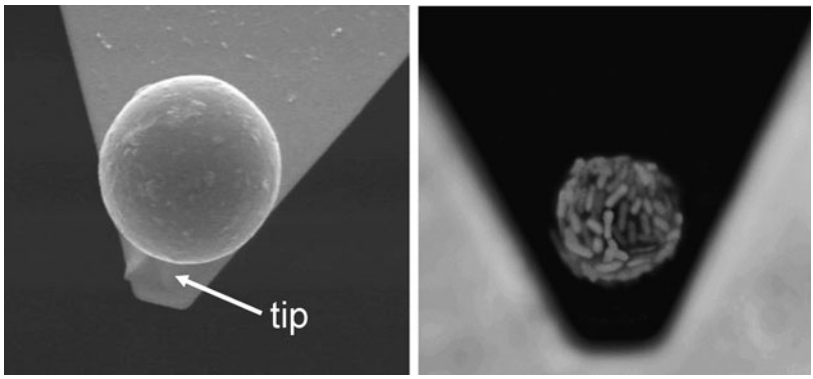

Fig. 18.3 (*Left*) Scanning electron microscopy image of a glass bead that is attached to the free end of the cantilever. (*Right*) Optical micrograph of a bacteria-coated bead on the end of the cantilever. The cells are expressing an intracellular green fluorescent protein so that they can be visualised on the cantilever

18.2.2 Collection and Analysis of Force Data

Each force curve consists of two parts: approach of the tip toward the sample and the subsequent retraction of the tip from the sample. The rate of the approach-retraction cycle may be controlled by the operator. A typical approach-retraction curve takes about 1 s.

In raw form, AFM force data are measured as (i) the output voltage from a photodiode detector in response to the deflection of the cantilever deflection, and (ii) the displacement (or movement) of the cantilever relative to the sample. To convert the raw measurements into meaningful physical quantities, the photodiode output voltage must be converted to force values and the displacement must be converted to distance or separation between the tip and sample.

18.2.2.1 Converting Photodetector Voltage into Force Values

The photodiode output signal, which is related to the position of the reflected laser spot (see Fig. 18.2), is measured in volts. These voltages correspond to the upwards or downwards movement of the free end of the cantilever in response to repulsive or attractive forces between the tip and sample. Detector voltage measurements must be converted into force values using the spring constant of the cantilever (N m^{-1}; see above) and a "volts to nm" conversion factor called the optical lever sensitivity (in nm V^{-1}).

The optical lever sensitivity allows the signal from the photodiode detector (in volts) to be converted into deflection (in nm) values for the cantilever. When the cantilever is pressed into contact with a hard surface, each unit of piezo movement ideally corresponds to an equivalent deflection of the cantilever. The inverse slope of the region of contact (also referred to as the region of constant compliance) is the optical lever sensitivity (Fig. 18.4). For the data shown in Fig. 18.4, the optical lever sensitivity is ~120 nm V^{-1}. Each voltage value is multiplied by the optical lever sensitivity to determine the upwards or downwards deflection of the cantilever in response to repulsive or attractive forces, respectively.

One important point to consider is that this conversion is accurate only if the cantilever itself is the most compliant or flexible component of the system. This includes not only the cantilever but also the sample and any cells or biological polymers that may be attached to the cantilever. This criterion may not be met for many soft materials such as biological cells. Therefore, it is best to calibrate the optical lever sensitivity on bare glass prior to measuring forces on bacteria that are deposited on the same piece of bare glass.

Once the photodiode signal (V) is converted into the deflection of the cantilever (m), the spring constant (N m^{-1}) is used to convert the deflection values into force data (N). The region of no contact is defined as zero force (see Fig. 18.4). Any value above this line (i.e. positive) indicates repulsion whereas any value below this line (i.e. negative) indicates attractive forces between the tip and sample.

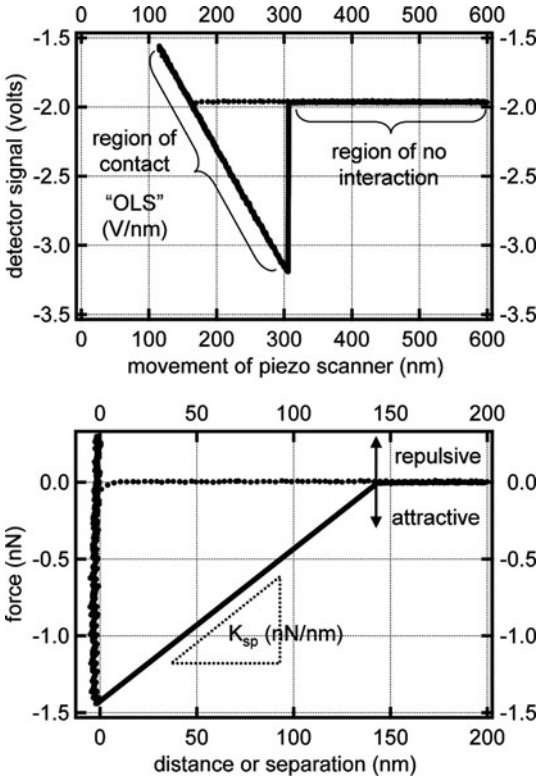

Fig. 18.4 (*Top*) The approach (*dotted*) and retraction (*solid*) curves for an AFM tip on a hard substrate. The y-axis shows the raw voltage output of the photodetector in response to the deflection of the free-end of the cantilever. The x-axis shows the vertical movement of the piezoelectric scanner, which translates the fixed-end of the cantilever. In the region of contact, each unit of piezo movement results in equivalent cantilever deflection (e.g. the cantilever deflects 1 nm if the piezo moves 1 nm). The inverse slope in this region yields the optical lever sensitivity, ~120 nm V^{-1}, which is a measure of how the photodetector responds to the flexure of the cantilever. (*Bottom*) The photodetector output (*top plot*) was converted to cantilever deflection (in nm) which in turn was converted to force, assuming a spring constant of 0.01 nN/nm. The piezo movement was corrected to account for deflection of the cantilever and yields the separation between tip and sample. By convention, repulsive forces are positive and attractive forces negative. The "jump-from" or "jump-to" contact features result from the mechanical instability of the cantilever relative to the forces it is probing. Jump-from contact features can be seen in retraction curves when the cantilever spring constant exceeds the actual force gradient at the tip-glass interface (K_{sp} label on *bottom figure*). Jump-to contact features may be present in approach data when the actual force gradient exceeds the spring constant of the cantilever (see distance from 0 to 10 nm in approach curve in the *bottom figure*)

18.2.2.2 Converting Piezoelectric Scanner Movement into Separation values

The movement of the piezoelectric scanner must be corrected by the deflection of the free end of the cantilever to obtain an absolute separation distance between a sample (e.g. a cell attached to a substrate) and the tip on the cantilever. The

separation between the tip and sample can be determined once the photodiode signal is converted into deflection values for the cantilever. Absolute separation is determined by correcting the movement of the piezoelectric scanner by the cantilever deflection. For example, if the piezoelectric scanner moves the cantilever 10 nm towards the sample, but the free end of the cantilever deflects upwards by 2 nm, the actual separation has changed by only 8 nm (Fig. 18.4).

The origin of the separation axis (i.e. distance of zero) is defined by using "jump-to-contact" and "jump-from-contact" events for approach and retraction curves, respectively (see Fig. 18.4). In instances where only repulsive forces are measured (i.e. no jump to/from contact) it is more difficult to define a separation distance of zero. This is typically accomplished by defining the initial point on the region of contact as the origin of the separation axis.

18.3 Examples of AFM Force Measurements on Living Bacteria

In the late 1990s, a few groups of researchers began to use AFM to study forces associated with bacterial adhesion (Camesano and Logan, 2000; Lower et al., 1999, 2000; Razatos et al., 1998). Since then there have been countless publications in which AFM has been used to probe forces and bonds associated with bacteria. Over the years, a number of researchers have led this effort, including Terrance Beveridge, Terri Camesano, Yves Dufrene, and the current author. Below I will provide two examples to illustrate how AFM can be used to gain a unique perspective of the forces, bonds, and macromolecules that operate at the interface between a bacterium and another surface.

18.3.1 Intermolecular Forces as Staphylococcus aureus Comes into Contact with Silica (SiO_2)

Quartz (SiO_2), or its amorphous form silica, is probably the most common surface that bacteria encounter in nature. This is mainly due to the fact that the two elements silicon and oxygen make up 74 wt% (95 vol%) of the Earth's crust (Klein and Hurlbut, 1985). On an atomic scale, the Earth's crust consists of a packing of oxygen atoms with interstitial metal ion, mainly Si. Quartz and silica are also found within humans in the form of implanted medical devices, like catheters for example. Bacteria are known to form infectious biofilms on such surfaces. Finally, silica glass slides are the substrate of choice for viewing bacteria with an optical microscope.

AFM can be used to measure the attractive or repulsive intermolecular forces that a bacterium experiences as it approaches a surface of quartz or silica. The following discussion will show force-distance curves that were collected between a glass bead attached to the end of a cantilever (Fig. 18.3, left panel), and living cells of *S. aureus*, which were sitting on a glass slide (Fig. 18.1, right panel). The observed force-distance relationship will be compared to theoretical models of two important

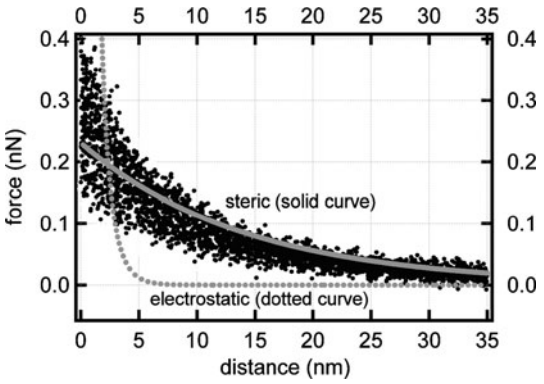

Fig. 18.5 Intermolecular forces (*dots*) measured as a 10 μm silica (SiO_2) bead approaches a *S. aureus* bacterium in 0.1 M NaCl solution at about pH 7. The electrostatic force was calculated using Eq. (1) with surface potentials of –35 and –6 mV for the silica and bacterium, respectively. The steric force was calculated using Eq. (2) with values of 90 nm and 3.4×10^{14} molecules per m^2 for the polymer thickness and density, respectively

intermolecular forces: the electrostatic force and the steric force. By comparing the measured and theoretical forces, one can determine which force type controls the initial adhesion of *S. aureus* to SiO_2 surfaces in an aqueous solution.

Figure 18.5 shows forces detected as a glass bead is brought into contact with a single cell or binary fission pair of *S. aureus*. Shown are 10–15 approach curves chosen at random from a total of ~500 curves collected for three different glass beads and three different cultures of the same strain of *S. aureus*. This figure reveals that the bead's surface must approach to within 30 nm of the bacterium before a measurable force is detected. As the distance between the cell and glass decreases, the bacterium experiences a repulsive force (positive sign) that appears to increase exponentially until the cell and glass make contact (i.e. a distance of zero).

Theoretical force-distance expressions can be used to interpret the observed force data. As mentioned in the Introduction, there are a few fundamental forces that may exist between surfaces in aqueous solution. The electrostatic force is one of these force types. A common mathematical expression for the electrostatic force is given as (Elimelech et al., 1995):

$$F(D) = \frac{2\,\pi\, r_1\, r_2\, \varepsilon\, \varepsilon_0\, \kappa}{r_1 + r_2} \left(\frac{k_B\, T}{z\, e_c} \right)^2 \frac{\phi_1^2 + \phi_2^2 + \left(2e^{D\kappa}\phi_1\phi_2\right)}{\left(e^{D\kappa} - 1\right)\left(e^{D\kappa} + 1\right)} \tag{1}$$

where F = force (in Newtons); D = distance between the two surfaces of interest (m); r = radius of the cell or bead (m), ε is the dielectric constant of water (78.54 at 298 K), ε_0 is the permittivity of free space (8.854×10^{-12} C^2 $J^{-1}m^{-1}$), k_B is Boltzmann's constant (1.381×10^{-23} J K^{-1}), T is temperature (298 K), z is the valence of electrolyte ions (1 for NaCl), and ec is the charge of an electron (1.602×10^{-19} C). The inverse Debye length (κ, in m^{-1}) describes the thickness of

the electrostatic double layer of counter-ions that surrounds charged particles (glass bead or bacterium) in solution. For monovalent electrolytes (e.g. NaCl) at 298 K, the Debye length (κ^{-1}, in nm) is given by $0.304/(c)^{-1/2}$, where c is the concentration of the electrolyte (mol L^{-1}). The final parameter is the surface potential (ϕ) described as [(zeψ)/(kT)], where ψ is the surface potential of the cell or glass bead (in V) and all other parameters are as described above.

For an aqueous solution at around pH 7 and ionic strength ~0.1 M, the surface potentials of a glass bead and *S. aureus* are, respectively, –35 mV (Ducker et al., 1992) and –6 mV (Prince and Dickinson, 2003). By using these values in Eq. (1), one may calculate the theoretical electrostatic force between an *S. aureus* bacterium and a glass bead. This theoretical force-distance relationship is shown in Fig. 18.5.

The electrostatic force is expected to be repulsive and short range (<5 nm) in a 0.1 M saline solution. While the observed interaction is repulsive, the measured forces are clearly longer range than expected based solely on electrostatic interactions. Therefore, another intermolecular force must also be involved in how this particular bacterium interacts with the surface of glass.

Staphylococcus cells, like all bacteria, have a surface that is studded with biological polymers. One of the most common biopolymers on *S. aureus* is β-1,6-linked glucosaminoglycan, also know as the polysaccharide intercellular adhesin (PIA) (Heilmann et al., 1996; Ziebuhr et al., 1997). Polymers such as these cause steric repulsion when they are confined to a narrow space (Israelachvili, 1992; Israelachvili and McGuiggan, 1988; Taylor and Lower, 2008). This repulsion is driven by a decrease in entropy that occurs when a polymer is no longer free to move at random. Polymers that are free to move and rotate in random orientations within a solution are in a higher state of disorder relative to the same polymer that has been confined to a smaller volume of space. This is precisely what occurs when a polymer on a bacterium is confined to a narrowing interface created by an approaching surface (e.g. a glass bead).

Like the electrostatic force (see Eq. (1)), the steric force (F) has been described as a function of the distance (D) between two surfaces. This expression, known as the modified Alexander-de Gennes equation, is given by (Butt et al., 1999; Taylor and Lower, 2008):

$$F(D) = 50\, r\, \mathrm{k_B}\, T\, L_0\, \Gamma^{3/2} e^{-2\pi D/L_0} \tag{2}$$

where r = radius of the cell (m), k_B is Boltzmann's constant (1.381 × 10–23 J K–1), T is temperature (298 K), L_0 is the equilibrium thickness of a polymer (in m) on the cell surface, Γ is the surface density of that same polymer on the cell surface (in m–2).

One can determine the theoretical steric force between *S. aureus* and glass by using the thickness and surface density of PIA. *Staphylococcus* have PIA molecules composed of at least 130 sugar residues (Mack et al., 1996), which corresponds to a value for L_0 of ~90 nm assuming 0.7 nm per glucose residue (Yongsunthon and Lower, 2006). While not measured directly, the surface density (Γ) of PIA on a staphylococci cell can be estimated from previous studies (Mack et al.,

1996; Madigan et al., 2003). Using these references, there are about 4300 PIA polysaccharides per bacterium. For a 2 μm bacterium (i.e. proxy for a fission pair of *Staphylococci* cells) this is equivalent to approximately 3.4×10^{14} PIA per m^2. Using these values for L_0 and Γ in Eq. (2) results in a theoretical expression of the steric force between a *Staphylococcus* cell and a glass bead (see Fig. 18.5).

Comparing the measured forces to the theoretical models reveals that the steric force and to a lesser extent the electrostatic force dominate the interactions between *S. aureus* and a glass surface in saline solution. The glass substrate must be within 30 nm of the bacterium surface before the forces between the two are measurable (above noise). Steric forces then cause the bacterium to be repelled until the cell is within ~5 nm of the glass. At this close distance, repulsive, electrostatic forces begin to impact the final approach.

18.3.2 Bonds that Form Between Staphylococcus aureus and a Silica Surface That Is Coated with a Protein Layer

The above example focuses only on the forces that occur as a cell approaches another surface. However, adhesion may occur and bonds may form once a cell comes into contact with another surface. AFM can be used to probe the force required to rupture a bond that forms between a biomolecule on a bacterium and a reactive site on a material surface. AFM can also be used the probe the biomechanical properties of cell wall macromolecules.

The following discussion will show force-distance curves that were collected as a protein coated probe was pulled from contact with living cells of *S. aureus*. For these measurements, the AFM tip was coated with fibronectin (Fn), a human protein that commonly coats implanted medical devices. The measured force-distance curves will be compared to a worm-like chain model, which predicts the force-distance trajectory for a protein that is mechanically perturbed into an unfolded conformation. By comparing the measured and theoretical forces, one can identify an adhesin and understand the intrinsic biomechanical properties of that adhesin.

Figure 18.6 shows the force-extension curves for Fn on a glass slide versus Fn in contact with a strain of *S. aureus* that overexpresses fibronectin-binding protein (FnBP) on its cell wall. Many of these curves exhibit a distinct, non-linear, sawtooth-shaped, force-distance relationship. For example, the Fn molecules (X-symbols in Fig. 18.6) unravel to approximately 200 nm where they rupture at a force of ~0.4 nN. This non-linear, sawtooth-shaped feature becomes more pronounced for Fn that has formed a bond with putative FnBPs on *S. aureus*.

Such signatures have been attributed to specific binding events mediated by proteins (Carrion-Vazquez et al., 1999; Lower et al., 2001a, 2005; Mueller et al., 1999; Müller et al., 1999; Oberdorfer et al., 2000; Oberhauser et al., 1999; Rief et al., 1997). The shape profile of the binding event can be explained by the unfolding mechanics of the bound protein. The worm-like chain (WLC) model approximates the biomechanical force-extension relationship of folded-polymers (e.g. proteins)

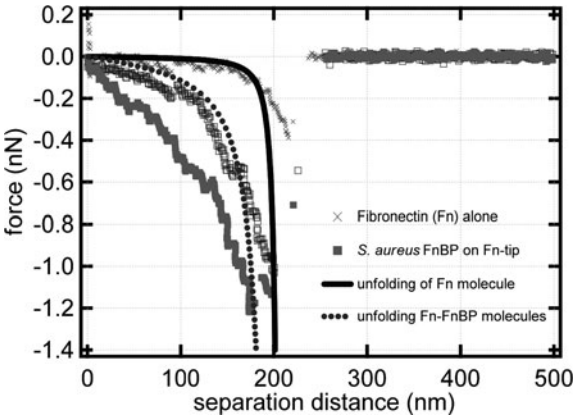

Fig. 18.6 Forces measured as a protein, which forms a bridging bond between two surfaces, is stretched or unfolded in a buffer solution. These retraction curves begin at the origin and proceed to the right on the distance axis. The "x" symbols correspond to a fibronectin (Fn) coated tip that is being pulled away from a glass slide. The *square symbols* correspond to an Fn-tip that has bonded to fibronectin-binding proteins (FnBP) on *S. aureus*. Equation (3) was used to calculate the theoretical force-extension relationship for a Fn molecule (*solid curve*) versus an Fn molecule that has formed parallel bonds with FnBP on the cell wall of a bacterium. For this calculation the contour length was 210 nm and the persistence length was 0.4 nm (*solid curve*) or 0.04 nm (*dotted curve*)

that are mechanically extended (or unfolded) into their linear form (Flory, 1989). The WLC equation is given as:

$$F(D) = [k_B T/p] \times [0.25\,(1 - D/L)^{-2} + D/L - 0.25], \tag{3}$$

where F (in Newtons) is the entropic restoring force generated when a protein is mechanically unfolded to distance D (in meters), k_B is Boltzmann's constant, and T is temperature (in Kelvins). The adjustable parameters of the WLC model are the persistence length (p) and the contour length (L).

The persistence length is a measure of the bending rigidity or stiffness of a polypeptide chain. For a single protein molecule, the persistence length is typically less than 2.0 nm (Carrion-Vazquez et al., 1999; Kellermayer et al., 1997; Müller et al., 1999; Oberhauser et al., 1999; Tskhovrebova et al., 1997), which is similar to the physical length of 0.4 nm between C_α atoms in the backbone of a protein (Mueller et al., 1999). The contour length is the extended length of either an entire protein molecule or a structural domain within a protein. A number of groups have studied the force-structure relationship of ligand-receptor pairs by comparing AFM force spectra to WLC models (Carrion-Vazquez et al., 1999; Lower et al., 2001a, 2005, 2007; Mueller et al., 1999; Oberdorfer et al., 2000; Rief et al., 1997).

For example, if Fn on the tip forms a bond with a receptor on the outer cell wall of a bacterium, an increasingly nonlinear force will be exerted on the tip as the tip is pulled away from the surface of the bacterium (i.e. the separation distance increases

from left to right in a force-distance profile). This process causes the mechanical unfolding of the protein(s) bridging the bacterium to the AFM tip. At some distance from the surface, the force exerted by the tip's spring constant will exceed the tolerance of the ligand/receptor interaction, and the bond will break or the load-bearing domain will unravel. At this point, the tip will "snap" back to its index position, producing a sawtooth-shaped profile or waveform.

Figure 18.6 (solid black curve) shows the WLC force-extension relationship for 525 amino acids ($L = 210$ nm) at the N-terminal domain of Fn. This is the region of Fn that binds to FnBP on *S. aureus* (Foster and Höök, 1998; Greene et al., 1995; Schwarz-Linek et al., 2004). The WLC prediction compares well with the force spectra corresponding to an Fn-coated tip on a glass substrate (Fig. 18.6). There is a nonlinear force-distance (or force-extension) relationship until the Fn breaks free of the glass slide at an extension distance of ~200 nm, which corresponds to the extended length of the N-terminal domains on Fn.

The WLC model can also be used to explain what happens when FnBP on *S. aureus* forms a bond with Fn molecules on the AFM tip. Parallel bonds that form along the length of Fn and FnBP would cause a stiffening (i.e. decreasing persistence length, p, in Eq. (3)) of the protein–protein bond. Figure 18.6 (dotted black curve) shows the hypothetical sawtooth-shaped binding profile for FnBP that forms parallel bonds with the N-terminal region of Fn. For this curve the persistence length was set at 0.04 nm, which is smaller than the physical dimension of an amino acid.

Others have attributed such small values for persistence length to a response caused by multiple protein chains acting in parallel (Bemis et al., 1999; Dugdale et al., 2005, 2006; Higgins et al., 2002; Kellermayer et al., 1997; Lee et al., 2006). For example, ten protein chains in parallel, each with the same contour length, would exert a force ten times that of a single chain. Fitting this response by a single chain model, such as the WLC, would result in one-tenth the true persistence length value. This may be the situation for *S. aureus* FnBP as other studies suggest that one FnBP has the capacity to bind to multiple copies (2–9) of Fn (Fröman et al., 1987; Huff et al., 1994).

18.3.3 Other Uses of AFM: Loading Rate and Affinity Maps

The two examples above provide only small glimpses into the possibilities that AFM offers to investigators who wish to explore the interface between a living bacterium and another surface. Recently, it was demonstrated that individual proteins on the surface of a living bacterium could be mapped across the cell wall (Lower et al., 2009). This was accomplished by tuning into a specific force-signature, like the one shown in Fig. 18.6. Other researchers have begun to use AFM to study the fundamental binding properties (e.g. dissociation rate constant) of protein bonds. These investigations rely upon the fact that the rupture force of a ligand–receptor pair should depend upon the loading rate (N s^{-1}) of the bond (Bell, 1978; Evans, 2001). The loading rate of a bond can be easily manipulated with the AFM by simply

varying the retraction velocity (m s^{-1}) and spring constant (N m^{-1}) of the cantilever. Benoit et al. (2000) and Hanley et al. (2003) provide an excellent description of this work on large eukaryotic cells. This type of research could also be applied to study fundamental aspects of bacterial adhesion.

References

Albrecht TR, Akamine S, Carver TE, Quate CF (1990) Microfabrication of cantilever styli for the atomic force microscope. J Vac Sci Technol A 8:3386–3396

Bell GI (1978) Models for specific adhesion of cells to cells. Science 200:618–627

Bemis JE, Akhremitchev BB, Walker GC (1999) Single polymer chain elongation by atomic force microscopy. Langmuir 15:2799–2805

Benoit M, Gabriel D, Gerisch G, Gaub HE (2000) Discrete interactions in cell adhesion measured by single-molecule force spectroscopy. Nat Cell Biol 2:313–317

Binnig G, Quate CF, Gerber C (1986) Atomic force microscope. Phys Rev Lett 56:930–933

Butt HJ, Kappl M, Mueller H, Raiteri R, Meyer W, Ruhe J (1999) Steric forces measured with the atomic force microscope at various temperatures. Langmuir 15:2559–2565

Camesano TA, Logan BE (2000) Probing bacterial electrosteric interactions using atomic force microscopy. Environ. Sci. Technol. 34:3354–3362

Cappella B, Dietler G (1999) Force-distance curves by atomic force microscopy. Surf Sci Rep 34:1–44

Carrion-Vazquez M, Oberhauser AF, Fowler SB, Marszalek PE, Broedel SE, Clarke J, Fernandez JM (1999) Mechanical and chemical unfolding of a single protein: a comparison. Proc Natl Acad Sci USA 96:3694–3699

Cleveland JP, Manne S, Bocek D, Hansma PK (1993) A nondestructive method for determining the spring constant of cantilevers for scanning force microscopy. Rev Sci Instrum 64:403–405

Craig VSJ, Neto C (2001) *In situ* calibration of colloid probe cantilevers in force microscopy: hydrodynamic drag on a sphere approaching a wall. Langmuir 17:6018–6022

Ducker WA, Senden TJ, Pashley RM (1991) Direct measurement of colloidal forces using an atomic force microscope. Nature 353:239–241

Ducker WA, Senden TJ, Pashley RM (1992) Measurements of forces in liquids using a force microscope. Langmuir 8:1831–1836

Dugdale TM, Dagastine R, Chiovitti A, Mulvaney P, Wetherbee R (2005) Single adhesive nanofibers from a live diatom have the signature fingerprint of modular proteins. Biophys J 89:4252–4260

Dugdale TM, Dagastine R, Chiovitti A, Wetherbee R (2006) Diatom adhesive mucilage contains distinct supramolecular assemblies of a single modular protein. Biophys J 90:2987–2993

Elimelech M, Gregory J, Jia X, Williams R (1995) Particle deposition & aggregation: measurement, modeling, and simulation. Butterworth-Heinemann, Oxford

Evans E (2001) Probing the relation between force – lifetime – and chemistry in single molecular bonds. Annu Rev Biophys Biomol Struct 30:105–128

Flory PJ (1989) Statistical mechanics of chain molecules. Hanser Publisher, Munich, Germany

Foster TJ, Höök M (1998) Surface protein adhesins of *Staphylococcus aureus*. Trends Microbiol 6:484–488

Fröman G, Switalski LM, Speziale P, Höök M (1987) Isolation and characterization of a fibronectin receptor from *Staphylococcus aureus*. J Biol Chem 262:6564–6571

Greene C, McDevitt D, Francois P, Vaudaux PE, Lew DP, Foster TJ (1995) Adhesion properties of mutants of *Staphylococcus aureus* defective in fibronectin-binding proteins and studies on the expression of fnb genes. Mol Microbiol 17:1143–1152

Hanley W, McCarty O, Jadhav S, Tseng Y, Wirtz D, Konstantopoulos K (2003) Single molecule characterization of P-selectin/ligand binding. J Biol Chem 278:10556–10561

Heilmann C, Schweitzer O, Gerke C, Vanittanakom N, Mack D, Götz F (1996) Molecular basis of intercellular adhesion in the biofilm-forming *Staphylococcus epidermidis.* Mol Microbiol 20:1083–1091

Higgins MJ, Crawford SA, Mulvaney P, Wetherbee R (2002) Characterization of the adhesive mucilages secreted by live diatom cells using atomic force microscopy. Protist 153: 25–38

Huff S, Matsuka YV, McGavin MJ, Ingham KC (1994) Interaction of N-Terminal fragments of fibronectin with synthetic and recombinant-D motifs from its binding-protein on *Staphylococcus aureus* studied using fluorescence anisotropy. J Biol Chem 269:15563–15570

Hutter JL, Bechhoefer J (1993) Calibration of atomic-force microscope tips. Rev Sci Instrum 64:1868–1873

Israelachvili JN (1992) Intermolecular and surface forces. Academic, London

Israelachvili JN, McGuiggan PM (1988) Forces between surfaces in liquids. Science 241: 795–800

Jericho SK, Jericho MH, Hubbard T, Kujath M (2004) Micro-electro-mechanical systems microtweezers for the manipulation of bacteria and small particles. Rev Sci Instrum 75: 1280–1282

Kellermayer MSZ, Smith SB, Granzier HL, Bustamante C (1997) Folding-unfolding transitions in single titin molecules characterized with laser tweezers. Science 276:1112–1116

Kendall TA, Lower SK (2004) Forces between minerals and biological surfaces in aqueous solution. Adv Agronom 82:1–54

Klein C, Hurlbut CS (1985) Manual of mineralogy. Wiley, New York, NY

Leckband D, Israelachvili JN (2001) Intermolecular forces in biology. Quart Rev Biophys 34: 105–267

Lee G, Abdi K, Jiang Y, Michaely P, Bennett V, Marszalek PE (2006) Nanospring behaviour of ankyrin repeats. Nature 440:246–249

Lower SK, Hochella MF, Beveridge T (2001a) Bacterial recognition of mineral surfaces: nanoscale interactions between *Shewanella* and alpha-FeOOH. Science 292:1360–1363

Lower BH, Shi L, Yongsunthon R, Droubay TC, McCready DE, Lower SK (2007) Specific bonds between an iron oxide surface and outer membrane cytochromes MtrC and OmcA from S*hewanella oneidensis* MR-1. J Bacteriol 189:4944–4952

Lower SK, Tadanier CJ, Hochella MF (2000) Measuring interfacial and adhesion forces between bacteria and mineral surfaces with biological force microscopy. Geochim Cosmochim Acta 64:3133–3139

Lower SK, Tadanier CJ, Hochella MF (2001b) Dynamics of the mineral-microbe interface: use of biological force microscopy in biogeochemistry and geomicrobiology. Geomicrobiol J 18: 63–76

Lower SK, Tadanier CJ, Hochella MF, Berry DF, Potts M (1999) The bacteria-mineral interface: probing nanoscale forces with biological force microscopy. Geol Soc Am Abstr Prog 31(7):A394

Lower BH, Yongsunthon R, Shi L, Wildling L, Gruber HJ, Wigginton NS, Reardon CL, Pinchuk GE, Droubay TC, Boily JF, Lower SK (2009) Antibody recognition force microscopy shows that outer membrane cytochromes OmcA and MtrC are expressed on the exterior surface of *Shewanella oneidensis* MR-1. Appl Environ Microbiol 75:2931–2935

Lower BH, Yongsunthon R, Vellano FP, Lower SK (2005) Simultaneous force and fluorescence measurements of a protein that forms a bond between a living bacterium and a solid surface. J Bacteriol 187:2127–2137

Mack D, Fischer W, Krokotsch A, Leopold K, Hartmann R, Egge H, Laufs R (1996) The intercellular adhesin involved in biofilm accumulation of *Staphylococcus epidermidis* is a linear beta-1,6-linked glucosaminoglycan: purification and structural analysis. J Bacteriol 178:175–183

Madigan MT, Martinko JM, Parker J (2003) Brock biology of microorganisms. Prentice Hall, Upper Saddle River, NJ

Mueller H, Butt HJ, Bamberg E (1999) Force measurements on myelin basic protein adsorbed to mica and lipid bilayer surfaces done with the atomic force microscope. Biophys J 76: 1072–1079

Müller DJ, Baumeister W, Engel A (1999) Controlled unzipping of a bacterial surface layer with atomic force microscopy. Proc Natl Acad Sci USA 96:13170–13174

Noy A, Vezenov DV, Lieber CM (1997) Chemical force microscopy. Annu Rev Mater Sci 27: 381–421

Oberdörfer Y, Fuchs H, Janshoff A (2000) Conformational analysis of native fibronectin by means of force spectroscopy. Langmuir 16:9955–9958

Oberhauser AF, Marszalek PE, Carrion-Vazquez M, Fernandez JM (1999) Single protein misfolding events captured by atomic force microscopy. Nat Struct Biol 6:1025–1028

Parsek MR, Fuqua C (2004) Biofilms 2003: emerging themes and challenges in studies of surface-associated microbial life. J Bacteriol 186:4427–4440

Prince JL, Dickinson RB (2003) Kinetics and forces of adhesion for a pair of capsular/unencapsulated *Staphylococcus* mutant strains. Langmuir 19:154–159

Razatos A, Ong Y-L, Sharma MM, Georgiou G (1998) Molecular determinants of bacterial adhesion monitored by atomic force microscopy. Proc Natl Acad Sci USA 95:11059–11064

Rief M, Gautel M, Oesterhelt F, Fernandez JM, Gaub HE (1997) Reversible unfolding of individual titin immunoglobulin domains by AFM. Science 276:1109–1112

Schwarz-Linek U, Höök M, Potts JR (2004) The molecular basis of fibronectin-mediated bacterial adherence to host cells. Mol Microbiol 52:631–641

Senden TJ, Ducker WA (1994) Experimental determination of spring constants in atomic-force microscopy. Langmuir 10:1003–1004

Taylor ES, Lower SK (2008) Thickness and surface density of extracellular polymers on Acidithiobacillus ferrooxidans. Appl Environ Microbiol 74:309–311

Tortonese M (1997) Cantilevers and tips for atomic force microscopy. IEEE Eng Med Biol Mag 16:2833

Tskhovrebova L, Trinick J, Sleep JA, Simmons RM (1997) Elasticity and unfolding of single molecules of the giant muscle protein titin. Nature 387:308–312

Watnick P, Kolter R (2000) Biofilm, city of microbes. J Bacteriol 182:2675–2679

Whitman WB, Coleman DC, Wiebe WJ (1998) Prokaryotes: the unseen majority. Proc Natl Acad Sci USA 95:6578–6583

Yongsunthon R, Lower SK (2006) Force measurements between a bacterium and another surface *in situ*. Adv Appl Microbiol 58:97–124

Ziebuhr W, Heilmann C, Götz F, Meyer P, Wilms K, Straube B, Hacker J (1997) Detection of the intercellular adhesion gene cluster (ica) and phase variation in *Staphylococcus epidermidis* blood culture strains and mucosal isolates. Infect Immun 65:890–896

Chapter 19
Assessing Bacterial Adhesion on an Individual Adhesin and Single Pili Level Using Optical Tweezers

Ove Axner, Magnus Andersson, Oscar Björnham, Mickaël Castelain, Jeanna Klinth, Efstratios Koutris, and Staffan Schedin

Abstract Optical tweezers (OT) are a technique that, by focused laser light, can both manipulate micrometer sized objects and measure minute forces (in the pN range) in biological systems. The technique is therefore suitable for assessment of bacterial adhesion on an individual adhesin-receptor and single attachment organelle (pili) level. This chapter summarizes the use of OT for assessment of adhesion mechanisms of both non-piliated and piliated bacteria. The latter include the important helix-like pili expressed by uropathogenic *Escherichia coli* (UPEC), which have shown to have unique and intricate biomechanical properties. It is conjectured that the large flexibility of this type of pili allows for a redistribution of an external shear force among several pili, thereby extending the adhesion lifetime of bacteria. Systems with helix-like adhesion organelles may therefore act as dynamic biomechanical machineries, enhancing the ability of bacteria to withstand high shear forces originating from rinsing flows such as in the urinary tract. This implies that pili constitute an important virulence factor and a possible target for future anti-microbial drugs.

19.1 Introduction

Infections remain a major cause of morbidity and mortality in the world. In particular, the widespread bacterial resistance to antibiotics is a ubiquitous and rapidly growing problem that needs to be addressed with no further delay. There is therefore an urgent need for new anti-microbial drugs. However, it is a general consensus that the development of new drugs requires the identification of new targets in bacteria

O. Axner (✉)
Department of Physics, Umeå Centre for Microbial Research (UCMR), Umeå University, Umeå, Sweden
e-mail: ove.axner@physics.umu.se

D. Linke, A. Goldman (eds.), *Bacterial Adhesion*, Advances in Experimental Medicine and Biology 715, DOI 10.1007/978-94-007-0940-9_19,

(Rasko and Sperandio, 2010), which, in turn, calls for detailed knowledge of microbial pathogenic mechanisms. Since adhesion of bacterial pathogens to host tissue is a prerequisite for infections, the adhesion mechanism is one possible target. It is therefore of importance to characterize the adhesion process in bacterial systems in detail.

The adhesion mechanism of bacteria has been found to be more complex than first anticipated (An and Friedman, 2000). For example, many types of bacteria have adhesins that bind to specific receptors on the host cell. Whereas some bacteria express their adhesins directly on the cell wall, others produce extended attachment organelles, often referred to as pili or fimbriae, on which their adhesins are expressed (Proft and Baker, 2009). It has been hypothesized that the biomechanical properties of these pili, in particular their unique elongation properties, play an important role for the adhesion of piliated bacteria, specifically in the presence of external rinsing forces.

The human body has a number of responses which remove bacteria that lack the appropriate adhesion capabilities. Since a bacterium detaches from its host only when all its adhesin-receptor interactions have ruptured, and bacteria use a variety of adhesins, it is in general non-trivial to fully characterize a given adhesion mechanism from bulk measurements; instead, the adhesion mechanisms should preferably be addressed on the single cell level. In addition, since bacteria often are exposed to shear flows that will expose different adhesins to dissimilar forces, a number of non-linear processes can arise, e.g. successive breakage of interactions and bacterial rolling (Thomas et al., 2004). Hence, in order to understand microbial adhesion from a basic point of view, one needs a technique that can assess individual adhesin-receptor interactions at the single-molecule level and characterize individual organelles. From such knowledge it is possible to comprehend the adhesion behaviour of individual bacteria adhering by several adhesins under various conditions.

Although a number of techniques for investigation of bacterial adhesion have been developed over the years, most address bacteria by population-based measurements, and so they are not applicable to the assessment of individual adhesion mechanisms. Static pictures of the structure of pili can be obtained from techniques such as atomic force microscopy (AFM) (Balsalobre et al., 2003), scanning electron microscopy (SEM) (de Breij et al., 2009), and X-ray diffraction (Knight et al., 2002). However, to obtain information about the dynamic properties as well as the force dependence of the adhesion mechanism, which has turned out to be of highest importance for the adhesion of piliated bacteria exposed to external forces, individual interactions need to be studied in real time. The techniques that predominantly are used for such studies are force measuring techniques such as AFM and optical tweezers (OT).

AFM utilizes a mechanical cantilever to assess the force to which a given object is exposed. Due to the mechanical properties of the cantilever, the technique is applicable to forces ranging from some tens of picoNewton (pN) to a few nanoNewton (nN). OT manipulates objects and measure forces solely by light, the latter by

assessing the movement of a trapped bead in the focus of a laser beam. This is then sometimes referred to as force measuring optical tweezers (FMOT), and is more sensitive than AFM; it can address forces from sub-pN to hundreds of pN, often with a sub-pN resolution. In addition, whereas AFM measures forces in the vertical direction, FMOT measures them predominantly horizontally. It also has a larger degree of freedom since the trapped object is not fixed to the surface; it can easily be moved in all three dimensions (3D). Moreover, in case of contamination, the AFM technique requires a change of the cantilever, while it suffices for FMOT to trap another bead. All this has made FMOT the most appropriate technique for quantitative studies of bacterial adhesion processes. Due to all its capabilities, a significant amount of knowledge has been gained during the last years about adhesion mechanisms in general, and the biomechanical properties of individual attachment organelles in particular, thus helping us comprehend the complex features of bacterial adhesion.

19.2 Optical Tweezers

OT is a tool by which micrometer-sized transparent objects, inorganic as well as biological, can be trapped in the focus of a laser beam by transfer of light momentum (Neuman and Block, 2004). A trapped object will be confined in the focal volume, which acts as a harmonic potential for small displacements, and allows for precise movement and manipulation in 3D. Since the first single gradient optical trap, which was built by Arthur Ashkin in the eighties (Ashkin and Dziedzic, 1987), numerous groups worldwide have constructed and used sensitive and user-friendly optical tweezers systems for optical micro-manipulation of a variety of objects, e.g. cell sorting (Grover et al., 2001), signal regulation in NK-cells (Ericsson et al., 2000), investigations of the spatial confinement and organization of cells (Haruff et al., 2003), manipulation of bacterial positions (Horner et al., 2010), and investigations of the bending stiffness of *E. coli* adhering to a surface (Wang et al., 2010).

OT can also be used for force measurement in biological systems. When a trapped bead is exposed to an external force, its position in the trap will shift, and so it can serve as a force transducer (Neuman and Block, 2004). By monitoring the position of the bead, the force to which the bead is exposed can be assessed. By coating the bead with a specific receptor it is possible to study individual adhesin-receptor interactions directly. Moreover, by attaching the bead to bacteria that express pili, the biomechanical properties of the pili can be characterized. Calibration of the optical trap can swiftly be made, for example, by monitoring the Brownian motion (Capitanio et al., 2002).

A typical characterization of the biomechanical properties of an attachment organelle is made by measuring its force (stress) response as it is exposed to a given elongation (strain). A schematic of a set-up is given in Fig. 19.1. Similar set-ups are used to assess the binding strength and lifetime of adhesin-receptor interactions.

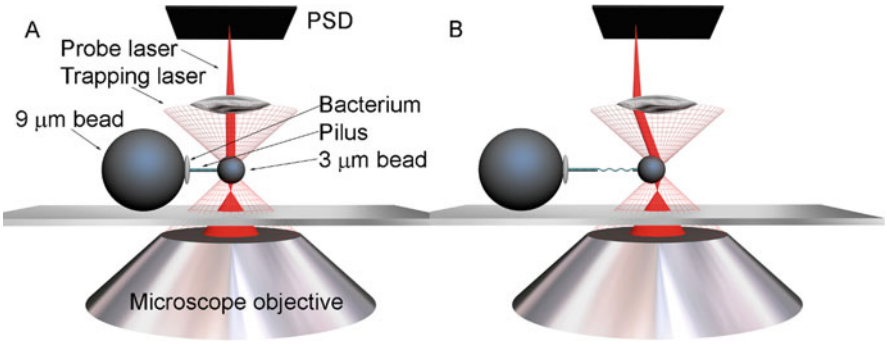

Fig. 19.1 Schematic of FMOT for assessment of the biomechanical properties of pili. (**a**) A single bacterium is mounted on a 9 μm large bead that is firmly attached to the microscope slide. A free floating single bacterium is trapped by the optical tweezers at low laser power and mounted onto the bead. A trapped bead, whose position is probed by a separate probe laser, and to which one or several pili are attached, is used as a force transducer. (**b**) Strain is applied by slowly translating the microscope slide. The force is assessed by detecting the deflection of the probe light by a position sensitive detector (PSD) whose output is converted to a force by a calibration process. Pilus dimensions not to scale

19.3 Bacterial Adhesion Systems Investigated by Optical Tweezers

Bacteria adhere to host cells initially by adhesins that bind specifically to receptors expressed on the surface of host cells. This implies that each type of bacteria adheres preferentially at particular locations. Each adhesin-receptor interaction has also a given strength, presumably optimized for its environment. It is weak enough for the bacterium not to be immobilized forever at a single position, which allows the bacterium to detach regularly so it can migrate to other locations, but it is simultaneously strong enough so that the bacterium avoids being removed by an external force, e.g. from a rinsing flow. An adhesin-receptor interaction can also have a specific susceptibility to various environmental conditions, e.g., to acidity or mechanical force. Hence, the properties of an adhesin-receptor interaction are of crucial importance for the ability bacteria to cause infections.

Interactions are often modelled in terms of a bond and an energy landscape, where the transition between the different states of the bond, i.e. open and closed, is a stochastic process that is strongly affected by the properties of the landscape, such as activation energy and bond length. The average time after which it opens is termed the lifetime and serves as a measure of its strength. The lifetime of a bond depends on the activation energy in an exponential manner. When a bond is exposed to an external force, the activation energy is lowered by an amount given by the product of the force and the bond length (Bell, 1978). Application of force to a bond thus provides a way to map out its energy landscape.

A common way to assess the properties of an individual bond is to probe its force dependence with a constant loading rate (i.e. with a force that increases linearly

with time), often referred to as *Dynamic Force Spectroscopy* (DFS) (Evans, 2001). Since the rupture event of a bond is stochastic, a given bond needs to be probed a large number of times. The bond strength is commonly defined as the force at which it most frequently ruptures (Björnham and Schedin, 2009). If measurements are performed at several loading rates, specific bond parameters, e.g. bond length and thermal off-rate, can be assessed.

The adhesion properties of piliated bacteria are determined by the properties of both the adhesin-receptor interaction and the pili. In order to simplify the assessment, pili are often characterized separately from the adhesin-receptor interaction on a single pilus level, by attaching the pilus non-specifically to the probe bead and probing its force-vs.-elongation behaviour. It has been found that the response from a pilus differs markedly from that of a single adhesin-receptor interaction; it depends strongly on the quaternary structure of the pilus. "Linear" or "coil-like" pili, predominantly found on Gram-positive bacteria, display a monotonically and progressively increasing force-vs.-elongation response. Conversely, helix-like pili, which predominantly are expressed by Gram-negative bacteria (Proft and Baker, 2009), show a more intricate response consisting of a combination of a constant elongation force, originating from an uncoiling of the helix-like structure, and a wave-like pseudo-elastic response, caused by a conformational change of the head-to-tail interaction that takes place in a random order. When the biomechanical properties of a pilus have been assessed, the properties of the adhesin-receptor interaction can be deduced from the combined pilus-adhesin response. With knowledge of both the biomechanical and the adhesion properties of a single pilus, and by the use of a model of the distribution of force among a multitude of pili on a bacterial cell binding with multiple pili, henceforth referred to as multipili-attaching bacteria, the adhesion behaviour of multipili binding bacteria can be estimated.

19.3.1 Non-piliated Bacteria

Bacteria that lack attachment organelles mediate binding to host cells by adhesins expressed directly on the cell wall. Adherence by non-piliated bacteria allows the colonizing bacteria to take up nutrients efficiently from host tissue and to escape clearance from peristaltic and rinsing actions more effectively (since the shear forces are smaller close to the surface). On the other hand, tight adherence makes the bacterium vulnerable to various host responses, e.g. toxins that directly can be delivered into the bacterium and thus knock it out (Rad et al., 2002).

One example of an adhesin-receptor interaction that has been studied with FMOT is that between the *Helicobacter pylori* blood group antigen binding adhesin (BabA) and its receptor on gastric epithelial cells (the Lewis b antigen). It was found that this interaction is dominated by a single energy barrier with a bond length and a thermal off-rate of 0.86 nm and 0.015 Hz, respectively (Björnham et al., 2005, 2009a). Other examples of individual bacterial adhesion interactions studied are *Staphylococcus epidermidis* binding to fibronectin (Simpson et al., 2002), and *Staphylococcus aureus* to fibrinogen and fibronectin (Simpson et al., 2003, 2004).

19.3.2 Piliated Bacteria

The adhesion properties of piliated bacteria depend both on the biomechanical properties of the pili and the adhesion properties of the adhesin-receptor interaction. When bacteria lacking pili, or bacteria expressing pili with little flexibility, are exposed to a shear force from the surrounding medium, the various adhesin-receptor interactions will, in general, experience significantly dissimilar forces. In contrast, for bacteria expressing extendable pili, any such force can be distributed more evenly among the various pili, so that the bacteria can maintain attachment despite being exposed to considerable rinsing forces. This implies that the lifetime of multipili-attaching bacteria strongly depends on the biomechanical properties of the pili. It is therefore of highest importance to characterize the structure, the biomechanical properties, and the role of various pili in the adhesion process in some detail.

Since the ability to distribute an external force among various pili, referred to as pili cooperativity (Björnham and Axner, 2009), is assumed to be significant for bacteria expressing helix-like pili, most work has up to now been done regarding the assessment of the biomechanical properties of such pili expressed by *Escherichia coli* (Andersson et al., 2008). The first type of non-helical like pili expressed by Gram-positive bacteria was scrutinized only recently (Castelain et al., 2009a).

19.3.2.1 Helical Like Pili

Uropathogenic *E. coli* (UPEC) is a type of bacterium commonly associated with community–acquired urinary tract infection. It expresses different kinds of helix-like pili, of which P pili and type 1 pili, which colonize the kidneys (Källenius et al., 1981) and the bladder (Jones et al., 1995), respectively, are the two best studied. They consist of a $\sim$1 μm long and 6–7 nm diameter rod that is composed of $\sim 10^3$ subunits, PapA and FimA, respectively, assembled via the chaperone-usher pathway (Sauer et al., 2000, 2004) by a donor-strand-exchange mechanism, and arranged in a right-handed helix-like quaternary structure with 3.28 and 3.36 subunits per turn, respectively (Bullitt and Makowski, 1995; Hahn et al., 2002). At the end of the helix-like rod, a short thin thread (a tip fibrillum) is expressed. It anchors the adhesin (PapG for P pili and FimH for type 1) that binds to receptor molecules on the host cells (Båga et al., 1987; Jacob-Dubuisson et al., 1993).

A few types of helix-like pili have been characterized with respect to their biomechanical properties by FMOT. Some typical force-vs.-elongation curves of F1C pili expressed by UPEC bacteria are shown in Fig. 19.2a, where the different curves represent dissimilar elongation velocities. The figure shows that a pilus has a force-vs.-elongation response that can be seen as composed of three regions; *Region I*, in which the response is basically linear; *Region II*, in which the force response is constant; and *Region III*, in which the response has a monotonically increasing but non-linear (wave-like) response.

Whereas the first region stems from a general elastic stretching of the pilus, the second originates from a sequential opening of the layer-to-layer (LL) interactions

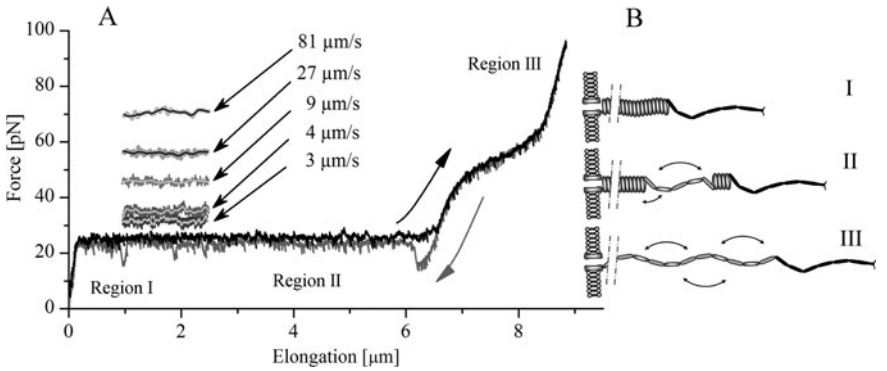

Fig. 19.2 (**a**) Force-vs.-elongation response of a single F1C pilus. *Black curve*: elongation under steady-state conditions: *Grey curve*: the corresponding retraction response; *Coloured curves*: parts of the uncoiling force under dynamic conditions. (**b**) Schematic illustration of the three elongation regions (I, II, and III) of helix-like pili

of the quaternary structure, often referred to as uncoiling of the pilus rod. The reason the opening of the LL interactions is sequential in this region is that each layer of the quaternary structure consists of several (∼3) LL interactions, each of which experiences a fraction of the force to which the pilus is exposed. The interaction connecting the outermost unit in the folded part of the rod, on the other hand, experiences the entire force. This implies that the opening of the LL interactions takes place in a sequential manner, which gives rise to the force plateau. Because each bond can open and close a number of times, the uncoiling of the helix-like structure is fully reversible. Since region II allows for a significant elongation of the pili length (5–7 times), it has been considered of special importance for the ability of a bacterium to redistribute an external shear force among a multitude of pili.

The third region, with its specific wave-like shape, arises from a combination of a stochastic conformational change of the interactions between consecutive subunits of the pilus in the linearized part of the rod and entropy (since this change can take place in a random manner). A schematic representation of the elongation of a pilus in the three regions is given in Fig. 19.2b.

The first demonstration that FMOT could be used to assess the forces that are involved in adhesion of UPEC bacteria was done by Liang et al. (2000) addressing type 1 pili adhering to mannose-presenting surfaces. Since then, a number of more quantitative assessments of the biophysical properties of a number of pili (all expressed by UPEC) have been made: P pili (Jass et al., 2004); type 1 (Andersson et al., 2007); S (Castelain et al., 2009b); and F1C (Castelain et al., 2011). It has been found that they have a similar general shape, although they differ quantitatively.

As was shown in Fig. 19.2a, the uncoiling force in region II depends on the elongation velocity. For velocities below a certain corner velocity, the uncoiling takes place at a force that is independent of the elongation velocity, referred to as the steady-state uncoiling force (the black curve in Fig. 19.2). The steady-state

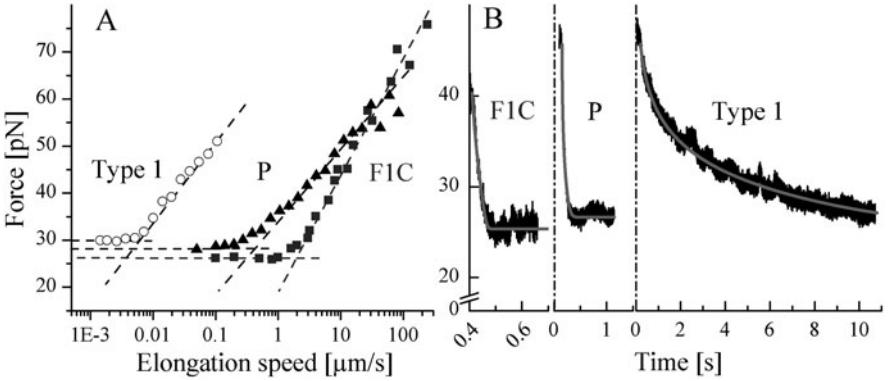

Fig. 19.3 (**a**) The uncoiling force versus elongation velocity for type 1, P and F1C pili, represented by open circles, filled *triangles*, and filled *squares*, respectively. The intersection of the two linear fits gives the corner velocity, representing the boundary between the steady-state and the dynamic regimes. (**b**) Relaxation curves for the same types of pili

uncoiling force for the various types of pili so far investigated ranges from 21 pN (for S_I) to 30 pN (for type 1). For larger elongation velocities, the uncoiling force increases logarithmically with the velocity. Figure 19.3a shows this dependence for three types of pili: type 1, P, and F1C. The corner velocity has been found to vary widely among various pili, ranging from 6 nm/s (for type 1) to 1.4 μm/s (for F1C).

The temporal response of pili can be assessed by relaxation measurements in which the pilus first is uncoiled at a speed that provides a dynamic response before the elongation is suddenly halted. The temporal response of three types of pili is given in Fig. 19.3b. It has been found that the relaxation rates vary extensively among various pili, ranging from 45 ms (for F1C) to 6.7 s (for type 1).

So far, only one specific adhesin-receptor interaction of helix-like pili has been assessed by FMOT, the specific PapG–galabiose binding mediated by P pili (Björnham et al., 2009b). However, the FimH-mannose interaction has recently been characterized by other techniques (Le Trong et al., 2010). The others remain to be characterized.

The biophysical properties of the pili assessed so far have been compared (Andersson et al., 2008; Castelain et al., 2011). It has been concluded that the biomechanical properties of UPEC pili reflect the host environment (Andersson et al., 2007). It has been hypothesized that as long as the pili uncoil in region II, an external force is evenly distributed among the various pili (Björnham and Axner, 2009). However, once one pilus reaches region III, elongation halts, so the force on the pili still in region II is lowered to their steady-state value, whereas the force on the one in region III increases considerably. For an interaction of ordinary slip bond type, this implies that it will rapidly rupture. Since the force thereafter is redistributed among the other pili, this can give rise to a runaway detachment process. The corner velocity for type 1 is significantly lower than that of F1C (6 nm/s and 1.4 μm/s, respectively), which implies that a type 1 pilus exposed to a force

slightly above the steady-state uncoiling force will elongate to its maximum length (a few micrometers) over a time-period of $\sim 10^2$ s, whereas a F1C pilus will fully uncoil within only a few seconds. This suggests that type 1 pili can maintain a force substantially longer than F1C (as well as P and S), which in turn agrees qualitatively with the in vivo conditions in which these bacteria are predominantly found (the lower and upper urinary tract, respectively). Moreover, the temporal response suggests that the pili that are mostly found in upper urinary tract (P, S, and F1C) have fast kinetics, presumably allowing them to accommodate for rapid changes of urine flow.

Modelling of the biomechanical properties of helix-like pili under stress has been made by both a sticky chain model (Andersson et al., 2006), as well as Monte Carlo simulations (Björnham et al., 2008). Both techniques provide excellent agreement with experimental data, thus verifying the underlying model as well as the model parameters assessed. A succinct presentation of the biomechanical modelling of helix-like pili has recently been given (Axner et al., 2009). By access to verified models of the biomechanical properties of pili, the complex phenomenon of multipili adhesion (illustrating the importance of pili-cooperativity) can be investigated by Monte Carlo simulations (Björnham and Axner, 2009). It has even been shown that bacterial catch bond behaviour can appear from piliated bacteria adhering solely by slip bonds (Björnham and Axner, 2010). These types of simulations indicate the importance of the biophysical properties of pili for the adhesion of bacteria and provide an important insight into the complex field of multipili-adhering bacteria.

19.3.2.2 Non-helical Like Pili

Bacteria mediate adhesion not only by expressing helical-like pili, but also by other complex machinery (Proft and Baker, 2009). For example, *Neisseria spp.* produce bundled pili through the type IV secretion pathway whereby the bacteria can both adhere and move using a polymerization processes (Maier, 2005). Gram-positive bacteria often produce pili with a simpler architecture than helix-like. So far, FMOT has only been used to assess the biomechanical properties of one type of pili, T4, expressed by *Streptococcus pneumoniae* (Castelain et al., 2009a), a class of bacteria colonizing the lower respiratory tract (Barocchi et al., 2006). The open coil-like backbone of the pilus is assembled by covalent-linked protein monomers while a single protein, RrgA, is the putative adhesin (Hilleringmann et al., 2009). The elongation properties of this type of pili agree with that of semi-flexible biopolymers chain, well-described by the interpolated worm-like chain (WLC) model (Bustamante et al., 1994). Figure 19.4 displays the force-vs.-elongation response from a bacterium adhering by a few pili, showing the elongation and subsequent rupture of pili. It was found that the persistence length of this type of pili was 2.1 $\pm$1.7 nm. Because of their monotonically increasing force-vs.-elongation response, this type of pilus is expected to express a lower degree of pili-cooperativity than helix-like pili. However, no quantitative analysis of pili-cooperativity in this type of pili has yet been performed.

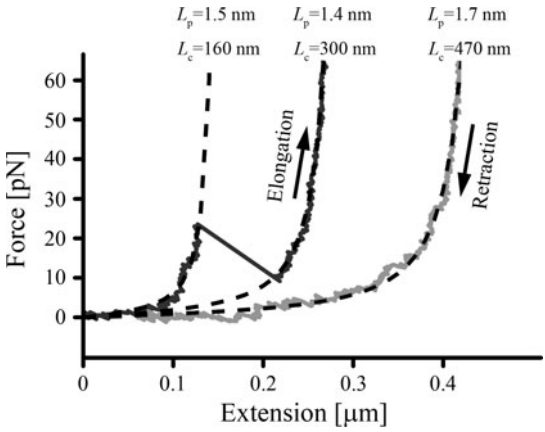

Fig. 19.4 Typical force-vs.-elongation of T4 pili fitted with the WLC model. Copyright Wiley-VCH Verlag GmbH & Co. KGaA. Reproduced with permission from Castelain et al. (2009a)

19.4 Conclusions

While traditional biological research has relied on population-based assessments and indirect techniques to assess the properties of bacterial adhesion, optical tweezers have provided the means to assess bacterial adhesion not only on the single cell level, but also at the single adhesion organelle and single adhesin-receptor interaction level. Using this technique, it is not only possible to assess interaction forces between single cells and various surfaces of interest; it can even be used to characterize the interactions of a given adhesin-receptor interaction or to assess the properties of individual macromolecules. The technique has so far been used to assess the biomechanical properties of a few types of pili, predominantly with a helix-like structure, expressed by UPEC bacteria.

These studies have revealed the importance of the biomechanical properties of pili for the adhesion properties of piliated bacteria. It has been conjectured that the large flexibility of helix-like pili could allow the redistribution of an external shear force among a large number of pili so each pilus is exposed to a force that can be sustained by the adhesin for an extended period of time, making the attachment organelles of crucial importance for the ability of bacteria to withstand rinsing actions. Systems with helix-like adhesion organelles may therefore act as dynamic biomechanical machines, enhancing the ability of bacteria to withstand high shear forces originating from rinsing flows, e.g. in urine. Pili thereby constitute an important virulence factor and a possible target for future anti-microbial drugs.

References

An YH, Friedman RJ (2000) Handbook of bacterial adhesion principles, methods, and applications. Humana Press, Totowa, NJ

Andersson M, Axner O, Almqvist F, Uhlin BE, Fällman E (2008) Physical properties of biopolymers assessed by optical tweezers: analysis of folding and refolding of bacterial pili. ChemPhysChem 9:221–235

Andersson M, Fällman E, Uhlin BE, Axner O (2006) A sticky chain model of the elongation and unfolding of *Escherichia coli* P pili under stress. Biophys J 90:1521–1534

Andersson M, Uhlin BE, Fällman E (2007) The biomechanical properties of *Escherichia coli* pili for urinary tract attachment reflect the host environment. Biophys J 93:3008–3014

Ashkin A, Dziedzic JM (1987) Optical trapping and manipulation of viruses and bacteria. Science 235:1517–1520

Axner O, Björnham O, Castelain M, Koutris E, Schedin S, Fällman E, Andersson M (2009) Unraveling the secrets of bacterial adhesion organelles using single-molecule force spectroscopy. In: Rigler R (ed) Nobel symposium, vol 138, chapter 18. Springer, Berlin, pp 337–362

Båga M, Norgren M, Normark S (1987) Biogenesis of *Escherichia coli* Pap pili – PapH, a minor pilin subunit involved in cell anchoring and length modulation. Cell 49:241–251

Balsalobre C, Morschhauser J, Jass J, Hacker J, Uhlin BE (2003) Transcriptional analysis of the *sfa* determinant revealing multiple mRNA processing events in the biogenesis of S fimbriae in pathogenic *Escherichia coli*. J Bacteriol 185:620–629

Barocchi MA, Ries J, Zogaj X, Hemsley C, Albiger B, Kanth A, Dahlberg S, Fernebro J, Moschioni M, Masignani V, Hultenby K, Taddei AR, Beiter K, Wartha F, von Euler A, Covacci A, Holden DW, Normark S, Rappuoli R, Henriques-Normark B (2006) A pneumococcal pilus influences virulence and host inflammatory responses. Proc Natl Acad Sci USA 103:2857–2862

Bell MG (1978) Models for the specific adhesion of cells to cells. Science 200:618–627

Björnham O, Axner O (2009) Multipili attachment of bacteria with helixlike pili exposed to stress. J Chem Phys 130:18

Björnham O, Axner O (2010) Catch-bond behavior of bacteria binding by slip bonds. Biophys J 99:1331–1341

Björnham O, Axner O, Andersson M (2008) Modeling of the elongation and retraction of *Escherichia coli* P pili under strain by Monte Carlo simulations. Eur Biophys J 37:381–391

Björnham O, Bugaytsova J, Borén T, Schedin S (2009a) Dynamic force spectroscopy of the *Helicobacter pylori* BabA-Lewis b binding. Biophys Chem 143:102–105

Björnham O, Fällman E, Axner O, Ohlsson J, Nilsson U, Borén T, Schedin S (2005) Measurements of the binding force between the *Helicobacter pylori* adhesin BabA and the Lewis b blood group antigen using optical tweezers. J Biomed Opt 10:044024

Björnham O, Nilsson H, Andersson M, Schedin S (2009b) Physical properties of the specific PapG–galabiose binding in *E. coli* P pili-mediated adhesion. Eur Biophys J 38:245–254

Björnham O, Schedin S (2009) Methods and estimations of uncertainties in single-molecule dynamic force spectroscopy. Eur Biophys J 38:911–922

Bullitt E, Makowski L (1995) Structural polymorphism of bacterial adhesion pili. Nature 373: 164–167

Bustamante C, Marko JF, Siggia ED, Smith S (1994) Entropic elasticity of lambda-phage DNA. Science 265:1599–1600

Capitanio M, Romano G, Ballerini R, Giuntini M, Pavone FS, Dunlap D, Finzi L (2002) Calibration of optical tweezers with differential interference contrast signals. Rev Sci Instrum 73: 1687–1696

Castelain M, Ehlers S, Klinth J, Lindberg S, Andersson M, Uhlin BE, Axner O (2011) Fast uncoiling kinetics of F1C pili expressed by uropathogenic *Escherichia coli* are revealed on a single pilus level using force-measuring optical tweezers. Eur Biophys J 40(3):305–316

Castelain M, Koutris E, Andersson M, Wiklund K, Björnham O, Schedin S, Axner O (2009a) Characterization of the biomechanical properties of T4 pili expressed by *Streptococcus pneumoniae* – a comparison between helix-like and open coil-like pili. ChemPhysChem 10:1533–1540

Castelain M, Sjöstrom AE, Fällman E, Uhlin BE, Andersson M (2009b) Unfolding and refolding properties of S pili on extraintestinal pathogenic *Escherichia coli*. Eur Biophys J 39:1105–1115

de Breij A, Gaddy J, van der Meer J, Koning R, Koster A, van den Broek P, Actis L, Nibbering P, Dijkshoorn L (2009) CsuA/BABCDE-dependent pili are not involved in the adherence of *Acinetobacter baumannii* ATCC19606T to human airway epithelial cells and their inflammatory response. Res Microbiol 160:213–218

Ericsson M, Hanstorp D, Hagberg P, Enger J, Nyström T (2000) Sorting out bacterial viability with optical tweezers. J Bacteriol 182:5551–5555

Evans E (2001) Probing the relation between force – lifetime – and chemistry in single molecular bonds. Annu Rev Biophys Biomol Struct 30:105–128

Grover SC, Skirtach AG, Gauthier RC, Grover CP (2001) Automated single-cell sorting system based on optical trapping. J Biomed Opt 6:14–22

Hahn E, Wild P, Hermanns U, Sebbel P, Glockshuber R, Haner M, Taschner N, Burkhard P, Aebi U, Müller SA (2002) Exploring the 3D molecular architecture of *Escherichia coli* type 1 pili. J Mol Biol 323:845–857

Haruff HM, Munakata-Marr J, Marr DWM (2003) Directed bacterial surface attachment via optical trapping. Colloids Surf B27:189–195

Hilleringmann M, Ringler P, Muller SA, De Angelis G, Rappuoli R, Ferlenghi I, Engel A (2009) Molecular architecture of *Streptococcus pneumoniae* TIGR4 pili. EMBO J 28:3921–3930

Horner F, Woerdemann M, Muller S, Maier B, Denz C (2010) Full 3D translational and rotational optical control of multiple rod-shaped bacteria. J Biophotonics 3:468–475

Jacob-Dubuisson F, Heuser J, Dodson K, Normark S, Hultgren S (1993) Initiation of assembly and association of the structural elements of a bacterial pilus depend on 2 specialized tip proteins. EMBO J 12:837–847

Jass J, Schedin S, Fällman E, Ohlsson J, Nilsson UJ, Uhlin BE, Axner O (2004) Physical properties of *Escherichia coli* P pili measured by optical tweezers. Biophys J 87:4271–4283

Jones CH, Pinkner JS, Roth R, Heuser J, Nicholes AV, Abraham SN, Hultgren SJ (1995) FimH adhesin of type-1 pili is assembled into a fibrillar tip structure in the Enterobacteriaceae. Proc Natl Acad Sci USA 92:2081–2085

Källenius G, Svenson SB, Hultberg H, Möllby R, Helin I, Cedergren B, Winberg J (1981) Occurrence of P-fimbriated *Escherichia coli* in urinary tract infections. Lancet 2:1369–1372

Knight SD, Choudhury D, Hultgren S, Pinkner J, Stojanoff V, Thompson A (2002) Structure of the *S pilus* periplasmic chaperone SfaE at 2.2 Ångstrom resolution. Acta Crystallogr D Biol Crystallogr 58:1016–1022

Le Trong I, Aprikian P, Kidd BA, Forero-Shelton M, Tchesnokova V, Rajagopal P, Rodriguez V, Interlandi G, Klevit R, Vogel V, Stenkamp RE, Sokurenko EV, Thomas WE (2010) Structural basis for mechanical force regulation of the adhesin FimH via finger trap-like beta sheet twisting. Cell 141:645–655

Liang MN, Smith SP, Metallo SJ, Choi IS, Prentiss M, Whitesides GM (2000) Measuring the forces involved in polyvalent adhesion of uropathogenic *Escherichia coli* to mannose-presenting surfaces. Proc Natl Acad Sci USA 97:13092–13096

Maier B (2005) Using laser tweezers to measure twitching motility in *Neisseria*. Curr Opin Microbiol 8:344–349

Neuman KC, Block SM (2004) Optical trapping. Rev Sci Instrum 75:2787–2809

Proft T, Baker EN (2009) Pili in Gram-negative and Gram-positive bacteria – structure, assembly and their role in disease. Cell Mol Life Sci 66:613–635

Rad R, Gerhard M, Lang R, Schoniger M, Rosch T, Schepp W, Becker I, Wagner H, Prinz C (2002) The *Helicobacter pylori* blood group antigen-binding adhesin facilitates bacterial colonization and augments a nonspecific immune response. J Immunol 168:3033–3041

Rasko DA, Sperandio V (2010) Anti-virulence strategies to combat bacteria-mediated disease. Nat Rev Drug Discov 9:117–128

Sauer FG, Barnhart M, Choudhury D, Knights SD, Waksman G, Hultgren SJ (2000) Chaperone-assisted pilus assembly and bacterial attachment. Curr Opin Struct Biol 10:548–556

Sauer FG, Remaut H, Hultgren SJ, Waksman G (2004) Fiber assembly by the chaperone-usher pathway. Biochim Biophys Acta-Mol Cell Res 1694:259–267

Simpson KH, Bowden MG, Hook M, Anvari B (2002) Measurement of adhesive forces between *S-epidermidis* and fibronectin-coated surfaces using optical tweezers. Lasers Surg Med 31: 45–52

Simpson KH, Bowden G, Hook M, Anvari B (2003) Measurement of adhesive forces between individual *Staphylococcus aureus* MSCRAMMs and protein-coated surfaces by use of optical tweezers. J Bacteriol 185:2031–2035

Simpson KH, Bowden MG, Peacock SJ, Arya M, Höök M, Anvari B (2004) Adherence of *Staphylococcus aureus* fibronectin binding protein A mutants: an investigation using optical tweezers. Biomol Eng 21:105–111

Sherlock O, Schembri MA, Reisner A, Klemm P (2004) Novel roles for the AIDA adhesin from diarrheagenic *Escherichia coli*: cell aggregation and biofilm formation. J Bacteriol 186: 8058–8065

Thomas WE, Nilsson LM, Forero M, Sokurenko EV, Vogel V (2004) Shear-dependent "stick-and-roll" adhesion of type 1 fimbriated *Escherichia coli*. Mol Microbiol 53:1545–1557

Wang S, Arellano-Santoyo H, Combs PA, Shaevitz JW (2010) Measuring the bending stiffness of bacterial cells using an optical trap. J Vis Exp 38. doi:10.3791/2012

Chapter 20
Short Time-Scale Bacterial Adhesion Dynamics

Jing Geng and Nelly Henry

Abstract In natural conditions many bacterial populations are found as surface-attached communities exhibiting features distinct from those of planktonic cells. We focus here on the question of initial adhesion, the mechanisms of which are still far from being fully understood. Recently, the frontier between microbiologists and physicists has become increasingly permeable, boosting implementation of new methodological approaches for better elucidating the intricate aspects of initial bacterial adhesion. After discussing briefly the main sources of complexity that confuse the understanding of the early steps of cell-surface attachment, we present a selection of physical methods enabling real-time measurement of early adhesion kinetics in live cells. We also discuss the limitations and pitfalls that might appear when applying such methodologies – initially designed for studying physically ideal systems – to analysis of these, more complex, living systems. We address mainly on the use of dispersed-surfaces flow cytometry (DS-FCM), quartz microbalance (QCM) and surface plasmon resonance (SPR) approaches, and give a brief survey of new perspectives in optical microscopy. We conclude that the use of combined and multiparametric technical approaches will lead to significant advances in providing a comprehensive understanding of the early events in bacterial adhesion.

20.1 Introduction

Historically, significant knowledge of bacteria has been obtained using cells living in suspension in liquid growth medium. However, with the increasing spread of molecular genetics, microbiologists have become aware that adherent cell populations exhibit features distinct from those of planktonic cells. This has stimulated research

N. Henry (✉)
Laboratoire Physico-chimie Curie (CNRS UMR 168), Université Paris VI Institut Curie,
75231 Paris Cedex 05, France
e-mail: Nelly.henry@curie.fr

D. Linke, A. Goldman (eds.), *Bacterial Adhesion*, Advances in Experimental Medicine and Biology 715, DOI 10.1007/978-94-007-0940-9_20,

to understand better the phenotypic shift associated with bacterial anchorage and growth on surfaces (Ghigo, 2003; Stewart and Costerton, 2001; Watnick and Kolter, 2000). Much work has been dedicated to biofilm development processes, and remarkable progress has been made in elucidating the molecular mechanisms involved in biofilm formation. However, the initial adhesion of bacteria to surfaces is still not understood.

Initial adhesion has been the object of a great deal of confusion in terms of both experimental observations and theoretical interpretations (Donlan, 2002). One explanation for this is that early bacterial adhesion is strongly multifactorial, depending on the adhesive substrate, the conditioning films forming on the surface, the hydrodynamics of the aqueous medium, the characteristics of the medium and other various properties of the cell surface. Moreover, all these properties vary with time, influencing each other by still indistinct interrelations.

Recently, the frontier between microbiologists and physicists has become increasingly permeable, boosting implementation of new methodological approaches for better elucidating the intricate aspects of initial bacterial adhesion.

In this chapter, we first examine the main sources of complexity in the initial process of bacterial adhesion. Next, we describe a selection of recent methodological approaches used for exploring the early steps in bacterial interactions with surfaces, focussing on physical methods enabling real-time measurement of early adhesion kinetics in live cells. We point out both the main contributions of the different approaches and the limitations and pitfalls that appear when applying such methodologies – initially designed for studying physically ideal systems – to analysis of more complex living objects. Atomic force microscopy (AFM), which has contributed much to microbiology during the last decade, will not be discussed here, but in Chapter 18 by Lower, this volume.

20.2 Embracing Complexity to Inch Closer to Reality

Before addressing the question of the appropriate methodological approach to gain insight into short time-scale adhesion dynamics, we begin by considering the principal sources of complexity in this process. We have selected a few issues likely to drive or affect initial adhesion dynamics.

20.2.1 General Heterogeneity

An initial source of complexity lies in the tremendous heterogeneity of bacteria themselves evolving in close interrelationships with a world that is itself heterogeneous. Heterogeneity is found in the intrinsic diversity of bacterial cell populations (Fraser et al., 2009) to exhibit all sorts of surface appendages (Klemm and Schembri, 2000), but also between genetically identical cells in which phenotypic variation may emerge stochastically (Brehm-Stecher and Johnson, 2004). Heterogeneity also

exists at the single cell level due to lateral variations in composition and physical properties, as revealed by spatially resolved atomic spectroscopy (Dufrêne, 2003), and to intrinsic shape asymmetry or pili polar location (Dufrêne, 2003; Ebersbach and Jacobs-Wagner, 2007; Kaiser and Yu, 2005). The bacterial environment also dynamically changes with different length scales and frequencies, inducing specific adaptation processes dictated by natural selection (Goller and Romeo, 2008).

20.2.2 Surface Conditioning Film

Over the past decades, numerous research groups have tried to relate artificial surface physicochemical properties to bacterial adhesion, leading to contradictory results. The confusion that has long prevailed in the field is well-illustrated by the debate surrounding the impact of surface hydrophobicity on bacterial initial adhesion. Eventually, using micropatterned surfaces, Bos et al. (2000) demonstrated that bacteria do not have a strong preference for adhesion to hydrophobic or hydrophilic surfaces.

The difficulty in finding an empirical relationship between the physico-chemical properties of a surface and bacterial adhesion is likely to arise at least in part from the formation of conditioning films. When a substratum is exposed to an aqueous environment, it actually adsorbs various organic molecules present in the medium, forming a layer called "conditioning film" (Bos et al., 1999; Chamberlain, 1992). The molecules in this layer include both small and polymeric compounds such as lipids, proteins, polysaccharides and inorganic salts (Neu, 1996). Once the surface has been conditioned, its physicochemical properties such as hydrophobicity and surface charge are quite different from the original bare surfaces. The main difficulty in clarifying this issue lies in the extraordinary variety of conditioning films, which can arise from the environment or from nutrients or adhering microorganisms themselves. Depending on the surface-active molecules involved, both adhesion-inhibiting and -enhancing effects can be expected (Dunne, 2002). For instance, most uropathogenic *Escherichia* (Chamberlain, 1992) can produce group II capsule, a soluble negatively charged polysaccharide, into the surrounding media. This drastically reduces the initial adhesion of a wide range of Gram-positive and Gram-negative bacteria (Valle et al., 2006). On the other hand, excreted exopolymeric substances produced by *Pseudomonas fragi* on the surface increased *Listeria monocytogenes* adherence (Sasahara et al., 1993). Shearing of bacterial cells from a surface may also result in bacterial footprints or bacterial surface polymer residues. When left behind on the surface, they might also play a role in further bacterial cell attachment (Palmer et al., 2007). The time scale in which these surface conversion processes occur is also highly varied, ranging from a few seconds to hours or days. Thus, characterising physicochemical properties of the surfaces actually being colonised by the cells remains a true challenge that would require implementation of a thorough research program in basic surface analytical physicochemistry.

20.2.3 Cell–Cell Aggregation

In Nature, many bacteria can self-aggregate in temperature-, pH- and growth-phase-dependent-processes. This ability has been closely related to the presence on the bacterial surface of various outer membrane proteins that induce rapid cell–cell aggregation and clump formation (Schembri et al., 2003). Among these structures, curli, which are flexible filaments on the surface of Enterobacteriaceae, have been clearly elucidated (Barnhart and Chapman, 2006), as has the family of proteins called self-associating autotransporters (SAAT), comprising the adhesin involved in diffuse adherence (AIDA-I), auto-aggregation factor antigen 43 (Ag43) and the TibA adhesin/invasin in *E. coli* (Girard et al., 2010; Sherlock et al., 2004). The presence of these appendages on the cell surface clearly increases strain pathogenicity and promotes biofilm development. Yet the impact of cell–cell aggregation per se on these phenomena and their influence on initial adhesion remain elusive. In addition, self-aggregation, or co-aggregation between two or several microorganisms of different species in suspension, are widespread in nature (Bos et al., 1999; Kjaergaard et al., 2000; O'Toole et al., 2000) and might also drastically affect the initial adhesion profile predicted from single species adhesion experiments.

The imprecision persisting concerning this issue arises from a lack of quantification and understanding of the bacterial self-aggregation process itself. This must be resolved before its role in initial surface colonisation dynamics can be accurately evaluated.

20.2.4 Early Adhesion-Induced Physiological Dynamics

In 1984 at the Dahlem Workshop on Microbial Adhesion and Aggregation, it was concluded: "Attachment to a surface can undoubtedly affect the activity of microorganisms, although sometimes in ways that are not readily predictable with our current knowledge" (Breznak, 1984). Since then, numerous investigations have demonstrated that adherent bacteria differ profoundly from planktonic bacteria in physiology and gene expression. This adhesion-induced physiological shift was suggested very early on (van Loosdrecht et al., 1990; Zobell, 1943). However, the question of the direct effect of a solid surface on bacterial activity is still open to debate. Bacterial cells might possess surface-sensing systems that trigger intracellular signalling directed towards physiological changes enabling cells to adapt to life on the surface (Jefferson, 2004; Prigent-Combaret et al., 1999). Alternatively, the physiological changes may result from interfacial physical or chemical gradients on the surface, creating ecological niches for the cells (Geesey, 2001). Finally, while a physiological shift is generally admitted in growing biofilm (Ghigo, 2003), the time scale of the process remains unclear and the advent of functional changes induced by short-term adhesion remains poorly documented. In *Pseudomonas aeruginosa*, expression of an alginate gene was increased after 15 min of cell surface attachment (Davies and Geesey, 1995).

20.2.5 Cell Motility

Cell motion is a non-trivial factor in bacterial adhesion and participates in its complexity. In addition to Brownian motion, many, but not all, bacteria exhibit motility, i.e. self-propelled motion mainly driven by flagella rotation depending on various stimuli and environmental circumstances. Near the surface, i.e. typically within the first few hundred nanometres above the surface, hydrodynamics and cell motion are affected by the presence of a stationary boundary (Frymier et al., 1995; Lauga et al., 2006). For instance, *E. coli* cells, which swim in solution in a random walk made of approximately straight trajectories alternating with rapid reorientations, trace circular trajectories near the surface (Lauga et al., 2006; Vigeant and Ford, 1997) that last for long periods of time (Vigeant et al., 2002). How these phenomena actually impact initial attachment to the surface is far from being understood. It is usually agreed that increasing the dwelling time near the surface increases the probability of cell-surface contact and thus may assist adhesion. However, in some cases, coupling between cell self-propulsion, Brownian motion and hydrodynamic interactions near the surface increases the mean distance of the cells from the surface (Li et al., 2008). In addition, hydrodynamic entrapment of cells close to the surface has been shown to be highly dependent on other factors like medium ionic strength (Vigeant and Ford, 1997), surface conditioning (McClaine and Ford, 2002) and bacterial cell surface polymers (Kogure et al., 1998; Merritt et al., 2007; Morisaki et al., 1999).

20.2.6 Cell Responses to Shear Stress

One of the main sources of confusion concerning cell responses to shear stress arises from the intricate role played by mechanical stress in bacterial attachment. While most of the time microbial adhesion is observed in an aqueous environment, the actual hydrodynamic conditions in which attachment and monitoring occur are seldom known – with their description being limited to the famous refrain, "gentle shaking – slight rinsing – dipping in fresh buffer", as pointed out elsewhere (Andersen et al., 2010; Busscher and van der Mei, 2006). Furthermore, even when the experiments are performed under the more controlled hydrodynamic conditions of a flow chamber, the actual shear forces experienced by the cells in the devices are not always evident, since not only flow value but also geometric details are needed to calculate them. Moreover, hydrodynamics near the surface involve an interplay of many physicochemical parameters (Lauga et al., 2007) which are, as we stated above, poorly defined due to the release of bacterial compounds in the medium and formation of surface conditioning films. Likewise, adhesion itself remodels the shape of the boundary and consequently changes the local hydrodynamics. In this context, the question of shear effects on bacterial adhesion remains unresolved. It has long been thought that increasing shear stress reduces bacterial adhesion, either preventing attachment or washing off already bound bacteria (Li et al., 2000; Mohamed et al., 1999; Shive et al., 1999; Wang et al., 1995). Several papers

nonetheless reported opposing observations where shear forces enhance bacterial adhesion (Brooks and Trust, 1983; Thomas et al., 2002). This is mainly for bacterial adhesion mediated by the specific receptor FimH, the tip domain of an *E. coli* type I fimbriae appendage that mediates mannose-sensitive adhesion (Thomas et al., 2004). The enhancement of bacterial binding to the surface upon shear stress increase was interpreted there in terms of catch-bonds, as in several eukaryotic systems previously described (Thomas et al., 2008). However, a recent communication on *P. aeruginosa* adhesion showed enhanced adhesion as shear stress increased over a wide range of shear rates independent of primary surface organelles or type of surface, suggesting that this might be a general but poorly understood phenomenon (Lecuyer et al., 2010).

20.3 Short Time-Scale Real-Time Methodologies

20.3.1 The Dispersed Surfaces-Flow Cytometry (DS-FCM) Approach

Flow cytometry (FCM) is a technique for analyzing particles suspended in a fluid stream of sizes between 1 and 100 μm. The particle suspension is injected into a sheath fluid that hydrodynamically focuses on micrometric objects in the beam waist of a laser one by one. Particles are then counted, analysed and possibly sorted on the basis of their individual light scattering and fluorescence emission properties (Fig. 20.1A). This provides large sets of multiparameter data from single object in a high-throughput mode (Brehm-Stecher and Johnson, 2004; Radcliff and Jaroszeski, 1998).

Fig. 20.1 DS-FCM assay illustration (**A**) Flow cytometry principles. For each object flowing one by one through the laser beam, the intensity of light forward scattered (FSC), side scattered (SSC) and the fluorescence emitted at different wavelengths (FLn) are collected simultaneously at high speed. For the DS-FCM assay, data were collected typically at several thousands of events per second. (**B**) FCM snapshots of a cell-particle suspension using the curli producing *E. coli* marked with GFP (MG1655*gfpompR234* kindly provided by J.M. Ghigo and C. Beloin from the Pasteur Institute, Paris, France) and 10 μm cationic particles (Polysciences, Eppelheim, Germany). *Dot plots* of GFP (FL1) and Propidium iodide (FL3) fluorescence intensities versus forward scattering are shown for *(a)* planktonic isolated cells. *(b)* Partially aggregated cells. *(c)* Bare particles in their initial state. *(d)* Particles with surface converted by bacterial medium components. Histograms are plotted from bare particles (*grey*) and propidium iodide-labelled particles (*red*) after surface charge conversion, *(e)* particles colonised by bacteria. Bright field and fluorescence microscope images are shown to illustrate the various situations. Each different population can be detected and quantified in the same suspension at given time enabling kinetics monitoring with a time resolution of a few seconds. (**C**) *(a)* The short time adhesion, *(b)* aggregation and *(c)* conversion kinetics obtained simultaneously on the same sample are shown for surface colonisation of 10 μm polyethyleneimine-coated particles by exponentially growing MG1655*gfpompR234* cells

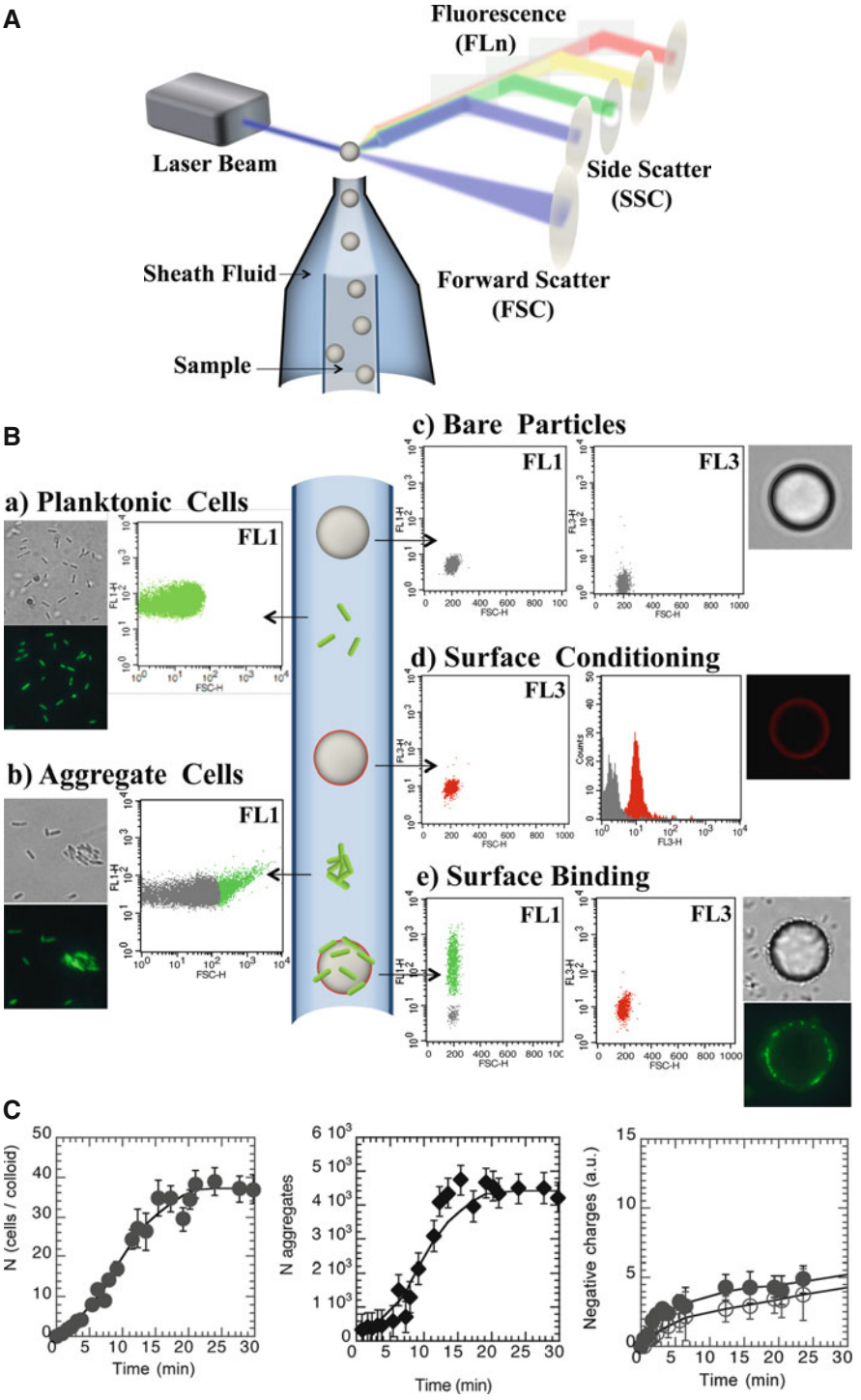

Fig. 20.1 (continued)

Initially, the technique was extensively used with mammalian cells, while its use in microbiology was limited because the bacteria were too small. Developments in light sources and optics, together with brighter, more spectrally diverse and genetically controlled dyes have, in recent years, enhanced the use of flow cytometry in microbiological research. Flow cytometry has become a valuable tool for rapid detection, identification and characterisation of bacteria in environmental samples, providing a broad range of information, from total counts and size measurements to quantification of specific molecular details, revealing the heterogeneity present in a population (Davey and Kell, 1996; Shapiro, 2000). However, until recently, the technique was considered unsuited for directly studying attached cells due to the necessity of putting the sample in flow.

Lately, we have introduced a simple approach bypassing this limit to take advantage of high-speed multiparametric acquisition and multivariate data analysis offered by flow cytometry in exploring bacterial adhesion, and especially the very first steps in the process (Beloin et al., 2008; Otto, 2008). The principle consists of using dispersed surfaces as adhesive substrates, typically particles 10–30 μm in diameter. Their surface may be engineered using various methods like polyelectrolyte deposit (Decher, 1997) or chemical functionalisation. These objects have a clear flow cytometry signature, both in the scattering channels (forward and side scattering) and in the fluorescence channels if surface characteristic labelling has been used. For instance, the surface charge may be easily checked using cationic or anionic fluorescent dyes that quickly bind to the surface by electrostatic interactions. Bacteria also have their own FCM signal that can be easily distinguished from those of particles due to their smaller size. In addition, cells tagged with fluorescent proteins, GFP or others, display very a clear fluorescence signal originating from single cells (Fig. 20.1B).

To monitor cell-surface attachment, bacteria and particles are brought into contact in suspension and aliquots are taken from the incubation sample within seconds and at given time points for immediate analysis in FCM. These aliquots all contain free particles, planktonic cells and particle-associated cells, as well as free-floating cell aggregates. Propidium iodide is added to the tube for FCM analysis just before data acquisition to label the particle surface by surface charge density. Then, for each time point, acquisition of individual scattering and fluorescence parameters of individual object in the suspension reports the following: (i) the respective abundance of each subpopulation present in the suspension, i.e. bare particles, bacteria-colonised particles, free cells and free-floating aggregates; (ii) the surface charge state of the particles, whether colonised or not; (iii) the number of adhering bacteria per particle, providing an instantaneous snapshot of both the adhesion level, with single cell precision, and surface conversion in parallel with the bulk state, with a time resolution of a few seconds, without any separation step (Fig. 20.1C). Moreover, due to the high throughput of FCM, data are obtained on the basis of high statistics, thus revealing cooperative effects via deviation from standard statistical Poisson's law.

Using this assay, it has been possible to show in *E. coli* that the thin fimbriae or so-called curli sustained early surface colonisation with an amplitude closely

correlated with curli overexpression and cell–cell aggregation. In contrast, Ag43, another *E. coli* surface appendage, which also promotes cell–cell aggregation, was unable to support cell surface initial attachment. This suggested that cell–cell aggregation acted as a surface colonisation amplification factor only in the presence of already-bound anchors (Beloin et al., 2008).

The DS-FCM adhesion assay enabled quantitative and multiparametric analysis of initial attachment kinetics. However, it has two main limitations: first, the sample is subjected to non-negligible shear stress. We evaluated this shear as being on the order of 50–100 s^{-1} based on Amblard et al. (1992) considerations, which is low. Moreover, the resulting forces are applied to the objects for no longer than a fraction of a second. When flow cytometry results were checked by microscopy, no significant difference was observed. This indicated that shear stress exerted by the apparatus did not disrupt the cell-particle association that formed. However, it is still possible that, in some cases, the instrument could disrupt very weak cell–surface or cell–cell interactions. Second, the DS-FCM approach requires fluorescently labelled cells. The tool box of genetic markers is now very large for laboratory strains (Giepmans et al., 2006) but exogenous labelling is needed to work with strains isolated from the natural environment, for instance dyes labelling either DNA or cytoplasm or even membranes (Czechowska et al., 2008).

At present, DS-FCM is a long way from achieving its full potential for elucidating early bacterial adhesion processes. For instance, the possibility of running single cell adhesion investigations with high statistics – typically several hundreds of thousands of events – has not yet been exploited. On the other hand, use of various fluorescent labelling techniques that target specific molecules, physiological or genetic pathways would shed new light on the complex processes occurring within the first few minutes of bacterial adhesion. We are currently developing a new assay to characterise possible metabolic changes occurring in the first few minutes of cell interaction with the surface, taking advantage of the fluorescence of the redox active dye 5-cyano-2,3-ditolyl tetrazoliumchloride (CTC). It would also be of interest to couple the DS-FCM adhesion assay with short lifetime fluorescent reporters of gene expression or fluorescence in situ hybridisation (FISH) techniques now available in living cells (Golding et al., 2005).

20.3.2 Quartz Microbalance (QCM)

QCM is an acoustic sensor initially conceived as a microweighing device to detect in real time the adhesion of a monolayer of label-free molecules to a surface (Sauerbrey, 1959). Briefly, the technique relies on electrical excitation of a quartz disk with a surface of about 1 cm^2, sandwiched between two metal electrodes typically made of gold. Due to the piezoelectric nature of the quartz material, the application of an alternating electric field induces acoustic waves that propagate across the quartz crystal perpendicularly to the surface with a decay length in the fluid of about 250 nm, depending on the applied electric field frequency. Constructive interference is created upon reflection at each sensor surface with a

resonance frequency f_0, depending on crystal thickness and acoustic wave velocity, i.e. on the properties of the propagating materials. Consequently, a small mass increase at the surface of the sensor induces a detectable proportional variation in resonance frequency Δf_0. For a review, see Ferreira et al. (2009).

In the initial model of Sauerbrey (1959), mass increase was assumed only to make the crystal thicker, not to lead to energy dissipation. However, more detailed analysis shows that when the crystal is immersed in a fluid, energy is lost through viscous coupling to the fluid near the surface, and the viscoelastic properties of the adsorbed layer, the surface roughness or the presence of charged species near the surface influence the variation in resonance frequency as well (Kanazawa, 1997). As a result, mass increase cannot always be differentiated from roughness or viscoelastic effects by simply measuring Δf_0. To determine the energy dissipation of the sensor and evaluate the viscoelastic component of the adsorbed film, one can monitor the decay in a crystal's oscillation after a rapid excitation close to the resonance frequency. On the basis of this phenomenon, a variation in the QCM technique called quartz crystal microbalance with dissipation monitoring (QCM-D) has been developed (Dixon, 2008).

Recently, several groups have used QCM or QCM-D to analyse bacterial adhesion, which appears to be attractive because continuous real-time measurements can be performed in a label-free system (Olofsson et al., 2005; Shen et al., 2007). However, an unambiguous relationship between actual bacterial attachment to the surface and the output parameters of QCM or QCM-D experiments could not be established. Indeed, bacterial attachment creates considerable alterations in the surface properties, like viscosity and rigidity, which are translated into resonant frequency variations in addition to those that are caused by mass deposition. Moreover, the fluid properties near the sensor surface might well be affected by the viscoelastic properties of the extracellular adhesives produced by adherent cells or by cell surface extensions, seriously complicating signal interpretation. Since such perturbations follow their own time dependence**,** which is different from true adhesion kinetics, analysis of dissipation does not really help to obtain information linked to the increase in the mass. Using the QCM-D technique to evaluate anti-adhesive surface treatment, Olofsson et al. (2005) found that the magnitude and kinetics of frequency and dissipation shifts were dependent on the life cycle stage of the bacteria. Moreover, the bacterial surface properties themselves also affect the magnitude of frequency and dissipation shifts. This was clearly shown by Olsson et al. (2009) who found, using CCD camera imaging in parallel with QCM-D measurements, that adhesion of a "bald" bacterium, completely devoid of surface appendages, is registered as a frequency decrease. On the other hand, adhesion of bacteria possessing surface appendages yields either a much smaller decrease or an increase in frequency despite the fact that they adhere in higher numbers. This behaviour was probably due to the influence of the distance at which the cell body was held from the sensor surface by its surface appendages upon the magnitude of frequency and dissipation shifts. QCM signals are thus not suitable for interpreting attachment kinetics and should not be used for quantitative analysis of bacterial adhesion itself.

In contrast, what constitutes a serious technical hindrance when seeking to quantitatively measure surface adhesion becomes a powerful tool for obtaining more

detailed information on adhering cells and maturation of the adhering layers. For instance, Otto et al. (1999) used the QCM-D technique to study adhesion of fimbriated and non-fimbriated *E. coli* mutants. They monitored resonance shift on an already formed cell layer after removing loosely bound cells and showed that the signal still changed, suggesting that firmly attached cells continue to undergo time-dependent surface interactions, possibly due to structural reorganisation of the cells, which is different for fimbriated and non-fimbriated cells. They also examined the influence of *ompX*, which does not influence cell surface attachment per se upon cell-surface contact following attachment. Deletion of *ompX* weakened the cell surface contact of non-fimbriated cells but reinforced that of fimbriated *E. coli* cells (Otto and Hermansson, 2004).

Eventually, QCM techniques might be excellent tools for determining subtle physical dynamics occurring in the first moments of bacterial cell adhesion, but not adhesion per se. To achieve their full potential, these approaches should be coupled with other techniques. Adaptation of optical systems enabling detector imaging, as already attempted by Olsson et al. (2009), should open up an interesting pathway in that direction.

20.3.3 Surface Plasmon Resonance (SPR)

SPR is another physical technique initially developed to characterise reversible interactions between biological macromolecules. Surface plasmons are waves of oscillating surface charge density travelling along a metal surface with amplitudes that decrease exponentially with distance perpendicular to the surface over a distance of a few hundred nanometres. On the basis of this phenomenon, Kretschmann and Raether (1968) proposed an SPR biosensor aimed at probing macromolecule adsorption on surfaces. The device consists of a glass prism coated with a thin gold or silver layer. The plasmons can be excited by light only at a well-defined angle of incidence, for which the wave vector of the light matches that of the surface plasmon. At that angle, resonance causes an energy loss in the reflected light which appears in the angle-dependent reflectance curve measured experimentally. The resonance angle strongly depends on the refractive index of the layer close to the metal surface enabling monitoring of material deposited on the surface with a time resolution up to ≈ 0.1 s. The shift in the resonance angle has been shown to be approximately proportional to the mass bound to the sensor surface up to a concentration of 50 ng mm^{-2}, and the signal is averaged from a surface area about 1 mm^2. Like QCM, SPR is label-free and real-time; it has become a popular tool for studying a wide range of molecular properties including antigen–antibody interactions, characterisation of protein targets or drug screening (Garland, 1996; Hoa et al., 2007). However, even in the simple case of ligand-receptor binding involving a mobile reactant and a reactive partner immobilised on the sensor surface, determination of kinetic rate constants is often complicated by deviation of the results from the fitting models (Schuck, 1997). In recent years, this technique has been applied to static or flow conditions to monitor and qualify processes involving whole bacterial cell interactions with the surface (Jenkins et al., 2005;

Oli et al., 2006). Taking into account these limitations, mainly qualitative questions, such as the demonstration of interactions with a specific receptor attesting its presence on the surface, can be accurately deduced from SPR experiments with whole cells (Pourshafie et al., 2004; Salminen et al., 2007). Indeed, several side-effects will affect the resonance of the incidence angle: adsorption of surface active molecules, or non-homogeneous deposition of the cells on the surface. Moreover, the fitting model obtained for extracting kinetic rate constants cannot adequately describe the entire situation, which again is far from thermodynamic equilibrium, precluding true competition experiments. In contrast, the technique might be further developed to explore surface conditioning. For example, it would be of great interest to design an experiment in which surface coating kinetics could be precisely measured in real time upon bacterial contact, while bacterial adhesion could be measured in parallel using another technique.

20.3.4 New Perspectives in Optical Microscopy

Previously, optical microscopy has been widely used to study the initial attachment of bacteria. The relevance of the technique to characterize initial adhesion per se was often questionable, with results mainly consisting of images obtained after immersion and rinsing steps, which could not be compared from one laboratory to another. Indeed, only the cells that had resisted the uncontrolled shear forces applied during rinsing appeared in the analysis. Moreover, cell counts were obtained using tedious and time-consuming counting of "randomly chosen" fields, which limits sample size and the statistical validity of the results.

Now, as light microscopy is coupled to other current methodologies, specific behaviour of cells on or near the surface can be described. For instance, several groups have implemented total internal reflection fluorescence (TIRF). As in SPR, the technique involves the total internal reflection at a specific critical angle obtained when a light beam propagating through a transparent medium of high index of refraction (e.g. a solid glass prism) encounters an interface with a medium of a lower index of refraction (e.g. an aqueous solution). In TIRF, molecules located close to the surface are excited by evanescent waves generated at the critical angle with a frequency identical to that of the incident light. The intensity of the evanescent waves exponentially decays with increasing distance z from the interface, typically fading away a few hundred nanometres from the surface (Trache and Meininger, 2008). Using this approach, it was possible to characterise better the behaviour of different bacterial species near the surface, and in particular, their swimming and hydrodynamic interactions near the surface (Li et al., 2008; Vigeant and Ford, 1997; Vigeant et al., 2001). These properties, while not exactly adhesion events, are likely to influence attachment significantly and so warrant further study to develop a comprehensive model of the initial steps of bacterial adhesion.

Using fast Fourier transform (FFT) analysis of digitised phase contrast images, Agladze and colleagues (Agladze et al., 2003; Agladze et al., 2005) observed that *E. coli* cells settling by gravity for 2 h on a glass surface were organised in periodic

spatial patterns suggesting a concerted adhesion mechanism based on differential diffusion of activator and inhibitor molecules.

Coupled with the most recent advances in imaging techniques and fluorescence labelling, light microscopy enables high-resolution single molecule detection (Gitai, 2009). It is now possible to label specific proteins of interest, while reporting cell function and gene activation in a single cell (Locke and Elowitz, 2009) and it would be of great interest to monitor genetic dynamics and initial adhesion dynamics in parallel. Moreover, automated image analysis and high-throughput data collection are now becoming possible for optical microscopy (Jones et al., 2009; Ljosa and Carpenter, 2009). Thus, information on rare events and stochasticity is in principle close at hand and should deliver new insights into short time bacterial adhesion dynamics.

20.4 Concluding Remarks

In the light of the research on bacterial adhesion over the past few years, the process of bacterial anchoring to artificial surfaces appears to occur via several types of dynamic processes that have often been confused: cell-surface association, surface link maturation and adhesive substrate property alterations. The overlapping of these phenomena means that bacterial adhesion is a highly out-of-equilibrium process and only a combination of approaches can permit its description and understanding.

The physical and physico-chemical methods discussed here will help clarify these phenomena if they are used in parallel. Thus, while QCM techniques seem better adapted to the analysis of maturation of initial attachment, the DS-FCM approach is suitable for measuring initial attachment kinetics, and SPR techniques should be very useful for analysis of conditioning film formation. We have not discussed here all the possible physical approaches, but rather, a selection of those that could be used widely. Nevertheless, several other physical techniques of surface analysis, such as X-ray photoelectron spectroscopy, ellipsometry and Fourier transform infrared spectroscopy, could also significantly contribute to clarifying questions related to the formation of conditioning films.

In the near future, it is to be hoped that we can significantly elucidate the complexity of these short-term bacterial adhesion phenomena using combined and multiparametric technical approaches. This should provide us with the means for predicting and controlling such phenomena.

References

Agladze K, Jackson D, Romeo T (2003) Periodicity of cell attachment patterns during *Escherichia coli* biofilm development. J Bacteriol 185:5632–5638

Agladze K, Wang X, Romeo T (2005) Spatial periodicity of *Escherichia coli* K-12 biofilm microstructure initiates during a reversible, polar attachment phase of development and requires the polysaccharide adhesin PGA. J Bacteriol 187:8237–8246

Amblard F, Cantin C, Durand J, Fischer A, Sekaly R, Auffray C (1992) New chamber for flow cytometric analysis over an extended range of stream velocity and application to cell adhesion measurements. Cytometry 13:15–22

Andersen TE, Kingshott P, Palarasah Y, Benter M, Alei M, Kolmos HJ (2010) A flow chamber assay for quantitative evaluation of bacterial surface colonization used to investigate the influence of temperature and surface hydrophilicity on the biofilm forming capacity of uropathogenic *Escherichia coli*. J Microbiol Meth 81:135–140

Barnhart MM, Chapman MR (2006) Curli biogenesis and function. Annu Rev Microbiol 60: 131–147

Beloin C, Houry A, Froment M, Ghigo JM, Henry N (2008) A short-time scale colloidal system reveals early bacterial adhesion dynamics. PLoS Biol 6:e167

Bos R, van der Mei HC, Busscher HJ (1999) Physico-chemistry of initial microbial adhesive interactions–its mechanisms and methods for study. FEMS Microbiol Rev 23:179–230

Bos R, van der Mei HC, Gold J, Busscher HJ (2000) Retention of bacteria on a substratum surface with micro-patterned hydrophobicity. FEMS Microbiol Lett 189:311–315

Brehm-Stecher BF, Johnson EA (2004) Single-cell microbiology: tools, technologies, and applications. Microbiol Mol Biol Rev 68:538–559

Breznak JA (1984) Activity on surfaces: group report, Dahlem Conference. In: Marshall KC (ed) Microbial adhesion and aggregation. Springer, Berlin, pp 203–221

Brooks DE, Trust TJ (1983) Enhancement of bacterial adhesion by shear forces: characterization of the haemagglutination induced by *Aeromonas salmonicida* strain 438. J Gen Microbiol 129:3661–3669

Busscher HJ, van der Mei HC (2006) Microbial adhesion in flow displacement systems. Clin Microbiol Rev 19:127–141

Chamberlain AHL (1992) The role of adsorbed layers in bacterial adhesion. In: Melo LF, Bott TR, Fletcher M, Capdeville B (eds) Biofilms-science and technology. Kluwer, The Netherlands, pp 59–67

Czechowska K, Johnson DR, van der Meer JR (2008) Use of flow cytometric methods for single-cell analysis in environmental microbiology. Curr Opin Microbiol 11:205–212

Davey HM, Kell DB (1996) Flow cytometry and cell sorting of heterogeneous microbial populations: the importance of single-cell analyses. Microbiol Rev 60:641–696

Davies DG, Geesey GG (1995) Regulation of the alginate biosynthesis gene algC in *Pseudomonas aeruginosa* during biofilm development in continuous culture. Appl Environ Microbiol 61: 860–867

Decher G (1997) Fuzzy nanoassemblies: toward layered polymeric multicomposites. Science 277:1232–1237

Dixon MC (2008) Quartz crystal microbalance with dissipation monitoring: enabling real-time characterization of biological materials and their interactions. J Biomol Tech 19:151–158

Donlan RM (2002) Biofilms: microbial life on surfaces. Emerg Infect Dis 8:881–890

Dufrêne YF (2003) Recent progress in the application of atomic force microscopy imaging and force spectroscopy to microbiology. Curr Opin Microbiol 6:317–323

Dunne WM Jr. (2002) Bacterial adhesion: seen any good biofilms lately? Clin Microbiol Rev 15:155–166

Ebersbach G, Jacobs-Wagner C (2007) Exploration into the spatial and temporal mechanisms of bacterial polarity. Trends Microbiol 15:101–108

Ferreira GN, da-Silva AC, Tome B (2009) Acoustic wave biosensors: physical models and biological applications of quartz crystal microbalance. Trends Biotechnol 27:689–697

Fraser C, Alm EJ, Polz MF, Spratt BG, Hanage WP (2009) The bacterial species challenge: making sense of genetic and ecological diversity. Science 323:741–746

Frymier PD, Ford RM, Berg HC, Cummings PT (1995) Three-dimensional tracking of motile bacteria near a solid planar surface. Proc Natl Acad Sci USA 92:6195–6199

Garland PB (1996) Optical evanescent wave methods for the study of biomolecular interactions. Q Rev Biophys 29:91–117

Geesey GG (2001) Bacterial behavior at surfaces. Curr Opin Microbiol 4:296–300
Ghigo JM (2003) Are there biofilm-specific physiological pathways beyond a reasonable doubt? Res Microbiol 154:1–8
Giepmans BN, Adams SR, Ellisman MH, Tsien RY (2006) The fluorescent toolbox for assessing protein location and function. Science 312:217–224
Girard V, Cote JP, Charbonneau ME, Campos M, Berthiaume F, Hancock MA, Siddiqui N, Mourez M (2010) Conformation change in a self-recognizing autotransporter modulate bacterial cell-cell interaction. J Biol Chem 285:10616–10626
Gitai Z (2009) New fluorescence microscopy methods for microbiology: sharper, faster, and quantitative. Curr Opin Microbiol 12:341–346
Golding I, Paulsson J, Zawilski SM, Cox EC (2005) Real-time kinetics of gene activity in individual bacteria. Cell 123:1025–1036
Goller CC, Romeo T (2008) Environmental influences on biofilm development. Curr Top Microbiol Immunol 322:37–66
Hoa XD, Kirk AG, Tabrizian M (2007) Towards integrated and sensitive surface plasmon resonance biosensors: a review of recent progress. Biosens Bioelectron 23:151–160
Jefferson KK (2004) What drives bacteria to produce a biofilm? FEMS Microbiol Lett 236: 163–173
Jenkins AT, Buckling A, McGhee M, Ffrench-Constant RH (2005) Surface plasmon resonance shows that type IV pili are important in surface attachment by *Pseudomonas aeruginosa*. J R Soc Interface 2:255–259
Jones TR, Carpenter AE, Lamprecht MR, Moffat J, Silver SJ, Grenier JK, Castoreno AB, Eggert US, Root DE, Golland P, Sabatini DM (2009) Scoring diverse cellular morphologies in image-based screens with iterative feedback and machine learning. Proc Natl Acad Sci USA 106:1826–1831
Kaiser D, Yu R (2005) Reversing cell polarity: evidence and hypothesis. Curr Opin Microbiol 8:216–221
Kanazawa KK (1997) Mechanical behaviour of films on the quartz microbalance. Faraday Disc 107:77–90
Kjaergaard K, Schembri MA, Hasman H, Klemm P (2000) Antigen 43 from *Escherichia coli* induces inter- and intraspecies cell aggregation and changes in colony morphology of Pseudomonas fluorescens. J Bacteriol 182:4789–4796
Klemm P, Schembri MA (2000) Bacterial adhesins: function and structure. Int J Med Microbiol 290:27–35
Kogure K, Ikemoto E, Morisaki H (1998) Attachment of *Vibrio alginolyticus* to glass surfaces is dependent on swimming speed. J Bacteriol 180:932–937
Kretschmann E, Raether H (1968) Radiative decay of non-radiative surface plasmons excited by light. Z Naturforsch A 23:2135–2136
Lauga E, Brenner MP, Stone HA (2007) Microfluidics: the no-slip boundary condition. In: Tropea C, Yarin A, Foss JF (eds) Handbook of experimental fluid dynamics. Springer, The Netherlands, isbn: 978-3-540-25141-5. Chap 19:1219–1240
Lauga E, DiLuzio WR, Whitesides GM, Stone HA (2006) Swimming in circles: motion of bacteria near solid boundaries. Biophys J 90:400–412
Lecuyer S, Rusconi R, Shen Y, Forsyth A, Stone HA (2010) Shear-enhanced adhesion of *Pseudomonas aeruginosa*. American Physics Society annual meeting, Portland, OR
Li ZJ, Mohamed N, Ross JM (2000) Shear stress affects the kinetics of *Staphylococcus aureus* adhesion to collagen. Biotechnol Prog 16:1086–1090
Li G, Tam LK, Tang JX (2008) Amplified effect of Brownian motion in bacterial near-surface swimming. Proc Natl Acad Sci USA 105:18355–18359
Ljosa V, Carpenter AE (2009) Introduction to the quantitative analysis of two-dimensional fluorescence microscopy images for cell-based screening. PLoS Comput Biol 5:e1000603
Locke JC, Elowitz MB (2009) Using movies to analyse gene circuit dynamics in single cells. Nat Rev Microbiol 7:383–392

McClaine JW, Ford RM (2002) Reversal of flagellar rotation is important in initial attachment of *Escherichia coli* to glass in a dynamic system with high- and low-ionic-strength buffers. Appl Environ Microbiol 68:1280–1289

Merritt PM, Danhorn T, Fuqua C (2007) Motility and chemotaxis in Agrobacterium tumefaciens surface attachment and biofilm formation. J Bacteriol 189:8005–8014

Mohamed N, Teeters MA, Patti JM, Hook M, Ross JM (1999) Inhibition of *Staphylococcus aureus* adherence to collagen under dynamic conditions. Infect Immun 67:589–594

Morisaki H, Nagai S, Ohshima H, Ikemoto E, Kogure K (1999) The effect of motility and cell-surface polymers on bacterial attachment. Microbiology 145(Pt 10):2797–2802

Neu TR (1996) Significance of bacterial surface-active compounds in interaction of bacteria with interfaces. Microbiol Rev 60:151–166

Oli MW, McArthur WP, Brady LJ (2006) A whole cell BIAcore assay to evaluate P1-mediated adherence of *Streptococcus mutans* to human salivary agglutinin and inhibition by specific antibodies. J Microbiol Methods 65:503–511

Olofsson AC, Hermansson M, Elwing H (2005) Use of a quartz crystal microbalance to investigate the antiadhesive potential of N-acetyl-L-cysteine. Appl Environ Microbiol 71:2705–2712

Olsson AL, van der Mei HC, Busscher HJ, Sharma PK (2009) Influence of cell surface appendages on the bacterium-substratum interface measured real-time using QCM-D. Langmuir 25: 1627–1632

Otto K (2008) Considering the first steps toward a stable and orderly way of bacterial life. PLoS Biol 6:e180

Otto K, Elwing H, Hermansson M (1999) Effect of ionic strength on initial interactions of *Escherichia coli* with surfaces, studied on-line by a novel quartz crystal microbalance technique. J Bacteriol 181:5210–5218

Otto K, Hermansson M (2004) Inactivation of ompX causes increased interactions of type 1 fimbriated *Escherichia coli* with abiotic surfaces. J Bacteriol 186:226–234

O'Toole G, Kaplan HB, Kolter R (2000) Biofilm formation as microbial development. Annu Rev Microbiol 54:49–79

Palmer J, Flint S, Brooks J (2007) Bacterial cell attachment, the beginning of a biofilm. J Ind Microbiol Biotechnol 34:577–588

Pourshafie MR, Marklund BI, Ohlson S (2004) Binding interactions of *Escherichia coli* with globotetraosylceramide (globoside) using a surface plasmon resonance biosensor. J Microbiol Methods 58:313–320

Prigent-Combaret C, Vidal O, Dorel C, Lejeune P (1999) Abiotic surface sensing and biofilm-dependent regulation of gene expression in *Escherichia coli*. J Bacteriol 181:5993–6002

Radcliff G, Jaroszeski MJ (1998) Basics of flow cytometry. Meth Mol Biol 91:1–24

Salminen A, Loimaranta V, Joosten JA, Khan AS, Hacker J, Pieters RJ, Finne J (2007) Inhibition of P-fimbriated *Escherichia coli* adhesion by multivalent galabiose derivatives studied by a live-bacteria application of surface plasmon resonance. J Antimicrob Chemother 60:495–501

Sasahara K, Zottola C, EA (1993) Biofilm formation by *Listeria monocytogenes* utilizes a primary colonizing microorganism in flowing systems. J. Food Protect 56:1022–1028

Sauerbrey GZ (1959) Use of quartz vibrator for weighing thin films on a microbalance. Z Phys 155:206–222

Schembri MA, Hjerrild L, Gjermansen M, Klemm P (2003) Differential expression of the *Escherichia coli* autoaggregation factor antigen 43. J Bacteriol 185:2236–2242

Schuck P (1997) Reliable determination of binding affinity and kinetics using surface plasmon resonance biosensors. Curr Opin Biotechnol 8:498–502

Shapiro HM (2000) Microbial analysis at the single-cell level: tasks and techniques. J Microbiol Methods 42:3–16

Shen Z, Huang M, Xiao C, Zhang Y, Zeng X, Wang PG (2007) Nonlabeled quartz crystal microbalance biosensor for bacterial detection using carbohydrate and lectin recognitions. Anal Chem 79:2312–2319

Sherlock O, Schembri MA, Reisner A, Klemm P (2004) Novel roles for the AIDA adhesin from diarrheagenic *Escherichia coli:* cell aggregation and biofilm formation. J Bacteriol 186:8058–8065

Shive MS, Hasan SM, Anderson JM (1999) Shear stress effects on bacterial adhesion, leukocyte adhesion, and leukocyte oxidative capacity on a polyetherurethane. J Biomed Mater Res 46:511–519

Stewart PS, Costerton JW (2001) Antibiotic resistance of bacteria in biofilms. Lancet 358:135–138

Thomas WE, Nilsson LM, Forero M, Sokurenko EV, Vogel V (2004) Shear-dependent 'stick-and-roll' adhesion of type 1 fimbriated *Escherichia coli*. Mol Microbiol 53:1545–1557

Thomas WE, Trintchina E, Forero M, Vogel V, Sokurenko EV (2002) Bacterial adhesion to target cells enhanced by shear force. Cell 109:913–923

Thomas WE, Vogel V, Sokurenko E (2008) Biophysics of catch bonds. Annu Rev Biophys 37: 399–416

Trache A, Meininger GA (2008) Total internal reflection fluorescence (TIRF) microscopy. Curr Protoc Microbiol Chapter 2:Unit 2A 2 1–2A 2 22

Valle J, Da Re S, Henry N, Fontaine T, Balestrino D, Latour-Lambert P, Ghigo JM (2006) Broad-spectrum biofilm inhibition by a secreted bacterial polysaccharide. Proc Natl Acad Sci USA 103:12558–12563

van Loosdrecht MC, Lyklema J, Norde W, Zehnder AJ (1990) Influence of interfaces on microbial activity. Microbiol Rev 54:75–87

Vigeant MA, Ford RM (1997) Interactions between motile *Escherichia coli* and glass in media with various ionic strengths, as observed with a three-dimensional-tracking microscope. Appl Environ Microbiol 63:3474–3479

Vigeant MA, Ford RM, Wagner M, Tamm LK (2002) Reversible and irreversible adhesion of motile *Escherichia coli* cells analyzed by total internal reflection aqueous fluorescence microscopy. Appl Environ Microbiol 68:2794–2801

Vigeant MA, Wagner M, Tamm LK, Ford RM (2001) Nanometer distances between swimming bacteria and surfaces measured by total internal reflection aqueous fluorescence microscopy. Langmuir 17:2235–2242

Wang IW, Anderson JM, Jacobs MR, Marchant RE (1995) Adhesion of S*taphylococcus epidermidis* to biomedical polymers: contributions of surface thermodynamics and hemodynamic shear conditions. J Biomed Mater Res 29:485–493

Watnick P, Kolter R (2000) Biofilm, city of microbes. J Bacteriol 182:2675–2679

Zobell CE (1943) The effect of solid surfaces upon bacterial activity. J Bacteriol 46:39–56

Chapter 21
Deciphering Biofilm Structure and Reactivity by Multiscale Time-Resolved Fluorescence Analysis

Arnaud Bridier, Ekaterina Tischenko, Florence Dubois-Brissonnet, Jean-Marie Herry, Vincent Thomas, Samia Daddi-Oubekka, François Waharte, Karine Steenkeste, Marie-Pierre Fontaine-Aupart, and Romain Briandet

Abstract In natural, industrial and medical environments, microorganisms mainly live as structured and organised matrix-encased communities known as biofilms. In these communities, microorganisms demonstrate coordinated behaviour and are able to perform specific functions such as dramatic resistance to antimicrobials, which potentially lead to major public health and industrial problems. It is now recognised that the appearance of such specific biofilm functions is intimately related to the three-dimensional organisation of the biological edifice, and results from multifactorial processes. During the last decade, the emergence of innovative optical microscopy techniques such as confocal laser scanning microscopy in combination with fluorescent labelling has radically transformed imaging in biofilm research, giving the possibility to investigate non-invasively the dynamic mechanisms of formation and reactivity of these biostructures. In this chapter, we discuss the contribution of fluorescence analysis and imaging to the study at different timescales of various processes: biofilm development (hours to days), antimicrobial reactivity within the three-dimensional structure (minutes to hours) or molecular diffusion/reaction phenomena (pico- to milliseconds).

21.1 Microbial Biofilms in Our Environment

Biofilms have a considerable impact on human existence and well-being because of their involvment in various beneficial ecological phenomena (Singh et al., 2006). Moreover, the ability of microbes to perform specific chemical reactions in surface associated consortia can be used to produce energy (Yadvika et al., 2004; Cournet et al., 2010). Nevertheless, bacterial communities are involved in a large number of detrimental processes such as biofouling or biocorrosion (Beech et al., 2005), and

R. Briandet (✉)
INRA, UMR 1319 MICALIS, Massy, France
e-mail: romain.briandet@jouy.inra.fr

D. Linke, A. Goldman (eds.), *Bacterial Adhesion*, Advances in Experimental Medicine and Biology 715, DOI 10.1007/978-94-007-0940-9_21,

in infectious diseases such as periodontitis, endocarditis, cystic fibrosis pneumonia and most hospital-acquired infections (Costerton et al., 1999). This phenomenon can be explained by the high resistance of biofilm-dwelling cells to antimicrobial agents (Mah and O'Toole, 2001), which enables pathogens to persist on medical devices or industrial equipment, leading thus to critical problems in terms of public health. Although the precise mechanisms of resistance remain unclear, it appears to be a multifactorial process directly or indirectly related to the architectural features of multicellular bacterial edifices. The depletion of active antimicrobial agents in the bulk of biofilm due to diffusion and/or reaction limitations (Huang et al., 1995; Campanac et al., 2002) illustrates the vital role of the shape of the matrix in the resistance of such communities. The biofilm matrix is also known to play a key role in protection against the human innate immune system by decreasing phagocytosis, for example (Vuong et al., 2004). In addition, the development of a complex three-dimensional (3D) biofilm architecture results in the appearance of nutrient and oxygen gradients. These lead to differential gene expression and specific physiological activities throughout the biofilm in response to local microenvironmental conditions (Stewart, 2003; Rani et al., 2007). Consequently, the emergence of phenotypic variants in biofilm subpopulations contributes to the expression of novel community functions such as tolerance to antimicrobial stress, which can increase population fitness (Lewis, 2005; Stewart and Franklin, 2008).

Until now, biofilm imaging has concentrated on identifying and understanding the sequence of events leading to biofilm formation and its structure (Lakins et al., 2009). Specifically, it is now appreciated that biofilm formation can be defined as a process that consists of defined stages including: reversible and irreversible attachment; surface motility and initiation of the formation of microcolonies or other arrangements; maturation, ageing and differentiation of microcolonies; and finally, biofilm dissolution and generation of specialised dispersal cells (Kjelleberg et al., 2007). Numerous studies have shown that this biological process involves a coordinated spatio-temporal expression of adhesion, motility, matrix or cell death genes in response to micro-environmental conditions and signalling molecules (Rieu et al., 2007; Vlamakis et al., 2008). The regulated death of bacterial cells in biofilms constitutes an important component of multicellular development and a telling example of temporal and spatial regulation (Bayles, 2007). In *B. subtilis* biofilms for example, Lopez et al. (2009) showed that matrix-producing cells exhibit cannibalistic behaviour by producing toxins that lyse a part of the population. The nutrients released are preferentially consumed by the surviving matrix-producing subpopulation as they are the only cells expressing resistance to toxins. This phenomenon leads to increase of matrix production and thus favours biofilm formation. The authors showed that this coordinated mechanism may constitute a defense mechanism of *B. subtilis* in adverse conditions. In *Pseudomonas aeruginosa*, some cells in the centre of the microcolonies undergo prophage-mediated autolysis, providing nutrients to the remaining cells that can disseminate and colonise novel ecological niches (Webb et al., 2003; Rice et al., 2009). Moreover, most dispersed cells exhibit specific phenotypes that are associated with increased resistance to environmental stress and higher virulence (Hall-Stoodley and Stoodley, 2005). Both these

competitive or altruistic behaviours are deleterious at the single-cell level, but benefit the global community fitness, demonstrating that biofilm typically results from a balance between these two social behaviours (Dunny et al., 2008; Nadell et al., 2009). It is important to consider that, even if most experimental studies are performed on single species models, biofilms usually contain multiple bacterial species, fungi, viruses and protozoa. This diversity increases the complexity of the relationships between dwelling organisms and can lead to the emergence of specific traits (Hansen et al., 2007).

The functional properties of biofilms therefore result from the complex spatial and temporal differentiation of cells in the dynamic three-dimensional structure in response to environmental signals and cell-cell interactions. The development of tools enabling in-situ observation of dynamic processes within biofilms is required to improve our understanding of biofilm traits and to develop advanced control strategies. Recent developments in confocal laser scanning microscopy (CLSM), and new fluorescent molecules and protein reporters allowing the labelling of specific matrix components or cell states, have deepened our knowledge of biofilms. These new tools allow researchers to explore non-invasively the dynamic architectural and physiological evolution in the three-dimensional structure of biofilms (Palmer and Sternberg, 1999). In this chapter, we review the use of fluorescence imaging for the study of biofilm structure and reactivity at different timescales. We first present the contribution of the method to analyse the 3D architecture and development of the biofilm (hours to days). We then discuss the use of fluorescence in monitoring biocide activity in biofilms by 4D imaging (minutes to hours). Finally, we describe the use of FRAP (Fluorescence Recovery After Photobleaching), FCS (Fluorescence Correlation Spectroscopy) and FLIM (Fluorescence Lifetime Imaging) in insitu molecular diffusion/reaction studies in biofilms (picoseconds to minutes).

21.2 From Free Cells to 3D Organised Multicellular Architecture

21.2.1 Laboratory Biofilms Assays

In laboratories, different devices are used to produce biofilms: we only present here the most commonly used systems in live-cell imaging studies. Two types of systems, “dynamic” or “static”, can be distinguished.

In “dynamic” systems such as flow-cells, biofilms are formed under the flow of medium, which enables continuous renewal of nutrients. This kind of device enables the elimination of planktonic cells by the flow and is particularly well adapted to the monitoring of biofilm development in “real time” using fluorescent strains and CLSM (Pamp et al., 2009). Different flow-cell designs exist, varying according to the number and the dimension of channels, as well as the nature of the base. One major drawback of these systems is the cumbersome and expensive nature of the growth protocol, which does not allow the screening of many samples. Furthermore, the difficulty of standardising biofilm growth in flow-cells and the weak control of

hydrodynamic parameters can limit the repeatability between different experiments or laboratories.

In "static" systems, biofilms are produced without any flow and thus result from the multiplication of attached cells on the surface and also partially from the sedimentation of the planktonic fraction. Static systems also suffer from a lack of standardisation, in particular in the key step of rinsing that can severely affect the biofilm 3D structure.

Using microtiter plates, many high-throughput static assays have been developed to quantify biofilm formation in a large number of strains (Peeters et al., 2008). These methods are very useful for screening mutants and identifying the genes involved in biofilm formation and maintenance, but they do not provide structural information. Recently, a method based on a microtiter plate compatible with high resolution imaging by CLSM was proposed to overcome this limitation (Bridier et al., 2010). The ability of some species to form a floating pellicle at the air-liquid interface or complex macrocolonies on agar can also be exploited to identify developmental steps and genes required in biofilm formation (Branda et al., 2005; Enos-Berlage et al., 2005).

The choice of growth protocol is a critical step in biofilm study because it greatly influences biofilm formation and architecture: this has been clearly illustrated by Yarwood et al. (2004), who demonstrated that mutating a gene involved in *Staphylococcus aureus* biofilm formation had opposing effects depending on the system (microtiter plate, rotating disk reactor or flow-cell).

21.2.2 CLSM for Multi-dimensional Biofilm Fluorescence Imaging

As mentioned previously, most of what makes microbial cells in a biofilm different from their planktonic counterparts is their multicellular spatial organization. The analysis of such structure/function relationships has considerably evolved during the last decade, in line with technical advances in microscopy. To gain access to in situ observations, much effort has been directed toward photonic microscopy associated with the fluorescent labelling of biofilm elements. Hence, in conventional widefield fluorescence microscopy, the biofilm is illuminated by a cone of light, thus obtaining almost uniform sample excitation and fast image acquisition. The drawback is poor depth resolution due to the collection of light coming from regions of the sample located at different depths. Practically, it means that only very thin biofilms (close to a monolayer in structure) can be adequately observed. Deconvolution can in some cases allow 3D imaging enhancement in such systems (Conchello and Lichtman, 2005).

The emergence of CLSM has radically transformed biofilm optical imaging, and in particular allows the analysis of thick biofilms. Due to the introduction of a "pinhole" in the path of the fluorescence light emitted by the sample, only the fluorescence coming from the focal plane reaches the detector and the contribution

of out-of-focus light is eliminated. This optical sectioning ensures a submicron resolution compatible with observation of a single bacterium within the biofilm. It is also now possible to add two other dimensions to these image stacks: time (t) for 2D or 3D dynamics analysis, and wavelength (λ) for spectral imaging, for example to unmix multi-fluorescent labels or subtract interference from a fluorescent background. Therefore, the introduction of CLSM has led to considerable progress in studying the architecture, physiology and molecular interactions within the biofilm without prior chemical fixation (in situ observations in aqueous medium).

The widespread use of lasers has led to the emergence of new methods, including approaches based on nonlinear optics. Hence, the limited depth penetration of CLSM can be overcome by employing two-photon laser scanning microscopy (2PLSM). Experimentally, two-photon excitation of the fluorescent molecule is obtained by the quasi-simultaneous absorption of two photons of half the energy of the photons used in CLSM (Vroom et al., 1999), typically using near-infrared lasers (Neu et al., 2010; Lakins et al., 2009).

These laser microscopy methods are constantly evolving to improve both image acquisition rate (fast confocal spinning-disk microscopes, multiphoton multifocal microscopy; Deniset-Besseau et al., 2007) and spatial resolution, for instance: structured illumination, total internal reflection fluorescence microscopy (TIRF), stimulated emission depletion microscopy (STED), photoactivation localisation microscopy (PALM), stochastic optical reconstruction microscopy (STORM) and 4pi microscopy. Researchers involved in the study of biofilms may benefit from these new developments in fluorescence microscopy.

The extensive use of CLSM in biofilm research is also intrinsically related to the development of dedicated specific fluorophores. Available fluorophores allow visualisation of different components of the biofilms, of individual cells and their local physiology or patterns of gene expression, or of the organic matrix and the existence of heterogeneous microdomains.

The analysed fluorescence can come either from fluorescent labels incorporated into the biofilm or from the microorganism. The main requirement is that it is a good fluorophore: i.e. that it has high brightness (product of fluorescence quantum yield and molar extinction coefficient ε) and suitable photostability.

The most widespread methods of fluorescent labelling of biofilm components are:

- Indicators of microbial membrane integrity, e.g. Live/dead stain (Pamp et al., 2008).
- Indicators of metabolic activity markers, e.g. Calcein AM (Takenaka et al., 2008).
- Fluorescent lectins to label extracellular polysaccharides, e.g. concanavalin A (Neu et al., 2001).
- Fluorescent in situ hybridisation (FISH) for identification of community members within complex biofilms (Amann et al., 1990).
- Expression of fluorescent proteins from the microbial genome: green fluorescent protein (GFP) has proven to be a powerful method to study in vivo gene expression in a broad range of hosts (Veening et al., 2004).

21.2.3 Time-Course Structural Analysis of Events Leading to Biofilm Formation

Tracking of the time-course of biofilm construction was pioneered in the last decade by the Tolken-Nielsen group on *P. aeruginosa* biofilms grown in flow-cells (Tolker-Nielsen et al., 2000; Klausen et al., 2006). The ideal situation for non-destructive time-course biofilm imaging is to grow bacterial cells expressing fluorescent reporter protein(s) for the biofilm assay on a transparent substratum compatible with in situ CLSM observation (i.e. flowcells or dedicated microtiter plates). In this configuration, it is possible to record 4D image series (3D images as a function of time) of the same microscopic field and to trace in "real time" the multicellular assemblage as a movie. This approach was used to identify the molecular determinants involved in biofilm construction. The experimental method compares the sequence of events involved in the formation of a wild type biofilm

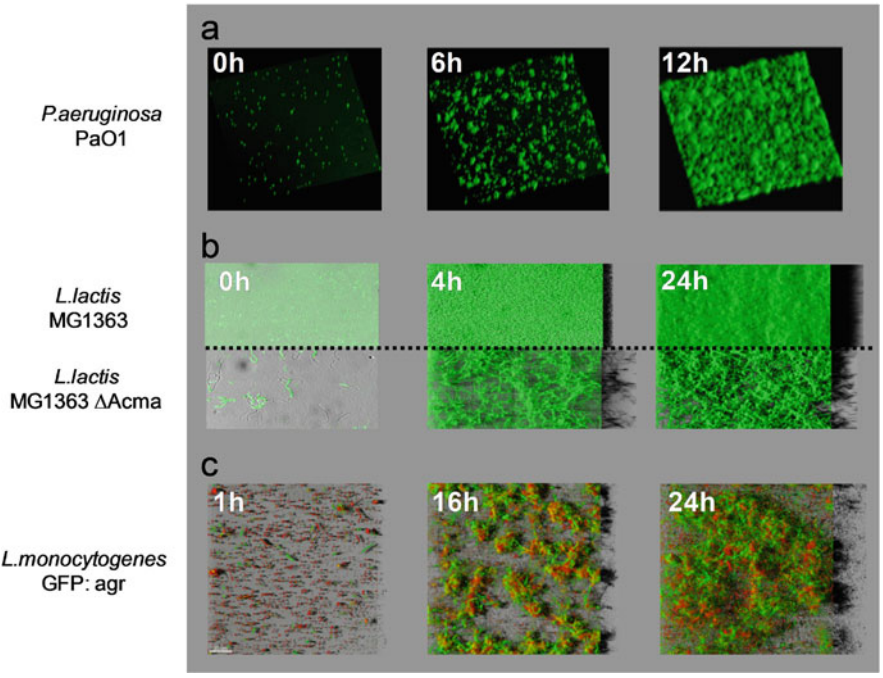

Fig. 21.1 3D reconstruction of biofilm development under flowing conditions from confocal image series. (**a**) Structural development of GFP-tagged *Pseudomonas aeruginosa* PaO1 biofilm using time-lapse CLSM. (**b**) Time-course CLSM of GFP-tagged WT *Lactococcus lactis* MG1363 (*top*) and its cell wall mutant, ΔacmA (inactivation of N-acetyl glucosaminidase) (*bottom*). The mutation leads to the development of cell chains forming a biofilm with different architectural properties than wild-type. Adapted from Habimana et al. (2009). (**c**) Sequence illustrating the spatiotemporal regulation of *agr* expression during biofilm formation by *Listeria monocytogenes*. *Green* indicates cells expressing GFP from the reporter plasmid pGID128, which contain a fusion of the *agr* promoter region with *gfp*. The red cells are stained with the nucleic acid SYTO61 dye (cells in red lacks *agr* activity). Adapted from Rieu et al. (2008)

with the sequence of events in a series of mutants. Using this scheme, it has been possible for example to identify the involvement of F plasmid, pilus and putative membrane proteins in *E. coli* biofilms (Beloin et al., 2004; May and Okabe, 2008), and the involvement of exopolysaccharide synthesis in *Lactococcus lactis* biofilms (Habimana et al., 2009).

As the understanding of biofilm complexity increases, "simple" descriptive architectural studies are being replaced by those in which the three-dimensional organization of the biofilm is related to other information, such as species composition, relationship with substrate or physiology (Palmer and Sternberg, 1999). Indeed, most studies of gene expression by bacteria in biofilms described levels that reflect the average gene expression over the entire population (Lenz et al., 2008). CLSM associated with fluorescent reporter fusions has recently been used to trace the spatio-temporal expression of specific genes at the single cell level in the overall biofilm structure. The approach has shown than some genes are specifically expressed on the interfacial layers of the biofilm (Lenz et al., 2008; Ito et al., 2009; Rieu et al., 2008), while others are expressed in more specific patterns, such as the *agr* system implicated in quorum sensing regulation in *Staphylococcus aureus* biofilms, which is expressed in patches within cell clusters and where the expression oscillates with time (Yarwood et al., 2004). Some examples of biofilm structural dynamics are presented in Fig. 21.1.

21.3 Real Time 3D Visualization of Biofilm Inactivation by Antimicrobials

The latest surge of interest in biofilms was triggered by the observation of their unprecedented microbial tolerance to antimicrobial agents e.g. antibiotics or biocides. Previous studies suggested that biofilm resistance is clearly multifactorial, and only a combination of different mechanisms could account for the observed resistance levels in biofilm communities (Anderson and O'Toole, 2008). Exopolymeric matrix can serve as a protective environment. For example, the activity of an antibiotic on mucoid *P. aeruginosa* biofilms can be significantly enhanced by addition of alginate lyase and DNAase, suggesting that alginate and extracellular DNA function as antibiotic barriers (Alipour et al., 2010; Harmsen et al., 2010). The heterogeneity of cell physiology within the biofilm matrix due to oxygen and nutrient gradients can also constitute a protective phenotype (Xu et al., 1998; Stewart and Franklin, 2008). In addition, regulated cell differentiation, collective coordinated behaviour and inter-cellular genetic exchange can contribute to the resistance of biofilm cells to antimicrobial stress. As a result, there is particular interest in developing biocides able to overcome such tolerance.

Conventional methods to study biofilm inactivation, such as bacterial enumeration on agar plates, are time-consuming, static and incompatible with structural observations. Therefore, the development of fast (minutes to hours), dynamic and non-destructive methods is required. Non-invasive direct time-lapse microscopic observation of biofilm viability was pioneered by Hope and Wilson (2004). Cells

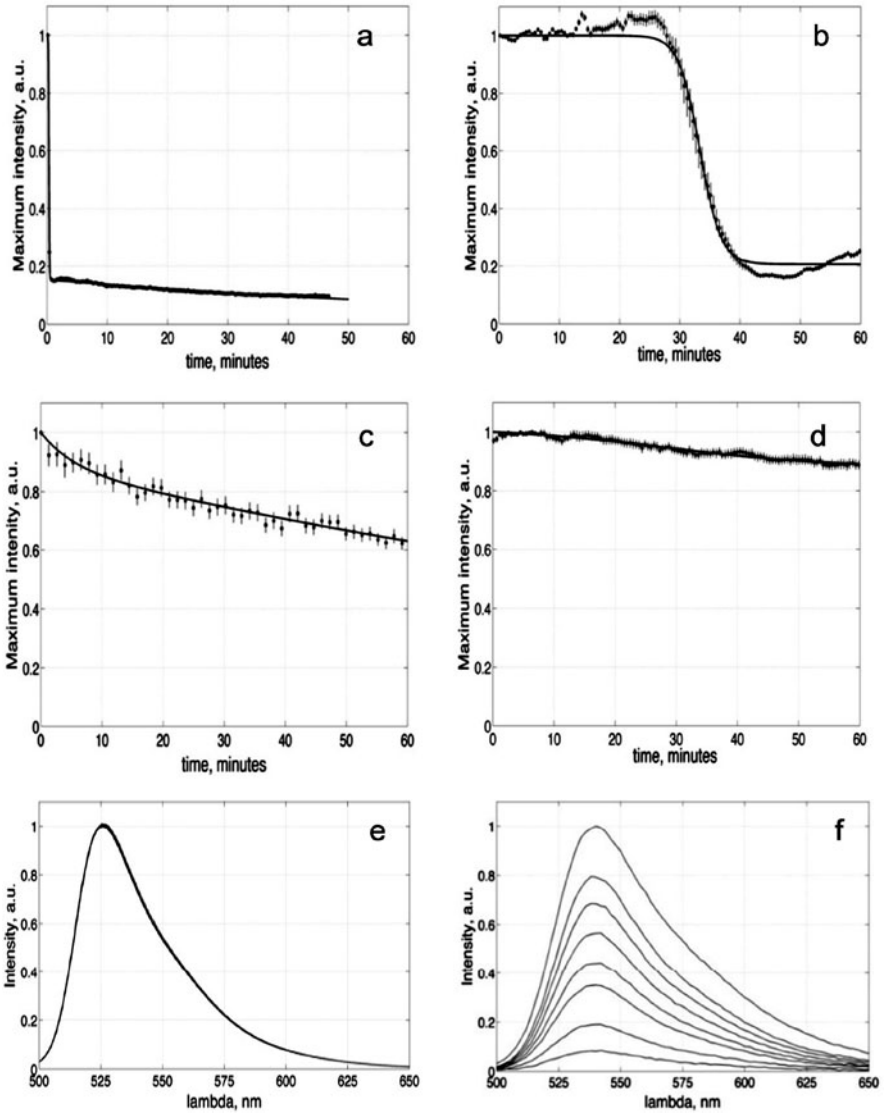

Fig. 21.2 Dynamics of *Staphylococcus aureus* biofilm inactivation by (**a**) 0.3% Peracetic Acid; (**b**) 0.05% C14-benzalkonium chloride; (**c**) 0.03% O-phthaldialdehyde and (**d**) saline solution. Fluorescent intensity of ChemChrome V6 is integrated over the image and normalized to the maximal value. Each *curve* represents the evolution of the mean fluorescent intensity of biofilm during biocide treatments. Dynamic profiles obtained illustrate the different modes of action of the three biocides tested. Fluorescent spectra ChemChrome V6 during: (**e**) C14-benzalkonium chloride and (**f**) 0.3% Peracetic acid action. Time between subsequent measurements (*curves*) is 5 min. Results show the loss of fluorescence intensity of the marker in presence of PAA showing an interaction between the two molecules. There was no interaction between ChemChrome V6 and the other biocides tested, as shown for C14-benzalkonium chloride as example

were visualised with the commercial BacLight Live/Dead kit (Invitrogen) composed of DNA-intercalating dyes, which is widely used for the time-independent measurements of bacterial membrane integrity. Later, the Stewart group (Takenaka et al., 2008) further improved the method by using the esterase activity marker Calcein-AM, which meets the basic requirements for cell viability tagging, i.e. it is stable and it efficiently tags the intracellular space in live cells without any changes in morphology or physiology of the cells and bacterial community structure. There is another essential requirement for "direct time-lapse microscopic observation": either the marker should not interact at all with the biocide, or the biocide-marker interactions should be fully understood and subtracted from the observed effect. Focusing on chemical biocides, there is evidence that such strongly reactive molecules and fluorescent dye or its target can interact (Phe et al., 2007). In this case, intracellular fluorescent reporters such as metabolic activity fluorophores are the most relevant. Their foremost advantage is that the marker is already inside cells, and is only affected by biocide after the biocide penetrates the cell or after the marker leaks out.

As an illustration, we measured the time and spatial inactivation of *Staphylococcus aureus* biofilms by three biocides used for disinfection of medical equipment and food processing areas (Fig. 21.2). In the absence of antimicrobials, the cell viability reporter used (esterasic marker V6 ChemChrome, AES Chemunex) stays inside the cell without any noticeable influence on the cell. When the plasma membrane is damaged during disinfection, the fluorophore leaks out of the cell, which allows direct visualization of biocide action within the 3D structure. The profiles of inactivation dynamics obtained underlined the specific mode of action of each biocide tested and enabled a deeper understanding of the treatment limitations. We could determine how well the dynamics of marker fluorescence intensity and biofilm cell inactivation correlate using model systems. For instance, using fluorescent spectroscopy in an in vitro system containing DNA and esterase enzyme to mimic the intracellular environment, we detected a strong biocide-marker interaction only with peracetic acid (PAA) (Fig. 21.2e–f). Consequently, the evolution of the intracellular marker fluorescent intensity under PAA action in biofilm tells us that the contact between marker and antimicrobial agent took place, and thus that the antimicrobial agent at least penetrated the cell. Moreover, the classical cell enumeration on agar was in good agreement with the fluorescent kinetics for the three biocides, including PAA.

CLSM 4D time-lapse experiments allow direct in situ visualization of antimicrobial action throughout the biofilm and the standardization of tools for the selection of active molecules in order to achieve efficient biofilm treatments.

21.4 Understanding the Process of Diffusion-Reaction Within Biofilms

Both the physiological properties of microorganisms and the structure of the extracellular polymeric substances play a crucial role in the reactivity of biofilms towards scattering entities. To analyse the molecular interactions within biofilms, it is

necessary to have non-invasive efficient methods of investigation in terms of spatial resolution, sensitivity and acquisition speed. Besides fluorescence intensity imaging techniques, more advanced fluorescence-based approaches can be implemented for in situ molecular diffusion/reaction studies within "live" biofilms, including FRAP (Fluorescence Recovery After Photobleaching), FCS (Fluorescence Correlation Spectroscopy) and FLIM (Fluorescence Lifetime IMaging).

21.4.1 Fluorescence Recovery After Photobleaching (FRAP)

As described previously, time-lapse imaging in CLSM allows following the diffusion of fluorescent molecules in such spatially organised biofilms (Rani et al., 2005; Takenaka et al., 2009). However, this method only allows estimating average and global diffusion coefficients over the macrostructure and ignores its heterogeneity (e.g. water channel, mushroom-like structures).

To measure local diffusion/reaction through a 3D biological structure, FRAP is a simple method that is now routinely implemented on commercial CLSMs (Waharte et al., 2010). FRAP is based on a brief excitation of fluorescent molecules by a very intense light source in the volume defined by the confocal microscope objective (for single spot FRAP) or in a user-defined region to quench their fluorescence (photobleaching) irreversibly (Fig. 21.3a,b). Fluorescence redistribution is then observed if the fluorophores are allowed to move in the sample. The analysis of the time course of fluorescence intensity recovery with proper mathematical models thus gives access to the quantitative mobility of the fluorescent molecules (determination of diffusion coefficient and/or rate of molecular association) (Fig. 21.3a).

FRAP typically requires micromolar concentrations of fluorescent tracers, and consequently gives access only to average diffusion coefficients unlike FCS (see below), potentially masking the effects of local heterogeneity. FRAP is not sensitive enough to detect the motion of a single molecule. Furthermore, the quantification of FRAP measurements requires mathematical models adapted to the experimental conditions and the geometrical/structural configuration of the sample; these difficulties explain why most FRAP studies are essentially based on a qualitative and relative analysis. Recently, an image-based FRAP protocol and its corresponding analysis that can be readily applied by anyone familiar with a CLSM has been published; it improves the accuracy and accessibility of FRAP measurements of molecular diffusion inside bacterial biofilms (Fig. 21.3d,e). The method was supported by an original representation that allows checking the presence of bacterial movement during image acquisition that would alter the measurements (Fig. 21.3c) (Waharte et al., 2010).

21.4.2 Fluorescence Correlation Spectroscopy (FCS)

FCS, on the other hand, is the most appropriate technique to analyse diffusion/reaction processes within biological entities with single molecule

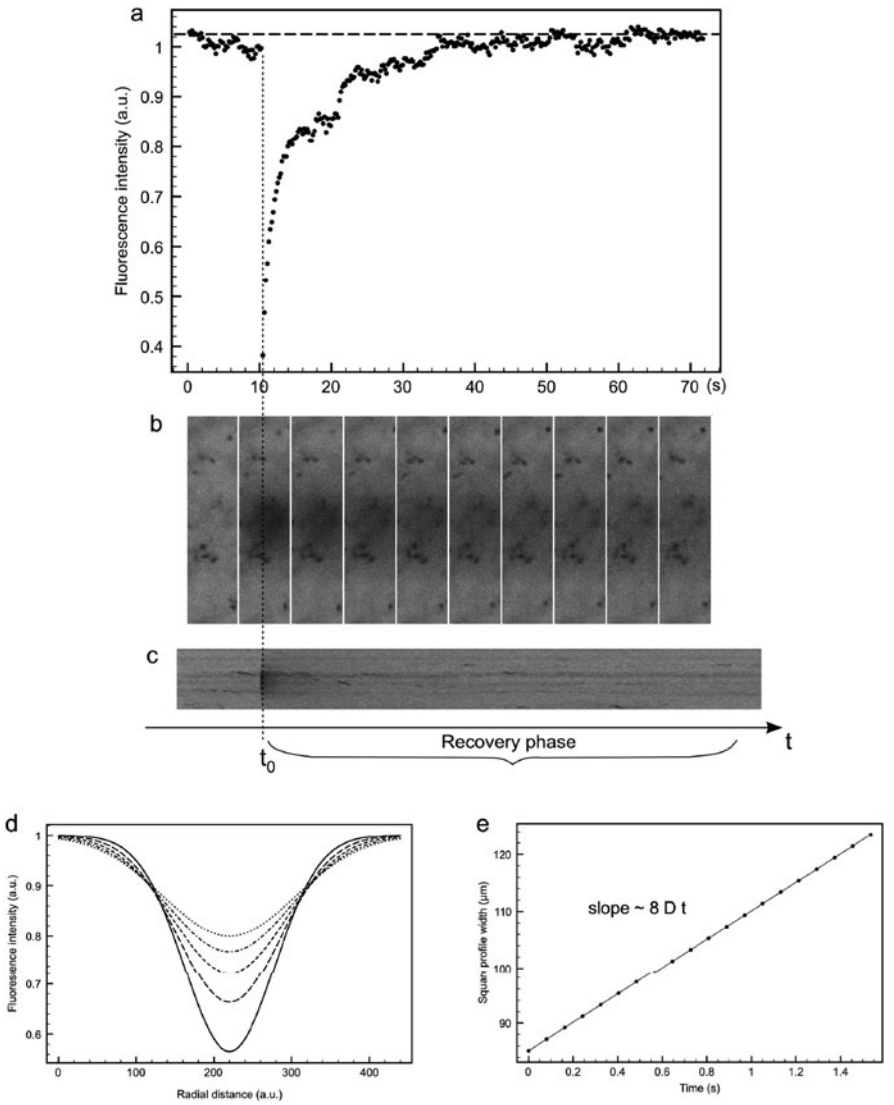

Fig. 21.3 Principle of molecular diffusion measurements in biofilms by FRAP (**a**) Example of fluorescence recovery curve. The *vertical points* show the start of the recovery phase just after photobleaching. The *horizontal dashed line* shows the initial level of fluorescence to estimate the mobile fraction (100% here). (**b**) Image sequence taken during the FRAP experiment on a *Stenotrophomonas maltophilia* biofilm loaded with FITC-dextran. The *dark area* in the centre of the images is the photobleached area. (**c**) Kymogram representation (intensity along a *vertical centered line* crossing the image for each time point) giving a graphical representation of spatial position over time. (**d**) Illustration of the evolution of the intensity spatial profile overtime (*dark line* is the initial profile after photobleaching and successive profiles in *dashed lines* with decreasing amplitudes with time). (**e**) Evolution of the squared intensity profile width with time showing the proportionality of the slope of the graph with the diffusion coefficient (profile analysis)

resolution. FCS is based on monitoring the emission intensity fluctuations due to a small number of molecules passing through the confocal excitation volume. These fluctuations can be quantified in their amplitude and duration by temporally autocorrelating the recorded intensity signal.

The experimental conditions required for this technique (a small number of fluorophores, characterization and control of the excitation volume) explain why FCS was mainly developed after the advent of confocal and two-photon microscopy (excitation volume < 1 fL) and of ultrasensitive new systems for detecting fluorescence photons (photomultipliers, avalanche photodiodes) allowing the use of low fluorophore concentrations (Guiot et al., 2000). Fluorescence intensity fluctuations reflect not only the diffusion of fluorescent molecules through the 3D structure of the biofilm, but also the photophysical and photochemical reactions that quench the fluorescence (charge transfer transition to the triplet state of the molecule), or conformational changes of molecules (molecular complexation, aggregate formation). Thus the FCS signal analysis quantifies a range of reaction parameters on a large time scale from microseconds to several seconds.

In practice, although this method is highly sensitive, has high resolution and is and non-invasive, it remains difficult to use and imposes some constraints. In particular, the fluorophores must have high fluorescence quantum yields and low photo-destruction yields. Furthermore, because of the small number of molecules involved, it is often necessary to temporally accumulate the fluorescence signal to obtain a representative statistic of fluctuation correlations with a satisfactory signal to noise ratio. This condition can be greatly improved by the use of two-photon excitation (TPE). The probability of fluorophore excitation by quasi-simultaneous ($<10^{-16}$ s delay) absorption of two photons is very low, thus significant TPE only occurs at the objective focal volume where the concentration of photons (also temporally concentrated by the use of femtosecond pulsed lasers) is very high. These properties give TPE microscopy several advantages over one photon excitation microscopy, in particular in a classical confocal setup: (i) intrinsic localisation of the excitation allows fluorescence detection with extremely low background noise and thus easier detection of single molecules, (ii) use of an infrared excitation wavelength (e.g. from a Titanium-sapphire laser) results in greater penetration of biological samples, (iii) photodamage is limited and restricted to the excitation volume and (iv) the excitation volume can easily be characterised and mathematically modelled.

FCS was first explored using homemade equipment and the associated specific know-how. The method has now been adapted to commercial CLSM and TPE setups. Whatever the setup used, FCS has allowed the following of the penetration, diffusion and reaction capabilities of fluorescent probes (latex beads and fluorescein isothiocyanate–dextran) of different sizes and electrical charge (Guiot et al., 2002), of fluorescently stained bacteriophages (Briandet et al., 2008), and of antimicrobial agents in models of static and dynamic biofilms with different EPS density. Steric hindrance and even total inhibition of diffusion have been observed, particularly in areas with a high cotent of extracellular polymeric substances. Alternative explanations for this were attractive electrostatic interactions between cationic particles and negatively charged bacteria, specific interactions between the diffusing fluorophore

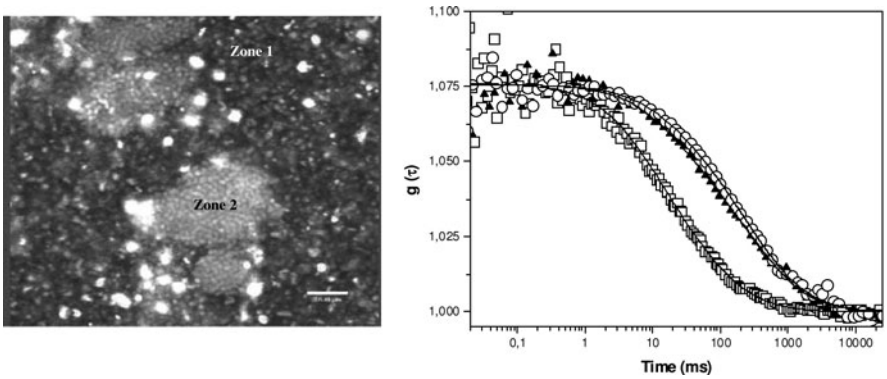

Fig. 21.4 (**a**) CLSM image of *S. maltophilia* biofilms near the substratum. Zone 1 and zone 2 correspond to homogeneous and heterogeneous parts of the biofilm respectively. Cells were stained with SYTO nucleic acid stain (scale bar = 20 μm). (**b**) Fluorescence correlation curves (g(τ)) corresponding to c2 bacteriophages stained with sytox green in solution (□), in zone 1 (▲) and zone 2 (◯) of *S. maltophilia* biofilms. The curve fits (*straight lines*) were obtained using a two diffusional component equation

and elements in the biofilm (e.g. sugar-matrix interaction, cell envelope and phage) (Fig. 21.4) or antibiotics. Such studies have given a better understanding of the role of the exopolymer matrix as a molecular "reservoir" and of its ability to modulate the transport and interaction of entities within the biofilm.

21.4.3 Fluorescence Lifetime Imaging (FLIM)

FLIM is well-suited for characterising such molecular interaction processes as fluorescence lifetime is an intrinsic property of a fluorophore, independent of its concentration. The fluorescence lifetime of a molecule varies locally depending on its reactivity with the biological environment. It is hence possible to build fluorescence lifetime images that allow assessment of the reactivity of a fluorophore at the molecular level throughout a 3D biological structure such as a biofilm. FLIM was used in biofilm studies to characterise the interaction between sugars in the exopolymeric matrix (Guiot et al., 2002), to probe the local pH (Vromm et al., 1999) and more recently to measure the differentiation of active and inactive bacteria by the estimation of the intracellular RNA:DNA ratio (Walcysko et al., 2008).

21.5 Conclusion

Recent advances in photonic microscopy, fluorophore design and molecular tools have dramatically transformed biofilm experimental analysis by making it possible to explore the dynamic structure and reactivity of these biological edifices non-invasively. The current development of high content screening automated systems

(Bridier et al., 2010), alternative label-free imaging methods such as scanning transmission X-ray microscopy (STXM) and magnetic resonance imaging (MRI) (Neu et al., 2010), and the development of correlative microscopy (Schaudinn et al., 2009) will dramatically improve our understanding of biofilm structure/function relationships, offering new perspectives in the field of biofilm research.

Acknowledgements Funding for our work from the French "Pole de Compétitivité Ile-de-France MEDICEN" is greatly appreciated. AES-Chemunex is warmly acknowledged for providing ChemChrom V6 fluorophore. We thank the "department of Essonne" for financial support of the confocal microscope (ASTRE n°A02137) and the INRA MIMA2 microscopic facilities for CLSM imaging. O. Habimana, P. Latour-Lambert and P. Piveteau are acknowledged for their contribution to image acquisition.

References

Alipour M, Suntres ZE, Lafrenie RM, Omri A (2010) Attenuation of *Pseudomonas aeruginosa* virulence factor and biofilms by co-encapsulation of bismuth-ethanedithiol with tobramycin in liposomes. J Antimicrob Chemother 65:684–693

Amann RI, Binder BJ, Chisholm SW, Devereux R, Stahl DA (1990) Combination of 16S rRNA-targeted oligonucleotide probes with flow cytometry for analyzing mixed microbial population. Appl Environ Microbiol 56:1919–1925

Anderson GG, O'Tolle GA (2008) Innate and Induced resistance mechanisms of bacterial biofilms. Curr Top Microbiol Immunol 322:85–105

Bayles KW (2007) The biological role of death and lysis in biofilm development. Nat Rev Microbiol 5:721–726

Beech IB, Sunner JA, Hiraoka K (2005) Microbe-surface interactions in biofouling and biocorrosion processes. Int Microbiol 8:157–168

Beloin C, Valle J, Latour-Lambert P, Faure P, Kzreminski M, Balestrino D, Haagensen JA, Molin S, Prensier G, Arbeille B, Ghigo JM (2004) Global impact of mature biofilm lifestyle on *Escherichia coli* K-12 gene expression. Mol Microbiol 51:659–674

Branda SS, Vik S, Friedman L, Kolter R (2005) Biofilms: the matrix revisited. Trends Microbiol 13:20–26

Briandet R, Lacroix-Gueu P, Lecart S, Renault M, Meylheuc T, Bidnenko E, Bellon-Fontaine M-N, Fontaine-Aupart M-P (2008) Fluorescence correlation spectroscopy to study diffusion-reaction of bacteriophages inside bacterial biofilms. Appl Environ Microbiol 74:2135–2143

Bridier A, Dubois-Brissonnet F, Boubetra A, Thomas V, Briandet R (2010) The biofilm architecture of sixty opportunistic pathogens deciphered using a high throughput CLSM method. J Microbiol Methods 82:64–70

Campanac C, Pineau L, Payard A, Baziard-Mouysset G, Roques C (2002) Interaction between biocide cationic agents and bacterila biofilms. Antimicrob Agent Chemother 46:1469–1474

Conchello J-A, Litchman J (2005) Optical sectioning microscopy. Nat Methods 2:920–931

Costerton JW, Stewart PS, Greenberg EP (1999) Bacterial biofilms, a common cause of persistent infections. Science 284:1318–1322

Cournet A, Delia M-L, Bergel A, Roques C, Bergé M (2010) Electrochemical reduction of oxygen catalyzed by a wide range of bacteria including Gram-positive. Electrochem Commun 12: 505–508

Deniset-Besseau A, Lévêque-Fort S, Fontaine-Aupart M-P, Roger G, Georges P (2007) Three-dimensional time-resolved imaging by multifocal multiphoton microscopy for a photosensitizer in living cells. Appl Optics 46:8045–8051

Dunny GM, Brickman TJ, Dworkin M (2008) Multicellular behavior in bacteria communication, cooperation, competition and cheating. BioEssays 30:296–298

Enos-Berlage JL, Guvener ZT, Keenan CE, McCarter LL (2005) Genetic determinants of biofilm development of opaque and translucent *Vibrio parahaemolyticus*. Mol Microbiol 55: 1160–1182

Guiot E, Enescu M, Arrio B, Johannin G, Roger G, Tosti S, Tfibel F, Mérola F, Brun A, Georges P, Fontaine-Aupart MP (2000) Molecular dynamics of biological probes by fluorescence correlation microscopy with two-photon excitation. J Fluoresc 10:413–419

Guiot E, Georges P, Brun A, Fontaine-Aupart MP, Bellon-Fontaine MN, Briandet R (2002) Heterogeneity of the diffusion inside microbial biofilms using fluorescence correlation microscopy under two-photon excitation. Photochem Photobiol 75:570–578

Habimana O, Meyrand M, Meylheuc T, Kulakauskas S, Briandet R (2009) Genetic features of resident biofilm determine attachment of *Listeria monocytogenes*. Appl Environ Microbiol 75:7814–7821

Hall-Stoodley L, Stoodley P (2005) Biofilm formation and dispersal and the transmission of human pathogens. Trends Microbiol 13:7–10

Hansen SK, Rainey PB, Haagensen JAJ, Molin S (2007) Evolution of species interactions in a biofilm community. Nature 445:533–536

Harmsen M, Yang L, Pamp SJ, Tolker-Nielsen T (2010) An update on *Pseudomonas aeruginosa* biofilm formation, tolerance, and dispersal. FEMS Immunol Med Microbiol 59:253–268

Hope CK, Wilson M (2004) Analysis of the effects of chlorhexidine on oral biofilm vitality and structure based on viability profiling and an indicator of membrane integrity. Antimicrob Agents Chemother 48:1461–1468

Huang CT, Yu FP, McFeters GA, Stewart PS (1995) Non-uniform spatial patterns of respiratory activity within biofilms during disinfection. Appl Environ Microbiol 61:2252–2256

Ito A, May T, Taniuchi A, Kawata K, Okabe S (2009) Localized expression profiles of rpoS in Escherichia coli biofilms. Biotechnol Bioeng 103:975–983

Kjelleberg S, Marshall KC, Givskov M (2007) The biofilm mode of life. In: Kjelleberg S, Marshall KC, Givskov M (eds) The biofilm mode of life, mechanisms and adaptations. Horizon Bioscience, Wymondham

Klausen M, Gjermansen M, Kreft J-U, Tolker-Nielsen T (2006) Dynamics of development and dispersal in sessile microbial communities: examples from *Pseudomonas aeruginosa* and *Pseudomonas putida* model biofilms. FEMS Microbiol Lett 261:1–11

Lakins MA, Marrison JL, O'Toole PJ, Van der Woude MW (2009) Exploiting advances in imaging technology to study biofilms by applying multiphotons laser scanning microscopy as an imaging and manipulation tool. J Microsc 235:128–137

Lenz AP, Williamson KS, Pitts B, Stewart PS, Franklin MJ (2008) Localized gene expression in *Pseudomonas aeruginosa* biofilms. Appl Environ Microbiol 74:4463–4471

Lewis K (2005) Persister cells and the riddle of biofilm survival. Biochemistry 70:267–274

Lopez D, Vlamakis H, Losick R, Kolter R (2009) Cannibalism enhances biofilm development in *Bacillus subtilis*. Mol Microbiol 74:609–618

Mah T-F C, O'Toole GA (2001) Mechanisms of biofilm resistance to antimicrobial agents. Trends Microbiol 9:34–39

May T, Okabe S (2008) Escherichia coli harboring a natural IncF conjugative F plasmid develops complex mature biofilms by stimulating synthesis of colanic acid and curli. J Bacteriol 190:7479–7490

Nadell CD, Xavier JB, Foster K (2009) The sociobiology of biofilms. FEMS Microbiol Rev 33:206–224

Neu TR, Manz B, Volke F, Dynes JJ, Hitchcock AP, Lawrence JR (2010) Advanced imaging techniques for assessment of structure, composition and function in biofilm systems. FEMS Microbiol Ecol 72:1–21

Neu TR, Swerhone GDW, Lawrence JR (2001) Assessment of lectin binding analysis for *in situ* detection of glycoconjugates in biofilm systems. Microbiology 147:299–313

Palmer RJ, Sternberg C (1999) Modern microscopy in biofilm research: confocal microscopy and other approaches. Curr Opin Biotechnol 10:263–268

Pamp SJ, Gjermansen M, Johansen HK, Tolker-Nielsen T (2008) Tolerance to the antimicrobial peptide colistin in Pseudomonas aeruginosa biofilms is linked to metabolically active cells, and depends on the pmr and mexAB-oprM genes. Mol Microbiol 68:223–240

Pamp SJ, Sternberg C, Tolker-Nielsen T (2009) Insight into the microbial multicellular lifestyle via flow-cell technology and confocal microscopy. Cytometry A 75:90–103

Peeters E, Nelis HJ, Coenye T (2008) Comparison of multiple methods for quantification of microbial biofilms grown in microtiter plates. J Microbiol Methods 72:157–165

Phe MH, Dossot M, Guilloteau H, Block JC (2007) Highly chlorinated *Escherichia coli* cannot be stained by propidium iodide. Can J Microbiol 53:664–670

Rani SA, Pitts B, Beyenal H, Veluchamy RA, Lewandowski Z, Buckingham-Meyer K, Stewart PS (2007) Spatial patterns of DNA replication, protein synthesis and oxygen concentration within bacterial biofilms reveal diverse physiological states. J Bacteriol 189:4223–4233

Rani SA, Pitts B, Stewart PS (2005) Rapid diffusion of fluorescent tracers into *Staphylococcus epidermidis* biofilms visualized by time lapse microscopy. Antimicrob Agents Chemother 49:728–732

Rice SA, Tan CH, Mikkelsen PJ, Kung V, Woo J, Tay M, Hauser A, McDougald D, Webb SA, Kjelleberg S (2009) The biofilm life cycle and virulence of *Pseudomonas aeruginosa* are dependent on a filamentous prophage. ISME J 3:271–282

Rieu A, Briandet R, Habimana O, Garmyn D, Guzzo J, Piveteau P (2008) *Listeria monocytogenes* EGD-e biofilms: no mushrooms but a network of knitted-chains structures. Appl Environ Microbiol 74:4491–4497

Rieu A, Weidmann S, Garmyn D, Piveteau P, Guzzo J (2007) Agr system of *Listeria monocytogenes* EGD-e: role in adherence and differential expression pattern. App Environ Microbiol 73:6125–6133

Schaudinn C, Carr G, Gorur A, Jaramillo D, Costerton JW, Webster P (2009) Imaging of endodontic biofilms by combined microscopy (FISH/cLSM – SEM). J Microsc 235:124–127

Singh R, Debarati P, Rakesh KJ (2006) Biofilms, implications in bioremediation. Trends Microbiol 14:389–397

Stewart PS (2003) Diffusion in biofilms. J Bacteriol 185:1485–1491

Stewart PS, Franklin MJ (2008) Physiological heterogeneity in biofilms. Nat Rev Microbiol 6: 199–210

Takenaka S, Pitts B, Trivedi HM, Stewart PS (2009) Diffusion of macromolecules in model oral biofilms. Appl Environ Microbiol 75:1750–1753

Takenaka S, Trivedi HM, Corbin A, Pitts B, Stewart PS (2008) Direct visualization of spatial and temporal patterns of antimicrobial action within model oral biofilms. Appl Environ Microbiol 74:1869–1875

Tolker-Nielsen T, Brinch UC, Ragas PC, Andersen JB, Jacobsen CS, Molin S (2000) Development and dynamics of *Pseudomonas* sp. Biofilms J Bacteriol 182:6482–6489

Veening JW, Smits WK, Hamoen LW, Jongbloed JD, Kuipers OP (2004) Visualization of differential gene expression by improved cyan fluorescent protein and yellow fluorescent protein production in *Bacillus subtilis*. Appl Environ Microbiol 70:6809–6815

Vlamakis H, Aguilar C, Losick R, Kolter R (2008) Control of cell fate by the formation of an architecturally complex bacterial community. Genes Dev 22:945–953

Vroom JM, De Grauw KJ, Gerritsen HC, Bradshaw DJ, Marsh PD, Watson GK, Birmingham JJ, Allison C (1999) Depth penetration and detection of pH gradients in biofilms by two photon excitation microscopy. Appl Environ Microbiol 65:3502–3511

Vuong C, Kocianova VJM, Yao Y, Fischer ER, DeLeo FR, Otto M (2004) A crucial role for exopolysaccharide modification in bacterial biofilm formation, immune evasion, and virulence. J Biol Chem 279:54881–54886

Waharte F, Steenkeste K, Briandet R, Fontaine-Aupart MP (2010) Local diffusion measurements inside biofilms by FRAP analysis with a commercial confocal laser scanning microscope. Appl Environ Microbiol 76:5860–5869

Walczysko P, Kuhlicke U, Knappe S, Cordes C, Neu TR (2008) *In situ* activity of suspended and immobilized microbial communities as measured by fluorescence lifetime imaging. Appl Environ Microbiol 74:294–299

Webb JS, Thompson LS, James S, Charlton T, Tolker-Nielsen T, Koch B, Givskov M, Kjelleberg S (2003) Cell death in *Pseudomonas aeruginosa* biofilm development. J Bacteriol 185: 4585–4592

Xu KD, Stewart PS, Xia F, Huang C-T, McFeters GA (1998) Spatial physiological heterogeneity in *Pseudomonas aeruginosa* biofilm is determined by oxygen availability. Appl Environ Microbiol 64:4035–4039

Yadvika S, Sreekrishnan TR, Kohli S, Rana V (2004) Enhancement of biogas production from solid substrates using different techniques – a review. Bioresour Technol 95:1–10

Yarwood JM, Bartels DJ, Volper EM, Greenberg EP (2004) Quorum sensing in *Staphylococcus aureus* biofilms. J Bacteriol 186:1838–1850

Chapter 22
Inhibition of Bacterial Adhesion on Medical Devices

Lígia R. Rodrigues

Abstract Microbial infections resulting from bacterial adhesion to biomaterial surfaces have been observed on almost all medical devices. Biofilm infections pose a number of clinical challenges due to their resistance to immune defence mechanisms and antimicrobials, and, regardless of the sophistication of the implant, all medical devices are susceptible to microbial colonisation and infection. Research efforts are currently directed towards eliminating or reducing infection of medical devices. Strategies to prevent biofilm formation include physiochemical modification of the biomaterial surface to create anti-adhesive surfaces, incorporation of antimicrobial agents into medical device polymers, mechanical design alternatives, and release of antibiotics. Nevertheless, the success of these alternatives has been modest, mainly due to the various environments into which devices are placed and the diversity of ways in which organisms can colonise surfaces. Biosurfactants have been reported as a promising strategy as they effectively inhibit bacterial adhesion and retard biofilm formation, and are thus potentially useful as a new generation of anti-adhesive and antimicrobial coatings for medical devices.

22.1 Introduction

Microbial adhesion and biofilm formation on medical devices is a common event that can have important medical and economic consequences. The use of temporary or permanent implants or prosthetic devices fabricated from polymeric biomaterials has increased dramatically in recent years. It is estimated that over 5 million medical devices or implants are used per year in the United States alone (Bryers, 2008). Medical devices are responsible for about 60–70% of hospital-acquired infections, particularly in critically ill patients (Bryers, 2008; Darouiche, 2001).

L.R. Rodrigues (✉)
IBB – Institute for Biotechnology and Bioengineering, Centre of Biological Engineering, University of Minho, 4710-057 Braga, Portugal
e-mail: lrmr@deb.uminho.pt

D. Linke, A. Goldman (eds.), *Bacterial Adhesion*, Advances in Experimental Medicine and Biology 715, DOI 10.1007/978-94-007-0940-9_22,

Bacterial colonisation of an indwelling device, followed by biofilm formation, can be a prelude to infection and consequently to tissue destruction, systemic dissemination of the pathogen and dysfunction of the device, resulting in serious illness and death (Hall-Stoodley et al., 2004). The process by which microorganisms colonise open and closed implants or prosthetic devices is fairly complicated and involves a series of steps starting with deposition of host substances (macromolecules such as collagen and fibronectin) onto the material (Costerton et al., 1999). Device-associated infections are resistant to immune defence mechanisms and are difficult to treat with antimicrobial agents because the organisms are encased within a protected microenvironment hampering the prevention and treatment of established biofilms (Habash and Reid, 1999). Bacteria that grow in association with medical devices always form slime-enclosed biofilms within which they are protected, to a large extent, from the bactericidal activity of chemical biocides and antibiotics. Removal of the device may be necessary, resulting in both attendant distress to the patient and cost. Considerable research endeavour is currently directed towards reducing, if not eliminating, infection of medical devices. Strategies under investigation include physiochemical modification of the biomaterial surface to create anti-adhesive surfaces, incorporation of antimicrobial agents into medical device polymers and the use of electric fields to improve antibiotic therapy (Darouiche, 2001; Hall-Stoodley et al., 2004; Hetrick and Schoenfisch, 2006). Nevertheless, the efforts to reduce adhesion using specially developed materials, with hydrophilic or heparin coated surfaces, have had only modest clinical success (Habash and Reid, 1999). The reason, at least for the most part, is the various environments into which devices are placed and the diversity of ways in which organisms colonise surfaces. A better understanding of the process is required, as well as the development of new alternatives to the traditional surface-modifying preventive approaches, which have largely focused on antimicrobial coating of devices and on employment of antibiotics (Darouiche, 2001; Habash and Reid, 1999).

This chapter focuses on adhesion and biofilm formation by bacteria on medical devices, strategies to inhibit bacterial adhesion and the potential use of biosurfactants as anti-adhesive and antimicrobial surface coatings.

22.2 Medical Biofilms

More than half of the infectious diseases that affect mildly immune-compromised individuals involve bacterial species that are commensal in humans or are common in our environment (Costerton et al., 1999). For example, the skin bacterium *Staphylococcus epidermidis* and the soil bacterium *Pseudomonas aeruginosa* can cause devastating chronic infections in immune-compromised hosts. Microbial infections have been observed on most, if not all, medical devices or implants including: prosthetic heart valves, orthopaedic implants, intravascular catheters, artificial hearts, left ventricular assist devices, cardiac pacemakers, vascular prostheses, cerebrospinal fluid shunts, urinary catheters, voice prostheses, ocular prostheses and

contact lenses, and intrauterine contraceptive devices (Bryers, 2008; Darouiche, 2001; Rodrigues et al., 2007). In non-surgical indwelling medical devices, such as central venous and urinary catheters, biofilm colonisation may originate either from the skin at the point of insertion, or by migration of the organism(s) through or around the catheter once implanted. As for surgical devices, tissue damage and clot formation associated with surgical implantation are correlated with enhanced rates of microbial biofilm colonisation (Donlan and Costerton, 2002; Hetrick and Schoenfisch, 2006; Lynch and Robertson, 2008; Zilberman and Elsner, 2008). At the cellular level, implant-associated infections are the result of bacterial adhesion to a biomaterial surface. Upon implantation, there is competition between integration of the material into the surrounding tissue and adhesion of bacteria to the implant surface (Gristina, 1987). For a successful implant, tissue integration occurs prior to appreciable bacterial adhesion, thereby preventing colonisation at the implant. However, host defences often can not prevent further colonisation if bacterial adhesion occurs before tissue integration (Gristina, 1987). A 6 h post-implantation "decisive period" has been identified during which prevention of bacterial adhesion is critical to the long-term success of an implant (Poelstra et al., 2002). Over this period, an implant is particularly susceptible to surface colonisation. Virtually all medical devices or tissue engineering constructs are susceptible to microbial colonisation and infection (Castelli et al., 2006).

Upon adhesion to a surface, replicating adherent bacteria secrete mostly insoluble gelatinous exopolymers, forming a biofilm (Bryers, 2008; Darouiche, 2001). From a medical perspective, both commensal and pathogenic microorganisms form biofilms that are associated with the epithelial or endothelial lining: embedded in the lung, intestinal or vaginal mucus layer; attached to the teeth or medical implant surfaces; or formed intracellularly (Costerton et al., 1999; Hall-Stoodley et al., 2004; Pizarro-Cerdá and Cossart, 2006; Reid 1999). Microorganisms involved in biofilms related to human infections are compiled in Lynch and Robertson (2008). Biofilm formation and persistence has profound implications for the patient, because microorganisms growing as biofilms are significantly less susceptible to antibiotics and host defenses than the planktonic forms of the same microorganisms (Bryers, 2008; Costerton et al., 1999). Sessile bacterial cells release antigens and stimulate the production of antibodies, but the antibodies are not effective in killing bacteria within biofilms and may cause damage to surrounding tissues (Costerton et al., 1999). Even in individuals with excellent cellular and humoral immune reactions, biofilm infections are rarely resolved by host defence mechanisms and commonly manifest themselves as chronic or recurrent infections (Bryers, 2008; Costerton et al., 1999; Gristina, 1987; Gottenbos et al., 2004). Biofilm infections constitute a number of clinical challenges, including disease, chronic inflammation, impaired wound healing, rapidly acquired antibiotic resistance, and the spread of infectious emboli (Bryers, 2008; Hall-Stoodley et al., 2004; Pizarro-Cerdá and Cossart, 2006). A number of physical, biological and chemical processes are involved in biofilm formation, with the relative contribution of each changing throughout biofilm development and depending on environmental and hydrodynamic conditions (Habash and Reid, 1999; Hall-Stoodley et al., 2004). Therefore, non-fouling biomaterials

ought to be developed; otherwise protein deposition onto the surfaces will occur with subsequent microbial adhesion and biofilm formation.

22.3 Prevention of Medical Device-Associated Infections

Prophylactic use of antibiotics and biocides can reduce the incidence of biofilm-associated infections with indwelling medical devices (Lynch and Robertson, 2008). Strategies to prevent biofilm formation range from systemic approaches controlling any bacterial invasion of sterile sites to local biofilm inhibition on medical devices (Fux et al., 2003). The latter focuses on the elimination of planktonic cells before they adhere to the surface and initiate biofilm formation. Both material properties and host factors determine bacterial adhesion to medical devices (Rodrigues et al., 2004a, 2006b, c, 2007). Bacterial adherence to silicone, for example, has been found to be significantly higher than to polyurethane or Teflon® (Lopez-Lopez et al., 1991). Host factors, such as fibronectin, fibrinogen or platelets may be deposited on the foreign body material and provide specific ligands for bacterial adhesins (Shenkman et al., 2002). A variety of approaches have proven to be effective in reducing biofilm-related infections by preventing bacterial adhesion, at least in high-risk populations (Fux et al., 2003). They include device coatings, device immersion, anti-septic irrigation of the surgical site, antibiotic loaded cements in orthopedic surgery (Zilberman and Elsner, 2008), and antibiotic catheter lock therapy containing vancomycin and heparin (Carratalà et al., 1999) or minocycline and EDTA (Raad et al., 2002). In antibiotic catheter lock therapy, a concentrated antibiotic solution is placed in a catheter in a volume adequate to fill the lumen. The catheter is then "locked" into place for an extended period while the catheter is not in use, with the goal of preventing it from becoming colonised and thereby reducing the risk of infection (Lynch and Robertson, 2008). Impregnation of catheter surfaces with antiseptics (Veenstra et al., 1999) or antibiotics (Zilberman and Elsner, 2008) has been shown to delay bacterial colonisation. Although the use of antibiotic prophylaxis is controversial because of its potential to increase antimicrobial resistance, it is increasingly common in high-risk patient groups (Lynch and Robertson, 2008). With regard to device coatings, Falagas and co-workers (2007) conducted a recent and comprehensive meta-analysis of randomised controlled trials of rifampin-impregnated central venous catheters and found that they are both safe and effective in reducing the rate of catheter colonisation and catheter-related bloodstream infections. Similarly, Manierski and Besarab (2006) performed six independent studies on the efficacy of antibiotic lock therapy in the prevention of catheter-related bloodstream infections in haemodialysis patients, and found an overall reduction of 64–100% in catheter-related bloodstream infections.

Furthermore, Rodrigues and collaborators (2004, 2006b, c, 2007) have shown that impregnation of silicone rubber surfaces with biosurfactants produced by several lactobacilli inhibits the adhesion of several microorganisms. In the specific case of voice prostheses, it is well-known that biofilms are resistant to a range of

antifungal agents currently in clinical use, including amphotericin B and fluconazole, thus new prophylactic treatments are being explored to prolong their lifetime. As antimicrobial resistance is becoming a source of concern in modern medicine and health-improving functional foods are gaining in popularity, the development of alternative prophylactic and therapeutic agents, including probiotics, has been investigated (Free et al., 2001). Lactobacilli are one of the most well-known probiotic bacterial genera and play an important role in the maintenance of a healthy intestinal and urogenital tract (Velraeds et al., 1998; Reid, 1999, 2000). Other bacterial genera known to have probiotic effects are *Lactococci*, *Enterococci* and *Streptococci*. The mechanisms by which probiotic bacteria exert their beneficial effects are not yet entirely understood. Possible mechanisms are competitive adhesion (Busscher et al., 1997), activation of the immune system (Perdigon et al., 1986), or nutrient competition (Free et al., 2001). Some strains are able to release biosurfactants, while others are known to have antimycotic effects by producing lactic acid or hydrogen peroxide.

22.4 Treatment of Medical Device-Associated Infections

Traditional treatment of microbial infections is based on compounds that inhibit growth of the microbe or kill it (Bryers, 2008). The major concern with this approach is the frequent development of resistance to antibiotics. For details on agents for treatment or prophylaxis of biofilm-associated infections, the reader is directed to the review by Lynch and Robertson (2008). Bacterial biofilms are inherently resistant to antimicrobial agents and the host immune system, and tend to be significantly less responsive to antibiotics and antimicrobial stressors than planktonic organisms of the same species (Bryers, 2008; Costerton et al., 1999). Prolonged and high-dose antibiotic therapy and the elimination of infected foreign-body material are the basis of successful therapy. Antibiotic treatment of bacterial endocarditis was shown to be more successful when serum antibiotic levels were held at least tenfold above the minimal bactericidal concentration (Joly et al., 1987); but even with 8 weeks of treatment, few patients have been cured by antimicrobial therapy alone (Hancock, 1994). The combination of rifampicin and a fluoroquinone has proven especially successful in the treatment of various *S. aureus* biofilm infections, ranging from infections of orthopaedic prostheses (Habash and Reid, 1999) to right-heart endocarditis (Heldman et al., 1996). On the other hand, the study reported by Bagge and co-workers (2004) showed that sub-lethal doses of β-lactam antibiotic can actually enhance biofilm formation by *P. aeruginosa*, increasing its volume and polymer matrix, which can lead to adverse consequences when treating cystic fibrosis patients. Also, Hoffman et al. (2005) reported that sub-inhibitory concentrations of aminoglycoside antibiotics induced biofilm formation by *P. aeruginosa* and *E. coli*.

As a consequence of this increase in resistance, researchers have turned to a number of alternatives to synthetic antibiotics including disinfectants (Hetrick and

Schoenfisch, 2006; Zilberman and Elsner, 2008), bacteriophage (Sulakvelidze et al., 2001) and bacteriophage lytic enzymes (Fischetti, 2005), probiotics (Hong et al., 2005), and human antimicrobial peptides (defensins, cathelicidins, and histatins) (De Smet and Contreras, 2005). Nevertheless, these are mostly synthetic compounds with the ability to inactivate or kill suspended bacteria but with poor efficacy when applied to biofilm infections (Stewart, 2002). It has been recently proposed that substances that specifically inhibit bacterial virulence should be developed. Such "antipathogenic" drugs, in contrast to antibacterial drugs, do not kill bacteria or stop their growth and are assumed not to lead to the development of resistant strains (Bryers, 2008). A very elegant approach comprises the inhibition of regulatory systems that govern the expression of a series of bacterial virulence factors: for example, anti-adhesion therapy [passive antibody therapy (Casadevall et al., 2004), and synthetic peptide vaccine and antibody therapy (Cachia and Hodges, 2003)], inhibition or negation of cell–cell signalling (Otto, 2004), negation of biofilm formation by disrupting iron metabolism (Kaneko et al., 2007), and up-regulation of biofilm detachment promoters (rhamnolipids) (Boles et al., 2005).

Replacement or removal of an infected indwelling medical device, combined with systemic antibiotic and/or antifungal therapy, is the most effective treatment in most settings (Trampuz and Zimmerli, 2006). For managing indwelling medical device infections in non-surgery patients, long-term antimicrobial suppressive therapy remains the only option (Lynch and Robertson, 2008). Recent reviews summarise current recommended practices for the treatment of infections of prosthetic joints (Trampuz and Zimmerli, 2006), arterial prostheses (Goeau-Brissonnière and Coggia, 2000), vascular catheters (Castelli et al., 2006), prosthetic heart valves (Karchmer, 2000), central nervous system shunts (Yogev and Bisno, 2000), pacemakers and defibrillators (Eggimann and Waldvogel, 2000), endotracheal and tracheotomy tubes (Dever and Johanson, 2000), and hemodialysis and peritoneal hardware (Oliver and Schwab, 2000), as well as treatment of foreign body infections of the urinary tract (Hessen et al., 2000).

22.5 Development of Anti-adhesive Biomaterials

The remarkable resistance of biofilms to conventional antibiotic therapy has prompted a great deal of research to produce anti-infective and anti-adhesive devices or implants by either (a) mechanical design alternatives, (b) modification of material surface features (biosurfactants, plasma, brushes), (c) anti-infective agents bound to the surface of the material (silver, quaternary ammonium, synthetic antibiotics, biosurfactants), or (d) release of soluble toxic agents (chlorhexidine, antibiotics) into the adjacent surroundings (Bryers, 2008; Hetrick and Schoenfisch, 2006). Mechanical design alternatives have had only marginal success and are only applicable for short-term indwelling catheters (Bryers, 2008). Coatings have been developed that reduce bacterial adhesion by altering the physicochemical properties of the substrate so that conditioning films do not form and/or bacteria-substrate

interactions are not favoured. These "passive" coatings include surfaces modified with poly(ethylene glycol) (Kingshott et al., 2003), poly(ethylene oxide) brushes (Kaper et al., 2003), and hydrophilic polyurethanes (Nagel et al., 1996), among many others. Unfortunately, the effectiveness of passive coatings for reducing bacterial adhesion is limited and varies greatly depending on the bacterial species (Hetrick and Schoenfisch, 2006). The physicochemical properties of the coating can be masked by an adsorbed conditioning film, thereby diminishing their effectiveness. Additionally, surface-bounded anti-infective agents are only toxic to the initial wave of incoming bacteria and provide little residual effects once layers of dead cells accumulate, which are also inflammatory (Bryers, 2008). Nevertheless, there are studies pointing to some success in retarding bacterial adhesion, which in turn inhibits or delays biofilm formation. One specific example is the development of anti-adhesive silicone rubber surfaces for voice prostheses. Voice prostheses are continuously exposed to saliva, food, and drinks that, together with the oropharyngeal microflora, contribute to valve failure and the need to replace the implant frequently (Mahieu et al., 1986). Therefore, improvement of the antifouling properties of the silicone rubber material is desirable. Rodrigues and collaborators (2007) reviewed the different approaches that have been undertaken to modify the silicone rubber surface as an obvious strategy to inhibit biofilm formation and consequently to prolong the lifetime of voice prostheses.

A recent alternative approach to reducing bacterial adhesion is based on coatings that actively release antibacterial agents. Such "active" coatings have been designed to temporarily release high initial fluxes of antibacterial agents during the critical short term post-implementation period (several hours) to inhibit adhesion of bacteria. Continued release beyond this short term period is desirable because protective fibrous capsule formation and tissue integration occur over a longer time period (weeks to months) (Anderson, 2001). Zilberman and Elsner (2008) reviewed the latest developments on antibiotic-eluting medical devices for various applications.

For example, non-degradable polymethylmethacrylate (PMMA) bone cements and spacer beads loaded with antibiotics have been employed clinically in various forms in joint replacements and in prevention or treatment of deep bone infections (osteomyelitis) (Webb and Spencer, 2007). Such systems slowly release the soluble drug from the solidified PMMA bone cement surrounding the implant over time. Moreover, the use of a bioactive ceramic coating containing hydroxyapatite (HA), calcium phosphate and other osteo-conductive materials as antibiotic carriers offers the added value of providing the physiochemical environment and structural scaffold required for bone-implant integration. In vitro release of antibiotics from HA-coated implants has been reported for several antibiotics (Teller et al., 2007). The conventional plasma spraying technique for HA-coating is associated with high processing temperatures and therefore does not enable the incorporation of antibiotics in the process. Most reported work therefore focuses on soaking antibiotics onto plasma-sprayed HA. Gollwitzer and collaborators (2003) studied biodegradable polymeric coatings made from polylactic acid and its copolymers with glycolic acid. An additional advantage of such coatings is the relative ease with which the polymer can be

applied to both alloys and plastics with polished, irregular or porous surfaces using a simple dip-coating technique (Schmidmaier et al., 2006).

Other examples of antibiotic-eluting medical devices include intravascular devices and vascular grafts. Infection of intravascular devices for vascular access and vascular prostheses for the replacement or bypass of damaged arteries is a rare but serious event (Zilberman and Elsner, 2008). The infection of a vascular graft is a rare complication, with an estimated incidence of 0.5–2.5% of bypass procedures. However, the mortality and morbidity rates due to this complication are high (Bryers, 2008). Once a prosthetic graft is infected, it must almost always be excised and replaced with a new prosthetic bypass. The development of infection-resistant vascular prostheses may therefore contribute to the prevention and treatment of this complication. PET (polyethyleneterephtalate, Dacron^{TM}) and ePTFE (expanded polytetrafluorethylene) vascular prostheses soaked in an antibiotic solution produce a wash-out release of antibiotics within minutes after placement (Blanchemain et al., 2005). Several approaches have been proposed for extending release over days and weeks. Antibiotics have been "bonded" by soaking collagen, albumin, and gelatin sealed grafts to produce extended antibacterial activity (Zilberman and Elsner, 2008).

Finally, regardless of the type of "drug release" method used (passive versus active), release of a toxic agent from a biomaterial of a soluble anti-infective agent will inevitably stop once the entrapped agent is depleted. Further, as discussed above, delivery of sub-lethal dosages of antibiotics can lead to accelerated biofilm formation and induced virulence factor expression (Bryers, 2008).

22.6 Biosurfactants: A Powerful Tool to Inhibit Bacterial Adhesion

Biosurfactants are microbial amphiphilic compounds with both hydrophilic and hydrophobic moieties and with a distinct tendency to accumulate at interfaces. For all interfacial systems, it is known that organic molecules from the aqueous phase tend to immobilise at the solid interface. There they eventually form a conditioning film, which will change the properties (wettability and surface energy) of the original surface (Neu, 1996). In an analogy to organic conditioning films, biosurfactants may interact with the interfaces and affect the adhesion and/or detachment of bacteria. In addition, the substratum surface properties determine the composition and orientation of the molecules conditioning the surface during the first hour of exposure. After about 4 h, a certain degree of uniformity is reached and the composition of the adsorbed material becomes substratum-independent (Neu, 1996). Adsorption of charged biosurfactants to interfaces is governed by a range of interactions that are not only hydrophobic. Most interfaces have an overall negative or, rarely, positive charge. Gottenbos et al. (2001) showed that positively charged biomaterial surfaces exert an antimicrobial effect on adhering Gram-negative, but not on Gram-positive bacteria.

Microbial surfactants constitute a diverse group of surface-active molecules and are known to occur in a variety of chemical structures, such as glycolipids, lipopeptides and lipoproteins, fatty acids, neutral lipids, phospholipids, and polymeric and particulate structures (Rodrigues et al., 2006a). Their use and potential commercial application in the medical field has increased during the past decade (Muthusamy et al., 2008; Rivardo et al., 2009; Rodrigues et al., 2006a), due to their antibacterial, antifungal and antiviral activities, which make them useful for combating many diseases and as therapeutic agents. In addition, their role as anti-adhesive agents against several pathogens indicates their utility as suitable anti-adhesive coating agents for medical insertional materials, leading to new and effective means of combating colonisation by pathogenic microorganisms without the use of synthetic drugs and chemicals (Rodrigues et al., 2006a). Mireles and collaborators (2001) pre-coated vinyl urethral catheters by running the surfactin solution through them before inoculation with media and found a decrease in the amount of biofilm formed by *Salmonella* Typhimurium, *Salmonella enterica*, *E. coli* and *Proteus mirabilis*. Moreover, the use of lactobacilli as a probiotic for the prevention of urogenital infections has been widely studied (Reid, 2000; Boris and Barbés, 2000). Velraeds et al. (1998) reported the inhibition of biofilm formation by uropathogens and yeast on silicone rubber with biosurfactants produced by *Lactobacillus acidophilus*. Also, Heinemann et al. (2000) showed that *Lactobacillus fermentum* RC-14 releases surface-active components that can inhibit adhesion of uropathogenic bacteria. Efforts to develop strategies to prevent the microbial colonisation of silicone rubber voice prostheses have been reported by Rodrigues and co-workers (2004a, 2006c). Biosurfactants obtained from *Lactococcus lactis* 53 and *Streptococcus thermophilus* A have been evaluated as anti-adhesive agents against several microorganisms isolated from explanted voice prostheses. Over 90% reductions in the initial deposition rates were achieved for most of the bacterial strains tested. The biosurfactant obtained from *S. thermophilus* A was more effective against *Rothia dentocariosa* GBJ 52/2B, which is one of the strains responsible for valve prosthesis failure. Nevertheless, the effect of the adsorbed biosurfactant was less pronounced for the initial deposition rates of the yeast strains. The authors also demonstrated that, when rinsing flow chambers designed to monitor microbial adhesion with a rhamnolipid solution, the rate of deposition and adhesion was significantly reduced for a variety of microorganisms (Rodrigues et al., 2006a, b). Thus, this rhamnolipid may be useful as a biodetergent solution for cleaning prostheses, prolonging their lifetime and directly benefiting laryngectomised patients.

Furthermore, the biosurfactants produced by the same strains (Rodrigues et al., 2004b) and by *Lactobacillus paracasei* ssp. *paracasei* A20 (Gudiña et al., 2010a, b) were found to possess antimicrobial and anti-adhesive activity against several microorganisms. For contact lenses (CL), maintaining the optical properties might limit the use of biosurfactants as coating agents. Consequently, Rodrigues and collaborators evaluated the influence of biosurfactants on refractive index (RI) and transmittance (T) (*unpublished data*). One conventional hydrogel (Etafilcon A) and two silicone-hydrogel (Galyfilcon and Lotrafilcon B) contact lenses were tested (Table 22.1). Prior adsorption of biosurfactants to silicone-hydrogel lenses had no

Table 22.1 Refractive index and transmittance in the visible spectrum of contact lenses with and without an absorbed biosurfactant layer. Biosurfactants from *Lactococcus lactis* (BS1), *Lactobacillus paracasei* ssp. *paracasei* A20 (BS2) and *Streptococcus thermophilus* A (BS3) were tested at 2 different concentrations (10 and 50 g/L). One conventional hydrogel CL (Etafilcon A) and two silicone-hydrogel (Galyfilcon and Lotrafilcon B) lenses were used. Experiments were done in triplicate. Refractive index values correspond within 1–2% and transmittance values correspond within 2–5%

		Treatment with biosurfactant						
		BS1 (g/L)		BS2 (g/L)		BS3 (g/L)		Untreated contact lenses
	Contact lenses	10	50	10	50	10	50	
Refractive index	Galyfilcon	1.408	1.411	1.408	1.409	1.410	1.411	1.408
	Lotrafilcon B	1.422	1.424	1.423	1.423	1.422	1.424	1.422
	Etafilcon A	1.414	1.436	1.406	1.418	1.408	1.418	1.398
Transmittance in the visible spectra (%)	Galyfilcon	86.2	82.8	89.7	88.5	83.0	82.2	91.0
	Lotrafilcon B	82.4	80.1	85.8	81.5	82.5	81.6	83.9
	Etafilcon A	90.3	86.5	89.1	88.9	90.2	81.6	88.7

effect on the RI. However, for the biosurfactant-conditioned hydrogel CL, a higher RI was obtained compared to the untreated lenses. This increase in RI is a consequence of the dehydration observed with the adsorption of the biosurfactants, which is not desirable. All treated contact lens types showed a decrease in transmittance levels in the visible spectra, the effect being more pronounced for higher biosurfactant concentrations as a result of their colour. Although the results obtained for the transmittance experiments were promising, further characterisation and purification of the biosurfactants is required to enable the use of lower concentrations, more active and colourless fractions.

In another study, the same authors explored the possibility of using the biosurfactant produced by *S. thermophilus* A to pre-condition silicone rubber surfaces to inhibit the adhesion of the two most frequent fungi isolated from maxillofacial prostheses, *Candida albicans* MFP 22-1 and *Candida parapsilosis* MFP 16-2 (*unpublished data*). Adhesion assays showed a reduction of 60–80% in the initial deposition rates (Fig. 22.1). These results represent progress towards designing new strategies for preventing microbial adhesion to silicone rubber maxillofacial prostheses.

Besides the screening of lactobacilli as biosurfactant producers, Rodrigues and collaborators (2006d) also characterised the anti-adhesive activity of these biosurfactants against several microorganisms including Gram-positive and Gram-negative bacteria and filamentous fungi (Gudiña et al., 2010a, b). For example, the biosurfactant produced by *L. paracasei* A20 showed anti-adhesive activity against *Streptococcus sanguis* (72.9%), *S. aureus* (76.8%), *S. epidermidis* (72.9%) and *Streptococcus agalactie* (66.6%) (Gudiña et al., 2010a). Additionally, the anti-adhesive activity of two biosurfactants produced by *Candida sphaerica* UCP 0995

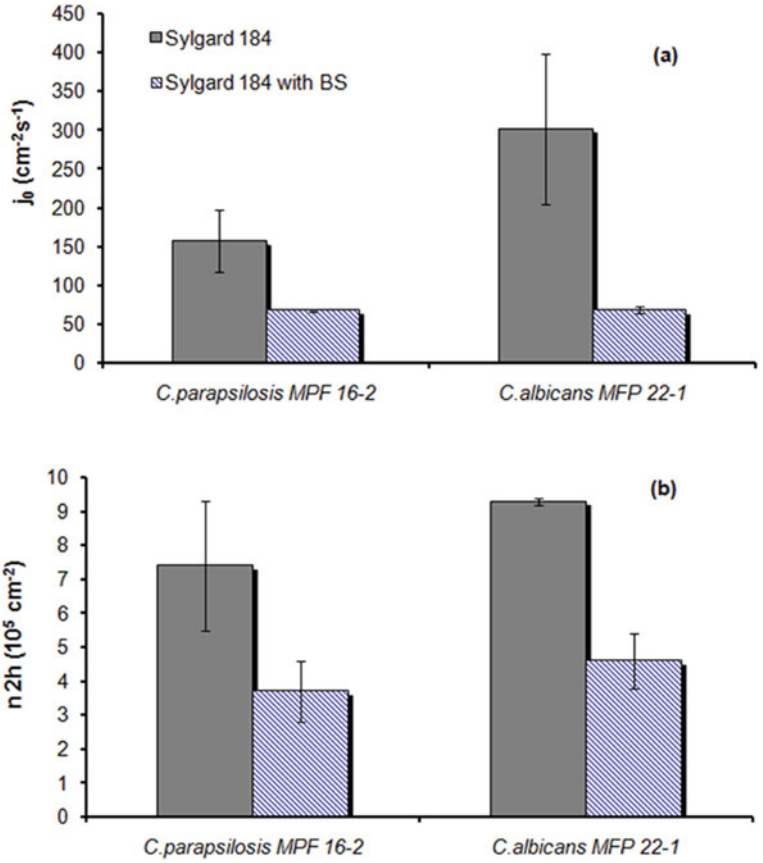

Fig. 22.1 (**a**) Initial deposition rates (j_0, cm^{-2} s^{-1}) of *Candida parapsilosis* MFP 16-2 and *Candida albicans* MFP 22-1 isolated from maxillofacial prostheses on Sylgard® 184 silicone rubber with and without an adsorbed biosurfactant (BS) layer; (**b**) Number of microorganisms adhering after 2 h ($n_{2\,h}$) on Sylgard® 184 with and without an adsorbed biosurfactant (BS) layer. Biosurfactant was produced by *Streptococus thermophilus* A, (see Rodrigues et al., 2006c). Results are averages of triplicate experiments and the standard deviation represented by *error bars*

and *Candida lipolytica* UCP 0988 was studied (*unpublished data*). The biosurfactant from *C. sphaerica* UCP 0995 was found to inhibit the adhesion of *P. aeruginosa*, *S. agalactiae*, *S. sanguis*, *C. tropicallis*, *E. coli*, and *S. salivarius* by between 80 and 92%. Inhibition of adhesion with percentages near 100% occurred for the higher concentrations of biosurfactant used (Table 22.2). Although less pronounced, similar results were obtained with the biosurfactant produced by *C. lipolytica* UCP 0988 for some of the microbial strains studied (Fig. 22.2). All these results open prospects for the use of biosurfactants against the adhesion of microorganisms responsible for diseases and infections in the urinary, vaginal and gastrointestinal tracts, as well as in the skin.

Table 22.2 Anti-adhesive properties of crude biosurfactant produced and extracted from *Candida sphaerica* UCP 0095. Negative controls were set at 0% to indicate the absence of biosurfactant. Positive percentages indicate the reductions in microbial adhesion when compared to the control, and negative percentages indicate increased microbial adhesion. Results are expressed as percentage means from triplicate experiments and correspond within 1–3%

	[Biosurfactant] (mg/L)				
Microorganism	0.3	0.6	2.5	5	10
Candida tropicalis	80	85	87	98	100
Escherichia coli	89	93	96	97	99
Pseudomonas aeruginosa	80	82	83	89	92
Streptococcus agalactiae	80	86	88	92	100
Streptococcus sanguis	80	83	87	98	100
Streptococcus salivarius	92	93	95	97	100

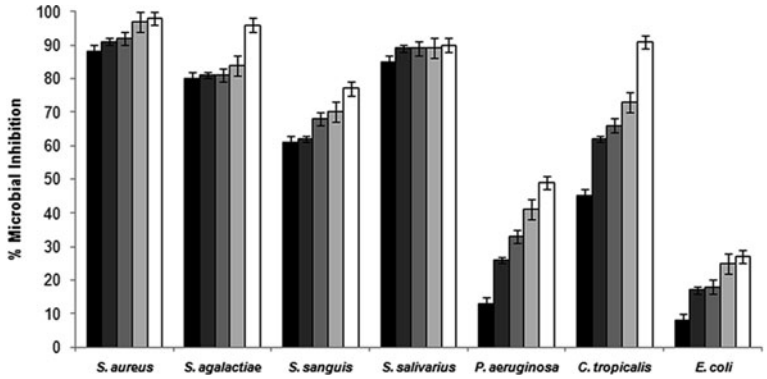

Fig. 22.2 Microbial inhibition percentages obtained from the anti-adhesion assays with the crude biosurfactant produced by *Candida lipolytica* UCP 0988 at different concentrations (0.75 mg/L [■], 1.5 mg/L [■], 3 mg/L [■], 6 mg/L [■] and 12 mg/L [■]). Results are averages of triplicate assays and *error bars* represent standard deviations

Based on the above, biosurfactants can play an important role in the development of anti-adhesive coatings for silicone rubber as they effectively inhibit bacterial adhesion and retard biofilm formation. Therefore, surface and bulk modification techniques, laser-induced surface grafting and the sequential method for interpenetrating polymer networks should be explored as ways to link the biosurfactants more strongly with the silicone rubber surfaces, thus avoiding their washout from the surfaces and prolonging their effect. Furthermore, biosurfactants are a suitable alternative to antimicrobial agents, and could be used as safe and effective therapeutic agents or probiotics. The use of biosurfactants as antimicrobial agents is currently of particular interest, since an increasing number of drug-resistant microorganisms are being encountered and there is a need for alternative lines of therapy. Some biosurfactant activities could be exploited by developing an alternative therapy for treating patients (Rodrigues et al., 2006a). Nevertheless, although the replacement

of synthetic surfactants by biosurfactants would provide advantages such as biodegradability and low toxicity, their use has been limited by their relatively high production cost, as well as scarce information on their toxicity in humans. The main limiting factor, however, for commercialisation of biosurfactants is the high cost of large-scale production. Several strategies have been adopted to reduce costs (Rodrigues et al., 2006e). The use of agro-industrial wastes as substrates, optimisation of medium and culture conditions, and efficient recovery processes all help. However, to compete with synthetic surfactants, effective microorganisms must be developed for biosurfactant production. The use of biosurfactant hyper-producer strains allows increasing biosurfactant production and reduces production costs. Strains producing higher amounts of biosurfactants can be obtained by screening high biosurfactant-producing microorganisms from the natural environment, or by engineering strains for biosurfactant production. Therefore, knowledge of the genes required for production of biosurfactants is critical for their application in industry. Once the genes have been indentified and isolated, they can be expressed in other microorganisms (e.g. to prevent pathogenicity), or they can be modified or placed under regulation of strong promoters to increase their expression and so enhance production. This knowledge will also allow the production of novel biosurfactants with specific new properties (designed by metabolic engineering) for different industrial applications. Genetic engineering of the known biosurfactant molecules could produce potent biosurfactants with altered antimicrobial profiles and decreased toxicity against mammalian cells.

22.7 Concluding Remarks

The processes governing biofilm formation are rather complex, involving several steps and almost all surfaces are susceptible of being colonised. Bacterial colonisation and subsequent biofilm formation on an indwelling device can lead to infection with severe economic and medical consequences. Device-associated infections are resistant to immune defense mechanisms and are difficult to treat with antimicrobial agents because the organisms are encased within a protected microenvironment. Therefore, non-fouling biomaterials ought to be developed. Several strategies based on the modification of the physicochemical properties of the substrate have been pursued. Nevertheless, the effectiveness of these coatings has been found to be limited and varies greatly depending on bacterial species, mainly due to the diverse environments into which the devices are placed and the multiplicity of ways in which organisms can colonise surfaces. Development of alternatives to the traditional surface-modifying preventive approaches, which have largely focused on antimicrobial coating of devices and employment of antibiotics, is required. Biosurfactants represent an interesting approach because it may be possible to modify the surface properties to make it simultaneously anti-adhesive and give it antimicrobial activity. However, although some studies have demonstrated the potential of biosurfactants in biomedical applications, the genetics and structure-function relationships of biosurfactants, and methods of binding them to surfaces, require further exploration.

References

Anderson JM (2001) Biological responses to materials. Annu Rev Mater Res 31:81–110

Bagge N, Schuster M, Hentzer M, Ciofu O, Givskov M, Greenberg EP, Høiby N (2004) *Pseudomonas aeruginosa* biofilms exposed to imipenem exhibit changes in global gene expression and β-lactamase and alginate production. Antimicrob Agents Chemother 48(4): 1175–1187

Blanchemain N, Haulon S, Martel B, Traisnel M, Morcellet M, Hildebrand HF (2005) Vascular PET prostheses surface modification with cyclodextrin coating: development of a new drug delivery system. Eur J Vasc Endovasc Surg 29(6):628–632

Boles BR, Thoendel M, Singh PK (2005) Rhamnolipids mediate detachment of *Pseudomonas aeruginosa* from biofilms. Mol Microbiol 57:1210–1223

Boris S, Barbés C (2000) Role played by lactobacilli in controlling the population of vaginal pathogens. Microbes Infect 2:543–546

Bryers JD (2008) Medical biofilms. Biotechnol Bioeng 100(1):1–18

Busscher HJ, Van Hoogmoed CG, Geertsema-Doornbusch GI, Van der Kuijl-Booij M, Van der Mei HC (1997) *Streptococcus thermophilus* and its biosurfactants inhibit adhesion by *Candida* spp. in silicone rubber. Appl Environ Microbiol 63:3810–3817

Cachia PJ, Hodges RS (2003) Synthetic peptide vaccine and antibody therapeutic development: Prevention and treatment of *Pseudomonas aeruginosa*. Biopolymers 71(2):141–168

Carratalà J, Niubó J, Fernández-Sevilla A, Juvé E, Castellsagué X, Berlanga J, Liñares J, Gudio F (1999) Randomized, double-blind trial of an antibiotic-lock technique for prevention of Gram-positive central venous catheter-related infection in neutropenic patients with cancer. Antimicrob Agents Chemother 43:2200–2204

Casadevall A, Dadachova E, Pirofski LA (2004) Passive antibody therapy for infectious diseases. Nat Rev Microbiol 2(9):695–703

Castelli P, Caronno R, Ferrarese S, Mantovani V, Piffaretti G, Tozzi M, Lomazzi C, Rivolta N, Sala A (2006) New trends in prosthesis infection in cardiovascular surgery. Surg Infect 7 (Suppl 2):S45–S47

Costerton JW, Stewart PS, Greenberg EP (1999) Bacterial biofilms: a common cause of persistent infections. Science 284:1318–1322

Darouiche RO (2001) Device-associated infections: a macroproblem that starts with microadherence. Clin Infect Dis 33(9):1567–1572

De Smet K, Contreras R (2005) Human antimicrobial peptides: defensins, cathelicidins and histatins. Biotechnol Lett 27(18):1337–1347

Dever LL, Johanson WGJ (2000) Infections associated with endotracheal intubation and tracheostomy. In: Waldvogel FA, Bisno AL (eds) Infections associated with indwelling medical devices. ASM Press, Washington, DC, pp 307–324

Donlan RM, Costerton JW (2002) Biofilms: survival mechanisms of clinically relevant microorganisms. Clin Microbiol Rev 15:167–193

Eggimann P, Waldvogel F (2000) Pacemaker and defibrillator infections. In: Waldvogel FA, Bisno AL (eds) Infections associated with indwelling medical devices. ASM Press, Washington, DC, pp 247–264

Falagas ME, Fragoulis K, Bliziotis IA, Chatzinikolaou I (2007) Rifampicin-impregnated central venous catheters: a meta-analysis of randomized controlled trials. J Antimicrob Chemother 59:359–369

Fischetti VA (2005) Bacteriophage lytic enzymes: novel anti-infectives. Trends Microbiol 13(10):491–496

Free RH, Van der Mei HC, Dijk F, Van Weissenbruch R, Busscher HJ, Albers FWJ (2001) Biofilm formation on voice prostheses: *In vitro* influence of probiotics. Ann Otol Rhinol Laryngol 110:946–951

Fux CA, Stoodley P, Hall-Stoodley L, Costerton JW (2003) Bacterial biofilms: a diagnostic and therapeutic challenge. Exp Rev Anti Infect Ther 1(4):667–683

Goeau-Brissonnière OA, Coggia M (2000) Arterial prosthetic infections. In: Waldvogel FA, Bisno AL (eds) Infections associated with indwelling medical devices. ASM Press, Washington, DC, pp 127–144

Gollwitzer H, Ibrahim K, Meyer H, Mittelmeier W, Busch R, Stemberger A (2003) Antibacterial poly(D,L-lactic acid) coating of medical implants using a biodegradable drug delivery technology. J Antimicrob Chemother 51(3):585–591

Gottenbos B, Busscher HJ, Van der Mei HC, Nieuwenhuis P (2004) Pathogenesis and prevention of biomaterial centered infections. J Mat Sci Mat Med 13(8):717–722

Gottenbos B, Grijpma D, Van der Mei HC, Feijen J, Busscher HJ (2001) Antimicrobial effects of positively charged surfaces on adhering Gram-positive and Gram negative bacteria. J Antimicrob Chemother 48:7–13

Gristina AG (1987) Biomaterial-centered infection, microbial *versus* tissue integration. Science 237:1588–1597

Gudiña E, Rocha V, Teixeira JA, Rodrigues LR (2010a) Antimicrobial and anti-adhesive properties of a biosurfactant isolated from *Lactobacillus paracasei* subsp. *paracasei* A20. Lett Appl Microbiol 50:419–424

Gudiña E, Teixeira JA, Rodrigues LR (2010b) Isolation and functional characterization of a biosurfactant produced by *Lactobacillus paracasei*. Col Surf B 76:298–304

Habash M, Reid G (1999) Microbial biofilms: their development and significance for medical device-related infections. J Clin Pharmacol 39:887–898

Hall-Stoodley L, Costerton JW, Stoodley P (2004) Bacterial biofilms: from the natural environment to infectious diseases. Nat Rev Microbiol 2:95–108

Hancock E (1994) Artificial valve disease. In: Schlant RC, O'Rourke RA, Roberts R, Sonnenblick EH (eds) The heart arteries and veins. McGraw-Hill, New York, NY, pp 1539–1545

Heinemann C, Van Hylckama V, Janssen D, Busscher HJ, Van der Mei HC, Reid G (2000) Purification and characterization of a surface-binding protein from *Lactobacillus fermentum* RC-14 that inhibits adhesion of *Enterococcus faecalis* 1131. FEMS Microbiol Lett 190:177–180

Heldman AW, Hartert TV, Ray SC, Daoud E, Kowalski T, Pompili V, Sisson S, Tidmore W, vom Eigen K, Goodman S (1996) Oral antibiotic treatment of right-sided staphylococcal endocarditis in injection drug users: prospective randomized comparison with parental therapy. Am J Med 101(1):68–76

Hessen MT, Zuckerman JM, Kaye D (2000) Infections associated with foreign bodies in the urinary tract. In: Waldvogel FA, Bisno AL (eds) Infections associated with indwelling medical devices. ASM Press, Washington, DC, pp 325–344

Hetrick EM, Schoenfisch MH (2006) Reducing implant-related infections: active release strategies. Chem Soc Rev 35:780–789

Hoffman LR, D'Argenio DA, MacCoss MJ, Zhang Z, Jones RA, Miller SI (2005) Aminoglycoside antibiotics induce bacterial biofilm formation. Nature 436(25):1171–1175

Hong HA, Ducle H, Cutting SM (2005) The use of bacterial spore formers as probiotics. FEMS Microbiol Rev 29(4):813–835

Joly V, Pangon B, Vallois JM, Abel L, Brion N, Bure A, Chau NP, Contrepois A, Carbon C (1987) Value of antibiotic levels in serum and cardiac vegetations for predicting antibacterial effect of ceftriaxone in experimental *Escherichia coli* endocarditis. Antimicrob Agents Chemother 31:1632–1639

Kaneko Y, Thoendel M, Olakanmi O, Britigan BE, Singh PK (2007) The transition metal gallium disrupts *Pseudomonas aeruginosa* iron metabolism and has antimicrobial and antibiofilm activity. J Clin Invest 117(4):877–888

Kaper HJ, Busscher HJ, Norde W (2003) Characterization of poly(ethylene oxide) brushes on glass surfaces and adhesion of *Staphylococcus epidermidis*. J Biomater Sci Polym Ed 14(4):313–324

Karchmer AW (2000) Infections of prosthetic heart valves. In: Waldvogel FA, Bisno AL (eds) Infections associated with indwelling medical devices. ASM Press, Washington, DC, pp 145–172

Kingshott P, Wei J, Bagge-Ravn D, Gadegaard N, Gram L (2003) Covalent attachment of poly(ethylene glycol) to surfaces, critical for reducing bacterial adhesion. Langmuir 19: 6912–6921

Lopez-Lopez G, Pascual A, Perea EJ (1991) Effect of plastic catheter material on bacterial adherence and viability. J Med Microbiol 34:349–353

Lynch AS, Robertson GT (2008) Bacterial and fungal biofilm infections. Annu Rev Med 59: 415–428

Mahieu H, Van Saene H, Rosingh H, Schutte H (1986) *Candida* vegetations on silicone voice prostheses. Arch Otolaryngol Head Neck Surg 112:321–325

Manierski C, Besarab A (2006) Antimicrobial locks: putting the lock on catheter infections. Adv Chronic Kidney Dis 13:245–258

Mireles JR, Toguchi A, Harshey RM (2001) Salmonella enteric serovar Typhimurium swarming mutants with altered biofilm-forming abilities: surfactin inhibits biofilm formation. J Bacteriol 183:5848–5854

Muthusamy K, Gopalakrishnan S, Ravi TK, Sivachidambaram P (2008) Biosurfactants: properties, commercial production and application. Curr Sci 94(6):736–747

Nagel JA, Dickinson RB, Cooper SL (1996) Bacterial adhesion to polyurethane surfaces in the presence of pre-adsorbed high molecular weight kininogen. J Biomater Sci Polym Ed 7(9): 769–780

Neu T (1996) Significance of bacterial surface active compounds in interaction of bacteria with interfaces. Microbiol Rev 60:151–166

Oliver MJ, Schwab SJ (2000) Infections related to hemodialysis and peritoneal dialysis. In: Waldvogel FA, Bisno AL (eds) Infections associated with indwelling medical devices. ASM Press, Washington, DC, pp 345–372

Otto M (2004) Quorum-sensing control in Staphylococci – A target for antimicrobial drug therapy? FEMS Microbiol Lett 241:135–141

Perdigon G, De Marcias ME, Alvaraz S, Oliver G, De Ruiz-Holgado AA (1986) Effect of perorally administrated lactobacilli on macrophage activation in mice. Infect Immun 53:404–410

Pizarro-Cerdá J, Cossart P (2006) Bacterial adhesion and entry into host cells. Cell 124:715–727

Poelstra KA, Barekzi NA, Rediske AM, Felts AG, Slunt JB, Grainger DW (2002) Prophylactic treatment of gram-positive and gram-negative abdominal implant infections using locally delivered polyclonal antibodies. J Biomed Mater Res 60:206–215

Raad I, Hachem R, Tcholakian RK, Sherertz R (2002) Efficacy of minocycline and EDTA lock solution in preventing catheter-related bacteremia, septic phlebitis and endocarditis in rabbits. Antimicrob Agents Chemother 46:327–332

Reid G (1999) Biofilms in infectious disease and on medical devices. Int J Antimicrob Agents 11:223–226

Reid G (2000) *In vitro* testing of *Lactobacillus acidophilus* NCFM as a possible probiotic for the urogenital tract. Int Dairy J 10:415–419

Rivardo F, Turner RJ, Allegrone G, Ceri H, Martinotti MG (2009) Anti-adhesion activity of two biosurfactants produced by *Bacillus* spp. prevents biofilm formation of human bacterial pathogens. Appl Microbiol Biotechnol 83:541–553

Rodrigues LR, Banat IM, Teixeira JA, Oliveira R (2006a) Biosurfactants: potential applications in medicine. J Antimicrob Chem 57(4):609–618

Rodrigues LR, Banat IM, Teixeira JA, Oliveira R (2007) Strategies for the prevention of microbial biofilm formation on silicone rubber voice prostheses. J Biomed Mat Res B 81B(2):358–370

Rodrigues LR, Banat IM, Van der Mei HC, Teixeira JA, Oliveira R (2006b) Interference in adhesion of bacteria and yeasts isolated from explanted voice prostheses to silicone rubber by rhamnolipid biosurfactant. J Appl Microbiol 100:470–480

Rodrigues LR, Moldes A, Teixeira JA, Oliveira R (2006d) Kinetic study of fermentative biosurfactant production by *Lactobacillus* strains. Biochem Eng J 28(2):109–116

Rodrigues LR, Teixeira JA, Oliveira R (2006e) Low cost fermentative medium for biosurfactant production by probiotic bacteria. Biochem Eng J 32:135–142

Rodrigues LR, Van der Mei HC, Banat I, Teixeira JA, Oliveira R (2006c) Inhibition of microbial adhesion to silicone rubber treated with biosurfactant from *Streptococcus thermophilus* A. FEMS Immunol Med Microbiol 46(1):107–112

Rodrigues LR, Van der Mei HC, Teixeira JA, Oliveira R (2004a) Biosurfactant from *Lactococcus lactis* 53 inhibit microbial adhesion on silicone rubber. Appl Microbiol Biotechnol 66(3): 306–311

Rodrigues LR, Van der Mei HC, Teixeira JA, Oliveira R (2004b) Influence of biosurfactants from probiotic bacteria on formation of biofilms on voice prostheses. Appl Environ Microbiol 70(7):4408–4410

Schmidmaier G, Lucke M, Wildemann B, Haas NP, Raschke M (2006) Prophylaxis and treatment of implant-related infections by antibiotic-coated implants: a review. Injury 37(Suppl 2): S105–S112

Shenkman B, Varon D, Tamarin I, Dardik R, Peisachov M, Savion N, Rubinstein E (2002) Role of agr (RNAIII) in *Staphylococcus aureus* adherence to fibrinogen, fibronectin, platelets and endothelial cells under static and flow conditions. J Med Microbiol 51:747–754

Stewart PS (2002) Mechanism of antibiotic resistance in bacterial biofilms. Int J Med Microbiol 292:107–113

Sulakvelidze A, Alavidze Z, Morris JG Jr (2001) Bacteriophage therapy. Antimicrob Agents Chemother 45(3):649–659

Teller M, Gopp U, Neumann H-G, Kuhn K-D (2007) Release of gentamicin from bone regenerative materials: an *in vitro* study. J Biomed Mater Res B 81(1):23–29

Trampuz A, Zimmerli W (2006) Antimicrobial agents in orthopaedic surgery: prophylaxis and treatment. Drugs 66:1089–1105

Veenstra DL, Saint S, Saha S, Lumley T, Sullivan SD (1999) Efficacy of antiseptic-impregnated central venous catheters in preventing catheter-related bloodstream infection: a meta-analysis. JAMA 281:261–267

Velraeds M, Van de Belt-Gritter B, Van der Mei HC, Reid G, Busscher HJ (1998) Interference in initial adhesion of uropathogenic bacteria and yeasts to silicone rubber by a *Lactobacillus acidophilus* biosurfactant. J Med Microbiol 47:1081–1085

Webb JC, Spencer RF (2007) The role of polymethylmethacrylate bone cement in modern orthopaedic surgery. J Bone Jt Surg Br 89(7):851–857

Yogev R, Bisno AL (2000) Infections of central nervous system shunts. In: Waldvogel FA, Bisno AL (eds) Infections associated with indwelling medical devices. ASM Press, Washington, DC, pp 231–246

Zilberman M, Elsner JJ (2008) Antibiotic-eluting medical devices for various applications. J Cont Release 130:202–215

ERRATUM

Erratum to: Bacterial Adhesion

Dirk Linke
Max Planck Institute for Developmental Biology, Department of Protein Evolution,
Spemannstr. 35, 72076 Tübingen, Germany,
dirk.linke@tuebingen.mpg.de

Adrian Goldman
University of Helsinki, Institute of Biotechnology, Viikinkaari 1,
FIN-00014 Helsinki, Finland,
adrian.goldman@helsinki.fi

D. Linke, A. Goldman (eds.), *Bacterial Adhesion*, Advances in Experimental Medicine and Biology 715, DOI 10.1007/978-94-007-0940-9, © Springer Science+Business Media B.V. 2011

DOI 10.1007/978-94-007-0940-9_23

The author noticed the following error in the book:

In the Table of Contents, List of Contributors and Chapter 17, the first author name should be Ilaria Ferlenghi.

The online version of the original book can be found at
http://dx.doi.org/10.1007/978-94-007-0940-9

Index

D. Linke, A. Goldman (eds.), *Bacterial Adhesion*, Advances in Experimental Medicine and Biology 715, DOI 10.1007/978-94-007-0940-9,